University of Venda

APPLICATION OF GIS AND REMOTE SENSING TECHNIQUES TO EVALUATE THE IMPACT OF LAND COVER AND LAND USE CHANGE ON THE HYDROLOGY AND WATER RESOURCES OF LUVUVHU RIVER CATCHMENT IN LIMPOPO PROVINCE, SOUTH AFRICA.

by

SINGO LUTENDO RHINAH
Student No: 11511585

A thesis submitted in fulfillment of the requirements for the degree of Doctor of Philosophy in Environmental Sciences in the Department of Hydrology and Water Resources at the University of Venda, Limpopo Province, South Africa

Promoter: **Dr. Peter Musula Kundu**

Co-promoter: **Prof. John Ogony Odiyo**

September, 2018

DECLARATION

I **SINGO LUTENDO RHINAH** hereby declare that this thesis submitted to the Department of Hydrology and Water Resources at the University of Venda, for the degree of Doctor of Philosophy in Environmental Sciences, has not been previously submitted for a degree at this or any other University, that it is my own work in design and execution and all the reference material contained herein has been duly acknowledged.

---------- ----------

Singo Lutendo Rhinah Date

Promoter: Dr. Peter Musula Kundu

……..

Co- promoter: Prof. John Ogony Odiyo

……..

SCIENTIFIC STATEMENT

Partial results contained in this thesis have given rise to different articles which have been presented at international and local conferences. Ten publications have been produced in referred proceedings as shown below. Paper manuscripts have been submitted to scientific Journals for consideration.

L.R. Singo, P.M. Kundu, F.I. Mathivha and J.O. Odiyo, (2016) Evaluation of flood risks using flood frequency models: A case study of Luvuvhu River Catchment in Limpopo Province, South Africa. In Proc. *5th International Conference on Flood Risk Management and Response*, 29 June - 01 July 2016, San Servolo, Venice, Italy. Published in the *WIT Transactions on The Built Environment,* Urban Water Systems & Floods, *Vol.165, pp215-226*, Published in http://www.witpress.com/elibrary/wit-transactions-on-the-built-environment/165/35567, ISSN 1743-3509, doi:10.2495/UW160191.

Mathivha, F.I, Kundu, P.M. and **Singo, L.R.** (2016) The Impacts Of Land Cover Change On Stream Discharges In Luvuvhu River Catchment, Vhembe District, Limpopo Province, South Africa. In Proc. *5th International Conference on Flood Risk Management and Response*, 29 June - 01 July 2016, San Servolo, Venice, Italy. Published in the *WIT Transactions on The Built Environment,* Urban Water Systems & Floods, *Vol.165, pp259-270,* Published in http://www.witpress.com/elibrary/wit-transactions-on-the-built-environment/165/35567, ISSN 1743-3509, doi:10.2495/UW160191.

Singo, L.R, Kundu, P.M. and Mathivha, F.I. (2016). Spatial variation of reference evapotranspiration and its influence on the hydrology of Luvuvhu River Catchment. *Research Journal of Agriculture and Environmental Management*, Vol. 5(6), pp. 187-196, Available at http://apexjournal.org/rjaem/archive/2016/July/fulltext/Singo%20et%20al.pdf, ISSN 2315-8719. Also available at GRIN Verlag, http://www.grin.com/en/e-book/323712/spatial-variation-of-reference-evapotranspiration-and-its-influence-on, ISBN: 9783656989769.

Singo, L.R, Kundu, P.M. and Odiyo, J.O. (2016). Impact of land use change on surface runoff and stream discharges in Luvuvhu River Catchment. *Research Journal of Agriculture and Environmental Management*, *Vol. 5(6), pp. 197-206*, ISSN 2315-8719. Available at http://apexjournal.org/rjaem/archive/2016/July/fulltext/Singo%20et%20al%202.pdf, ISSN 2315-8719.

Kundu P.M, **Singo L.R**, Odiyo J.O. (2015). Impact of land cover change on stream discharges and water resources in Luvuvhu River Catchment, Vhembe District, Limpopo Province, South Africa. *In Proc. 18th International Conference on Bioinformatics and Biomedicine*, Istanbul, Turkey, 21-22 May 2015. *World Academy of Science, Engineering and Technology, Bioengineering and Life Sciences*, *Vol: 2, No: 5 2015*; *International Scholarly and Scientific Research & Innovation - International Science Index* 2(5) 2015, Available at https://waset.org/abstracts/23083.

L.R. Singo, P.M. Kundu, J.O. Odiyo, F.I. Mathivha and T.R. Nkuna, (2015). Hydrologic modeling using Remote Sensing and GIS in Luvuvhu River Catchment, South Africa. In *Proc. 1st Disaster Risk Sciences and Management Conference*, 2-3 March 2015, Polokwane, South Africa. *DRS&M Conference Proceedings 2-3 March 2015* –www.univendrmc.co.za/index.

Kundu P.M, **L.R Singo**, J.O. Odiyo and T.R Nkuna, (2014). An evaluation of the effects of climate change on flood frequency in Luvuvhu River catchment, Limpopo Province, South Africa. In *Proc. 5th International Conference on Sustainable Irrigation and Drainage: Management, Technologies and Policies.2014, Poznan, Poland.* Published in the *WIT Transactions on Ecology and the Environment, Vol.185: pp157-168, ISBN: 978- 84564-788-9*. Available at http://www.witpress.com/Secure/elibrary/papers/SI14/SI14015FU1.pdf.

Kundu P.M, **L.R Singo**, J.O. Odiyo and T.R Nkuna, (2014). Effects of climate change on flood risk and sustainable developments in South Africa. In *Proc. 6th International Conference on Flood Management*, 16th-18th Sept. 2014, Sao Paulo, Brazil. Available at http://www.abrh.org.br/icfm6/proceedings/papers/PAP014716.pdf.

P.M. Kundu, **L.R. Singo**, J.O. Odiyo, F.I. Mathivha and T.R. Nkuna, (2013). Extraction and analysis of geomorphologic and hydrologic properties for Luvuvhu River Catchment in Limpopo Province, South Africa. In *Proc. 2nd International Conference on Water and Society 2013, New Forest, UK*. Published in *WIT Transactions on Ecology and the Environment, Vol. 178: pp29-39. ISBN: 978-1-84564-743-8.* Available at http://library.witpress.com/pages/PaperInfo.asp.PaperID=25052.

L.R Singo, P.M Kundu, J.O Odiyo, F.I Mathivha and T.R Nkuna, (2012). Extraction and analysis of morphologic and hydrologic properties for Luvuvhu River Watershed in Limpopo Province, South Africa. Paper presented at the *13th Waternet/WARFSA/GWP-SA Symposium*, Birchwood Hotel and O.R Tambo Conference Centre, Johannesburg, 31 October - 02 November 2012.

L.R. Singo, P.M. Kundu, J.O. Odiyo, F.I. Mathivha and T.R. Nkuna, (2012). Flood Frequency Analysis of Annual Maximum Stream flows for Luvuvhu River Catchment, Limpopo Province, South Africa. *Proceedings of the 16th SANCIAHS National Hydrology Symposium*, University of Pretoria (Hatfield Campus), Pretoria, South Africa, 1-3 October 2012. Available at http://www.ru.ac.za/static/institutes/iwr/SANCIAHS/2012/documents/050Singo.pdf. Also available at https://www.yumpu.com/en/document/view/25893157/flood-frequency-analysis-of-annual-maximum-stream-flows-for-.

L.R. Singo, P.M. Kundu, J. O. Odiyo and T.R. Nkuna (2011). Hydrologic modeling on a messo scale using GIS and imagery in Luvuvhu River Catchment, South Africa. Paper presented at the *12th Waternet/WARFSA/GWP-SA Symposium*, 26-28 October 2011, Joaquim Chissano International Conference Centre, Eduardo Mondlane University, Maputo, Mozambique.

DEDICATIONS

This thesis is dedicated to my entire family, in appreciation for their understanding and moral support. A special dedication goes to my parents, **Mr. Edwin and Mrs. Elizabeth Singo**, whose vision and interest in mainstream education enabled me to overcome the challenges associated with hard of hearing.

ACKNOWLEDGEMENTS

I would like to express my appreciation to Dr. P.M Kundu for the excellent supervision that made this thesis possible. Without his constructive criticisms, tireless supports and advice, this work would have been more difficult to accomplish. I acknowledge Prof. J.O Odiyo for his co-supervision and continued support throughout the research period. I give special thanks to Prof. T.A Kabanda (North West University) for paving a way towards my PhD and for being such an inspiring role model.

I acknowledge the South African Weather Services (SAWS) for providing rainfall data; the South African's Department of Water Affairs (DWA) for providing hydrological data; Statistics South Africa (StatsSA) for providing population and socio-economic data; the Regional Centre for Mapping and Resources for Development (RCMRD) for providing Landsat and ENVISAT images; the South African National Space Agency (SANSA) for providing free satellite images; the Agricultural Research Council (ARC) for providing meteorological data, as well as land use and soil maps. I acknowledge the financial support I received from the National Research Foundation (NRF), the Research and Publication Committee (RPC) and the Work-Study Programme (WSP) at the University of Venda.

I acknowledge the following individuals for the invaluable support they provided towards this research. T. Makondelela of Vondo Water Scheme; B. Mhlongo and C. Muzerengi of University of Venda's Mining and Environmental Geology department; M.P Tshidada of University of Venda's Department of Soil Sciences; M.T Mafune of University of Venda's Transport Department; V.F Mushiana of University of Venda's Urban and Regional Planning Department; and the late Norah Machaba of the University of Venda's Research and Innovation Department.

I acknowledge the support I received from my fellow postgraduate students: Ms. R. Makungo, Ms. H.J. Nemudivhiso, Ms. P. Nemaxwi, Mr. T.R. Nkuna, Ms. C. Kaseke, Mr. H.S Ogombe, Ms. O.J. Bassey and Dr. A. Mommoh. I acknowledge the companionship of Mr. Matidze T.M, Ms. Nemandiwe L, Ms. Nemapate M, Mr. Sengani M, Mr. Sambo S and Mr. Masombuka B

during primary data collection. Ms. Nevhushoma Nditsheleni is acknowledged for her enthusiasms and cheerful encouragements.

Last but not least, I would like to acknowledge and pay my special thanks to Ms. F.I. Mathivha for her incredible support. She served as the interpreter between myself and Dr. Kundu and removed a huge obstacle that would have made the challenges associated with my condition of deafness more difficult. She assisted me during field work and lab analysis and also accompanied me to local and international conferences where I presented my partial results.

ABSTRACT

Luvuvhu River Catchment (LRC) exhibits diverse land use and land cover patterns that are influenced by seasonality and socio-cultural practices of the local communities. From 1950, the catchment has been undergoing land cover changes caused by expanding villages, new urban centres and clearing forest land for agriculture. Conversion of natural landscape for agricultural and urban purposes degraded the catchment by negatively affecting the hydrologic processes. This study was therefore conducted to evaluate the impact of land cover and land use change on the hydrology and water resources of LRC. Geographical Information Systems (GIS) and remote sensing techniques were applied to evaluate the impact of the changes on the catchment. Remotely sensed imagery was used as the primary sources of data for classification and detection of changes. Digital Elevation Models (DEMs) were used for hydrologic and geomorphic modeling in combination with information from remotely sensed imagery. Field data sets for soil and meteorology were obtained from selected sampling segments, based on the area frame sampling. The method of direct expansion was used to quantify land use classes. Flood frequency was analysed using probability distribution methods at recurrence intervals of 2, 5, 10, 20, 25, 50, 100, and 200 years. The FAO CROPWAT software based on Penman-Montheith equation was used to assess the impact of land cover changes on evapotranspiration regimes. To study the hydrological response of land cover change in the catchment, the Soil Conservation Services-Curve Number (SCS-CN) method was first used independently to simulate surface runoff and investigate the impact of land use change on runoff under historical land cover regimes. The Soil and Water Assessment Tool (SWAT) model was then applied in the Tshakhuma-Levubu subcatchment to assess the impact of land management practices on the soil and water bodies in the catchment.

The results indicated that changes were having negative impacts on the hydrology of the catchment. The impact of land use and land cover change on hydrology of LRC was manifested in stream flow, surface runoff, suspended sediment and flood frequency and magnitudes. There was significant land cover and land use change from forestland, woodland and open grassland to medium size farms, subsistence agriculture and built-up land. These developments were concentrated on hillsides and hilltops in the catchment and they were of concern as they were

impacting on the hydrological processes. Throughout the 2000's, land use change revealed a decrease in natural forest from 32.15% to 20.67%, giving rise to agriculture which rose to 38.57% in 2010. Runoff was observed to be highly variable during the month of February with maximum runoff records of 1.63 m^3 and 3.84 m^3 upstream and downstream, respectively. Flood frequency results showed that an increase in the peak discharges was to be expected, especially for the discharge range corresponding to smaller and medium flood magnitudes. The use of imagery and DEMs within GIS was found to efficiently represent ground surface and allow automated extraction of features, thus bringing advantages in terms of processing efficiency, cost effectiveness, and accuracy assessments. This technique could therefore be adopted to improve land use planning, water management, and rapid identification of slopes and elevations in consideration for their functional and structural requirements. Analysis showed that the SWAT model was suitable for predicting the location and extent of pollution in the catchment. It assumed sheet and rill erosion as the dominant erosion type contributing to siltation and water pollution in rivers. The study recommends close monitoring and sustained enforcement of the rural land use regulations to prevent the conversion of land to urban land use.

TABLE OF CONTENTS

LIST OF FIGURES

LIST OF TABLES

LIST OF APPENDICES

LIST OF SYMBOLS

A	Area of cross section [m^2]
a_s	Fraction of extraterrestrial radiation reaching the earth on overcast days
b	Slope
b_s	Fraction of extraterrestrial radiation reaching the earth on clear days
C	Runoff coefficient
CN_m	Runoff curve number
CN_w	Weighted curve number
c_s	Soil heat capacity [MJ m-3 $°C^{-1}$]
C_v	Coefficient of variation
d_r	Inverse relative distance Earth-Sun [rad]
e_a	Actual vapour pressure [kPa]
e_s	Saturation vapour pressure [kPa]
ET	Evapotranspiration (mm)
ET_o	Reference evapotranspiration [mm/day]
F	Cumulative infiltration [mm]
f	Infiltration rate [mm/h]
G	Skewness coefficient
G_{sc}	Solar constant [MJ m^{-2} day^{-1}]
h	Elevation [m]
i	Rainfall intensity [mm]
I_a	Initial abstraction [mm]
J	Number of the day in the year
K	Frequency factor
k	Decay constant specific to the soil in hours
t_p	Ponding time
m	Order number of event
MC	Moisture content of the soil
n	Number of events
P	Rainfall [mm]
$P(x_m)$	Probability of exceedance
Q	Discharge [m^3/s]
Q_T	Discharge for a given year [m^3/s]
r	Regression coefficient
R_a	Extraterrestrial radiation [MJ m^{-2} day^{-1}]
RH	Relative humidity (%)
R_n	Net radiation of the crop surface in [MJ m^{-2} day^{-1}]
R_s	Solar or shortwave radiation [MJ m^{-2} day^{-1}]
R^2	Co-efficient of determination
T	Mean daily air temperature [°C]
T_r	Return period [years]
u_2	Wind speed at 2 m above ground surface [m s^{-1}]
u_z	Measured wind speed at z m above ground surface [m s^{-1}]
$V(t)$	Cumulative volume of the ordinate of the mass curve at any time t
$\hat{w}$	Profile curvature
W_d	Dry weight of the soil
W_{Sieve}	Sample weight per sieve

W_{Total}	Weight of soil sample
W_w	Wet weight of the soil
X	Curvature
$\bar{x}$	Multi-year average value
X_{av}	Mean of the LP3 series
x_i	Data in the *i*th year
x_p	Quantile estimates
X_T	Logarithm of discharge
y_n	Gumbel's reduced mean
y_T	Value of peak discharge for a given recurrence interval
Z	Height of measurement above ground surface [m]
ω_s	Sunset hour angle [rad]
θ	Latitude
θ_w	Water content
Δt	Length of time interval [day]
Δz	Effective soil depth
δ	Solar declination [rad]
ψ	Wetting front soil suction head
$\Delta\theta$	The difference between initial and final moisture contents of the soil
Δ	Slope vapor curve [kPa/^{0}C]
γ	Psychtometric constant [kPa/^{0}C]
σ_n	Gumbel's reduced standard deviation
σ_x	Standard deviation of the series
β	Slope
φ	Aspect
Φ	Plan curvature

LIST OF ABBREVIATIONS

ARC	Agricultural Research Council
ASCE	American Society of Civil Engineers
ASTER	Advanced Spaceborne Thermal Emission and Reflection Radiometer
ASTM	American Society for Testing and Materials
CANEGRO	Canesugar Crop Growth
CMAs	Catchment Management Agencies
CEEPA	Centre for Environmental Economics and Policy in Africa
CN	Curve Number
DEM	Digital Elevation Model
DWA/S	Department of Water Affairs/ and Sanitation
ENVI	Environment for Visualizing Images
ESRI	Environmental Systems Research Institute
ESRL	Earth System Research Laboratory
ET	Evapotranspiration
ET_o	Reference Evapotranspiration
ETM+	Enhanced Thematic Mapper Plus
FAO	Food and Agricultural Organization
FFA	Flood Frequency Analysis
FFT	Fast Fourier Transform
GIS	Geographical Information System
GPS	Global Positioning System
HSG	Hydrologic Soil Group
IDW	Inverse Distance Weighted
ISRIC	International Soil Reference and Information Centre
ISSS	International Society of Soil Science
IUSS	International Union of Soil Sciences
GEV	Generalized Extreme Value
GIS	Geographical Information System
GLOVIS	Global Visualization Viewer

HEC-HMS	Hydrologic Engineering Centre- Hydrologic Modeling System
ITCZ	Inter-tropical Convergence Zone
KNP	Kruger National Park
LP3	Log Pearson Type III
LRC	Luvuvhu River Catchment
MCA	Mass Curve Analysis
MERIS	Medium Resolution Imaging Spectrometer
MLC	Maximum Likelihood Classifier
MODIS	Moderate Resolution Imaging Spectrometer
MSS	Multispectral Scanner
NASA	National Aeronautics and Space Administration
NEMA	National Environmental Management Act
NGA	National Geospatial-Intelligence Agency
NOAA	National Oceanic and Atmospheric Administration
NRCS	Natural Resources Conservation Services
RBF	Radial Basis Function
RCMRD	Regional Centre for Mapping and Resource Development
SANSA	South African National Space Agency
SAWS	South African Weather Services
SCS	Soil Conservation Services
SPOT	Systeme Probatoire d'Observation de la Terra
SPSS	Statistical Package for the Social Sciences
SSC	Suspended Sediment Concentration
SWAT	Soil and Water Assessment Tool
SRTM	Shuttle Radar Topography Mission
TM	Thematic Mapper
USACE	United States Army Corps of Engineers
USCS	Unified Soil Classification System
USDA	United States Department of Agriculture
USEPA	United States Environmental Protection Agency
USGS	United States Geological Survey

CHAPTER 1
INTRODUCTION

1. Background

Luvuvhu River Catchment (LRC) exhibits diverse land use and land cover patterns that are influenced by seasonality and socio-cultural practices of the local communities (Hope *et al*., 2004; Jewitt and Garratt, 2004). From the 1950s, the catchment has been undergoing land cover changes associated with expanding urban centres and villages and clearing forestland for agriculture (Van der Waal, 1997). Land cover in the catchment has been extensively altered by human activities, such as increasing settlements, increasing area under agriculture, increasing and shifting populations, changing national and regional policies, and the introduction of macro-economic activities that negatively impact on the environment. A combination of these alterations impact upon the hydrological system at different temporal and spatial scales (Schulze *et al*., 2004; Calder, 2005). Land cover changes, together with land use changes and associated hydrological disturbances are common reasons for land degradation around the world today (Zacharias *et al*., 2003). The impact of changing land cover associated with deforestation and agricultural transformation on water resources has created increasing concern in the catchment. Studies by Griscom *et al*. (2010) and DWA (2013) have shown that population growth in the LRC has increased rapidly over the years. In order to evaluate the impacts of land cover changes on the hydrological regime, it was necessary to consider the physiological and hydrological factors of LRC.

This study focused on the application of Geographic Information Systems (GIS) and remote sensing to evaluate the impacts of land cover changes on hydrology and water resources. In addition, a number of watershed models were incorporated to achieve automated catchment delineation. Largely, remote sensing was used for land use/cover mapping; GIS was used for data manipulation; and the Digital Elevation Models (DEMs) generated from contours and from the Shuttle Radar Topography Mission (SRTM) data were used for morphological analysis. A rainfall-runoff model based on the US Soil Conservation Services-Curve Number (SCS-CN) was used to determine surface runoff while CROPWAT model based on FAO Penman-Montheith equation was used to evaluate the meteorological factors in the study area.

Remote sensing and GIS have been used by hydrologists to deal with large scale, complex and spatially distributed hydrological processes. The combination of derivatives from remotely sensed data into GIS and their analysis has been seen as the primary tool for operational, efficient acquisition of input parameters for distributed hydrological modeling (Meijerink *et al*., 1994). The technique has held a great deal of promise for hydrology, mainly because of the potential to observe areas and entire river basins rather than mere points (Baldyga, 2004). Due to the variable nature of water resources in the LRC, continuous assessment and monitoring of hydrological system components is important. Lack of appropriate land and water management strategies in the catchment leads to land degradation by soil erosion, increased runoff and sedimentation processes during rainfall events (DWA, 2003). To date, there still exists lack of objective methods to ensure the overall sustainability of land and water resources in the catchment, although there are legal frameworks for management of land (such as the National Environmental Management Act (NEMA) and water resources (such as the Catchment Management Agencies (CMAs) to combat land degradation and water quality monitoring and management. It is therefore imperative that studies to investigate, detect and quantify the land cover and land use changes and their potential impact on the hydrological processes be carried out to enable informed decisions for management purposes.

1.1 Statement of the Problem

Land use affects land cover and changes in land cover affect land use. It affects a wide range of environmental and landscape attributes including the quality of water, land and air resources, ecosystems processes and functions, and climate system (Sylla *et al*., 2012). In the Limpopo Province of South Africa, land cover change resulting from land use changes is a major cause of environmental concern. The water resources are gradually getting depleted due to uncontrolled anthropogenic activities by the rising human population. Due to the rapid population growth and development in areas of Vhembe District of the Limpopo Province, the LRC has been subjected to considerable land use change over the past decades. The rapid land use change can accelerate land degradation and impact negatively on the hydrology and water resources (Forsyth, 2005; Matano, 2015). This is a global problem affecting many countries and the only widely used assessment according to ISRIC-World Soil Information (ISRIC, 2016), has been to map the

perceptions on the type and degree of degradation. Mapping land use/land cover and their changes is crucial for planning and sustainable management of land and water resources (Butt *et al*., 2015). This study used a combination of GIS, remote sensing techniques and watershed models to evaluate the past, present and possible future impacts of land cover change on the hydrology and water resources in the catchment.

This study was conducted in an area with great scientific interest, the LRC, where important land cover alterations have been observed during recent decades, coupled with substantial degradation of land resources (soil, water, vegetation, climate, relief). The hydrologic processes in LRC have not received the necessary scientific attention to identify any relationships between them and the spatio-temporal changes in land use and land cover. The lack of both spatial and temporal land cover data has limited investigation into hydrological processes in the catchment. Studies to understand the dynamics of such changes and their long term effects are therefore important in order to enable water resource planners and managers to formulate strategies to minimize the undesirable impact of future land use and land cover changes on the hydrology and water resources in the catchment.

Recent researches by Lee *et al*. (2011) and Deng *et al*. (2013) suggest that land use activities that significantly change the regional land cover may lead to climate change by influencing evapotranspiration and altering the extremes in temperature and precipitation. Climate change is known to exacerbate the impacts of land cover changes by causing erratic and unpredictable weather, which could drastically diminish the supply of water coming from precipitation. The majority of the people in the LRC are faced with problems of inadequate water resources due to erratic rainfall, coupled with the Intertropical Convergence Zone (ITCZ). Since the large portion of the catchment is under subsistence agriculture, the rainfall variability puts a substantial strain on food security and water resources. As a result, farming (the major economic driver in the catchment) is drastically impacted upon due to sporadic rainfall patterns.

Over the years, the catchment has been affected by severe floods and droughts that have resulted in destruction of property, loss of life, loss of biodiversity and reduced water availability

respectively. Wetlands in the LRC are being threatened in some parts of the study area by being drained to pave way for residential and industrial establishments. These wetlands are crucial in the area as they can help reduce flooding and reduce damage from storm surge, recharge groundwater, control pollution, harbor wildlife and regulate temperatures of the surrounding environment (Junk *et al*., 2012); they further act as water storage for the catchment that can recharge rivers in the event of drought. Large tracks of land along the main river are being degraded by brick manufacturing as well as mining of platinum and quarrying. These activities have affected hydrological processes in many aspects including change in runoff volume, peak flow characteristics, water table levels, and water quality.

While land use and land cover changes are a present-day global phenomenon, the severity of their impacts on both hydrology and water resources might pose serious concern on the future water resources use in a catchment if the existing impacts are not taken into consideration. There is a need to understand how land use activities can alter the state of land cover, which can significantly impact on the hydrological cycle consisting of rainfall, evapotranspiration, surface runoff, infiltration, and river discharge. It was therefore crucial to undertake this intervention to study land cover change and its impact on the hydrology and water resources of the LRC for the expansion of comprehensive integrated land and water management practices.

1.2 Motivation

The application of GIS and remote sensing techniques to evaluate the impact of land cover change on a catchment is important to enhance the available data for sustainable development in water catchments. An assessment evaluating the impact or effects of land use and land cover changes on hydrologic variations is important to enable water resource planners and managers to formulate strategies to minimize the undesirable effects of future land use and land cover changes in the catchment. This study applied remotely sensed imagery data in combination with ancillary data in ArcGIS (ESRI, 2011b) environment to produce the result necessary for timely decision making, which is needed for environmental monitoring, planning and design. This approach makes use of various algorithms to extract and represent watershed structure from Digital Elevation Model (DEM) data. Land surface attributes are then mapped into the watershed

structure as estimated directly from remote sensing imagery, digital terrain data, and digitised soil maps.

1.3 Objectives

The overall objective was to evaluate the impact of land cover changes on the hydrology and water resources by using GIS, remotely sensed imagery and ancillary data. The study was further aimed at evaluating hydrologic processes and flood frequency for the catchment.

The specific objectives were:

i. To detect and quantify land cover and land use changes and examine their impact on the hydrology and water resources in the catchment
ii. To analyse morphologic and hydrologic properties and evaluate their effects on the hydrologic processes in the catchment
iii. To analyse hydrometeorological trends for a period of 50 years and evaluate the annual flood frequency for the catchment

1.4 Research Questions

i. How can land cover and land use changes and the associated change dynamics be detected and quantified?
ii. How can analysis of morphologic and hydrologic properties be carried out to enhance hydrologic modeling of catchments?
iii. How do hydrological measurements lead to the selection of the best method for analysing annual flood frequency for meso scale catchments?

1.5 The Study Area

1.5.1 Location and Topography

The study area shown in Figure 1.1 is located between latitudes 22°17'S and 23°17'S and longitudes 29°49'E and 31°23'E in Vhembe District in Limpopo Province of South Africa.

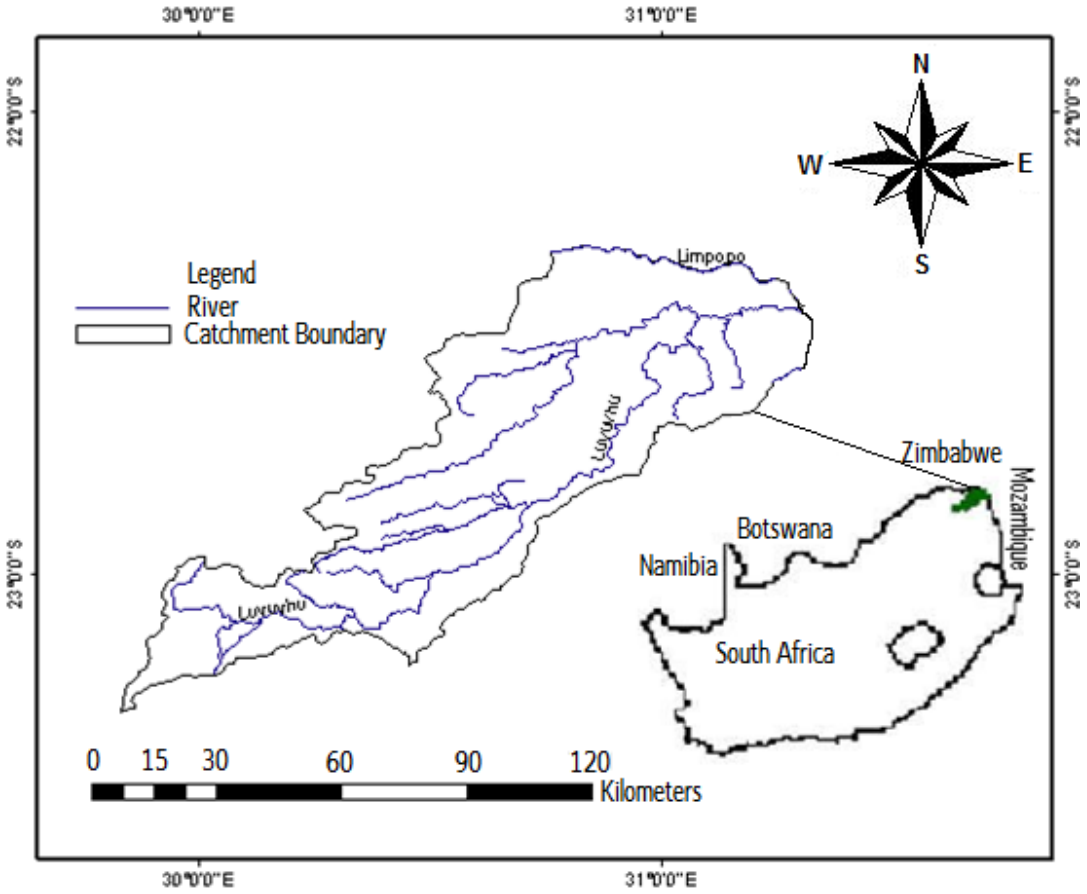

Figure 1.1: The study area

It covers an area of approximately 5941km^2 and is situated on a plateau of 1 312 meters above sea level (DWA, 2002). The catchment consists of a relatively rolling landscape, which gives rise to shallow storage dams, which have large water surfaces exposed to evaporation. The catchment lies at the periphery of the southernmost position of the Intertropical Convergence Zone (ITCZ) during the southern summer with average January position at about 15°S. The river rises as a steep mountain stream in the southeasterly slopes of the Soutpansberg Mountain complex range, which features the west-east direction, flows through Kruger National Park (KNP) (an important conservation and ecotourism area), and empties into the Limpopo River at the border with Mozambique and Zimbabwe. It is located within a zone that is critically affected by seasonal meridional (north-south) shift in the Indian Ocean High (Tshehla, 2009).

The topographic feature that characterises the study area is the Soutpansberg mountain range in the east of the catchment, which reaches an elevation of 1,700m above mean sea level before dropping off into the Limpopo River Valley (LRV) and the border between South Africa and Zimbabwe. The topography of the LRC is softly undulating with a few prominent ridges extending in an east-west direction; whereas the monotony of the area is relieved by separated hills and ranges. The general terrain of mean ridge height of approximately 800-1200 m is common in some places while in some places the peak reaches above 1500 m.

1.5.2 Climate

Generally, the climate of the catchment is strongly influenced by the east-west orientated Soutpansberg mountain range (Weiner, 2006), which represents an effective barrier between the south-easterly maritime climate influences from the Indian Ocean and the continental climate influences (predominantly the ITCZ and the Congo Air Mass) coming from the north (Macdonald *et al*., 2003). The mountains give rise to wind patterns that play an important role in determining local climates. Due to the extreme topographic diversity and altitude changes over short distances within the Soutpansberg, the climate of LRC varies dramatically (Mostert *et al*., 2008).

Rainfall is characterised by large intraseasonal, interannual and longer-scale variability and is associated with the ITCZ with its position being determined by the position of the sun (Reason *et al*., 2005). It is also characterised by the distribution of land and sea (Shongwe, 2007) and orographic uplift as a result of east-west orientation of the Soutpansberg mountain range, due to moisture-laden air from the Indian Ocean, driven by the prevailing south-easterly winds on to the southern scarp of the Soutpansberg. The ITCZ follows distinct seasonal meridional propagation across the region, and is often associated with rainfall because of extensive convection and cloud development that occur at the location of the ITCZ. The study area however, receives one cycle of rainfall that extends from October of the previous year and ends in April of the following year; wherein the dry season runs from May to September. The mean annual temperature ranges from 18°C to 40°C with high variability. Maximum temperatures are experienced in January and minimum temperatures occur on average in winter.

The catchment is characterised by high evaporation rates which increase gradually from 1400 mm to 1900 mm per annum (DWA, 2004a). Evaporation is highest (about 60%) during rainfall season (during the period October to January) and it significantly reduces effective rainfall, runoff, soil infiltration and groundwater recharge. This high evaporation has been known to cause water loss from water bodies leading to an increase in the concentration of sediments. The lowest evaporation (about 40%) occurs in June (DWA, 2002). The high levels of evaporation means that the soil dries up quickly and this reduces the amount of water available for plant intake, leading to drought (FAO, 2004). Thus, evaporation is one of the fundamental elements in hydrology (Keskin *et al*., 2009). It affects the yield of a river basin, the capacity of reservoirs, the consumptive use of water by crops and the yield of underground water. Tyson (1986) noted that evaporation in South Africa varies from a minimum in winter to a maximum in summer over the year. These two periods correspond with the position of the sun at the particular time, i.e. during the summer season the sun is in the southern hemisphere while during winter the sun is in the northern hemisphere. The sun being overhead in summer is also associated with convective rainfall which offsets strong evaporation (Kabanda, 2004).

The wind gust usually blows from east to west, suggesting an eastward or easterly wind movement. Prevailing wind tends to blow from east in summer and the south-west in winter (Schulze, 1965 as cited by Illgner, 2004). The north-south meridional propagation of the ITCZ is associated with the dominant wind flow in the area, which include the South West Indian Ocean (SWIO) and the North West (NW) monsoon winds (Kanyanga, 2008). The overlying ITCZ induces high NW monsoon (from the tropical sub-regions of north-western southern Africa, e.g. Angola) intensity convection over northern Madagascar during austral summer as monsoon winds flow southward over the western Indian Ocean (Nassor and Jury, 1998). Convective clusters associated with the ITCZ are believed to produce very strong wind gusts and torrential rainfall, which result into flooding (Moolchan, 2010). During January (when the ITCZ is in the Southern Hemisphere), the prevailing winds, together with local topographic characteristics, are south-easterly winds from the Indian Ocean. These winds can give rise to maximum monthly rainfall experienced when the ITCZ is located in its most southern position. However, during July (when

the ITCZ is in the Northern Hemisphere (NH); that is, during summer in the NH) the dominant winds are dry south-westerly winds (Nieuwolt, 1997).

Weiner (2008) noted the importance of wind patterns in determining the climate of a region, modified by climatic factors such as rainfall, ambient humidity and extended drought. These climatic factors affect surface moisture. The South African Weather Services (SAWS) (2001) estimated that the average wind speed in LRC was 11km/h; high-speed winds occur occasionally with long intervals. Figures 1.2 and 1.3 show the wind vectors for the catchment during summer and winter seasons.

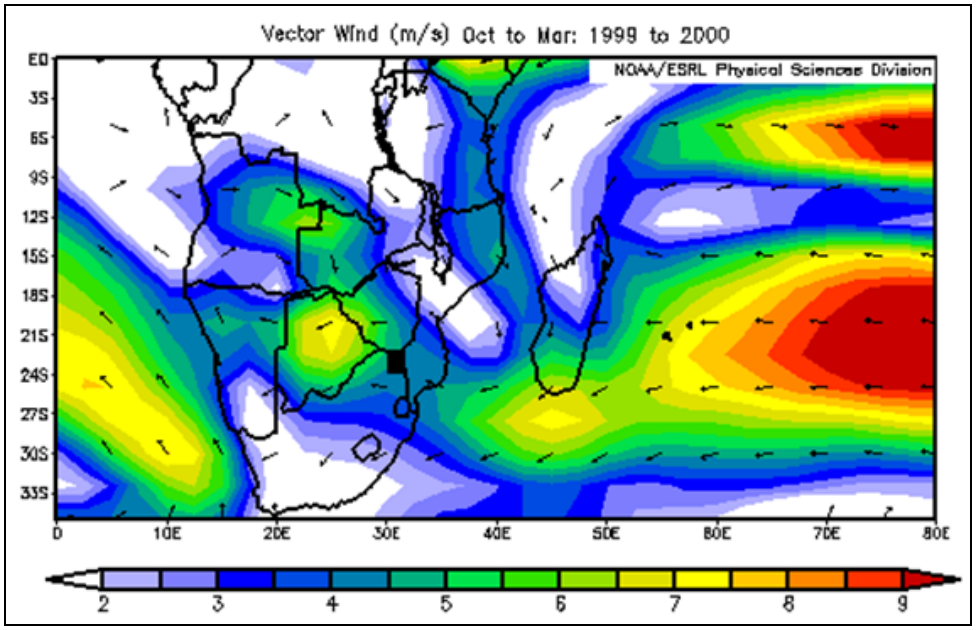

Figure 1.2: Wind vectors during summer season (Source: NOAA/ESRL)

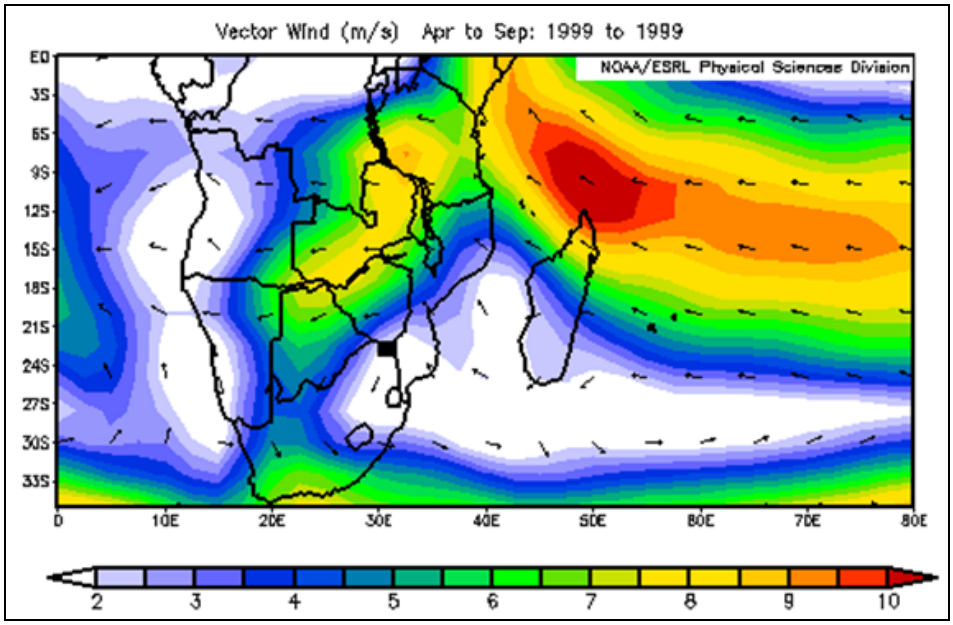

Figure 1.3: Wind vectors during winter season (Source: NOAA/ESRL)

1.5.3 Soils

The area is generally characterised by limited high potential agricultural soil. A wide spectrum of soils found in LRC are sandy (Sa), clay (Cl) and loamy (Lm) with sandy soils most common in other parts of the catchment as shown in Figure 1.4. Due to the combination and diversity nature of soils, the area is also characterised by loamy sand (LmSa), sandy loamy (SaLm), sandy clay (SaCl), and sandy clay loamy (SaClLm). The soils in the study area vary in productivity and are also vulnerable to various forms of degradation, either physical, chemical or biological and hence appropriate management strategies are critical if productivity of the soils is to be improved and sustained.

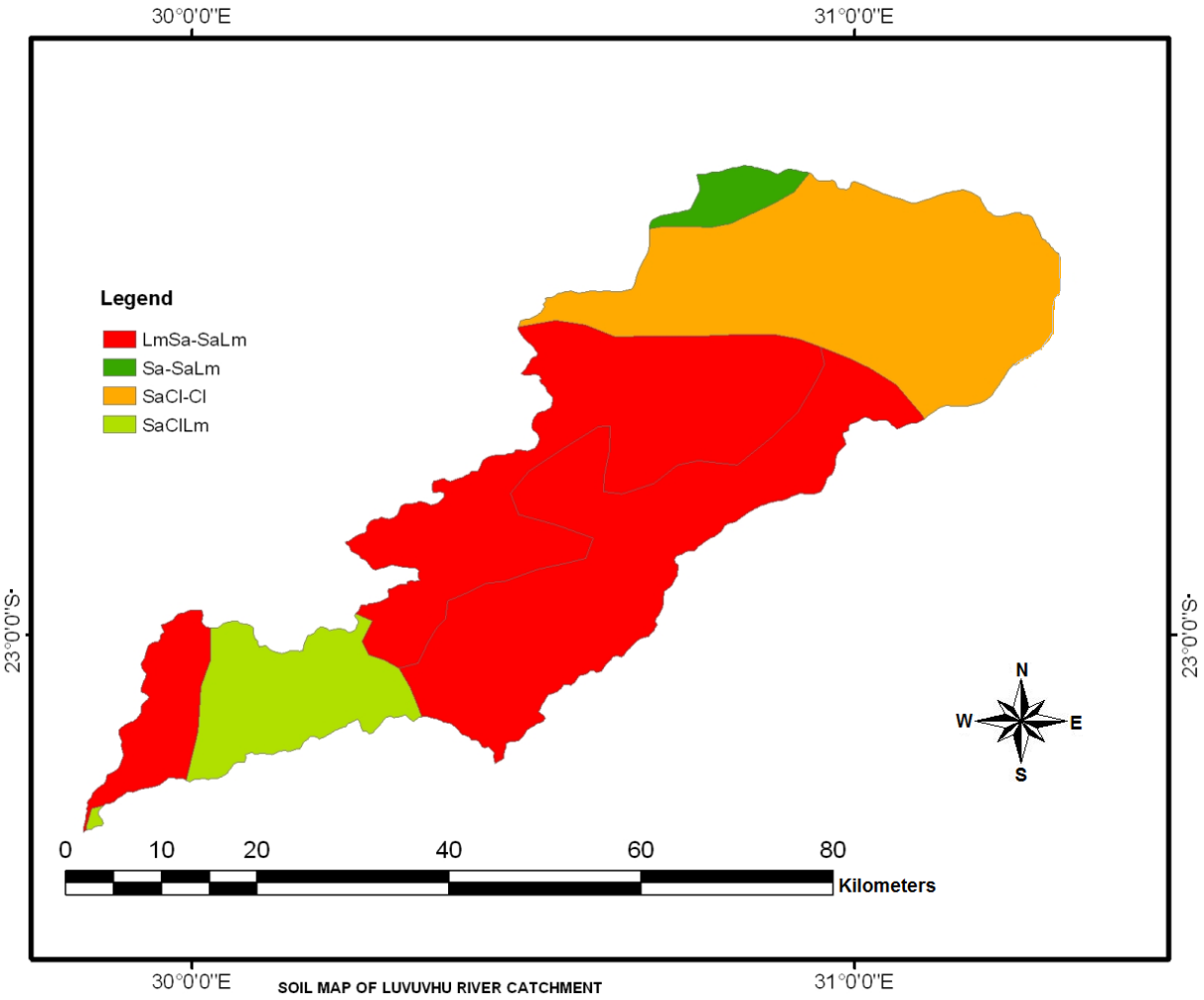

Figure 1.4: Soil Map (Source: FAO-ISRIC-ISSS, 1998)

1.5.4 Geology

The geology is varied and complex and dominated by deep basaltic rock overlain with sedimentary and quartzite layers that block-faulted to the north 150 million years ago (Brandl, 2000). Prior to this faulting, approximately 1800 million years ago, the Soutpansberg geological basin was formed as an east-west trending asymmetrical rift along the palala shear belt (Brandl, 2002). Numerous north-south extensional faults truncate the Spoutpansberg strata, and the landscape in LRC today was formed by erosional forces (Brandl, 1999). Minerals found in the study area, include complex flake granite, ironstone, marble, fire clay, surficial limestone, magnesium and barile mineralisation. Mining is believed to exert significant pressure on water

resources, especially groundwater quality (DWA, 2001). For example, platinum mines can affect the surrounding environment due to acid mine drainage problems from mine residue and waste dumps. Large scale withdrawals of groundwater from mined areas also affect hydrology of both surface and groundwater systems. Surface streams often act as recharge sources for underlying aquifers and groundwater transfers are sometimes severely compromised. Figure 1.5 shows the geological map of the study area.

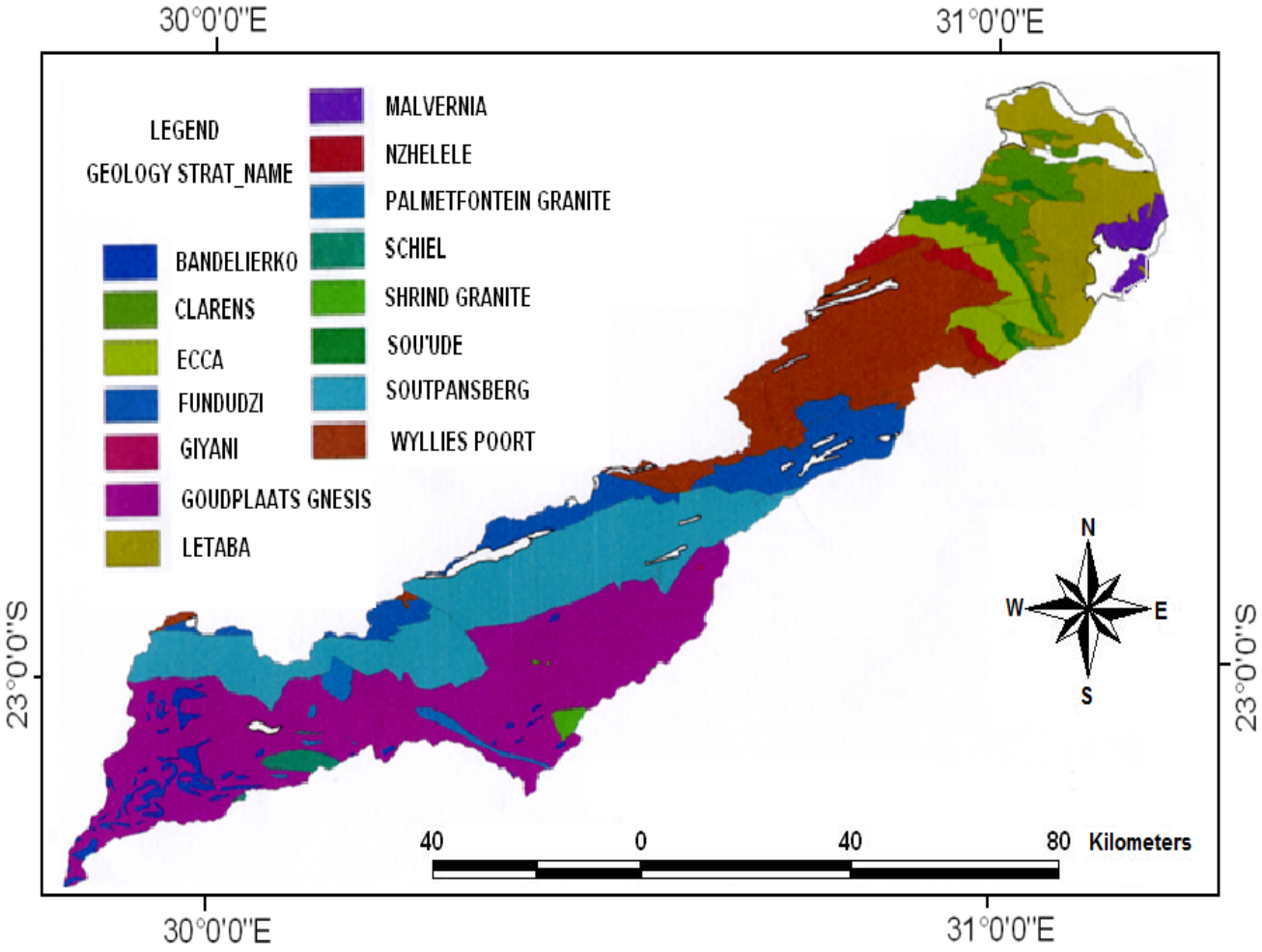

Figure 1.5: Geology of the study area (Source: GIS Resource Centre, University of Venda)

1.6 Scope, Limitations and Outline

1.6.1 Scope

An application of GIS, remote sensing and hydrological modeling in ArcGIS environment was adopted to evaluate the impact of land cover changes on the hydrology of Luvuvhu River

catchment. Land cover changes were analysed over a period of 30 years using data from Landsat Multispectral Scanner (MSS), Landsat Thematic Mapper (TM), and Landsat Enhanced Thematic Mapper Plus (ETM+) and ground survey. The ground survey was conducted for a two year period from 2011 to 2012. A statistical sampling methodology based on Area Frame Sampling (AFS) was adopted to quantify land cover and land use change based on ground data. Physically based distributed hydrological models of different complexity were used to simulate hydrological processes. Representations of surface runoff, evapotranspiration, flood frequency, and infiltration were used as indicators to assess the human impact on the catchment.

1.6.2 Limitations

The different resolutions in imagery data presented a major limitation for the study. For example, Landsat MSS acquired from 1972 had 80 meters spatial resolution whereas Landsat TM acquired from mid-80's and Landsat ETM+ acquired from 1999 had spatial resolution of 30 meters. DEMs obtained from the SRTM have shortcomings that must be understood before using them in water resources modeling applications. A major limitation with the direct expansion method was that the only information used was the one deduced from digitisation of the segments. While it was necessary to provide meteorological products as maps or gridded datasets, the observation network for the different meteorological variables was not constant in time and space, which provided challenges and consequences for the interpolation approach chosen, since each variable requires a specific interpolation technique.

1.6.3 Research Outline

The study was divided into five chapters where chapter one highlighted the background, the problem statement, motivation and objectives of the study. Chapter two gives a review of literature on aspects of the impact of land cover change on hydrology and water resources. It outlined the theoretical framework that informed the study and presented a broad review of the different approaches to understanding impacts of land cover change on the hydrology and water resources of a catchment. Chapter three provides an account of the research methodology focusing on the objectives of the study. Chapter four comprise the results and discussion based on the outcomes while Chapter five provides the conclusions and recommendations.

CHAPTER 2

LITERATURE REVIEW

2. Land Cover and Land Use

Land cover is the observed (bio)physical cover on the earth's surface (Di Gregorio and Jansen, 2000; Ippoliti *et al*., 2012; Sodov *et al*., 2015). When considering land cover in a very pure and strict sense it should be confined to describe vegetation and man-made features. Consequently, areas where the surface consists of bare rock or bare soil are describing land itself rather than land cover. Land use is characterised by the arrangements, activities and inputs people undertake in a certain land cover type to produce, change or maintain it (Di Gregorio and Jansen, 2000; 2005). Definition of land use in this way establishes a direct link between land cover and the actions of people in their environment. Land cover and land use change may alter surface permeability characteristics, through soil compaction associated with human land use and addition of impervious surface to watersheds. Evidence has shown that long-term forest conversion reduces baseflows; because the intensive soil compaction and increases in impervious surface that accompany human land uses decrease infiltration rates and subsurface storage recharge (Price *et al.*, 2010).

2.1 Determination of Land Cover and Land Use Change

In many catchments, application of remote sensing techniques and GIS is widely used to inventorise of land cover changes. Hydrological models are also used to predict the impact of management of water, sediment, surface runoff and other processes through land cover change detection. When classifying land cover and land use, land covers are used as baseline maps, which can then be compared to subsequent classification to detect changes in land cover. Land use information on the other hand can be inferred from land cover data such that it is used in many situations and for various purposes, including the development of strategies to balance conservation and developmental issues (Ackermann, 2011).

A study by Briassoulis (2000) has shown that determination of land cover change revolves around identifying the drivers/causes and the impacts of land cover change. This is done to detect the origins of the drivers of land cover change, which may be either bio-physical or socio-economic drivers; as well as a categorisation of the various factors and processes that contribute

to land cover change through certain human actions, which are known as human driving forces. The bio-physical drivers include characteristics and processes of the natural environment such as: weather and climate variations, landform, topography, and geomorphic processes, volcanic eruptions, plant succession, soil types and processes, drainage patterns, availability of natural resources (Briassoulis, 2000). Bio-physical drivers usually do not cause land use change directly. Mostly, they do cause land-cover change (or changes) which, in turn, may influence the land use decisions of land owners/managers (e.g. no farming on marginal lands) (Sivakami *et al*., 2010). The socio-economic drivers comprise demographic, social, economic, political and institutional factors and processes such as population and population change, industrial structure and change, technology and technological change, the family, the market, various public sector bodies and the related policies and rules, values, community organisation and norms, property regime. Olaleye *et al*. (2012) singled out human population as a very important factor or agent of change in land use/cover in an area. For instance, as population increases, construction of dwellings increases, thus engendering conversion of cropland and forest land to settlements. Turner and Meyer (1994) noted that land use change that drives land cover change is shaped by human driving forces that determine the direction and intensity of land use.

In semi-arid areas such as LRC, land use/cover change is influenced by a variety of bio-physical and societal factors operating on several spatial and temporal levels. Land cover changes therefore produce environmental and socio-economic impacts that frequently feedback and modify the bio-physical and societal factors causing them. Briassoulis (2000) provided numerous interdependent factors influencing land cover changes in semi-arid areas. Such factors include demographic traits (age and gender of the head of family and members of household, family status including fertility and mortality, migration); economic considerations (profits from the exploitation of land and unequal distribution of wealth); natural availability (droughts and floods); technological factors (technical assistance and traditional knowledge); as well as socio-cultural (education, urban and rural life, employment status and personal traits); organisational (integrated world markets and population growth); and institutional factors (land ownership and tenure). Determination of land cover change in LRC is therefore of significance in ensuring environmental and water resources management.

In order to clearly understand the impact of land cover change on hydrology and water resources, modern techniques of modeling are needed. Modeling is an important tool for understanding the physical and hydrological impacts of land use/cover change (Ndlovu *et al*., 2012). Generally, quantification of runoff and other hydrological components can be done in many ways with hydrological modeling being the only efficient way for consistent long term behavioural studies. Hydrological modeling is a mathematical representation of natural processes that influence primarily the energy and water balances of a watershed. The fundamental objective of hydrological modeling is to gain an understanding of the hydrological system in order to provide reliable information for managing water resources in a sustained manner (Dadhwal *et al*., 2010). Methods for transforming various land cover and land use characteristics into distributed hydrologic model parameters are not well developed for a wide range of conditions. For management purposes, many approaches rely largely on empirical studies of small plots and watersheds to relate land cover and land use to hydrologic model parameters. Analysis of trend detection on hydro-meteorological data is also critical for assessing whether climatic factors and human activities have had significant effect in the hydrological regimes and land use change in a watershed. A number of statistical tests are commonly used to detect trends in hydrological data to test whether there is an increase or a decrease in the data. Such statistical methods of trends detection in hydro-meteorological data are either numerical, graphical or curve fitting analysis.

2.1.1 Field Survey

Field survey is used routinely in remote sensing studies as 'ground truthing', primarily used for ground checking and validating, but rarely feeds back directly to modify the definitions of land classifications determined from satellite images or aerial photography (Bunce *et al*., 1992). Field surveys are traditional ways of obtaining information about the ecological characteristics of land; often based upon observing vegetation, and mapping in the field.

In the present study ground truthing involved taking geographic coordinates of the ground resolution cell with Global Positioning System (GPS) technology and comparing them with the coordinates of the pixel being studied on remotely sensed digital image to understand and analyse the location errors and how it may affect the study area. Ground truthing was used in the initial supervised classification of an image to identify and locate land cover types. The spectral

characteristics of these areas were used to train the remote sensing software and a Maximum Likelihood Classification technique to classify an image. Ground truth sites allowed the remote sensor to establish an error matrix which was used to validate the accuracy of the classification method used.

2.1.2 Image Interpretation

The remotely sensed imagery is one of the widely used primary sources of data for land cover classification and change detection analyses. The data also provides information on many of the hydrological parameters and variables requested by hydrological models including land use, topography, evapotranspiration and vegetation characteristics (Stisen *et al*., 2008). The use of multi-temporal satellite images to detect land cover change and its spatial and temporal pattern has been proven an efficient approach in a number of studies including those of Herold *et al*. (2003) and Maktav and Erbek (2005). Remote sensing coupled with GIS is being extensively used for real time and long-term monitoring of the environment. Numerous investigators have used classifications of land cover from Landsat and other remote sensing sources as input to various water resources studies. Interpretations of remotely sensed images are widely used when detecting land use changes in an area. Since the spatial and spectral resolutions of different sensors vary significantly, it is widely practiced to use data from two or more sensors for land use/cover change detection (Rango, 1994).

The United States Geological Survey (USGS) website *http://glovis.usgs.gov/* has a Spectral Characteristics Viewer (SCV) file that helps visualize the different satellite bands of Landsat and other sensors, along with selected spectra and convolving capabilities. The USGS's Global Visualisation Viewer (GLOVIS) website allows satellite and aerial data of the world to be downloaded from 1984 to date. GLOVIS consists of more than 50 metadata queries for Luvuvhu River catchment alone. The satellite images downloaded from the USGS website were acquired through Landsat 4-7 spectral bands, which consists of combined metadata and scenes for remotely sensed images of all the Landsat sensors that utilize World Reference System-2 (WRS-2). Each of the Landsat images has its own scene ID, latitudes and longitudes, and the dates the images were acquired.

Representing land cover information in spatial and temporal form derived from remotely-sensed multispectral satellite digital data has been an increasingly common approach for decades. The procedure includes deriving land cover information that includes performing a discrete classification of remotely-sensed digital data. It comprises of three stages; namely, pre-processing stage, image classification stage, and post-processing stage. A GIS platform software with image processing capabilities can help to automate the process of interpreting remotely-sensed multispectral satellite digital data to identify and delineate various characteristics of the earth's surface (Senseman *et al*., 1995).

2.1.3 Area Estimation by Direct Expansion Method

Remote sensing techniques can be applied to perform crop area estimation by integrating area frame sampling and classification of satellite images. The technique has been applied successfully by the national statistics service of US, department of agriculture during the 1980-1987 period with satisfactory results (Allen and Hanuschak, 1988). Other successful applications have been carried out in Canada (Ryerson *et al*., 1985), France (Meyer-Roux, 1992), Australia (Daubin and Beach, 1981), Argentina (Badhwar *et al*., 1986) and Brazil (Moreira *et al*., 1986). In Africa, successful applications have been carried out in Nigeria (Holland, 2012), Tanzania (Jinguji, 2012), Ethiopia (Central Statistical Agency (CSA) of Ethiopia ((2008; 2010; 2011; 2012); Gutu, 2009), and South Africa (von Hagen, 2001; Von Hagen *et al*., 2002).

2.1.4 Impact of Land Cover and Land Use Change on Hydrology and Water Resources

Land cover change in a watershed can impact on hydrology and water resources by altering hydrological processes such as runoff, stream flow, infiltration, soil moisture, baseflow, and groundwater recharge (Prachansri, 2007). Land cover conversions such as the change from forests or vegetated areas into urban land uses have many significant ecological, hydrological, and sociological effects. Such changes reduce interception, infiltration, surface and subsurface flow, evapotranspiration, storm water storage, and the time required for water to travel over and through a hill slope to a stream (Trinh and Chui, 2013; Albhaisi *et al*., 2013). Water resources are inextricably linked with climate change, population growth and rainfall variability (IPCC, 2001). Any change in land cover has correlated effects in the hydrological regime, and possible impacts on the habitats and ecological communities (Calder, 1992).

Studies by Zieglar (2004); Siriwardena *et al*. (2006); White and Greer (2006); Palamuleni *et al*. (2011) and Albhaisi *et al*. (2013) have paid attention on land use/cover changes with respect to impacts on water supply and hydrological processes. In these studies, agricultural lands, vegetation, impervious surfaces, and deforestation have been reported to alter hydrological processes in a catchment. Deforestation together with agricultural practices have been reported to cause damage to ground cover and surface soil resulting in decrease in water infiltration capacity, increase in the rate of surface runoff, increase in stream flow; and increase in sediment discharge in rivers. Large increases in runoff volumes have been regarded as the cause of severe flooding in downstream portion of watersheds. Urbanisation on the other hand has been reported to cause increases in surface runoff by creating impervious surfaces that do not allow percolation of the water through the soil to the aquifer.

The Luvuvhu River Catchment has been undergoing land cover and land use change over the years. Considerable land cover changes have occurred since the late 80's as the growing population is increasingly putting pressure on water resources. A number of studies on the hydrological effects of land cover change have affirmed that the intensity of land cover change effects on hydrology depends on the changes of vegetation type, especially the effects of deforestation and afforestation on the dry season flow. Kiersch (2000) noted that land use practices can have important impacts on water quality, which in turn may have negative or, in some cases, positive effects on downstream uses of water.

Land cover changes have been known to trigger changes around dams especially after the dams have started operation (Syvitski *et al*., 2005). Anthropogenic land use/cover changes such as urbanisation, agriculture, and deforestation erode land faster than ever before. As the previously dry landscape will instantly be filled with the reservoir water; the area becomes prone to open water evaporation and enhancement of moisture supply for precipitation. Quantification of the relationship between land cover and land use changes and hydrological regimes in the LRC is therefore necessary for sustainable resources management in the catchment.

Surface runoff information is needed for watershed management purposes, which include flood control, stream flow forecasting, and design of hydrological structures and morphology of

drainage systems. A study by Pao-Shan *et al*. (2003) found that the change of land cover type has a considerable impact on the nature of runoff and related hydrological characteristics in a catchment. For example, evapotranspiration may decrease after trees and vegetation are removed in the process of urbanisation. Later, an impervious area due to the construction of houses, streets and culverts may reduce infiltration and shorten the time of concentration.

It is widely accepted that flow regimes can be negatively affected by urbanisation due to increased withdrawal and reduced recharge (Cho *et al*., 2009). Land use condition is an important factor to influence the storm-flood process including surface runoff formation and concentration (Coutu and Vega, 2007). The change in land use structure and pattern not only affects the runoff coefficient in the drainage basin, but also affects the runoff concentration process evidently. Thus, simulation of the impacts of change in land use structure and pattern on the drainage basin runoff generation and concentration process give details on the flood effect of change in land use structure and pattern in urbanisation areas (Shi *et al*., 2007). Such information is important as it provides knowledge on the practice of flood disaster prevention and reduction in urban areas. A study by Solín *et al*. (2011) has shown that increased frequency of high-intensity precipitation events in the effect of global warming and land cover changes (urbanisation, deforestation, or intensification of agriculture) have been generally considered the principal causes of frequent flood events over the last two decades. Dramatic changes and the impact of urbanisation or deforestation on the discharge process that have been identified as the main causes of frequent flood events include the change of agricultural or forest landscape into an urbanised landscape or the change of forest landscape into agricultural landscape (Solín *et al*., 2011).

2.2 Extraction and Analysis of Morphologic and Hydrologic Properties

In many water resource management studies, morphologic and hydrological features such as terrain slope, drainage network, and catchment boundaries are commonly investigated by the use of distributed watershed models. A spatial hydrology model is one which simulates the water flow and transport on a specified region of the earth using GIS data structures (Maidment, 1996). Traditionally, these features are determined from topographic maps, field surveys and sometimes photographic processing and interpretation (Garbrecht and Martz, 1999a; Anornu *et al*., 2012),

which are tedious, time consuming and prone to errors (Moore *et al*., 1991; Martz and Garbrecht, 1992). Over the years, these features have been increasingly derived directly from digital representations of the topography. A study by Harrower (2010) noted that a Digital Elevation Model (DEM) is frequently a crucial source of information in GIS and is essential for GIS hydrological modeling.

2.2.1 Digital Elevation Modeling

A DEM has been found to efficiently represent ground surface and allow automated extraction of hydrological features, thus bringing advantages in terms of processing efficiency, cost effectiveness, and accuracy assessment, compared with traditional methods based on topographic maps, field surveys, or photographic interpretations (Bolch *et al*., 2005). DEM data are now being imported and analysed by GIS tools such that variation in natural characteristics such as physiography, climate, geology, soils and vegetation can be used to delineate the ecoregions of a study area because they provide convenient boundaries within which to do ecological assessments and set quality objectives. A DEM therefore provides the most convenient way of extracting topographic information such as watershed properties (DeVantier *et al*., 1993; Garbrecht and Martz, 1999b). Today, DEM generation using satellite images is becoming a very advantageous method which offers updated information, large area coverage, quick data access and it is cost effective. However, there are disadvantages of a DEM in comparison to the satellite imagery such that a DEM has coarser resolution comparing to the resolution of satellite images (Podobnikar, 2010). On the other hand, grid-based DEM cannot handle abrupt changes in elevation and the size of grid mesh affects the obtained results and the computational efficiency (Moore *et al*., 1991; Vieux, 2004).

In water resources projects, DEMs are used to identify drainage related features such as channel networks, surface drainage patterns, valleys, and ridge bottoms; and to quantify sub-catchment and channel properties such as size, length and slope. DEMs are also used to make calculations to describe, understand and predict water storage and movements. A study by Bolch *et al*. (2005) has presented the SRTM and Advanced Spaceborne Thermal Emission and Reflection Radiometer (ASTER) as the two most recent widely free and globally available DEM data. The SRTM is a project of U.S National Geospatial-Intelligence Agency (NGA) and U.S National

Aeronautics and Space Administration (NASA). The elevation models derived from the SRTM data are used in GRID and can be downloaded from the USGS website *http://www.usgs.gov/*. ASTER is a multispectral optical sensor on board of Terra satellite and has been used to obtain detailed maps of land surface temperature, emissivity and elevation (USGS, 2012). Bolch e*t al*. (2005) noted that high resolutions DEMs are better for delineation of watersheds since they provide denser stream networks. Hydrological modeling with DEM involves modeling flow directions to identify streams that flow to each basin outlet; calculating down-gradient flow accumulations and flow distances; inferring stream network from flow accumulations; and identifying the sub-catchments feeding individual segments of the stream network. These analyses are important as they demonstrate strategies for designing riparian buffers to protect streams from agricultural runoff.

DEMs can be interpolated from contour lines digitised from topographic maps or from irregularly spaced three-dimensional points collected from field surveys, photogrammetry, radar interferometry, laser altimetry, and others. In some regions of the world, DEMs generated using these techniques are readily available at multiple resolutions in digital format. Interpolation is the process of predicting the values of a certain variable of interest at unsampled locations based on measured values at points within the area of interest (Burrough and McDonnell 1998). Interpolation methods can be classified into deterministic and geostatistical. Deterministic interpolation methods use mathematical functions to calculate the values at unknown locations based either on the degree of similarity (e.g. Inverse Distance Weighted (IDW) or the degree of smoothing (e.g. Radial Basis Function (RBF) in relation with neighboring data points. Geostatistical techniques use both, mathematical and statistical methods to predict values at unknown locations and to provide probabilistic estimates of the quality of the interpolation based on the spatial autocorrelation among data points (Burrough and McDonnell, 1998; Johnston *et al*., 2001).

The usual process followed to derive DEMs from such data sources involves the digitising of contour lines from the maps, and the interpolation of elevation values for every pixel in the surface function of the values of neighboring cells where contours exist. The interpolation methods commonly used include the Inverse Distance Weighted, Radial Basis Function, ordinary

Kriging (KRG) and TOPOGRID (TOPO). Stream networks derived from automated drainage analysis techniques can be used as a proxy of DEM quality. The modeled networks can be compared with a reference network digitised from a topographic map. The accuracy of each DEM can then be evaluated using the Kappa coefficient of agreement (Cohen, 1960) between the modeled and the reference stream networks. The TOPOGRID method is the preferred approach where contours provide the data for DEM generation.

2.2.2 The TOPOGRID Method

The TOPOGRID method implements a locally adaptive interpolation approach proposed by Hutchinson (1989). The algorithm implemented in TOPOGRID optimises the use of contour lines by using them to build a generalised drainage model (ridges and streams) at the beginning of each iteration. The definition of these features is based on the identification of areas of maximum curvature in each contour.

The procedure couples a drainage enforcement algorithm that removes spurious sinks and pits, with a finite difference interpolation technique based on the minimisation of a terrain specific, rotation invariant roughness penalty. The interpolation algorithm was designed to have the computation efficiency of local methods and the continuity in the interpolated surface generated by global methods. The algorithm is designed to minimize a discretised rotation invariant roughness penalty defined in terms of the first and second order partial derivatives of the interpolating function. It acts in an iterative fashion, which calculates grids at increasingly finer resolutions from a coarse initial grid until the user-defined resolution is achieved. The values in the initial coarse grid are the average of all data points, and for subsequent iterations, they are linearly interpolated from the preceding grid. The data point values are assigned to the nearest cell grid, and for those grids without data points inside (i.e. cells between contour lines), the values are calculated by Gauss-Seidel iteration with overrelaxation subject to the roughness penalty (Hutchinson, 1989). The roughness penalty is defined in function of the first and second order partial derivatives of the interpolation function f by the following functions:

$$J_1(f) = \int (f_x{}^2 + f_y{}^2)dxdy \qquad 2.1$$

$$J_2(f) = \int (f_{xx}{}^2 + 2f_{xy}{}^2 + f_{yy}{}^2)dxdy \qquad 2.2$$

where, f_x and f_y are the grids in the spatial frequency domain

dx and dy are the grid spacing in the x and y direction

Minimising J_1 in its discretised form conduces to discretised minimum potential interpolation, while minimising J_2 conduces to the minimum curvature interpolation of thin-plate splines in their discrete form. If only J_2 was minimised, the resulting surface would be unrealistically smooth, whereas minimising J_1 gives rise to sharper local maxima and minima at data points as grid resolution becomes finer.

Hutchinson (1996) incorporated a spatially varying statistical assessment of the error introduced by the use of squared grids to represent elevation. This modification forces the amount of smoothing in the interpolation to be locally adaptive to the slope of the terrain. The goal of the drainage enforcement algorithm is to identify and remove spurious sinks in the data. It is also possible to identify natural sinks in the input elevation data so that the algorithm will not attempt to remove them.

The algorithm basically removes sinks by inferring drainage lines to the lowest saddle point in the area surrounding each sink. The algorithm does not remove sinks that have elevation differences of more than a user-defined vertical tolerance (usually set to half the contour interval). Drainage enforcement is implemented iteratively along with the interpolation of the DEM at increasingly finer resolutions. When a more accurate delineation of streams is needed, the algorithm allows the inclusion of stream line data, which are used to ensure that each stream lies in the bottom of its valley.

2.2.3 Automated Catchment Delineation

In broad terms, catchment delineation refers to determination of the boundary of a catchment based on morphologic indicators (e.g. soil, vegetation, land use/cover, terrain, and slope) and/or hydrological indicators (e.g. streams). The study of catchment delineation and characterisation obtains its relevance and importance making it a worthwhile pursuit in the field of hydrology and water resources management. Data acquisition is followed by data processing, which leads to

initial watershed delineation (Allred, 2001). Automatic catchment delineation tool uses and expands ArcView and Spatial Analyst extension functions in GIS to operate watershed delineations. The delineation process requires a DEM in ArcInfo grid format, and optionally a pre-digitised stream network in shapefile (polyline) format. Once the delineation is finished a detailed topographic report is added to the current project and the resulting themes that include Sub-basins, Streams, Outlets and (optional) reservoirs are added to the Basins View. The tools are accessed through the Arc Hydro Tools toolbar, where they are grouped by functionality into toolbar menus (USEPA, 2001).

The procedure for automated catchment delineation starts by eliminating the sinks or depressions in the DEM. The sinks are known as higher-elevation cells, which interrupt the calculation of off-map flow directions. The flow direction map, which provides the input data for most of the watershed analysis and stream inference tools, is then created to identify the basins that flow to each outlet point on the map edge. To create a stream network, the "FLOWACCUMULATION" tool is used to calculate the number of upslope cells flowing to a location. The output flow direction raster created in a previous step is used as input. The "STREAMORDER" tool, from either Shreve or Strahler techniques, is then used to represent the order of each of the segments in a network. Using the "FLOWLENGTH" tool, the length of the flow path, either upslope or downslope, from each cell within a given watershed can be determined. This is useful for calculating the travel time of water through a watershed. The stream link map can be used as input pour point targets for the "WATERSHED" tool. The "WATERSHED" tool uses the flow direction map and "pour point" targets to determine the sub-basins within the basin that flow to each stream link (ESRI, 2011a).

2.3 Hydrometeorological Factors in a Catchment

2.3.1 Rainfall

Rainfall plays a major role in determining agricultural production and hence the economic and social wellbeing of rural communities. Luvuvhu catchment is a predominantly semi-arid region where precipitation is the limiting factor. In the study, rainfall exhibits distinct seasonality within each year with a large quantity of rainfall received between October and March (Mason, 1996). Studies such as those of Mason and Joubert (1997) and Mason *et al*. (1996) have shown that

there is an increase in the frequency of high rainfall events in some parts of southern Africa. The SAWS reported that the 2000 floods, which hit Mozambique, eastern Zimbabwe and northeast South Africa have been linked to the Tropical Temperate Troughs (TTTs), which have been previously linked to high rainfall intensities in these parts. The TTTs are a dominant conduit for moisture (and momentum) from the tropics into the mid-latitudes (Harrison, 1984; Tyson and Preston-Whyte, 2000). They have been associated with the ITCZ and are regarded as the significant contributors of rainfall to the summer rainfall regions of South Africa and Zimbabwe.

Other weather systems linked to ITCZ in the study area during summer include tropical cyclones and easterly waves and lows (Taljaard, 1994; Tyson, 1984; Dyson *et al*., 2002). Tropical cyclones provide only a minimal percentage of the total rainfall during summer and are more frequently associated with dry conditions over the region. Easterly waves and lows are influenced by northward penetrating mid-latitude disturbances, but also exert a reciprocal influence on the mid-latitude circulation. These weather systems that contribute to rainfall in the study area often originate from the SWIO in the Mozambique Channel. The cut-off-lows (COLs) and the ridging anticyclones have been shown to affect the eastern and southern parts of South Africa during the summer season. They often originate from maturing of anticyclones from the South Atlantic Ocean (SAO) and are associated with the ITCZ (Dube, 2002; Kelbe, 1984).

South Africa is a water stressed country, with a natural climate of low rainfall and high evaporation and rainfall variability, which contribute to the low water availability (DWA, 2004a). The average rainfall in South Africa is considerably lower than the global average of 850 mm per annum (Mukheibir, 2005). There are few years of average rainfall or river flows, with extremes of drought or floods being the norm. This variability is coupled with one of the lowest conversions of rainfall to runoff in the world (O'Keeffe *et al*., 1992). Typically around 20 to 30 percent of rainfall is converted to runoff. Only around 10 percent of the country's rainfall is converted to runoff largely due to the high rates of evaporation experienced in the country. Potential evaporation rates of 2,000 – 3,000 millimetres per year are common in parts of the country – many times higher than the average rainfall (Earle *et al*., 2005).

2.3.2 Rainfall Estimation and Analysis

It is necessary to provide climatological and meteorological data products covering the whole country as maps or gridded datasets. To achieve this, observations and records from meteorological stations need to be interpolated. The problem is that observation network for the different meteorological variables are not constant in time and space, which provides challenges and consequences for the interpolation approach chosen, since each variable requires a specific interpolation technique.

Yearly, monthly and daily maps can be generated for a number of meteorological elements like precipitation, temperature, wind and insolation. The maps should be based on the measurements of automatic meteorological stations. Based on records from meteorological stations, many rasterised products can be calculated, provided that definition of the grid size (cell size of 1 to 10 km) the geographical projection/coordinate system, time-steps, processing method and delivery method are specified.

Many different interpolation methods exist under deterministic and probabilistic approaches. Deterministic methods create a continuous surface by only using the geometric characteristics of point observations. Probabilistic methods use the concept of randomness, and allow the inclusion of the variance in the interpolation process and in the computation of the statistical significance of the predicted values. For each method, its applicability, algorithm, efficiency and advantage should be evaluated. There is no absolutely best method but only the optimal choice under certain circumstances. The characteristic and theorem of each method as well as the property and spatial analysis of data should first be reviewed before selecting the one which is relatively best suited for certain situations.

The inverse distance weighting (IDW) approach is an exact local deterministic interpolation technique. The method assumes that the value at an unsampled location is a distance-weighted average of values at sampled points within a defined neighborhood surrounding the unsampled point (Burroughs and McDonnell, 1998). In this sense, IDW considers that points closer to the prediction location will have more influence on the predicted value than points located farther away (Johnston *et al*., 2001). IDW uses:

$$\hat{Z}(S_0) = \sum_{i=1}^{N} \lambda_i . Z(S_i) \qquad 2.3$$

where, $\hat{Z}(S_0)$ is the predicted value of the unsampled location S_0

N is the number of measured sample points within the neighborhoods defined for S_0

λ_i is the distance-dependent weight associated with each sample point

$Z(S_i)$ is the observed value at location S_i

Weights are calculated as:

$$\lambda_i = \frac{{d_{10}}^{-p}}{\sum_{i=1}^{N} {d_{10}}^{-p}} \qquad 2.4$$

$$\sum_{i=1}^{N} \lambda_i = 1 \qquad 2.5$$

where, d_{10} is the distance between the prediction location S_0 and the measured location S_i

p is the power parameter that defines the rate of reduction of the weights as distance increases

In many hydrometeorological studies, frequency analysis, regression analysis, and trend analysis are the most common statistical methods of analysing rainfall data. Frequency analysis is used as a tool for determining design rainfalls for drainage works and drainage structures, especially in relation to their required hydraulic capacity. Regression analysis is used as a tool for detecting relations between two or more variables to test whether such relation is statistically significant (Oosterbaan, 1994). Trend analysis is carried out to examine the long term trends in rainfall over different spatial and temporal scales, and to detect frequency and magnitude of extreme rainfall events. Recent study by Maragatham (2012) noted that trend analysis of rainfall is very crucial for the economic development and hydrological planning for an area. In the present study, the annual averages were used to analyse rainfall data to detect trends in rainfall variations. It is necessary to check if the data meets the required test assumptions or whether the method selected is likely to correctly find a change when it is present. As noted by Lee (2005), analysis of rainfall enhances the management of water resources applications as well as the effective utilisation of

water resources. Such information can be used to prevent floods and droughts, and applied to the planning and designing of water resources related engineering, such as reservoir design, flood control work, drainage design, and soil and water conservation planning.

2.3.3 Evaporation and Evapotranspiration

Evaporation refers to loss of open water systems like natural lakes and man-made pools and reservoir, streams, bare soil with water tables at or close to the land surface, the impervious surfaces like roofs and roads. It accounts for the movement of water to the air from sources such as the soil, canopy interception, and water bodies, while transpiration accounts for the movement of water within a plant and the subsequent loss of water as vapor through stomata in its leaves. In hydrological studies, the process of evaporation is important as it affects the yield of river basins, the necessary capacity of reservoirs, the consumptive use of water by crops and the yield of underground supplies (Wilson, 1990), and it forms part of the abstraction of rain water (Das, 2002). For evaporation to occur, it is necessary to have a supply of water, a source of heat and vapour pressure deficit (Reddy, 2011).

The evapotranspiration (*ET*) on the other hand refers to the evaporation from vegetated surfaces, forests and woodlands where evaporation is accompanied by the process where water vapour escapes from the living plant through the leaves and enters the atmosphere. In simple term, *ET* is the sum of evaporation and plant transpiration from the Earth's land surface to atmosphere. The *ET* is influenced by local conditions that range from precipitation and meteorology to soil moisture, plant water requirements and the physical nature of the land cover (Dunn and Mackay, 1995; Abdullahi, 2013). Estimation of *ET* is an important issue for proper water management both at the farm and the irrigation project level (Yang and Wang, 2011); it is also important in almost every water resources engineering including water supply, distribution, management irrigation, agriculture and hydrological practices (Moghaddamnia *et al*., 2008). In many watersheds, the return of moisture to the atmosphere through the process of *ET* is a large proportion of the input to precipitation (Jain *et al*., 2008). In southern Africa where natural vegetation has been highly modified by urbanisation, overgrazing, crop cultivation, and deforestation, up to 91% of the rainfall returns to the atmosphere through evapotranspiration (Gondwe and Jury, 1997), significantly greater than the global average of 65-70% (Martyn,

1992). A study by Jovanovic *et al*. (2015) estimated the dynamics of evapotranspiration in South Africa using MOD16 evapotranspiration satellite-derived data. It was estimated that evapotranspiration is strongly dependent on plant transpiration in all climatic regions, and occasionally on soil evaporation in dry areas with sparse vegetation. However, annual evapotranspiration was strongly dependent on rainfall and potential evapotranspiration in some climatically different regions.

In many hydrological studies, evapotranspiration is defined as a 'consumptive use of water', which refers to the evaporation and transpiration from vegetation covered land areas only, frequently with respect to horticulture and agriculture and associated irrigation requirements. The consumptive use of water in an area is controlled by factors such as meteorological conditions, the supply of soil moisture, land use, type of soil, soil characteristics, geology, topography, altitude, growing vegetation, characteristics of the surface and canopy, and methods of land management (Wilson, 1990; Andersen, 2008). In semi-arid regions such as the Luvuvhu River catchment where rainfall occurs on limited basis, estimation of *ET* is crucial for management of water resources. As a result of spatial variability of landscape characteristics such as topography, soils, land use/cover, and vegetation, evapotranspiration will likely exhibit a spatial variation in the catchment (Güntner and Bronstert, 2004). Estimates of evaporation and evapotranspiration are therefore required in the design of reservoirs, irrigation systems, scheduling and frequency of irrigation and water balance and simulation studies (Reddy, 2011).

Land use and land cover change has a direct effect on hydrology through its link with the evapotranspiration regime (Dunn and Mackay, 1995). Changes in vegetation cover in forested watersheds affect the generation of runoff and stream flow as a result of increased transpiration and/or evaporation of precipitation intercepted by the vegetation canopy (Waring and Running, 1998; VanShaar *et al*., 2002). Changes in vegetation with succession and reforestation may also influence evaporation. Putuhena and Cordery (2000) studied the hydrological effects of clearcutting a watershed covered by a native, dry, sclerophyll eucalypt forest and replacing it with radiate pine. The study results showed that evaporation decreased after clearcutting and then increased with increasing pine age. A study by Zhang *et al*. (2014) has shown that economy,

population and macro-policy are main factors responsible for driving the land use changes that led to the decrease in woodland area corresponded with an increase in evapotranspiration.

Gondwe and Jury (1997) and Zeng *et al.* (1999) have shown that vegetation removal results in higher albedo and reduced evapotranspiration. Reduced evapotranspiration results in increased soil moisture, which in turn increases the extent of saturation and hence can lead to more runoff during snow melt or heavy rainfall events (VanShaar *et al*., 2002). The processes for vegetation removal are largely anthropogenic and may include drivers such as overgrazing, agricultural extension and fuel wood extraction (Taylor *et al.,* 2002). Griscom *et al*. (2009) observed that land cover change in LRC has the potential to impact on river hydrology through evapotranspiration. He found that the increase in evapotranspiration caused by more fruit orchards in the Levubu farm district may be compensated by the decrease in evapotranspiration from vegetation clearing elsewhere, and could potentially result in greater river yields. Any change of natural landscapes can affect catchment hydrology by altering the rate of evapotranspiration resulting in changes in timing and amounts of surface and river runoff (Miller *et al*., 2002).

2.3.4 Estimation of Evaporation

A number of methods have been developed to estimate the rate of evaporation from a reservoir. These include the water budget method, energy budget method, mass transfer methods and empirical formulae. The selection of the "best" technique to use for a particular computation is largely a function of the data availability, type or size of the water body, and the required accuracy of the estimated evaporation. Historically, class-A evaporation pan was used as an estimate of evaporation, however with improvements in computer technology and simulation techniques this estimate is now frequently obtained using simulation models like Canesugar Crop Growth (CANEGRO) and the Food and Agricultural Organisation (FAO) based Penman Monteith type estimates (Mcglinchey and Inman-Bamber, 2002).

The CANEGRO based Penman Monteith is one of the leading sugarcane crop growth models, which is used to estimate sugarcane reference evapotranspiration (*ET*cane) and is used extensively to schedule irrigation (McGlinchey and Inman-Bamber, 1996). The FAO based

Penman Monteith is used to evaluate rainfed production and drought effects, as well as the efficiency of irrigation practices (FAO, 1992; 2002a; 2003). The FAO Penman-Monteith method uses CROPWAT for windows programme, a decision support system developed by the Land and Water Development Division of the FAO. Its main functions are to calculate reference evapotranspiration (ET_o), crop water requirements (*CWR*) and crop irrigation requirements (*CIR*) to develop irrigation schedules under various management and water supply conditions (FAO, 1992; 2002; 2003).

Estimation of changes in evapotranspiration with computer technology and simulation techniques has been rare in LRC. Evaporation pan coefficients from Symon's pan and Class-A pan have been used by DWA and SAWS, respectively, to estimate total annual evaporation losses in the study area. These methods are often not reliable for estimating the seasonal variation in evaporation losses due to heat storage in deep lakes. However, with due considerations and proper care, the use of an evaporation pan coefficient may be a suitable method for assessing evaporation losses for both present and future reservoirs (Harding, 1962; Kohler *et al*., 1955). The reference evapotranspiration (ET_o), which forms the basis of *ET* estimation in the study area, is used to study the evaporative demand of the atmosphere independently of crop type, crop development and management practices. As water is abundantly available at the reference evapotranspiration surface, soil factors do not affect *ET*. Relating *ET* to a specific surface provides a reference to which *ET* from other surfaces can be related. The site specific water requirement can be estimated, if climatic data recorded at weather station are available in different sites of a region, through CROPWAT 8.0 model which is based on FAO-guidelines (Allen *et al*., 1998).

2.3.5 Estimation of Evapotranspiration

The reference evapotranspiration (ET_o) is the evapotranspiration rate from a reference surface, not short of water; and is a hypothetical surface with extensive green grass cover with specific characteristics (FAO, 2003). It expresses the evaporating power of the atmosphere at a specific location and time of the year and does not consider the crop characteristics and soil factors. The ET_o values can be considered equal to evaporation from a large body of water, such as a pond or lake. However, for smaller, shallower bodies of water this relationship does not apply. Allen *et*

al. (1998) proposed the CROPWAT for Windows version 4.3 (now incorporated to 8.0) to calculate ET_o by the Penman-Monteith equation, which assumes the ET_o as that from hypothetical crop with an assumed height of 0.12 m, having a surface resistance of 70 s/m and an albedo of 0.23, closely resembling the surface of green grass of uniform height, actively growing and adequately watered.

When estimating ET_o using CROPWAT for Windows, full climatic data sets that include radiation (MJ/m-^{2}day^{-1}), sunshine hours (hours), minimum and maximum temperatures (°C), air humidity (%), and wind speed (m/s) are used. Other data that are needed to compute radiation and sunshine hours for use in ET_o include soil heat flux (MJ/m-^{2}day^{-1}), vapour pressure (kPa), saturated vapour pressure (kPa), and vapour pressure deficit (kPa). However, this data cannot be used as input in Penman-Monteith climate data table. The units of ET_o are millimeters of water per day (mm/day). Allen *et al*. (1998) provided the equation for extraterrestrial radiation (R_a) for each day of the year and for different latitudes, which can be estimated from the solar constant, the solar declination and the time of the year by:

$$R_a = \frac{24}{\pi}(60)G_{sc}d_r[\omega_s \sin(\theta)\sin(\delta) + \cos(\theta)\cos(\delta)\sin(\omega_s)] \qquad 2.6$$

where,

R_a = extraterrestrial radiation [MJ m^{-2} day^{-1}]

G_{sc} = solar constant = 0.0820 MJ m^{-2} day^{-1}

d_r = inverse relative distance Earth-Sun (rad) $= 1 + 0.0033\cos\left(\frac{2\pi}{365}J\right)$

where,

J is the number of the day in the year between 1and 365 or 366 days (i.e. 1 January – 31 December).

ω_s = sunset hour angle (rad) $= \arccos[-\tan(\theta)\tan(\delta)]$

θ = latitude (rad) $\theta = \frac{\pi}{180}$ x [*decimal degrees*]

δ = solar declination (rad) $= 0.409\sin\left(\frac{2\pi}{365}J - 1.39\right)$

If the area under study has no radiation data, it can be calculated with the Angstrom formula (Angstrom, 1924), which relates solar radiation to extraterrestrial radiation and relative sunshine duration given by:

$$R_s = \left(a_s + b_s \frac{n}{N}\right) R_a \qquad 2.7$$

where,

R_s = solar or shortwave radiation (MJ m^{-2} day^{-1})

n = actual duration of sunshine (hours)

N = maximum possible duration of sunshine or daylight hours (hours)

n/N = relative sunshine duration (unitless)

R_a = extraterrestrial radiation (MJ m^{-2} day^{-1})

a_s = regression constant, expressing the fraction of extraterrestrial radiation reaching the earth on overcast days (n = 0),

a_s+b_s = fraction of extraterrestrial radiation reaching the earth on clear days (n = N), known as the angstrom coefficients. The a_s and b_s are only applied when no actual solar radiation data are available and no calibration has been carried out; the values a_s = 0.25 and b_s = 0.50 are recommended in the radiation formula.

The average hours of sunshine represents the average number of hours of bright sunshine per day for each month, rounded to the nearest hours. Sunshine hours (N) are commonly recorded where the cost and practicability of maintaining radiation meters are limiting. The ratio that expresses the cloudiness of the atmosphere is the relative sunshine duration (n/N). The ratio is also known as fraction of sunshine hours or cloudiness fraction, and it varies daily and seasonally (Augustine and Nnabuchi, 2009). Snyder (2001) has shown that it is possible to convert radiation data to sunshine hours in cases where there is no sunshine hour's data. This involves first estimating extraterrestrial radiation and potential (maximum) sunshine hours which both depend on the astronomical calculations. The ratio (n/N) is calculated as a function of the ratio of surface extraterrestrial solar radiation (R_s/R_a) after Snyder (2011) as follows:

$$\frac{n}{N} = 2\left(\frac{R_s}{R_a} - 0.25\right) \qquad 2.8$$

Alternatively, the following equation can be also used to derive daylight hours in terms of latitudes and solar declinations:

$$N = \frac{24}{\pi}\omega_s \qquad 2.9$$

To derive the actual bright sunshine hours, the ratio (*n/N*) should be multiplied by the N estimated from astronomical calculations as shown in equation 2.9.

Maximum and minimum temperatures are used to calculate mean daily values for use in *ET* estimations. The solar radiation absorbed by the atmosphere and the heat emitted by the earth increase the air temperature. The sensible heat of the surrounding air transfers energy to the crop and exerts as such a controlling influence on the rate of *ET*. In sunny, warm weather the loss of water by *ET* is greater than in cloudy and cool weather. For standardisation, the daily mean temperature (T_{mean}) for 24-hour periods is defined as the mean of the daily maximum (T_{max}) and minimum temperatures (T_{min}) rather than as the average of hourly temperature measurements. The unit of temperature is given in degrees Celsius (°C) or Fahrenheit (°F) or in Kelvin scale. The later can be obtained by adding 273.16 to the temperature expressed in degrees Celsius. The daily mean temperature is computed as:

$$T_{mean} = \frac{T_{\max} + T_{\min}}{2} \qquad 2.10$$

The moisture status of the air has a strong influence on rates of soil *ET* and open water evaporation, both of which are greater when the humidity of the air is low. Relative humidity (*RH*) is considered important in ET_o estimation. It is the ratio between the amount of water the ambient air actually holds and the amount it could hold at the same temperature. It is dimensionless and is commonly given as a percentage. *RH* expresses the degree of saturation of the air as a ratio of the actual (e_a) to the saturation (e_s) vapour pressure at the same temperature (*T*). *RH* values are widely used in *ET* equations. *RH* is expressed following Allen *et al*. (1998) as follows:

$$RH = 100\left(\frac{e_a}{e_s}\right) \qquad 2.11$$

where, *RH* is the relative humidity in percentage

e_a and e_s are the actual and the saturation vapour pressures, respectively, in kPa.

The process of vapour removal depends to a large extent on wind and air turbulences, which transfer large quantities of air over the evaporating surface. If this air is not continuously replaced with drier air, the driving force for water vapour removal and the *ET* rate decreases. For the calculation of evapotranspiration, wind speed measured at 2 m above the surface is required. However, in some weather stations wind speed data is obtained from instruments placed at elevations other than the standard height of 2 m. Such data are adjusted with a logarithmic wind speed profile given by Allen *et al*. (1998); which is used for measurements above a short grassed surface as follows:

$$u_2 = u_z \frac{4.87}{In67.8z - 542} \qquad 2.12$$

where,

u_2 = wind speed at 2 m above ground surface [m s^{-1}]

u_z = measured wind speed at z m above ground surface [m s^{-1}]

z = height of measurement above ground surface [m]

Water vapour is a gas and its pressure contributes to the total atmospheric pressure (Hall *et al*., 2013) and is therefore used in ET_o estimation (FAO, 2012). The amount of water in the air is related directly to the partial pressure exerted by the water vapour in the air and is therefore a direct measure of the air water content. As saturation vapour pressure is related to air temperature, it can be calculated from the air temperature (T) whereas an actual vapour pressure is related to dew point temperature (T_{dew}) and can be calculated from the dew point temperature (Ahrens *et al*., 2012). The actual vapour pressure (e_a) is the vapour pressure exerted by the water in the air. When the air is not saturated, the actual vapour pressure will be lower than the saturation vapour pressure (e_s) (Ahrens *et al*., 2012). The vapour pressure deficit is the difference between the saturation and actual vapour pressure and is an accurate indicator of the actual evaporative capacity of the air. It is also called saturation deficit and is given by e_s - e_a (Ahrens *et al*., 2012). The dew point temperature is the temperature to which the air needs to be cooled to make the air saturated. The equations for expressing e_s and e_a were given by Allen *et al*. (1998) as follows:

$$e_s = 0.6108 \exp\left[\frac{17.27T}{T + 237.3}\right] \qquad 2.13$$

$$e_a = 0.6108 \exp\left[\frac{17.27 T_{dew}}{T_{dew} + 237.3}\right] \qquad 2.14$$

where, es and e_a are as defined in equation 2.11.

Soil heat flux (G), which is the energy that is utilised in the heating of the soil, is also important in ET_o estimates. The G is regarded as positive when the soil is warming and negative when the soil is cooling. Measurements of the rate of energy transferred through a given surface are made by heat flux sensors. Complex models are available to describe the G, such as that proposed by Allen *et al*. (1998) based on the idea that the soil temperature follows air temperature, as follows:

$$G = c_s \frac{T_i + T_{i+1}}{\Delta t} \Delta z \qquad 2.15$$

where,

G = soil heat flux [MJ m^{-2} day^{-1}]

c_s = soil heat capacity [MJ m-3 $°C^{-1}$]

T_i = air temperature at time i [°C]

T_{i-1} = air temperature at time i-1 [°C]

Δt = length of time interval [day];

Δz = effective soil depth [m]

2.3.6 Runoff

Runoff is the portion of precipitation which appears as flowing water in the drainage network of a watershed following a storm event. It is generated by the topographic flow of water from precipitation to stream channels located at lower elevations. A very small portion of rainfall falling on land surface may either evaporate back to the atmosphere, be transpired by plants or flows out through the small natural channels on the land surface to the main drainage channel and becomes *surface runoff* or *overland flow*. The other portion of rainfall will infiltrate into the soil and travel laterally through the upper soil horizons towards the stream channels above the main groundwater table and become *subsurface/groundwater runoff* or *interflow*. Hence, some of the infiltrated water that percolates down to long-term storage becomes part of stream flow that responds slowly to precipitation variations known as *baseflow*. Figure 2.1 shows a schematic representation of runoff process as derived by Reddy (2011).

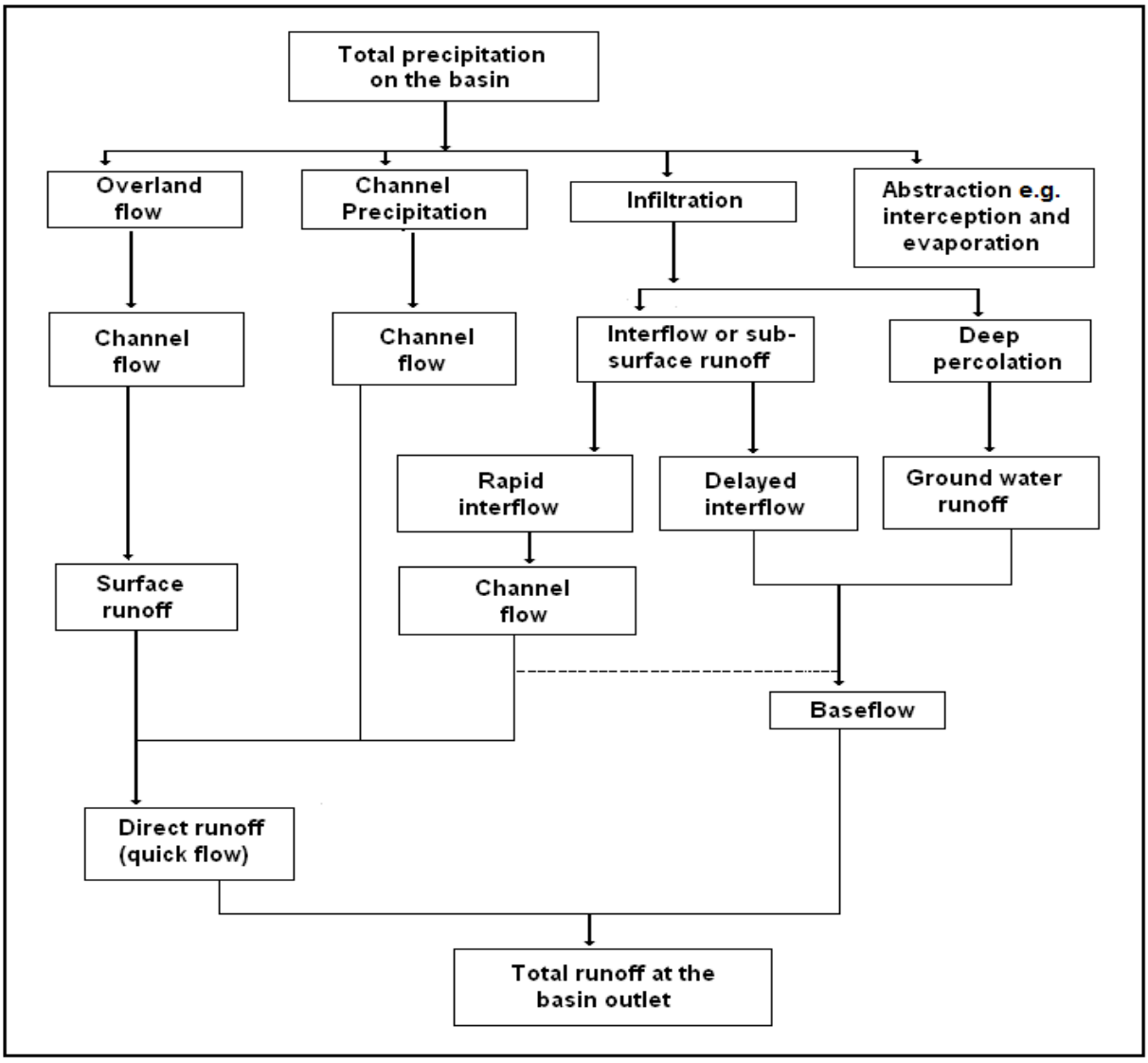

Figure 2.1: Schematic representation of runoff process (Source: Reddy, 2011)

McGee (1991) provided a number of climatic and physiographic factors affecting the volume and distribution of runoff in a catchment. These include climatic factors such as precipitation, solar radiation, evaporation, temperature, humidity, and transpiration. Physiographic factors on the other hand include local topography, geology, land use/cover, type of soil, shape of basin, slope, and type of drainage network. Of the climatic factors affecting runoff, precipitation is the only factor that directly affects runoff depending upon the type of precipitation, rainfall intensity, duration, distribution, and direction of prevailing wind (McGee, 1991). The other climatic factors

affect the water losses from watershed area; they determine how much of precipitation that falls on the catchment shall be transpired and evaporated with the residual only being available for runoff. Of the physiographic factors mentioned above, land use/cover is the most important factor that affects the runoff of any area through its influence on interception, evapotranspiration, and soil moisture movement. Runoff in rural areas produces low discharges than in urban areas due to the magnitude of infiltration and transpiration in urban areas.

Chapman and Lake (2003) described precipitation as the potential source of water that may run off the surface of small watersheds. The extent of the storm and the distribution of rainfall during the storm are two major factors, which affect the peak rate of runoff. The direction of movement of storm over the catchment area has a definite effect on runoff such that if the storm moves in the direction of the flow, the base period of the hydrograph will be less and more peak flow may be expected (Deodhar, 2009). If the rainfall is distributed evenly over a large portion of the watershed, it causes less runoff than the one that is distributed over small portion of a watershed. This is because evenly distributed rainfall over the whole watershed is less damaging to soil than the sudden, sharp and heavy rainfall. As a result, it would rarely cause a flood as floods are caused by excessive rainfall, which is unevenly distribution across the catchment (Das and Saikia, 2012).

Land cover is a factor that affects runoff volume through its influence on the infiltration rate of the soil. Vegetation, including ground litter, forms numerous barriers along the path of the water flowing over the surface of the land, which slows the water down and reduces its peak rate of runoff. Covering areas with impervious material reduces surface storage and infiltration and thus increases the amount of runoff. Recent studies such as those of Siriwardena *et al*. (2006) and Giertz and Diekkruger (2003) have shown that agricultural land use results in lower infiltration rate than natural vegetation, which results in higher runoff. However, interception of rainfall by plants may substantially reduce runoff peaks since most of the rain water is intercepted by plants at the beginning of the storm events (McGee, 1991).

The catchment size and antecedent moisture condition are two factors that affect the peak flow and minimum flow in a catchment. For peak flow in a stream, large basins are likely to

experience less intense storms and peak discharge per unit area of the basin. The shape of the catchment area also has a definite effect on the runoff. For instance, fewer hydrographs and more peak flows will occur in a fan-shaped (semi-circular) catchment area whereas more hydrograph, more infiltration losses and less runoff will occur in an elongated catchment area. It is estimated that fan-shaped catchments give high peak and narrow hydrographs while elongated catchments give broad and low peaked hydrographs (Subramanya, 2013).

In terms of antecedent moisture condition, Wilson (1990) noted that the soil moisture conditions of the basin existing at the time of the occurrence of a storm will greatly influence the runoff peak resulting from that storm. However, the soil moisture conditions of the basin during very intense rains falling in late summer rarely produce high discharges because most of the water enters the soil surface under the existing high infiltration capacity and will be held there. Local topography and geology together with soil types are regarded as factors that influence both the timing and quantity of runoff (McGee, 1991). Steep slopes and impervious strata will enhance the rate and quantity of runoff, while flat pervious deposits offer substantial opportunity for infiltration and less runoff (Akbarimehr and Naghdi, 2012). The type of soil has direct influence on its infiltration capacity rate and it consequently affects runoff. Open textured sandy soils will tend to have higher infiltration rates and therefore tend to produce less peak discharges. Fine-textured soils such as clay and closely compacted clay soils produce a higher rate of runoff than course-textured soils such as sand (Reddy, 2011).

In the study area, the DWA is responsible for conducting surface runoff measurements and storing large amount of data that can be used in change detection and trend analysis. The measurement of runoff is carried out using current meters and calibrated or rated channel cross sections, flumes or standardised weirs, together with water level readings, often by automatic recorders. Although in-situ measurements of runoff are considered more accurate, they cannot be operated anytime and anywhere when needed. This is due to the fact that runoff data is measured on limited basins and this leads to lack of data in most basins. In order to fill the gap, state of art surface runoff modeling have been developed for use in a more convenient and less time consuming procedure.

Shit *et al*. (2014) has noted that runoff volumes are influenced primarily by the total amount of rainfall; while runoff rates resulting from a given rainfall, including peak rate or discharge, are influenced primarily by the rainfall distribution as well as variability of the rainfall rate or intensity over a period of time. Through the use of simplifying assumptions and empirical data, there are several mathematical models and equations that can simulate these processes and predict resultant runoff volumes and rates with acceptable accuracy. Runoff methods that include the Rational method and the U.S Natural Resources Conservation Service or Soil Conservation Service (NRCS/SCS) method, rely on a hypothetical rain event known as a design storm for their rainfall input. The rational method can only be used to produce estimates of peak runoff rates while the NRCS methods can accurately predict both total runoff volume and peak rate, and even entire runoff hydrographs. Generally, runoff computation methods attempt to mathematically reproduce or simulate the hydrologic cycle (Karamouz *et al*., 2012). They treat rainfall as an input, converting it into estimates of resultant runoff volume and/or rate. The use of rainfall-runoff modeling methods may either require limited rainfall and drainage area data, or extensive data needs, including long-term rainfall and temperature data as well as drainage area soils, subsoil, and ground cover information.

2.3.7 Runoff Modeling

Over the years, assessment of the impacts of land cover change on surface runoff dynamics of river catchments has been an area of interest for hydrologists with hydrological models being widely used with different approaches to assess the impacts of land use/cover changes (Mueller *et al*., 2009). Hydrological models for runoff generation, transformation and channel flow routing have been applied for simulations using semi distributed modeling techniques. Ward and Robinson (1990) have distinguished surface runoff models as either stochastic or deterministic models; with the former taking into consideration the chance of incidence or probability distribution of the hydrological variables and are derived from time series analysis of historical data. They can then be used for the generation of long hypothetical sequence of events with the same statistical properties as the historical data. The latter simulate the physical processes operating in the catchment to transform precipitation into runoff. Such models can either be empirical, conceptual, or physically based (Beven, 2012). In the present study, physically based spatially distributed runoff models that describe the effects of soil, vegetation and topography on

the movement of water at and near the land surface have been adopted. These models are based on mathematical modeling representing the physical basis underlying the hydrological system by a series of equations.

The impact of land cover change on surface runoff are mostly simulated by the use of empirical hydrological models that include the U.S Soil Conservation Service (SCS) model and the rational model which are regarded as rainfall-runoff methods. The SCS model is widely-used internationally for the water resources management and planning (Lewis *et al*., 2000). The model uses runoff Curve Number (CN) coefficients to calculate direct storm runoff or excess precipitation; or rather effective precipitation from storm rainfall (Reshma *et al*., 2010). The CN is based on hydrological soil group (HSG), land use, and hydrologic condition (i.e. Antecedent Moisture Condition; AMC) (Lewis *et al*., 2000). The Curve Number method of the SCS (SCS-CN) has been found useful in South Africa for simulating runoff and designing catchments greater than 25 km^2 (Tsheko,2006). The SCS-CN model has been applied in urban and suburban as well as agriculture lands. Since major input parameters for the SCS model are land use, soil type and terrain slopes, the SCS model is potentially compatible with remote sensing input (Lewis *et al*., 2000) and can reflect the impact of human activities on runoff yield (Liu and Li, 2008).

The process of CN estimation is that the volume of runoff (Q) depends on the volume of precipitation (P) and the volume of storage that is available for the retention (Lewis *et al*., 2000; Singh and Xu, 2006). For a storm as a whole, the depth of excess precipitation or direct runoff (Q) is always less than or equal to the depth of precipitation (P) (Reshma *et al*., 2010). After the beginning of runoff, the additional depth of water retained in the watershed (F), known as actual retention, will be less than or equal to some potential maximum retention (S). The actual retention (F) is regarded as the difference between the volumes of precipitation and runoff. Some amount of rainfall (I_a), known as the initial abstraction before ponding, will not occur as runoff. As a result, the potential runoff will be the difference between precipitation (P) and the initial abstraction (I_a), given by P- I_a (Reshma *et al*., 2010). Thus, precipitation loss is calculated based on supplied values of CN and initial abstraction (I_a), which are related to a total runoff depth for a storm. The initial abstraction (I_a) refers to all losses before runoff begins. It includes water

retained in surface depressions, water intercepted by vegetation, evaporation, and infiltration (Shadeed and Almasri, 2010; Strom *et al*., 2013). The I_a is highly variable but generally is correlated with soil and cover parameters. Precipitation loss is calculated based on supplied values of CN and initial abstraction (I_a), which are related to a total runoff depth for a storm by the following SCS (1986) relationships:

$$Q = \left(\frac{(P - I_a)^2}{(P - I_a) + S} \right) \qquad 2.16$$

where,

Q = Runoff (mm)

P = daily rainfall (mm)

I_a = initial abstraction (mm)

S = potential maximum retention after runoff begins or weighting factor (mm)

The procedure used in CN determination and computation of runoff volumes involves a few steps. The analysis begins with collecting daily rainfall data from a number of stations for different sub-catchments. As the CN method estimates runoff volume from inches of rainfall per day, the daily rainfall data is then converted to inches from mm following NRCS (1999). The second step involves identifying the soil type from the SCS soil classification table to determine the Hydrologic Soil Group (HSG) for each sub-catchment. The land use/cover types for each sub-catchment are identified and the CN values for each land use/cover type are determined using the SCS (1986) runoff CN tables. The potential maximum retentions (S), which represents infiltration occurring after runoff has started are computed at each sub-catchment with respect to the corresponding CN value. The water retained in surface depressions, intercepted by vegetation, evaporation, and infiltration at each sub-catchment, also known as the initial abstraction (I_a), is also determined. Thereafter, the runoff volumes are computed in mm/day (SCS, 1986). Regarding the manner in which the physical catchment characteristics are incorporated, inconsistencies in the application of the SCS method are the result of choosing a relevant CN (Smithers and Schulze, 2002). The method is also recommended for design flood estimation when no recorded stream flow data are available at the site of interest, or if the

records are inadequate (Smithers and Schulze, 2002). For carrying out the flood study the runoff has to be converted into m^3/s.

In many hydrological studies, the SCS-CN method is commonly known as the NRCS TR–55 method (SCS, 1986). The TR-55 utilises the SCS runoff equation to predict the peak rate of runoff as well as the total volume, and also provides a simplified "tabular method" for the generation of complete runoff hydrographs. It provides a number of techniques that are useful for modeling small watersheds. TR–55 considers hydrologic parameters such as slope of the watershed and channel, channel roughness, water losses, rainfall intensity, soil type, land use, and time. Thus, TR-55 presents simplified procedures to calculate storm runoff volume, peak rate of discharge, hydrographs, and storage volumes required for floodwater reservoirs. The method assumes that rainfall is uniformly imposed on the watershed over a specified time distribution (NRCS, 2007). TR-55 has a disadvantage of its restriction to the use of the 24-hour storm and is based on open and unconfined flow over land or in channels. The discharge can be assumed constant until another flow is encountered at a junction or another inlet (NRCS, 2007). The CN method was found suitable for use in LRC as it only requires daily rainfall data, which is readily available, together with the combination of catchment characteristics. In the SCS method, land use or cover categories for cultivated agricultural watersheds are distinguished after Gary (1973); SCS (1986) and Chow *et al.* (1988).

The preceding relative moisture of the previous surfaces prior to rainfall event, known as the antecedent moisture condition (AMC), has significant effect on both the volume and rate of runoff (Schiariti, 2010). As a result, the SCS developed three AMCs, namely, AMC I (low or dry moisture condition), AMC II (average moisture condition) and AMC III (high or wet moisture condition). AMC I is an option condition of watershed soils, where soils are dry but not to the wilting point and when satisfactory cultivation takes place; AMC II is the average case for annual floods; whereas AMC III is for when a heavy rainfall or light rainfall and low temperatures have occurred during the five days previous to the storm. AMC is considered to be low when there has been little preceding rainfall and high when there has been considerable preceding rainfall prior to the modeled rainfall event. All watersheds are considered to have AMC II which is regarded as the average moisture condition, therefore, the equivalent curve

numbers for both dry (AMC I) and wet (AMC III) conditions can be determined using CN (I) and CN (III) (Schiariti, 2010) as follows:

$$CN(I) = \frac{4.2CN(II)}{10 - 0.058CN(II)} \quad 2.17$$

$$CN(III) = \frac{23CN(II)}{10 + 0.13CN(II)} \quad 2.18$$

Application of the rational method has been neglected in many South African catchments as most of the catchments are predominantly rural areas with large catchment areas. The rational model is widely used to design storm runoff in watersheds with small catchment areas less than 50 km^2, and is used for computing peak rates of runoff. However, the method is generally recommended to be used in catchments smaller than 15 km^2 because of accuracy; but can be used for large catchments by experienced engineers (SANRAL, 2006). The method can also be used to calculate runoff coefficient, which indicates water release unit in a watershed. Mathematically, the rational method relates the peak discharge (m^3/sec) to the drainage area (A, km^2), the rainfall intensity (I, mm/hr), and the runoff coefficient (C) (SANRAL, 2006; Gupta, 2011) as follows:

$$Q = CIA \quad 2.19$$

where,

Q = Maximum rate of runoff

C = Runoff coefficient

I = Average intensity of rainfall

A = Contributing watershed area

Robust spatially-distributed models that include Soil and Water Assessment Tool (SWAT), MIKE-SHE, Variable Infiltration Capacity (VIC) model, Hydrologic Engineering Centre-Hydrologic Modeling System (HEC-HMS), Agricultural Catchments Research Unit (ACRU) and the Pitman model are commonly used in runoff simulation. Distributed hydrological models are based on physical principles governing the movement of water within a catchment area, but they need detailed high-quality data to be used effectively.

The SWAT model is a river basin or watershed, scale model developed by Arnold in 1990 for the United State Department of Agricultural Research Service (ARS). SWAT was developed to predict the impact of land management practices on water, sediment and agricultural chemical yields in large complex watershed with varying soils, land use and management condition over long periods of time (Neitsch *et al*., 2002). Land use components are first modeled by a raster based model, which produces land use maps for use in the SWAT model (Neitsch *at al*., 2002). The model uses the Curve Number (CN) method to simulate surface runoff and it requires data to produce reliable predictions in ungauged settings. The SWAT can be used for identifying the landscape factors that may be contributing towards the drying of the river (Miller *et al*., 2007).

The SWAT model uses GIS and DEM to delineate watersheds and extract the stream network (Neitsch *et al*., 2011). SWAT is available within EPA's BASINS 3.0 (the BASINS version is ArcSWAT2000) (EPA, 2012). To set up the SWAT model, the ArcSWAT (an ArcGIS-ArcView extension and a graphical user input interface for the SWAT) is used. Normally, a SWAT model can be built by using the ArcMap (Arc Hydro) in ArcGIS interface which provides suitable means to enter data into the SWAT code (Obiero *et al*., 2011; Samad *et al*., 2016). Arc Hydro contain some of the data structure which are not available in SWAT data structure, such as the cross sections and profile lines, the stream geometric network, and some drainage elements. SWAT model on the other hand include many land and stream parameters which are not included in Arc Hydro. In most cases when an area is flat, the ArcSWAT stream extraction function cannot get the right streamlines. The Arc Hydro supports independent hydrologic models like SWAT by providing a geospatial and temporal data structure for describing surface water hydrology and hydrogarphy (Maidment, 2002). ArcSWAT breaks pre-processing into four main steps, namely, watershed delineation, HRU analysis, weather data definition and SWAT simulation (Neitsch *et al*., 2011). When using SWAT, a watershed is partitioned into a number of sub-watershed or sub-basins. The use of sub-basins in a simulation is particularly beneficial when different areas of watershed are dominated by land uses or soils dissimilar enough in properties to impact hydrology. By partitioning the watershed into sub-basins, the user is able to reference different areas of watershed to one another spatially. Input information for each sub-basin is grouped or organised into different categories: climate; ponds/wetlands, groundwater; and the main channel, draining the sub-basin. In the ArcSWAT, the SWAT input data (lup.dat)

file allows the hydrologic response units (HRUs) fraction updating during a simulation run, therefore, the HRUs are also considered input information. The HRUs are portions of subbasins comprising of unique land use, land cover, management, and soil attributes (Conaghan, 2010). The land area in the subbasin may be subdivided into HRUs which comprise of geographic position in the watershed and are spatially related to each other. Hence, a subbasin will contain at least one HRU, a tributary channel and a main channel (Neitsch *et al*., 2002; Neitsch *et al*., 2011). To describe the relationship between input and output variables, SWAT requires specific information about weather, soil properties, topography, vegetation and land management practices occurring in watershed (Malunjkar *et al*., 2015).

The advantages of the SWAT model includes modelling of ungauged catchments, prediction of relative impacts of scenarios (alternative input data) such as changes in management practices, climate, vegetation on water quality, quantity or other variables (Arnold *et al*., 1998). As a semi-distributed model, SWAT is attractive for its computational efficiency as it offers some compromise between the constraints imposed by the other model types such as lumped, conceptual or fully distributed, physically based models (Watson *et al*., 2003). SWAT incorporates a kinematic storage model for subsurface flow (Sloan and Moore, 1984). In this study, SWAT model was applied to predict the impact of land management practices on the hydrology and water resources of LRC as well as to set up the SWAT model for the catchment condition and run the model and assess its performance. These characteristics can be used to provide information on the hydrological behaviour of the catchment when subjected to climatic and land management forcing inputs.

The SWAT model, both calibrated and uncalibrated, has been applied in various studies to assess watershed response to land use/cover changes, including those of Kepner *et al*. (2004); Ncube and Taigbenu (2007); Githui *et al*. (2009); Obiero *et al*. (2011) and Samad *et al*. (2016). Kepner *et al*. (2004) assessed the impacts of land use change in San Pedro River in Mexico using uncalibrated SWAT model and found that land cover changes associated with increasing urbanization and replacement of vegetated surfaces with imperviousness will significantly alter the hydrological response to watershed in the future. In South Africa, a study by Ncube and Taigbenu (2007) has applied the sensitivity analysis in SWAT model to assess the impacts of

land use/cover changes on the hydrologic response of Oliphants Catchment. The study detected correlation between land cover and hydrologic response with an increase in land cover and a reduction in stream flow. Githui *et al*. (2009) estimated the impacts of land cover changes on runoff of Nzoia catchment in Kenya using the calibrated SWAT model. They found that land use, particularly agricultural land use, had strong effects on the runoff regime in the catchment. A study by Obiero *et al*. (2011) assessed the performance of SWAT to predict stream flow on the Naro Moru river catchment in Ewaso Ng'iro river basin, Kenya, based on monthly simulations. They found that improved simulations can be achieved by the use of better and more detailed data and better parameter calibration efforts. With better parameter calibration techniques and better quality data, the model may be used to predict the effect of climate change on river flows as well as the effect of land use changes on the hydrologic response of a catchment. Samad *et al*. (2016) used calibrated SWAT model to estimate discharge and sedimentation in the Rawal Dam Catchment in Pakistan. It was found that there was a reduction in discharge and an increase in sedimentation in the dam as a result of clearing large forest land while constructing an expressway along the dam.

MIKE-SHE model solves the partial differential equations for the processes of overland and channel flow, unsaturated and saturated subsurface flow, and the model is completed by a description of the processes of snowmelt, interception and evapotranspiration. The flow equations are solved numerically using finite difference methods (Sørensen *et al*., 1996). The VIC model has been used for modeling the river flow regime. It is a physically based, macroscale hydrological model, which represents the partitioning of incoming (solar and long wave) radiation at the land surface into latent and sensible heat, and the partitioning of precipitation (or snowmelt) into direct runoff and infiltration. VIC explicitly represents vegetation, and simultaneously solves the surface energy and water balances (Liang e*t al*., 1994). HEC-HMS was designed to simulate the surface runoff resulting from precipitation over a watershed by representing that watershed as an interconnected system of components. These components consist of surface runoff, stream channels, and reservoirs. Each component is represented by a set of parameters, which specify its characteristics, and the mathematical relations, which describe its physical processes. The end result of the HEC–1 modeling process

is the computation of runoff hydrographs for the sub-basins and stream channels (USACE, 1981).

The ACRU model (Schulze, 1995) is a multipurpose model that integrates water budgeting and runoff components of the terrestrial hydrological system with risk analysis. It is a physical-conceptual model which operates on a daily time step and where the simulated stream flow and peak discharge are sensitive to rainfall, soils, land cover and catchment characteristics. Hence, the model can be applied in crop yield modeling, design hydrology, reservoir yield simulation and irrigation water demand/supply, regional water resources assessment, planning optimum water resource allocation and utilisation, climate change, land use and management impacts, and resolving conflicting demands on water resources (FAO, 2014). The ACRU modelling system was developed and refined by Smithers *et al*. (2006) in a number of areas to improve simulated peak discharges and related design flood estimation. The ACRU model revolves around multi-layer soil water budgeting with specific variables governing the atmosphere-plant-soil water interfaces. Runoff is generated as quick flow, which responds to the magnitude of daily rainfall in relation to dynamic soil water budgeting, i.e. the antecedent moisture conditions.

The Pitman model (Pitman, 1973) is a conceptual rainfall-runoff model consisting of storages linked by functions designed to represent the main hydrological processes prevailing at the catchment scale. It has interception, impervious area runoff, catchment absorption and surface runoff, soil and ground water runoff and evaporative loss functions. The model runs on a monthly time step. As it was designed for water resource assessment purposes in managed catchments, it also includes functions to account for losses and abstractions from small dams and direct abstractions from the river itself. The model uses eleven user-specified parameters to account for the processes involved in rainfall-runoff transformation. In this model, surface runoff calculations are based on a symmetrical triangular distribution of absorption rates (Pitman, 1973).

2.3.8 Drainage

A stream can be defined as a flow channel which drains the runoff from a drainage basin (Linsley *et al*., 1958). Stream flow on the other hand is the main mechanism by which water

moves from the land to the water bodies such as oceans (Wetzel and Likens, 2009). It is regarded as the volume of water moving past a cross-section of a stream over a set period of time. Stream flow is crucial in hydrology as it forms the most important data for hydrologists since they are concerned mainly with estimating rates and volumes of the stream flow to be used in the design of water resources projects, or the changes in these values resulting from the man-made causes. Stream flow is also used by hydrologists in the scientific investigations such as establishing the rainfall-runoff relations, unit hydrograph studies and design flood estimates.

The LRC, being one of the semi-arid regions of South Africa and a summer rainfall area, faces water constraints due to insufficient rainfall and changing land use/cover patterns. However, the degree of scarcity has been the subject of research by hydrologists, in an attempt to quantify and understand the relationships between rainfall and stream flow as well as between rainfall and groundwater recharge. The run-off in rivers in the country is very unsteady due to the fact that there are large areas, which are either summer or winter rainfall areas as rainfall do not occur on a regular basis, but rather random during a specific rainfall season. The variation in rainfall duration and intensities in the country also contribute to the unsteadiness of flow (Meyer *et al*., 2000).

In order to quantify water resources in the catchment, it is essential to assess the availability of water resources as accurately as possible. This may include measuring discharge in a stream continuously over a period of time. Two different flows are encountered in the LRC due to seasonal variations in precipitation. For example, during summer (October to March), flows are caused by heavy local rains attributed to orography, ITCZ and localised effects. During this time, peak flows are usually short term with high volumes of runoff causing flash floods. During winter (April to September), flows are diminished as there is always little or no rainfall in the catchment. This in turn leads to droughts and death of aquatic species. Extra-tropical incursions are believed to bring minimal rainfall during this period.

Gordon (2004) noted that river flow may change both seasonally and inter-annually forcing river species to adapt to ever changing conditions. The quality and quantity of water in rivers changes due to seasonal and inter-annual rainfall changes (Mukheibir, 2005). The seasonal rainfall

however, is important in the recharging of the river catchment as it provides water for both surface and subsurface abstractions. Long term flow variations, on the other hand, are affected by a combination of rainfall variations and human-related changes such as changing water use and land use patterns and such changes can have effects on various stream flow characteristics. For example, depleted land cover can significantly affect both low and high flows in such a way as to cause substantial flood volumes during the wet period and reduced flows during the dry period (Valimba, 2004). A study of changes in stream flow is therefore important in catchment hydrology because it directly influences the management of land and water resources as changes in intensity and distributions of stream flow can potentially affect human settlements, water supply, designs of drainage systems and river management (Chiew and McMahon, 1995).

Studies that relate changes in land cover with changes in stream flow indicate that deforestation causes an increase in the annual mean discharge. However, a few studies that evaluated the effects of changes in land cover in tropical meso- or large-scale river basins usually could not find similar relationships (Bruijnzeel, 1990). A study by Bosch and Hewlett (1982) reviewed the results of 94 (mostly paired) catchment experiments throughout the world and concluded that removal of forest almost invariably leads to high stream flow, and reforestation of open lands generally leads to a decline in the overall stream flow and increased runoff volumes. A study by Calder (1992) identified afforestation to be the main land use change impacting on the hydrological cycle. It is believed that the conversion of vegetation such as tropical forest or savanna to grassland disrupts the hydrological cycle of a drainage basin by altering the balance between rainfall and evaporation and, consequently, the runoff response of the area.

The higher surface albedo, the lower surface aerodynamic roughness, the lower leaf area and the shallower rooting depth of pasture compared with forest all contribute to reduced evapotranspiration and increase the long-term discharge (Costa and Foley, 1997). Also, Chen *et al*. (1994) noted that land use/cover in the urbanisation process can cause change of characteristics of steam flow in a drainage basin. In urbanised areas, rainfall detention in the drainage basin may decline sharply while the runoff coefficient increases evidently due to expansion of the city. The large area of urbanised land may lead to decrease of the surface coarseness. The building of road and drainage system may also contribute to the rapid growth of

runoff concentration speed and greatly shortened time of runoff concentration. Also, the wave shape of flood may become more susceptible to high precipitation intensity in short time due to the detention capability in the drainage basin declines. As a result, the runoff concentration may speed up and the original capability of smoothing the flood wave shape in the drainage basin may decrease, leading to an evident growth of the flood peak discharge (Chen *et al*., 1994).

2.3.9 Stream Flow Variation

A considerable number of initiatives such as those of Le Maitre *et al*. (1996; 2000; 2001) and Middleton and Bailey (2008) have shown that dense forests affect stream flow variation in South Africa. The studies have shown that alien plants such as *pines*, *acacia*, *eucalyptus*, *lantana camara*, and *jacaranda mininosifoli* reduce stream flow because they consume large amount of groundwater (Le Maitre *et al*., 1996; 2000; 2001). Alien vegetation is known to reduce stream flow to less than that which would occur under naturally vegetated conditions. This is due to the additional biomass and greater rooting depth than indigenous species, resulting in greater evapotranspiration (Mallory *et al*., 2011). Pine and eucalyptus trees alone can consume up to 35 liters and 50 liters of water per day, respectively, (DWA, 1999). Studies by Smithers and Schulze (1995); Gush *et al.* (2002) and Jewitt *et al.* (2009) showed that afforestation of different forestry species (primarily pines, eucalypts and wattles) also reduce stream flow in catchments.

Suspended sediment load can affect the life of a stream to such an extent that the flow of water in the stream may be reduced. The majority of sediment loads in streams is carried out in solution (dissolved load) or suspension leading to some of the loads to be accumulated at the bottom of the stream. The change of seasons can also affect stream flow in such a way that catchments produce high stream discharges during high rainfall in wet seasons whereas little or no rains as experienced during dry season will produce opposite effects. Climate parameters that include precipitation, temperature, sunshine, humidity, and wind also affect stream flow variation with precipitation and temperature as critical factors.

Human activities, such as changing land use and water use patterns due to high population, is exerting high pressure on limited water resources. The changes in land-cover and water use patterns affect both the surface and groundwater hydrology and stream flow in sub-basins,

altering the hydrological cycle and flood vulnerability (Hernandez *et al*., 2000). If a watershed has high human activities, water flow might thus be depleted by withdrawals for irrigation, domestic or industrial purposes. Abstractions of water from a river, such as irrigation water, industrial water and domestic water, can cause a decline in stream flow. As there is a steadily increasing demand for food and water in various parts of South Africa, there is an increase in water abstractions to sustain expanding agricultural activities and this constantly changes river flow regimes.

2.3.10 Measurement of Stream Flow

A widely used practice in the stream flow measurement is to record the river stage and to convert the stage data to discharge data. The river stage is defined as the height of water surface in the river at a given section above any arbitrary or random datum and is usually expressed in meters. This process is achieved through the stage-discharge relationship, which is first established by actual measurement of discharge in the river at different stages. Once a stable stage-discharge relationship is established at a gauging site, the discharge measurement is discontinued and only the stage is recorded continuously (Wilson, 1990). In the study area the DWA measures flow rates, flow volumes and water levels in rivers. This is done by using a network of flow gauging stations which are monitored on daily basis. The existing network of flow gauging stations consists mainly of compound gauging weirs which become inaccurate when high discharges occur because they are not built large enough to cope with very high flows. These gauging stations are usually restricted to lower flows in terms of their capacity and as a result, measurements of high flows have become a concern since most gauging stations cannot cope with these flows. Thus, measurements of high flows are important because observed stream flow data will be needed to analyse and predict the occurrence of floods more accurately. By quantifying high discharges accurately, the calculation of flood levels and potential damage can be made more accurately. Given that the country is water stressed, accurate knowledge of the discharge of water for use as well as for the temporal storage of floodwater becomes a priority.

A study by Meyer *et al*. (2000) highlighted that only two methods are reliable for measurements of high discharges in South African rivers. These include the slope–area method and bridge contraction method, which are used in conjunction with flow measurement data from gauging

stations and reservoir spillway. The slope–area method is based on the assumption that the flow is uniform (cross-section's geometry relatively constant) for the reach where flow measurement is being undertaken. The method assumes that the flow depth is a function of the average bed slope S_o, bed roughness (Manning *n*-value) and cross sectional geometry and is not influenced by cross sectional geometry and by control sections and/or obstructions elsewhere along the river (Meyer *et al*., 2000). In this method, it is very difficult to observe the water surface levels accurately since there are oscillations in the water surface. The bridge contraction method in the form of continuity equation is used reliably in most South African bridges because the drops in surface levels are too small to measure with sufficient accuracy (Meyer *et al*., 2000). In this method, flows approaching a bridge will experience contraction due to the bridgeheads and undergo an associated drop in water surface level upon passing through the bridge openings.

Other flow measuring techniques that are being practised in South African rivers but not reliable involve the measurement of flows through near uniform river reaches and the derivation of stage-discharge relationships. The latter involves conducting a number of discharge measurements at a gauging station along with simultaneous stage (depth) observations. A calibration or rating curve is then drawn on a single graph with discharge on the x-axis and stage on the y-axis. Such curve plotted between the discharge and stage is used to predict the flow discharge when the stage is known.

2.3.11 Suspended Sediment

Surface runoff is the main source of pollution to surface water. Runoff from impervious areas degrades receiving waters by increasing the quantity of polluted water in river systems in a short period of time. Common pollutants in stormwater include heavy metals, petroleum products, bacteria, and suspended sediments (USEPA, 2007). These pollutants degrade the quality of surface water and impair fish/macro invertebrate habitat.

Methods for monitoring suspended sediment includes grab and composite sampling techniques taken manually or by automatic sampler, total suspended solids (TSS) and suspended sediment concentration (SSC) analytical analysis, and turbidity and tri-laser diffraction (light obstruction).

Suspended sediment characteristics can be reported as sediment event mean concentrations (EMC), total sediment load, particle size distribution (PSD), and specific gravity.

The manual sampling method contains what may be presumed to be the true suspended sediment concentration and particle size distribution to which all other monitoring methods can be compared. Sediment can originate from different sources within the river system such as landscape erosion, channel erosion, bank failure and bed scour. Sediment that moves in suspension in water is maintained by the upward components of turbulent currents or by colloidal suspension. Akrasi (2011) noted that sediment particles are transported through river system as a result of runoff from rainfall through the processes of sheet, rill and gully erosion. The mass of sediment transported by a river changes constantly based on natural change in the hydrological regime and manmade alterations to the landscape. A change in runoff regime from a drainage basin may concentrate or disperse sediments in the stream channel and, in turn, affect the flow capacity of the stream.

In semi-arid areas like the LRC, the transport of suspended sediments in rivers and streams is a natural process increasingly influenced by human activities. Nordin (1985) showed that streams in semi-arid areas have more highly variable sediment loads than those in humid regions. In these areas, sediments can either be transported to streams or rivers through rainfall or agricultural practices. Soil erosion is mainly generated by irrigation runoff, which has hydrological properties distinct from those caused by flooding (Peng *et al*., 2006).

The transport of fine sediment, carried in suspension by water, is central to the hydrology, geomorphology, and ecological functioning of river floodplains and deltas (Pavelsky and Smith, 2009). The suspension, transport, and deposition of sediment rank among the most important geomorphic processes in shaping the physical landscape and regulating ecological systems (Knighton, 1998). They are particularly critical in floodplain and deltaic environments, where most landscape features are formed by the movement of sediment and water (Gomez *et al*., 1995). The transport of sediment and associated contaminants in streams is a water-quality issue of national concern with ecological as well as economic impacts. Sedimentation reduces reservoir storage capacity for flow regulation and with it all water supply and flood control

benefits, plus hydropower, navigation, recreation, and environmental benefit that depend on releases from storage (Sumi *et al*., 2002). In order to evaluate the effect of land cover change on hydrology, observation of spatial and temporal patterns in sediment transport is helpful in understanding the formation and function of these environments and how they may respond to natural and anthropogenic perturbations in the future (Pavelsky and Smith, 2009).

Land cover change in southern Africa has a significant influence in the erosion processes (Walmsley and Bruwer, 1980). Many rivers in this region carry high concentrations of suspended material due to soil erosion which can be a result of the sparse vegetation, erratic rainfall and easily-weathered sedimentary rock. Anthropogenic influences such as the clearance of natural vegetation, agriculture, and other disturbances to the soil are considered as well; most regions of southern Africa can be described as being susceptible to soil erosion (Beckedahl *et al.*, 1988). In addition, reservoirs can have a considerable influence on the suspended sediment concentrations in fluvial systems, by reducing the magnitude and frequency of run-off, increasing evaporation, restricting sediment transport and increasing downstream scour (Slabbert, 2007). The construction of a dam and the creation of an impounded river reach area usually change the stream natural conditions. Concerning the sedimentological aspect, the dams cause a reduction on the flow velocity, thus causing the gradual deposition of those sediments carried by the stream resulting in the sedimentation, gradually diminishing the reservoir storage capacity (Slabbert, 2007).

A number of studies such as those of Mavima (2011) and Walling *et al*. (2001) have singled out land use and land cover changes as the main contributing factors to sediment discharge in streams and reservoirs. Much of the human induced erosion is caused by negligence and lack of understanding and can be successfully avoided to certain extent (Pavelsky and Smith, 2009). Anthropogenic activities such as land clearance for agriculture and subsequent intensification of agricultural land use are only some of the many ways in which human activity can change the natural vegetation cover and disturb the catchment surface, thereby increasing erosion and sediment yields.

Unlike natural erosion, most of the anthropogenic loss occurs at low elevations, where people live, build, and farm. Agriculture takes up about 40 percent of Earth's surface, and most of that land lies less than 2 km above sea level (Wilkinson, 2004). Generally, variability in sediment yield can result from a number of factors, such as geological and climatic variations, intermittent bank or hill slope collapse, channel incision into alluvium of carrying composition, the impact of fire or volcanic activity, change in land use, variable patterns of stream flow and activity in the channel such as dredging (Schumm, 1977).

In South Africa, the DWA is responsible for measuring the sedimentation in all the large storage basins in the country. Through surveys of specific dams at different time, DWA makes it possible to calculate the volume of sediment deposited between measurements, providing a historical basis for prediction of sedimentation. Haarhof and Cassa (2009) mentioned three distinct steps in estimating sedimentation of storage basins in South Africa including estimating the mass rate at which sediment is flushed towards the storage basin; estimating the trap efficiency of the storage basin; and converting the sediment mass to sediment volume.

2.3.12 Measurement of Suspended Sediment

Sediment discharge in runoff water is measured by collecting samples of the runoff water and analysing them for sediment discharge (Das, 2002). The other approach to obtaining sediment discharge in streams is based on relations developed between hydraulic parameters and sediment transport potential (Gray and Simões, 2008). However, the methods and equipments used to measure suspended sediments are not the same as those used to measure deposited sediments. This is because suspended sediment samples are collected from running water in streams and rivers, whereas deposited sediments are measured at the bottom of streams. The reason for the differences between suspended and deposited sediments reflects the fact that sediment quantity must include the sand-size fractions, which are unequally distributed in depth, whereas sediment quality is commonly focused on the silt and clay fraction, which is not depth dependent. Accurate measurements of suspended sediment concentration are difficult to obtain, since suspended sediment loads are highly variable in both time and space. As shown by Schindl *et al*. (2005), measurements of sediment transport commonly involve many simplifying assumptions. This is largely because sediment transport is a dynamic phenomenon and measurement

techniques cannot register the ever changing conditions that exist in water bodies, particularly in river systems.

In the study area, past records of suspended sediments were rare. There is no regional or national monitoring programme that monitors sediment yield/load. However, a toxicity monitoring programme linked to sediment is in the planning phase at the Resource Quality Services (RQS) directorate of the DWA but it is not clear when the programme will be put into practice. DWA recommended that the only best way to get sediment discharge data that will provide an indication of the sediment yield/load of South African rivers is through the surrogate of the dam/river sedimentation surveys. Other records of sediment discharge are derived from data collected with sufficient frequency to obtain reliable estimates for the computational interval and period.

Before 1920, an *ad hoc* sediment monitoring programme was started by the South African Directorate of Water Affairs and regular sampling programmes during 1929 were done. In an attempt to generate sediment yield figures, mean annual runoff or mean annual precipitation were used to represent the capacity of the transporting medium in the form of runoff. However, comprehensive sets of data achieved indicated that such simple relationships are unfortunately not generally valid. A study by Rooseboom and Annandale (1981) provided two main methods of measuring sediment loads in southern African rivers since 1920. These include daily "bottle" sampling and measurement of sediment deposit volumes. The average sediment loads in rivers can either be determined through sampling of streams or by monitoring of the accumulated sediment deposits in impoundments. The stream sampling method involves lowering an open sampling bottle 300 mm below the stream surface by hand and allowing it to fill. In the measurement of sediment deposit volumes, average sediment loads in rivers are measured indirectly by monitoring changes in storage capacity of existing reservoirs. In this method, data on volumetric changes of sediment deposits in reservoirs form the best basis for the prediction of sedimentation rates in planned reservoirs.

Das (2002) gave three distinct methods used for collecting the samples of the runoff water; namely, the Multislot divisor, the Coshocton wheel sampler and the Depth integrating samplers

(bottle samplers). The use of these samplers has usually been restricted to watersheds that are less than 1 ha, primarily because of their limited capacity. After the water samples are taken, they should be brought to the laboratory and analysed to determine the concentration of suspended sediment in water. In the Multislot divisor method, runoff is routed from the collector through a conveyance channel to a sludge tank where the heavier sediment particles are deposited (Pathak, 1991). The device is based on the principle that a uniform horizontal velocity of approach will be maintained in the divisor box throughout the entire head variations, to obtain equal division of flow and sediments. Any variation in the velocity distribution is likely to result in unequal division of flow, which in turn will introduce varying degrees of error in measurement (Pathak, 1991). Water passing out from one of the slots is led into a collecting drum and measured. Water from the remaining slots is allowed to drain away. The device is generally useful for low discharge rates and has some advantages: it is simple in design and operation; there is no risk of mechanical failure; data processing is relatively simple; and it can measure both runoff and soil loss. But its use is limited to the determination of total runoff volume and soil loss only, so it is little used in research where detailed information is required on variations with time in runoff and soil loss (e.g., peak runoff rate, runoff duration, and sediment concentration) (Das, 2002).

In the Coshocton wheel sampler method, water discharge from this channel falls on a- water wheel, which is inclined slightly therefore causing the wheel to rotate. An elevated sampling slot mounted on the wheel extracts a sample of water-sediment mixture with the representative proportion (Das, 2002). For Bottle samplers, a water-sediment sample is taken isokinetically by submerging bottles or dipping an open bottle to obtain samples in stream flow and is later analysed. In some Depth-integrating samplers, a glass bottle is inserted in a fish-shaped frame mounted on a rod when gauging small streams or suspended on a cable for large streams. For the bottle to fill smoothly and evenly when below the surface it is necessary to have one nozzle or orifice for entry of water, and a second pipe through which the displaced air is ejected. A few trial runs will establish how long is required for the bottle to fill during this double journey. The method has advantages that it is widely accepted, time tested techniques, allows determination of concentration and size distribution, most other techniques calibrate against bottle samplers

(Gordon *et al*., 2004). Its drawbacks are that it requires laboratory analysis to extract data and it also requires on site personnel.

Sediment rating curves are commonly used to estimate suspended sediment loads, regardless of the method of data collection. The rating curves model the logarithm of sediment response as a linear function of the logarithm of the simultaneous water discharge. This model can give highly biased estimates, especially for small streams (Walling, 1977a; 1977b; Walling and Webb, 1981).

2.3.13 Flood Frequency and Magnitude

A flood can be described as an event during which the water surface in a river rises to such an extent that the river is no longer flowing only in the main channel, but also fills the floodplains on the sides, therefore rising above the normal flow boundaries (Meyer *et al*., 2000). Floods are expressions of the temporal variability in rainfall interacting with physical, chemical and biological characteristics of river catchment. Floods occur for many reasons, such as long-lasting rainfall over a broad area, locally intense thunderstorm-generated rainfall, or rapid melting of a large snow pack with or without accompanying rainfall. Because floods result from many different circumstances, not all floods are equal in magnitude, duration, or effect (USGS, 2010).

Dilley *et al.* (2005) estimated that more than one-third of the world's land area is flood prone affecting some 82 percent of the world's population. A survey study by the United Nations Development Programme (UNDP) (2004) estimated that about 196 million people in more than 90 countries worldwide are exposed to catastrophic flooding. The UNDP (2004) evaluated that 70,000 deaths in those 90 countries were associated with floods worldwide between 1980 and 2000. The South African National Disaster Management Center (NDMC) estimated that at least 50 000 people, and possibly more than 100 000 are living along rivers and streams in South Africa below levels reached by previous floods. Because of their proximity to the river banks, they are at risk of flooding in years of above average floods.

The need to accurately predict extreme flood events is imperative in designing for not only the safety of infrastructure, but also people's lives. This helps provide warnings to riparian users of

LRC when heavy rains are anticipated to occur to avert damage. These characteristics are determined almost by the nature of the catchment and activities (anthropogenic and natural) that take place in it (Davies and Day, 1998).

A flood frequency is defined as the number of time a flood above a given magnitude is likely to be equaled or exceeded in a given number of years on the average. The objective of the frequency analysis of hydrologic data is to relate the magnitude of extreme events to their probability of occurrence, and this relationship is described by a probability distribution of extremes. The results of flood frequency analysis are used for many engineering purposes, such as design of flood control structures or delineation of flood plains. Thus, in planning a flood protection system for a river basin, which consists of embankments, it is necessary to determine the magnitude of the flood corresponding to a specified exceedance probability or return period (Tanaka and Takara, 2002).

The present study attempts to estimate flood peaks using frequency models. The LRC is one of the regions in South Africa where floods have caused enormous damage to both property and life and impacted negatively on fauna and flora. Over the years, the catchment has experienced floods resulting from heavy rainfall associated with the ITCZ. Risk of floods has been felt in the past, with the major occurring during the 1999/2000 rainy season. Meteorologists and weather observers from the SAWS have managed to develop some mitigation strategies such as tracking the paths of ITCZ using radar and satellite imageries and providing early warnings in time when heavy rainfalls are anticipated.

A study by Van Zyl (2006) noted that climatic extremes, especially excessive rainfalls, were the most common cause of floods in South Africa. They vary from semi-predictable seasonal rains over wide geographic areas, which gives rise to the annual wet-season floods in tropical areas, to almost random convectional storms over small basins. Prolonged rainfall over large drainage basins is also associated with tropical cyclones or the intense depressions of mid-latitudes. Duaibe (2006) noted that a number of human induced factors contribute to floods in a catchment. These include factors such as land degradation; deforestation of catchment areas; increased population density along river banks; inadequate land use planning; zoning and control of

floodplain development; inadequate drainage, particularly in cities, and inadequate management of discharge from river reservoirs. Such activities can also alter the natural state of lands and rivers in a catchment (Thorvat and Mujumdar, 2010).

The floods that have had some effect on Limpopo Province of South Africa were associated with tropical cyclones that moved inland from the Mozambique Channel near the southwest Indian Ocean (SWIO) (Tyson (1986); Dyson (2000); Dyson and Van Heerden (2001; 2002); Dyson *et al*., (2002)). In January 1958, tropical cyclone Astrid caused heavy rainfall where severe flooding occurred over Musekwaspoort washing away Wyllie's Poort bridge just north of Makhado. The cyclone resulted in large scale devastation of homes, bridges and crops. Cyclone Caroline caused heavy rains over the Kruger National Park in February 1972 with between 68 to 158 mm rainfall being measured. In February 2000, Cyclone Eline brought heavy rainfall in Limpopo province causing extensive flooding and damage. The areas affected most by flooding were Thohoyandou, Giyani, Messina and Makhado. It is estimated that 23 people died in the flooding and thousands were left homeless. The realistic estimation of the magnitude of a design flood peak with a chosen probability of exceedance that can be expected at a given site in a given region is fundamentally important in the planning, design and operation of hydraulic structures and for the preservation of human life and property (Pegram and Parak, 2004).

A study by Dilley *et al*. (2005) highlighted that floods are among the most devastating natural hazards in the world, claiming more lives and causing more property damage than any other natural phenomena. Flood estimation is therefore essential in hydrologic analysis for the design of engineering projects (Rahman *et al.*, 1998), such as flood control, irrigation and hydro power projects (Das, 2002). The latter represents the generation of electricity by using the natural force of water. Historical information of hydrologic events need to be reviewed as they can lead to a better understanding of the factors that lead to extreme flood events. The analysis of information on historic floods can also provide better insight into the seasonality of flood occurrence and the effects of land-use change on catchment flood regime. The use of historical flood data is important in hydrologic studies, with benefits of understanding flood-producing mechanisms, land use/cover change and flood seasonality, and food frequency analysis (Bayliss and Reed, 2001). It is therefore necessary to provide information on the probability of such events so that

hydraulic structures are built accordingly. Accurate estimation of flood frequency discharge increases safety of the structures and minimize risks.

A number of frequency distribution models have been used in the past for hydrologic frequency determination. Though several probability models have been developed to describe the frequency distribution of extreme hydrologic events, major problems arise when selecting the best method to use since there is no general agreement as to which distribution, or distributions, that should be used for the frequency analysis of extreme hydrologic events. Therefore, the selection of an appropriate model depends mainly on the characteristics of available data at the particular site (Olofintoye *et al*., 2009). In flood frequency analysis, statistical and deterministic models are commonly used to estimate future floods. The statistical approach uses probabilistic methods to model flood events, while the deterministic approach requires the use of physically-based approach. Of the two approaches, statistical probability methods remain the most widely used in the scope of hydrology (Helsel and Hirsch, 2010). A statistical estimate based on a flood record for the stream of interest is typically the preferred method since it is most closely based on floods that have actually occurred on the stream (NOAA, 2011).

The common statistical methods used for analysing hydrologic data include, frequency analysis, regression analysis, and time series. Frequency analysis is the most suitable to predict the occurrence and exceedance of a variable to assess the reliability of the prediction. It is used as a tool for determining design values for rainfall and discharge for drainage infrastructure in relation to the required hydraulic capacity. Design discharge should be based on the frequency with which the high values will be exceeded. The design frequency represents the acceptable risk, where smaller the risk, will imply more costly drainage works and structures, since the occurrence and exceedance of the design variable will rarely be reached.

Flood hazard depends on many parameters such as flooding depth, flood duration, velocity of flood flow, timing and frequency of occurrence. Human settlement and land use practice in LRC have an impact on the above named processes. Since human activities can be controlled, the focus should be primarily directed towards managing the causes of flooding. But it should be

noted that climate change is likely to increase both the magnitude and frequency of extreme weather events, which will lead to greater flooding and associated damage.

2.3.14 Flood Frequency Models

Statistical models used in flood frequency analysis (FFA) includes three groups, namely the Normal (Normal/Gaussian, lognormal, lognormal-III), Generalised extreme value (EV1/Gumbel's, EVII/Frechet's, EVIII /Weibull's) and Exponential/Pearson type (Exponential, Pearson type III, Log-Pearson type III) distributions (Chow *et al*., 1988). Normal distribution is useful in hydrology for describing well-behaved phenomena such as average annual rainfall and stream flow. Studies by Chow *et al*. (1988), Merwade (2006) and Das *et al*. (2010) recommended the use of lognormal model as the representative for hydraulic conductivity, raindrop size distributions in storm, and sediment size data. The Log-Pearson type III (LP3) distribution is used for anticipating flood of high recurrence interval and the standard practice for estimating annual probability of exceedance of peak flows with a common-logarithmic transformation of discharges. Gumbel's distribution is the most widely used probability analysis for extreme values in hydrologic and meteorological studies. The EVIII distribution is often used in hydrology to analyse extreme low river flows (Ware and Lad, 2003).

The accuracy of peak-flood frequency estimates depends on the frequency distribution selected to estimate peak-flow magnitudes, and how well the population parameters, which include the mean, standard deviation, and skew, are estimated from the sample data. Benson (1960) studied the accuracy of peak-flow frequency estimates and found that longer period of record (observed peak flows) at a station should be used to estimate reliably peak-flow frequencies. Large errors in the estimates can occur when the period of record is short. Thus, the longer the period of record (observed peak flows) at a station, the more reliably peak-flow frequencies can be estimated. Benson (1960) indicated that the magnitude for 10-, 25-, 50-, or 100-year floods can be computed from 18-, 31-, 39-, or 48-year records, respectively, to peak-flow frequency value of 95 percent of the exceedance probability. Conversely, short period of records should also be applied to peak-flow frequency value of 80 percent of the exceedance probability. The magnitude for 10-, 25-, or 50 year floods can be computed from 8, 12 or 15-year records

respectively. Confidence limits about the annual exceedance probabilities can be used to evaluate the uncertainties inherent in the estimates (USGS, 2003).

A study by Ponce (1989) highlighted the importance of selecting return periods for various flood magnitudes. The choice of return period depends on various factors, including the size of the drainage area, the risk of failure, the importance of the structure, and the desired degree of conservatism. The lowest return period, which is only applicable in urban drainage, is 5 to 10 years. Typically, these return periods are associated with drainage areas smaller than 100 ha (low risk). For these areas, the rational method may be used to develop a peak discharge. In certain cases, particularly for areas exceeding 100 ha (high risks), long return periods may be warranted. For places where generalised probable maximum precipitation (PMP) have not been developed, and where risk of failure places human life in jeopardy, return periods in excess of 100 years, to include 200, 500, 1000, 2000, 5000, and 10,000 are warranted. Values up to 10,000 years are used for emergency spillway and freeboard hydrographs in dam design (Ponce, 1989). Pilon (2004) noted that reliable estimates for peak flow values with various return periods (on the mesoscale: drainage area of roughly 10–1000 km^2) are an indispensable prerequisite for planning measures, which reduce or even prevent flood damage. Table 2.1 below shows the guidelines for the selection of return periods for various hydrological projects:

Table 2.1: Guidelines for the selection of return period (Source: Ponce, 1989)

Type of project or feature	**Return Period (Years)**
Urban drainage [low risk] (up to 1km^2)	5 to 10
Urban drainage [medium risk] (more than 1km^2)	25 to 50
Road drainage	25 to 50
Principal spillways (dams)	25 to 100
Highway drainage	50 to 100
Levees [medium risk]	50 to 100
Urban drainage [high risk] (more than 10 km^2)	50 to 100
Flood plain development	100
Bridge design (piers)	100 to 500
Levees [high risk]	200 to 1000
Emergency spillways (dams)	100 to 10,000 (PMP)
Freeboard hydrograph [for a dam where the PMP is used to calculate the PMF]	10,000 (PMP)

The U.S Water Advisory Committee (WAC) on Water Data (1982) and the US Water Resources Council (U.S WRC, 1981) have recommended the use of the Log-Pearson Type III (LP3) distribution as a base method for flood flow frequency analysis. Mays (2001) clarified that this was an attempt to promote a consistent, uniform approach to flood flow frequency determination for use in all federal planning involving water and related land resources. This distribution is useful in predicting the likely values of discharges to expect in the river at various recurrence intervals based on the available historical record. This is important and helpful when designing structures in or near the river that may be affected by floods. It is also helpful when designing structures to protect against the largest expected event (Mays, 2001). Alexander (1990; 2001) recommended the use of the LP3 probability distribution for design flood estimation in South Africa while Singo *et al*. (2013) showed that the LP3 distribution provides good estimates for floods in the LRC. LP3 distribution differs from most of the distributions in that, three parameters (mean, standard deviation and coefficient of skew) are necessary to describe the distribution.

Gumbel (1941) introduced EV1 as a concept of extreme value distribution and as a model for prediction of hydrologic events such as flood peaks, maximum rainfall, maximum wind speed, etc. This distribution has a downfall in that the function is unbounded on either side, which could lead to the calculation of negative flows, however, this is unlikely. In hydrology, the Gumbel's distribution is used to analyse such variables as monthly and annual maximum values of daily rainfall and river discharge volumes and also to describe droughts.

2.3.15 Dams and Reservoirs

Dams are large physical barriers constructed across rivers to withhold the flow of river water for economic use. Dams may be built to accommodate unregulated random flows provided by nature that exceed the customary deterministic water demands required by society (Campos, 2010). As the world population is growing rapidly, artificial reservoirs are being created by damming rivers upstream of catchments to trap a sufficiently large amount of water from the local or regional water cycle to make up for a shortfall when demand exceeds the supply from nature (Hossain, 2012). Dams are important as they serve many functions that include flood control, the generation of hydroelectric power, and the impoundment of water for irrigation, drinking, and

recreation (Poff and Hart, 2002). They play an important role in flood management because they reduce high flow rates entering the dam to lower flow rates exiting to the river downstream (Xiaohong and jiying, 2004; Dinçergök, 2007).

Three major dams have been constructed within the study area; these include Albasini, Vondo and Nandoni Dams. The Albasini dam was built in 1952 and was raised (by means of spillway gates) in 1970/71 with a maximum capacity of 25.6 million m^3/a. This dam was built primarily to supply the Levubu Irrigation Scheme. Vondo dam was completed in 1982 to provide domestic/industrial water for Thohoyandou and its surrounding areas. This was then raised in 1992 to increase the dam's storage capacity six-fold to 30.5 million m^3/a. Nandoni Dam was initially known as the Mutoti Dam, but the name was changed to Nandoni dam in 1995. Its main purpose was to supply water for domestic use. The areas and communities that benefit are the urban areas of Makhado and Thohoyandou and the rural communities in the northern part of the Limpopo. It has a net storage capacity of 164 million m^3/a.

2.3.16 Dam Capacity

Dam capacity refers to the amount of water that is being stored in dams, particularly during winter when dam water levels drop and demand from irrigation and other uses remain high. The dam storage capacity of a river catchment refers to the quantity of water that can be stored in man-made dams in that catchment and availed for different uses (Tshikolomo *et al*., 2013). Water is stored in dams during high rainfall seasons when and where the economic value of the resource is low and is reallocated to times and places when and where its economic value is high. To mitigate against the challenge of scarcity, water resources should be more efficiently managed by assessing the amount of runoff/stream flow in a specific area, which depends on the availability of storage infrastructure such as dams (Mostert, 2008). It is therefore important to develop water storage through analysis of current runoff/stream flow and storage capacity relationships of river catchments. Measuring dam volume is crucial for water planning and budgeting, and for providing early warning of water shortage problem.

Sharma and Sharma (2002); Mays (2001); and Reddy (2011) have identified mass curve analysis (MCA) as widely used methods for determining storage-demand relationship for a specific

location along the river. A mass curve is defined as a graphical method that is often used in calculations of reservoir storage capacities. It is a curve of the accumulated total flow or rainfall against time and it serves as a very useful tool to determine the required storage capacity for any uniform rate of demand. The method is used in planning stages to determine the capacity of a single-surface reservoir for a specific release pattern; enabling researchers and engineers to develop storage-yield curves for the reservoir under consideration. It is useful in determining preliminary size of a reservoir required to satisfy a simplified pattern (i.e, time sequence) of water demand. Mass curves are useful in reservoir design studies since they provide ready means of determining storage capacity necessary for particular average rates of runoff and draw off (Mays, 2001). As active storage capacity of a reservoir depends on various hydrologic elements whose contributions to the mass balance are a function of unknown reservoir storage, it is important to account mass curve and sequent peak analysis to develop storage-yield relationship.

Systematic investigation for determining the capacity of a dam dates back from the work of Rippl (1883) who determined the capacity of a dam by mass curve method. This method is based solely on the historical inflow record. A recent study by Ndiritu *et al*. (2011) used mass curve analysis to model inflows from the complete monthly and long-term monthly average rainfalls as well as inflows from long-term daily average rainfall in Siloam village. Residual mass curve method (which is computationally identical to the mass curve) was also applied for the case using the complete monthly time series in order to improve graphical accuracy. Ndiritu *et al*. (2011) also demonstrated the limitations of using the simple mass curve analysis and the effect of applying a monthly time step. The implication of the mass curve method assumes that the time interval includes the critical period, which is the time period over which the flows have reached a minimum, causing the greatest drawdown of a river. This assumes that the total release over the time interval of analysis does not have to exceed the total reservoir inflows. A critical period always begin at the end of a preceding high-flow period that leaves the reservoir full; this critical period ends when the reservoir has refilled after a drought period. The critical drawdown period however, begins when the reservoir is full and ends when the reservoir is empty (Mays, 2001). As the critical period could occur at the beginning or the end of the time series, the inflows are doubled up for the mass curve analysis (McMahon and Adeyole, 2005). Double mass curves are created using cumulative values of one variable against the cumulation of another quantity

during the same time period. A mass curve is a plot of cumulative values against time. The importance of employing double mass curve is to correct any data inconsistencies. The MCA was adopted for this study to detect the impact of human population on dam capacity in LRC. Reddy (2011) presented the following formula for determining MCA of a river:

$$V(t) = \int_0^t Q(\tau).d\tau \qquad 2.20$$

where,

$V(t)$ = cumulative volume of flow up to time t from the start of the record, i.e., the ordinate of the mass curve at any time t.

$Q(\tau)$ = the discharge as a function of time, i.e., the ordinate of the hydrograph

τ = a dummy variable

2.4 Geomorphological Factors

Evaluation of the relative influences of land cover change on geomorphic factors is important in order to fully understand how land cover change affects hydrology and water resources in semi-arid regions with variable topography such as the LRC. Soil physical properties are the most important factors influencing the rate of water that can infiltrate into the soil. In turn, the infiltration serves as indicators for the influence of land use on soil (Zimmermann *et al*., 2006). The water infiltration rate can thus be considered as an important soil water property, which significantly influences the amount of surface runoff in a catchment and hence, the degree of soil erosion (Alhassoun, 2009). The infiltration capacity of soil, together with initial soil moisture content is important in this study as it plays a major role in the occurrence of flash flood events. Human activities that alter land cover which affect the properties of soils also contribute to flash flood. Such activities are considered to be a possible cause for changes in runoff peak flow behaviour, which in turn affect the magnitude of flooding in lowland areas.

2.4.1. Soil

Soil functions essentially as a pervious medium that provides a large number of passageways for water to move into the surface. The effectiveness of the soil to transport water depends on the size and permanency of the channels. The size of the conduits depends on the size of the soil

particles, the degree of aggregation between particles and the arrangements of particles and aggregates (Tsheko, 2006). A study by Jewitt and Garrat (2004) demonstrates soil as a geomorphological factor that plays a crucial role in catchments' hydrological response by either acting as a store of water, which makes soil water available to plants; or redistributing water, both within the soil profile and out of it. A study by Prachansri (2007) showed that land use/cover changes due to population pressure from forest to agricultural land, can result in major changes in soil physical properties such as bulk density, soil structure, and organic carbon content that affect soil hydraulic properties and water retention characteristics. Das (2002) reviewed soil properties that include soil texture and soil moisture as two of various important hydrological processes that play an important role in hydrology and water resources by influencing infiltration, evaporation and evapotranspiration.

Soil texture refers to the relative size distribution of the primary particles in a soil such that particles are grouped according to their size into what are called soil separates. These separates are typically named clay, silt, and sand. Soil textures are classified by the fractions of each soil separate (sand, silt, and clay) present in a soil. Classifications are typically named for the primary constituent particle size or a combination of the most abundant particles sizes, e.g. "sandy clay" or "silty clay." Soil texture affects the water-holding capacity, water movement through the soil, soil strength, and soil fertility. It is an important indicator of the ability of soil to absorb and hold both water and plant nutrients (Gee and Bauder, 1986). Soil texture affects several soil properties such as soil structure, aeration, water holding capacity, nutrient storage, water movement, and bearing strength.

A number of soil classification systems have been developed to classify soils of different profiles; the most widely known are the United States Department of Agriculture (USDA), the International soil classification System; the Unified Soil Classification System (USCS); the American Association of State Highway and Transportation Officials (AASHTO); and the PHI Scale System (McKenzie, 2004). The USDA is a widely used soil classification method since it is based on relative proportions of Sand, Silt and Clay. Determining the soil textures is often aided with the use of a soil texture triangle (also known as a ternary plot) as shown in Figure 2.2. The triangular diagram is subdivided into several soil textural classification types, with each soil

type comprising a range of percentages of the three particle types. The soil classification type is determined by plotting the percentages of each of the three soil particle classes found within the soil sample on the triangular diagram. The point of intersection of each of these three particle class percentages will fall within one of the soil classification types (Pfannkuch and Paulson, 2005). Twelve major soil texture classifications are defined by the USDA system, namely sand (Sa), loamy sands (LoSa), sandy loams (SaLo), loam (Lo), silt loam (SiLo), silt (Si), sandy clay loam (SAClLo), clay loam (ClLo), silty clay loam (SiClLo), sandy clay (SaCl), silty clay (SiCl), and clay (Cl). Subclasses of sand are subdivided into coarse sand, sand, fine sand, and very fine sand. Subclasses of loamy sands and sandy loams that are based on sand size are named similarly.

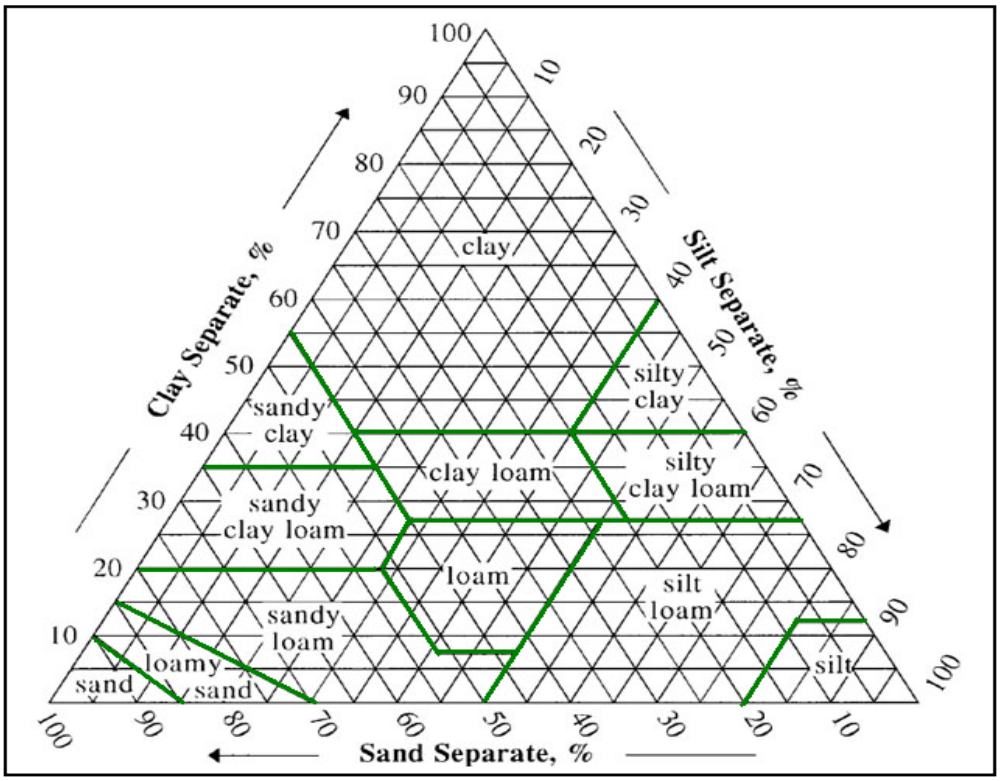

Figure 2.2: USDA Soil textural triangle plot

The most commonly used methods to determine soil texture include: hand texture method, separation by sieving and separation by sedimentation which include the pipet and the Bouyoucos hydrometer methods. The hand texture method involves taking a small sample of soil and moistening it, then rubbing it between the palms of the hand. The result rhymes with the

features of sand, clay and silt analysed previously. The hydrometer and pipette methods are sedimentation procedures that are accepted as standard methods of particle-size analysis (Gee and Bauder, 1986). The pipet method was introduced in the early 1920s by Jennings and Robinson and is often used as the standard to which other methods are compared (Sheldrick and Wang, 1993; Gee and Bauder, 1986). The Bouyoucos hydrometer method is somewhat less accurate than the pipet method, but is easier to perform. The theory of the hydrometer method is similar to that of the pipet method except for the manner of determining the concentration of solids in suspension (Dance and Hynes, 1980).

Soil moisture influences a number of environmental systems and the water resources management and is complex because of its spatial and temporal variability. Its interactions influence many of the ecological functions of soils and practices of soil management (Western *et al.*, 2002). These interactions determine how much rainwater runs into and through the soil and how much runs off the surface. The control of these processes in turn determines the movement of chemicals in groundwater, and of both chemicals and eroded soil particles to streams and lakes. These interactions affect the rate of water loss through leaching and evapotranspiration, the balance between air and water in soil pores, the rate of change in soil temperature, the rate and kind of metabolism of soil organisms, and the capacity of soil to store and provide water for plant growth (Brady and Weil, 2002). Soil moisture is influenced to some extent by climate and topography in a particular geographic region.

Brady and Weil (2002) provided two general kinds of soil water measurements that include direct and indirect methods. A direct method measures the amount of water present in soil (measurement of water content in the soil/wetness) whereas an indirect method measures the energy status of the water (measurement of soil water potential or stress or tension under which water is held by the soil). When these measurements are done, soil water characteristic curves (in a logarithm scale) are drawn to show results obtained by slowly drying completely saturated soils. Soil moisture measurements in the field have been shown to be spatially and temporally highly variable. The variability is driven by vegetation, soil type and topography (Scipal *et al.,* 2005). In the study area, soil water contents are widely obtained from direct method measurements where measurements of the amount of water present in the soil are done. Direct

methods are applied when water content is directly measured using a known mass or volume of the soil, and a drying oven.

The most common instruments used for estimating soil moisture by direct methods include soil water content expressed on a gravimetric or volumetric basis. The gravimetric method involves removing a sample of soil and bringing it to the lab. In this method, basic measurements of soil moisture are made on soil samples of known weight or volume. The volumetric water content on the other hand is defined as the volume of water associated with a given volume of dry soil. This method is applied when one is dealing with water transport. In this method, a soil sample is taken with a core sampler or with a tube auger whose volume is known. The method is though accurate and simple; it is used mainly for experimental purpose. Studies such as those of Lull and Reinhart (1955); Reynolds (1970a, b, c); Wagner *et al*. (1999); Robock *et al*. (2000) and Western *et al* (2002) have recommended the gravimetric method as the basic technique for measuring soil water content. The reason being that this method is based on direct measurements, it is the standard with which all other methods are compared. Unfortunately, gravimetric sampling is destructive, rendering repeat measurements on the same soil sample impossible. Another demerit of gravimetric sampling is that it is time consuming. Sampling, transporting and repeated weighing give errors. It is also laborious and time consuming (AgriInfo, 2011).

In this study, grain size distribution curves were plotted to separate particles size from sand, silt and clay as well as to identify the shapes of the grading curves for the study area. The shapes of the grain size distribution curves for the study area are indicative of the nature of the soil tested. A study by Murthy (2009) confirmed that these shapes can either be classified as uniform graded; well graded; and gap graded or poorly graded. Uniform soils are represented by nearly vertical lines. Such soil possesses particles of almost the same diameter (size) and will have almost vertical curve. A well graded soil possesses a wide range of particle sizes ranging from gravel to clay size particles. Such soil will have a curve spread evenly across the chart. A gap graded soil on the other hand has some of the sizes of particles missing within the curve. Such soils are poorly graded and stretch across but show deficiency of some intermediate sizes.

2.4.2 Infiltration

Infiltration is the process by which water enters into a soil from rainfall, snowmelt or irrigation. The rate of infiltration is a measure of the rate at which soil is able to absorb rainfall or irrigation water, and is a factor in the estimation of flood peaks and yields of catchments (Thomas and Goudie, 2000). A study by Horton (1933) shows that when rainfall reaches the ground surface, it infiltrates the surface soil at the rate that decreases with time, until a final, constant value known as the steady water infiltration rate, is reached. Infiltration capacity has been defined by Slatyer (1967) as the maximum rate at which the soil, in a given condition, can absorb falling rain. The infiltration capacity is expressed in terms of the infiltration curve (Horton, 1940). The capacity decreases with time after the onset of rainfall and ultimately reaches an approximately constant rate.

Infiltration is usually maximum at the beginning of a storm due to low antecedent moisture condition (AMC) and large pores. As the soil becomes wet, the infiltration rate slows to the rate at which water moves through the most restrictive layer, such as a compacted layer or a layer of dense clay. Prior to rainfall, infiltration is controlled by three factors, namely, entry, storage and transmission; which are mostly controlled by rainfall characteristics (Kuells *et al*., 1995). On the one hand channel infiltration is controlled by the properties of the alluvium, but on the other hand it is tied to the surface flow, because water levels and flood duration influence infiltration rates and amounts (Parissopoulos and Wheater, 1991).

Rogasik *et al*. (2004) presented a number of factors affecting infiltration rate and infiltration capacity. These include factors such as the type and extent of vegetal cover; condition of surface crust, temperature; rainfall intensity; soil properties including porosity, hydraulic conductivity, moisture content and water quality. The rate of infiltration is also affected by different chemical, biological and physical soil properties, like organic matter content, biological activity, earthworms, soil sealing and crusting, and compaction. Agricultural management practices like tillage, fertilisation and crop rotation also affect the infiltration of water into the soil. Numerous studies such as those of Hubbard *et al.* (1999); Schmidt *et al.* (2003) and Rogasik *et al*. (2004) have revealed that land use and management practices are the essential factors affecting soil structure and infiltration characteristics. Of all the above factors mentioned, soil properties have

been regarded as the predominant factor in affecting water infiltration rate. A study by Mangangka (2008) noted that infiltration capacity of soil mainly depends on two factors; the particle size and the moisture content of the soil. These properties include degree of compaction, soil structure, composition and texture. The latter has been reported as being the principal soil factor influencing infiltration rate (Saxton *et al*., 1986).

Soil infiltration is measured in a number of ways, either in the laboratory or under field conditions. It is suggested that measurements under field conditions are more reliable than laboratory measurements. When conducting field measurements, an infiltrometer that duplicates the system being investigated must be selected. The ring-infiltrometers (single-ring and double-ring infiltrometer) are the common method that are used today to measure infiltration of the soil (Maidment, 2002). In most studies, the double-ring infiltrometer is used more frequently than any other techniques. As only a small area is used, this technique is very sensitive to worm and root holes and other cracks in the soil (Maidment, 2002). Any crack in the soil surface will result in much faster flow than would otherwise be achieved. As these cracks are often not visible at the surface it is not always possible to avoid them when choosing a site (Burgy and Luthin, 1956). The infiltration rate decreases as the soil becomes saturated. If the precipitation rate exceeds the infiltration rate, runoff will usually occur unless there is some physical barrier (Maidment, 2002). The infiltration rate varies with different soil types, which can affect the accuracy of the results. The double ring method is not reliable on soils with vertic properties (McKenzie *et al*., 2002), such as roots, which are able to extract water during infiltration (Van Zyl, 1988).

The advantages of the double-ring infiltrometer are that only a small area is needed when undertaking measurements; it is simple to run; and does not have a high water requirements. This method usually produces higher steady-state infiltration rates than rainfall simulators (American Society of Civil Engineers (ASCE), 1996). Some draw-backs of the double-ring infiltrometer are that it is very time consuming, requiring frequent attention, either by recording measurements or by maintaining equilibrium in the height between the rings. The practicality of the instrument is reduced by the fact the rings are extremely heavy to move. It also requires a flat undisturbed surface which sometimes is not available (McKenzie *et al*., 2002). The method is suitable for use

in semi-arid areas characterised by high rainfall, relative humidity, temperature and evapotranspiration, such as the LRC. Singo (2010) in a study carried out in Khalavha Village found that sandy clay loam soil has the highest infiltration rate of 33 mm/hr while the sites characterised by clay and sandy loam soil have the lowest infiltration rate of 20 mm/hr. The infiltration rate of clay soil was higher than the Hillel (1980) steady state infiltration rates for clay soils due to large openings, which were observed.

2.4.3 Infiltration Rates

A number of infiltration models are used to determine infiltration rate, infiltration capacity, cumulative infiltration, time of ponding, and infiltration after ponding. Numerous formulations, some entirely empirical and others theoretically based, have been proposed over the years in repeated attempts to express infiltration rate as a function of time or of the total quantity of water infiltrated into the soil. Simplified approaches include empirical models such as Horton (1940), Holtan (1961); and approximate physically based models like those of Green and Ampt (1911) and Philip (1957). The physically based equations rely more heavily on the soil hydraulic and physical properties occurring within the profile, such as saturated hydraulic conductivity, soil moisture gradient, and suction at the wetting front. Empirical infiltration models on the other hand are generally obtained by curve-fitting measured data obtained from abundant field measurements. The cumulative infiltration is the cumulative amount of infiltration over a given time period. As shown in Mays (2001) and Chow *et al*. (1988), the cumulative infiltration F is the depth of water infiltrated, defined mathematically by:

$$F(t) = \int_0^t f(t)dt \qquad 2.21$$

where t is the time. The infiltration rate as the time derivative of the cumulative infiltration given as:

$$f(t) = \frac{dF(t)}{dt} \qquad 2.22$$

2.4.4 The Green and Ampt equation

The Green and Ampt equation is used to explain infiltration rate of time evolution in cumulative infiltration depth and rate. The method involves the simulation of rainfall loss as a two-phase

process. The first phase of rainfall loss is called initial abstraction (I_a) or surface retention loss, which involves vegetation interception, evaporation, and surface depression storage. The second phase of the rainfall loss process is infiltration of rainfall into the soil. The infiltration is assumed to begin after the surface retention loss is completely satisfied. The infiltration rate f and the cumulative equation F of the Green and Ampt equation are related by the following equations:

$$\int_0^{F(t)} \frac{1-\psi\Delta\theta}{F(t)+\psi\Delta\theta} dF = \int_0^t K dt \qquad 2.23$$

$$f(t) = K\left(\frac{\psi\Delta\theta}{F(t)}+1\right) \qquad 2.24$$

where,

$F(t)$ = total volume already infiltrated (cumulative infiltration)

ψ = wetting front soil suction head

θ = water/moisture content

$\Delta\theta$ = the difference between the initial and final moisture contents of the soil

f = infiltration rate

K = Hydraulic conductivity

Soliman (2010) presented a method for determining the ponding time with infiltration into the soil described by the Green and Ampt equation. This is done for rainfall intensity i starting instantaneously and continuing indefinitely to determine (i) infiltration before ponding where all the rainfall is infiltrated; (ii) the potential infiltration rate f as a function of cumulative infiltration F; and (iii) infiltration after ponding when the potential infiltration rate is less than or equal to the rainfall intensity. Soliman (2010) provided the equation for the time of ponding with the Green and Ampt method as follows:

$$t_p = \left(\frac{K\psi\Delta\theta}{i(i-k)}\right) \qquad 2.25$$

where,

ψ, θ, K are as shown above

i = rainfall intensity

$$i = K\left(\frac{\psi\Delta\theta}{it_p} + 1\right)$$

2.4.5 The Horton Equation

The Horton equation defines the infiltration capacity *f* as the maximum rate at which rain can be absorbed by the soil in a given condition (Beven, 2004). When the rainfall intensity *i* falling on the ground is less than *f,* then all of the rain infiltrates. When *i* is greater than *f,* then only *f* infiltrates, and the excess of *i* over *f* becomes overland flow. The equation states that infiltration starts at a constant rate, f_0, and is decreasing exponentially with time, *t*. After some time when the soil saturation level reaches a certain value, the rate of infiltration will level off to the rate f_c. It indicates that if the rainfall supply exceeds the infiltration capacity, infiltration tends to decrease in an exponential manner (Beven, 2004). The infiltration rate and cumulative infiltration *F* are expressed as follow:

$$f_t = f_c + (f_0 - f_c)e^{-kt} \qquad 2.26$$

$$F_t = f_c + \frac{(f_0 - f_c)}{k}(1 - e^{-kt}) \qquad 2.27$$

where,

f_t = the infiltration rate at time *t* in mm/h

f_0 = the initial infiltration rate or maximum infiltration rate in mm/hr.

f_c = the constant or equilibrium infiltration rate after the soil has been saturated or minimum infiltration rate in mm/hr.

F_t = cumulative infiltration in mm

k = the decay constant specific to the soil in hours. It represents the rate of decrease in the infiltration capacity (decay coefficient) and depends on soil characteristics. If vegetation is present, then *k* is small.

The Horton equation represents a family of curves fitted to experimental results derived from the observed behaviour of natural soils. The influence on infiltration of soil texture and structure, root system development and earthworm perforations is taken into account in evaluating the

parameters (Fischer *et al*., 2014). The equation captures the basic behavior of infiltration but the physical interpretation of the exponential constant is uncertain. One difficulty with Horton's equation is that it is difficult to predict how it would change if the soil were initially a little wet. Another drawback is that variations in antecedent conditions cannot readily be taken into account (Jiafeng, 2008).

Horton also provided an equation for calculations of time of ponding which is the elapsed time between the time rainfall begins and the time water begins to pond on the soil surface. The process of ponding time as provided by the Horton equation starts with a relatively dry soil at the beginning of a storm. If the rainfall persists and is maintained at a high enough intensity at some point in time, the rainfall intensity becomes equal to the falling value of the infiltration capacity. Beyond this time, called the ponding time t_p, t_p becomes larger than f; meaning that not all the rainfall can infiltrate. Therefore water begins to pond up at the surface, forming puddles, and eventually starts to flow downslope, thus producing sheet-like overland flow. The time to ponding is also regarded as the time between the start of the rainfall and the initiation of runoff given by:

$$t_p = \frac{-1}{k} In\left(\frac{1-f_c}{f_0-f_c}\right) \qquad 2.28$$

where,

t_p = the time of ponding

2.5 Application of GIS and Remote Sensing in Hydrology

A GIS can be described as a computer system capable of capturing, storing, analysing, and displaying geographically referenced information (Burrough, 1986). The use of GIS as a significant support tool for hydrologic modeling emerged during the late 1990s and has now been accepted as a tool for assembling water resources information. It has become a useful and important tool in hydrology for the scientific study and management of water resources.

Application of GIS and Remote Sensing can provide detailed, quantitative land surface information at large spatial coverages and at frequent temporal intervals. It allows for the

synthesis and integrated analysis of an extremely varied range of spatial, temporal and attributes information related to hydrology, land cover, land use, utilities, protected areas, political boundaries, economic patterns, transportation, telecommunications, biodiversity, resource extraction, agriculture, etc. (Yeh, 1999). This capacity for quantitative land-surface monitoring over large areas makes remote sensing well-suited for a very wide range of disciplines, including that of land-use planning (Prenzel, 2004). GIS provides the most effective information synthesis and analysis tools for incorporating detailed spatial information for planning. The widespread availability, and decreased cost, of remotely sensed imagery and GIS allow for efficient and quantitative resource mapping and land cover change detection. This is of particular value in developing nations where trained personnel and finances are limited, or where many areas are inaccessible (Sheng *et al*., 1997).

Advances in remote sensing and GIS techniques have broadened the scope of global data acquisition, providing the capacity to quantify and estimate spatially distributed hydrological processes (Moore *et a*l., 1991; Carpenter, 1999). Studies such as those of Hong *et al*. (1998) and Santillan *et al*. (2010), to cite a few, have demonstrated that remotely sensed data provide both actual and areal information for hydrological catchment modeling. Satellite sensors including Landsat Enhanced Thematic Mapper plus (ETM+), SPOT HRV (High Resolution visible), Moderate Resolution Imaging Spectrometer (MODIS), Medium Resolution Imaging Spectrometer (MERIS) and National Oceanic and Atmospheric Administration (NOAA) among others, now provide repetitive land surface data and have made it possible to quantify multitemporal variability of land cover (Coppin *et al*., 2004). Hydrogeophysical catchment parameters can be derived from the global digital soil and topographic datasets after which, computer-based hydrological models are applied to solve complex hydrological problems. In order to realize the synergism between remotely sensed digital data and GIS for land surface analysis and modeling, multispectral and multitemporal remotely sensed data are integrated with ancillary and hydrogeological data for spatial analysis and modeling within GIS (Coppin *et al*., 2004).

Ellis (2013) reinforced remote sensing as an essential tool of land-change science because it facilitates observations across larger extents of Earth's surface than is possible by ground-based

observations. Baldyga (2004) showed that remotely sensed imagery provides up-to-date, as well as over time, natural resource information such as land cover change caused by resource exploitation or renewal, available resource estimates, and how land cover changes are affecting surrounding areas. Such technologies can be used by developing nations to alleviate or predict resource scarcity and improve overall ability for self-sufficiency. Prenzel (2004) noted that sectors and activities that stand to benefit from remote sensing-derived change information for planning and management include: agriculture (e.g. irrigation, cropping, fertilising, and harvesting), forestry (e.g. harvesting, silviculture, pest management, and distribution), urban planning (e.g. utilities, transportation, telecommunications, and housing development), oil and gas (e.g. exploration, pipeline development, drilling, and refining), conservation (e.g. species at risk, protected areas, habitat monitoring, and rehabilitation), and environmental monitoring (e.g. ice extent, biomass, urbanisation, drought, and fire).

A study by Jensen *et al*. (2005) has shown that maps and measurements of land cover can be derived directly from remotely sensed data by a variety of analytical procedures, including statistical methods and human interpretation. Both types of land use/cover datasets may be compared between time periods using GIS to map and measure land use/cover at local, regional, and global scales. The ability of satellite sensors to provide repetitive land surface data normally difficult to obtain on the ground has permitted the quantification of multitemporal variability in the states of land cover (Miline, 1998; Coppin *et al*., 2004). Besides, physically based catchment parameters can be derived from the availability of global digital soil and topographic datasets (Reuter and Jarvis, 2007). Based on space-time representations, the models can be categorised on distributed or lumped basis (Chow *et al.,* 1988; Singh, 1995). Physically based models, distributed or lumped, relate model parameters to observable land surface characteristics and have hence been extensively utilised in studies of land surface changes and sub-surface hydrologic processes (Saghafian *et al*., 2007; McColl and Aggett, 2007).

Since Griscom *et al*. (2009) mapped land cover changes of the LRC, changes in land cover that include urban/built-up areas and agricultural lands have been developed to accommodate the increasing population. It is therefore important to include recent developments in land cover change analysis, through the integration of GIS and remote sensing to assess the changes in land

cover and their impacts on hydrology and water resources. Due to the variable nature of large proportion water resources in the catchment, continuous assessment and monitoring of hydrological system components is important. The use of GIS and remote sensing combined with hydrologic modeling makes it possible to evaluate hydrologic processes and catchment behavior under various conditions of cover change.

CHAPTER 3

MATERIALS AND METHODS

3. The Research Approach

The research approach adopted for this study was divided into three phases, namely, pre-fieldwork phase, fieldwork phase and post fieldwork phase. Figure 3.1 depicts the flow chart showing the research procedure used in this study.

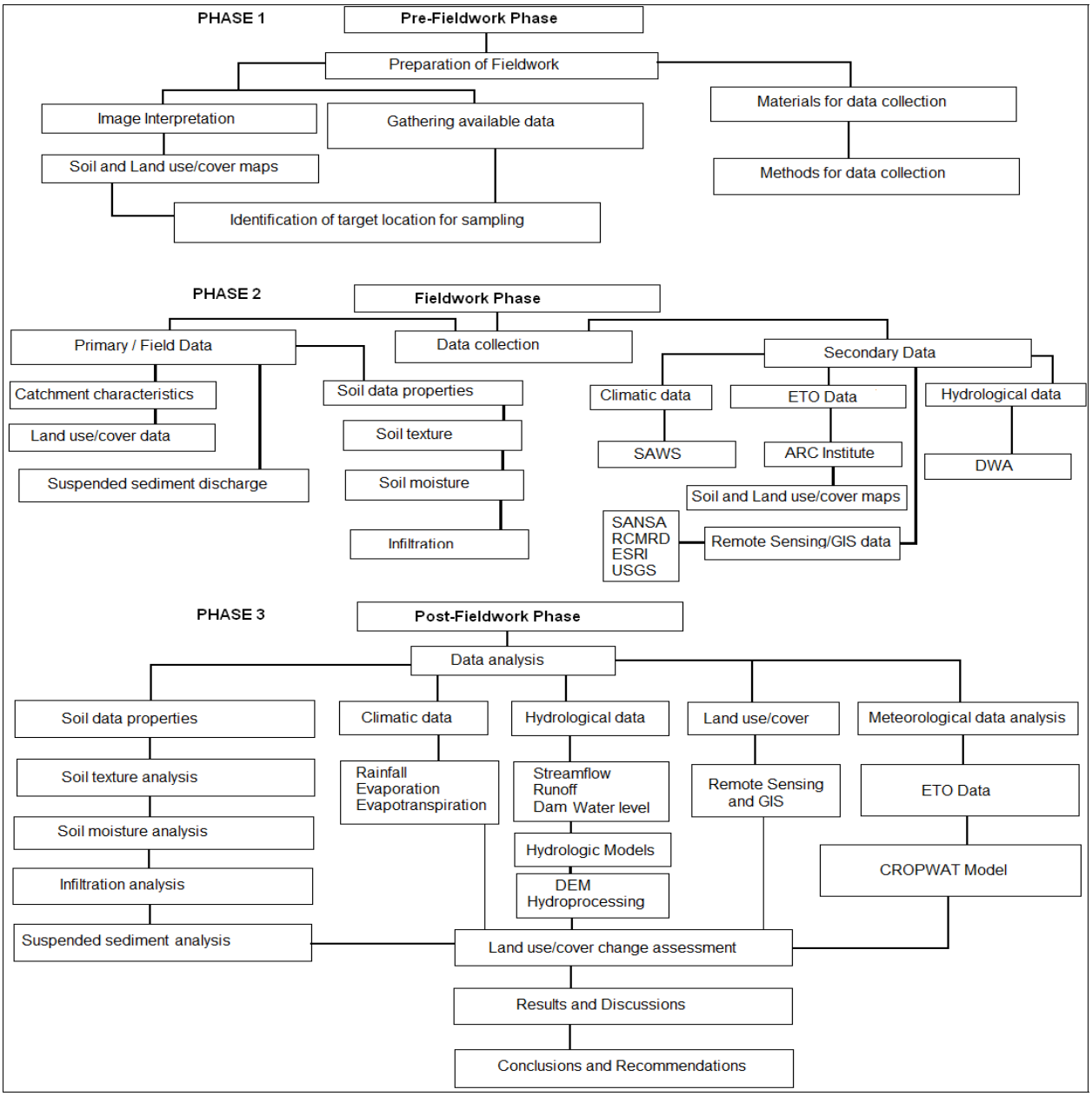

Figure 3.1: Flow chart showing the research procedure used for the study

3.1 The Conceptual Framework

The previous chapters have reviewed that changes in land use are associated with changes in land cover. The conceptual framework of this study focused on the concept of the dynamic interactions of land use and water resources in the catchment. Such dynamic interactions may cause significant changes in the location of land use or water resources, and the components of land use (e.g. residential, deforestation, agriculture) or water resources (e.g. precipitation, surface runoff, evapotranspiration, stream flow) may affect the other. This concept takes into account that land use changes is the driver of land cover change, and is affected by various factors, such as the environmental (e.g. weather, soil type, topography) and socio-economic factors (e.g. population growth and urbanisation). The framework serves as an understanding of the dynamic interactions of land use and water resources in the catchment to improve the livelihood and sustainable use of land and water resources in the catchment.

The conceptual framework for the study shown in Figure 3.2 was developed based on the above concept using an integrated approach to evaluate the impacts of land cover changes on the hydrology and water resources of the LRC through the application of GIS, remote sensing, and hydrological models. By applying remote sensing data and making use of the advances in GIS technology, the spatial dynamic of these impacts was assessed. Remote sensing and GIS analysis were used to describe the alterations of land use/cover from the late 80's to 2010 using aerial photographs and satellite images through visual interpretation of the aerial photographs and supervised classification of the satellite images. Distributed hydrological models such as SWAT and Arc Hydro were then used to simulate hydrological components of land use/cover maps from remote sensing images under various climatic conditions. Empirical hydrological models such as rainfall-runoff models were used to predict a relationship between input and output based on hydrometeorological data. The combination of GIS, remote sensing, and hydrological models related the influence of the identified land use/cover classes on the catchment and assessed their hydrological impacts on sub-catchments. This approach of linking a hydrological model to remote sensing image analysis into a GIS to evaluate the impacts of land use/cover changes on hydrology and water resources may provide quantitative information for decision making for both land and water resources management in the catchment.

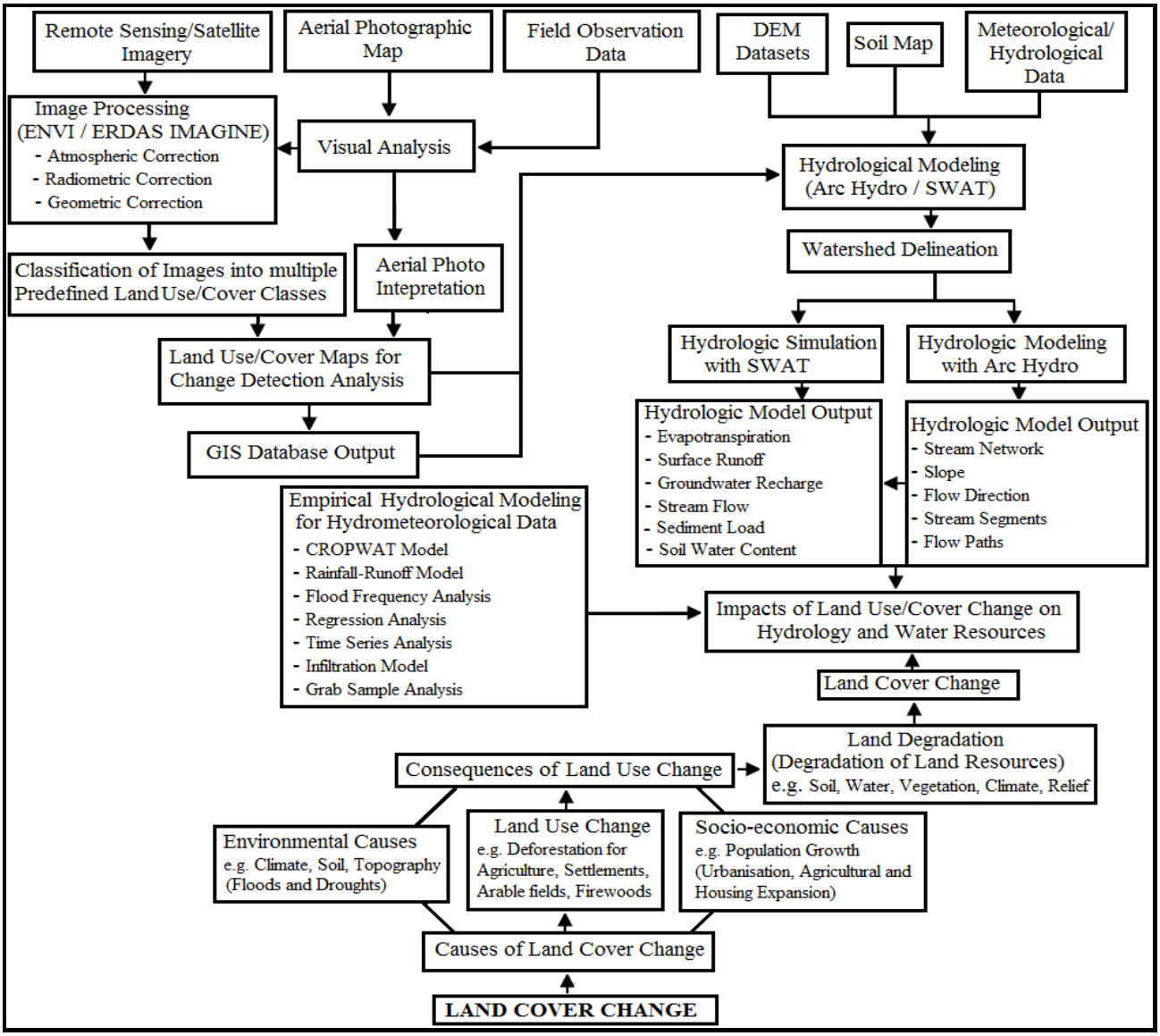

Figure 3.2: A conceptual framework for the study

3.2 Deriving Land Cover Information from Remotely Sensed Data

The remotely sensed images covering the study area (path 169, row 76) for a period of 30 years (1980-2010) were acquired from the Regional Centre for Mapping of Resources for Development (RCMRD). The study used Landsat Multispectral Scanner (MSS), Landsat Thematic Mapper (TM), and Landsat Enhanced Thematic Mapper plus (ETM+) images to derive land cover information for the study area. A total of 23 satellite images, each with its own Landsat scene identifier, were used for the production of land cover maps for the study area.

Topographic maps were used as ancillary data to assist in image analysis and classification as well as to populate metadata.

Geospatial Analysis tools were used for data capture and image analysis. The algorithm was conducted in ArcMap 10 (ESRI, 2011b) and ENVI 4.5 (ITT Visual Information Solutions, 2008) geospatial image processing and analysis software packages. Images were georeferenced to define their spatial position and coordinate reference system. After georeferencing the images, classification tools in ArcGIS 10 were used to provide primary information about land use/cover features such as forest, bare grounds, rivers, settlements, grasslands, shrublands, plantation, and agriculture. To obtain consistent classes for semi-distributed hydrological modeling, a per-pixel image classification approach was adopted where the images were classified based on guided clustering as described by Yuan *et al*. (2005). To minimise distorting spectral characteristics caused by mosaicking multi-data images before classification, the scenes were independently classified. The images were first resampled to a common spatial resolution of 80 m using the nearest neighbor interpolation technique as described by Jensen (2005). Coarse resolution data of 80m spatial resolution are widely used to acquire basic land cover and land use information over large areas (Köhl *et al*., 2006).

For better extraction of land use information classes, interactive supervised classification was used as an image training tool where the Maximum Likelihood Classifier (MLC) was used to classify the images in ArcMap 10. The required land-cover classes were originally identified by examining the needs of the 'end user' for the product. In this way, pixel categorisation was carried out by establishing numerical descriptors of one or more land use/cover types. The images were then converted to polygons to identify the number of land use/cover classes in the catchment. To determine whether the selected pixels were grouped into the correct features of land use/cover classes in the catchment, an accuracy assessment was done using the Area Frame Sampling (AFS) technique. This involves comparing the pixels with ground based data such as topographical maps and aerial topography. The error matrix and kappa coefficient were then used as standard methods of assessment of image classification accuracy. This method involves resampling classified imagery against ground truth field samples often obtained by a GPS. After georeferencing and classification of images, the shapefiles covering the study area were used to

clip the catchment area, after which land use maps for different temporal resolution were produced. Overlaying of maps generated through image classification was used to generate base maps for detecting land use change in the catchment. The land cover and land use statistics were used in identifying the percentage change, trend and rate of change in the study area.

3.2.1 Quantifying Land Cover and Land Use Change

The spatio-temporal land cover and land use changes in LRC were determined using 1980 satellite images as the baseline. Hydrologically discrete (individually separate and distinct) land use/cover classes (Jensen, 2005) within each quaternary catchment were estimated from remotely sensed images. The impact of land cover change was assessed using two time window periods where the 1980's were taken as the period before change, and the 2000's as the period after change. Studies of assessment of land use and land cover impacts using before and after change periods have been documented in the past, including recent studies by Zilassi *et al*. (2010); Li *et al*. (2014); Odongo (2014) and Mwangi *et al*. (2016). Historical aerial images are important to retain past ground surface information while recent images explain where change is occurring and what land cover types are changing. The images selected for land cover classification were divided into winter and summer seasons. The winter season in the study area runs from April to September whereas the summer season runs from October to March. Predominant land cover classes were identified by using a combination of image classification and visual interpretation with the aid of ArcGIS Spatial Analyst Extension Tools.

A statistical sampling methodology based on Area Frame Sampling (AFS) was adopted for this study. It relied on satellite imagery and maps being divided into small segments of the study area. The unaligned systematic random AFS scheme was preferred in order to capture representative samples of the heterogeneous land use in the catchment. The samples were chosen based on one square kilometer fixed size ground segments which have been found to be the most bias-free sampling design (Berry and Baker, 1968). A 1 km x 1 km grid corresponding to the 1:50,000 map sheet was overlaid upon the images, after which the locations of ground segments were chosen randomly from each block based on square grids. Each segment had unique and identifiable boundaries outlined on images and maps. Field enumerators visited the segments and recorded information about agricultural activity within the segment boundaries. Individual land

parcels, land use and ground cover classes were identified in each sample segment. Data on crops, homesteads, animals, and environmental factors were collected. Their locations were accurately determined by using conspicuous land marks and features such as road junctions and planted eucalyptus and first hand knowledge of the area by the author. By the method of direct expansion (Cochran, 1977; Allen and Hanuschak, 1988; Taylor and Eva, 1992) the area for each land use and land cover class was determined for the entire study area.

3.2.2 Area Estimation by Direct Expansion

The study employed the method of Area Frame Sampling (square grid method) proposed by the Institute for Remote Sensing Applications (IRSA) of the EEC (Earth Engineering Center) in Ispra (Institute for Environmental Protection and Research) (Alonso *et al*., (1991); Gallego (1995; 1999)). The main objective was to develop a method of estimating the surface cover for different land use classes through the combined use of remote sensing techniques and field work. The ground survey was conducted for a two year period from 2011 to 2012. The surface cover estimation was done for several classes of land cover and land use including forest, maize, macadamia, bananas, subsistence agriculture and build up areas. To estimate the area of the different land cover and land use, the stratified random sample formulas by Cochran (1977) were estimated by the following equations:

$$\hat{T} = \sum_{i=1}^{h} \hat{T}(i) \qquad 3.1$$

where,

$$\hat{T}(i) = D(i)\,\bar{y}(i)$$

$$\bar{y}(i) = [\frac{1}{n}(i)]\sum_{j=1}^{n(i)} y(i,j)$$

$$\hat{V}(\hat{T}) = \sum_{i=1}^{h} \hat{V}(\hat{T}(i)) = \sum_{i=1}^{h} D^{2}(i)\hat{V}(\bar{y}(i)) \qquad 3.2$$

$$\hat{V}(\bar{y}(i) = [1 - \frac{n(i)}{N(i)}][\frac{1}{n}(i)][\frac{1}{n}(i) - 1] * \sum_{j=1}^{n(i)} [y(i,j) - \bar{y}(i)]^{2}$$

and,

h= number of land use strata

$\hat{T}$ = estimated total of cover area for the study zone

$\hat{T}(i)$ =estimated total of cover area for the *i*th stratum

$N(i)$ = number of elementary area frame units in the *i*th stratum

$n(i)$ = number of segments sampled in the *i*th stratum

$D(i)$ = surface of the *i*th stratum

$\bar{y}(i)$ = average proportion of cover area per segment in *i*th stratum

$y(i, j)$ = proportion of cover area in the *j*th sample in the ith stratum as deduced from digitisation

$\hat{V}(\hat{T})$ = estimated variance of $\bar{y}(i)$

$\hat{V}(\hat{T}(i))$ = estimated variance of the total for the *i*th stratum

$\hat{V}(\bar{y}(i))$ = estimated variance of $\bar{y}(i)$

It is important to note that in the direct expansion method; only the information deduced from digitisation of the segments is used.

3.2.3 Regression Estimation

The regression estimator consists of the correction of the estimated average of a variable *Y* as a function of the results obtained from an auxiliary variable *X*. In this case, for a given cover for each segment in the sample, *Y* is the proportion occupied by the cover as deduced from digitizing the ground survey and *X* is the proportion of pixels of the satellite image classified as being of the given cover. A linear regression can be fitted in each stratum between these two variables. This linear model and the fact that the entire satellite image is classified are used for the regression estimation. The formulas as described by Cochran (1977) are as follows:

Total area *T* can be estimated as:

$$\hat{T}_{reg} = \sum_{i=1}^{h} D(i)\, \bar{y}_{reg}(i) \qquad 3.3$$

$$\bar{y}_{reg}(i) = \bar{y}(i) + \hat{b}(i)[m_x(i) - \bar{x}(i)]$$

where,

$D(i)$ = surface of the *i*th stratum

$\bar{y}(i)$ = average proportion of cover area per segment in *i*th stratum

$\hat{b}(i)$ = the estimated regression coefficient for the *i*th stratum when regressing proportion of ground reported cover area on proportion of classified pixels for the *n(i)* sample units in the *i*th stratum

$$\hat{b}(i) = \frac{\sum_{j=1}^{n(i)}[y(i,j) - \bar{y}(i)][x(i,j) - \bar{x}(i)]}{\sum_{j=1}^{n(i)}[x(i,j) - \bar{x}(i)]^2}$$

$m_x(i)$ = the proportion of pixels classified as a particular cover, in the *i*th stratum.

$\bar{x}(i)$ = the average proportion of pixels classified as a particular cover, per segment in the *i*th stratum

$x(i,j)$ = the proportion of pixels classified as a particular cover, in the *j*th sample unit in the *i*th stratum

The estimated variance for the regression estimator is:

$$\hat{V}(\hat{T}_{reg}) = \sum_{i=1}^{h} D(i)^2 \hat{V}(\bar{y}_{reg}(i)) \qquad 3.4$$

where,

$$\hat{V}(\bar{y}_{reg}(i)) = \hat{V}(\bar{y}(i))[1 - \hat{r}(i)^2]$$

and

$\hat{r}(i)^2$ = sample coefficient of determination between the variables *y(i,j)*and *x(i,j)* in the *i*th stratum

$$\hat{r}(i)^2 = \frac{\{\sum_{j=1}^{n(i)}[y(i,j)-\bar{y}(i)][x(i,j)-\bar{x}(i)]\}^2}{\{\sum_{j=1}^{n(i)}[y(i,j)-\bar{y}(i)]^2\}\{\sum_{j=1}^{n(i)}[x(i,j)-\bar{x}(i)]^2\}}$$

Note that:

$$\hat{V}(\hat{T}_{reg}) = \sum_{i=1}^{h} D(i)^2 \hat{V}(\bar{y}(i))[1-\hat{r}(i)^2]$$

$$= \sum_{i=1}^{h} \hat{V}(\hat{T}(i))[1-\hat{r}(i)^2]$$

and so,

$$Lim\,\hat{V}(\hat{T}_{reg}) \to 0 \qquad \text{as} \qquad \hat{r}(i)^2 \to 0$$

If the coefficient of determination is large for most strata, it will lower the estimated variance for the regression estimator.

In order to determine the success associated with the regression estimator, its Relative Efficiency (RE) is calculated as described by Allen and Hanuschak (1988) as:

$$RE = \frac{\hat{V}(\hat{T})}{\hat{V}(\hat{T}_{reg})} \qquad 3.5$$

A Relative Efficiency that equals 2.0 means that the same precision would have been obtained if the ground data sample size had been doubled and the satellite image had not been used.

3.3 Extraction and Analysis of Geomorphologic and Hydrologic Properties

3.3.1 DEM Generation

Topographic information was gained from maps obtained from the National Geospatial Services of South Africa. Two shapefiles, one corresponding to digitised contours and the other to the stream network for the study area were used to interpolate the DEMs. The nominal scale of the datasets was 1:50,000 and the vertical interval of the contour lines was 20 m. The dataset was projected to UTM and geographic coordinates. Since the interpolation methods available in the

Geostatistical Analyst extension of ArcMap uses points as input data, the contour lines were clipped to the study area and then converted to points. To define the study area, a preliminary DEM was generated using interpolation methods. The sub-catchments corresponding to the study area were derived and merged into a single polygon. To avoid spurious edge effects in the modeling of stream networks, a buffer of 300 m from the previous polygon was used to define the final study area.

The TOPOGRID model was adopted for the creation of hydrologically correct DEMs from selected elevation and stream coverage for the study area. Surface modeling was undertaken to translate discrete points into continuous surface that represented the geographic distribution of topographic features. Terrain analysis using Arc Hydro tools in ArcGIS (ESRI, 2011c) was performed to generate catchment delineations and extract hydrological properties including drainage pattern, stream order, stream segmentation, river profile, catchment boundary, flow direction and flow accumulation. The surface modeling or morphology from which drainage networks were automatically extracted was created using the Fast Fourier Transform (FFT) models as described by Frederiksen (1981). It is based on the concept that functions defining the surface of a DEM can be abstracted into sets of trigonometric series (Clarke, 1988). The FFT models that were used to create the morphology from which drainage networks were automatically extracted were of the form presented in equations 3.6 and 3.7, respectively.

$$\sigma_s^2 = 2\sum_{k=1}^{N/2}\{1 - H(v_k)\}^2 \mid F(v_k) \mid^2 \qquad 3.6$$

where,

$$|F(V_k)|^2 = |F(k)|^2 = RF(k)^2 + LF(k)^2$$

$$v_k = kv_1 = \frac{k}{L}; \text{ and } H(v_k) = 0 \text{ for } v_k > \frac{1}{2\Delta x}$$

Generalised as:

$$e(x,y) = f(x,y) - (f'x.y) \qquad 3.7$$

where,

$$f(x,y) = \sum_{k1=0}^{k1} \sum_{k2=0}^{k2} a_{k1k2} \sin(2\pi v_{k1} x + 2\pi u_{k2} y + \varphi_{k1k2})$$

where,

σ_s = variance of a sampled signal

F = the magnitude or the frequency space function of Fourier Transform/ drainage frequency

N = the number of equally spaced samples

H =the average altitude/elevation

k = imaginary unit ($k = \sqrt{-1}$)

R = Relief

L = watershed length/ length of the series

v_k = energy surfaces

$f(x, y)$ = a bivariate interpolation function fitted to the DEM to calculate the terrain derivatives

u, v are spatial frequencies variables, a = watershed area; φ = the phase, e = DEM error.

3.3.2 DEM Hydro-processing

The main objective for DEM hydro-processing was to obtain the automated extraction of morphologic and hydrologic properties. Since DEM quality and resolution affect the accuracy of derived hydrological features, a derived DEM with a 30x30m spatial resolution was used to estimate land-surface inputs. DEM hydro-processing procedures were used within ArcGIS environment where Arc Hydro tools were used to extract the physical properties such as drainage lines, slopes, and sub-catchments. The TOPOGRID interpolation process was used to modify the roughness penalty to allow the fitted DEM to follow abrupt changes in terrain, such as streams and ridges. A schematic representation of DEM analysis adopted for this study is shown in Figure 3.3.

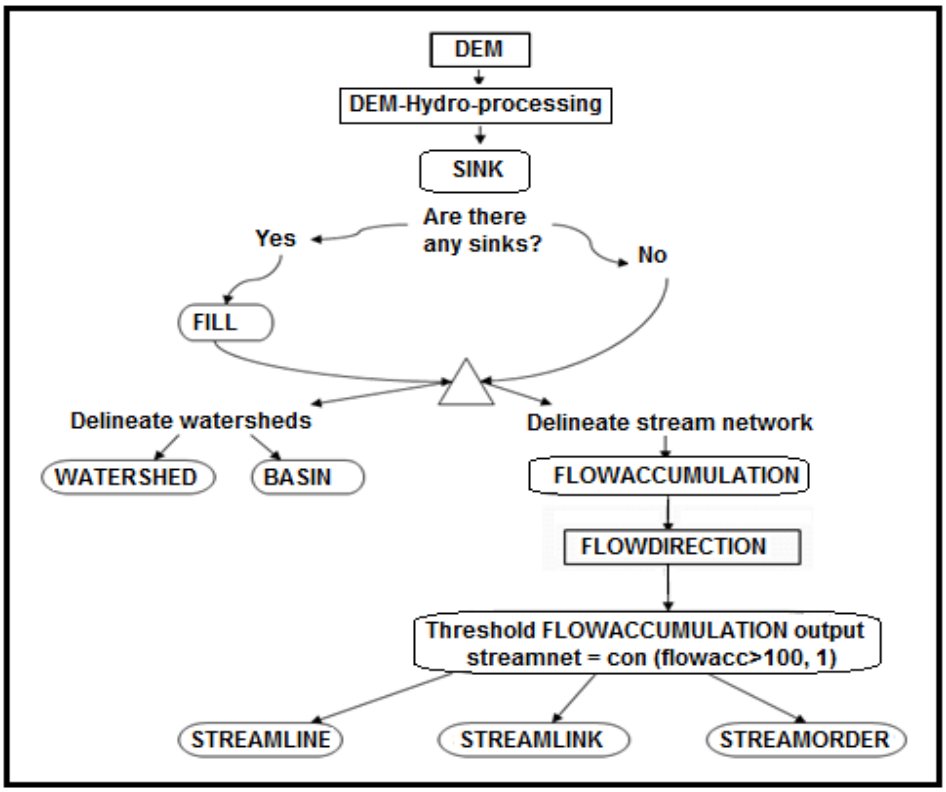

Figure 3.3: Schematic representation used in creating a hydrologically correct DEM analysis

Spatial analysis was carried out using ArcGIS Spatial Analyst extension to determine stream patterns, longest flow paths, average slopes, time of concentration and catchment orientation. The deterministic eight neighbour (D8) algorithm (O'Callaghan and Mark, 1984; Garbrecht and Martz, 1999b) was used to extract the morphologic and hydrologic properties and was able to rapidly extract stream networks in a straightforward and consistent manner. Most landscapes have many hill tops (local maximums) and few sinks (local minimum) resulting in connected drainage pattern. The sinks are seen as obstructions of flow paths by overestimated elevations, therefore, a DEM was smoothed prior to analysis to reduce the size and number of sinks using the fill sinks tool. Once the sinks in a DEM were filled, the resulting flat surface was used to define the surface drainage pattern. Removing sinks was done to ensure that flow direction will be found in every grid in the map. Flow direction and flow accumulation layers were then calculated using flow direction and flow accumulation tools. Flow accumulation model performed the cumulative count of the number of pixels that naturally drain into the outlets. The stream grid was then segmented into sections representing headwater tributaries or segments

between confluences, with each segment assigned a unique grid code identifier. The resulting link grid was used in the next step to generate a catchment grid based on the values held by each stream segment. The number of catchments was equal to the number of stream segments defined in the previous step. These catchment grids were converted to polygon vector features in the next step, with single cell catchments automatically dissolved within the process topology.

Additionally, the link grid from earlier processing was converted to a line feature class using the drainage line-processing tool in the next step. Each of these line segments is assigned an ID value corresponding to the catchment polygon in which it resides. Through watershed tools, stream layers were created using flow direction and pour point as input layers resulting in identification of flood inundation areas. Drainage points which are point features placed at the transfer points between adjacent catchments were also generated. Each point was assigned a unique identifier based on the catchment it drains. For general watershed analysis, the adjoint catchments contain the watershed elements of the selected catchments and adjacent downstream catchments in the watershed, thus delineating the watershed boundary based on the selected catchment. The measurable terrain and morphometric attributes shown in Table 3.1 were derived based on quadratic computations shown in equation 3.8.

$$h = Af^2g^2 + Bf^2g + Cfg^2 + Df^2 + Eg^2 + Ffg + Gf + Hg + I \qquad 3.8$$

where, f and g are spatial coordinates and h is elevation. The nine parameters, A, B, C, D, E, F, G, H and I were determined from the nine elevations on the 3 x 3 window using Lagrange polynomials as described by Zevenbergen and Thorne (1987).

Primary attributes that include aspect, slope, catchment area, flow-path length, as well as plan and profile curvatures, were calculated directly from the elevation data. Topographic attributes were calculated from the directional derivatives of the topographic surface in order to use them to describe the morphometry, catchment position, and surface attributes of hill slopes and stream channels comprising drainage basins. Secondary attributes that included Compound Topographic Index (CTI), Stream Power Index (SPI), and Slope Aspect Index (SAI) were computed to characterise the spatial variability of specific processes occurring in the landscape such as soil wetness river erosion.

Table 3.1: Derivation of primary and secondary attributes from DEM

Attribute	Category	Calculation method
Elevation (h)	TIN	DEM
Slope (β)	Primary	$\arctan\left[\sqrt{(G^2+H^2)}\right]$
Aspect (φ)	Primary	$180-\arctan\left[\frac{H}{G}\right]+90\frac{G}{\lvert G\rvert}$
Plan curvature (Φ)	Primary	$-2\frac{DG^2+EH^2-FGH}{G^2+H^2}$
Profile curvature (ŵ)	Primary	$2\frac{DH^2+EG^2-FGH}{G^2+H^2}$
Curvature (χ)	Primary	$2E+2D$
Contributing area (*Ai*)	Primary	$\frac{1}{b}\sum_{i=1}^{n}a_i$
Compound Topographic Index (CTI)	Secondary	$\ln\left[\frac{A_j}{\tan\beta}\right]$
Stream Power Index (SPI)	Secondary	$A_j\tan\beta$
Slope Aspect Index (SAI)	Secondary	$\varphi\tan\beta$

The CTI was used to describe the effects of topography on location and size of saturated areas. It provided an indication of relative moisture condition (wetness or dryness) associated with the accumulation of surface and near-surface runoff of rainfall. The SPI was used as the primary surrogate for critical area detection in the catchment. It is the product of flow accumulation and slope and it was used to measure the erosive power of flowing water, assuming discharge is proportional to a specific catchment area; as well as to identify places of accumulated overland flow within the delineated sub-catchments. The SAI was used to combine the measurements of slope and aspect into a unique scalar value, and was incorporated with the multispectral imagery to further refine the classification of forested lands, especially within areas of the state that exhibit dissected surface topography.

3.3.3 Hydrological Modeling with GIS

Hydrological modeling for this study utilised terrain processing tools of the Arc Hydro module within ArcGIS. Topological and morphometric characteristics of the catchment were derived from the global digital elevation model developed by the Shuttle Radar Topographic Mission

(SRTM). Surface water flow was modeled in GIS based on topography by defining flow direction from higher to lower elevation DEM grid cells. GIS was used to collect, digitise, organise, model and analyse data on watershed delineation and to create a geo-database to incorporate physical, environmental and socio-economic information on the watersheds. In the study area, higher resolution DEMs were generated from contours, which were digitised as polylines from topographic maps in one layer and tagged. Drainage was digitised, followed by other morphologic facets of the landscape. Since contours formed the source data for modeling, the TOPOGRID algorithm was selected to create DEMs upon which surface features were draped.

Areas of high elevations were first identified with “SINK” tool in Arc Hydro and eliminated with “FILL” tool to create a raster spatial layer or a "filled" DEM coverage for the study area. “FLOWDIRECTION” tool on the filled DEM was used to calculate the direction in which water would flow out of each cell. The “FLOWLENGTH” tool was used to determine the total flow distance from each cell to the outlet point of the catchment. The “FLOWACCUMULATION” tool was used to calculate the number of up-gradient cells that drain through each cell in the catchment. Lower accumulation values were ridge tops while higher accumulation values were valleys and stream channels. The “STREAMORDER” tool was used to calculate the order of each segment or link in the stream network. For purposes of adopting classifications and water quality standards, the streams and water bodies were identified according to river basin and specific water segments. After extraction was completed, the catchment was then delineated through the use of “STREAMLINK” and “WATERSHED” tools. All these analyses were entirely derived from 30x30m resolution DEM.

The river profile was determined from DEM data file consisting of distance from source versus elevation. River profile determination for the present study involved using DEM data and the rivers as input in ArcGIS where a route topology was first assigned to the set of arcs comprising a river starting at the river source. The total river length was then checked, and an appropriate profile interval was determined. The river longitudinal profile was then derived from the DEM and the x and y co-ordinates of the profile were used to generate a coverage of points at equal intervals along the length of the river. The elevation of the DEM at each profile point was

determined. The route topology was then used to derive the distance of each profile point from the river source and the output of data file consisting of distance from source versus elevation was produced. A graph showing distance along the length of the river, and the associated elevation at each distance was then drawn to interpret the longitudinal profile of a river.

3.4 Hydrometeorological Data

Hydrometeorological data for a period of 50 years were obtained from different agencies, including the South African Weather Services (SAWS), the Department of Water Affairs (DWA) and the Agricultural Research Council Institute (ARC-Institute). The data, which comprised of daily, monthly and annual averages, were subjected to quality check for missing data, consistency and stationarity. To evaluate the impact of land cover and land use change, the data was split into two sets to represent the pre-change (1960-1985) and post-change periods (1985-2010) based on the analysis of the hydrometeorological data and previous studies, including those of Singo (2008); Maramba (2011) and Dagada (2012). The post-change period represents the analysis of trends corresponding to major land cover changes that have taken place in the catchment while the pre-change period represented the scenario before the occurrence of major changes.

3.4.1 Rainfall

The mean annual rainfall was estimated by use of geostatistical techniques involving interpolation and regression within a GIS environment. After comparing the results from different methods, the inverse distance weighting (IDW) method was selected to perform the interpolation for mean annual rainfall. The rainfall data used was obtained from SAWS. Trends in rainfall data were examined between the two time periods, and the influence of changes in land use/cover on hydrologic response of the catchment were assessed.

Given that the bulk of the weather stations were located to the west of Vondo and Nandoni dams and the insignificant correlation of the intra-quaternary rainfall patterns, uncertainties were expected in the estimation of aerial rainfall. Due to the inadequacy of interpolation and regression techniques when the spatial distribution of stations is skewed, a “driver” station approach was selected for use, where Nooitgedacht and Rambuda weather stations (Fig. 3.4)

were selected to represent the upstream and downstream, respectively. From a hydrologic perspective, the upstream station is selected at the most upstream location of the catchment, while the downstream station should be located far enough downstream from the upstream so that the flow is uniformly distributed (WMO, 1994).

Effective rainfall data was used to study its variation in comparison with evapotranspiration in the study area. The FAO CROPWAT version 8.0 software was used to estimate effective rainfall for the catchment. Table 3.2 and Figure 3.4 show the physiognomies of the eight weather stations used:

Table 3.2: Weather stations

Station No	Name	Compound No	Latitude (°S)	Longitude (°E)	Elevation (m)
0723070 7	Elim Hosp	8228	-23°15'	30°05'	808
0766480 2	Entabeni Bos	8471	-23°00'	30°27'	1376
0723363 X	Klein Australie	8248	-23°05'	30°22'	702
0723334 X	Nooitgedacht	8245	-23°07'	30°20'	762
0766779 6	Palmaryville	8482	-22°98'	30°43'	570
0766827 4	Rambuda	8483	-22°78'	30°43'	762
0723513 X	Tshakhuma	8252	-23°05'	30°30'	1158
0723603 0	Tsianda	8256	-23°00'	30°35'	671

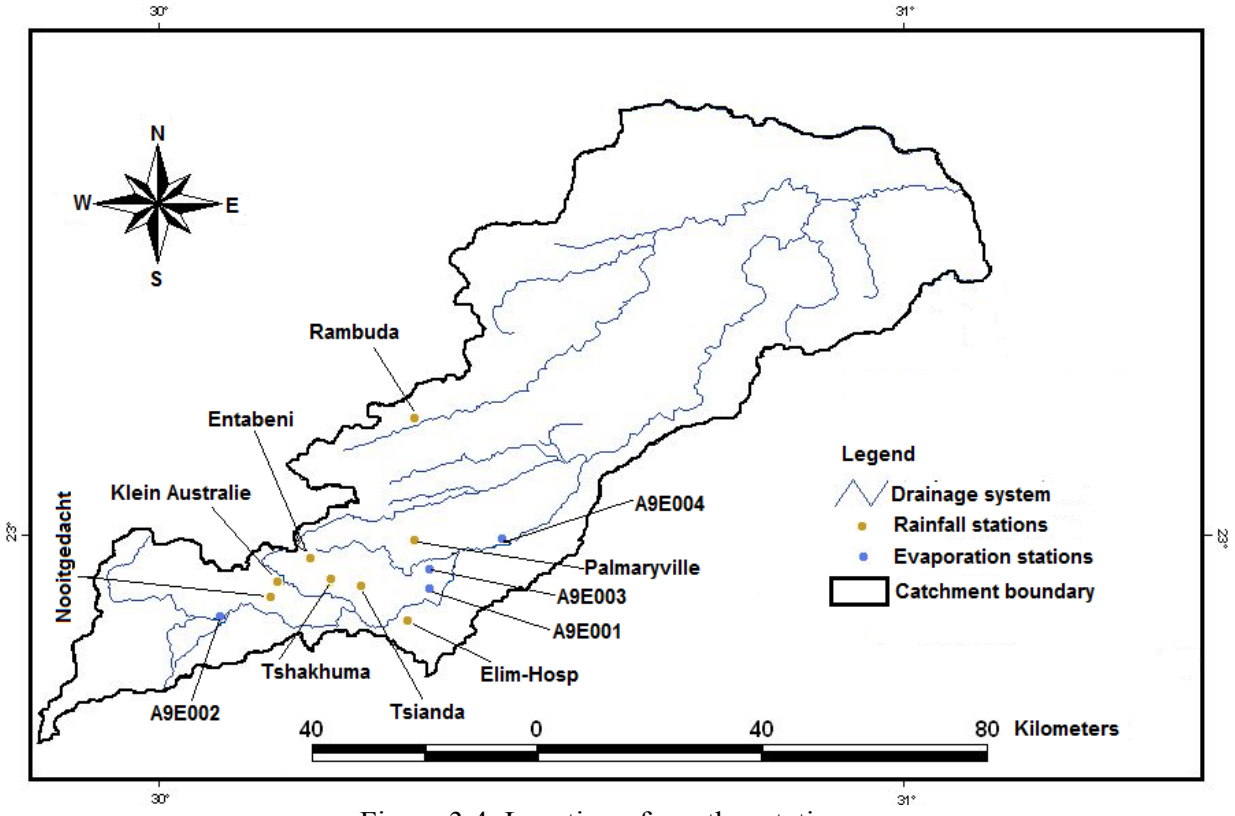

Figure 3.4: Location of weather stations

3.4.2 Evaporation

Evaporation measurements were obtained from four measuring stations as supplied by the DWA. Class A-Pan measurements are often discontinuous and sparse over much of South African regions, but station A9E002 in Luvuvhu River catchment had evaporation records for a period of 50 years. Table 3.3 below and Figure 3.4 above show the location and spatial distribution of the stations in the study area. Two Levubu settlement stations that consist of different station numbers were comprised.

Table 3.3: Evaporation stations

Station No	Name	Latitude (°S)	Longitude (°E)	Area (Km^2)	Drainage Region	Available Data Period
A9E001	Levubu Settlement	-23°10.1'	30°28.31'	N/A	A91C	1948-1952
A9E002	Goedehoop at Albasini Dam	-23°10.5'	30°12.37'	N/A	A91C	1952-2011
A9E003	Levubu Settlement	-23°08.4'	30°28.31'	30	A91D	1966-1980
A9E004	Nandoni Dam Evaporation	-22°97.2'	30°59.37'	30	A91F	2009-2012

3.4.3 Evapotranspiration

Evapotranspiration (*ET*) was determined as daily values that represented the removal of water from the soil by evaporation and plant transpiration. The reference evapotranspiration (ET_o) which represents the evaporative demand of the (*ET*) formed the basis of ET estimation in the study area. It was estimated using CROPWAT 8.0 model developed by the Food and Agriculture Organisation (FAO). The estimation of *ET* were used to predict its response to land use/cover change since the amount of water available for evaporation and plant transpiration is affected by changing land use/cover, such as urbanisation, which leads to imperviousness that enhances runoff. Climatic data that contain daily measurements of radiation (R_s; MJ/m-^{2}day^{-1}), sunshine hours (*N*; hours), minimum and maximum temperatures (*T*; °C), air humidity (*RH*; %), and wind speed (*u*; m/s) were obtained from the SAWS and ARC-Institute. The ET_o was then calculated using the full set of these climatic data as input into CROPWAT, in millimeters of water per day (mm/day). Other data included soil heat flux (*G*; MJ/m-^{2}day^{-1}), actual vapour pressure (e_a; kPa), saturated vapour pressure (e_s; kPa), and vapour pressure deficit (e_s - e_a; kPa). However, these data were not used as input in the ET_o climate table; rather they were used to derive parameters such as radiation, humidity and sunshine hours in stations with limited data.

Each of the evaporation stations used reported no cases of missing data. Of the six meteorological stations, Levubu and Lwamondo stations were the only stations having sunshine hour's records whereas the other four had radiation data. It can be seen from Table 3.4 and Figure 3.5 that the Levubu and Lwamondo data records started in the late 80's when measurements of bright sunshine hours used to be accomplished by use of sunshine recorders.

Table 3.4: Weather stations for ET_o analysis

Comp No	Station Name	Latitude (°S)	Longitude (°E)	Altitude (m)	Available Data Period	% of Missing Data
19937	Levubu	-23°08.33'	30°28.33'	610	1986-1996	Non-missing (0%)
19983	Lwamondo	-23°04.40'	30°37.36'	648	1986-2006	Non-missing (0%)
22411	Madzivhandila	-22°98.62'	30°55.48'	517	1999-2002	Non-missing (0%)
30753	Thohoyandou	-22°94.62'	30°48.80'	730	2007-2010	Non-missing (0%)
30720	University of Venda	-22°97.78'	30°44.01'	712	2006-2010	Non-missing (0%)
30759	Mhinga-Xikundu	-22°79.68'	30°84.22'	460	2007-2011	Non-missing (0%)

Nowadays, solar radiation is measured with pyranometers, radiometers or solarimeters and then converted to sunshine hours using astronomical equations. Thus, other station's radiation data was converted to sunshine hours using the formula expressed by Allen *et al*. (1998) and FAO (2003) as:

$$N = \frac{24}{\pi}\omega_s \qquad 3.9$$

where,

N = daylight hours

ω_s = sunset hour angle (radians)

$\omega_s = \arccos\left[-\tan(\theta)\tan(\delta)\right]$

θ = latitude (radians)

where,

$$\theta = \frac{\pi}{180} \text{ x } [decimal\ degrees]$$

δ = solar declination (radians)

$$\delta = 0.409\sin\left(\frac{2\pi}{365}J - 1.39\right)$$

The Penman-Monteith equation used to calculate ET_o by CROPWAT model assumes the ET_o as that from hypothetical crop with an assumed height of 0.12 m, having a surface resistance of 70 s/m and an albedo of 0.23, closely resembling the surface of green grass of uniform height, actively growing and adequately watered (Allen *et al*., 1998). The equation is given by:

$$ET_o = \frac{0.408\Delta(R_n - G) + \gamma\frac{900}{T+273}u_2(e_s - e_a)}{\Delta + \gamma(1 + 0.34u_2)} \qquad 3.10$$

where,

ET_o = is the reference evapotranspiration in mm/day

R_n = is the net radiation of the crop surface in MJ/m^2/day

G = is the soil heat flux density MJ/m^2/day

T = is the mean daily air temperature at 2 m height in ^{0}C,

u_2 = is the wind speed at 2 m height in m/s or km/day

e_s = is the saturation vapour pressure in kPa

e_a = is the actual vapour pressure in kPa

(e_s-e_a) =is the saturation vapour pressure deficit in kPa

Δ = is the slope vapor curve in kPa/^{0}C and

γ = is the psychtometric constant in kPa/^{0}C.

Figure 3.5 shows the spatial distribution and location of the meteorological stations where ET_o measurements were made.

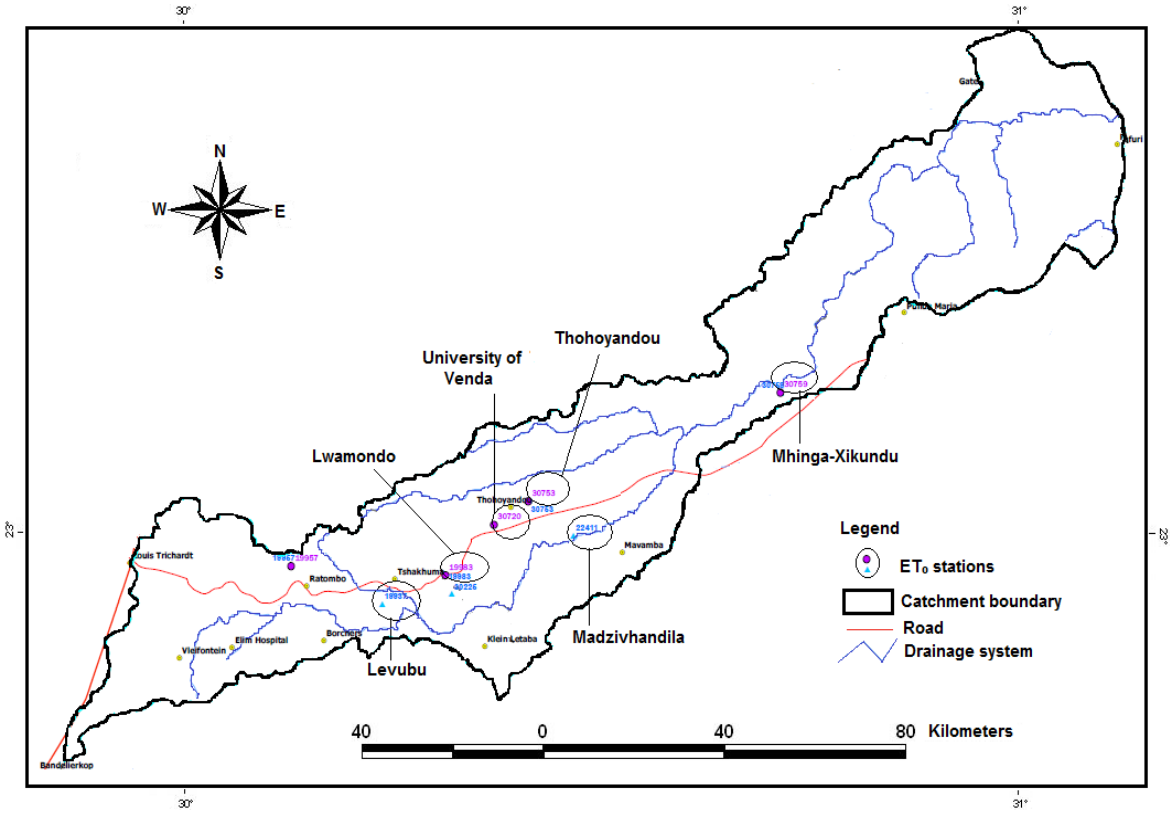

Figure 3.5: Locations of weather stations for ET_o analysis (Source: SANSA)

3.4.4 Runoff

Surface runoff data from seven gauging stations were used in this study as indicated in Table 3.5 and Figure 3.6. In this study, the surface runoff gauging stations used are the same as stream flow (section 3.4.5) gauging stations except that runoff was measured in cubic meters (m^3) whereas stream flow was measured in cubic meters per second (m^3/s). Runoff represented the

volume of precipitation that flows over the land surface and is not absorbed into the ground while stream flow represented the flow of water in a stream or river. Of the stations used, A9H001 was not included in runoff analysis as its historical records are no longer in existence. The data covering a period of 50 years (1960-2010) was provided by the DWA. The data was analysed to to examine significant hydrological trends and shifts in runoff time series and related them to land cover change. Accurate measurements of runoff from South African catchments are of utmost importance in order to quantify the country's water resources. As the gauging stations are usually restricted to lower flows in terms of their capacity, the determination of high flows are of importance as the gauging stations cannot cope with high flows. The hydrological model which was adopted for event based runoff simulations included the Soil Conservation Service-Curve Number (SCS-CN). The purpose of modeling runoff with curve number was to simulate the effect of rainfall on different soil types and detect if changes in rainfall will lead to changes in land use/cover, and impact on surface runoff. Daily rainfall data from selected rainfall events that occurred in the catchment during the study period were used to estimate daily runoff volume.

Curve number estimates for antecedent moisture conditions were obtained from standard curve number tables where estimates for agricultural land use were used and later adjusted into antecedent moisture condition (AMC) III, prevalent during floods. The calculated curve numbers were obtained using equation 2.16 and equation 3.11 as described by SCS (1986). Based on experiences from previous studies, the initial abstraction was assumed to be 20% of the maximum potential retention (S), which was related to the mean curve number parameter, by:

$$S = \left(\frac{25400}{CN_m} \right) - 254 \qquad 3.11$$

The CN_m is the SCS runoff curve number obtained by adding all the curve numbers for each land use. It is also known as the weighting factor. The initial abstraction (I_a), which refers to all losses before runoff begins, was obtained using the formula expressed below:

$$I_a = 0.2S \qquad 3.12$$

3.4.5 The Weighted Curve Numbers

To calculate the runoff for the subcatchments in their natural state under antecedent moisture condition III, the Weighted Curve Number method was used. This composite method was able to finds the area-weighted average curve number for each subcatchment and basin averaged curve number was used to calculate the runoff. The weighted curve numbers for were computed by summing all the area covered for each land use and their corresponding curve numbers selected from their corresponding soil group. For each subcatchment, the weighted curve number for LRC was computed by taking the sum of each CN value multiplied by its fraction of the total sub-catchment area. The area-weighted CN was calculated according to SCS (1986) as:

$$CN_w = CN_1 A_1 + CN_2 A_2 ..... + CN_j A_j \qquad 3.13$$

where,

CN_w = weighted curve number

$A_1\ A_2 .. + A_j$ = area of each land cover

$CN_1\ CN_2 .. + CN_j$ = curve number for each land cover

The composite custom CN was computed by taking the sum of each CN value multiplied by the area of each land cover and divided by the total area covered by all land use classes in the catchment as follows:

$$CN_c = \frac{CN_1 A_1 + CN_2 A_2 .... + CN_j A_j}{A_1 + A_2 ..... + A_j} \qquad 3.14$$

where,

CN_c = composite curve number

3.4.6 Stream Flow

Stream flow data from eight pluviometeric stations were used. The data spanning a period of 50 years (1960-2010) was provided by the DWA. The data was analysed to to examine significant hydrological trends and shifts in stream flow time series and relate them to land cover change over the years. The method of moving averages was used to filter and reduce the effects of random variations in the data. A 5-year smoothing interval was preferred because a 3-year

interval was not sufficient to clearly show the trend, and intervals longer than 5 years did not improve the results. The method is based on the premise that the systematic component of a time series exhibits autocorrelation while the random fluctuations are not autocorrelated. Therefore, the averaging of adjacent measurements eliminates the random fluctuations, with the result converging to a qualitative description of any systematic trend that is present in the data. In general, the moving-average computation uses a weighted average of adjacent observations to produce a new time series that consists of the systematic trend. For a given time series Y_i, the filtered series is derived as:

$$\hat{Y}_1 = \sum_{j=1}^{m} W_j Y_{i-k+j-1}, \qquad \text{for} = (k+1), (k+2), \ldots, (n-k) \qquad 3.15$$

where,

m = the number of observations used to compute the smoothing interval

w_j = the weight applied to value j of the series Y

A moving-average filter can be used to identify the presence of either a trend or a cycle. The smoothed series enables the form of the trend or the period of the cycle to be estimated. Trend analysis plays an important role in evaluating the effects of land cover and land use change and other time dependent parameters. Often through the use of trend analysis, future events can be estimated more rationally while past events can be better understood. However, moving-average filtering has several disadvantages. The approach for example loses two observations, which may be a very serious limitation for short record lengths.

A study by Jewitt and Garrat (2004) noted that LRC had insufficient data for stream flow and that measurements were done through the use of standard gauging stations. Table 3.5 and Figure 3.6 show the physiognomies of the gauging stations used.

Table 3.5: Gauging stations

Station No	Name	Measurment	Latitude (°S)	Longitude (°E)	Area (Km^2)	Data Period	% of Missing Data	
							Runoff	Stream flow
A9H001	Luvuvhu River	Weltevreden	-23°06'	30°23'	902	1960-2006	NA	1.3%
A9H003	Tshinane River	Chibase	-22°89'	30°52'	62	1960-2010	7.8%	6.2%
A9H006	Livhungwa River	Barotta	-23°03'	30°27'	16	1960-2010	7.2%	7.5%
A9H015	Canal From Livhungwa River	Barotta	-23°03'	30°27'	N/A	1960-2010	1.5%	2.2%
A9H016	Canal From Latonanda River	Levubu	-23°05'	30°24'	N/A	1960-2010	5.4%	4.3%
A9H017	Left Principal Canal From Dam	Goedehoop	-23°10'	30°12'	N/A	1960-2010	0.9%	1.0%
A9H020	Luvuvhu River	Goedehoop	-23°09'	30°13'	509	1960-2010	5.4%	5.1%
A9H023	Canal From Luvuvhu River	Nooitgedacht	-23°08'	30°17'	N/A	1960-2010	4.2%	2.9%

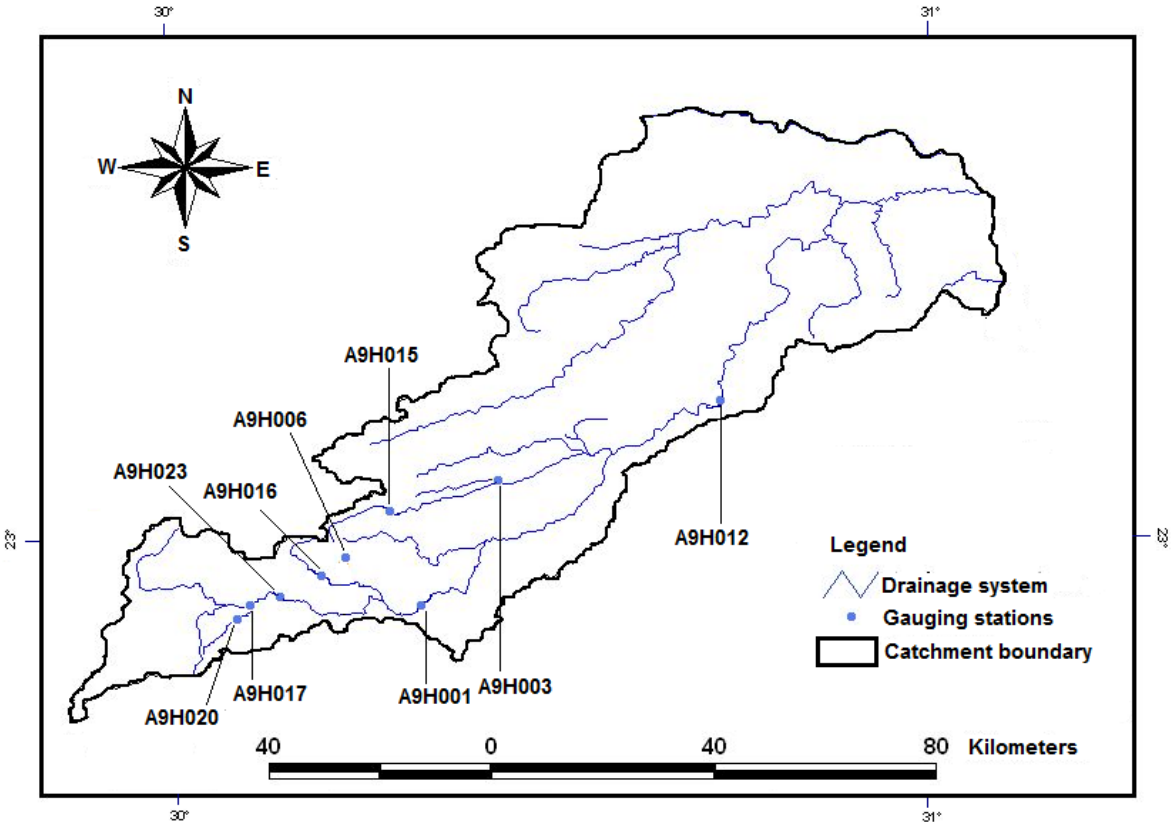

Figure 3.6: Location of gauging stations

3.5 Suspended Sediment

Suspended sediment measurements were done at selected points along streams within the catchment. The purpose of measuring suspended sediment in this study was to examine its response to changes in land use/cover and climate (i.e. rainfall) in the catchment and its effect on river regime and water quality in the catchment. Due to lack of historical records of suspended sediment discharge data, in-situ measurements were carried out in a number of streams in the

study area. Measurements were conducted during the rainy season of 2011/2012 (Oct-January) in two ways: (i) during or after heavy rainfall events; and (ii) during no rain days. This was because sediment-discharge measurements are usually available on a discrete or periodic basis. Visual observations were made during and after each rainfall event, in order to identify possible sources of sediments transport in streams. Eleven streams were selected for sampling during rainy days on the basis that they were located upstream of the catchment. During no rain days, a total of four streams were visited for sediment sampling. Sediment discharge by rivers is a major problem in arid and semi-arid regions, particularly in those regions underlain by friable soils and in mountainous regions where, for engineering applications, the amount of sediment loads should be known (WMO, 1994). The LRC, being an arid and semi-arid region itself is no exception for being prone to sediment discharging in rivers. Table 3.6 shows the locations where samples were collected while Figure 3.7 shows the spatial distribution of the sampling sites.

Table 3.6: Locations for suspended sediment sampling

Date of Sampling						
During Rainfall	**No rainfall**	**Sample Site**	**Latitude (°S)**	**Longitude (°E)**	**Drainage Region**	**Elevation (m)**
2011/10/05	2012/04/22	Madanzhe River at Ngovhela	-22°58'	30°27'	A91E	581
2011/11/01	2012/04/17	Mutshindudi River at Phiphidi	-22°56'	30°23'	A91G	775
2011/11/02	2012/04/21	Dzindi River at Dzwerani	-23°01'	30°24'	A91E	550
2011/11/14	2012/04/16	Tshinane River at Gondeni	-22°54'	30°26'	A91G	651
2011/11/15	…….	Mutshindudi at Dzingahe	-22°54'	30°31'	A91G	542
2011/11/22	…….	Mbwedi River at Khubvi	-22°48'	30°33'	A91G	582
2011/12/02	…….	Luvuvhu River at Tshino	-23°06'	30°24'	A91F	570
2011/12/08	…….	Nyahalwe River at Thengwe	-22°45'	30°32'	A92A	632
2012/01/13	…….	Mudaswali at Matangari	-22°48'	30°33'	A92A	591
2012/01/13	…….	Mutale River at Thengwe	-22°46'	30°32'	A92A	598
2012/01/24	…….	Luvuvhu River at Mhinga	-22°45'	31°28'	A91H	461

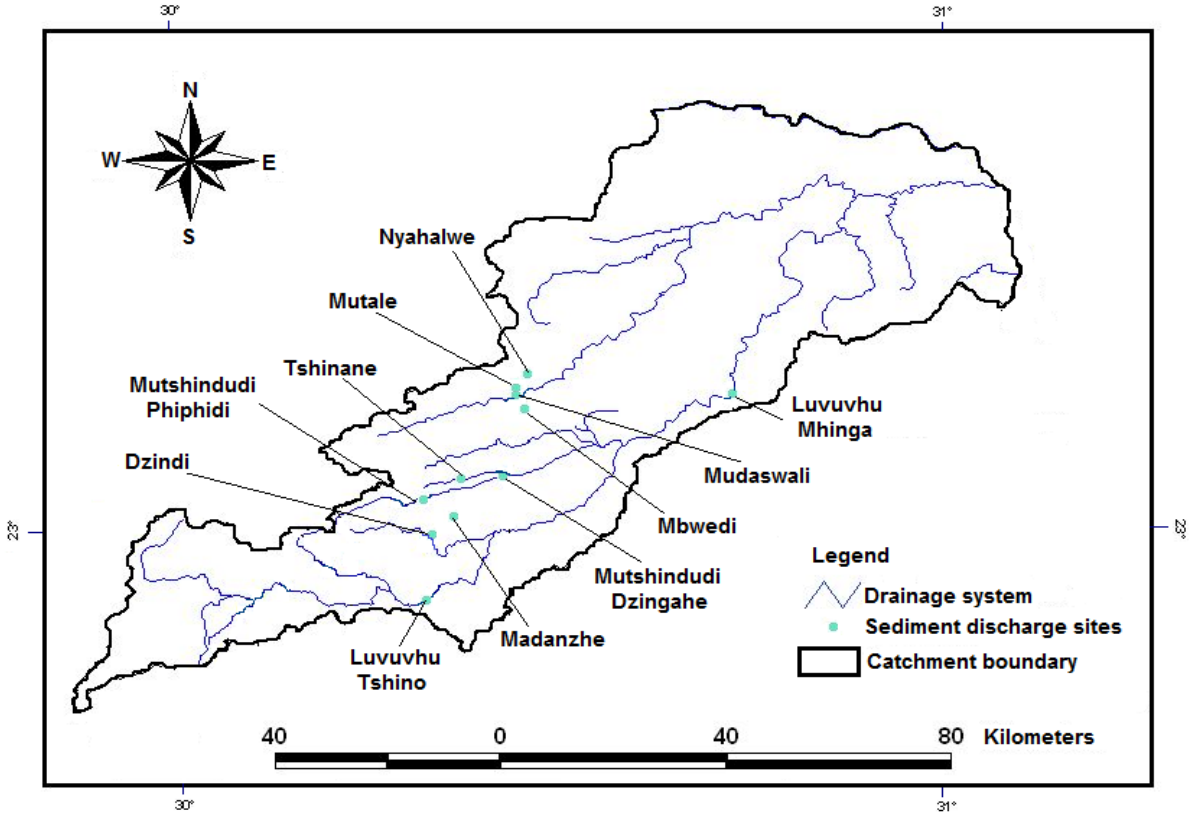

Figure 3.7: The spatial distribution of the suspended sediment sampling sites

3.5.1 SWAT Analysis

The SWAT model was adopted to simulate surface runoff from storm events in the LRC as well as to determine the effectiveness of the model in simulating runoff from storm rainfall. The model was applied to assess the impact of land use/cover change on surface runoff in the catchment. The basic datasets that were used in SWAT model are topography, climate, soil, slope and land use data. The hydro-processing of DEM during SWAT modeling was performed using Arc Hydro and ArcSWAT GIS interface similar to steps shown in section 3.3.3. The Arc Hydro and ArcSWAT first delineated and divided the catchment into a number of sub-catchments, which were further subdivided into HRUs. For delineation purpose, the SWAT model used input data including a Digital Elevation Model (DEM), a digital soils map, a land use /land cover map, as well as a number of tables and text files. Surface runoff was calculated in SWAT model as a function of rainfall, initial abstraction of rainfall, and soil retention parameter

and curve number, as described in Equations (2.16) and (3.11). The spatial datasets used include the 30m x 30m DEM data, 1:50,000 land cover map and 1:1 Million scale digital soil data.

The LRC was delineated from a DEM and the Levubu-Tshakhuma subcatchment formed the base of all spatial data and SWAT model set-up. The land use and soil data were then clipped in the basin using the facility provided within the SWAT ArcGIS platform. Climatological time series data such as daily rainfall, temperature, radiation, wind speed and relative humidity were also used in the SWAT model. The soil spatial data was related to the soil hydraulic properties which are important for determination of the amount of water available for runoff and the plants in the soils, and were taken from the United States Department of Agriculture (USDA) database. The flow chart of methodology for the rainfall-runoff modelling using the SWAT model is as shown in Figure 3.8. The main procedure and various steps followed in model application included SWAT Project set up, Watershed delineation, HRU Analysis, Write input tables, Edit SWAT inputs and SWAT simulation. The Edit SWAT Inputs menu allowed the editing of the database file in the model. The SWAT model was then applied to assess the impact of land management practices on the soil and water bodies in the catchment.

The SWAT model used the SCS-CN method to estimate the amount of runoff from daily rainfall based on local land use, hydrological soil group, and antecedent soil moisture, surface. The CN for each sub-catchment were selected based on the soil and land use type combination. Runoff simulation was carried out using two time periods for the years 1960-1985 and 1985-2010. The resulting runoff was then routed through the channel network of the watershed to the basin outlet. The SWAT method provides the Muskingum-Cunge (Cunge, 1969; Chow *et al*., 1988; Ponce, 1989; HEC, 2000) method, a flow routing method which has been incorporated into the SCS-CN model. The Muskingum-Cunge method was applied in SWAT to evaluate the effects of land cover changes on flood volumes and peak discharges in the catchment.

While the SCS-CN method is useful for engineering design purposes, the CN approach has been shown to be less than ideal when used to model runoff both spatially and temporally (Garen and Moore, 2005). The CN has problems in representing spatial variability of runoff and differentiating between runoff generating processes as it was developed by curve fitting rainfall-

runoff data only from the United States and is not necessarily accurate for all landscapes. In monsoonal climates, the original CN method can be replaced by a more mechanistic approach that uses soil water balances to calculate when the soil is saturated and consequently produces runoff (White *et al*., 2009). The use of the SCS-CN method in SWAT has provided a relatively easy way of adapting the model to a wide variety of hydrologic conditions; and has proved successful for many applications (Bansode and Patil, 2016).

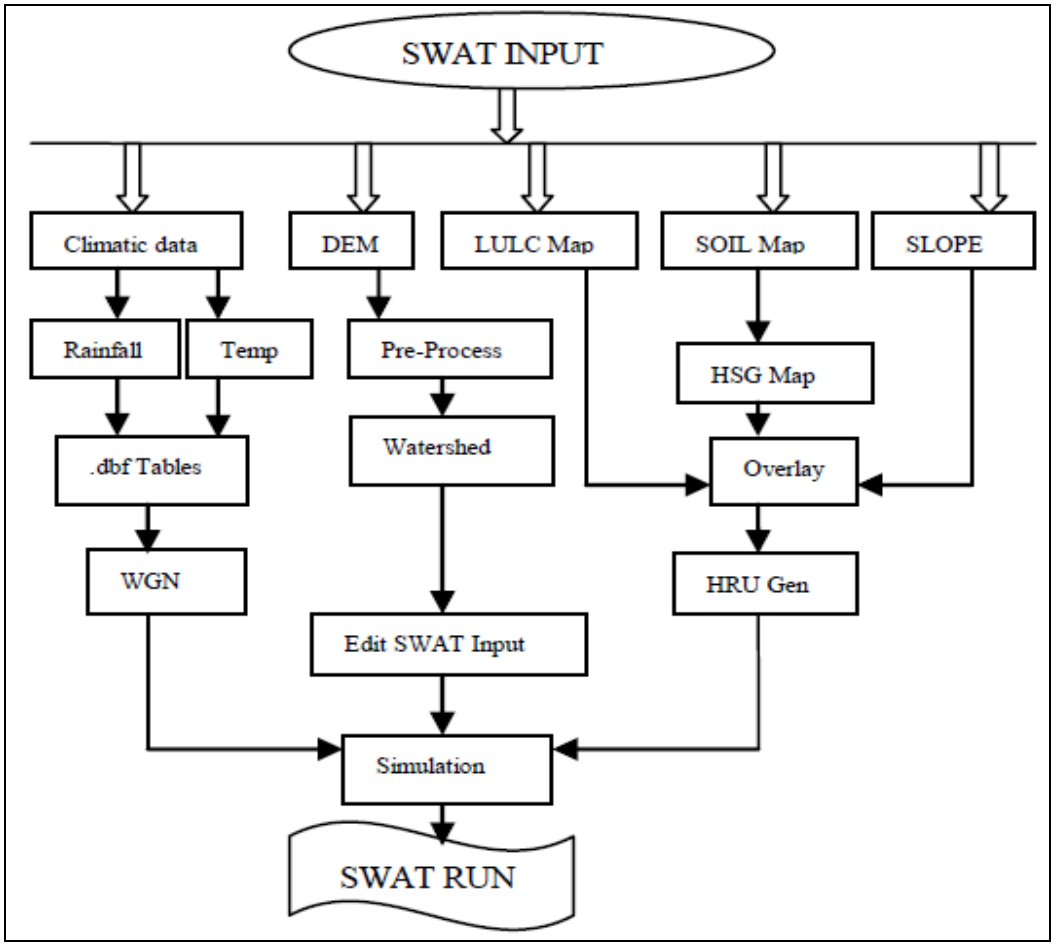

Figure 3.8: ArcSWAT methodology for rainfall-runoff modelling (Source: Shivhare *et al.*, 2014)

The computational components of SWAT can be grouped into different divisions including hydrology, weather, sedimentation, soil temperature, crop growth, nutrients, pesticides and agricultural management (Shivhare *et al*., 2014). SWAT uses a new water balance approach which replaces the CN method. The modified model known as SWAT-Water Balance or SWAT-

WB uses a new water balance approach which replaces the CN method, based on the following water balance equation:

$$SW_t = SW_0 + \sum_{t=1}^{t}\left(R_{day} - Q_{surf} - E_a - W_{seep} - Q_{gw}\right) \quad 3.16$$

where,

SW_t = the final soil water content

SW_0 = the initial soil water content

t = time in days

R_{day} = the amount of precipitation on day i

Q_{surf} = the amount of surface runoff on day i

E_a = the amount of evapotranspiration on day i

W_{seep} = the amount of percolation and bypass exiting the soil profile on day i

Q_{gw} = the amount of return flow on day i

To determine the amount of storage available for any given area of the watershed for every day of simulation, SWAT's soil moisture calculations were used. SWAT's soil moisture routine grossly simplifies processes that govern water movement through porous media (in particular, partly-saturated regions). For a daily model, the water balance has been shown to be proficient (Guswa *et al*., 2002). SWAT's soil moisture storage (mm) is given by:

$$\tau = D\left(\varepsilon - \theta\right) \quad 3.17$$

where, D is the effective depth of the soil profile (unit-less), ε is the total soil porosity (mm), and θ is the volumetric soil moisture for each day (mm).

3.5.2 The Grab Sample

The bottle sampling method was adopted for suspended sediments within the study area. Various 1.5 litres plastic bottles were used to collect samples of the runoff water in the streams as shown in Figure 3.9. For each stream, a total of three samples were collected at different points of the stream; at middle where possible and near the edges of the stream. Samples were taken at the water surface and 30 cm below the stream surface by hand. Samples were collected from

locations likely to have been impacted by significant land use such as anthropogenic activity and human settlements. The samples were then sent to the laboratory and oven-dried for 24 hours at 105 °C. In the laboratory, sample wet weight, sample dry weight, and water loss during drying were accurately estimated. The measured sediment data was then used to compute suspended sediment concentrations (quantity of sediment that can be carried by flowing water) and suspended sediment load (sediment particles carried by stream and stays in suspension). The sediment data for this study serves as baseline data to aid in understanding the effects of future land use/land cover on river water quality in the catchment. The weights of suspended sediments were estimated as shown below:

Sample Wet Weight (g) = Weight of empty bowl with Wet Sample –Weight of Empty bowl

Sample Dry Weight (g) = Weight of empty bowl with Dry Sample –Weight of Empty bowl

Suspended sediment loads in rivers were then computed by multiplying the volume of water discharge with the sediment concentration number. These refer to the soil particles that were transported through the stream channel by stream flow. Equation 3.18 gives a measure of the concentration of sediment and when combined with the rate of flow gives the rate of sediment discharge.

$$Sediment\ Concentration = \frac{SampleDryWeight}{SampleWetWeight} X100 \qquad 3.18$$

Figure 3.9: Suspended sediment sampling in Mhinga

The SAWS provided rainfall images corresponding to the dates on which the sediment samples were collected. The SAWS runs atmospheric component of the Unified Model (UM) over different domain sizes. The domain of the UM run on South African computers is between 0.48°N and 44°S, and 1°W and 56°E, with an East/West resolution of 0.11° and a North/South resolution of 0.1112°. This domain covers the whole of Southern African region including Madagascar and adjacent oceans. At the SAWS, the UM runs operationally at a horizontal resolution of 12 km and is scheduled to run twice daily to provide hourly numerical forecasts of atmospheric conditions for up to 48 h ahead. Data displayed are in grib format, and has been displayed using GrADS software. Using 12 km by 12 km grids, the rainfall images for the study area were then constructed through the UM from 3-hourly storms up to 15 hours on the day of the sampling.

3.6 Flood Frequency and Magnitude

The study used a 50-year record of rainfall and stream flow data to determine the recurrence of floods in the catchment. A flood frequency analysis was adopted to estimate the occurrence of

extreme events in the catchment. A comparison of different flood frequency models was made using EasyFit software version 5.5 from Mathwave Technologies (2011) in order to select the distribution(s) that could be used to model design floods in the study area. EasyFit supports the entire family of extreme value distributions, including the Gumbel, Fréchet, Weibull, and GEV models. It provides cumulative distribution probability which helps in simulation and also provides statistic distribution behaviour of each model. It uses Goodness of fit tests including Kolmogorov-Smirinov, Anderson-Darling, and Chi square tests as described in Jäntschi and Bolboacă (2009), to determine whether or not a certain distribution is fitted properly to the data.

The sequential steps used to estimate the floods of given recurrence intervals involved selecting the highest peak flood in a hydrological year. The peaks were then arranged in descending order of magnitudes and ranked. Within a single data series, some discharge values occurred more than once and were given the same rank. The frequency modeling for seven different flood levels, the 2, 5, 10, 25, 50, 100 and 200-year floods, was performed for flood prevention and protection in the catchment. Determination of the return periods and probabilities of exceedance for use in the selected probability distributions were computed using the Weibull's method as follows:

$$T_r = \frac{n+1}{m} \qquad 3.19$$

where,

T_r = the return period

m = order number of event

n = total number of events in the data series

The probabilities of events at which a flood is equaled or exceeded were computed as

$$P(x_m) = \frac{1}{T_r} \qquad 3.20$$

where, $P(x_m)$ = the probability of exceedance

3.6.1 The Log Pearson Type III (LP3) Distribution

The LP3 method consists of three parameters including mean, standard deviation and skewness, which were computed from the number of observations in annual maximum series (AMS) of

rainfall and stream flow data. The skew represents the degree of curvature to the flow-frequency curve and is an important hydrological characteristic, which gives a measure of shape of a sampling distribution. A skew of zero results in a straight-line flow frequency curve. A negative skew value produces a flow-frequency curve with lesser flows than the zero skew line, and a positive skew produces a flow-frequency curve with greater flows than the zero skew line (Marek, 2011). The LP3 distribution table of Haan (1977) was used to select the frequency factors based on the computed skewness coefficient of each data series. The frequency factor is a function of the specified probability (or return period) and of the skew of the logarithms of the sample. If the frequency factor was not corresponding to the skewness coefficient of the data, extrapolation of the values for events with return periods well beyond the observed flood events was made. The series means, standard deviations and skewness coefficients were computed using equations 3.21, 3.22, and 3.23 respectively:

$$X_{av} = \frac{\sum x}{n} \qquad 3.21$$

$$\sigma_x = \left[\frac{n}{n-1} \left(\frac{\sum x^2}{n} - X^2{}_{av} \right) \right]^{\frac{1}{2}} \qquad 3.22$$

$$G = \left[\frac{n^2 \left(\sum x^3 \right) - 3n \left(\sum x^2 \right) \left(\sum x \right) + 2 \left(\sum x \right)^3}{n(n-1)(n-2)\sigma_x{}^3} \right] \qquad 3.23$$

where,

X_{av} = mean of the series

$\sum x$ = sum of the series

n = number of the years in the data series

σ_x = standard deviation of the series

G = skewness coefficient

Maximum values per each year were first selected and transformed into logarithm scales of base 10 as follows:

$$X_T = \log 10 \qquad 3.24$$

where, Q_T = the discharge for a given year and X_T = the logarithm of discharge.

The estimated discharge values for a given period were evaluated using the logarithm of the design flood given by the following formula:

$$X_T = \log Q_T = X_{av} + K\sigma_x \qquad 3.25$$

where,

Q_T = the discharge for the estimated T-year return period

K = the probability factor based on n-years recurrence intervals

X_{av}, X_T and σ_x are as defined above.

The design flood itself was then given by:

$$X_T = anti\log Q_T \qquad 3.26$$

3.6.2 Gumbel's Extreme-Value Type I (EVI) Distribution

The Gumbel's distribution is a two parameters method consisting of the mean and the standard deviation. It ignores the logarithms of discharges and the coefficient of skew. The probability of occurrence of a Gumbel's extreme event, equal or larger than a value, is given by:

$$P(X \geq x_0) = 1 - e^{-e^{-y}} \qquad 3.27$$

where,

P = the probability of occurrence, X = the event of the hydrologic series, x_0 = the desired value of the event and y = the reduced variate: $y = \alpha(x - a)$

where,

x = the variate value, $a = \bar{x} - 0.45005\sigma_x$ and $\alpha = 1.2825/\sigma_x$, where σ_x = standard deviation of variate X and $\bar{x}$ = mean of the variate X.

The reduced variate is calculated as:

$$y = \frac{1.2825\left(x - \bar{x}\right)}{\sigma_x} + 0.577$$

where values 1.2825 and 0.577 are the constants for reduced mean and reduced variate, respectively. The estimated peak discharges in Gumbel's distribution at each return period are computed as from equation 3.28.

$$x_\tau = \bar{x} + K\sigma_x \qquad 3.28$$

$$K = \frac{y_T - \bar{y}_n}{\sigma_n} \text{ and } y_T = -In\left[In\left(\frac{T_r}{T_r - 1}\right)\right]$$

where,

K = the frequency factor, y_T = the value of peak discharge for a given recurrence interval,

y_n = Gumbel's reduced mean and σ_n = Gumbel's reduced standard deviation.

To estimate whether the frequency models used were best for LRC, a 99% confidence interval for LP3 and Gumbel's models were determined using SPSS software. A regression (r) method together with the co-efficient of determination (R^2) and the coefficient of variation (Cv) were used to detect the relationship between flood magnitudes and their recurrence. The developed equations could be used to estimate flood magnitudes at selected exceedance probabilities for sites along the streams. The C_v was used as a measure of consistency in the data and was determined algebraically as the standard deviation expressed as a percentage of the mean (the ratio of the standard deviation to the mean) as:

$$Cv = \left(\frac{\sigma}{\bar{x}}\right) \qquad 3.29$$

where,

Cv = coefficient of variation

σ = the standard deviation

$\bar{x}$ = the mean

3.6.3 Goodness of Fit Measures

The goodness of fit tests were used to analyse how well the data fitted the given distributions. The tests described the differences between the observed values and calculated values from the distribution and could be used to reject possible distributions. The skew coefficient of the station record is sensitive to extreme events and is a good indicator of changes in the catchment. It was difficult to obtain accurate skew estimates from small samples since it required the use of at least

40 stations. The mean skew coefficient was used as it provided the most accurate estimate. Where the station skew was greater than +0.4, tests for high outliers were considered first. Where the station skew was less than -0.4, then tests for low outliers were considered first. Where the station skew was between 2 and 0.4, tests for both high and low outliers were applied before eliminating any outliers from the data set. Based on the probability plots, the distribution with the highest frequency was selected to ensure that designs would be based on the highest safety standard for the probable maximum flood.

3.6.4 Dam Water Levels

The monthly dam water level data was obtained from DWA and used to compute reservoir storage yields. They included data from stations A9R001, A9R002 and A9R004. The data was used to analyse trends in dam water levels and assess the impact of land use/cover change on dam water levels in the catchment. Land cover changes caused by human activities such as construction and forest clearing may cause changes in dams and reservoirs water levels if they are constructed close to residential areas. These activities may impact on water resources due to the ever increasing water resource demands attributable to growing human populations. Built dams may also fail during heavy rainfall events causing an uncontrollable release of water, resulting in loss of human life, fauna and flora. Reservoir storage yield was used to determine the storage volume required to meet a particular demand (yield) pattern with a specified (small) probability of failure. A mass curve analysis (MCA) was used to estimate the reservoir yield in the study area. In MCA, the total flow in a stream at a point of a proposed reservoir was summed and plotted against time. The water demand was plotted, and the difference between the total water flowing in and the water demanded was the quantity that the reservoir must hold if the demand was to be met (Vesilind *et al*., 2009). Table 3.7 and Figure 3.10 show the locations of dams in the catchment and their spatial distribution.

Table 3.7: Dams in the study area

Station No	Station Name	Location	Latitude (°S)	Longitude (°E)	Area (km²)	Data Period
A9R001	Albasini Dam	Luvuvhu River at Goedehoop	-23°10.67'	30°12.48'	509	1960-2010
A9R002	Vondo Dam	Mutshindudi River at Vhutanda	-22°95.06'	30°35.17'	51	1985-2010
A9R004	Nandoni Dam	Luvuvhu River at Nandoni	-22°97.34	30°59.27'	1446	2006-2010

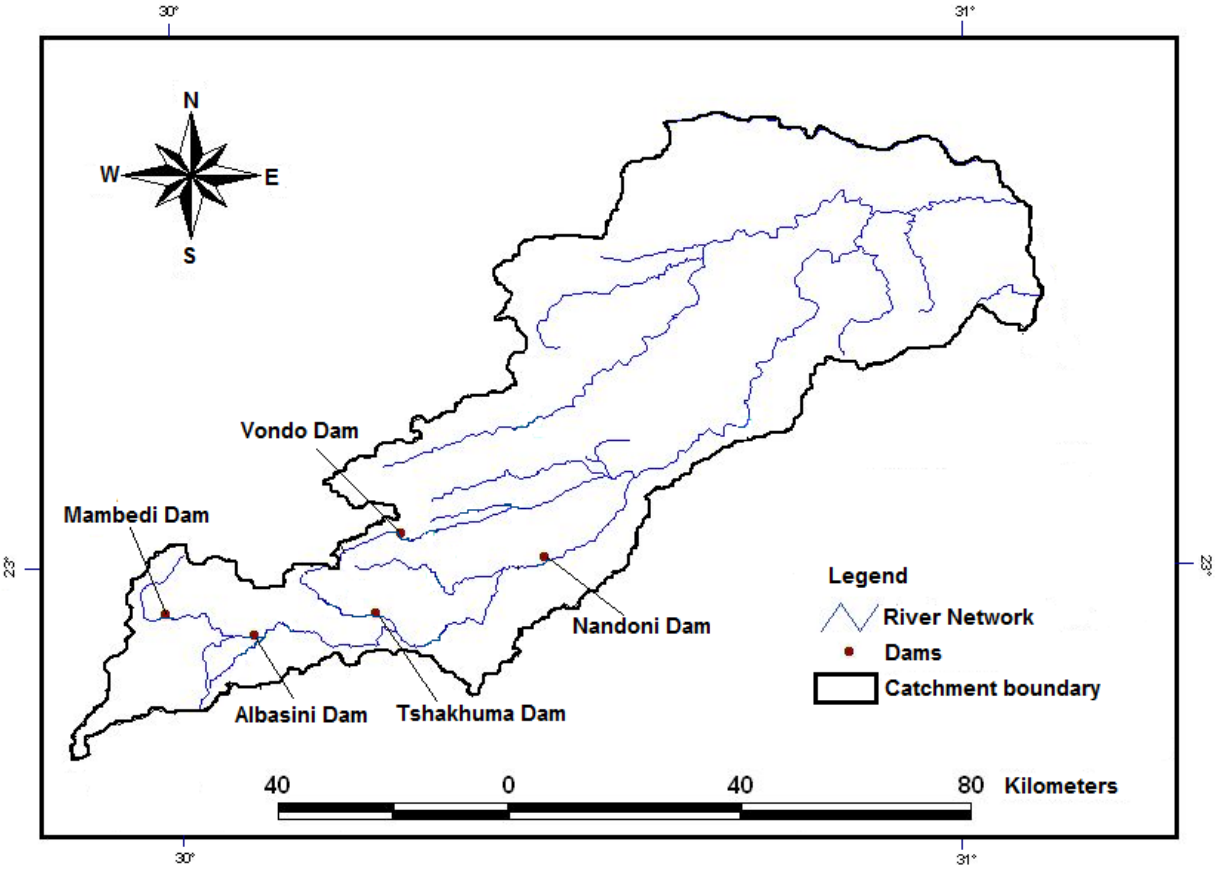

Figure 3.10: Location of major dams

3.7 Soil Data

The impacts of land use/cover change on hydrology and water resources depend on a host of natural factors including soil structure. In terms of soils, the impact of land use/cover change on surface runoff, peak flow, dry season flow, groundwater recharge, water quality, erosion and sediment load is a function the water regime of the plant cover in terms of evapotranspiration, the ability of the soil to hold water (infiltration capacity), and the ability of the plant cover to intercept moisture (FAO, 2002b).These impacts may affect many downstream uses, including providers of drinking water, industries, fisheries and other agricultural uses. In this study, soil data was used to assess the impact of land use/cover on the water resources as a result of changes in soil cover in the catchment. Digital soil data was used as input in hydrological modeling while in-situ measurements were used to assess the effect of different land use types on infiltration capacity and soil water content in the catchment. Digital soil data at a scale of 1:2 Million, were

acquired from the Global Environment Facility Soil Organic Carbon database for the SADC countries. This dataset was an upgraded version developed by national experts from the global Soil and Terrain (SOTER) database. Soil data were reclassified into the major hydrological soil groups (HSG) of the catchment with the help of FAO/UNESCO revised manual for soil maps of the world based on their drainage characteristics. The World Reference Base for Soil Resources (WRB) classification (FAO, 1998) was used as a unifying medium of communication.

The soil properties for the study area were assessed in relation to different physiographic conditions such as soil type, land use, topography, geology, climate and agricultural management practices. Soil samples for analysing soil texture, bulk density and soil moisture were collected in-situ around the infiltration test points. The sampling areas were selected based on specific attributes; such as cultivated land, grassland, woodland and built-up settlements. An extendable soil auger was used for obtaining the soil samples. The soils were extracted at 0-30 cm; 30-60 cm; 60-90 cm; and 90 cm-1 m depths. The soil physical properties such as colour and consistency were tested by the hand-feel method and recorded. An estimate of more than 40 soil samples was collected at various locations within the study area. The soil samples were collected when the soil was dry and sealed in plastic bags to prevent evaporation. The soil samples were then sent to the lab for analysing the initial soil moisture, soil texture, and bulk density. Soil texture and soil moisture are the most important factors influencing the rate of water that infiltrate into the soil thereby reducing the generation of runoff in the catchment. The coordinates of the sampling points were taken by Global Positioning System (GPS) and entered in GIS. Table 3.8 and Figure 3.11 show the locations of the test sites.

Table 3.8: Soil sampling sites

Site Name	Latitude (°S)	Longitude (°E)	Drainage Region	Height (m)	Land Use	Topography
Piesanghoek Slopping land	23°03'30.7"	30°04'27.7"	A91 A	832	Farmland	Undulating relief
Piesanghoek Valley Bottom	23°03'53.7"	30°04'10.1"	A91 A	836	Farmland	
Piesanghoek Hill Top	23°03'15.3"	30°04'26.7"	A91 A	856	Farmland	
Tsianda	23°02'92.0"	30°20'50.2"	A91E	710	built up settlements	Steep slope
Elim (Mpheni)	23°08'57.6"	30°03'19.1"	A91B	880	built up settlements	Flat terrain
Levubu (Lakomkom Farm)	23°05'27.0"	30°18'08.6"	A91C	646	Farmland	Steep terrain
Univen Agric (Disturbed)	22°58'44.6"	30°26' 20.3"	A91E	594	Arable land	Flat slope
Univen Residence (Undisturbed)	22°58'24.0"	30°27'2.0"	A91E	595	Residential area	Sloppy terrain
Thengwe (Mutale)	22°44'28.4	30°31'51.4"	A92A	626	built up settlements	Flat to sloppy land
Mhinga	22°46'45"	30°52'46.0"	A91H	460	Arable land, built up	Flat terrain
Punda Maria Gate	22°44'41.3"	30°58'41.3"	A91J	559	built up, woodland	Flat slope
Mukula	22°51'19.5"	30°33'63.0"	A91G	580	built up settlements	Flat slope
Levubu Settlement	23°04'28.4"	30°18'08.2"	A91D	628	Arable land, built up	Sloppy land
Sterkstroom Slopping Land	23°04'3.5"	30°04'35.7"	A91A	844	Farmland	Slopping to low land relief
Sterkstroom Low Lands	23°04'6.1"	30°04'38.2"	A91A	827	Farmland	

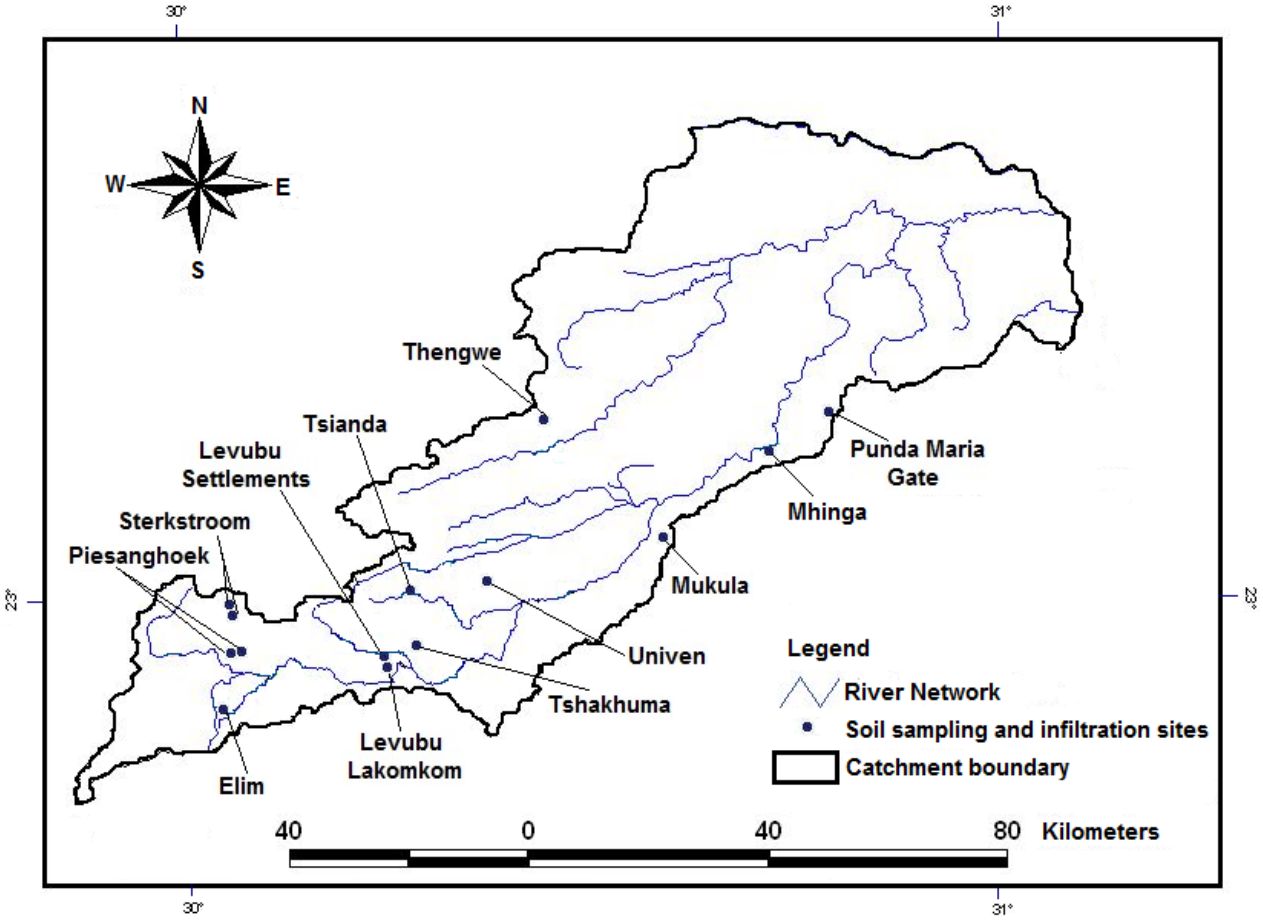

Figure 3.11: Spatial distribution of sampling sites

A set of sieves of sizes, 4mm, 2mm, 1mm, 500µm (0.5mm), 250µm (0.25mm), 125µm (0.125mm), 75µm (0.075mm), and 32µm (0.032mm) was used for particle sizes analysis. Accumulated weight of the samples and the weight for each sieve were recorded before samples were placed on a mechanical sieve shaker machine. The total accumulated weight of aggregates retained from each sieve was then recorded. The percentage retained on each sieve was computed as:

$$\%\,\mathrm{Re}\,tained = \frac{W_{Sieve}}{W_{Total}} \times 100\% \qquad 3.30$$

where,

W_{Sieve} = Sample weight per sieve (g)

W_{Total} = weight of soil sample (g)

Soil grading curves for each material retained during sieving were then plotted from the percentage finer of sand, silt and clay obtained from each soil sample. A D-Plot version 3.1 software for scientists and engineers, was then used to classify the soils according to the USDA soil textural classes. A gravimetric method was adopted to determine the water content in soil. The method involved taking a physical sample of the soil, weighing it before any water is lost, and drying it in an oven before weighing it again as follows:

$$MC = \frac{W_w - W_d}{W_d} X100 \qquad 3.31$$

where,

MC = Moisture content of the soil (%)

W_w = Wet weight of the soil (g)

W_d = Dry weight of the soil (g)

3.7.1 Infiltration Tests

The double ring infiltrometer method was used to conduct infiltration tests. The tests were carried out on various contrasting sites in order to estimate infiltration rates of different physiographic conditions such as soil type, land use, topography, geology, and agricultural

management practices. The tests were conducted for two hours in varying time steps till the values became constant. The experiments in Piesanghoek, Thohoyandou and Tsianda were done during the months of May 2011 to August 2011. More experiments in Thohoyandou and Mhinga were conducted during the spring period (from August to mid-October) while experiments in Mukula, Thengwe, Levubu, Punda Maria, Elim and Sterkstroom were conducted during November-December 2011 and January 2012. A total of seventeen tests were conducted and used to compare infiltration rates of different soil types. Three tests were conducted at each site on varying topography representing sloping land, valley bottoms and hill tops where applicable. However, some of the test sites were difficult to run the tests on due to rock restrictions. It is important to conduct as many field tests as possible in any catchment so that the data is representative. The problem is that infiltration rates vary widely over relatively short distances. It is therefore necessary to carry out many measurements throughout the catchment. In this study, infiltration data was used to assess the impact land use/cover of different soil types and their effects to soil water infiltration and soil water contents. Cultivation of the land and clear cutting of forests may change infiltration and runoff characteristics, which may affect groundwater recharge, sediment and water yield, and evapotranspiration (FAO, 2002a). Figure 3.12 shows infiltration measurements being conducted at the sites.

Figure 3.12: Infiltration measurements

3.7.2 Infiltration Rates

The Horton's equation was used to predict infiltration rates and cumulative infiltration based on the values of the field experimentation method. The *k*-value was determined empirically using a procedure described by Reddy (2011). This procedure involves taking logarithms of the natural base on both sides of the Horton's equation as shown below:

$$In\left(f_t - f_c\right) = In\left(f_0 - f_c\right)^{-kt} \qquad 3.32$$

where,

$$y = In\left(f_t - f_c\right) \text{ and } c = In\left(f_0 - f_c\right)$$

f_t = the infiltration rate

f_0 = the initial infiltration rate

f_c = constant or equilibrium infiltration rate

k = decay constant

The k-value was thus determined from the regression line equation as follows:

$$k = r.\frac{s_y}{s_t} \qquad 3.33$$

where,

r = regression coefficient fitted in the data in the form:

$$r = \frac{1}{n}\frac{\sum\left(y_i - \bar{y}\right)\left(t_i - \bar{t}\right)}{s_t.s_y}$$

where,

$$s_t = \sqrt{\frac{\left(t_i - \bar{t}\right)^2}{n}} \text{ and } s_y = \sqrt{\frac{\left(y_i - \bar{y}\right)^2}{n}}$$

y_i= logarithm of the left hand side of equation 3.33

$\bar{y}$ = mean of the logarithms for y_i

t_i = time recorded during infiltration measurements

$\bar{t}$ = mean of t_i

n = number of samples

s_t and s_y are the standard errors estimates for both y and t

The data collected from the field was also used to determine the time of ponding which is regarded as the elapsed time between the time rainfall begins and the time water begins to pond on the soil surface. The Horton method using equation 3.34 was used:

$$t_p = \frac{-1}{k} In\left(\frac{1 - f_c}{f_0 - f_c}\right) \qquad 3.34$$

where,

t_p is the time of ponding

CHAPTER 4

RESULTS AND DISCUSSION

4. Land Cover Change

There was significant land cover and land use change from forestland, woodland and open grassland to medium size farms, subsistence agriculture and built-up land. It was observed that hills around Tshakuma, Tsianda, and Lwamondo which were covered by natural forest in the pre-change period (1980's) were largely covered by small portions of trees and bushes at higher levels, interspersed agriculture at the middle and built up, mixed with agroforestry on hill-sides as shown in Figure 4.1. The notable farms within the catchment were Levubu, Tsianda, Piesanghoek, and Sterkstroom while the expanded built up area was around the greater Thohoyandou, Mhinga, and Elim. Figure 4.2 showed the land cover classes based on Landsat images for the 80's, 90's and 2000's while Table 4.1 showed the major land cover classes.

Figure 4.1: Built up and agroforestry on hill-sides at Tshakhuma (May, 2012)

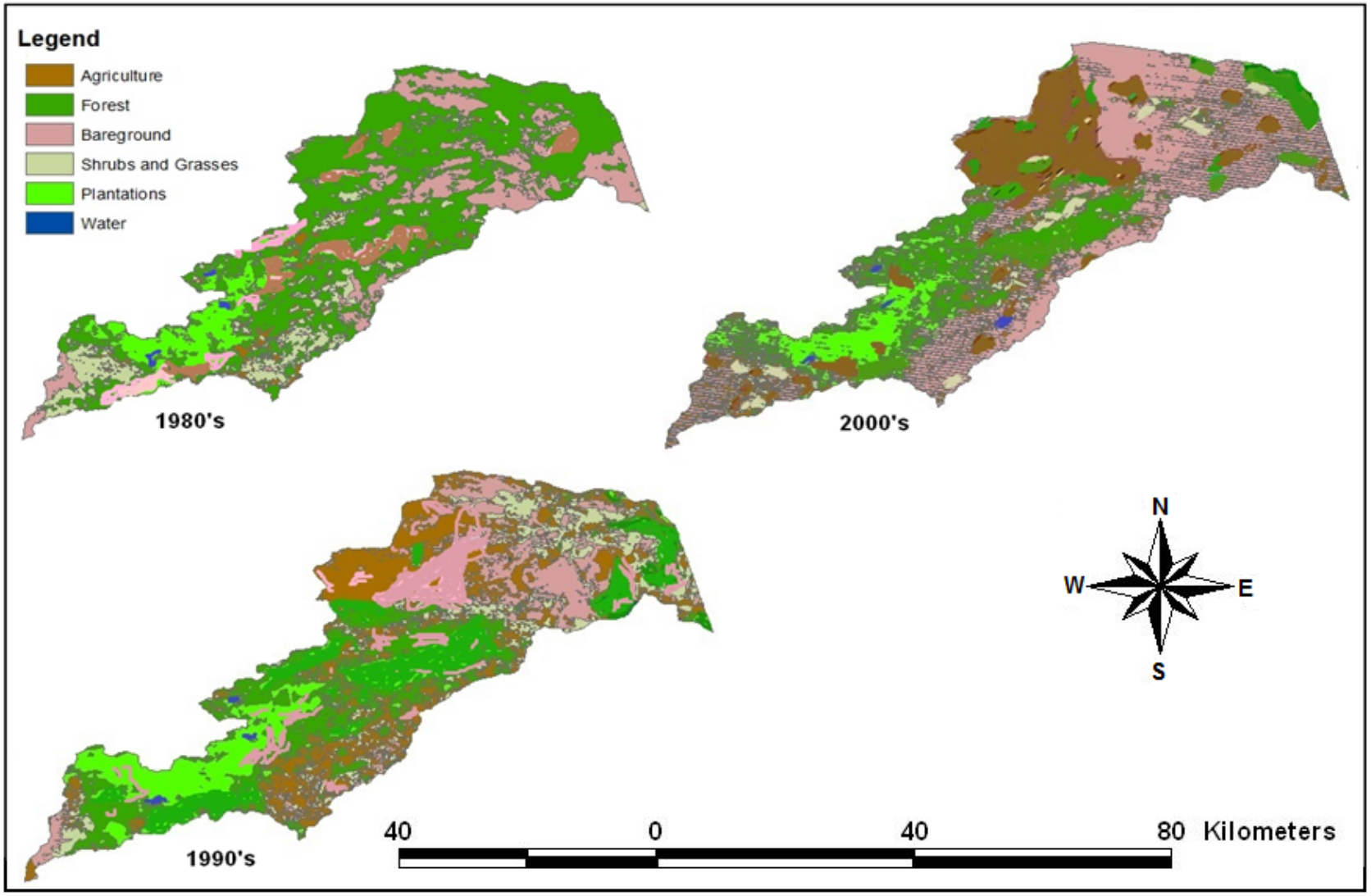

Figure 4.2: Land cover change in the Luvuvhu River Catchment

Table 4.1: Major land use classes

Class Name	**Description**
Agriculture	This included cumulative land under different crops
Natural Forest	Included the natural vegetation and shrubs
Bare Ground	This represented virgin land, unoccupied land, settlements and other buildings, including all residential areas in rural and peri-urban
Water Bodies	This class included all the dams and other bodies containing clear open water
Plantation	These were mainly planted commercial trees.
Shrub and Grass	Represented all the areas covered by tall grass and bushes of all types

The pre-change geo-topes of planted forests and farms showed clear corridors, sizes, shapes and connectivity. A limiting factor in the use of imagery was that due to decrease of spatial resolution on the images as a result of geometric characteristics of the images, the dominant land use cover types of forest and mixed farming exhibited a rapid increase and overestimation at the coarse levels of spatial aggregation at the expense of non-dominant land use cover types like rural built-up lands. The dominant land use cover types were overestimated due to spatial mixing of covers hence the high variances.

The coverage classified as Agriculture in the KNP was established, during ground truthing and field completion to be shrubland with scattered trees. The KNP is an area surrounded by impoverished rural communities, with high concentration of game farms with some parts of the region used for cattle and commercial farming. It was classified as Agriculture by the digital image classification and pattern recognition method, based on the maximum-likelihood classifier. The classifier works on the principle that the physical basis of remote sensing relies on the synoptic characteristic of reflected energy from target to sensor. Variations in photon energies are tied to the wavelength or frequency. When any target material is excited by interaction with incoming radiation, it emits photons of wavelengths whose radiometric quantities may be similar at different wavelengths. In this case, the target material in KNP emitted photons of wavelengths whose radiometric quantities were similar to land use target materials in the human populated area of the catchment.

4.1 Estimation of Land Cover and Land Use Change

The estimation of land cover and land use was done at level I and level II where categories which were spatially and temporally similar were grouped under one class. The diversity of the land use in the catchment was related to the diversity of agroclimatic zones, landform, water resources, topography, and human activities. The dominant land use categories concentrated specifically on the agricultural application, which was considered the most important human economic activity in the area. Table 4.2 shows the major land cover classes identified, based on modified Anderson (1977).

Table 4.2: The major land cover classes

Level I		**Level II**	
Code	Class Name	Code	Class Name
1.	Agriculture	11	Maize
		12	Bananas
		13	Subsistence agriculture
		14	Agroforestry
		15	Macadamia
		16	Avocados, Guavas, Mangoes, Litches
2.	Urban/Built-up Area	21	High density residential (above 90% imperviousness)
		22	Middle density residential (65-90% imperviousness)
		23	Low density residential (55-65% imperviousness)
		24	Industrial areas
		25	Rural villages (< 55% imperviousness)
3.	Water	31	River
		32	Pond, pool
		33	Lake
		34	Wetlands
4.	Coniferous forest	41	Dense Stand (above 80% tree coverage)
		42	Middle Stand (60-80% tree coverage)
		43	Loose Stand (40-40% tree coverage)
5.	Eucalyptus forest	51	Dense Stand (above 80% tree coverage)
		52	Middle Stand (60-80% tree coverage)
		53	Loose Stand (40-40% tree coverage)
6.	Mixed forest	61	Dense Stand (above 80% tree coverage)
		62	Middle Stand (60-80% tree coverage)
		63	Loose Stand (40-40% tree coverage
		64	Brushwood (20-40% tree coverage)
7.	Grassland and Bushland	71	Improved Pasture
		72	Meadow
		73	Open grassland with Individual trees
		74	Dense bush and thickets
8.	Park and Garden	81	Park and Garden

In a preliminary field check, a few classes corresponded to structural vegetation groups such as grassland or forest. The remaining classes appeared to be complex mixtures of vegetation and

built-up areas. The same spectral class represented different cover combinations at different locations. Although using more classes may have separated these heterogeneous groups into consistent subclasses, extensive field checking would have been required to verify that each spectral class represented the same vegetation in each polygon.

4.1.1 Area Estimation by Direct Expansion

The results obtained by direct expansion and regression estimation are as shown in Table 4.3. At the level of individual classes, the best results were obtained for bananas with a coefficient of variation of 10.22% and a regression coefficient of 5.07%. This could be due to the structure of the banana plant where the broad leaves provided a smooth texture and tone hue that gave a distinct feature class under supervised classification. The other crops and tree plantations had smaller leaves which provided mottled structure and poor tone hue that led to mixed and sometimes unidentifiable classes on imagery. The eucalyptus plantations had the lowest reliability with a coefficient of variation of 70.65. This could be due to the mixed reflectance from fire corridors and the contiguous woodlots and tree crops such as avocados, guavas and macadamia.

Table 4.3: Land cover and land use statistics for 2010

Land cover and land use within segments		**Total surface area (ha)**	**Variance**	**σ**	**CV**	**RE**
Maize	direct expansion	1,352	2,815,101	1245	60.12	
	regression estimation	1,009	833,650	650	29.90	4.95
Macadamia	direct expansion	3,799	4,896,099	1989	58.85	
	regression estimation	3,298	899,795	918	30.52	5.08
Bananas	direct expansion	25,664	9, 984,885	3170	10.22	
	regression estimation	28,727	2,369,960	1447	5.07	3.98
Agroforestry	direct expansion	3,144	581,419	893	30.53	
	regression estimation	2,945	286,655	623	25.22	1.95
Eucalyptus	direct expansion	2,005	1,887, 722	155	70.65	
	regression estimation	2, 442	52, 354	219	8.06	21.88
Built up area	direct expansion	12,558	15,554,215	3979	38.76	
	regression estimation	8,009	1,340,942	1255	18.32	15.11
Grass/bushland	direct expansion	30,550	16,868,711	3766	13.08	
	regression estimation	35,537	14,174,091	1473	11.74	2.90
	TOTAL	61,072				

Based on secondary data, the results in Table 4.4 showed that during the 80's, land cover patterns constituted 15.81% agriculture, 29.34% natural forest, 32.15% bare ground, 0.06% water bodies, 8.28% plantations and 14.36% shrubs and grasses. During this period, natural forests and bare ground dominated the study area covering almost 60%. During the 90's, a decrease in forest cover was noted with a major increase in bare ground revealing change in land use in the area. Forest cover declined from 29.34% to 16.8%. Notable was agriculture and bare ground which rose from 15.81% to 21.73% and from 32.15% to 37.16%, respectively. The area covered by plantations also increased by about 1.7% from 8.28% to 9.93%. Insignificant change was noted in water bodies, shrubland and grassland.

Table 4.4: Area covered by land cover classes

Land Cover Class	**Area Covered (%)**		
	1980	**1990**	**2000**
Bareland	32.15	37.16	20.68
Natural Forest	29.34	16.8	20.67
Water Bodies	0.06	0.06	0.08
Grass and Shrubs	14.36	14.32	10.07
Agriculture	15.81	21.73	38.57
Plantation	8.28	9.93	9.93
Total	100	100	100

A formal accuracy assessment for all land cover types was conducted using field surveys to verify how accurate the maps are in order to use the data more correctly and efficiently. Although aerial imagery were used to develop reference data for comparison to land cover datasets, field verification was by conducting site visits to compare actual land cover with land cover classifications dataset. To compare field verification data to the classified land cover data, the user's accuracy, producer's accuracy, and overall accuracy were determined to relate to each of the land cover categories. The accuracy was also evaluated using the *Kappa* index of agreement, which is a measure for quantifying the level of agreement between two maps with equal number of classes. These accuracy measures are described in an error matrix, where the land cover assessed in the field corresponds to the dataset classifications. The error matrices developed to assess the accuracies of the classifications indicated values between 78-86% for the overall accuracy and 67-80% for *Kappa* index as shown in Table 4.5. These values were used as

the measure of actual agreement and the expected output in the sense that values within these ranges normally indicate good representations of the actual land use and land cover.

Table 4.5: The Error matrix for image classification

Land cover	Landsat MSS (1980)		Landsat TM (1990)		Landsat ETM+ (2010)	
	Producer's (%)	User's (%)	Producer's (%)	User's (%)	Producer's (%)	User's (%)
Forest	96	77	97	79	98	90
Buildup land	88	78	98	79	100	89
Shrub land	55	87	86	65	87	82
Agriculture	81	92	85	94	89	97
Grassland	50	86	75	86	86	88
Bananas	85	70	94	89	98	82
Water	100	100	100	100	100	100
Overall accuracy (%)	78		81		86	
Kappa index (%)	67		67		80	

Throughout the 2000's, land use change revealed a decrease in natural forest from 29.34% to 20.67% and resulting in increased agriculture which rose to 38.57% as shown in Table 4.4 above. An increase in water bodies from 0.06% to 0.08% was observed. This may be due to the construction of Nandoni dam which started operating in 2005 with the mandate to supply water to rural and peri-urban communities within the catchment. Originally, only Lake Fundudzi, Vondo dam and Albasini dam as well as some tributaries of Luvuvhu River were the dominant water bodies in the catchment. Lake Funduzi, whose existence is unknown, presumably 800AD, is an ancient sacred heritage site of the Vhavenda people which is fed by Mutale River yet does not appear to have an outlet. Vondo dam was constructed in 1982 and raised in 1992 to supply domestic/industrial water for Thohoyandou and its surrounding areas, while Albasini dam was built in 1952 and was raised in 1970/71 to supply the Levubu Irrigation Scheme (DWA, 2004).

An increase in population may have led to clearing of forests to make way for new activities in the area, such as agricultural fields and human settlements. Since the early 2000's, the government of South Africa implemented the Rural Development Programme (RDP) where the

majority of natural forests were cleared to pave way for human settlements, leaving the area bare and susceptible to soil erosion.

4.2 Extraction and Analysis of Morphologic and Hydrologic properties

The major catchment characteristics were based on geomorphology, geology and vegetation. The geomorphology determined the catchment size (drainage area), steepness of slopes, the shape (elongated or pear-shaped) and the drainage-network configuration (related to shape). The size of the drainage basin determines the amount of water that is supplied to its rivers. If the basin slopes are steep, water from precipitation will tend to be delivered to the rivers more quickly than would be the case for more gentle basin slopes. An elongated basin tends to deliver water to the basin outlet over a prolonged period of time whereas a more compact pear shaped basin tends to deliver precipitation from all parts of the basin to the outlet in about the same time so that water from a single storm arrives in an abrupt pulse of flow. River channels are much more efficient at conveying water than surface slopes. As a result, if the drainage density is high (many channels per unit drainage area), water tends to be delivered to the basin outlet more quickly than if there are fewer channels to deliver it.

4.2.1 Automated Catchment Delineation

The method of automated catchment delineation involved automatically creating the boundaries of the study area using DEM-based GIS algorithms. Figure 4.3 shows the hydrologically correct DEM with a 30x30m resolution that was generated and used for automated catchment delineation. Since contour lines were used for DEM creation, they largely influenced the final product due to data imperfections created during data capture. Assessment of data quality involved extracting frequency histograms of the elevations. Figure 4.4 shows the frequency distribution curve for the DEM, which indicates that the DEM had a representative number of pixels with constant standard values, and did not therefore have a large number of flat regions dominating. Imperfections contained in the DEM could directly compromise the results of analysis for hydrological modeling and should therefore be as little as possible.

The minimum, maximum, mean, variance, and total values of the wavelength distributions were summarised in Figure 4.4. The maximum and minimum elevations were 1,588 and 194 m

respectively. The lowest areas with minimum elevations were characterised by valleys while maximum elevations were characterised by hills. The values of frequency distribution related directly to the topography of the study area. As shown in Wolock and Price (1994), higher values of frequency indicate greater potential for development of saturation. These values occur at locations where upslope areas are drained.

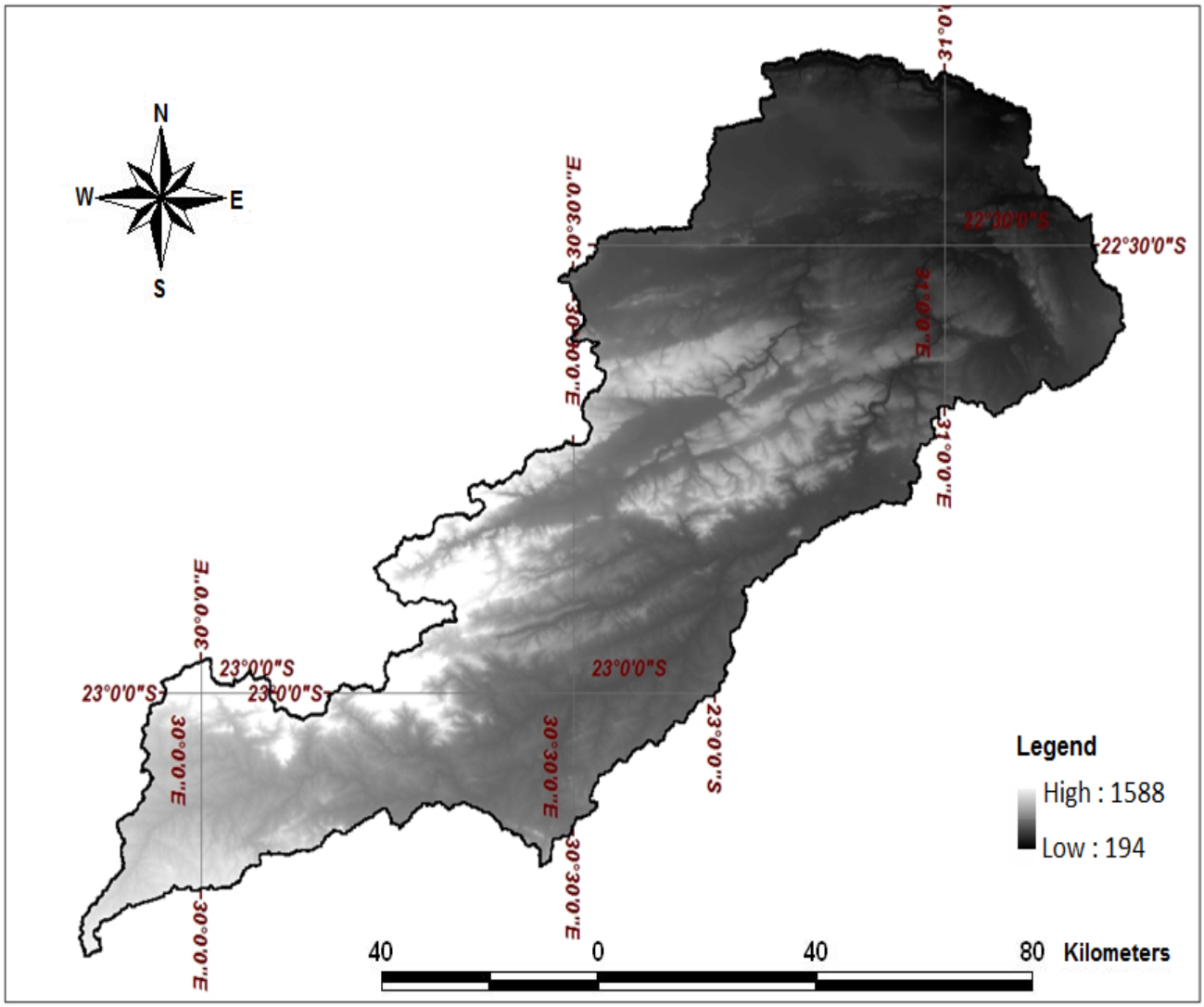

Figure 4.3: Hydrologically corrected DEM for the catchment

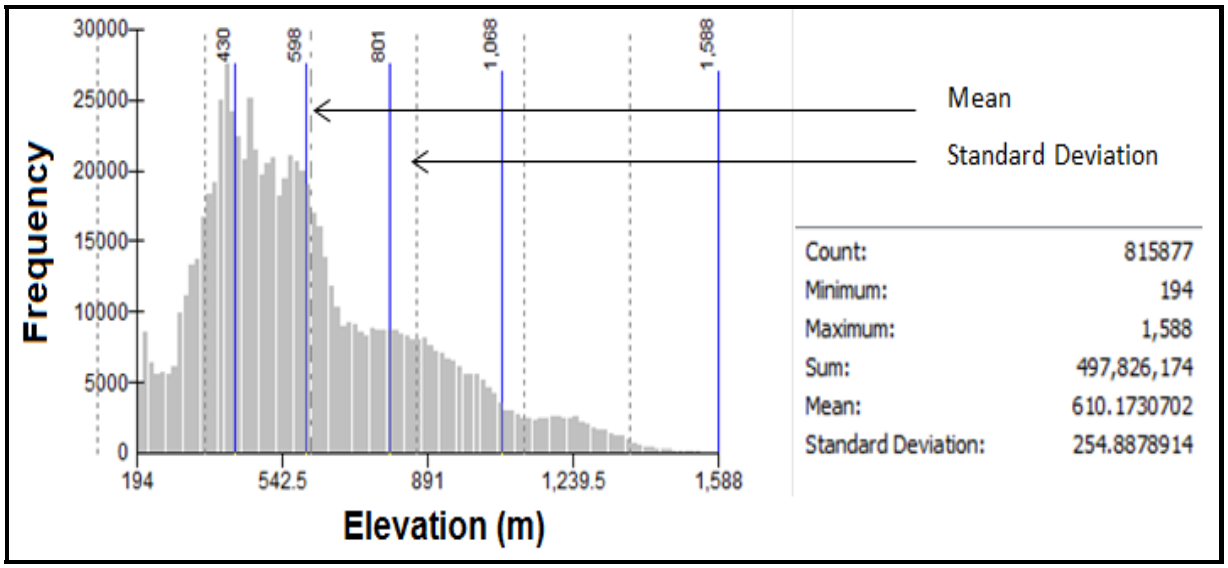

Figure 4.4: Frequency distribution of heights in the catchment

Figure 4.5 shows sub-catchment areas and their topographic attributes including shape and length needed for all physically based hydrological models. The sub-catchments indicate the location and spatial distribution of 1st order streams. Features such as terrain slope, drainage network, and catchment boundaries are essential input parameters for distributed catchment modeling. Mapping their spatial distribution is crucial to ensure that human activities do not inhibit the flow of water to natural systems and hence sustain biodiversity at the smallest sub-catchment unit. Based on this, the technique could be used for hydrological analysis of similar catchments and thereby open the planning process to the full advantages of GIS technology. Automated catchment delineation makes it possible for more responsive water resources management programs to be taken at local micro scales.

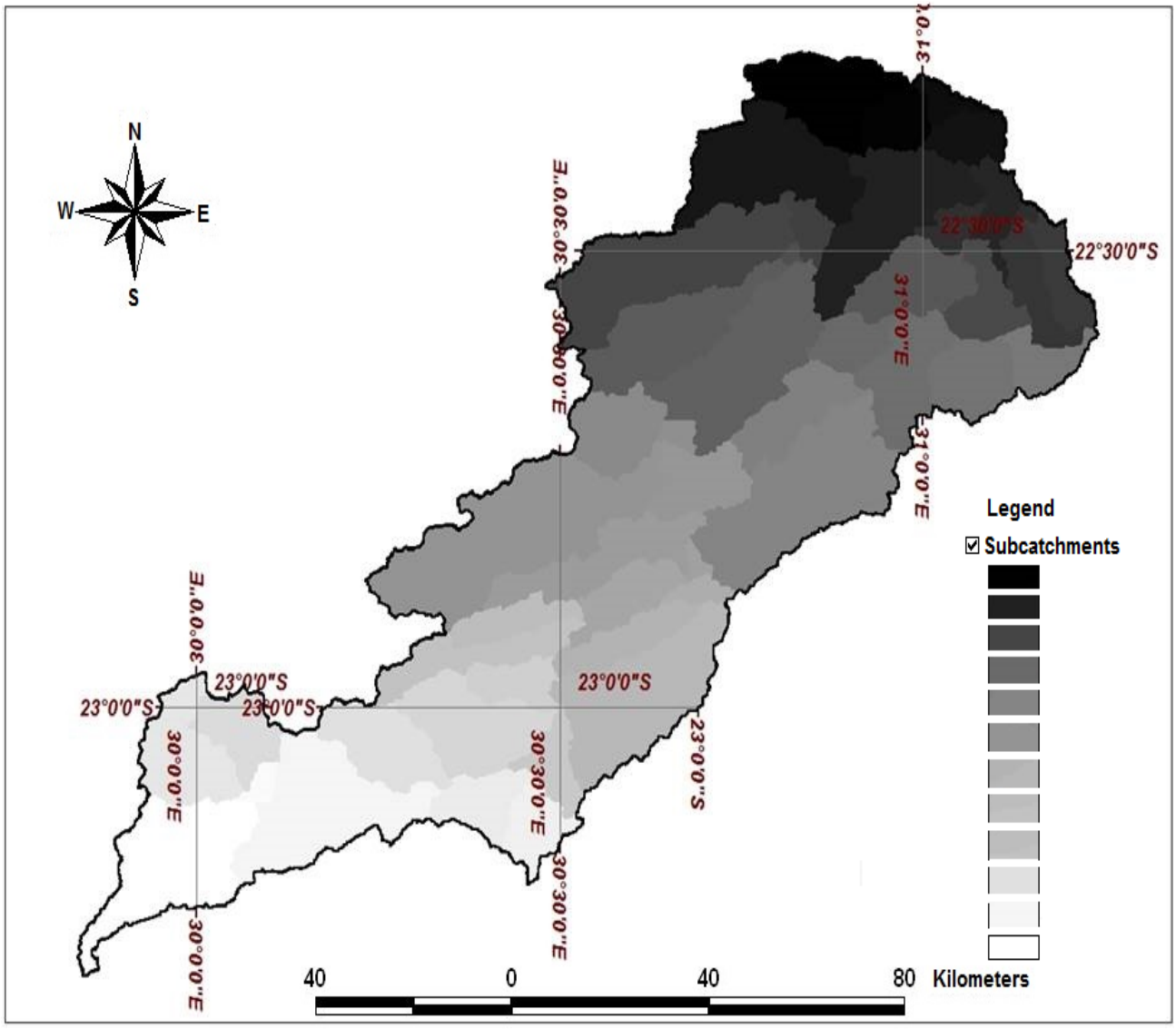

Figure 4.5: Sub-catchment delineation

4.2.2 Stream Network

In this study, the analysis of stream networks from a DEM was done to fix the direction of the flow line as well as the inlets and outlets, and the precise positioning of channels in the digital landscape. This is useful in calculating morphometric characteristics such as the river frequency, stream length, stream density and drainage ratio as well as the spatial pattern of the drainage lines. The characteristics of the extracted network depend on the definition of channel sources on the digital land surface topography.The extracted drainage pattern shown in Figure 4.6 was of the

parallel type. The drainage network was generated using a constant-threshold method based on the evolution mechanism of Luvuvhu River and landform characteristics of the catchment. The method calculated the number of upstream cells that contributed surface flow to any cell. The identified "pour points" for the LRC were shown in Figure 4.7. The headwater streams were extracted to the Strahler stream order 3, which allows a stream to increase in order only when two streams of the same order intersect. It is important to identify and protect all streams because they require the near-stream vegetation for environmental flow. When vegetation is removed along stream banks, water temperature increases. This brings about a shift in the micro-ecological structure that may result in resident species being replaced by less desirable ones that are more tolerant to increased temperatures.

The characteristics of the extracted networks showed the hillslope travel distance and network link lengths. These properties are important in catchment management as they influence the effects of channel morphology on water quality through the unit stream power (USP), which is the stream power per unit channel width. Generally, a stream power is the rate of energy dissipation against the bed and banks of a river or stream per unit downstream length. It is normally derived by the fact that if water is not accelerating and the river cross-section stays constant, all the potential energy lost as the water flows downstream must be used up in friction or work against the river bed. Hence, potential energy equal to the work done to the river bed and banks is the stream power. In models of landscape evolution and river incision, unit stream power is extensively used because it evolves dimensional downstream profile of the river channel. However, it can also be used in river channel migration and sediment transport (Bagnold, 1966). Stream power is important in basin hydrology studies because it can be used to predict the rate of erosion of a river into its bed. Knowledge of stream power assists engineers in designing waterways structures, which could be used to collect runoff from contour banks for erosion control.

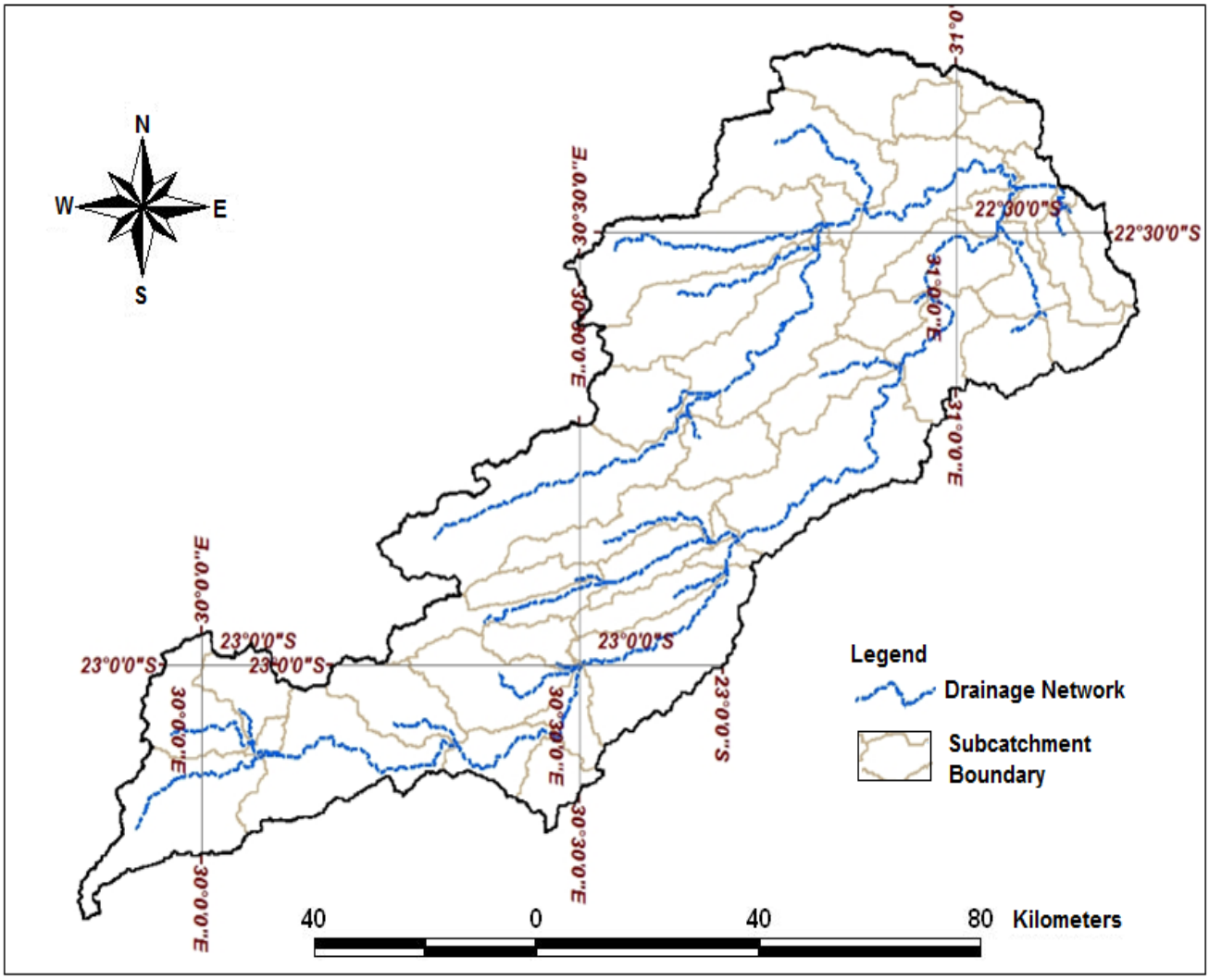

Figure 4.6: Automated extraction of river network

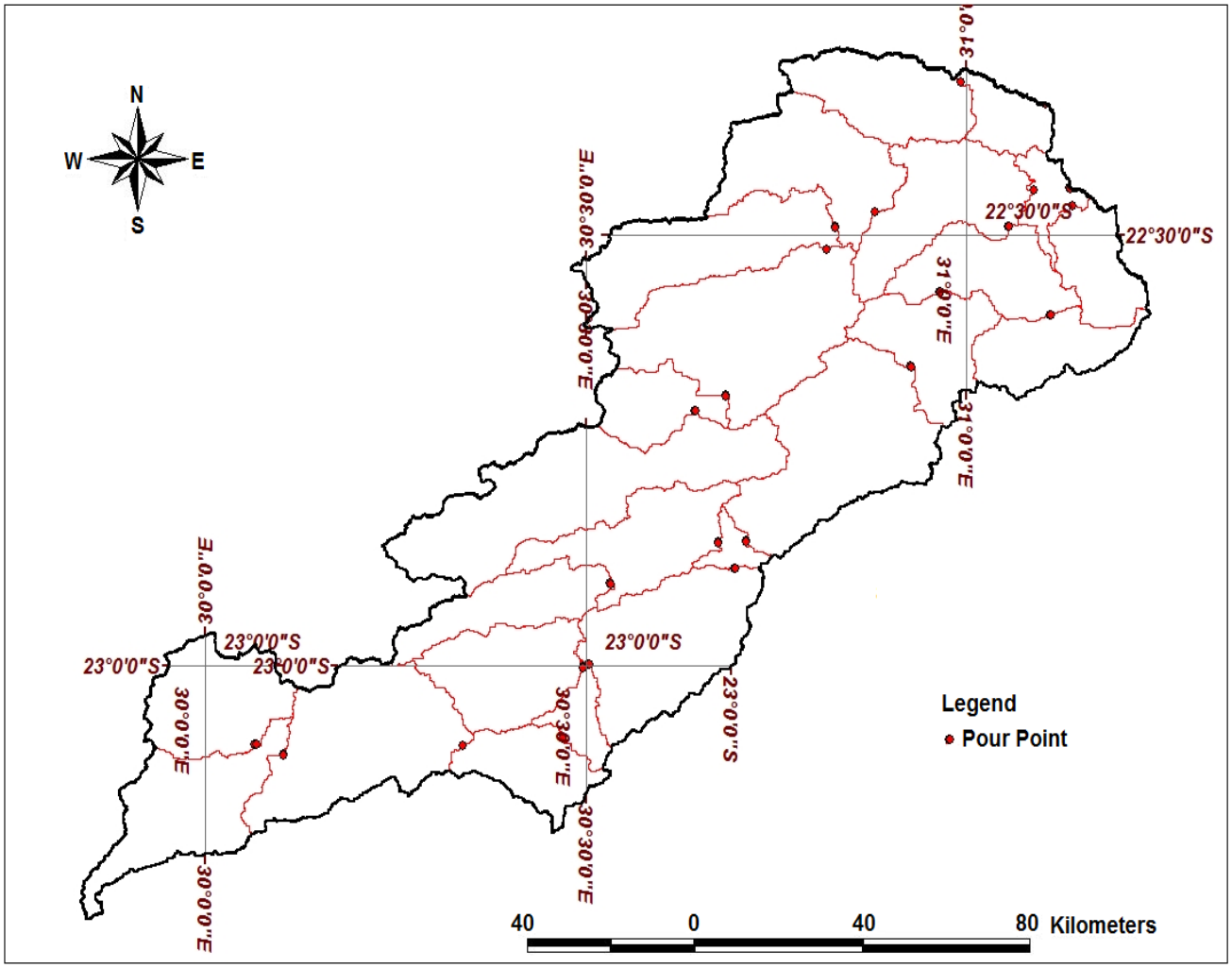

Figure 4.7: Pour points

4.2.3 Slope

The slope of terrain, together with the direction of the steepest slope, was useful to provide the most important information to assess how geology affects topography. This function allows generating a slope grid in percent or degree for a given DEM. The average travel distance slope was taken as the average of the slope from each point in the sub-catchment to the next adjacent downslope channel. A slope is the maximum derivative in any direction of a plane tangent to the surface as modeled by a DEM. The spatial distribution of local slopes for Luvuvhu River catchment is as shown in Figure 4.8. The slopes affected the overall rate of downslope movement for processes such as runoff, erosion hazard, moisture balance and landslide hazards.

Extraction of this property is therefore important as it allows overland and near-surface water flow to be modeled using DEMs if we assume that surface topography is the sole factor in the distribution of water. This would help check the processes of acceleration and deceleration and reduce the effects of erosion and deposition in the catchment.

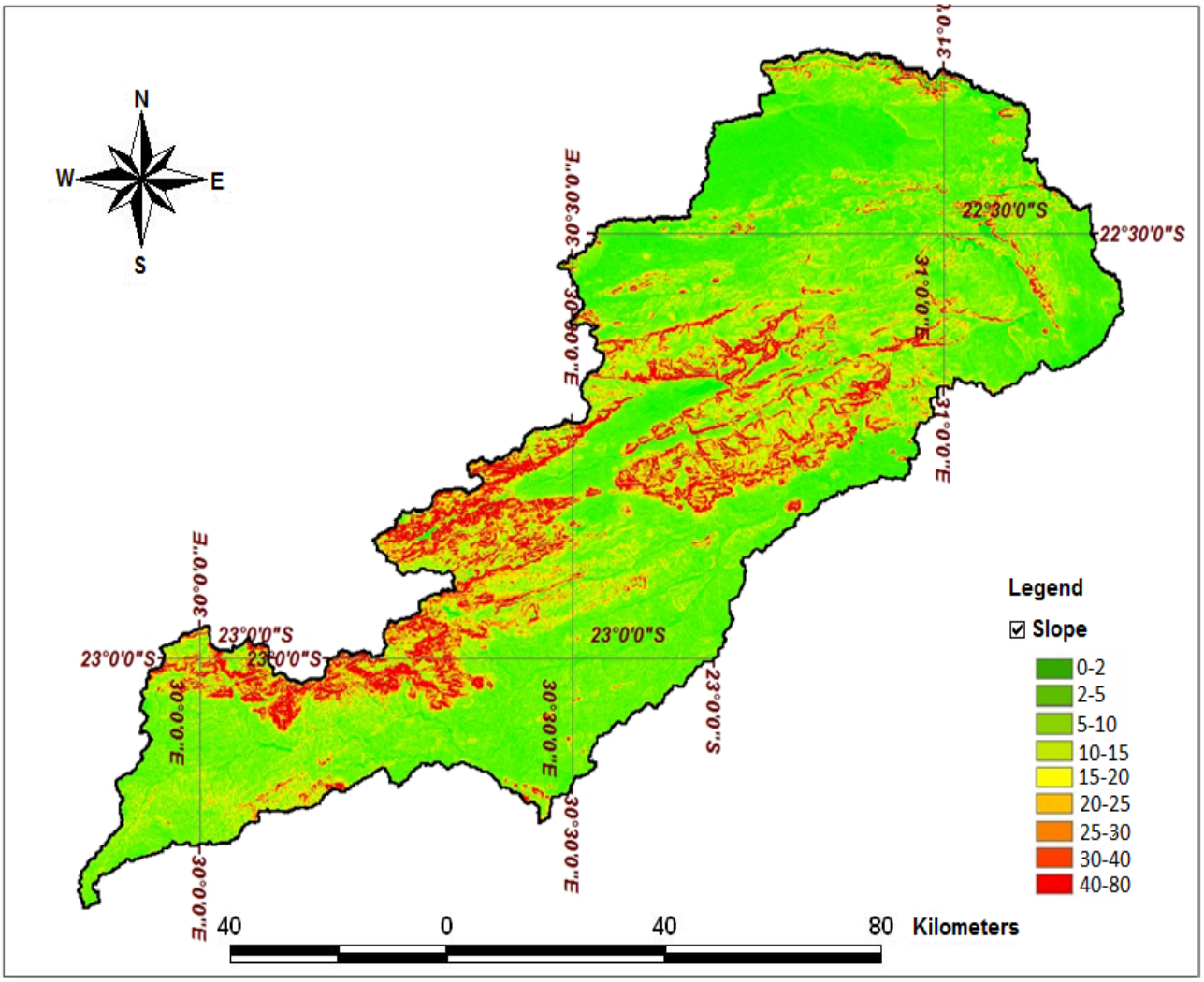

Figure 4.8: Spatial distribution of local slope

4.2.4 Topographic Indices

Knowledge of the compound topographic index (CTI) (Moore *et al.*, 1991) as a derived attribute/aspect is important as it provides the wetness index which could be used to predict zones of saturation in catchments whereas the stream power index (SPI) provides a measure of

the erosive power of overland flow. In the study area, the soil properties varied laterally with topography resulting in patterns of soil development, a relationship that allows for prediction of soil attributes from landscape position. As a result, topography may influence soil erosion and runoff. The dominance of aspect, elevation and the slope aspect index (SAI) reflected the fact that the surface horizon was deepest on the plateau followed by the escarpment and plains. The thinnest surface horizons occurred on the ridges and hills. This information is vital for managing farmland in the hilly areas within the catchment such as Piesanghoek macadamia cropland and Tsianda mango farms.

4.2.5 Flow Direction

Flow direction was useful in this study in order to determine where a landscape drains. The flow direction model showed the direction of the steepest downslope neighbour for each cell by colour coded direction. The "FLOWDIRECTION" model was similar to the slope direction and was in conformity with the fact that water takes the shortest path to find its own level. The pour points in Figure 4.9 represented the locations where water would most likely be found throughout the year even during droughts. Such points would be the best sites for developing community water supply projects as they would serve as reliable sources of water to ensure availability throughout the year. These properties are important for water resource management studies where geomorphic and hydrological features such as terrain slope, drainage network, and catchment boundaries are essential input parameters for distributed catchment modeling. This information is crucial to ensure that human activities do not inhibit the flow of water to natural systems. This would help sustain biodiversity at the smallest sub-catchment unit.

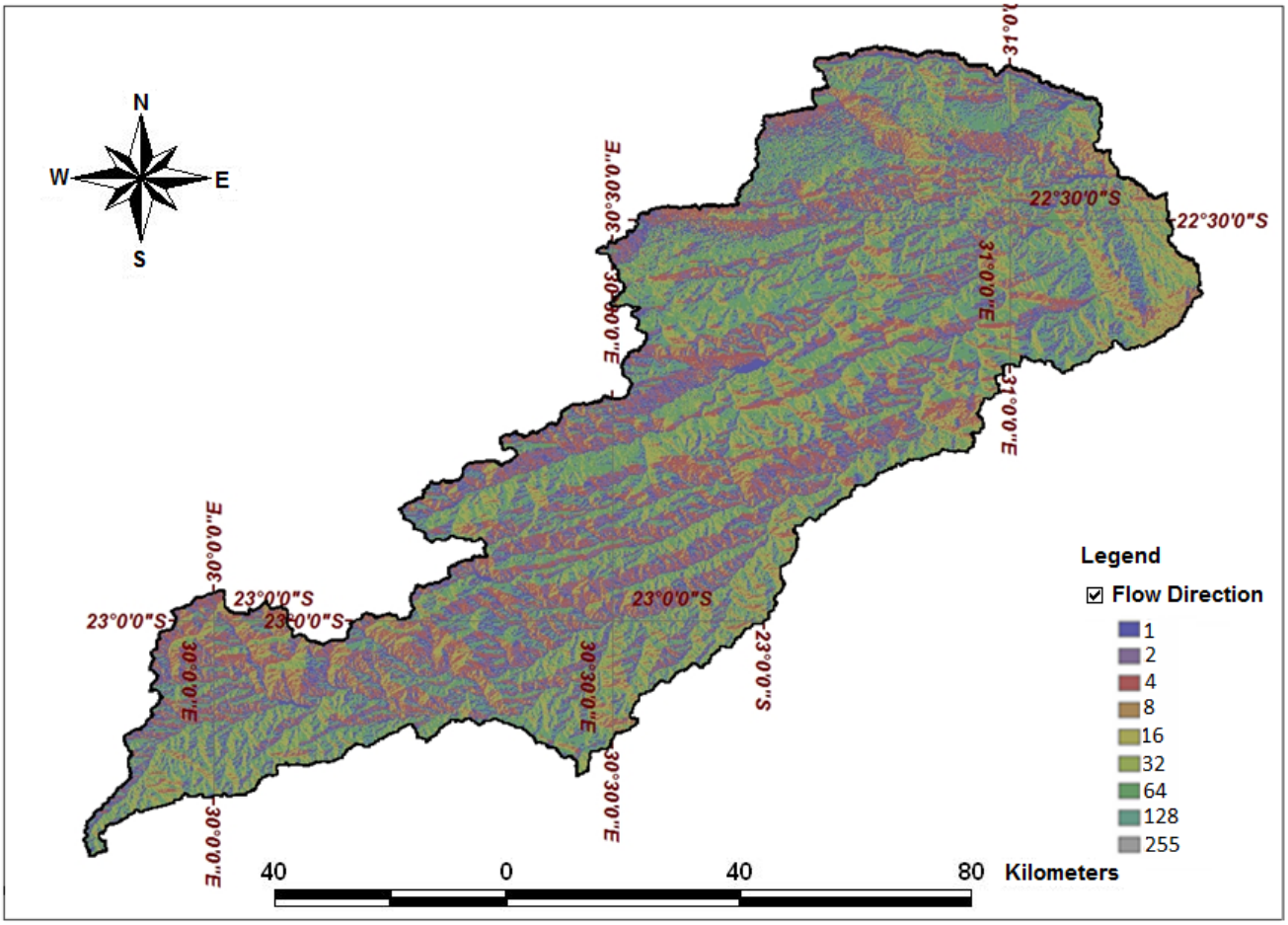

Figure 4.9: Spatial distribution of flow direction

4.2.6 Stream Segmentation

Streams in the catchment were automatically segmented and used as a background to create input flow direction and drainage networks. Stream layers were created using flow direction and pour points as input layers resulting in identification of flood inundation areas. The stream grid was segmented into sections representing headwater tributaries or segments between confluences, with each segment assigned a unique grid code identifier. The resulting link grid was used to generate a catchment grid based on the values held by each stream segment. During segmentation, other streams in the catchment did not appear in the map and were treated as first order stream segments. As streams were segmented, polygons were first used to create centerlines to adjoining or merging the streamlines. In this way, the lower order catchments could be merged to a higher order, which might be useful for basin scaling. Stream segmentation

is important in the catchment as streams and water bodies are identified for purposes of adopting classifications and water quality standards; in order to protect public health or welfare, and enhance the quality of water.

4.2.7 Flow Accumulation

The flow direction grid and associated "FLOWACCUMULATION" function were used to accumulate any spatial variable above any location. The drainage area above the location was calculated simply by translating the flow accumulation value (in pixels) into an appropriate area in square miles (mi^2). Use of the function in this way assumes that the weight given the flow accumulation function is one. All upstream pixels were counted or weighted in the same manner. Flow accumulation model performed the cumulative count of the number of pixels that naturally drain into the outlets. The "FLOWACCUMULATION" layer adds up all the upstream water available for runoff using the flow direction information layer along the steepest slope. Thus, the water was accumulated along the flow paths while being directed by topography.

4.2.8 Flow Paths

The flow length model was used to estimate the length of the longest flow path within the LRC, which could be used for inundation mapping and floodplain delineation. The longest flow path data could also be used in the rainfall-runoff analysis to determine the time of concentration value necessary for computing surface runoff. Thus, the flow length model was used to determine the route that is followed by runoff during rainfall starting at a divide and ending at the first adjacent downslope channel. In this study, the average travel distance slope was taken as the average of the slope from each point in the sub-catchment to the next adjacent downslope channel. Adjacent catchments were identified in order to associate topologic information for upstream and downstream connections. Figure 4.10 shows the adjacent catchment longest flow path while Figure 4.11 shows the longest flow paths within each delineated sub-catchment. This links up the outlet for a major basin to the furthest point upstream of the drainage line for each sub-catchment.

The stream networks showed the hillslope travel distance and network link lengths. The channel lengths estimated the streams following twists and turns as closely as possible. Since the

upstream end of the streams are often incorrectly shown on maps, this approach was appropriate and could be used to measure channel lengths from a stream's mouth in an upstream direction. In general, the actual length of the stream is usually underestimated from maps, because twists and turns of the channel are increasingly smoothed at smaller map scales. The smaller the map scale, the more length is underestimated. This model would provide the advantage of calculating the length of the upstream and downstream flow path from each cell. Past studies have demonstrated that lengths of stream classified on the basis of geomorphic and hydrologic properties are associated with specific riparian communities. Such associations are often interpreted as vegetation responses to flooding or flood disturbance (Harries, 1985; 1987).

The waterways in the LRC are mainly influenced by run-of-river and point source discharge mostly during significant rain events. The majority of waterways are susceptible to deterioration and transport of dispersive soils within the catchment through soil erosion. Most of the waterways in the catchment have little to no native riparian vegetation in continuous stands; as a result they tend to reduce its capacity to filter sediments from overland flow and they increase the risk of bank instability. The State of the Rivers Report (Angliss *et al.*, 2001) for the Luvuvhu/Letaba Water Management areas established that widespread clearing, particularly of the riparian vegetation and in areas vulnerable to soil erosion, resulted in higher than natural sediment loads to many rivers in the catchment. Forestry, poor agricultural practices and deforestation along the LRC affect rainwater run-off from the land. Human impacts on the landscape are often observed with synchronous changes in erosion and suspended sediment concentration in rivers. For example, within the LRC in some areas where land use practices are poor and where riparian vegetation has been or is being removed; floods accelerate bank and donga erosion.

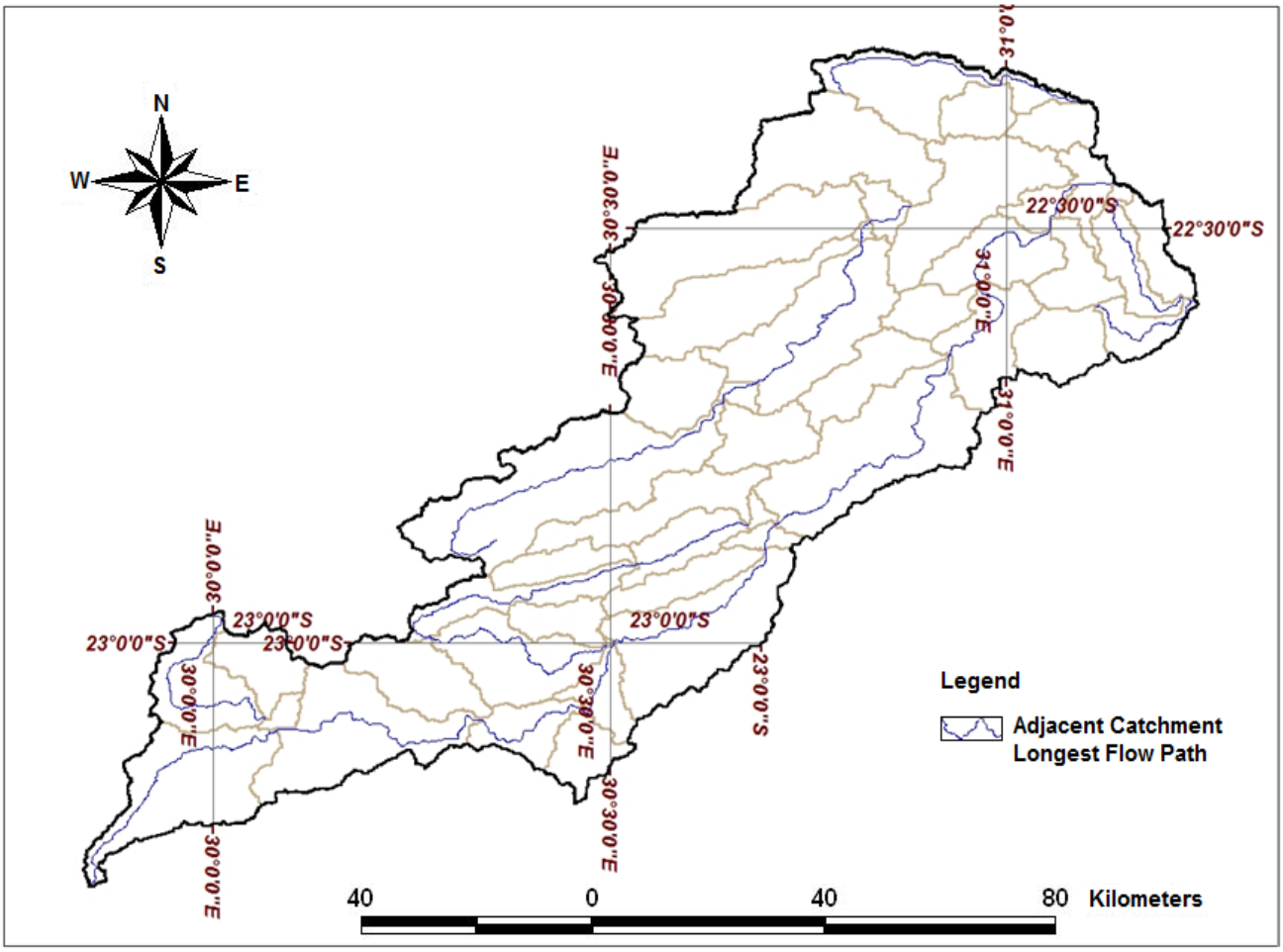

Figure 4.10: Adjacent catchment flow path model

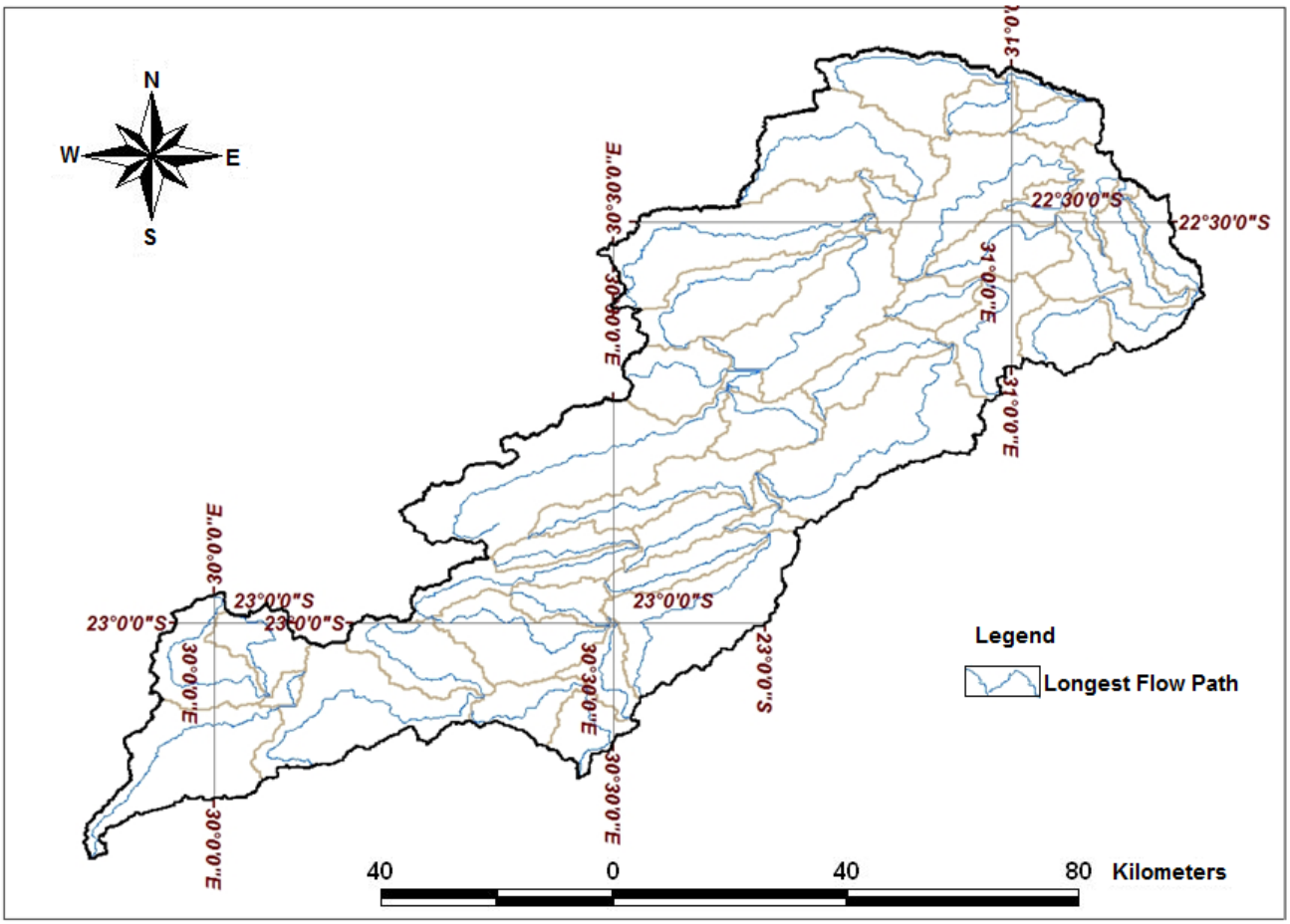

Figure 4.11: Longest flow path for the catchment

4.2.9 The Longitudinal Profile

Figure 4.12 shows the distances and elevations from the source of the river, downstream to the mouth or confluence with the next large river. The Luvuvhu River rise in the Soutpansberg Mountains and flows for about 200 km through a diverse range of landscapes before it joins the confluence of the Limpopo River near Pafuri in the Kruger National Park (DWA, 2004). The long river profile was used to obtain slopes between points intervals along the main river channel. Results showed that the profile of the LRC is a concave shape, with a steeper upper section and a gentle lower section. Change in altitude from the upper course of the river to its lower course was noted. All along its course, the river used energy to carry out erosion, transport and deposition of sediment. This energy was produced when water flowed down a slope.

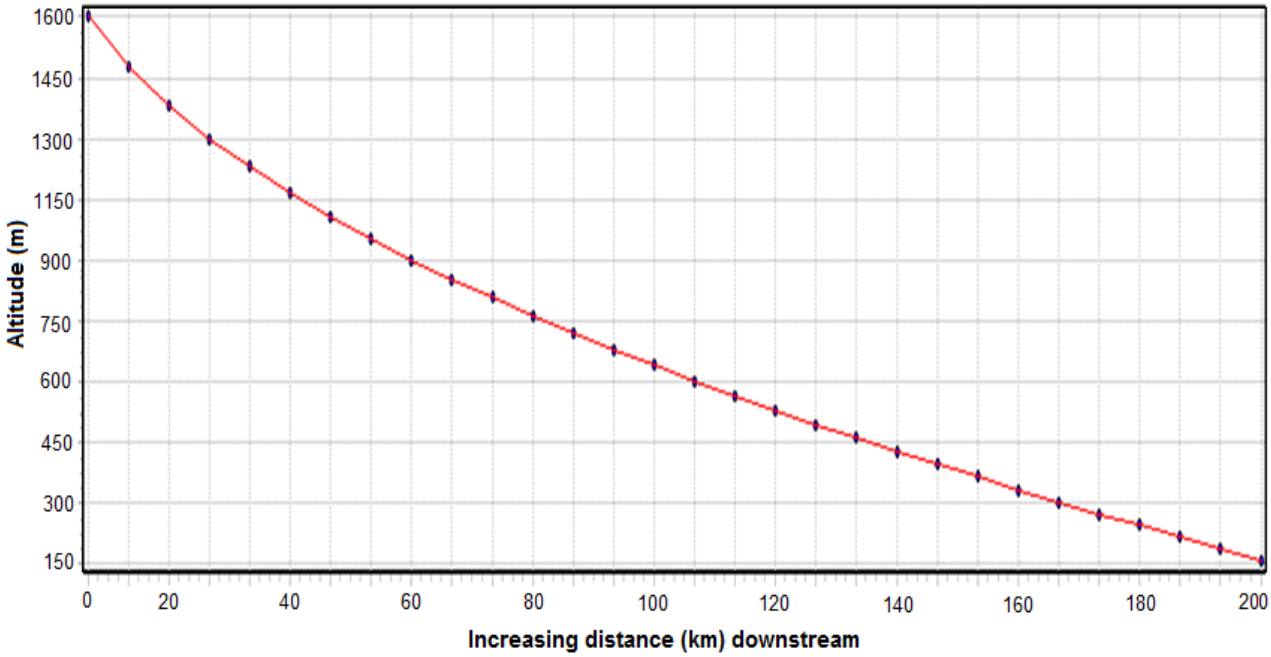

Figure 4.12: Longitudinal river profile for Luvuvhu River Catchment

TOPOGRID produced good results that closely matched the actual environment. The modeled rivers were comparatively very accurate when overlayed upon the digitised rivers even in areas with relatively flat slopes. TOPOGRID consistently produced high quality results for both landscapes corroborating the appropriateness of the locally adaptive approach used in this algorithm.

However, the reconditioned DEMs are reliable only to the extents of the reference river network used in the AGREE process. If an accurate and more detailed hydrological network is needed then an equally detailed reference stream network should be used or a good interpolation approach should be applied to produce reliable results. From a hydrological standpoint, the time efficiency and a locally adaptive approach make TOPOGRID a powerful tool to model hydrologically correct DEMs, and makes it the best interpolation technique for catchment.

4.3 Hydrometeorological Data Analysis

4.3.1 Mean Annual Rainfall

The spatial distribution of mean annual rainfall showed that rainfall was higher on the western side and lower on the eastern side ranging from a maximum of 251 mm to a minimum of 85 mm

(Figure 4.13). The middle section of the catchment, i.e. Levubu Valley, had maximum of 202 mm. The western side corresponded to the upstream while the eastern corresponded to the downstream parts of the catchment. The rainfall received at upstream is crucial within the catchment because it impacts on the flow of the river downstream. Variations in interannual rainfall may result in low river flows for much of the year with periodic high flows, thereby limiting the availability of water resources through the dry season (Mukheibir and Sparks, 2003).

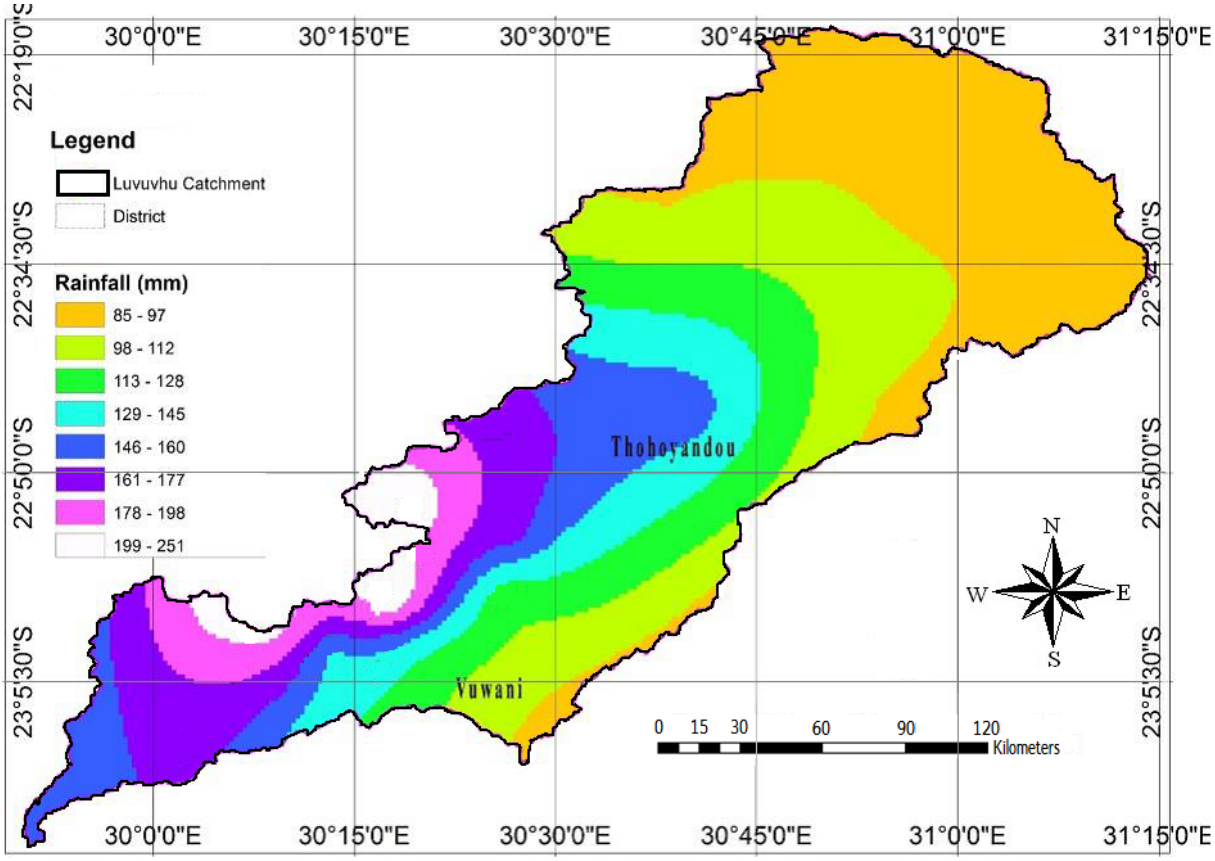

Figure 4.13: Spatial distribution of mean annual rainfall in the catchment

The trend analysis showed that the annual rainfall differed across the catchment. Some stations displayed a decreasing trend while others showed increasing trends. The trends during the 1960 and 1985 phase revealed an increase in rainfall upstream of catchment at Nooitgedacht and a decrease in rainfall downstream at Rambuda as shown in Figure 4.14. The figure revealed the temporal fluctuations in rainfall during the study period. Other stations which indicated an

increasing trend included Klein Australie, Entabeni Bos, Tshakhuma and Palmaryville. Three major peaks were observed in 1971/72, 1976/77 and 1977/78 hydrological years at Rambuda and Nooitgedacht, revealing the temporal fluctuations in rainfall. A study by Mukheibir (2005) has shown that South African regions experience seasonal and interannual variations in rainfall. These variations have a great impact on the agricultural sector in the country. For example, the timing of rainfall during the onset of rainfall in October is crucial for planting of crops whereas the timing of rainfall in early February is crucial for the growth of crops (Jury *et al*., 1997). During the period 1985 to 2010, Nooitgedatcht, together with Elim Hospital, Klein Australie, Entabeni Bos, Palmaryville, and downstream catchment at Tshakhuma, Tsianda, and Rambuda indicated increasing rainfall trends with unimodal peak in 1999/2000.

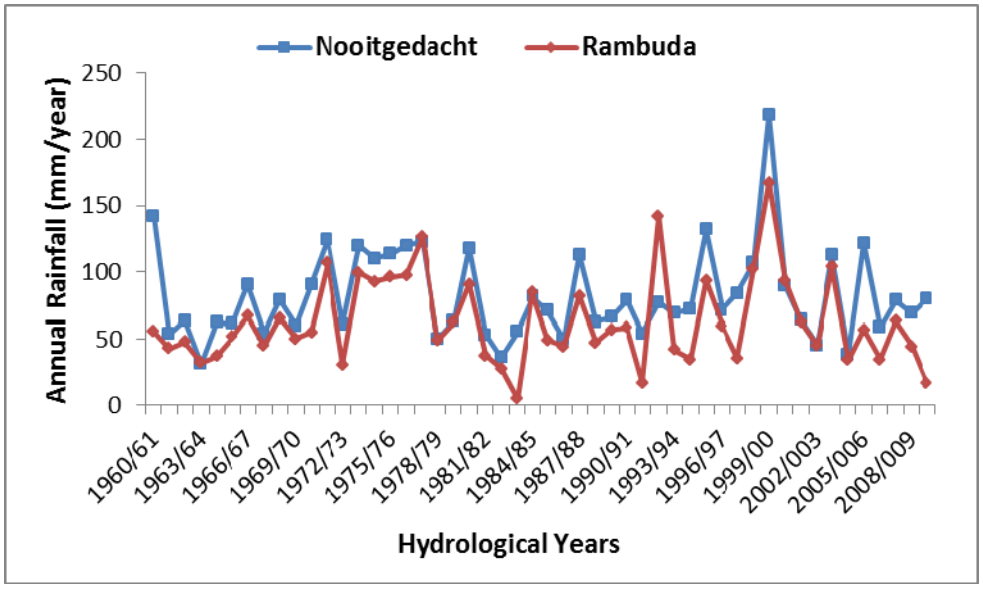

Figure 4.14: Rainfall trends for Nooitgedacht and Rambuda: 1960-2010

The wet season (October to March) trends in the catchment for the period 1960-1985 revealed a long-term annual mean rainfall of 1144.8 mm with a minimum rainfall of 476.1 mm in 1982/83 but a maximum rainfall of 2142.1 mm in 1976/77 hydrological year (Figure 4.15). Average rainfall during the dry season (April to September) for the same period was 215.1 mm with a minimum of 58.2 mm in 1963/64 and a maximum of 355.8 mm in 1973/74 hydrological year (Figure 4.15). Towards the end of each series, the wet season series showed an increasing trend

while the dry seasonal rainfall series revealed a consistent trend. The wet seasonal trends for the period 1985-2010 revealed a long-term average rainfall of 1125.5 mm with a maximum rainfall of 3074.2 mm in 1999/2000 hydrological year (Figure 4.16). During the same period, the dry season received a yearly average of 191.6 mm with a minimum rainfall of 62.15 mm in 1993/94 and a maximum rainfall of 480.5 mm in 1985/86 hydrological year (Figure 4.16). Again, the wet season revealed an increasing trend whereas the dry season showed a consistent trend towards the end of the series.

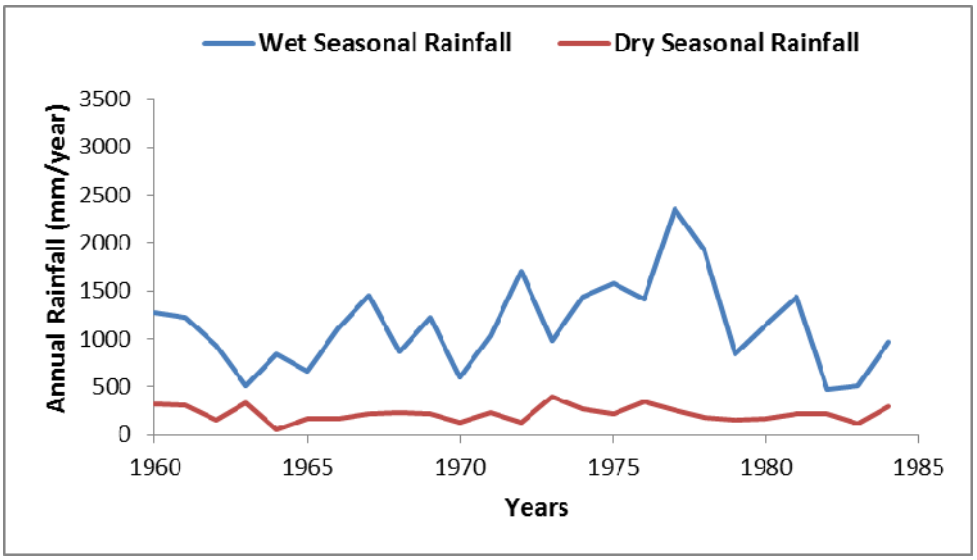

Figure 4.15: Average wet and dry seasonal rainfall for the study area: 1960-1985

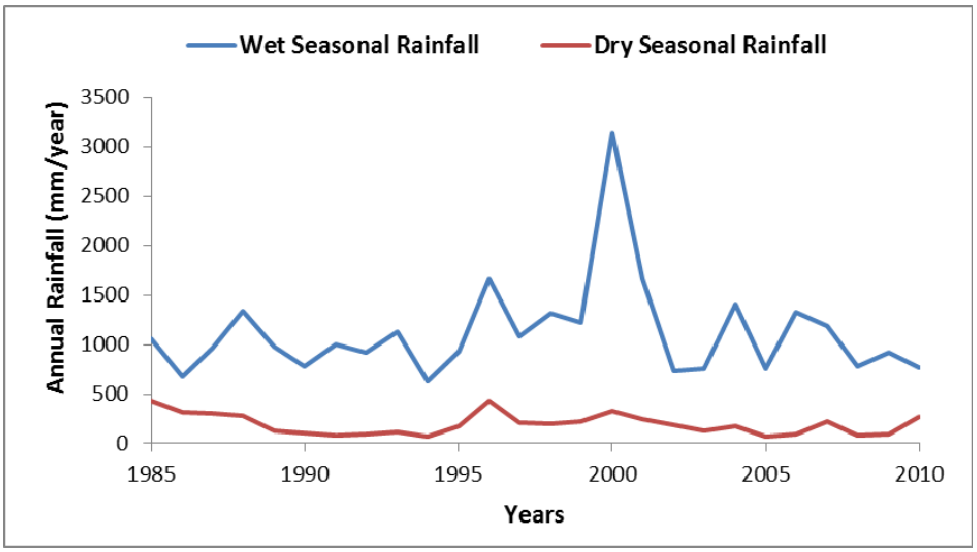

Figure 4.16: Average wet and dry seasonal rainfall for the study area: 1985-2010

4.3.2 Average Class-A Pan Evaporation

Results showed that evaporation as measured from Class-A pan was highly variable during the summer season (October to March), whereas it showed a gradual decrease during the winter season (April to September). The average monthly rainfall and evaporation for areas at Levubu, Lwamondo, Goodehoop, and Madzivhandila were as shown in Figure 4.17. These areas are located in the vicinity of A9E001, A9E002 and A9R003, A9E004 respectively (Figure 3.4) The peak evaporation months were highlighted around summer during November, October and January, with mean daily A-pan evaporation values of between 5 and 6 mm/day, respectively. During the dry season, evaporation and abstractions by plants reduce runoff and decrease the amount of subsurface and interflow that support stream flows.

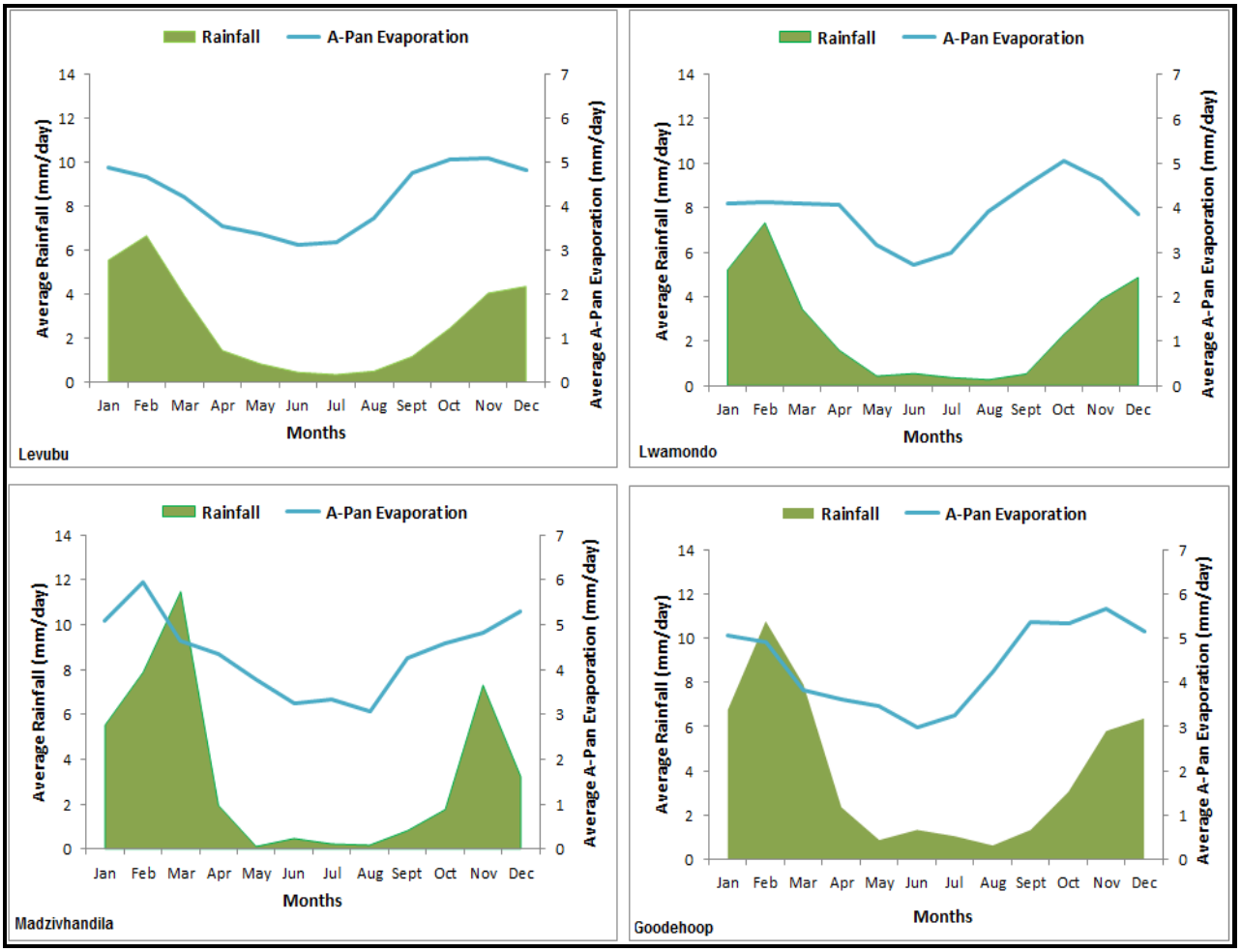

Figure 4.17: Average monthly evaporation

Figure 4.18 shows the spatial variation of evaporation in the study area, where evaporation increased from west (upstream of the catchment) at a rate of 1 400 mm/a to east (downstream) of the catchment at a rate of 2000 mm/a. For example, stations A9E001, A9E002 and A9E003 falls within a zone of equal mean annual evaporation (1500-1600 mm) and have comparable mean daily evaporations; whereas station A9E004 is in a zone of higher mean annual evaporation and has the highest mean daily evaporation (1700-1800 mm). These variations in evaporation could be linked to land use activities in the upstream (mostly plantations and agricultural) and downstream (mostly settlements) of the study area.

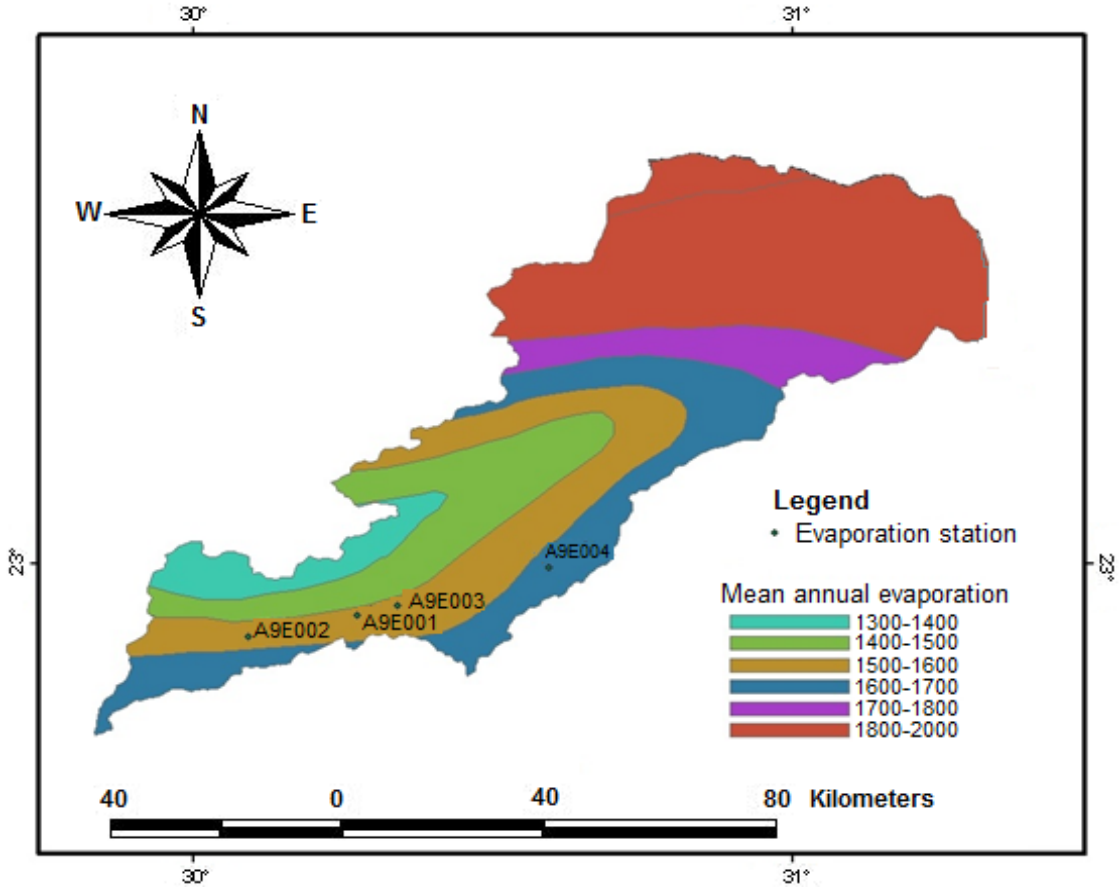

Figure 4.18: Spatial variation of evaporation

Land cover changes may have impacts on the evaporation rate by either reducing or increasing it. An increase in forestry area may increase the levels of evapotranspiration from vegetation and may tend to reduce bare ground evaporation. Humidity on the other hand has a tendency of

reducing evaporation rates. When relative humidity of the air increases, its ability to absorb water vapour decreases, leading to a decrease in evaporation rates. Conversely, when there is less humidity, the air becomes "hungry" for more moisture and hence more evaporation takes place. When the level of wind speed is low, the rates of evaporation tend to decrease due to saturated air above the ground surface. Also, high temperatures may increase evaporation rates which in turn increase the water losses in rivers and dams. These can be exacerbated by land cover changes which affect local temperatures thereby increasing the rate of evaporation.

4.3.3 Evapotranspiration

Evapotranspiration (*ET*) estimation for semi-arid South African regions like the LRC is a major challenge for researchers and water managers due to scarce and/or inadequate data. Through the use of given local meteorological data, reference evapotranspiration (ET_o) formed the basis of evapotranspiration (*ET*) estimation in the study area. While *ET* represents the combination of evaporation from soil and open water sources, and transpiration through plants; the ET_o was determined as daily values that represented the environmental demand for *ET* without considering the crop characteristics and soil factors, but rather evaporation from large open bodies of water. The ET_o was included in this study as it is the most important hydrometeorological variable to reflect climate change and detailed land-surface conditions (Ellen *et al*., 1998). The ET_o was determined using the FAO based Penman-Monteith equation within the CROPWAT software. Figure 4.19 shows the distribution of reference evapotranspiration (ET_o) for the study area. The onset of the rainy season in October at each climate station starts with relatively high ET_o values which then increases gradually until January. Thereafter, ET_o values declined gradually from February and reached minimum in June. It then rose again from July towards the early rainfall season in October. The peak ET_o months were recorded in January, February and March, throughout for different climatic stations (Appendix 9). During the wet season, Levubu, Lwamondo, Thohoyandou, and Univen observed the high ET_o values of more than 4.0 mm/day as shown in the data (Appendix 1). These areas are situated at the middle section of the catchment surrounded by many rivers and dams. The lowest ET_o values were observed during the dry months at Mhinga and Madzivhandila areas which are located at the lower section of the catchment and are surrounded by natural veld for grazing camps. Schaffer (2005) noted that high evapotranspiration occurs when high available energy

interacts with high soil moisture and robust plant health. Such high *ET* may constitute a threat to agriculture and to water storage, supply, management and quality. Areas with higher *ET* rates were near rivers and streams, which generally have more abundant vegetation. Conversely, areas with the lowest *ET* rates were relatively dry, where pasture and grasslands dominate the landscape. A study by Mölders (2011) showed that evapotranspiration was low in deforested areas due to reduced surface roughness length and it significantly decreased net radiation. Such low *ET* subsequently modifies the water and energy cycles within the deforested area. In areas that are characterised by low rainfall, the rate of evapotranspiration is low as some water will be lost due to percolation and surface runoff.

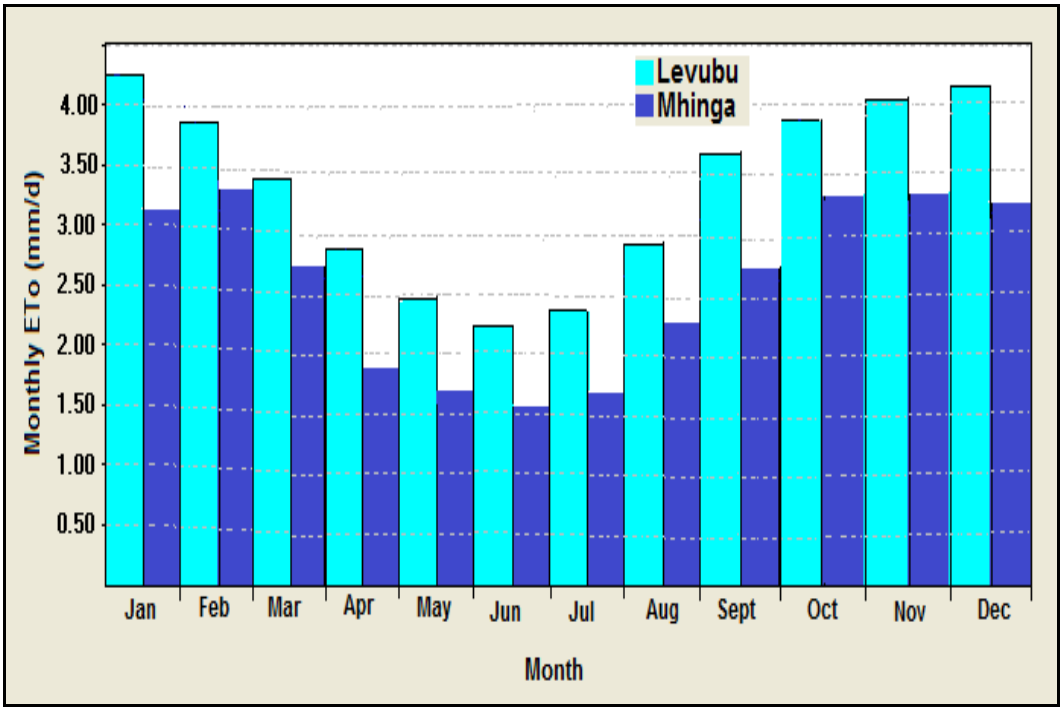

Figure 4.19: Average monthly ET_o upstream and downstream of catchment

Analysis of the effective rainfall, which equals to the difference between total rainfall and evapotranspiration, was as shown in Figures 4.20 and 4.21. Comparable trends were observed at three stations located near upstream including Levubu, Lwamondo, and Madzivhandila. The effective rainfall values for upstream and downstream are provided in Appendix 3. The highest effective rainfall was observed in summer between November and February while the lowest

effective rainfall were observed in winter between May and September, which corresponds to the total rainfall distribution during the study period. Hence, effective rainfall was lower than the total rainfall, revealing higher moisture deficit in the study area.

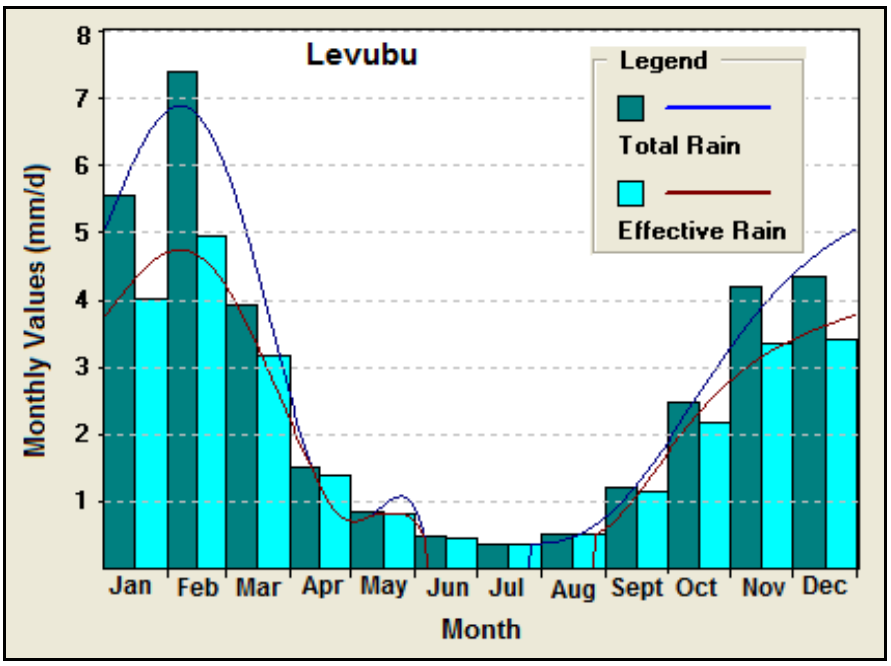

Figure 4.20: Total and effective rainfall distribution upstream

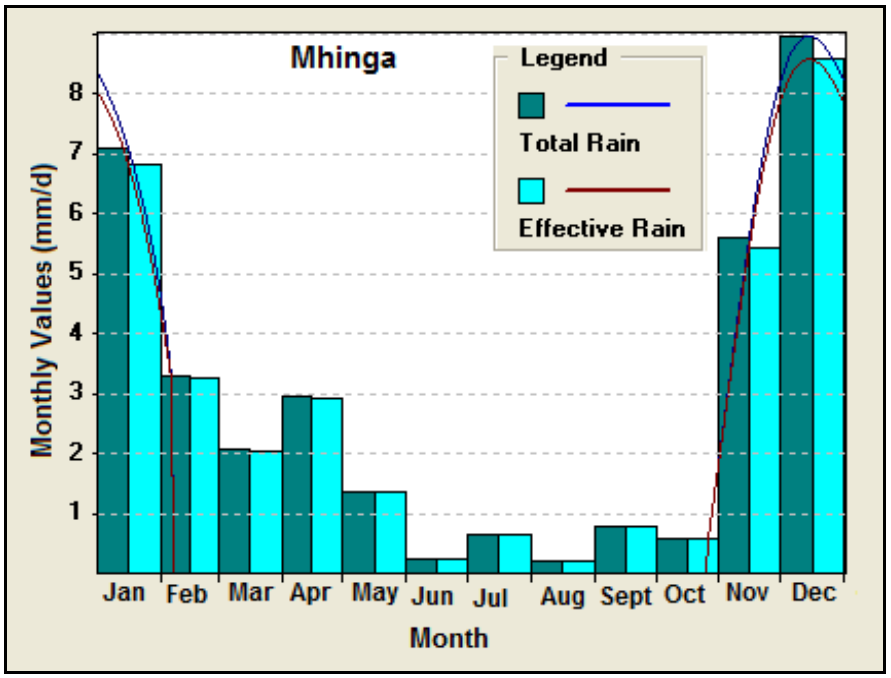

Figure 4.21: Total and effective rainfall distribution downstream

Surface wind velocities in the study area increased gradually from May to October and declined during the rainy season from November to April as shown in Figures 4.22 and 4.23. The Figures depict the relationship between average monthly wind speed, total rainfall and ET_o upstream and downstream of the catchment respectively. Calculated ET_o was compared to total rainfall in order to obtain water deficit for both upstream and downstream. The Figures show that the peak wind speed month was October with the least wind velocities occurring in April; with more winds velocities being experienced upstream than downstream. Appendix 5 shows that about 80 km/day (0.96 m/s) to more than 129 km/day (1.5 m/s) wind velocities were experienced in the catchment, with a maximum average of 99.1 km/day (1.2 m/s) and a minimum of 5.2 km/day (0.1 m/s). High winds tend to increase the rate of evapotranspiration as the rate of evaporation increases with the moving air. Such wind will also clear the air of any humidity produced by the plants' transpiration thereby increasing the rate of evapotranspiration. Levubu valley showed high wind velocity of more than 100 km/day during the summer months from October to December while minimal wind speed were experienced downstream of the catchment. Winds are known to remove the moist air around the plants and soil, and as a result, increase evapotranspiration and depletion of vegetative cover on the land by soil erosion. The more the wind speed, the more is the erosive power of the air mass and hence, more evapotranspiration.

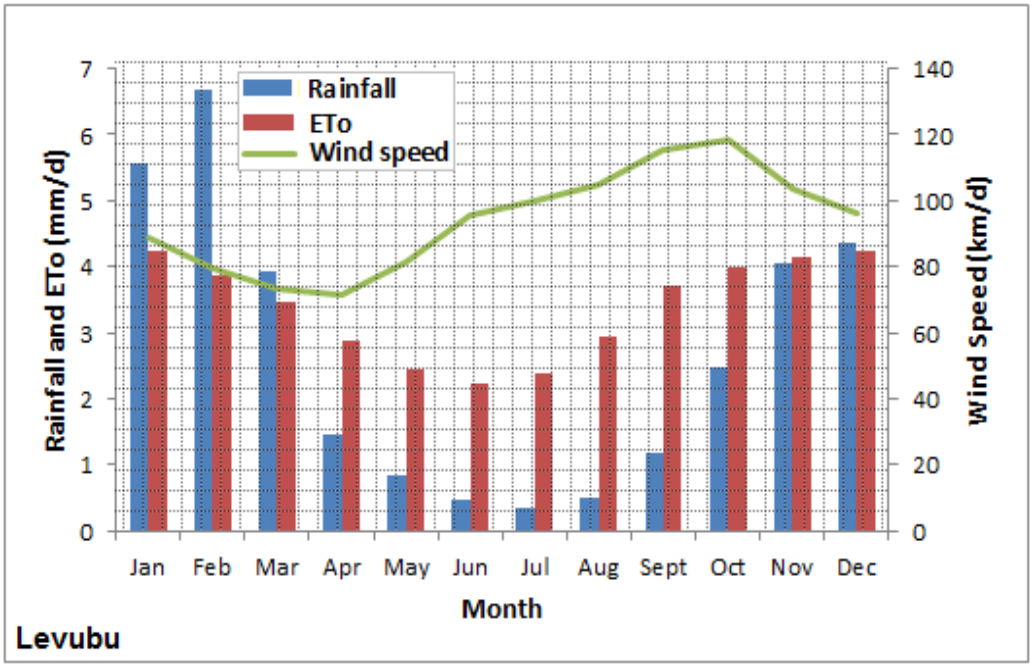

Figure 4.22: Average monthly wind speed, rainfall and ET_o for upstream of the catchment

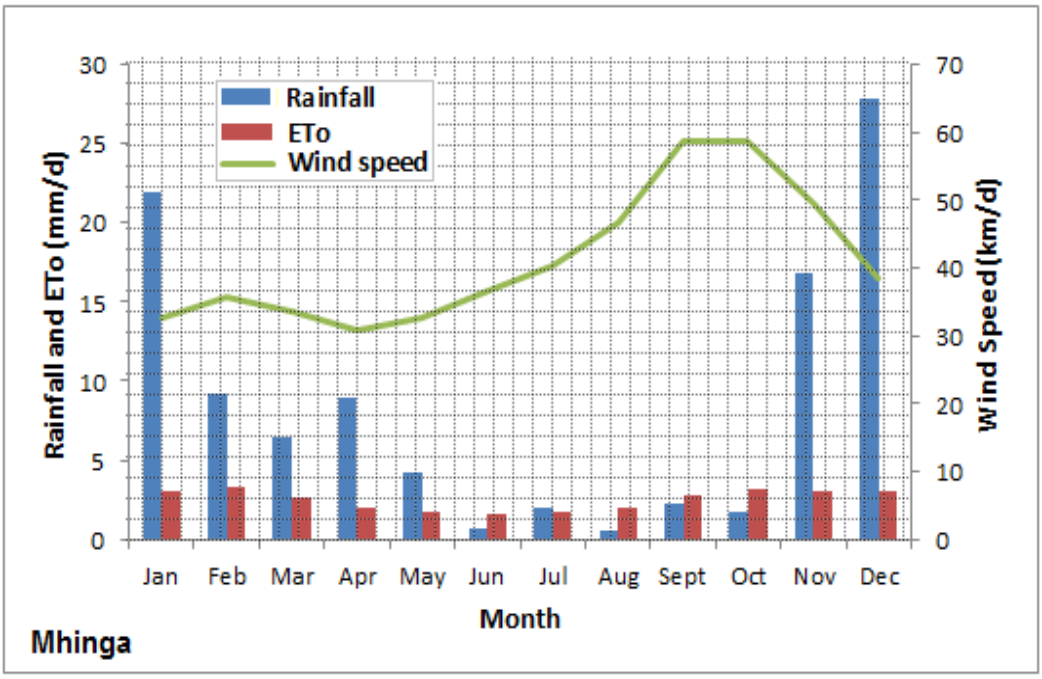

Figure 4.23: Average monthly wind speed, rainfall and ET_o for downstream of the catchment

Minimum and maximum temperatures showed greater variability during the rainy season from October to March while lesser temperatures were experienced in June and July. There appears to be a relationship between the increase in temperatures during the rainy reason and the increase in evapotranspiration rates in the study area. This could be due to the fact that high amount of energy was available during the summer months when temperatures were high. High temperatures lead to conversion of liquid water to vapour, and plants open up their stomata to release more vapour. Figure 4.24 and 4.25 show the average monthly minimum (lower dashes) and maximum (upper dashes) temperatures used for determining ET_o. Downstream catchment (Mhinga) revealed higher temperature values in comparison with upstream (Levubu).

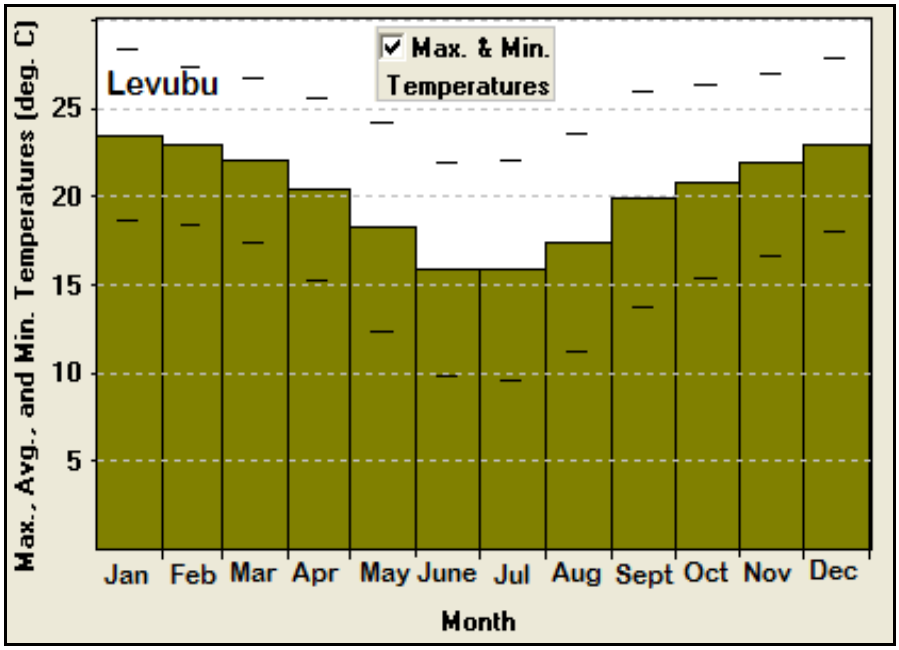

Figure 4.24: Average monthly minimum and maximum temperatures

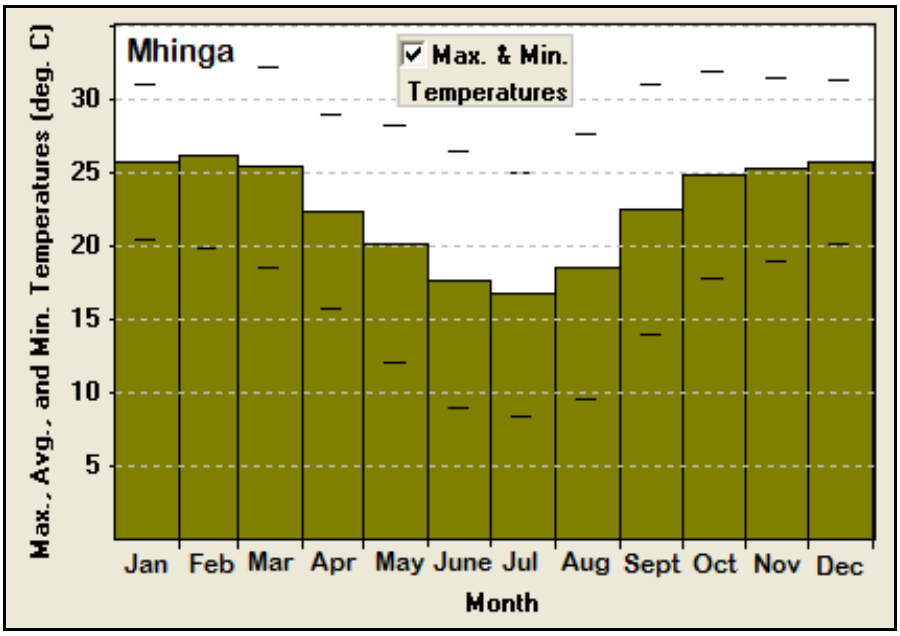

Figure 4.25: Average monthly minimum and maximum temperatures

Figures 4.26 and 4.27 compared the relative humidity and wind speed for the study area. The figures show that the humid season in the area extended from November to April. During the rainy season, average relative humidity was above 60%. Evaporation and transpiration rates

tended to drop to low levels when the air around the plants was too humid. When the air was drier, the rate and quantity of water vapour entering the atmosphere was higher, thereby increasing the rate of evapotranspiration in the study area.

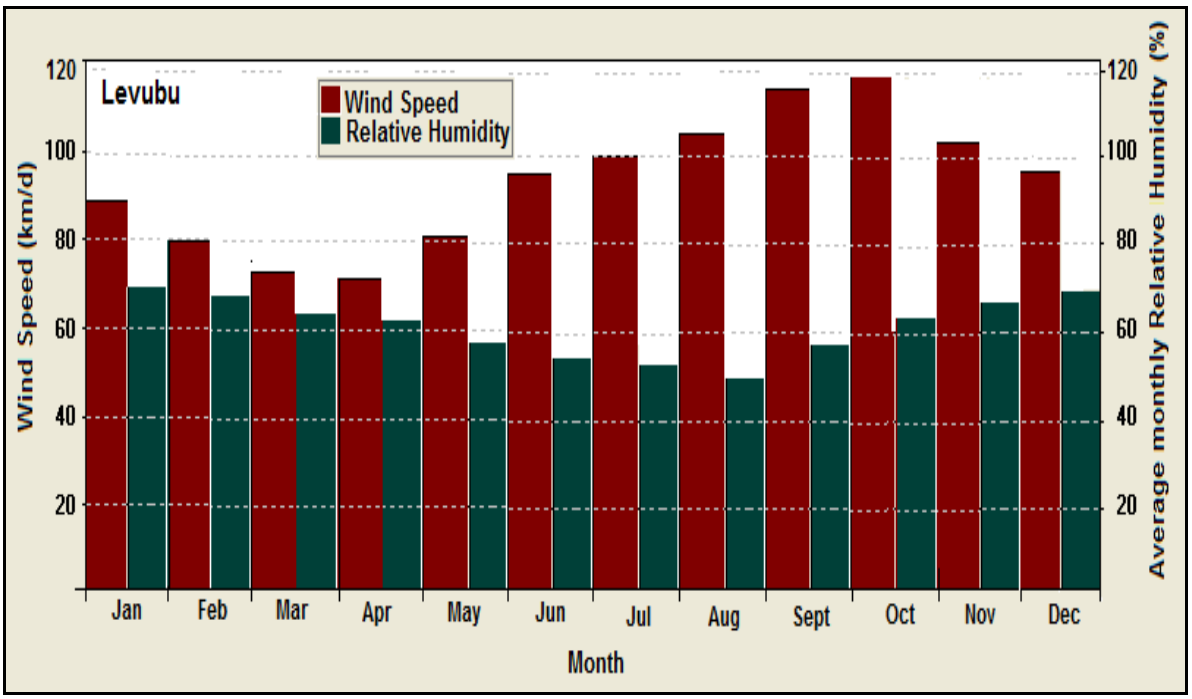

Figure 4.26: Average monthly relative humidity and wind speed upstream

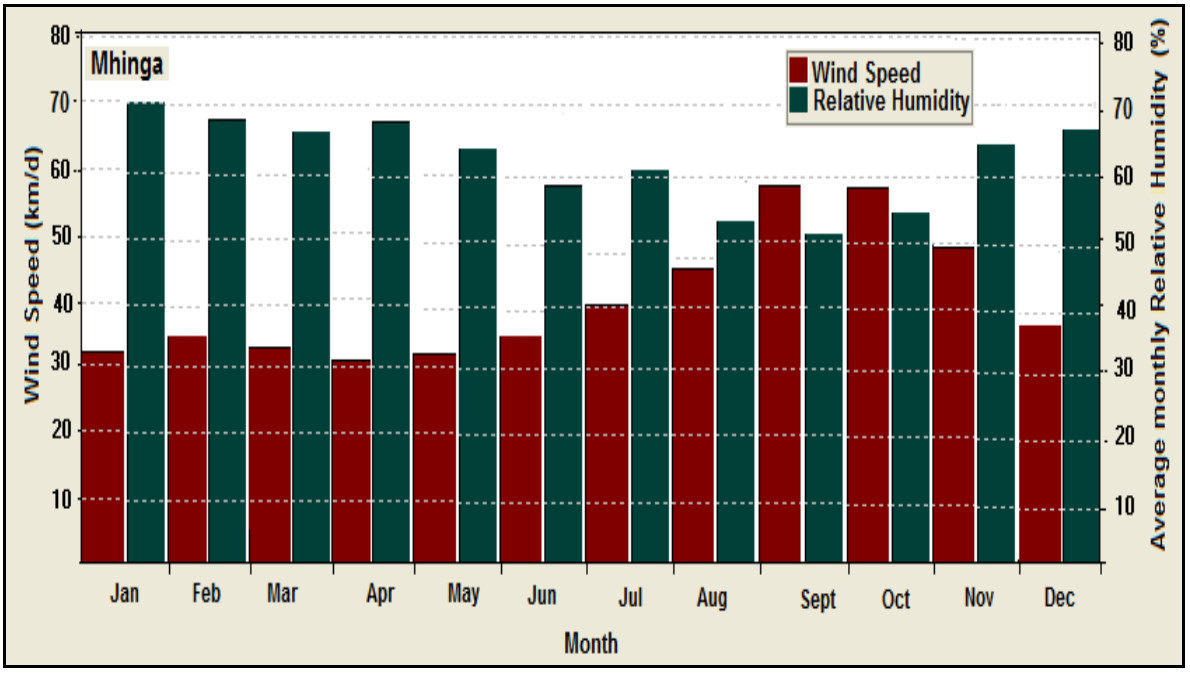

Figure 4.27: Average monthly relative humidity and wind speed downstream

Figures 4.28 and 4.29 show that solar radiation in comparison with rainfall and ET_o. The figures showed that solar radiation in the area was highly variable during the rainy months, with peaks either in January, February or March. Lesser amounts of radiation were experienced in the coldest months of June and July in Levubu. The upstream catchment (Levubu) received higher solar radiation and greatest ET_o as compared to downstream of the catchment (Mhinga). The results showed that the more energy available, the greater the rate of rainfall and evapotranspiration.

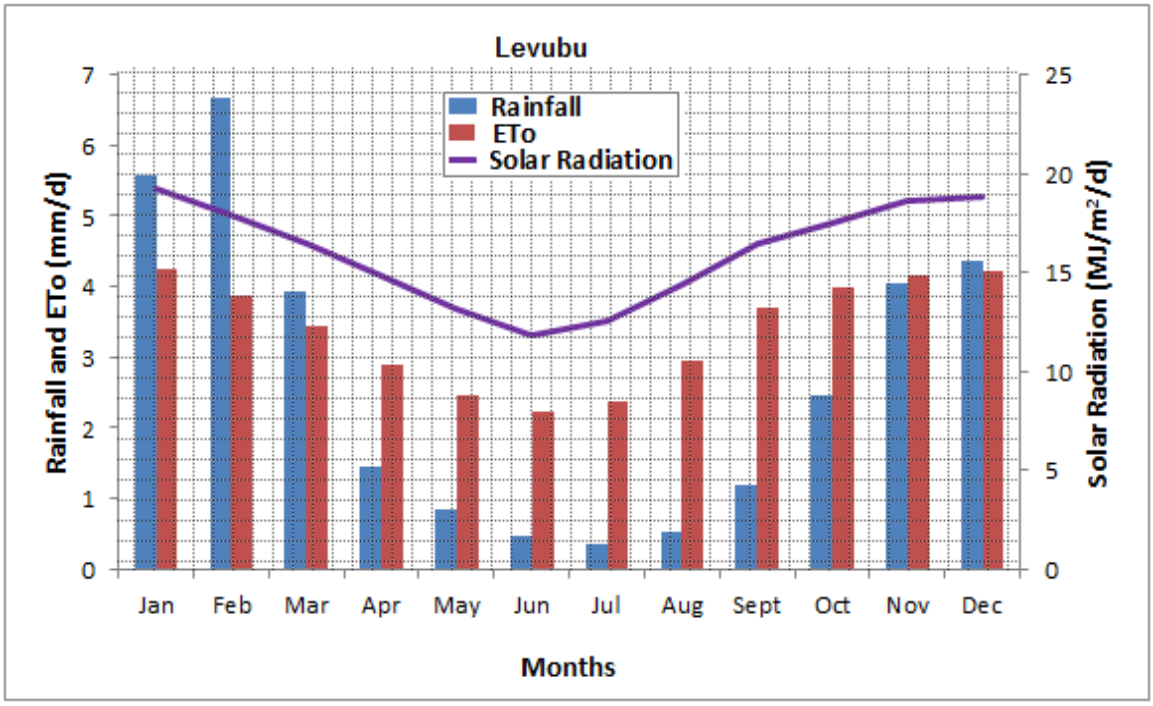

Figure 4.28: Average monthly radiation for upstream

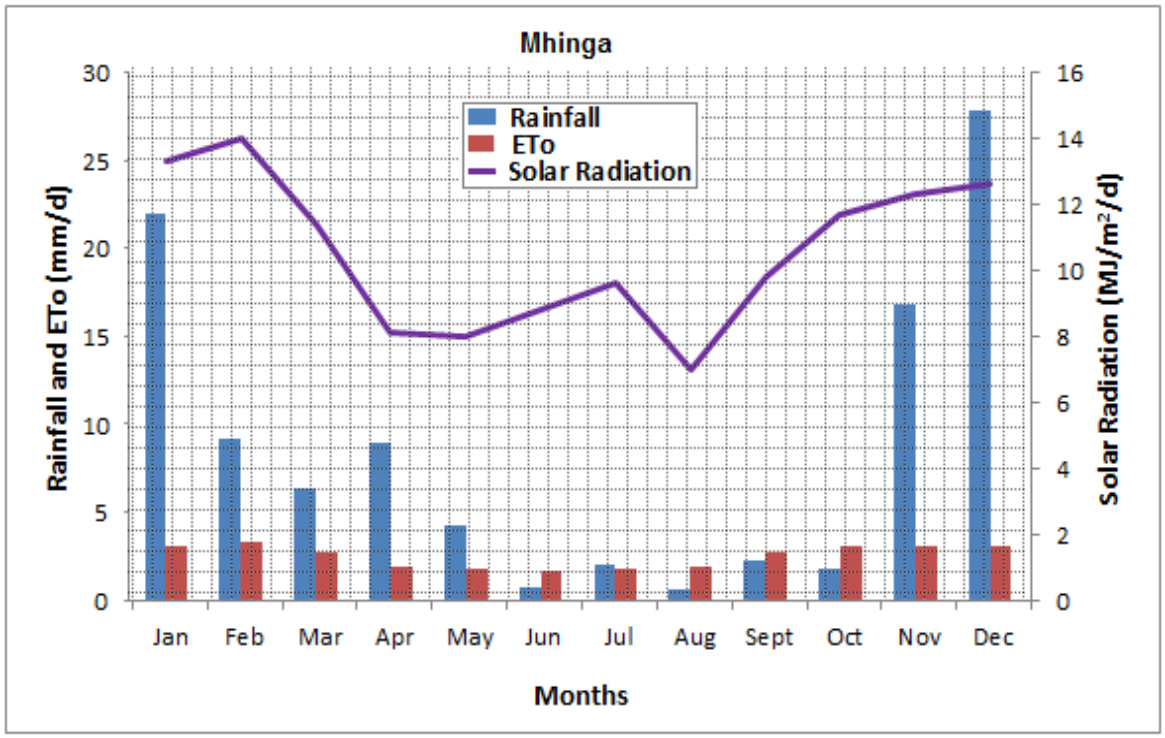

Figure 4.29: Average monthly radiation for downstream

Figure 4.30 shows the spatial distribution of sunshine hours in the study area. Long sunshine hours were experienced both in summer and winter months as shown in Appendix 8. Thohoyandou experienced highest sunshine hours in summer during the late rainy season from January to March. In other areas sunshine hours showed alternating trends such that Levubu, Lwamondo, Madzivhandila and Univen received long sunshine in winter regardless of the season. In winter, Limpopo province continues to experience plenty of sunshine due to absence of clouds but temperature remains cool. During this time of the year, days usually start with a chill in the air which progresses to a warm midday and cool, dry afternoon. At night the temperature drops dramatically. The annual averages of sunshine hours ranged from 1.6 hours/day to 6.8 hours/day. Lwamondo received more sunshine than other areas. Appendix 8 showed that ET_o was directly proportional to sunshine hours, such that when the hours of sunshine increased, it caused an increase in ET_o. The longer sunshine hours enhanced evapotranspiration in the study area, causing plants and environment to be exposed for longer and increase in the amount of moisture to be evapotranspirated.

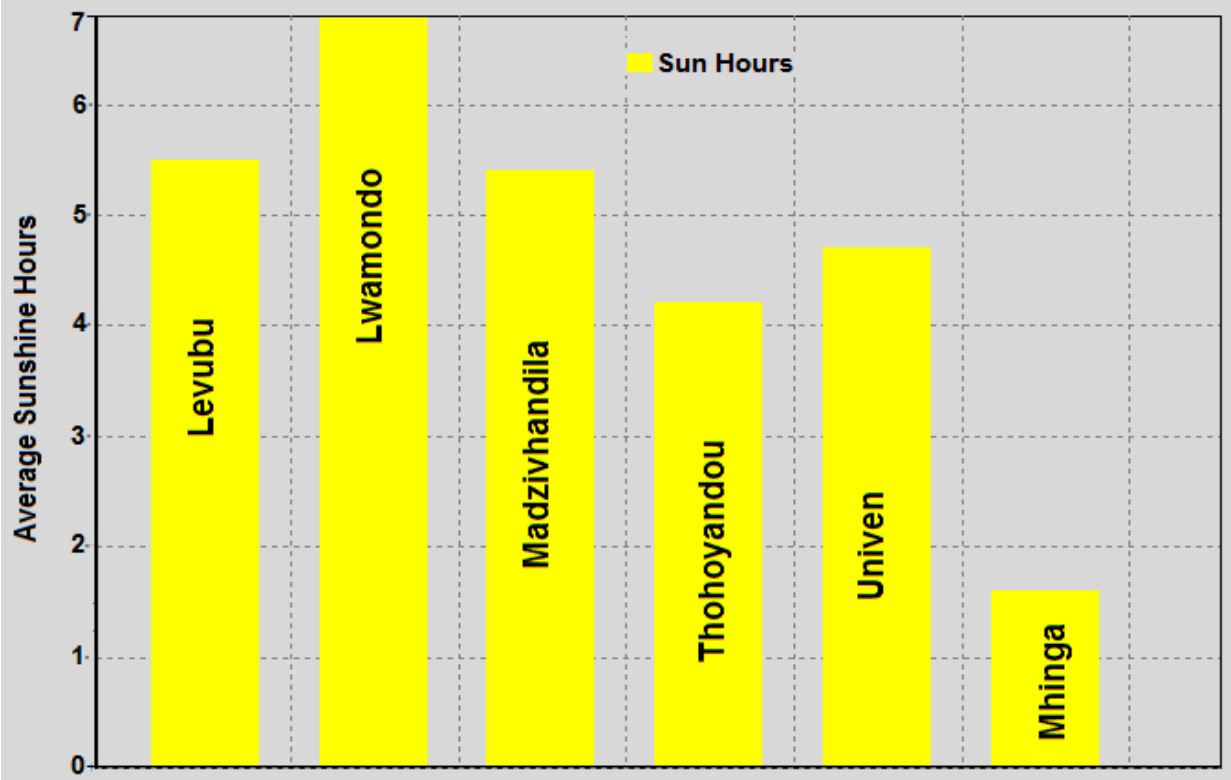

Figure 4.30: Annual average sunshine hours

4.3.4 Runoff

Gauging station number A9H020 (Figure 3.6) was chosen to represent the upstream catchments in the study area while station A9H003 (Figure 3.6) represented downstream of the catchment. Most rivers in the catchment sustain flows only during the wet season especially between December and April following intense rainfall events. Figure 4.31 showed the distribution of average runoff upstream and downstream of the catchment. The results showed that runoff was highly variable during the month of February with maximum runoff records of 1.63 m^3 and 3.84 m^3 upstream and downstream, respectively. The results showed that upstream catchments had lesser amounts of runoff while abundant runoff volumes were received downstream of the catchment. A study by Bisri *et al*. (2008) found that land use changes from pervious layer to impervious layer in a catchment area can change the hydrological system thereby altering the runoff in downstream area of a catchment. The change in runoff in the study area is an indication of land use/cover change, as a result, runoff volumes downstream can lead to flooding in low land areas.

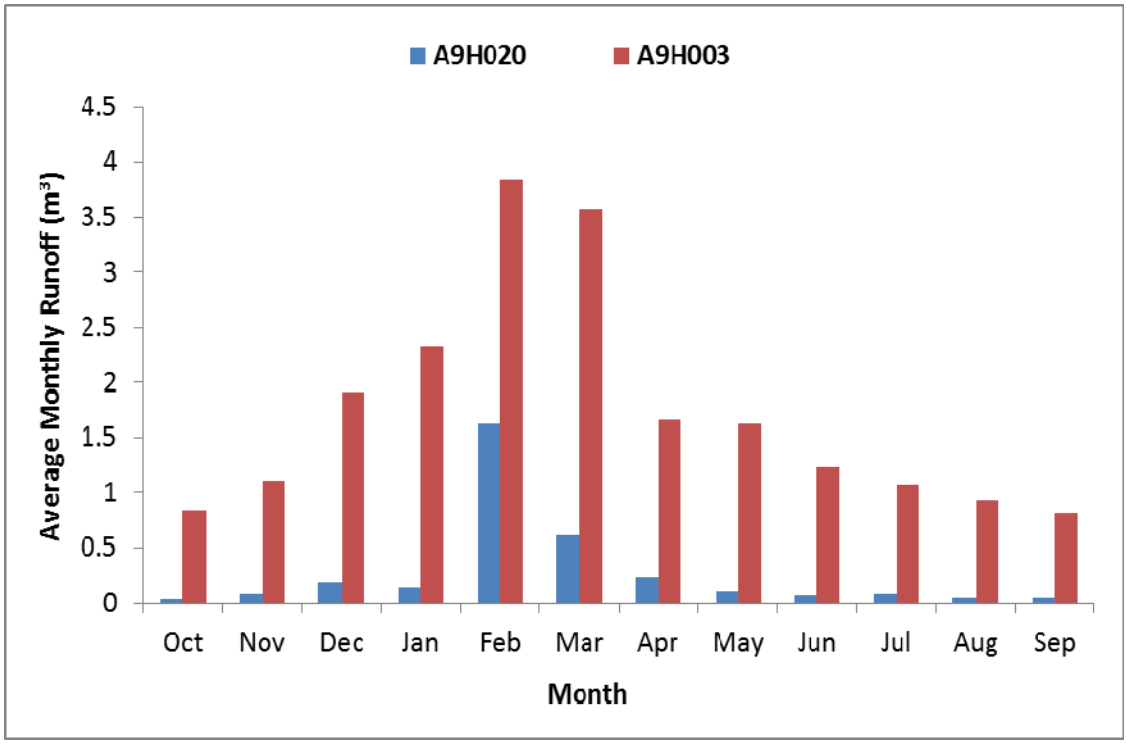

Figure 4.31: Average monthly runoff volumes for A9H020 and A9H003

In order to display a rainfall-runoff relationship in the sub-catchments, annual rainfall data was plotted against annual runoff data on a secondary axis. Sub-catchment A9H003 (Figure 3.6) was represented by Palmaryville rainfall station (Figure 3.4) as they fall within quaternary catchment (drainage region) A91G whereas sub-catchment A9H016 (Figure 3.6) was represented by Entabeni rainfall station (Figure 3.4), both under quaternary catchment A91D. It can be noted in Figures 4.32 and 4.33 that when rainfall is high at each sub-catchment, runoff also tends to be high. However, there were some cases where an increase in rainfall led to a decrease in runoff values. For example, the onset of rainfall trend at both sub-catchments and their corresponding rainfall stations started with an increase in rainfall and a decrease in runoff. Also, when rainfall peaked in 2005/06 hydrological year, runoff was at its lowest during that period. Notable was an increase in rainfall at Palmaryville and a decrease in runoff trend at its corresponding sub-catchment A9H003 between 2008/09 and 2009/10 hydrological years. This can be attributed to evapotranspiration and groundwater use which can result in a depletion or capture of both rain and surface water in a river catchment.

Average annual surface runoff during the 1960-1985 phase showed temporal variations. It can be noted from Figure 4.32 that average annual runoff trends at each gauging station varied from year to year and from place to place. The downstream catchment recorded highest runoff volumes than upstream catchments. Notable was the increase in runoff trends at A9H003 and A9H006 (Appendix 10) which were located downstream of the catchment. As shown in Figure 4.32, annual runoff for A9H003 downstream ranged from 4.95 m^3 to 38.9 m^3 during the 1960-1985 phase. A9H016 upstream had average runoff values of 1.10 m^3 to 6.15 m^3 revealing lesser runoff amounts. Appendix 10 shows unvarying trends at A9H015 and alternating trends at A9H017, A9H020 and A9H023 (Appendix 10) which were located upstream of the catchment was evident. Both trends revealed unimodal peaks centred around the hydrological year 1976/77 at A9H003 and A9H006; and hydrological year 1977/78 at A9H020; 1978/79 and at A9H016 and A9H023 respectively. During the dry periods of 1981/82 and 1982/83, stations A9H015 and A9H017 (Appendix 10) had record peak flow volumes while the rest of the catchment received little or no runoff.

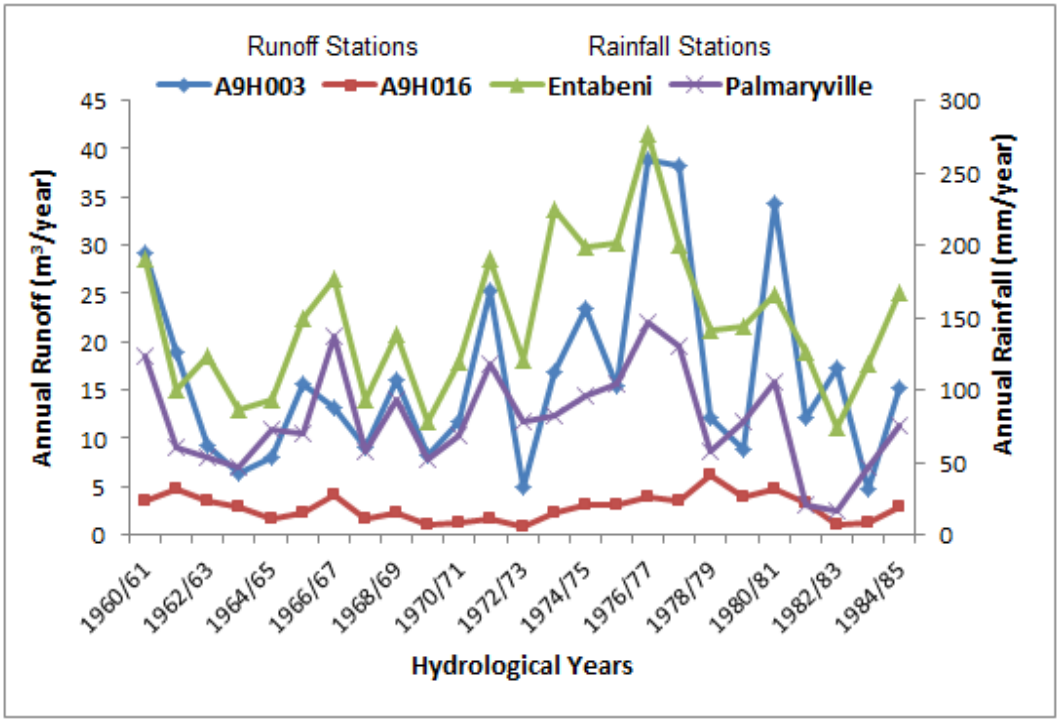

Figure 4.32: Rainfall-runoff trends upstream (A9H016 and Entabeni) and downstream (A9H003 and Palmaryville): 1960-1985 phase

Trends in surface runoff during the 1985-2010 phase shown in Figure 4.33 indicated an increase in runoff downstream of the catchment at A9H003, with lesser amounts upstream at A9H016. Appendix 11 shows that a hydrograph peak that lasted for about 5 years was evident upstream of the catchment at station A9H020. During this phase, the station recorded erratic runoff trend between 1995/96 and 2002/03. Highest flood peak were recorded during 1996/97 both upstream and downstream of the catchment. However, runoff trends downstream of the catchment revealed greater variability. Trends in surface runoff revealed unimodal flow peaks at different hydrological years. Such peaks were recorded during 1996/97 at A9H015; and hydrological years 1999/2000; 2001/02 at A9H016; and 2003/04 at sub-catchments A9H006 and A9H017 respectively, revealing temporal fluctuations in surface runoff in the study area.

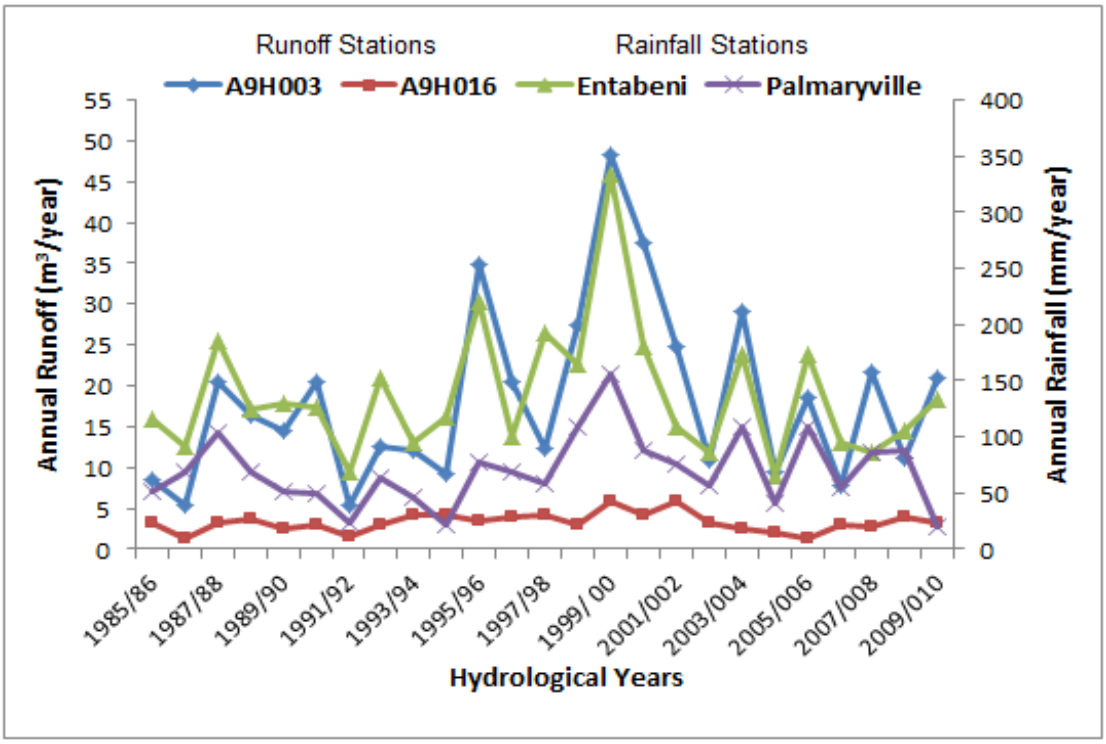

Figure 4.33: Rainfall-runoff trends upstream (A9H016 and Entabeni) and downstream (A9H003 and Palmaryville): 1985-2010 phase

General trend analyses during the wet (October-March) and dry season (April-September) in the catchment were as shown in Figure 4.34. Average daily runoff for the wet season during the

1960 - 1985 period was 5.03 m^3/day with a minimum flow of 1.02 m^3/day in 1983/84 hydrological year and maximum water discharge volume of 17.6 m^3/day observed in 1977/78 hydrological year. Average daily runoff during the dry season for the same period was 3.19 m^3/day with a minimum of 0.87 m^3/day in 1983/84 hydrological year and a maximum of 6.49 m^3/day in 1960/61 hydrological year. During the wet season when the area received abundant rainfall, the increase in runoff may have been due to the decrease in the amount of water available for evapotranspiration and infiltration, which are directly related to the health and presence of natural vegetation. Such increase in runoff volumes may accelerate channel erosion, degrade aquatic habitat, impair stream water quality, and increase the risk flooding and drought (Delidjakova *et al*., 2014). During the phase 1985-2010, observed runoff data in Figure 4.34 showed a reduction in runoff with maximum water volume of 12.8 m^3/day in 1999/2000 and 5.87 m^3/day in 2000/2001 hydrological years during the wet and dry seasons respectively. Human activities such as clearing of forest covers to give way to new activities such as agriculture and human settlements may lead to decreased infiltration of water and consequently higher runoff and increased peak water discharge following rainfall events and reduced runoff during dry seasons (Palamuleni *et al*., 2011).

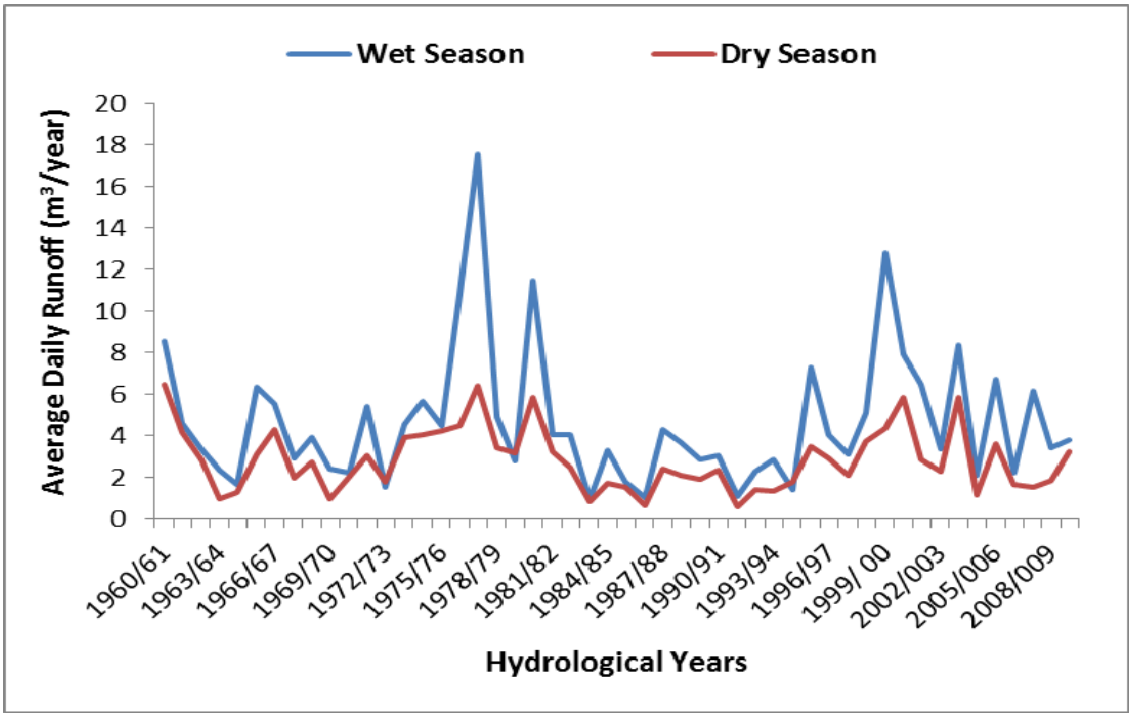

Figure 4.34: Average daily wet and dry seasonal runoff for the study area (1960-2010)

4.3.5 Runoff computation by Curve Number (CN) method

Curve number estimates for antecedent moisture conditions were obtained from standard curve number table (NRCS TR–55 Table: SCS, 1986) where estimates for agricultural land use were used and later adjusted into AMC III, prevalent during floods. The Curve Numbers for different soil groups and land use at each sub-catchment were as shown in Table 4.6.

Table 4.6: Curve Numbers for different sub-catchments

Q_{catch}	Sub-catchment	Land Use	Soil Group	Curve Number	Weather Station
A91A	A9H017	Cultivated Agricultural Land	A	67	Nooitgedacht
A91D	A9H015	Cultivated Agricultural Land	A	67	Entabeni-Bos
A91D	A9H016	Built-up Settlements	A	74	Tsianda
A91F	A9H001	Residential and Cultivated Land	B	83	Elim-Hosp
A91G	A9H003	Degraded, Forest	A	30	Palmaryville
A92A	A9H004	Built-up Settlements	A	74	Rambuda

Figures 4.35-4.38 show the observed daily rainfall and runoff depths in comparison with simulated daily runoff volumes performed by the SCS-CN method for 1960-1984 and 1985-2010 periods at different sub-catchments within the study area. Observed runoff depths were calculated using daily stream flow data at each sub-catchment. Appendices 12 and 13 show simulated and observed daily runoff volumes at different sub-catchments within the study area. The CN number method was used autonomously outside SWAT model to generate surface runoff and investigate the impact of land use change on runoff under historical land cover regimes. This approach (also described in SWAT model documentation) was based on converting the CN2 (AMC II) value in CN3 (AMC III) values using equation 2.18 described in this study. The SCS-CN model gave values of different runoff volumes close to the observed ones. During the study period, cultivated land upstream at sub-catchment A9H017 produced peak flood volumes of 127.3 mm/day in 1971 and 229.1 mm/day in 2000 during the two periods. Degraded and forested area downstream at sub-catchment A9H003 produced peak flood volumes of 135.7 mm/day in 1961 and 87.3 mm/day in 2004 respectively. Residential and cultivated areas at sub-catchment A9H001 produced peak flood volumes of 117.1 mm/day in 1967 and 343.7 mm/day in the year 2000 respectively; while built-up areas at sub-catchment A9H004 produced peak flood volumes of 95.9 mm/day in 1981 and 280.9 mm/day in 2000 during the two periods (Appendix 12). The runoff depths increased abundantly during the 1985-2010 period. Although

the simulated runoff volumes are higher than the observed ones, it is not all runoff that reaches the catchment outlet, as a fraction of it is trapped by wetlands, ponds, or infiltration. It should be noted that runoff calculated from the CN number method gives higher values than observed runoff and stream flow. It could be seen from simulated runoff and rainfall that there was a strong relationship between rainfall and runoff in the catchment. Notable was the increase in both runoff and rainfall during the phase of 1985-2010. Drier areas of a catchment are widely identified by lower CN values (Suprit *et al*., 2012). Shi *et al*. (2001) regards land use condition as an important factor to influence the storm-flood process including surface runoff formation and concentration. A study by Merz and Blöschl (2009) showed that runoff coefficients vary in space depending on the long-term controls such as climate and catchment information. They also vary in time depending on event characteristics such as antecedent soil moisture condition (AMC) and rainfall depth. The AMC for the study area ranged from 72.90 mm to 201.69 mm; high enough to represent the high runoff potential of the catchment.

Figure 4.39 shows a comparison of observed and simulated flows based on linear regression with indicated values of the y-intercept and coefficient of determination (R^2). The R^2 measured the linear dependence of observed and simulated values, where a positive R^2 indicate satisfactory results. The values of R^2 were found to range from 0.001 to 0.019 reflecting a poor linear relationship between the observed and predicted values based on daily simulations as shown in Appendix 13. This may be attributed to small differences in the timing of observed and simulated hydrographs likely to occur when using daily rainfall data. It must be noted that the daily simulations do not provide values that are expected to compare reasonably well with the predicted ones.

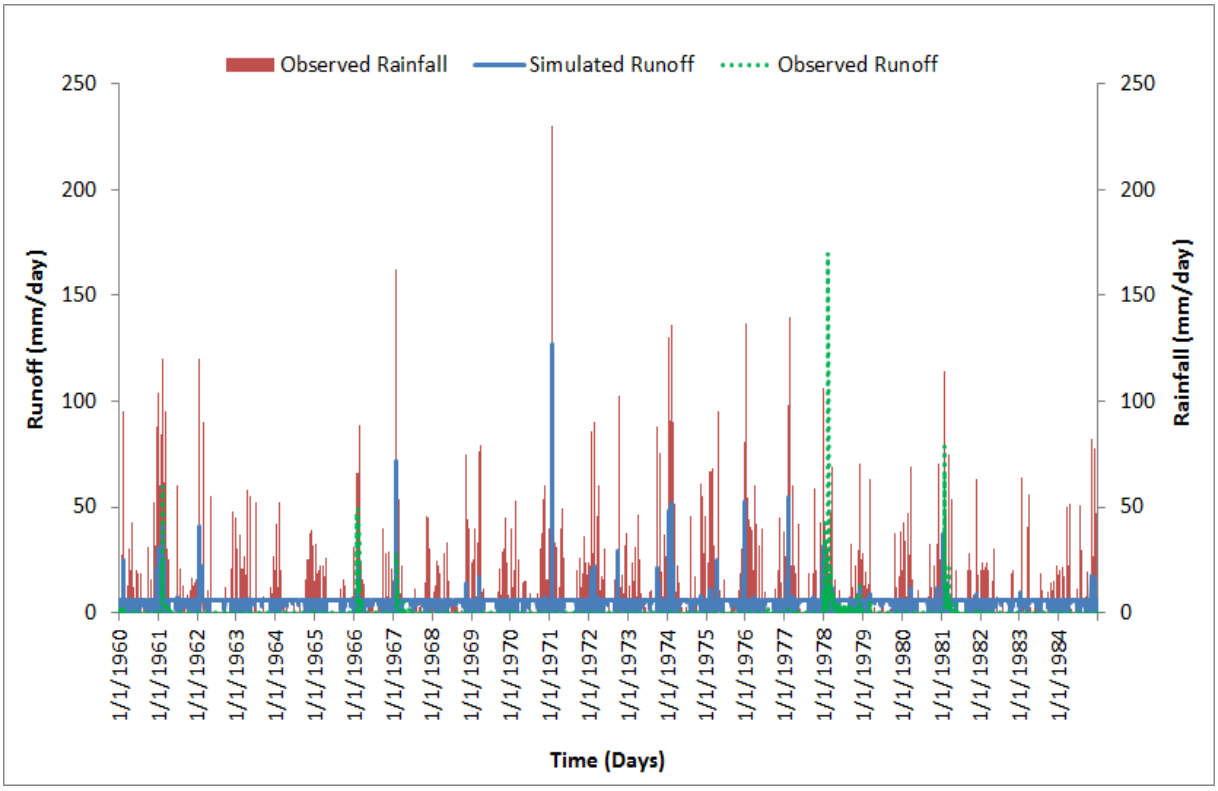

Figure 4.35: Observed and simulated runoff upstream in comparison with rainfall at A9H017: 1960-1984

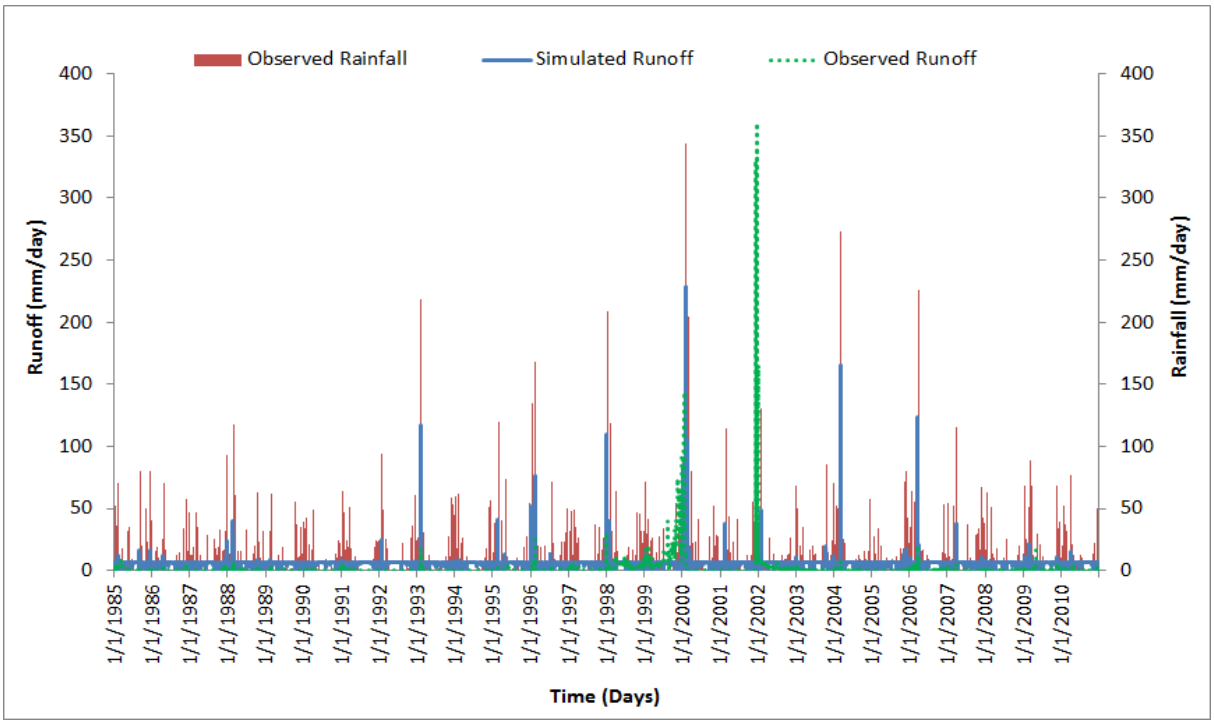

Figure 4.36: Observed and simulated runoff upstream in comparison with rainfall at A9H017: 1985-2010

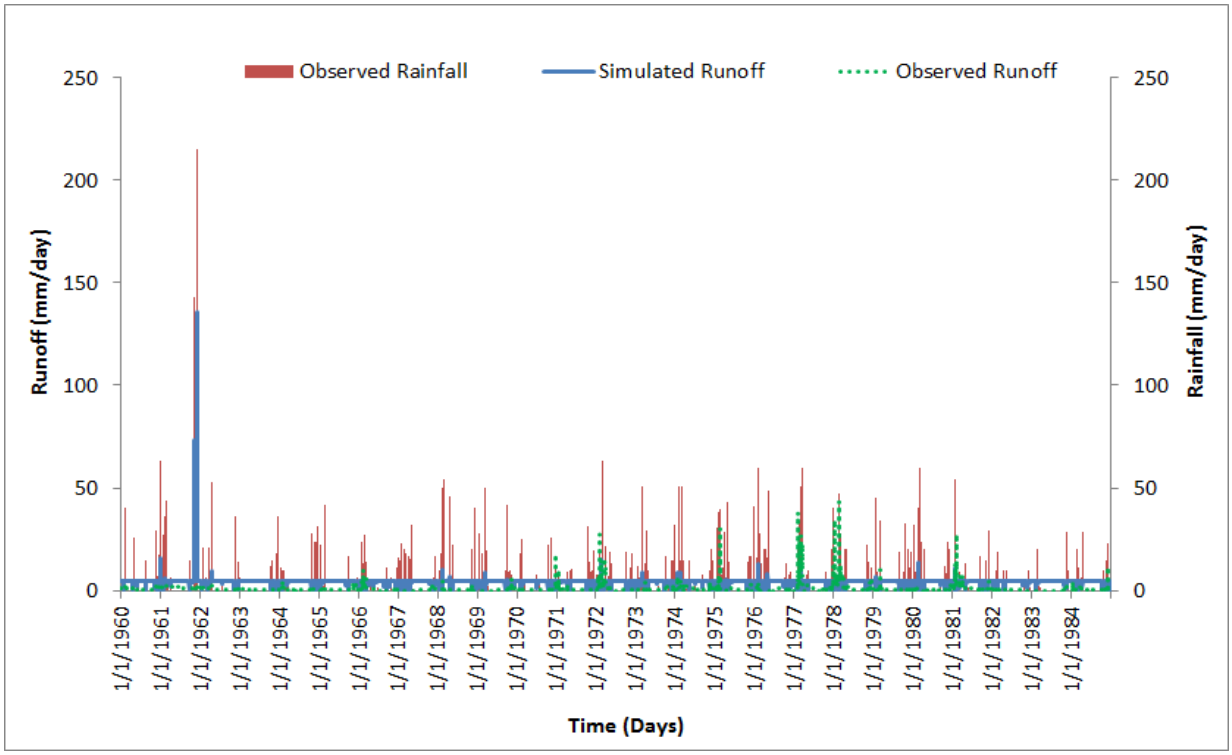

Figure 4.37: Observed and simulated runoff downstream in comparison with rainfall at A9H003: 1960-1984

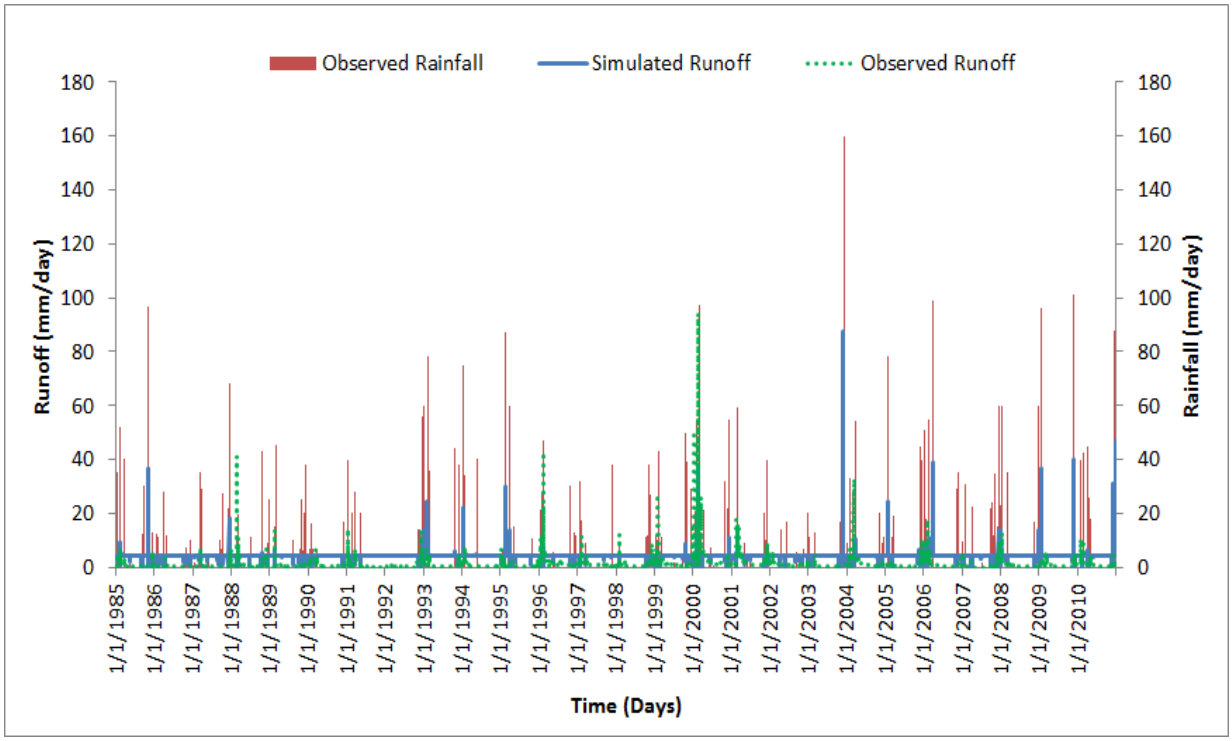

Figure 4.38: Observed and simulated runoff downstream in comparison with rainfall at A9H003: 1985-2010

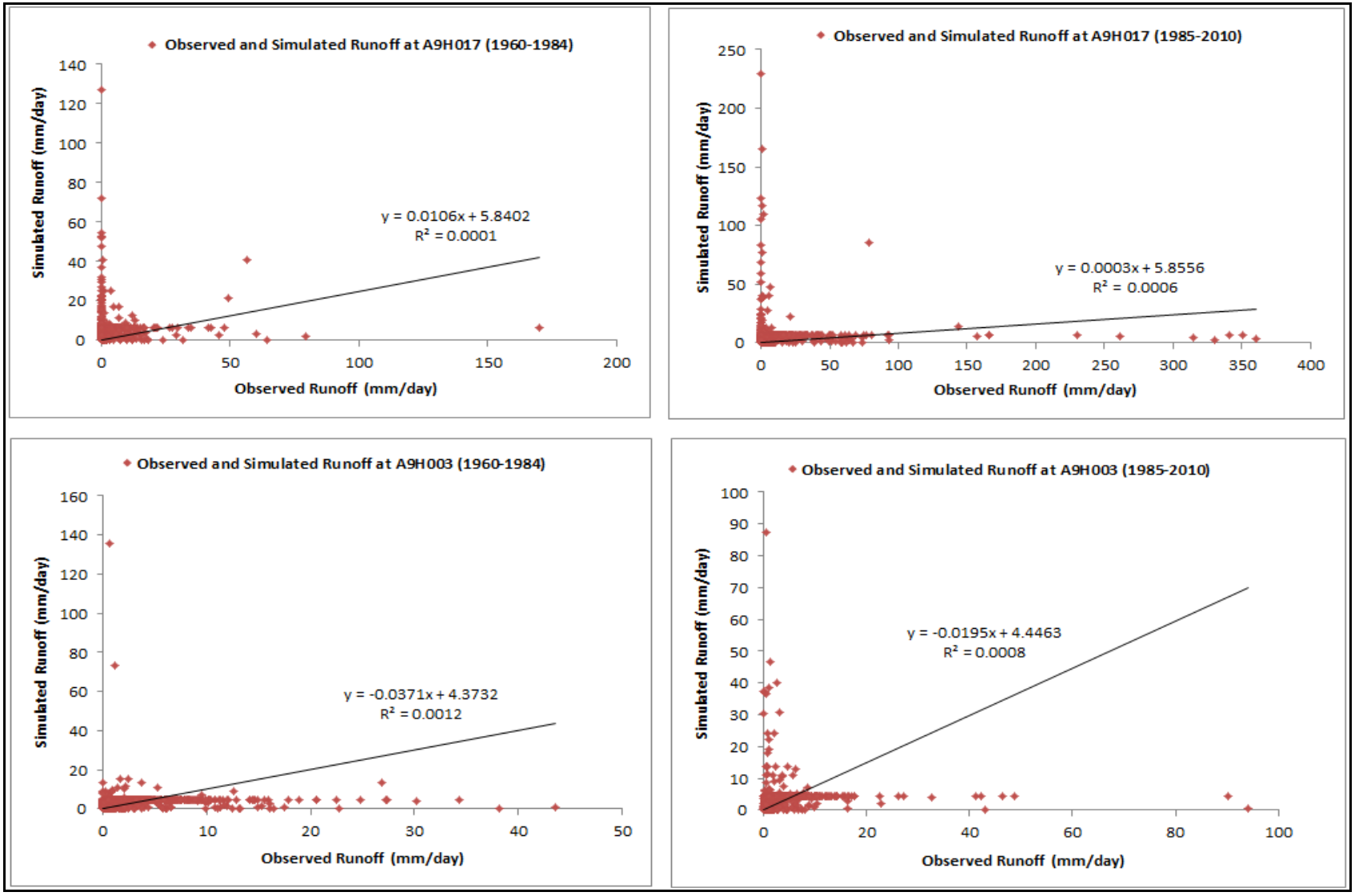

Figure 4.39: Comparison of observed and predicted mean daily runoff upstream (A9H017) and downstream (A9H003)

To relate the amount of rainfall or storm water that appears as runoff from a surface, runoff coefficients were calculated following the rational method by dividing stream flow and rainfall. The changes in the runoff coefficients during the study period were noted in all sub-catchments. High runoff coefficients ranging from 0.1 to 0.68 were noted at sub-catchment A9H003, which is located in the downstream of the catchment. Degraded areas, such as sub-catchment A9H003, were characterised by low infiltration capacity, high runoff coefficients and high stream discharges. High runoff coefficient values are an indicator of flash flooding in an area during storms as water moves fast overland (Merz and Blöschl, 2009). The California Environmental Protection (CEP) (2011) noted that areas with permeable soils, flat slopes and dense vegetation have low runoff coefficient values. This was concurrent with the results of this study as the area was mostly dominated by relatively flat slope and dense vegetation resulting in low runoff coefficients in some areas. Such evidence was noted at sub-catchment A9H016 located upstream, which recorded low runoff coefficient values ranging from 0.01 to 0.06. A decreasing trend was noted at sub-catchment A9H017 with a mean value of 0.05. Vegetation is important, not only because it determines evapotranspiration losses from the basin, but also because it can be an important control on slowing runoff (most evident in forested versus non-forested slopes) to the river channels. Vegetation amount and type within the channels may also exercise an important control on the efficiency of stream flow.

Though the SCS-CN method is widely used for estimating floods on small to medium-sized catchments, it has limitations that need to be evaluated whenever the method is used. Some of the limitations include:

i) The SCS-CN equation predicts decreasing runoff for increasing rainfall for low values of precipitation. However, this situation rarely occurs when the method is used to model cumulative runoff since the accumulated amount typically exceeds a few millimetres in value.
ii) The basic assumption of the SCS-CN method is that, for a single storm, the ratio of actual soil retention after runoff begins to potential maximum retention is equal to the ratio of direct runoff to available rainfall.
iii) The equation does not contain an expression for time and, therefore, does not account for rainfall duration or intensity

vi) Curve Numbers describe average conditions that are useful for design purposes. If the rainfall event used is a historical storm, the modeling accuracy decreases.

4.3.6 Average Stream Flow

Eight gauging stations with a 50-year record of stream flow data were used to estimate average stream flow for the study area. Figure 4.40 shows the distribution of average stream flow upstream (A9H020) and downstream (A9H003) of the catchment. The results showed that flow in the catchment was highly variable during the month of February with records of 0.68 m^3/s and 1.75 m^3/s respectively. Lesser flow records were evident upstream, while high flows were experienced downstream. There was a notable shift in the seasonality of LRC stream flow over time, with a detectable positive trend in mid and late summer (December to April) and negative trend in winter (May to September).

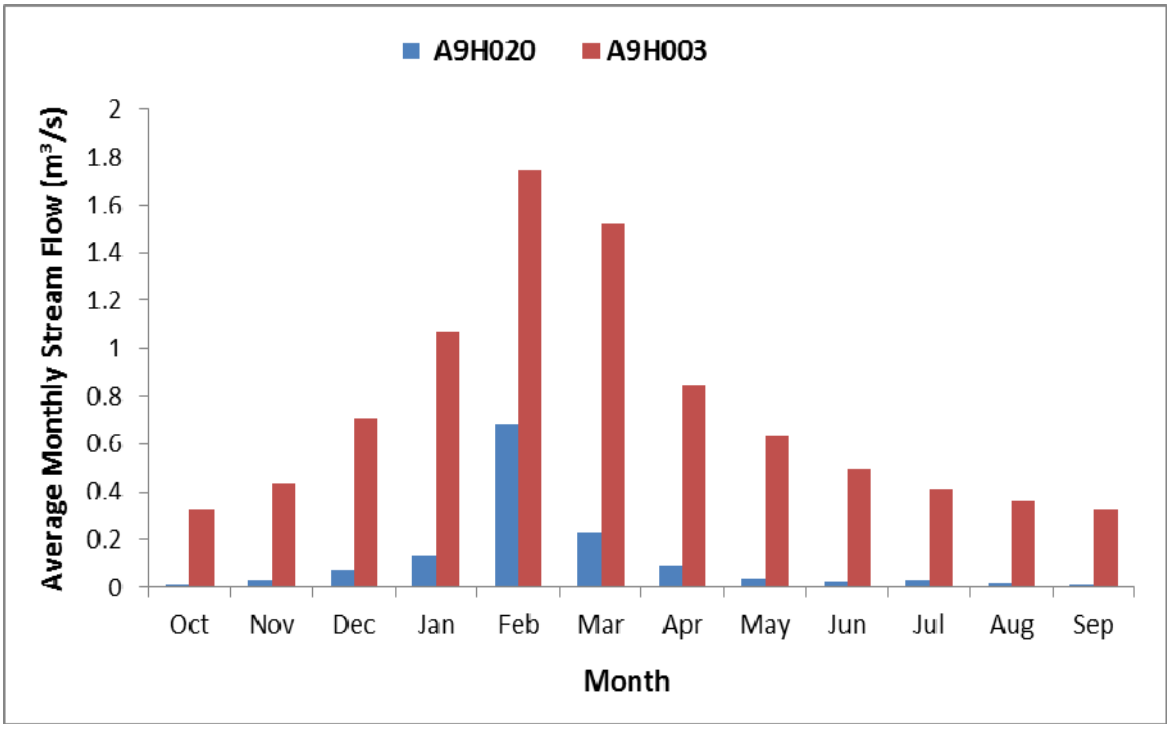

Figure 4.40: Average monthly stream flow for A9H020 and A9H003

Stream flow patterns in the catchment showed temporal variations upstream at A9H023 and downstream at A9H006 as shown in Figure 4.41. Stations A9H023 and A9H006, which are

located closer to A9H020 and A9H003 were adopted for this comparison as they showed clear trends. During both periods, discharges at upstream were generally less than the discharges downstream, however, sometimes the flows upstream was greater downstream as shown in appendix 14 and 15, revealing contrasting trends. Appendix 14 shows the annual stream flow trends for different gauging stations in the catchment during the 1960-1985 phase. Notable was the increase in discharges at sub-catchment A9H006; a slight increase in flows at sub-catchments A9H001, A9H015, A9H016; and lesser amounts in flows at A9H017, A9H020 and A9H023. Both revealed unimodal peaks centred around 1976/77, 1977/78 and 1978/79 except for stations A9H015 and A9H017 whose peaks centred on hydrological years 1981/82 and 1982/83 respectively. Sub-catchment A9H001 recorded high flows ranging from 0.38 to 22.7 m^3/s while other stations recorded 0.01 to 2.47 m^3/s. Appendix 15 shows stream flow trends for various sub-catchments during the 1985-2010 phase while Figure 4.42 shows the annual variation of stream flow during the 1985-2010 phase. During the second phase of 1985-2010, trends indicated an overall increase in stream flows at sub-catchments A9H001, A9H003, A9H006, A9H016 and A9H020 stations with unimodal flow peaks centred around 1999/2000 hydrological year except for A9H015, A9H017, and A9H023 whose peaks were observed during 1996/97, 2003/04 and 2005/06, respectively. These gauging stations show contrasting trends in stream flows. As streams are fed by runoff from rainfall events, it can be seen from the preceding section of runoff graphs that in years where runoff was high, stream flow trends were also high. The variation in stream flow peaks in the catchment could be attributed to the intensity and duration of rainfall events, including anthropogenic activities and impoundments, such as removal of alien vegetation which was initiated in 1995 in the catchment by DWA as well as deforestation for RDP settlements which began in 2000. A study by Chunzhen (2009) noted that detection of a trend in a hydrological time series are much more difficult because changes in runoff are affected not only by rainfall, but also by non-climate factors, such as increases in water use and water consumption resulting from population growth, economic development, and changes in land use and land cover. The large stream flow variation at A9H001 during the 1960-1985 phase was impacted upon by construction of Albasini dam, which was raised in 1970/71. Construction often involve removing vegetation and soil, these activities tend to accelerate runoff to streams, thereby increasing the flows. As a result of forest clearing, more runoff and high rates of stream flow were generated as more areas were left bare or covered with impervious materials. Since

1995, DWA started an initiative called Working for Water Programme (WWP) where a large fraction of the ground was left bare or covered by pavements resulting in high runoff and stream flow rates, giving rise to built-up areas and agricultural development.

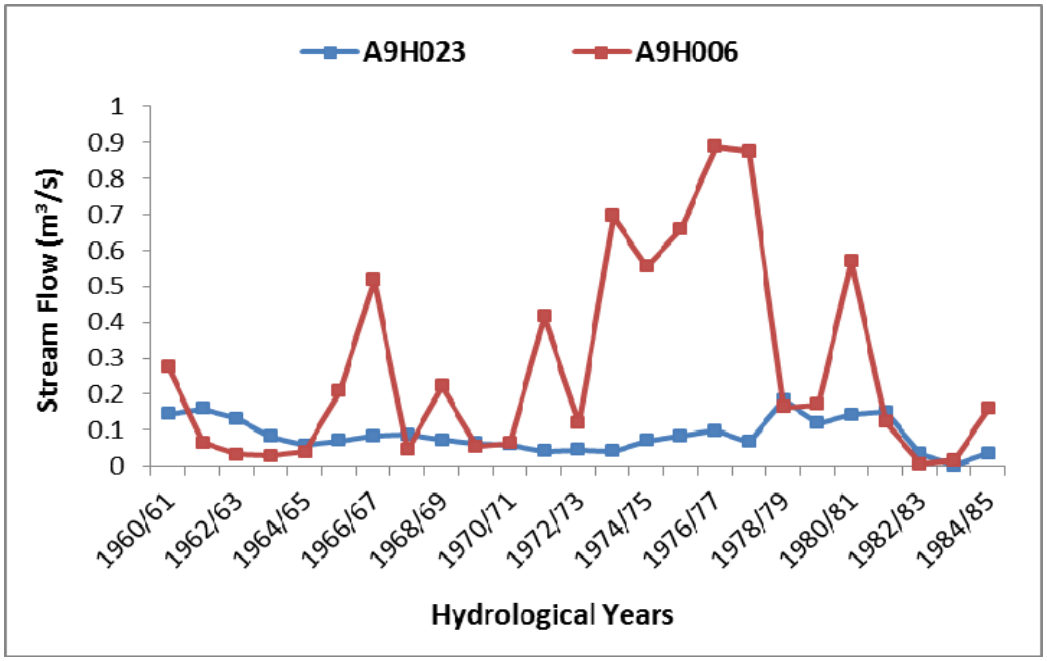

Figure 4.41: Stream flow trends for A9H006 and A9H023: 1960-1985

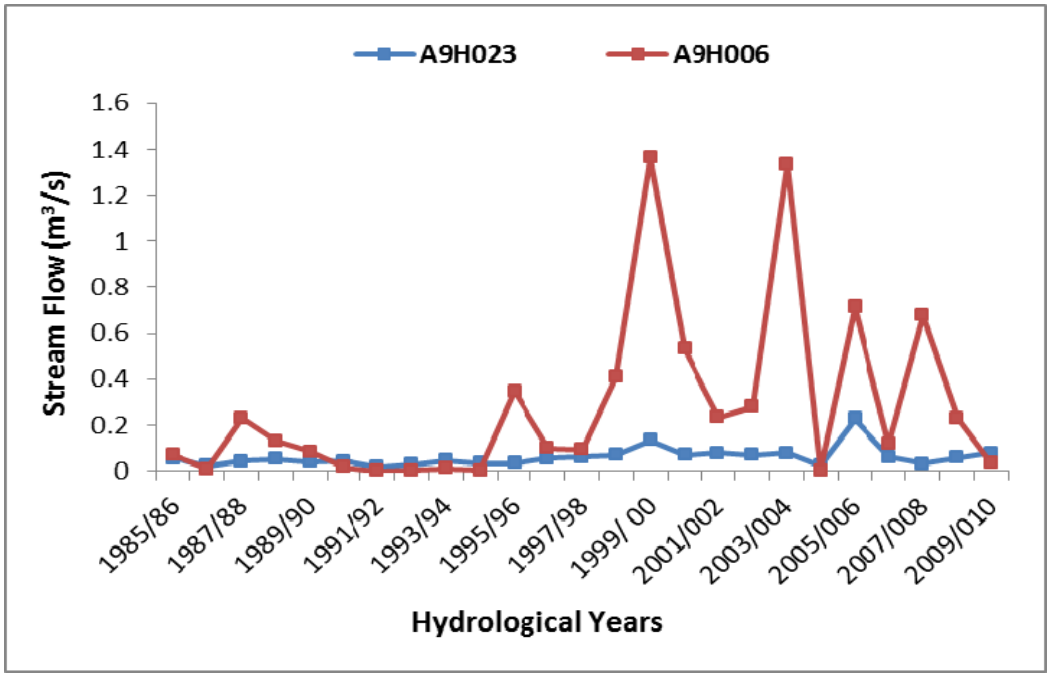

Figure 4.42: Stream flow trends for A9H006 and A9H023: 1985-2010

General stream flow trend analyses during the wet (October-March) and dry season (April-September) in the catchment were as shown in Figure 4.43. Stream flow trends for the 1960-1985 phase shown in Figure 4.43 revealed a long-term wet seasonal mean of 10.0 m^3/s with a minimum flow of 0.67 m^3/s in 1983/84 and a maximum flow of 36.8 m^3/s in 1976/77 hydrological year. Average stream flow during the dry season was 5.58 m^3/s with a minimum of 0.80 m^3/s in 1983/84 and a maximum of 15.9 m^3/s in 1976/77. During the phase of 1985-2010, stream flow tended to increase. The wet seasonal flow showed a long-term average flow of 7.63 m^3/s with a minimum flow of 0.64 m^3/s in 1991/92 hydrological year and a maximum flow of 19.9 m^3/s in 1999/2000. During the same period, dry seasonal stream flow received a yearly average of 4.0 m^3/s with a minimum of 0.25 m^3/s in 1991/92 and a maximum of 3.31 m^3/s in 1999/2000. It could be concluded that summer rainfall was the main driver of responses in stream flow, over time and space at different sub-catchments. Davies and Day (1998) maintained that South African rivers experienced high water recharge during the summer rainfall season, resulting in abnormal stream flows. However, much of the summer rainfall recharges the groundwater reservoir and is not lost to the system but feeds the rivers during the winter period of water deficit.

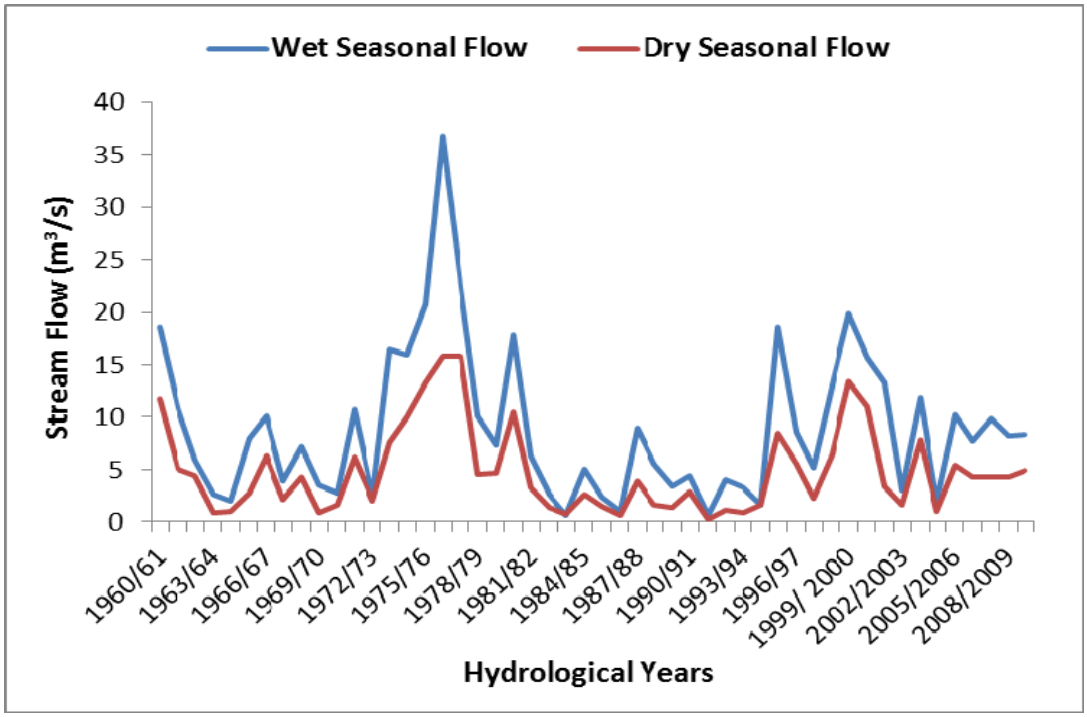

Figure 4.43: Average wet and dry seasonal stream flow for the study area: 1960-2010

Schulze (2008) presented the maps of stream flow variations in South Africa over a 50 year period (1950-1999). The images in Figure 4.44 showed that stream flow in the country was highly variable, with the highest annual flows ranging from less than 10 to 300 mm. The coefficient of variation however, ranged from <50 to <150 % of the annual total variations. Luvuvhu River catchment on the north-eastern corner of the country showed greater stream flow variability. Alemaw *et al*. (2006) and Chiew and MacMahon (2002) found that the variability of stream flows in southern Africa could be associated with the regional and global weather phenomenon. For example, a decline in stream flow regime could be associated with drought related phenomenon while a rise in stream flow regime is associated with flood-related phenomenon. Past studies such as those of Singo (2008) and Reason *et al*. (2000) have found interactions between El Nino Southern Oscillation (ENSO) cycles and stream flow trends. Other studies have found the ITCZ as being the regional driver of increased flow in many catchments.

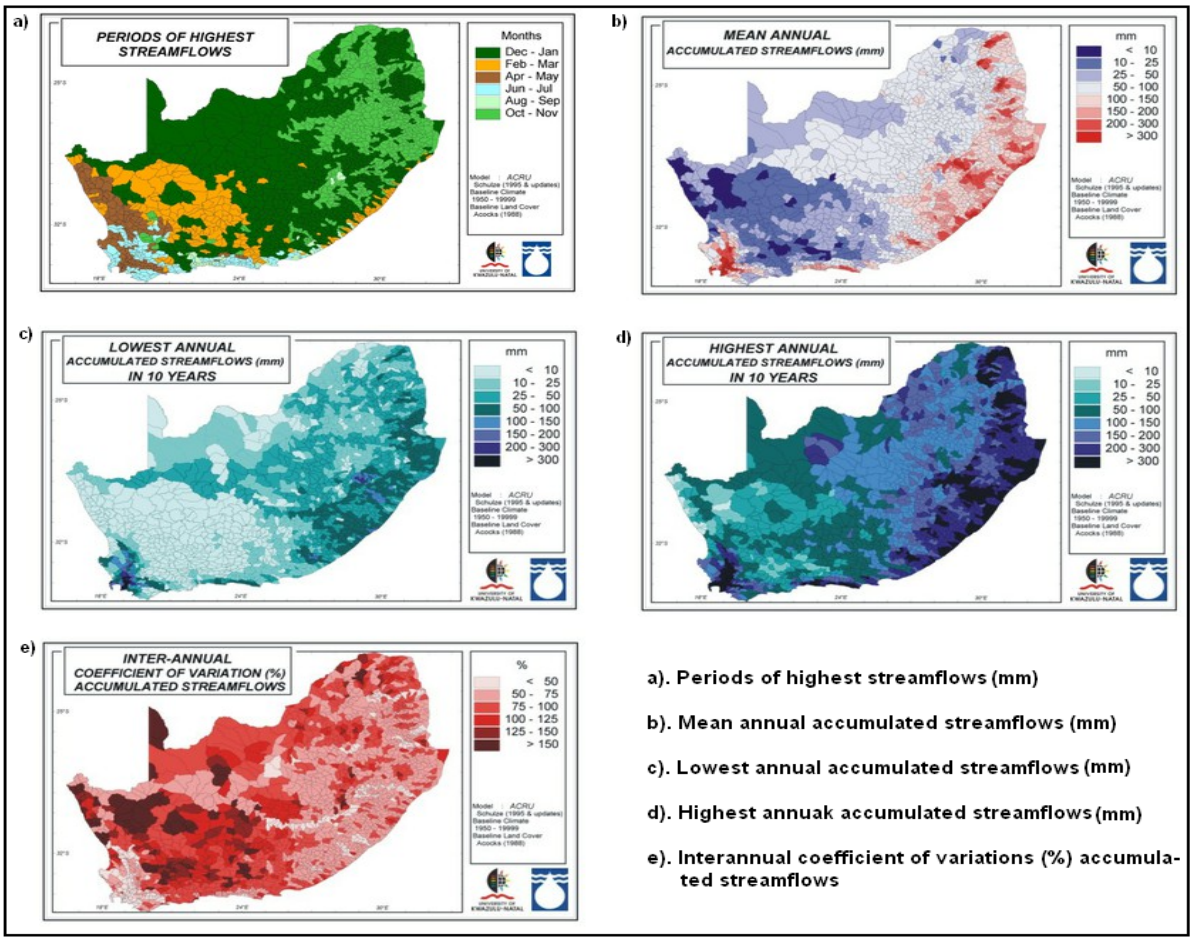

Figure 4.44: Stream flow variations in South Africa (Source: Schulze, 2008).

4.3.7 Dam Capacity Analysis

For each station, average dam water levels were calculated from October of one year to September of the following year. Figure 4.45 showed that the area experienced high dam water levels of ≥29 meters from October to September at Nandoni dam (A9R004) while lesser averages of ≥12 meters are highly visible at Albasini dam (A9R001). Vondo dam (A9R002) received minimum average dam water levels of 25 meters. Results of dam water levels show that the area has high water levels in dams from late February to September with a peak in either March (A9R002) or April (A9R001 and A9R004). Since 1960s, dams, together with water abstraction have been blamed for drying rivers in the LRC. For example, during the drought of 1991/1992, Luvuvhu River at Pafuri dried for 10 months and approximately 50% of outer riparian zone trees died. Such alterations have impacted on ecological community and threatened human communities (Griscom *et al.*, 2010). Dams, together with rapid socio-economic developments have also been blamed for flooding and widespread of diseases in the LRC. In the summer rainfall season of 2013, Nandoni Dam overtopped its banks and flooded the riparian zones causing malaria as well as deaths of fauna and flora.

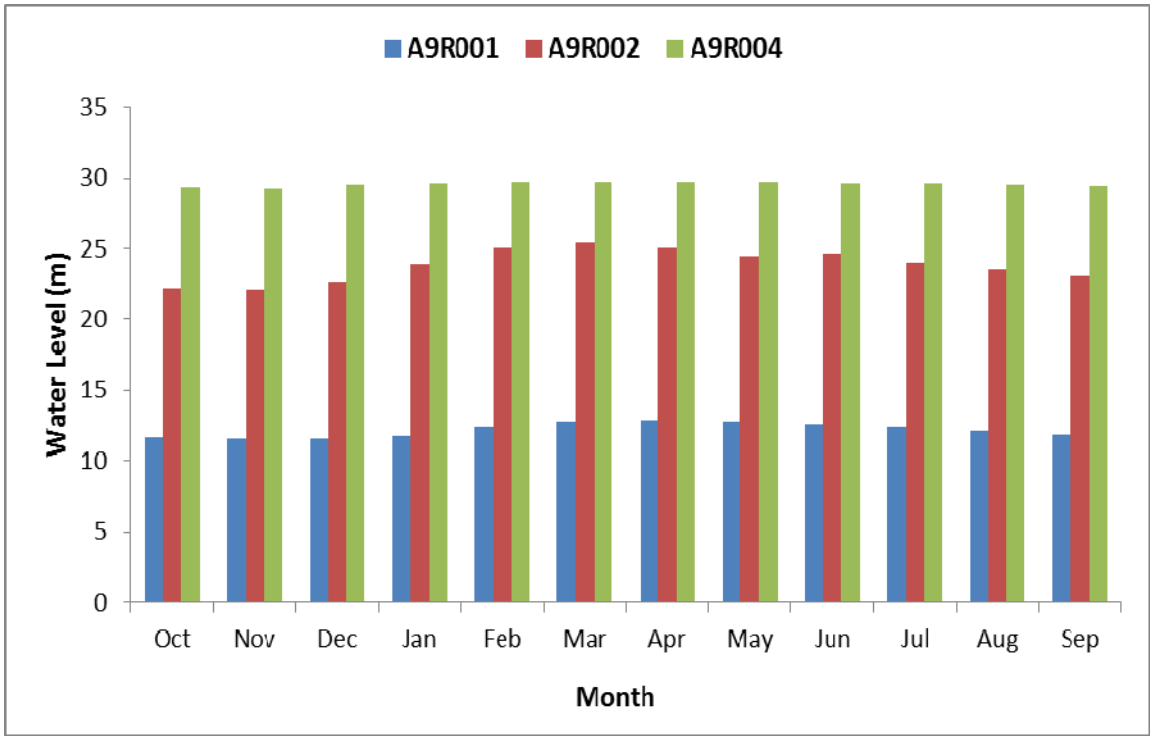

Figure 4.45: Monthly fluctuations of water levels at Albasini (A9R001), Vondo (A9R002) and Nandoni (A9R004) dams

This study used multitemporal Landsat images to evaluate the effects of land cover changes on dam water levels in the catchment. Landsat images used to assess the effects of land cover changes in LRC detected significant changes in dam water levels. The 1986 images showed that there was no support for ecological flow in the catchment and rivers may have been drying until the completion of Nandoni dam in 2005. By the end of 2008 high changes in dam water level could be seen as in Figure 4.46. The dam is well managed and now supports ecological flows in the catchment, and stores some of the water from the Luvuvhu River which is used for irrigation in the commercial farming industry.

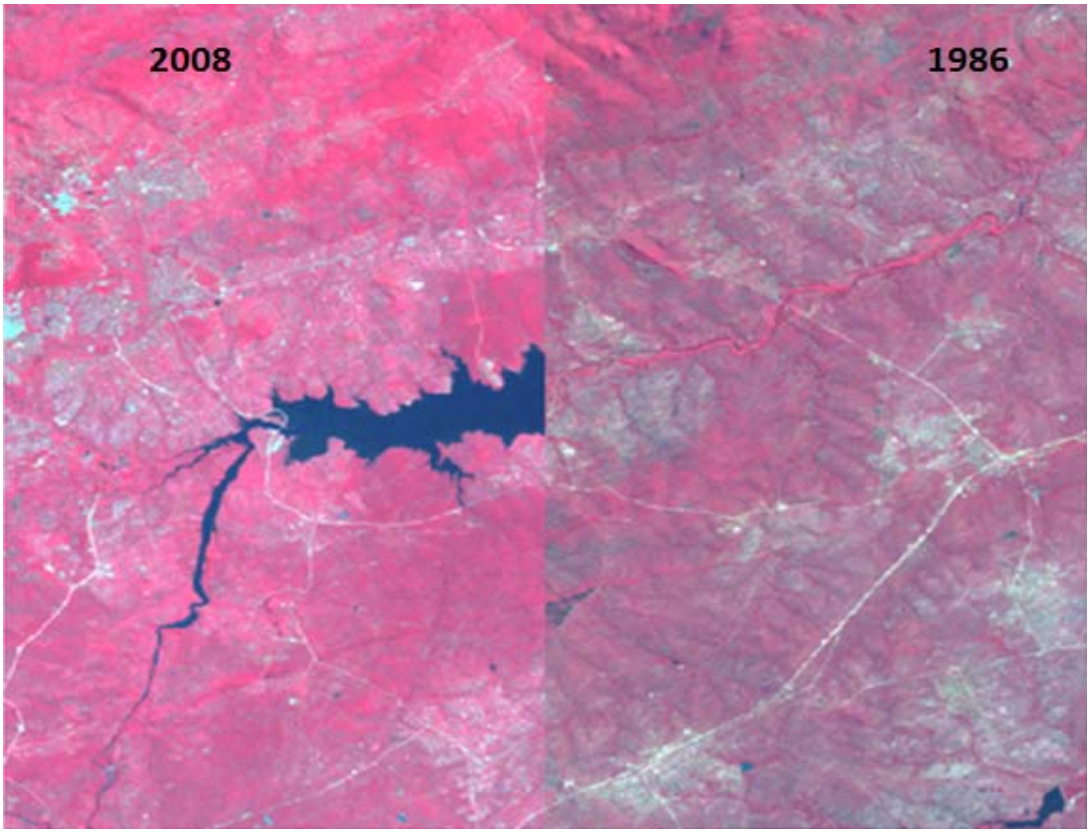

Figure 4.46: Land cover change before and after Nandoni dam was built

4.3.8 Mass Curve Analysis

To assess the impact of land use/cover change on water availability, a mass curve analysis (MCA) was used to estimate the reservoir storage-yield in the study area. The 1993-2010 Space-Time Research population data for the study area was used to estimate water demand in the

catchment. The data was obtained from Statistics South Africa (Stassa) in Pretoria. The villages rely heavily on water from Vondo, Nandoni and Albasini dams. Figure 4.47 showed that the highest average population in an area could be quite high as was the case for Shayandima where it stood at 15 379.

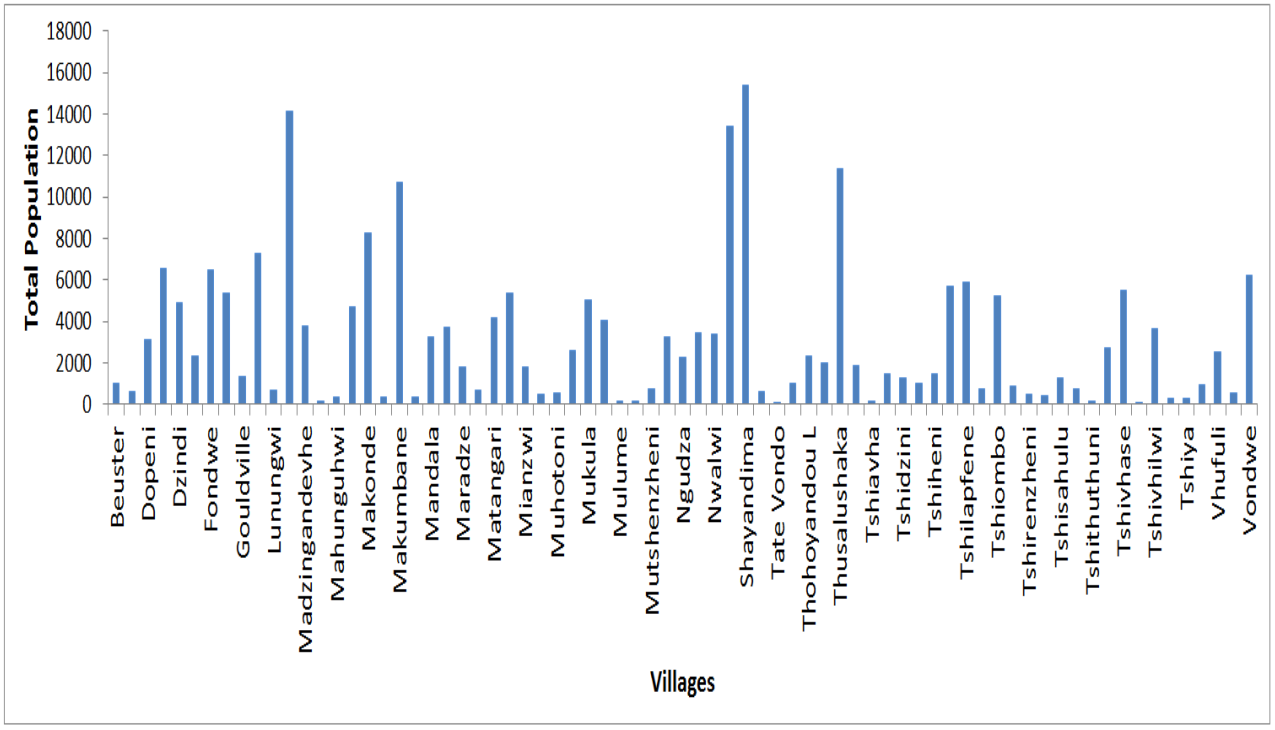

Figure 4.47: Total population by villages

As the dams are central to human population growth and technological innovation in the catchment, it was important to link the population data to land use/cover impacts which may threaten the future sustainability of water demand in the catchment. For example, Nandoni Dam was supposed to bring water to villages outside Thohoyandou in Limpopo's Vhembe district, but 10 years after being completed, human activities such as fishing, bathing and washing of cars were profiting the rich rather than the dam being used as a water source for the poor. Riparian vegetation was removed and the dam's serene banks were dotted with state-of-the-art houses and guesthouses under construction. In areas where riparian vegetation was removed, flood events accelerated bank and donga erosion. Clay soils were removed from the riverbank for use in brick manufacturing. These pressures were damaging the channel banks and impacted on the water

quality. There may be problems with water supply at the moment, but to date, there is a purification plant right next to the dam that supply villages that are located close to the dam with portable water.

Figure 4.48 showed the storage-yield relationship formulated from mean daily stream flow for Nandoni dam. Combined daily flows from selected gauging stations were used to determine storage capacity of the quantity that the reservoir must hold to meet the demand. The figure showed that about 226 545 m^3/day storage capacity is required to meet the water demand in the study area. This is evident in Figure 4.48 where a storage capacity was noted from the onset of rainy season to mid-summer season. In order to meet basic water demand for the increasing human population in the catchment, 50 litres of water per day per capita should be recommended as it will greatly enhance people's lives. Uniform demand could be assured for water resource utilisation like domestic water supply and irrigation.

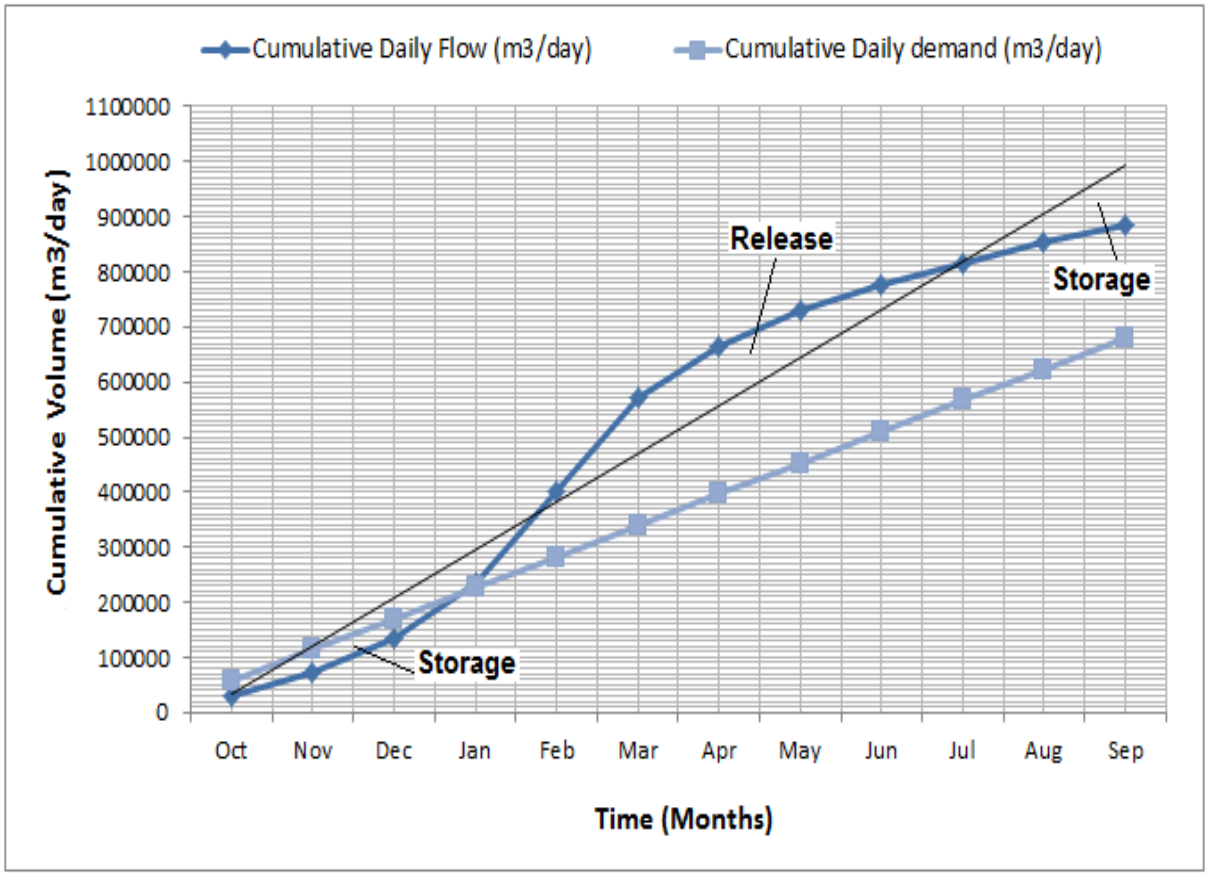

Figure 4.48: Mass curve for Nandoni dam

In the study area the maximum and minimum river flows occur in summer (October-March) and winter (April-September) respectively, with the peaks in mid-summer months (December-January-February). Winter flow is low as a result of little or no rainfall, such that the precipitation is either retained as fog. As shown in Figure 4.48, it is therefore important for the water storage in the dam to be implemented during the onset of the rainfall season when agricultural activities are being practiced. The release in the dry period will be able to sustain the water demand needed for other activities such as construction. As the population in the catchment is growing rapidly, the demand is growing for people wanting to build holiday houses near the banks of the dam, and people are losing agricultural lands in the process. People should be trained to limit land use practices especially during the onset of the rainfall season in order to prevent water pollution and scarcity. Storage of water and capture of sediment by dams can cause profound downstream changes in the natural patterns of hydrologic variation and sediment transport, including distribution of diseases and reduction in riparian species. Figure 4.49 further shows an aerial view of Nandoni dam overflowing and its surrounding Thohoyandou villages. Due to rapid land use, slope, and soil type, the dam is meandering, posing potential threat to humans and livestock. Rapid land use activities (such as rapid increase in housings) and erosion of soils are also posing threat to the water quality of the dam. These degradations are of concern as the alterations have changed the morphology and natural dynamics of dam which is used to provide inflow for use during dry periods as well as controlling flooding during the wetter periods. Ahmed and Fawzi (2011) noted that the conditions of river meandering and the associated processes of erosion and deposition accelerated with human activities may lead to the reduction of agricultural lands and loss of property as well as navigation problems. Effective and sustainable management of the dam is therefore crucial for economic development and alleviation of poverty.

Figure 4.49: Nandoni dam overflowing (Source: Wikipedia, 2009)

4.4 Suspended Sediment Analysis

4.4.1 The Grab Sample Analysis

Analysis of suspended sediments on rainy days showed that sediment concentration in rivers tended to increase with the rainy season. The highest concentration of sediment transported in streams was at Mutshindudi River at Dzingahe, Mutale River at Thengwe, and Luvuvhu River at Mhinga. The results showed that suspended sediment accumulations ranged from 0.01 to 0.33% as shown in Table 4.7 and Figure 4.50. This indicated that less than 1% of the sediment mobilised by erosion was subsequently deposited within the streams. During the onset of rainfall season, soil particles tended to become loosely attached to each other and were more erodible resulting in high chances of detachment and transportation in streams leading to high sediment concentrations. The months of November and December which exhibited a tremendous increase

in sediment concentrations were dominated by rainfall associated with tropical circulation features. These features are much more prevalent over South Africa during the early summer months of November and December (Dyson and Van Heerden, 2002). Hejduk and Banasik (2010) noted that intensive suspended sediment transport to rivers occurs mainly during flood runoff, caused by heavy rainfall events, leading to an increase of suspended sediment concentration. Such increase has a negative influence on biological life in river, on economic use of water and on recreation conditions of reservoirs.

In the study area no historical record on suspended sediment discharge data was available. The Department of Water and Sanitation (DWAS) had not been keeping records of sediment surveys in rivers across the catchment. As a result, sediment discharge samples used in this study were collected during surveys in various rivers (Figure 3.7) from 2011 to 2012, during rainy and non-rainy days. Samples were analysed for suspended sediment loads and concentrations. Lack of sediment data in the catchment enforced Gerber *et al*. (2015) to survey the Luvuvhu, Letaba, and Oliphants River Catchment to collect sediment samples during low and high flow periods from 2009 to 2011. Regrettably, their aim was to assess and monitor the quality of sediments in the rivers, and to determine the concentrations and distributions of metals in surface sediments of the selected rivers within the Kruger National Park (KNP) area. They found that the Luvuvhu River at KNP had low to medium percentage organic matter found in sediments in 2009, moderate to low organic content in 2010, and low to high levels of organic content in 2011. In their 2009, 2010, and 2011 surveys, the river was dominated by medium, large grain size, and fine sand to mud respectively. Their comparisons made with Oliphants and Letaba Rivers agree with Angliss *et al*. (2001) that the Luvuvhu River is considered to a lesser extent to be impacted by sediment pollution resulting from human activities in terms of its water quality. Both the Oliphants (urban, agricultural, industrial and mining), Letaba (subsistence farming, urban, deforestation, sand mining and overgrazing) and Luvuvhu (mostly agricultural and forestry practices, with fewer mining impacts and urban impacts limited to rural settlements) Rivers were found to be impacted upon upstream of the KNP by various human activities. Luvuvhu Rivers (post-high flows) had the potential to become highly contaminated because of the dominance of small grain size sediment particles and higher organ content deposited during the high flows of 2010 and 2011.

Average suspended sediment loads in rivers shown in Table 4.7 revealed a decreasing trend from October 2011 to January 2012. The trend started with low sediment load at the onset of rainfall season in October which then increased and reached a highest peak in early November. A gradual decrease was experienced towards the end of the rainfall season. The highest loads of suspended sediments were recorded in early November at Mutshindudi River at Phiphidi followed by Luvuvhu River at Tshino and Madanzhe River which recorded 3269.5; 2365.7; and 2313.3 mg/l, respectively. Luvuvhu River at Mhinga recorded the lowest suspended sediment loads of 87.07mg/l followed by Mutale River at Thengwe, Mutshindudi River at Dzingahe, Mudaswali River at Matangari, Nyahalwe River at Thengwe and Mbwedi River at Khubvi which recorded less than 500 mg/l of suspended sediment loads. About 500 mg/l were recorded at Dzindi River at Dzwerani and Tshinane River at Gondeni which constituted 509.2 and 535.6 mg/l respectively. It must be noted that suspended sediment load herein refers to the sediment particles carried by stream as described by Strahler and Strahler (2006) and stays in suspension for an appreciable length of time; while suspended sediment concentration is the quantity of sediment relative to the quantity of fluid that can be carried by flowing water.

Table 4.7: Average suspended sediment load and sediment concentration

Sampling Site	Date	Sediment Load (g/l)	Sediment Load (mg/l)	Sediment Concentration (%)
Madanzhe River	2011/10/05	2.31	2313.29	0.23
Mutshindudi River at Phiphidi	2011/11/01	3.27	3269.55	0.33
Dzindi River at Dzwerani	2011/11/02	0.51	509.24	0.05
Tshinane River at Gondeni	2011/11/15	0.54	535.61	0.05
Mutshindudi River at Dzingahe	2011/11/15	0.19	192.22	0.02
Mbwedi River at Khubvi	2011/11/22	2.29	2291.88	0.23
Luvuvhu River at Tshino	2011/12/02	2.366	2365.70	0.24
Nyahalwe River at Thengwe	2011/12/08	0.43	429.28	0.04
Mudaswali River at Matangari	2012/01/13	0.25	247.83	0.03
Mutale River at Thengwe	2012/01/13	0.10	99.89	0.01
Luvuvhu River at Mhinga	2012/01/24	0.09	87.07	0.01

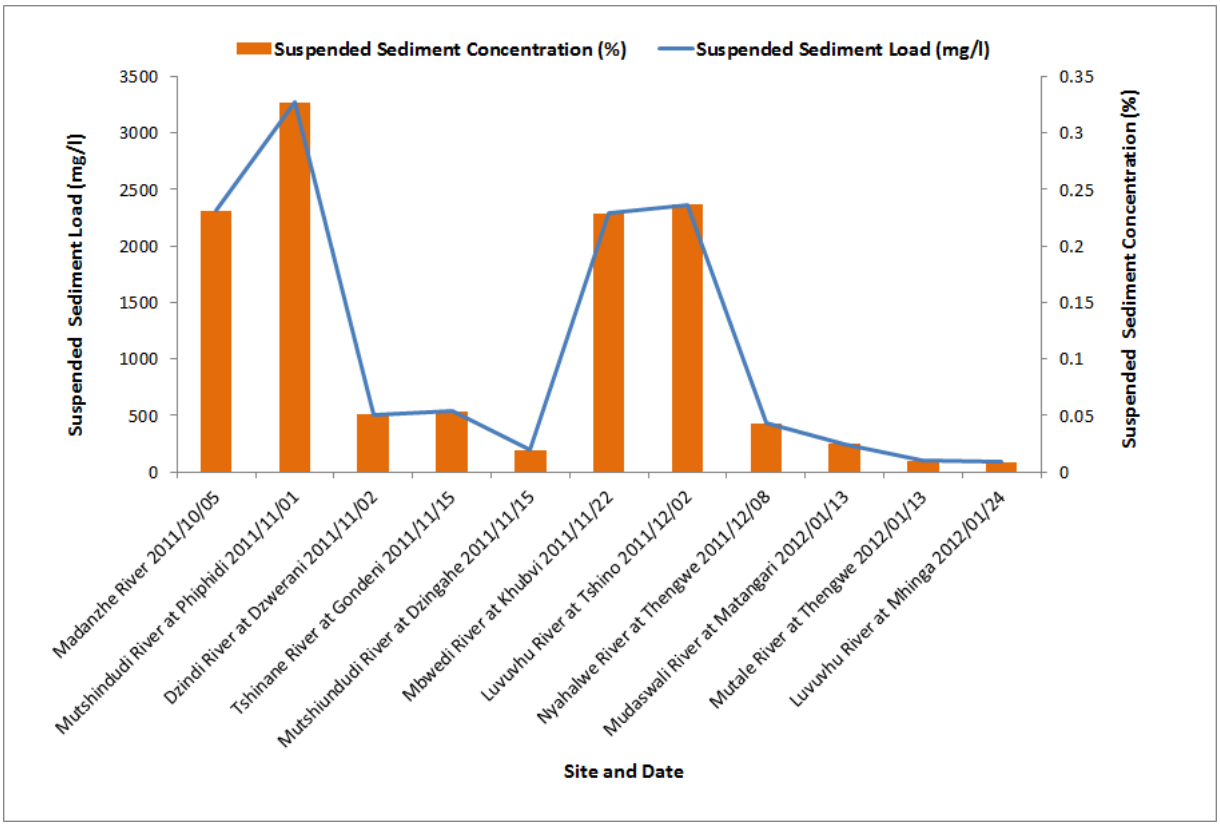

Figure 4.50: Suspended sediment load and sediment concentration

A study by Kamtukule (2008) showed that suspended sediment loads below 3000 mg/l indicated a well conserved catchment while those ranging from 3000 -10 000 mg/l indicated a catchment prone to erosion. This is concurrent with the results of this study such that suspended sediment loads of below and above 3000 mg/l were recorded. Mutshindudi River at Phiphidi which is located along steep slopes where soil erosion is highly variable, recorded more than 3000 mg/l of suspended sediment load. People have been allocated empty stands and housing infrastructures were being built along the river and this may have triggered the erosion of sediments to the river. Land use activities such as agricultural practices or deforestation were prominent. This makes the area prone to water pollution, exacerbated by related natural causes such as soil erosion. Widespread clearing of forest and trees, particularly of the riparian vegetation and in areas vulnerable to soil erosion, results in higher than natural sediment loads.

In their State of River Report (SRR), Angliss *et al*. (2001) reported that along the upper reaches of the Mutshindudi River where Phiphidi is located, the riparian vegetation is over-utilised, mainly for firewood, fence construction, furniture, medicinal purposes and food. In some areas, the riparian vegetation has been completely replaced by crops and as a result, siltation of the river which was scoured from the hillsides by sheet and rill erosion was increasing. The resultant health of the riparian zone along the Mutshindudi River was deteriorating, and sediment inflows into the Mutshindudi River were likely to increase. These distresses were causing loss of in-stream habitats and eventual loss of fish and invertebrate species from the river.

Kleynhans (1996) assessed the riparian zone and in-stream habitat integrity of the Luvuvhu River based on a qualitative rating of the impacts of major disturbance factors such as water abstraction, flow regulation, bed and channel modification among others. In the reaches along Mutshindudi and Tshinane Rivers, Kleyhans (1996) noted that stream bank erosion was often apparent and removal of clay from the river bank for brick manufacturing occurred occasionally. Consequently, riparian vegetation was being largely destroyed with large trees and dense stands of trees occurring only sporadically and several remaining trees have been pruned down for firewood. Small, hand irrigated lands and goat and cattle pens often occur right on the river's edge. During that time, Kleynhans noted that the area was mainly used for subsistence farming, which was associated high degree of catchment and river mismanagement as a result of removal of riparian vegetation, erosion, and sedimentation. Currently, rampant land use practices such as construction of houses and recreational activities dominate the riparian zones.

For example, sediment loads at Tshinane River at Gondeni showed that the water was easily polluted by sediments during high rainfall events as shown in Figure 4.51. This may be attributed to agricultural activities, which are widely practiced along the river. During times of floods, the Luvuvhu River may overtop its bank and sufficiently drop eroded materials such as alluvium (loose gravel, sand, silt, or clay). This can lead to the formation of floodplains which provide storage for flood flow, help reduce the velocity and peak flow and reduce deposition of sediment in stream channels. Figure 4.52 shows agricultural practices along Mutshindudi River at Dzingahe which trigger transportation of sediments to rivers after soil erosion. The water in the rivers will become turbid and affects both fauna and flora as the water will be unsuitable for use

in respect with their biological requirements. Sediments will get trapped at the bottom of the streams and result in deaths of aquatic animals. Turbid water results from the presence of suspended and dissolved matter such as clay, silt, finely divided organic matter, plankton, other microscopic organisms, organic acids, and dyes which are transported to streams either by wind, water, or soil erosion (ASTM, 2007). Collection and computation of suspended-sediment concentrations and suspended sediment loads in water is therefore important in the management of water resources. Suspended sediment can adversely affect water supply, recreation, aquatic life, flood control, transportation, fisheries, reclamation, and navigation (Angino and O'Brien, 1968).

Meyer *et al*. (2000) stressed that sediment problems are experienced in various South African rivers; with agricultural runoff constituting about 75% of sediment discharges. This is due to the fact that communities mostly practice subsistence farming during rainfall seasons especially along the river banks. The accumulation of sediments at existing flow gauging stations poses serious problems, especially during high discharges when flooding rivers carry heavy loads of sediments. Thus, it is important to quantify the impacts of land use and land cover changes as they are the driving forces that contribute to sediment discharges in streams and rivers. Monitoring of sediment loadings in streams and rivers within the LRC is needed in order to provide measures to minimize sediment discharge loadings in rivers.

The suspended sediments on dry days were insignificant. Such evidence could be seen along Tshinane River at Gondeni and Madanzhe stream as shown in Figure 4.53. Examples of the images taken during sediment samplings are shown in Figure 4.54 (during a rainfall event) and Figure 4.55 (no rain event). The area circled with a rectangle in each image represents the location surrounding the study area. Figure 4.54 showed that the catchment experienced floods resulting from heavy rainfall of intensities exceeding 15 mm per hour associated with ITCZ.

Figure 4.51: Sediment pollution in Tshinane River at Gondeni

Figure 4.52: Agricultural practices along Mutshindudi River at Dzingahe

Figure 4.53: Clear water at Tshinane River bridge at Gondeni and Madanzhe stream

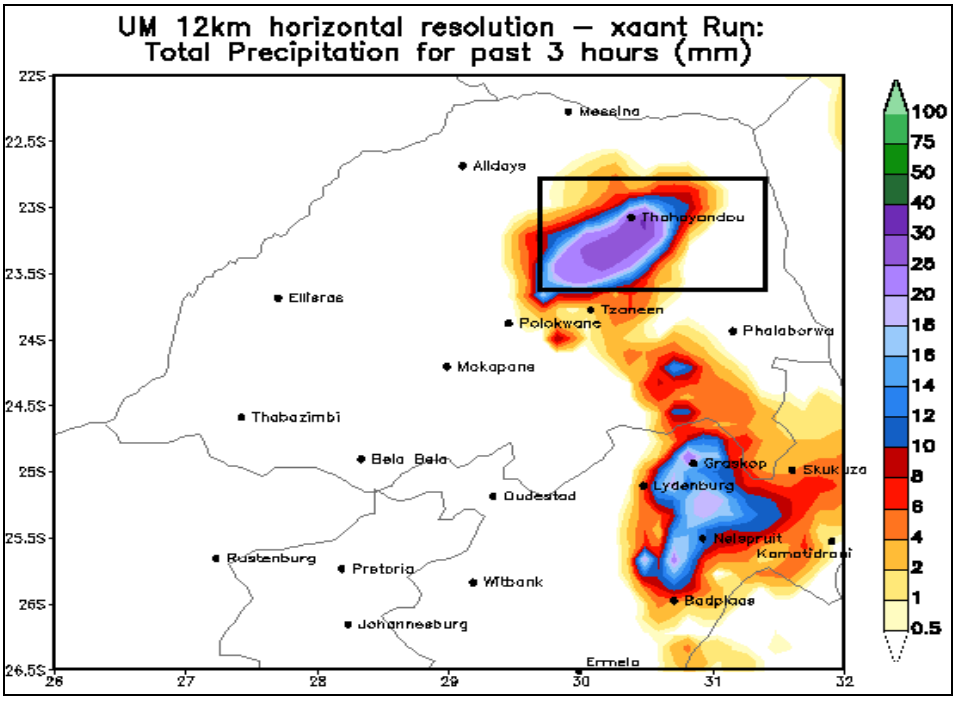

Figure 4.54: 3-hourly rainfall image during a rainfall event around Thohoyandou area

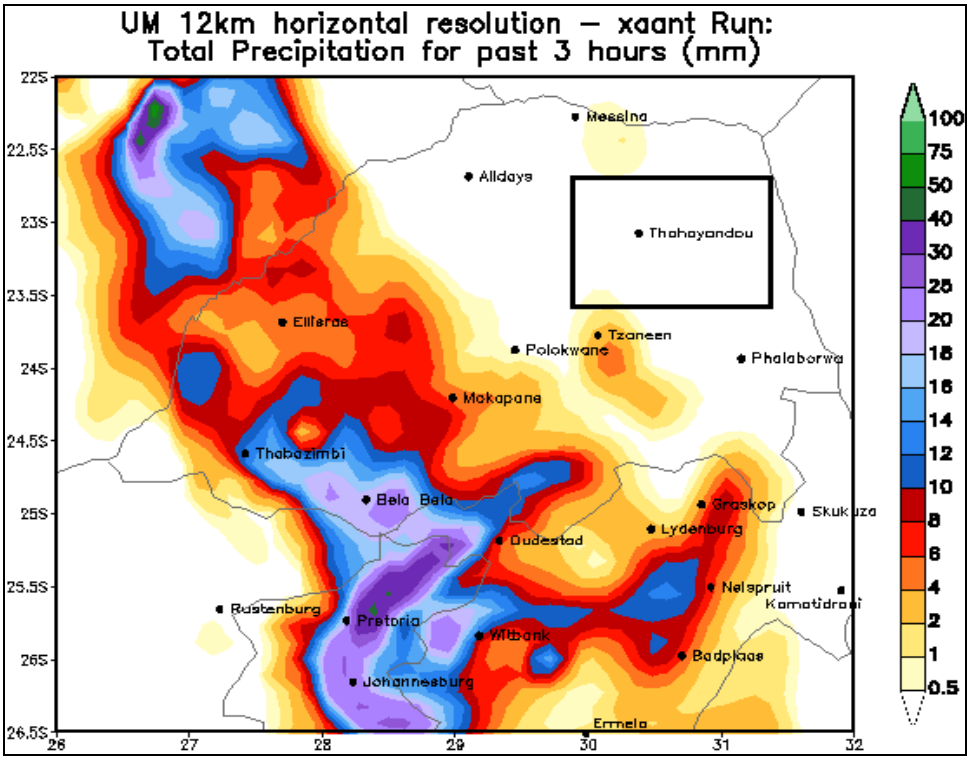

Figure 4.55: 3-hourly rainfall image during a no-rain event around Thohoyandou area

4.4.2 SWAT Analysis for Levubu-Tshakhuma sub-catchment

The calibration and validation procedures for discharge in this study were based on the recommendations as given in the SWAT user manual (Neitsch *et al*., 2002). The process involved comparing the model results generated by simulation and those obtained by observation and measurement. The split data method was used, where the discharge data for the period 1985 to 1996 was used for calibration while data for the period 1997 to 2010 was used for validation, as shown in Figures 4.56 and 4.57 shown below.

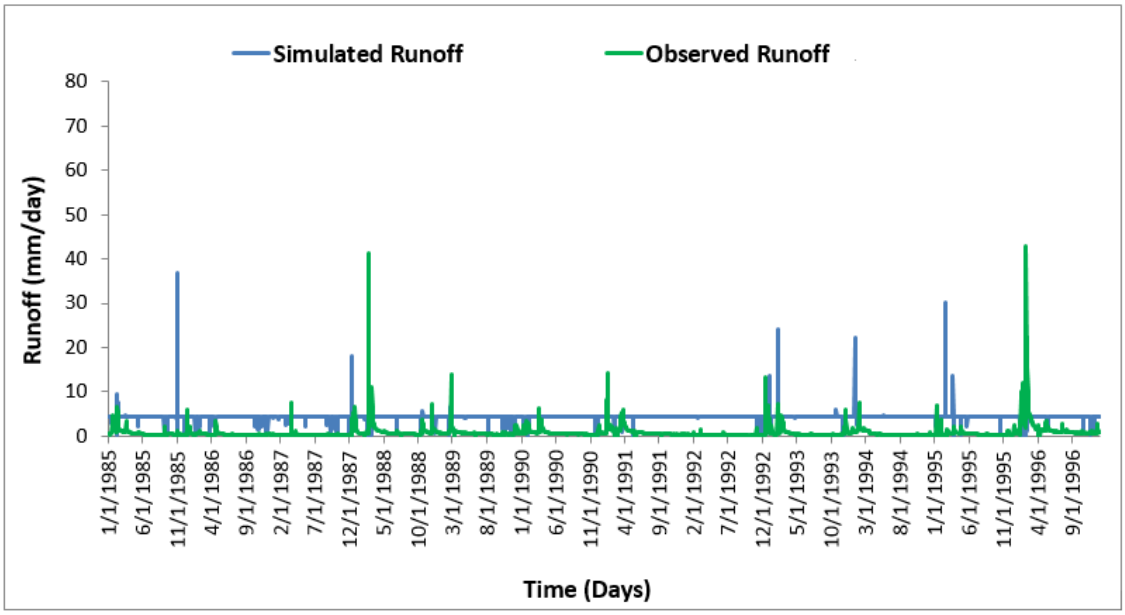

Figure 4.56: Calibration results for daily discharges

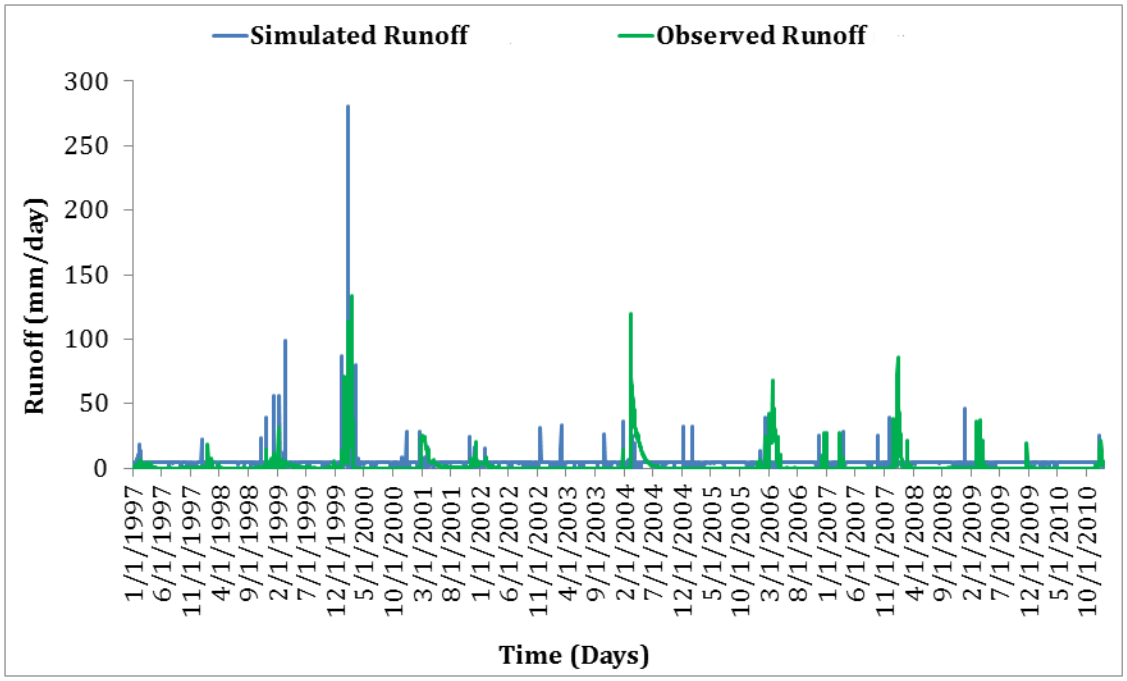

Figure 4.57: Validation results for daily discharges

The statistics results for calibration and validation in Table 4.8 showed that there was a good agreement between simulated and observed discharges. The calibration results showed coefficient of determination, R^2 of 0.85 and an environmental sensitivity of 0.85 while the

validation results showed coefficient of determination, R^2 of 0.83 and an environmental sensitivity of 0.83. The results fulfilled the requirement that R^2 should be greater than 0.6 while environmental sensitivity, E_{NS} should be greater than 0.5 for the simulation results to be reliable.

Table 4.8: Calibration and validation statistics for simulated and observed discharge

		Standard error (m^3/s)				
	Period (Years)	Observed	Simulated	% Error	R^2	E_{NS}
Calibration	1985-1996	6.55	6.04	+2.0	0.85	0.67
Validation	1997-2010	8.95	10.02	-5.6	0.83	0.51

Overall, the SWAT model performed well in simulating discharges of the catchment, hence the calibrated parameter values could be considered for further simulation of discharges for LRC.

The analysis showed that the water-balance-based SWAT model was suitable for predicting the location of runoff-generating areas of a watershed due to the inclusion of soil topographic indices. Figure 4.58 shows the hydrologically correct DEM that was used as a source of height data for modelling altitude-correlated properties. Figure 4.59 shows the upper Luvuvhu River at Levubu-Tshakhuma catchment (sub-catchment A91D), where the SWAT Tool was used to analyse the impact of land cover change. The land use map of the area was reclassified based on the available topographic map, aerial photographs and satellite images. This was done to represent the land use according to the specific land cover types such as type of crop, pasture and forest.The figure is a DEM with a 3-times magnification in altimetry and draped with a 2008 Landsat image.

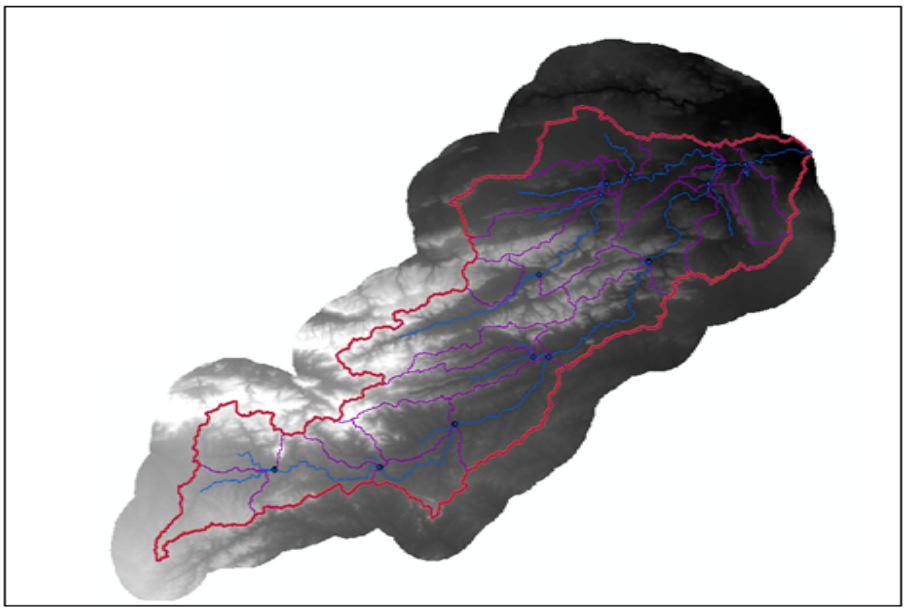

Figure 4.58: Hydrologically corrected DEM with buffer zone for the catchment

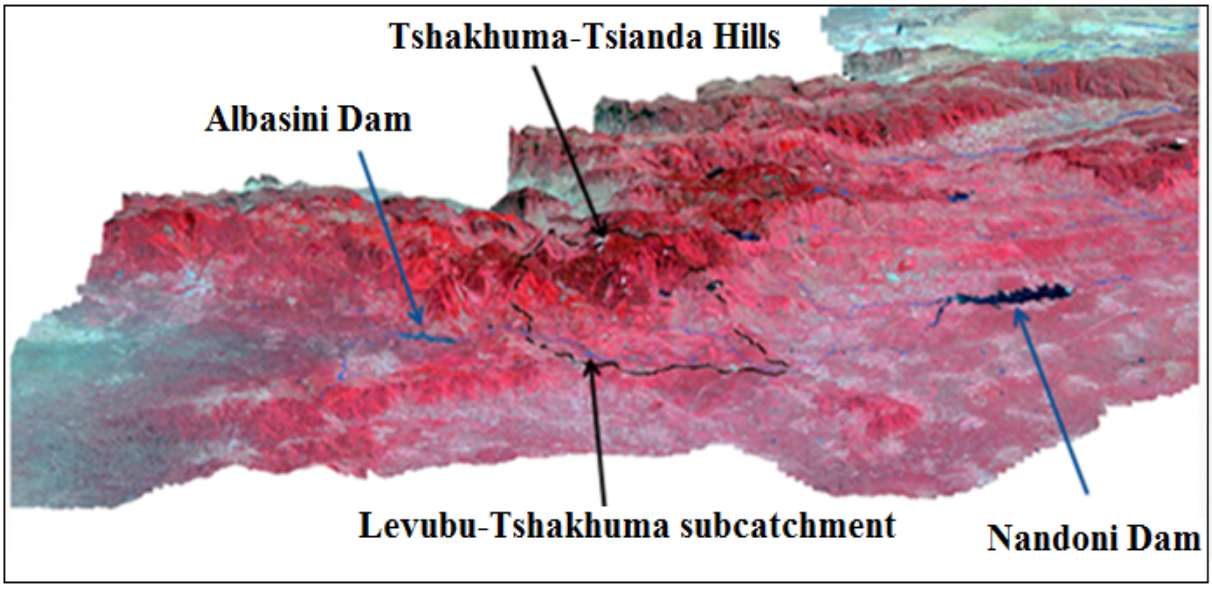

Figure 4.59: Location of Levubu-Tshakhuma sub-catchment

Figure 4.60 shows the different land cover classes from forestland, woodland and open grassland to medium size farms and built-up land. It was observed that hills around Tshakhuma and Tsianda which were covered by natural forest in the pre-change period were largely covered by small portions of trees and bushes at higher levels, interspersed with agriculture at the middle and built up areas, mixed with agroforestry on hill-sides.

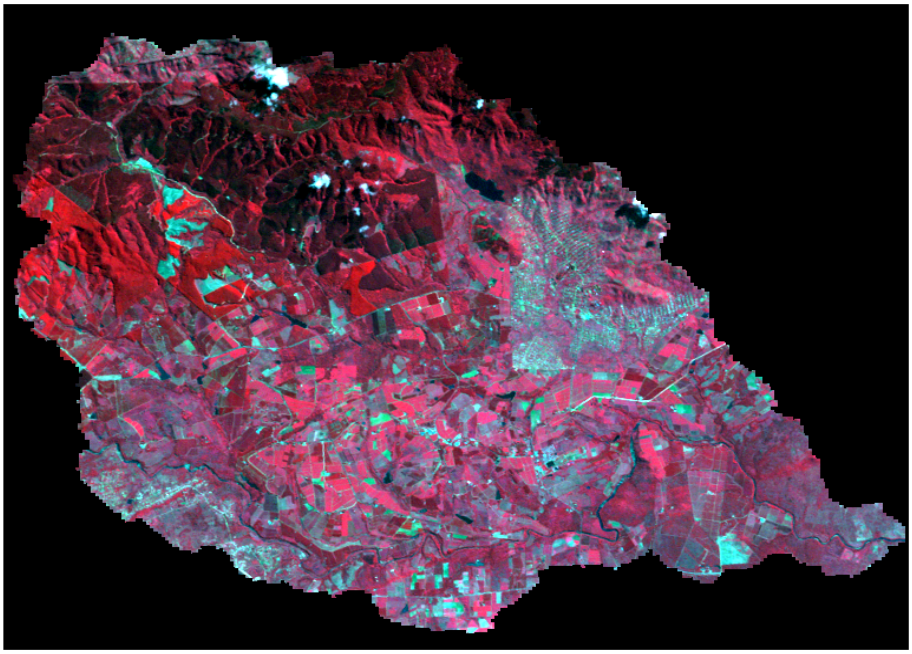

Figure 4.60: 2008 Landsat ETM+ image clip for Levubu-Tshakhuma sub-catchment

The extracted drainage pattern shown in Figure 4.61 was of the parallel type. The flow lines showed the longest paths in upper sub-catchment, which could be used for inundation mapping and floodplain delineation. The longest flow path data could also be used in the rainfall-runoff analysis to determine the time of concentration value necessary for computing surface runoff.

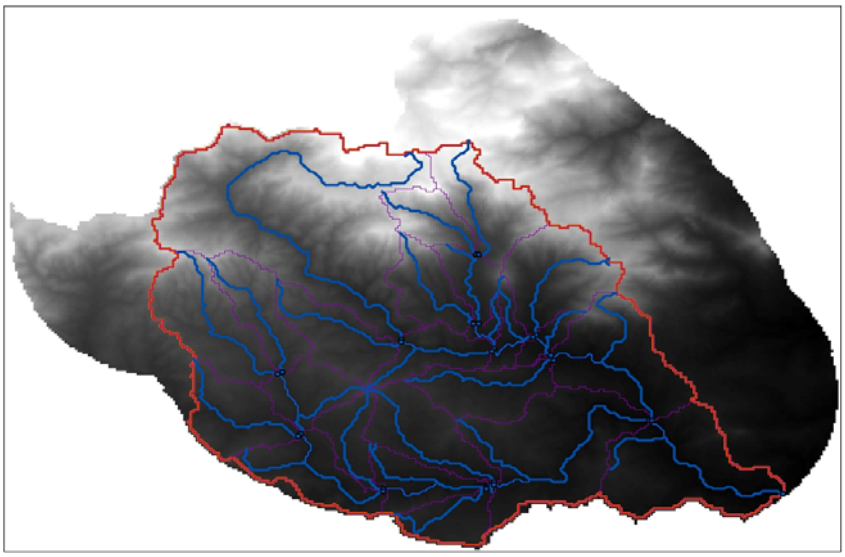

Figure 4.61: Levubu-Tshakhuma sub-catchment drainage system

The spatial distribution of local slopes for the sub-catchment was as shown in Figure 4.62. The slopes affected the overall rate of downslope movement for processes such as runoff, soil erosion, moisture balance and landslide hazards. Average slopes for the sections from the valley floors to the catchment divides for the Levubu-Tshakhuma sub-catchment. For up to 63% per cent area of the sub-catchment, average slopes are between 1 and 10%. Slopes tend to be steepest along the ridges and sub-catchment divides with some areas exceeding 10%. According to Gupta *et al*. (2015), a significant shift in slope is assumed to be an indication of land use and land cover changes. Extraction of this property is therefore important as it allows overland and near-surface water flow to be modeled using DEMs where surface topography is the sole factor in the distribution of water. This would help check the processes of acceleration and deceleration and reduce the effects of erosion and deposition in the catchment. The population in the sub-catchment depends on irrigated agriculture directly or indirectly. The SWAT application in the sub-catchment assumed sheet and rill erosion as the dominant erosion type contributing to siltation and water pollution in rivers.

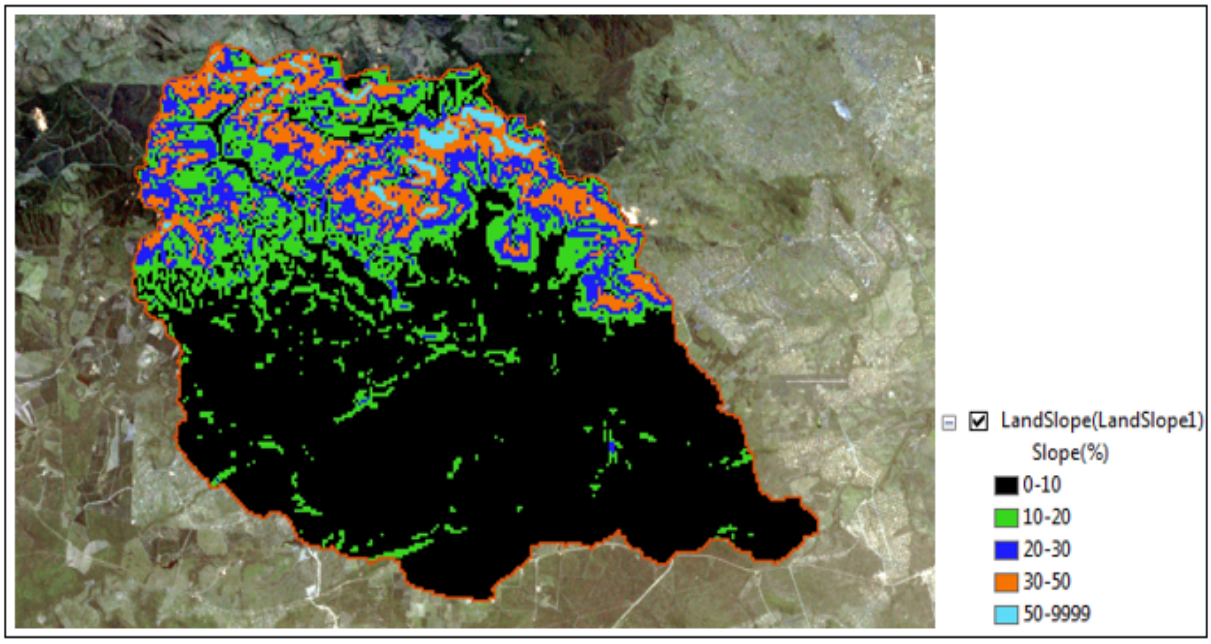

Figure 4.62: The spatial distribution of local slopes for Levubu-Tshakhuma sub-catchment

The SWAT's soil classification showed that the vast majority of the soils in the Levubu-Tshakhuma sub-catchment were cross-listed HSGs such as A/D, B/D and C/D, which

represented areas that were naturally poorly drained (D), but could be improved to the first listing (A, B or C) with appropriate management. Figure 4.63 shows the soil classification for the Levubu-Tshakhuma sub-catchment.

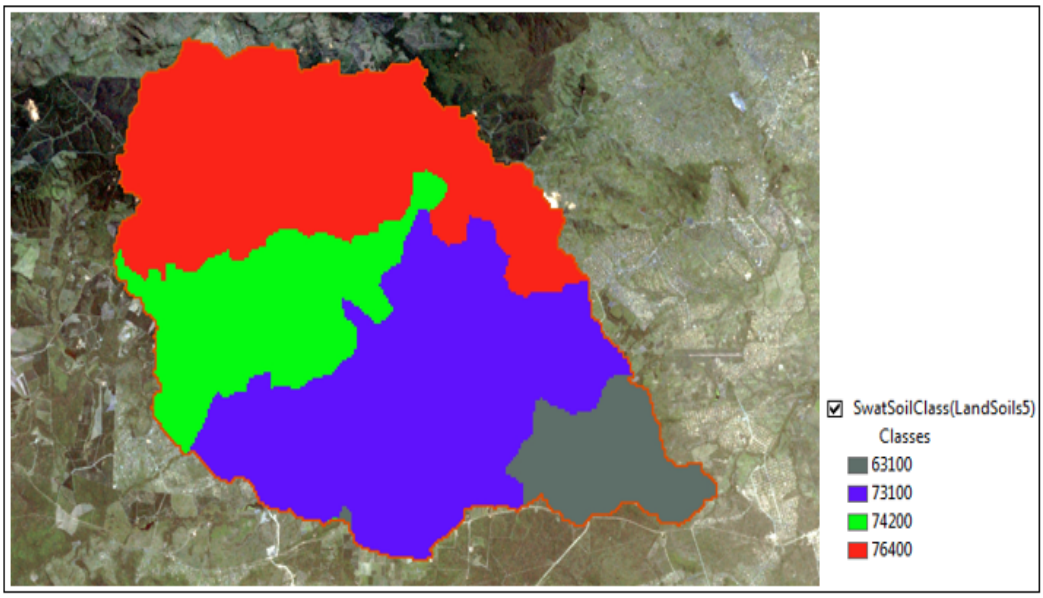

Figure 4.63: Soil classification for Levubu-Tshakhuma sub-catchment

The soil classification followed the Map Unit Key (MUKEY) system, as a soil type identifier from the SOTER-ISRIC data base. The numerical key is used to join tabular data and spatial data for each soil series or complex mapped. The MUKEY dataset contained 4 soil types, although each map unit may be composed of more than one component. The MUKEY system had a higher spatial resolution and showed more details than the ARC classification, which showed that the entire area was under soil class LmSa-SaLm. Figure 4.64 showed the soil-landscape relationship for Levubu-Tshakhuma sub-catchment. The proportion covered by areas A, B, C, and D was 34.90%, 17.76%, 37.99%, and 9.34% respectively. The dominant soils in the sub-catchment were situated in lowland plains.

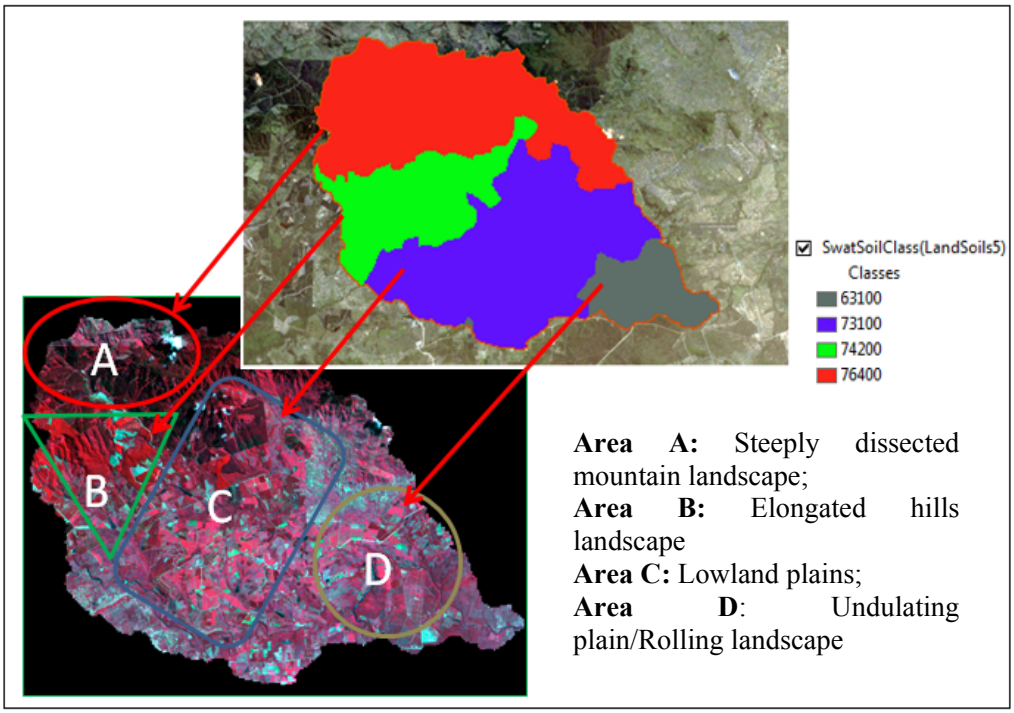

Figure 4.64: Soil-landscape relationship for Levubu-Tshakhuma sub-catchment

Since dominant Hydrologic Response Units (HRUs) distribution was used, the SWAT tool created 25 sub-catchments with 502 hydrologic response units (HRUs) for the catchment. The HRU showed lumped areas within the sub-catchment that are comprised of unique land cover, soil, and management combination. Figure 4.65 shows the location of the sub-catchments. The area is subdivided into smaller sub-catchments based on DEM data, land use and soil type data. Figure 4.66 shows the 502 hydrologic response units while Figure 4.67 shows the land cover and land use for Levubu-Tshakhuma sub-catchment, consisting of pastures, deciduous forests, agriculture, water bodies, and urban. Over-parameterisation is a major problem in the application of models hydrologic analysis. The use of sensitivity analysis for reducing the number of parameters to be adjusted during calibration is important for simplifying the use of these models.

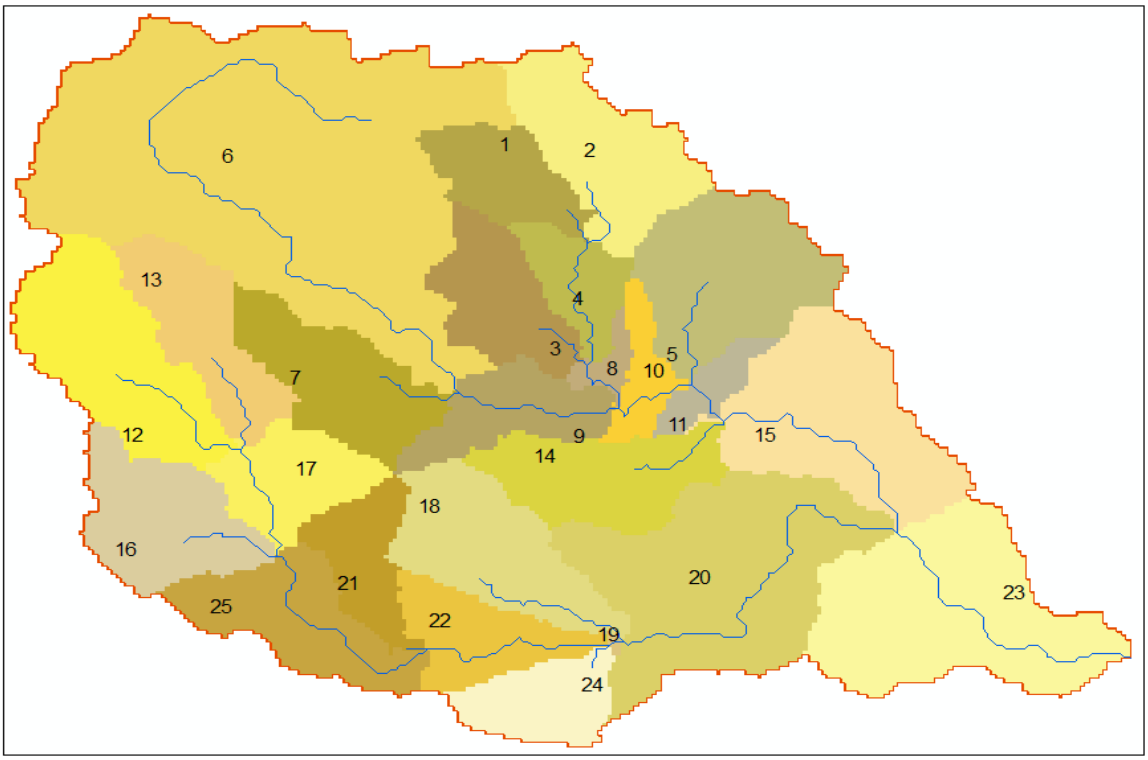

Figure 4.65: SWAT delineated sub-catchments for the Levubu-Tshakhuma sub-catchment

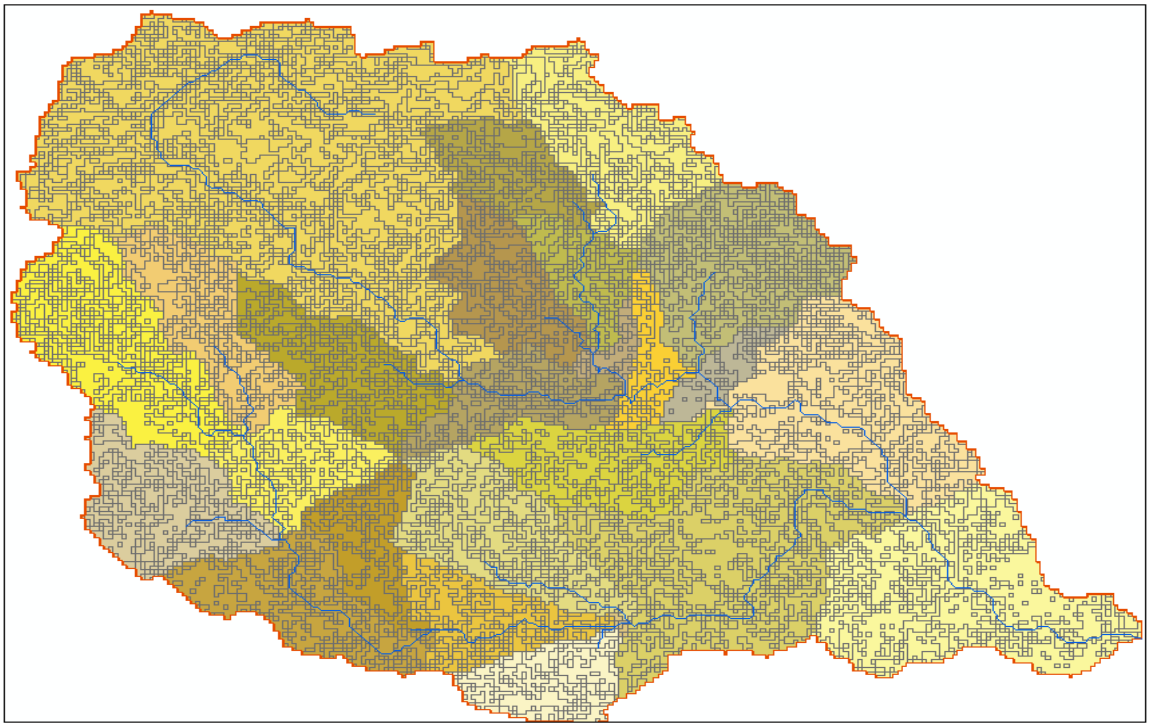

Figure 4.66: The hydrologic response units for Levubu-Tshakhuma sub-catchment.

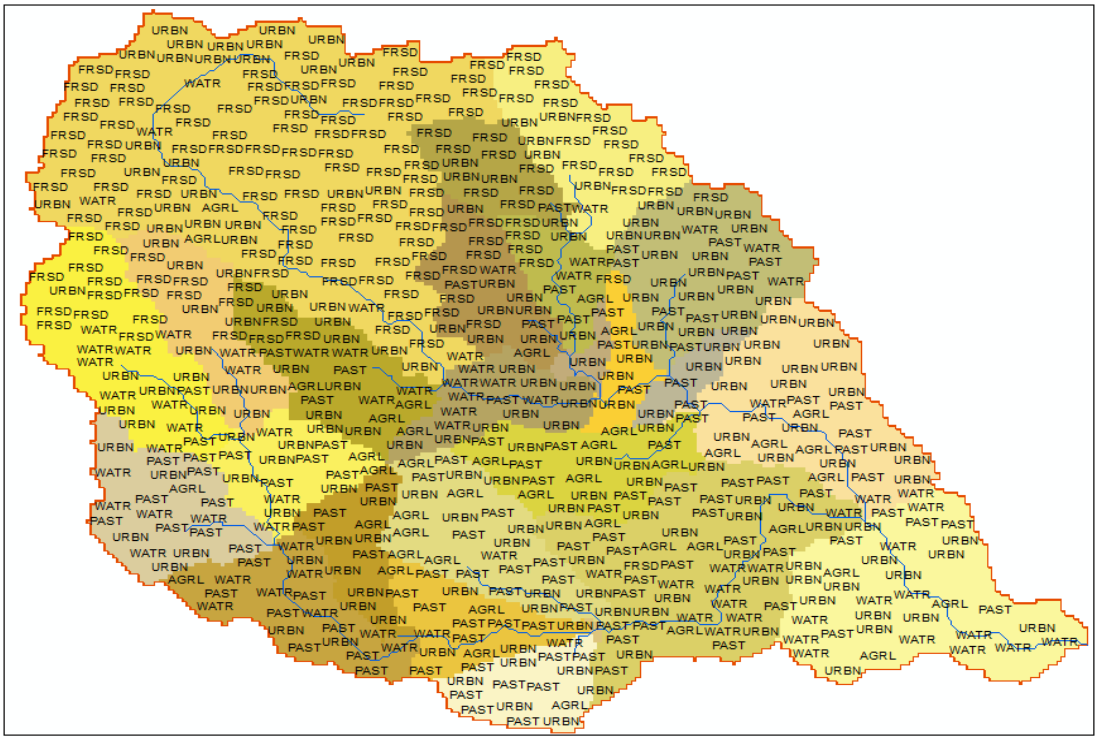

Figure 4.67: Land cover and land use for Levubu-Tshakhuma sub-catchment.

SWAT tool provided statistics for land use, soils and slope (Table 4.9). Five land use categories were the default classes defined by the SWAT tool. The dominant class was found to be residential/urban (35.35 %) followed by pasture (22.19 %), followed by deciduous-forest (21.78 %), water (14.67 %) and generic agricultural land (6.2 %). Pasture represented all land under open grassland and wooded grassland. Deciduous-forest represented plantation forest and tree crops. The area under agriculture appears to be small because some was covered under pasture and deciduous forest. A limitation to recognize for the SWAT tool is that the large spatial resolution of HRUs for this study could have led to biased results.

Table 4.9: Hydrologic response units report

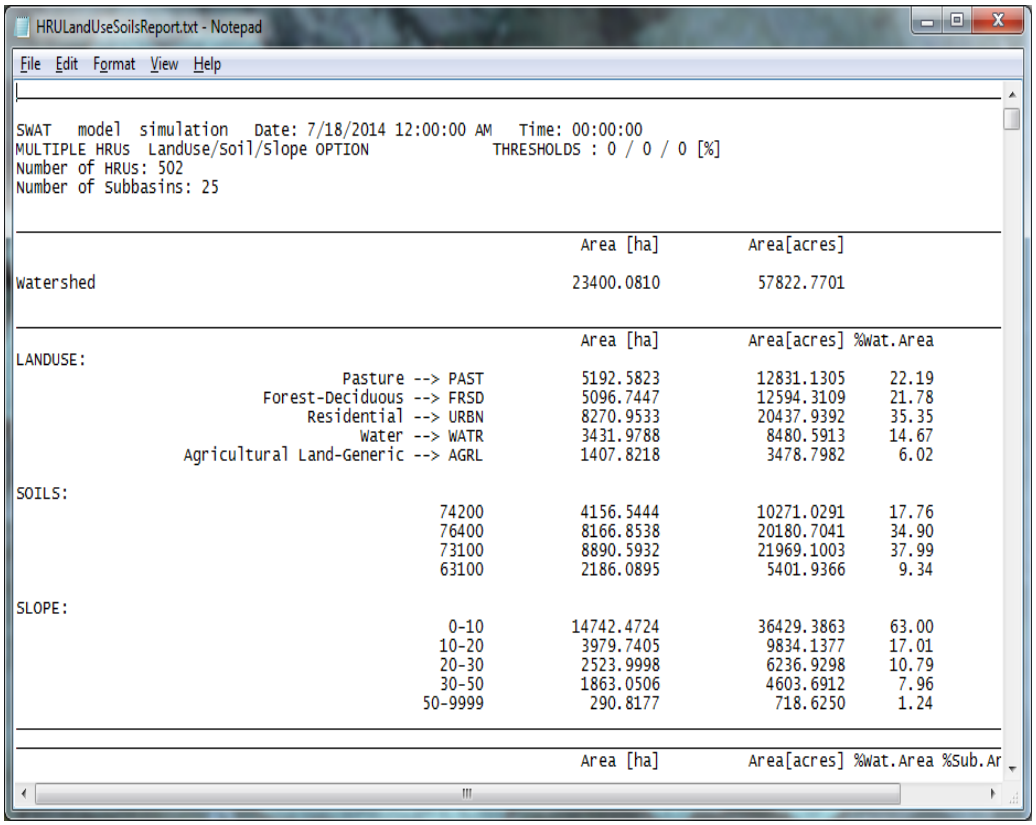

HRULandUseSoilsReport.txt - Notepad

File Edit Format View Help

SWAT model simulation Date: 7/18/2014 12:00:00 AM Time: 00:00:00
MULTIPLE HRUs LandUse/Soil/Slope OPTION THRESHOLDS : 0 / 0 / 0 [%]
Number of HRUs: 502
Number of Subbasins: 25

	Area [ha]	Area[acres]	
Watershed	23400.0810	57822.7701	
	Area [ha]	Area[acres]	%Wat.Area
LANDUSE:			
Pasture --> PAST	5192.5823	12831.1305	22.19
Forest-Deciduous --> FRSD	5096.7447	12594.3109	21.78
Residential --> URBN	8270.9533	20437.9392	35.35
Water --> WATR	3431.9788	8480.5913	14.67
Agricultural Land-Generic --> AGRL	1407.8218	3478.7982	6.02
SOILS:			
74200	4156.5444	10271.0291	17.76
76400	8166.8538	20180.7041	34.90
73100	8890.5932	21969.1003	37.99
63100	2186.0895	5401.9366	9.34
SLOPE:			
0-10	14742.4724	36429.3863	63.00
10-20	3979.7405	9834.1377	17.01
20-30	2523.9998	6236.9298	10.79
30-50	1863.0506	4603.6912	7.96
50-9999	290.8177	718.6250	1.24

	Area [ha]	Area[acres]	%Wat.Area	%Sub.Ar

4.4.2.1 Runoff-sediment Simulation in SWAT

The SWAT tool was used to route runoff-sediment in the channel of Levubu-Tshakhuma sub-catchment. The model determined the area and hydrologic parameters of each land-soil category, land use and soil maps of the catchment were overlaid and the dominance of land use and soil definition was used to create the dominant HRU for each sub-catchment. The hydrologic information was distributed within the sub-catchment and entered into SWAT interface independently for river/reach. The lengths of the river reaches and their slopes were derived from the DEM. The SWAT model was then applied in a major runoff-sediment contributing sub-catchment of Levubu-Tshakhuma as shown in the preceding section (Section 4.4.2) of this study. The suspended sediment data collected during the rainy season of 2011/2012 from 05/10/2011 to 24/01/2015 was used to study the dynamics of sediment load whereas the hydro-meteorological data was used to simulate surface runoff in the sub-catchment. The SWAT simulator for this

study used a modification of the SCS-CN method which determined the surface runoff based on the AMC for each of the HRU.

River routing was performed by the variable Muskingum-Cunge method which has been incorporated into the SCS-CN model. Thus, the hydrologic inputs derived from SWAT were routed downstream via Muskingum-Cunge method. The Muskingum-Cunge method was found useful where multiple channel slopes were found. The Muskingum-Cunge method was determined from four stream gauge data which were used to evaluate the runoff simulations; namely A9H001, A9H015, A9H016 and A9H023 (Figure 3.6) which are located at sub-catchments A91F, A91D and A91A respectively. These sub-catchments were selected from various altitude zones in the catchment. Simulations were performed for the period between 1960-2010. The Muskingum-Cunge method was related to estimation of routing coefficients and method of mathematical solution based on the selection of reference discharge for which routing coefficients were computed and the varying time step to reflect flow characteristics of the rising and receding flood wave. The time of concentration was estimated from the lag time while the storage coefficient was estimated by relating the parameter to the time of concentration and the geometrical properties of the catchment. Estimates for the bank full depth, width of the river channel bottom and other flow characteristics such as water abstractions were acquired from the Department of Water Affairs and Sanitation (DWS).

The SWAT model identified erosion sources as sheet and rill erosion but due to lack of available suspended sediment data at the watershed inlet, it could not capture the dynamics of sediment load in the catchment but was able to capture the observed hydrologic and erosive processes quite well across multiple scales. The most sensitive parameters controlling erosion in the catchment were those used for manipulating the amount of sediment that can be entrained during channel routing. For example, the previous Figure 4.62 showed that the slopes affected the overall rate of downslope movement for processes such as runoff, soil erosion, moisture balance and landslide hazards. Identification of sediment sources and erosion processes was also done through visual inspection during collection of the sediment discharge data in a number of the catchment's tributaries. Establishing a strategic suspended sediment concentration (SSC)

monitoring programme in the catchment could therefore enable the relative contribution of sheet and rill erosion sources to be assessed for better management of the quality of water in rivers.

The flood hydrographs shown in Figure 4.68 illustrated how the three scenario analysis namely, 1980-1989 (Sc.1), 1989-1999 (Sc.2) and 1999-2009 (Sc.3), were compared in terms of flood peak discharges and the associated volumes with the state of 2009 land cover (Lc. 2009). The 60 mm synthetic storm represented a typical storm event related to ITCZ for the respective sub-catchments in the catchment. From the simulations, the derived composite values for Curve Number values significantly changed the sub-catchments hydrologic response over the period. During the study period, the runoff coefficients increased in a similar way in the sub-catchments. Increasing the CN resulted in increased runoff which represented low infiltration, low detention and retention hence high surface runoff, while reducing it had the opposite effect. This could be attributed to their higher rates of deforestation during the three scenarios as shown in Figure 4.69. The figure presented the relative changes in the land cover classes during the three scenarios. Agricultural fields were noted to have increased from 61% to 77% during the periods under consideration. Using the above, and the flow routing parameters, the local flow due to runoff and routed floods occurring during the storm events were simulated within the sub-catchments and stream gauge locations of the catchment.

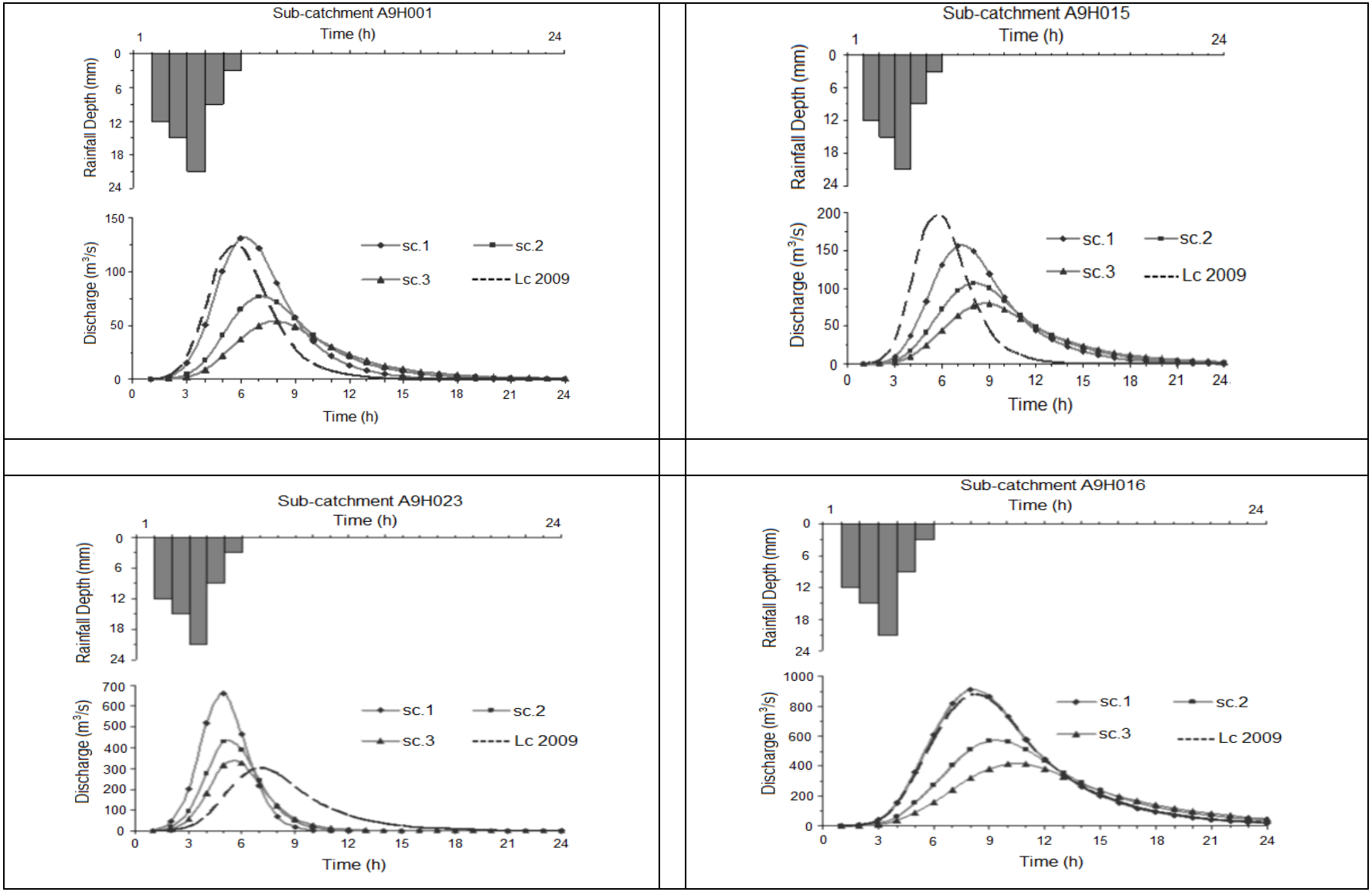

Figure 4.68: Flood hydrographs for the 60 mm synthetic storm event for the respective sub-catchments

Results of simulated runoff volumes in above Figure 4.69 showed that gauging stations A9H016 and A9H023 at sub-catchments A91D and A91A respectively had the highest increase in peak discharges. These stations are located upstream of the catchment adjacent to the Entabeni Forest, an Afro-temperate Mist-belt Forest that makes for an interesting combination of Afromontane and tropical vegetation elements. It was also noted that these sub-catchments were larger in area and hence provided a wider collecting surface and disposed more water at the outlets in response to the degraded land cover conditions. Sub-catchment A91F at gauging station A9H001 produced low peak discharges compared to the rest of the sub-catchments. The highest change in the runoff coefficient during the land cover state in 2009 was noted at gauging station A9H015 (A91D) which is located in the middle upland of the catchment in the Levubu-Tshakhuma sub-catchment. This area has largely experienced one of the highest conversion rates of forestland into commercial agriculture. Sub-catchment A9H015 produced peak discharges of 50 m^3/s in 1980, 56 m^3/s in 1989 and 65 m^3/s in 2009 state of land cover. The runoff depths also increased over the same period. The sub-catchment draining at A9H015 produced peak discharges of 117 m^3/s, 140 m^3/s and 160 m^3/s. The simulated floods for the sub-catchment draining at A9H015 conforms approximately to a normal flood event with a return period of 2 years in the catchment. Peak discharges of 472 m^3/s, 420 m^3/s and 470 m^3/s were obtained in 1980, 1989 and 2009 respectively. These values represented an increase of 20% between 1980 and 2009, with 11% occurring in the first period of 1980 and 1989. Also noted were the decreasing times to peak, with the same event in 1980 taking one hour more to reach the peak than in 2009. Flood volumes on the other hand increased by 11% over the entire period of study. The simulated flood event for January, 1984 conformed to a return period of about 10 years. Simulated peak discharges of 1517 m^3/s, 1550 m^3/s and 1750 m^3/s were obtained for this event, representing increases by 10%, 7% and 17% between 1980-1989, 1989-1999 and 1999-2009 respectively. The flood time to peak indicated a decreasing trend, in the range of 0.5 to 1 hour within the years. This represented a deteriorating situation in land cover conditions with increasing cultivation and expanding villages. The results indicated that in scenario 1 (1980-1989), the sub-catchments experienced an increase in peak discharges as compared to scenario 2 (1989-1999) and 3 (1999-2009), given the results of the land cover state in 2009. In terms of flood runoff volume however, scenario 3 experienced lowest peaks and would be the most appropriate change for the sub-catchments representing extreme case where forest cover was converted to agricultural fields.

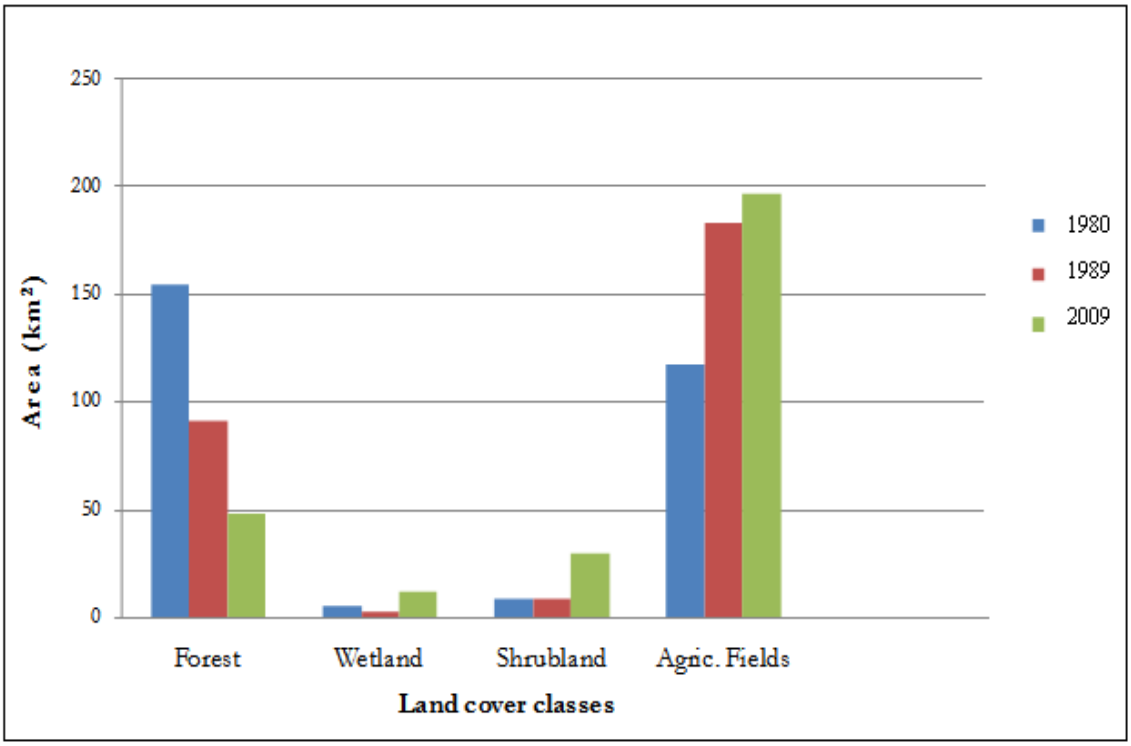

Figure 4.69: Relative changes in the land cover classes

4.5 Flood Frequency Analysis

4.5.1 Annual Maximum Flood

A 5-year moving average was smoothed in both rainfall and stream flow data to highlight significant changes in the trends. It also provided valuable insight into the trends of the past, and presented a foundation for predicting future trends. The smoothed trends showed significant hydrological conditions which may suggest that erratic rainfall and catchment characteristics such as land use may have caused flood peaks to increase in the area. The results showed that the area depicted unimodal peak floods recorded during the 1999/2000 at Nooitgedatcht and Palmaryville. The two stations detected standard variates of 304.4 mm and 270 mm and mean coefficient of variability (*Cv)* of 0.64 and 0.52, respectively. The highest measured flood of 1364.1 mm was recorded upstream of the catchment at Nooitgedacht during the 1999/2000 hydrological year, with the lowest flood of 98.9 mm recorded in 2004/05. Downstream catchment showed highest measured flood of 846.9 mm at Palmaryville during the 1999/2000 hydrological year, with the lowest flood of 68.5 mm recorded in 1983/84 hydrological year.

Appendix 16 shows that the highest measured rainfall occurred during the 1999/2000 rainfall season with lesser amounts in the early 80's and 90's. Tsianda recorded highest peak flood during 1966/67 hydrological year with low averages in 1994/95.

Figure 4.70 showed the annual maximum series for rainfall and stream flow at selected stations in the catchment. The highest measured stream flow of 9.91 m^3/s was recorded downstream at gauging station A9H003 during 1976/77 hydrological year, with the lowest flow of 0.23 m^3/s in 1991/92. Upstream catchment at gauging station A9H020 showed highest flow of 9.43 m^3/s during 1977/78 hydrological year, with lowest flows of less than 1.0 m^3/s recorded in various hydrological years. The two stations detected standard variates of 2.13 m^3/s and 0.7 m^3/s 3 and mean coefficient of variability (*Cv)* of 0.94 and 2.81, respectively. The results indicated in Appendix 17 show that some sub-catchments experienced peak flows from 1999/2000 hydrological year to the end of the series with *Cv* values ranging from 0.40 to 0.99. The results of both annual maximum rainfalls and stream flows showed spatial and temporal characteristics. This may be due to land use activities in the catchment as well as climate change which impact on stream hydrology. For example, stream flow patterns were affected by a combination of anthropogenic disturbances such as abstraction and impoundments (Hannaford and Marsh, 2006).

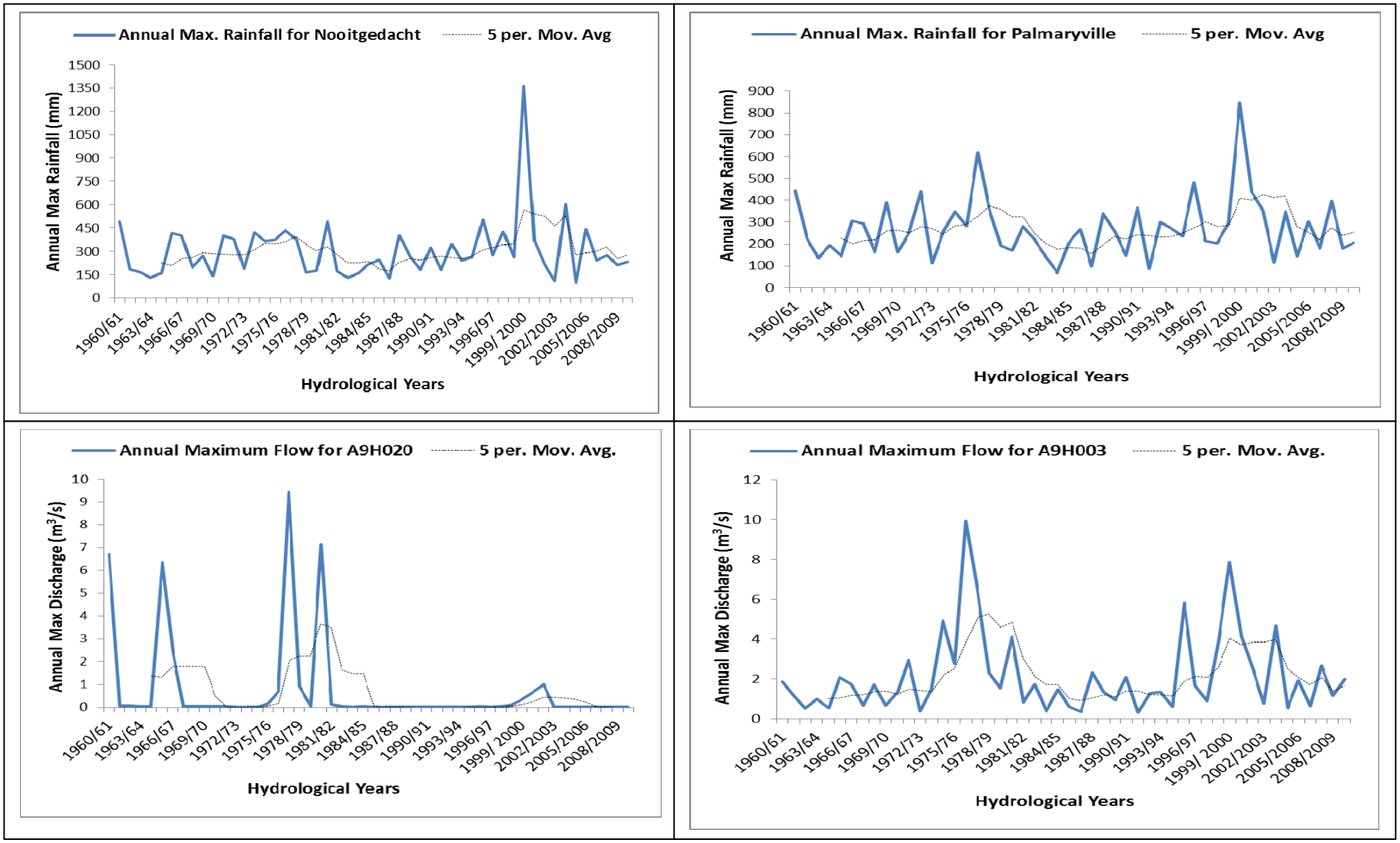

Figure 4.70: Annual maximum series for rainfall and stream flow

4.5.2 Frequency and Probability of Events

Land cover and land use change such as urbanisation and deforestation can alter the flood-frequency characteristics that would be expected to occur in a natural or rural watershed. A study by Takara (2009) showed that the 50-year event had a non exceedance probability of 0.98 (98%) which agreed with the results of this study. Figure 4.71 showed the return periods for rainfall and stream flow for both upstream and downstream catchments. A regression equation was fitted in the data to detect a relation between annual maximum series and their corresponding return periods, to test whether such a relation, either assumed or calculated, was statistically significant. The coefficient of determination (R^2) for rainfall series upstream at Nooitgedatcht and downstream at Palmaryville detected correlation values of 0.83 and 0.96, respectively, while correlation values of stream flow upstream and downstream at gauging stations A9H020 and A9H003 were detected as 0.68 and 0.97, respectively. The highest correlation values for rainfall were detected at Palmaryville with an R^2 of 0.960 and at station A9H003 with an R^2 of 0.973. The range of significant correlations for rainfall data varied from 0.68 to 0.97 while those of stream flow data varied from 0.77 to 0.97 as shown in Appendices 18 and 19, respectively. The R^2 values herein described the proportion of the variance in the observed rainfall and stream flow data. The R^2 in both rainfall and stream flow had correlations of 0.7 and higher, suggesting a strong relationship between annual data and simulated return periods.

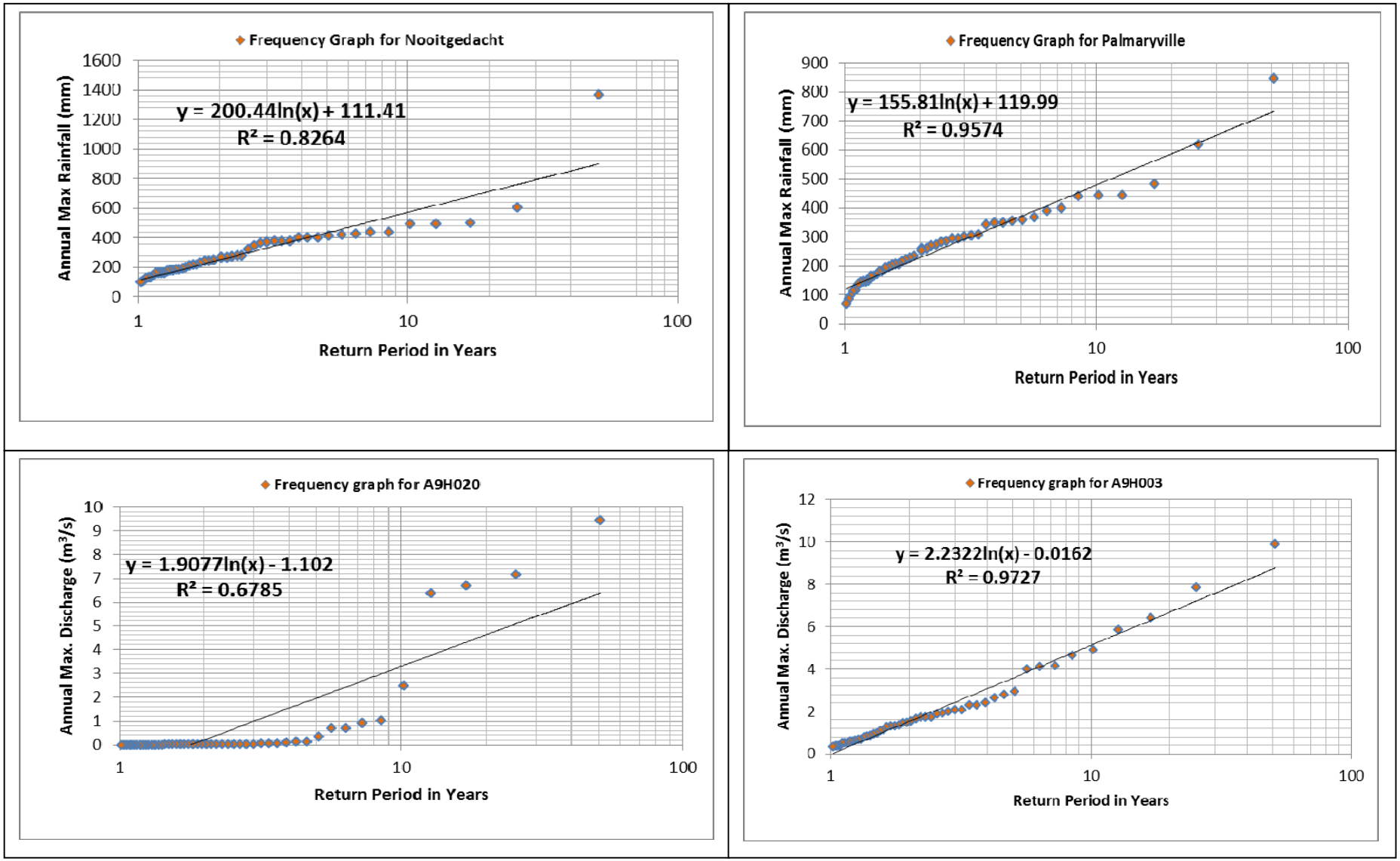

Figure 4.71: Return periods for rainfall and stream flow

4.5.3 The Log-Pearson III Distribution Analysis

Flood peaks corresponding to return periods and probability of occurrences for each hydrological year were as shown in Figure 4.72. The comparison between the annual maximum rainfall series (measured by SAWS) and estimated flood flows for upstream and downstream catchments showed no significant changes. The skewness observed showed that the distribution of flood in the catchment was both positively and negatively skewed for LP3 distributions. A significant change was detected at Tshakuma station which produced a large skew of 3.7 mm. The skew was used as a measure of asymmetry or lack of symmetry of stream flow and rainfall data. When the skew coefficient is small, the LP3 distribution approximates a normal distribution. If values are further from the mean on one side than the other, the distribution will have a large skew. Tshakhuma station failed to measure the irregularity of the frequency distribution; hence its relationship with simulated return periods was significant with an R^2 value of 0.94.

Figure 4.72 shows that there was a high variability in the flow magnitudes of sub-catchments A9H003 and A9h020 with peaks ranging from 10.75 m^3/s to 110.7 m^3/s and 0.01 m^3/s to 107.6 m^3/s, respectively. Sub-catchments A9H015, A9H016, A9H017 and A9H023 showed much lower estimated discharges, while sub-catchments A9H006 and A9H003 exhibited discharges of less than 20 m^3/s. Estimated flood magnitudes for various selected return periods based on LP3 distribution are shown in Figure 4.73 and Appendices 20 and 21. Each computed flood magnitude was determined at 95-percent confidence interval. This interval was the range that contained the true flood magnitude for a particular exceedance probability. The coefficient of determinations (R^2) at each station showed statistically significant relations between estimated flood peaks and assigned return periods.

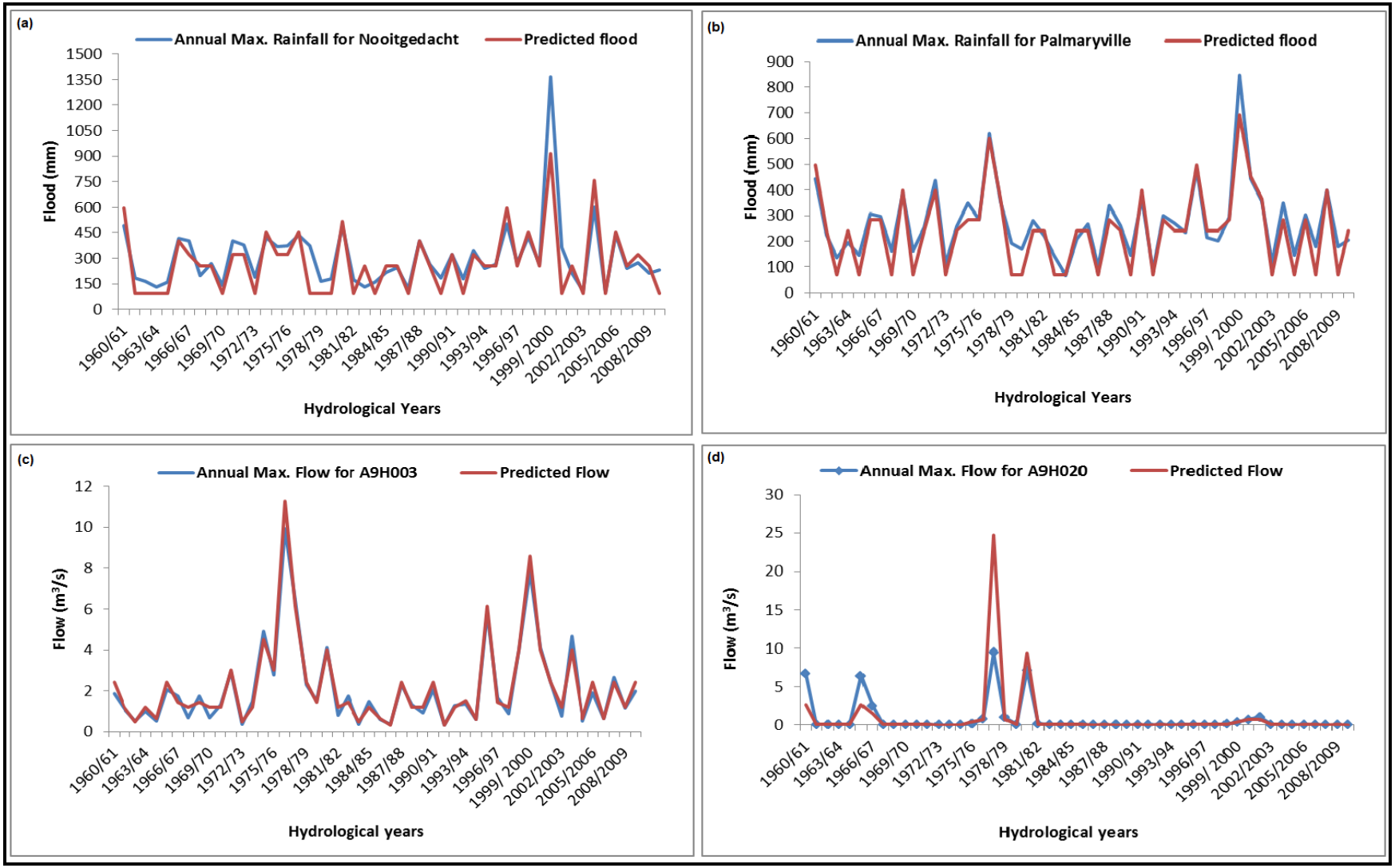

Figure 4.72: Measured and predicted annual floods for LP3 distribution

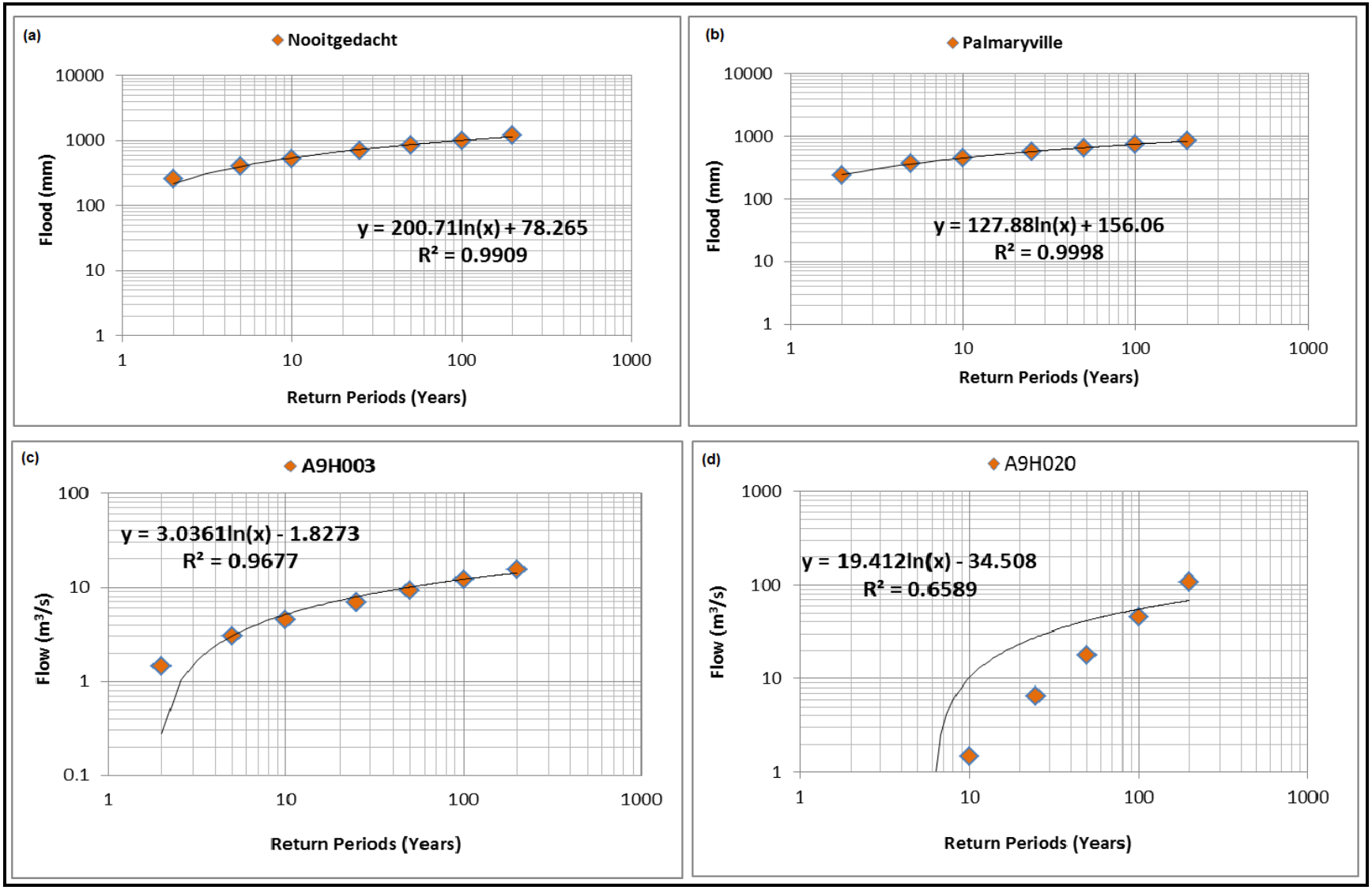

Figure 4.73: Estimated flow magnitudes for 2, 5, 10, 25, 50, 100 and 200 years return periods using LP3 distribution

In peri-urban areas such as the LRC, design life of structures for low risks (10-year return periods) and medium risks (50-year return periods) catchments are important to manage flood risks. The flood magnitudes of rainfall computed by the LP3 distribution associated with the 10-year floods ranged from 453.03 mm to 852.77 mm. Flood magnitudes of discharges ranged from 0.28 m^3/s to 39.62 m^3/s with sub-catchment A9H001 portraying highest flood peaks. Similarly, the floods associated with a recurrence interval of 50 years ranged from 0.39 m^3/s to 75.6 m^3/s. The amounts detected could be taken as the estimated limiting values for design purposes in the catchment, except for sub-catchment A9H001 which showed very large amounts for the 10- and 50-year return periods.

4.5.4 Gumbel's Distribution Analysis

Flood peaks corresponding to return periods and probability of occurrences for each hydrological year were estimated. Figure 4.74 showed the comparison between the annual maximum series and estimated flood flows for upstream and downstream catchments. Similar to LP3 distribution, no significant changes were detected between the annual maximum series and the estimated flood flows in upstream and downstream catchments. The analysis showed that there was a high variability in the flood magnitudes for both rainfall and stream flow series. Estimated flood magnitudes showed similar distribution curves, with flood peaks ranging from 186.45 mm to 1734 mm. Sub-catchment A9H001 depicted largest floods with peaks ranging from 14.30 m^3/s to 86.66 m^3/s. Sub-catchments A9H003, A9H006, A9H015, A9H016, A9H017 and A9H023 showed much lower estimated discharges ranging from 0.13 m^3/s to 9.64 m^3/s.

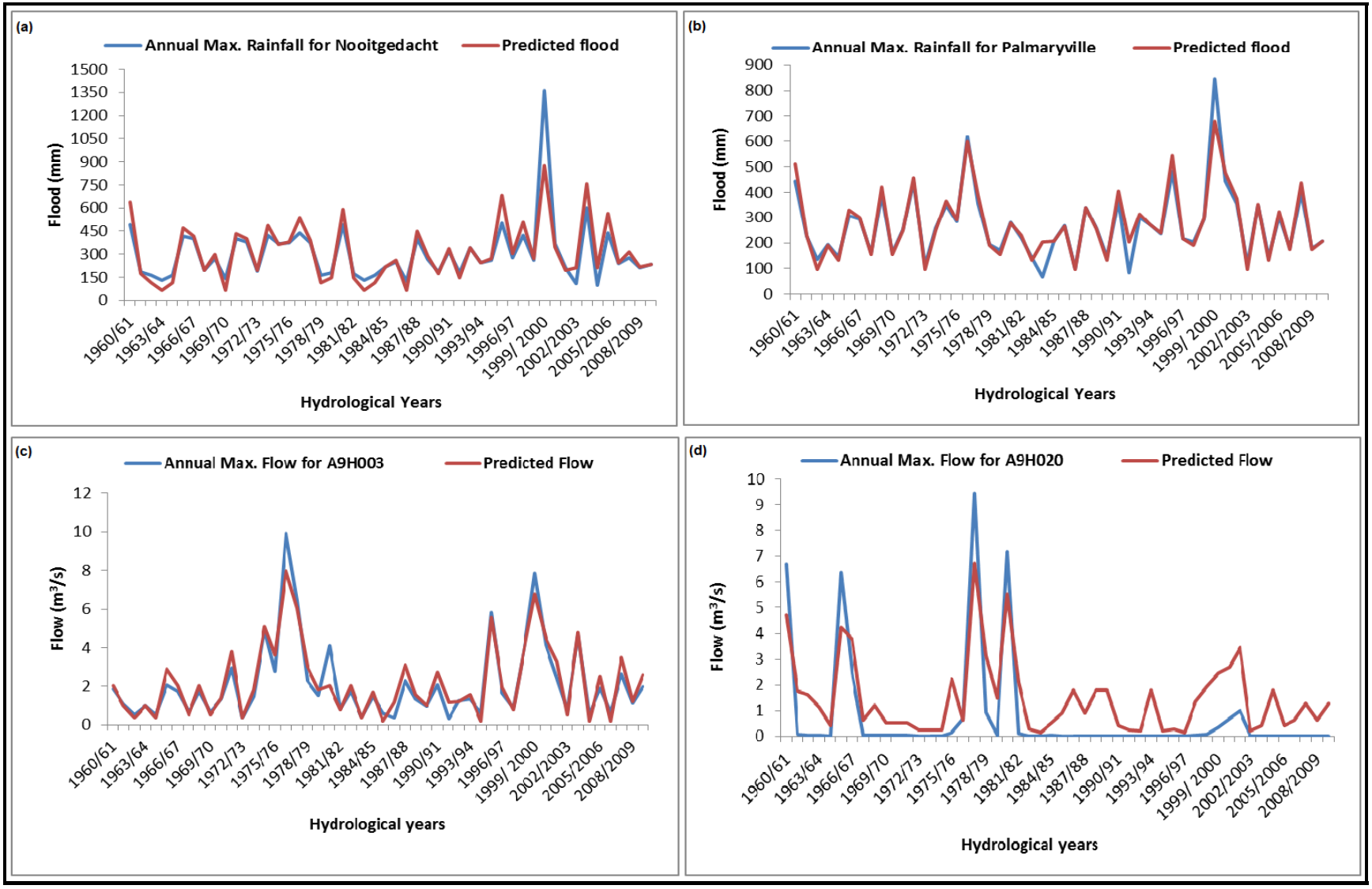

Figure 4.74: Measured and predicted floods using Gumbel's distribution

Estimated flood magnitudes for various selected return periods were as shown in Figure 4.75 and Appendices 22 and 23. Similar to LP3 distribution, each computed flood magnitude was determined at 95-percent confidence interval. The coefficient of determinations (R^2) at each station were extremely high suggesting very strong correlations between estimated flood peaks and assigned return periods. The flood magnitudes computed by the Gumbel's distribution that are associated with the 10- and 50-year events depicted both higher and lower magnitudes than those estimated by the LP3 distribution. The 10-year rainfall events ranged from 454.39 mm to 939.92 mm while flood magnitudes of 10-year discharge events ranged from 0.31 m^3/s to 41.92 m^3/s. Similarly, the floods associated with a recurrence interval of 50 years had flood magnitudes ranging from 478.84 mm to 1370.16 mm and discharge magnitudes ranging from 0.41 m^3/s to 66.14 m^3/s. These predictions can also be considered beneficial to people of the LRC and their environment at large as they can save the destructions caused by floods. Similar to LP3, the amounts detected could be taken as the estimated limiting values for design purposes in the catchment, except for sub-catchment A9H001 which showed very large amounts for the 10- and 50-year return periods.

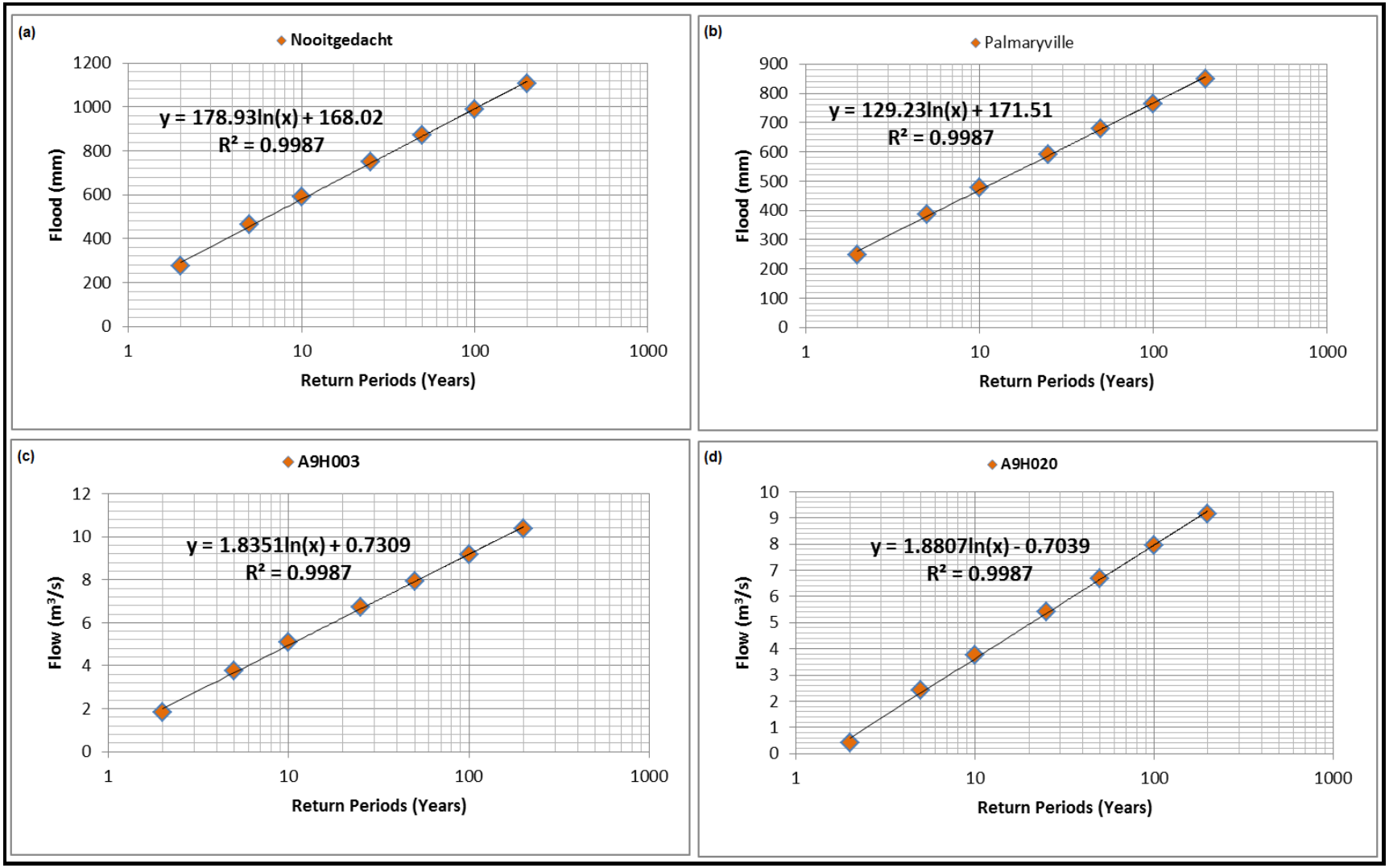

Figure 4.75: Estimated flow magnitudes for 2, 5, 10, 25, 50, 100 and 200 years return periods using Gumbel's distribution

4.5.5 Goodness of Fit

The histogram of annual maximum flood in Figure 4.76 showed a unimodal distribution which was skewed to the right. The probability density function showed that the LN and LP3 exhibited similar probability densities with higher frequencies than that of GEV and EV1 distributions. The skew in this study was found to be -0.4, which made it necessary for tests of low outliers to be considered first. Based on the probability plots, the distribution with the highest frequency was selected to ensure that designs would be based on the highest safety standard for the probable maximum flood. In this study, the LN and LP3 probability distributions were selected as the best valid distributions to model flood probability in the catchment. The Probability-Probability plots for LN and LP3 showed less bias and provided more linear graphs than GEV and EVI.

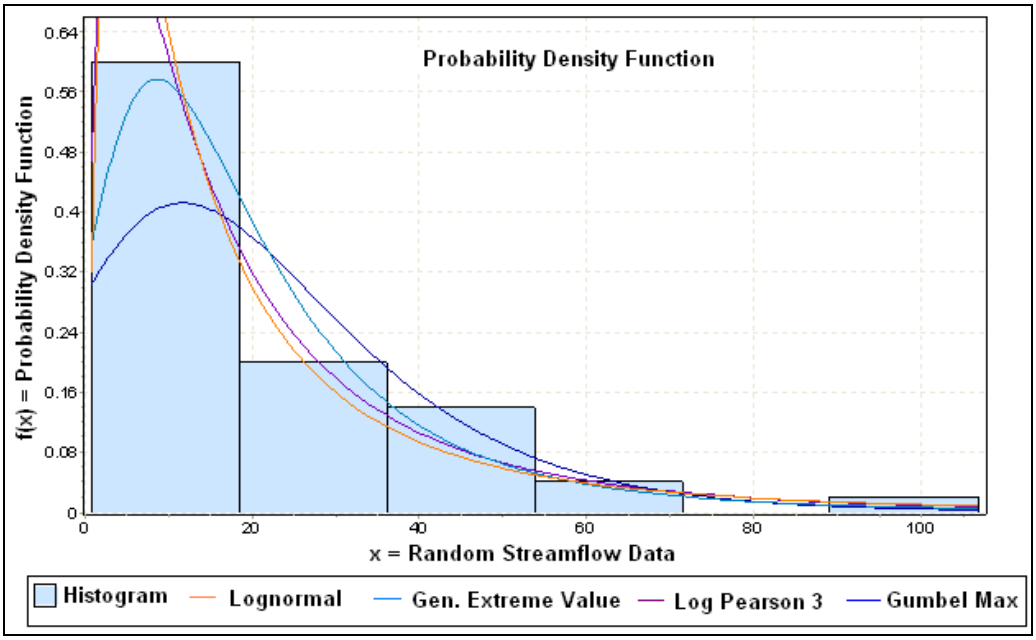

Figure 4.76: Histogram and probability density functions

The cumulative distribution function in Figure 4.77 showed the non-exceedance probability for a given magnitude. The right-skewness of each data set was shown by their concave shapes of their graphs. The calculated probability from the density function was further refined by the cumulative frequency distribution, which made it possible to directly compute the non-

exceedance probability for a given magnitude. The linearity of the probability plot indicated the goodness of fit as shown in Figure 4.78. The Probability-Probability plots for LN and LP3 showed less bias and provided more linear graphs than GEV and EVI.

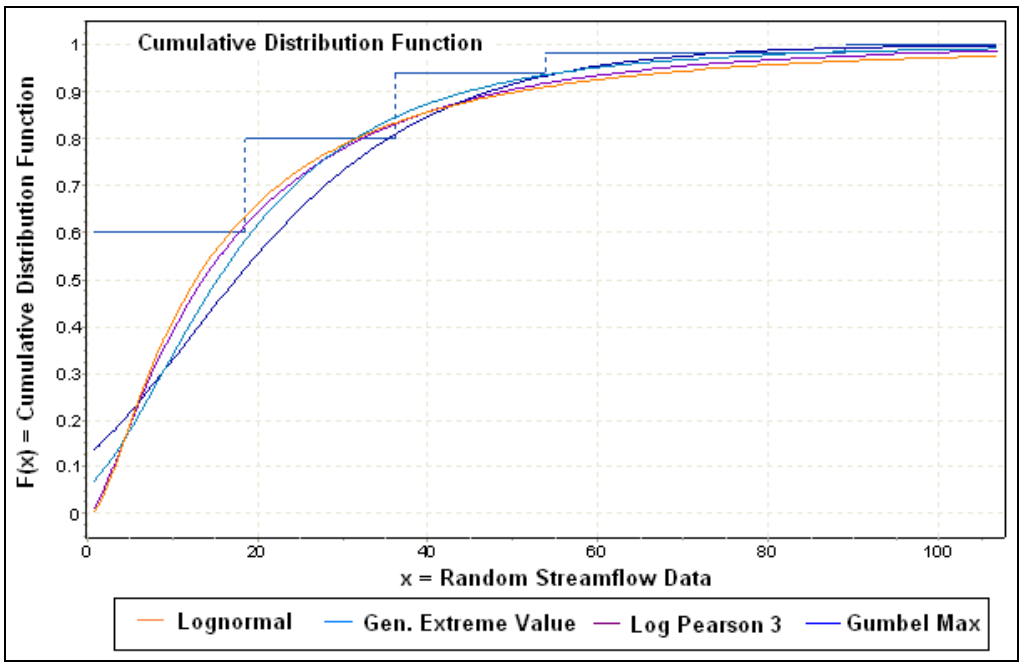

Figure 4.77: Cumulative distribution functions

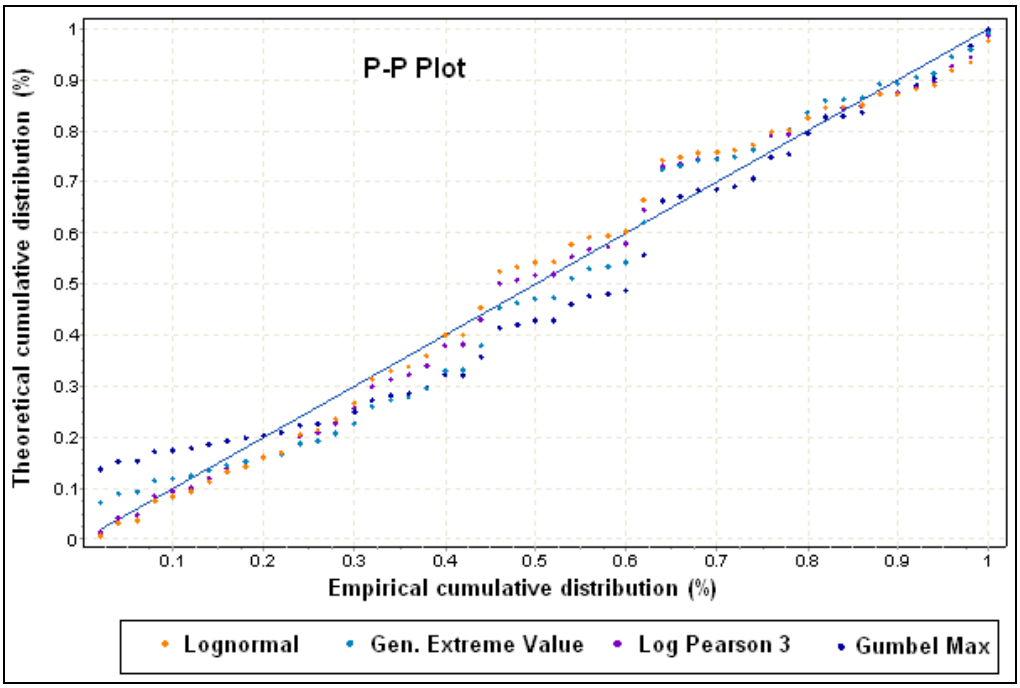

Figure 4.78: Probability-Probability plots

The parameters were estimated in order to make probability statements about the likelihood of future flood magnitudes. In general, a distribution with a larger number of parameters would be able to model the input data more accurately than a distribution with a lesser number Cunnane, (1989). In this case, GEV and LP3 had three parameters while EVI and LN had two parameters of location and scale, which indicated that they had a shape value of zero. The scale parameter was dominating in all cases, indicating large variance of extreme events, except for LN which had small-scale values that indicated relatively little variance.

The four models showed increasing discharges at higher probabilities of exeedence for all return periods, which could be associated with the effects of land cover and land use change. The EVI and LP3 models showed the highest discharges which could be taken as the estimated limiting values for design purposes, especially for the 100 and 200 year return periods. Based on the results, the computations showed that an increase in the peak discharges was to be expected, especially for the discharge range corresponding to small and middle floods. Given the rapid land use changes in the catchment, a significant rise in dam water levels would lead to an increase in potential flood damages, particularly for flood events of lower to medium extremity, reducing flood security for existing protection facilities. The effect would however be less for events with a lower probability of occurrence involving large floods.

Flood frequency and magnitude analyses were used to predict design floods along the course of Luvuvhu River. The estimated statistical values including mean, standard deviation, recurrence intervals and discharge were used to construct frequency distributions, which showed the likelihood of various discharges as a function of exceedance probability. These estimations could be used to assign hydrological and hydraulic dimensions to hydraulic structures like bridges.

In general, a distribution with a larger number of parameters would be able to model the input data more accurately than a distribution with a lesser number. In this case, GEV had a positive (k) parameter which showed that it belonged to the EV3 distribution. The EVI and LN distributions had two parameters, (u) and (σ) which indicated that they had a k-value of zero. The LP3 distribution provided the likely values of discharges to expect in the river at various recurrence intervals. This is helpful when designing structures in or near the river that may be

affected by floods. It is also helpful when designing structures to protect against the largest expected event.

Flood hazard depends on many parameters such as flooding depth, flood duration, velocity of flood flow, and frequency of occurrence. Since human activities can be controlled, the focus should be primarily directed towards managing the causes of flooding in LRC. But it should be noted that climate change is likely to increase both the magnitude and frequency of extreme weather events, which will lead to greater flooding and associated damage.

4.6 Soil Factors

4.6.1 Soil Analysis

The results showed a high proportion of sandy loam and silt loam, where sandy loam contained 50-88% silt, 0-27 clay, and 0-50 sand. Silt loam on the other hand contained 50% silt, 7-20% clay and more than 52% sand. In semi-arid regions like the LRC, sandy loams are well drained soils and are good for plant growth, though the constant renewal leads to deeper, more nutrient-enriched soils which are favorable to the development of forests. Available soil surveys in the catchment indicated that 17% of the soils of the basins (960 280 ha) were potentially suitable for afforestation. However, only 14% of this area (14 750 ha) has been planted (Hope *et al*., 2004). Silt loams on the other hand are poorly drained and are easily eroded into streams and rivers from cultivated lands. Many rivers in the catchment fill with silt and die as exotic timber plantations in the catchment consume more water than indigenous trees. Where these plantations are in river catchments, silting may occur but more often the rivers run dry. Clearing of trees also expose the shallow soils which wash away in heavy rain. In these cases, the sponge effect is destroyed, soil is loosened, and the silt-laden water races down to deposit its load of mud in the rivers further downstream. The sponge effect, which is created by plant roots, allows water to penetrate slowly and be stored underground. They can therefore help prevent soil being washed away by rain and rivers, and safeguard against flooding (Bruijnzeel, 2004).

The grain size distribution curves for Mukula and Levubu were as shown in Figure 4.79 and Figure 4.80 respectively. The soil grading curves for different sampling sites were as shown in appendix 24. The grading curves showed that the soils at the sampling sites comprised of

smooth, concave distribution curves revealing well graded soils. The soil classification triangle for the catchment was as shown in Figure 4.81.

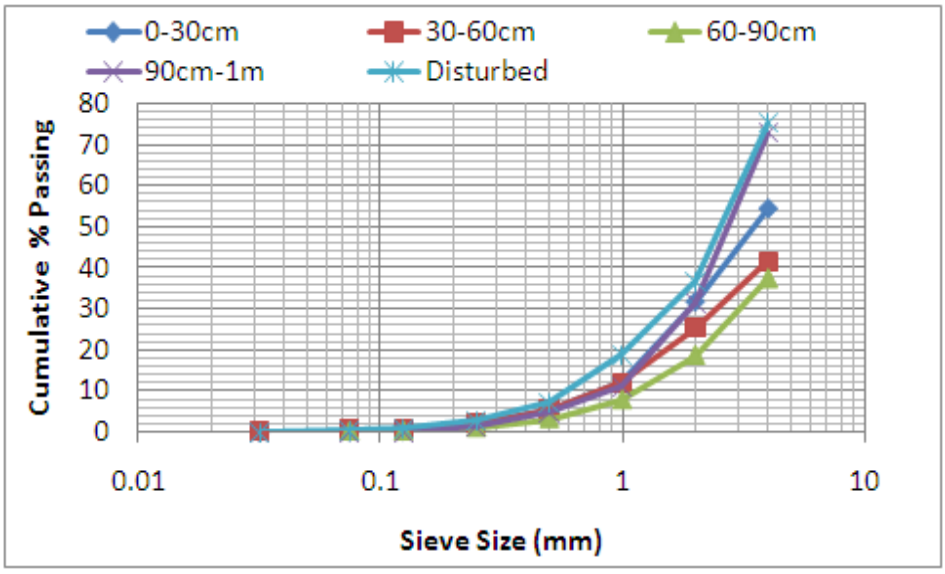

Figure 4.79: Grain size distribution curves for Mukula

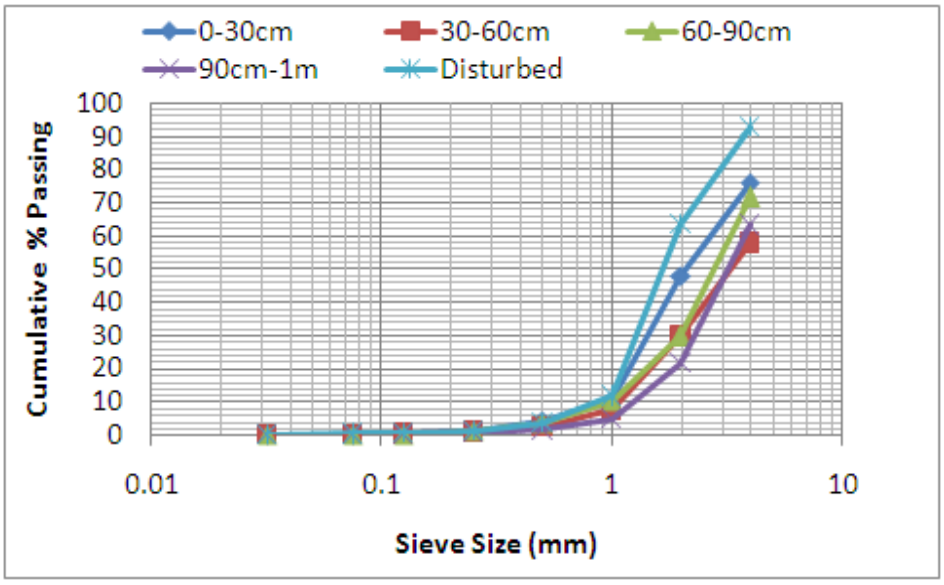

Figure 4.80: Grain size distribution curves for Levubu Settlements

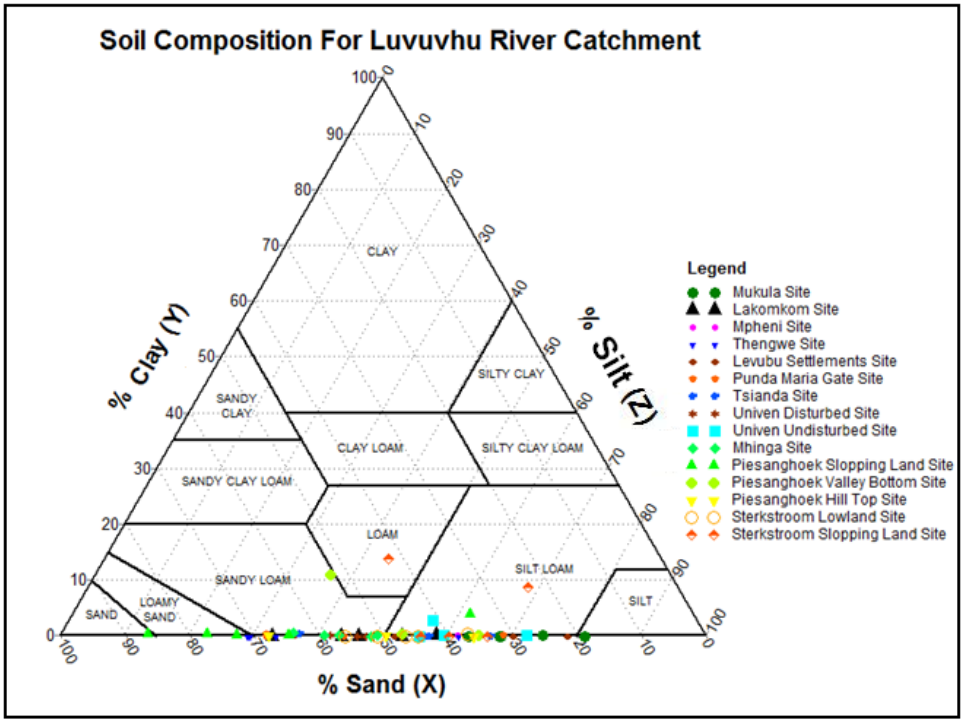

Figure 4.81: Soil classification

A study by Bumby (2000) found that the upland areas of the catchment were dominated by soils derived from quartzite and sandstones (Leptosols), which are generally shallow, gravely and well drained, with low nutrient content and acidic characteristics. The lowland areas are dominated by clay-rich soils which shrink and swell with changes in moisture content (Vertisols) and clay accumulation horizon, or argic B-horizon (Acricsols) (FAO-ISRIC-ISSS, 1998). In other words, soils in lowland areas are characterised by clay-enriched lower horizons and weakly developed organic horizons (IUSS, 2006). The lowveldt areas however, are dominated by soil consisting of unconsolidated material from freshly deposited alluvium or sand (Regosols). Thus, the soils in the study area vary in productivity and are also vulnerable to various forms of degradation, either physical, chemical or biological and hence appropriate management strategies are critical if productivity of the soils is to be improved and sustained.

4.6.2 Soil Moisture Analysis

The results showed that soil moisture was variable in space and time within the catchment being influenced by soil texture, vegetation, topography, and other hydrological components. At all

sites, the soil moisture increased with an increase in soil depth up to 90cm, and then declined to 1m depth as shown in Figure 4.82. An increase after 90cm was noted at Levubu settlements site 1, Mhinga, Univen disturbed site, and Sterkstroom. At Tsianda site 1 and Elim, soil moisture leveled off at 60cm. The gravimetric soil moisture content was very high at Tsianda site 2 reaching an estimate of 92.64% at 60-90cm depth. For other average values, the soil surface moisture content was less than 40% at all other sites. The lowest soil water content was found at Thengwe with a minimum average of 8.19, 7.03 and 6.48 percent at site 1, 2, and 3 respectively. The higher evapotranspiration capacity associated with plantation, forest and shrub vegetation may have resulted in lower soil moisture contents in these parts. Changes to land cover may therefore altered the soil moisture content such that re-vegetated in cultivated lands area may impede surface flows within the catchment. Throughout the study area, the surface soil moisture showed both increasing and decreasing trends. The mass of wet soils at each site was higher than the dry soils. This was due to the fact that the moisture in the wet soil was lost when the soil was being oven dried in order to estimate the water contents in soil. Extremes in weight of wet and dry soils were noted at Tsianda, Lakomkom, and Univen disturbed/undisturbed sites which recorded between 500 and 900 grams. As demonstrated by Hillel (1980) and Maidment (1992), the extreme in wet soil occurred when plants suffered because of decreased aeration whereas the dry soil extreme occurred when vegetation had difficulty obtaining the water they need (Hillel, 1980). Dry weight could be used as a measure of vegetation growth stress in the catchment to prevent erosion caused by excessive rain that results in surface runoff.

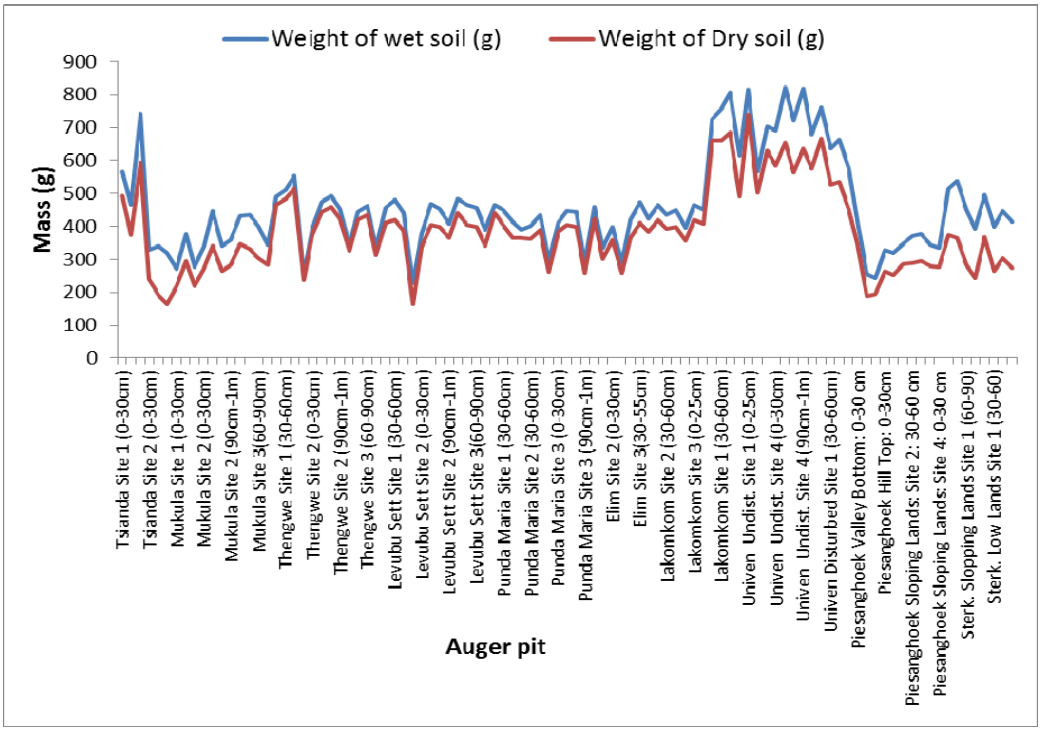

Figure 4.82: The mass of wet and dry soils

4.6.3 Infiltration Rates

Cumulative soil infiltration rate was higher with lower initial soil water content, and higher with higher soil saturated hydraulic conductivity. Cumulative infiltration indicated the variability in water intake rates of soils units within the experimental sites. In general, the initial infiltration rate was high when water was applied to dry soil. In the study area there was removal of indigenous vegetation which leaves the ground exposed to the surface. Since most areas of land were used for agricultural production, a small loss in the infiltration capacity of agricultural soils may have serious impacts on flood intensity. Results of this study indicated that infiltration rates for vegetated and grassy surfaces were higher than those of the bare grounds and sparsely vegetated surfaces. Such results agree with studies of Rietkerk *et al*., (2000) and Li *et al*., (2004) who have showed that vegetation covered soil has a relatively higher infiltration than the bared soil, because plant roots tend to increase the infiltration. This implies that the vegetated landuse and land cover contributes better to soil protection against surface runoff and erosion than bare grounds and sparsely vegetated surface in the study area. It is believed that porosity, which is a

measure of the water bearing capacity of a soil, plays a role in the determining the capability of the soil to transmit water.

Hillel (1980) showed that an infiltration rate of less than 15mm/h is a low infiltration rate; medium infiltration rate ranges from 15mm/hr to 50 mm/hr; whereas high infiltration rates are those greater than 50mm/hr. Infiltration rates above 100mm/hr are associated with coarse texture (i.e. sandy or gravel soils) whereas values of less than 50mm/hr are mostly likely on medium fine textures (i.e. silty clay) (Diamond, 2003). Figure 4.83 showed that the study area was characterised by low, medium and high infiltration rates. At some sites, whose locations were highlighted in Figure 3.11, infiltration rates were very high exceeding 100mm/hr. The figure showed that the initial infiltration rates for the study area were high, ranging from 81.6mm/hr to 114.0 mm/hr. The overall measured infiltration rates for the study area ranged from 0.5mm/hr to 114.0 mm/hr. The steady state infiltrations were attained at different times between all the measured points. This may be due to the spatial variability of the infiltration rates at different selected sites. The steady state infiltration rates at Tsianda, Univen sites and Sterkstroom sites ranged between 20 mm/hr to 25mm/hr while Lakomkom farm, Levubu settlements, Punda Maria, Piesanghoek hill-top and slopping land had steady state infiltration rates of less than 15mm/hr. Areas of Mpheni, Mhinga and Piesanghoek farmlands had steady state infiltrations between 15 - 20mm/hr. This indicates that the water storage was taking place in the vicinity 20 mm/hr throughout the rainfall. Accumulated infiltrations for the study area ranged from 0.68 – 49.78 mm/hr. The time of ponding estimated by the Horton's equation during the infiltration experiments ranged from 0.23 hours to 0.35 hours. This refers to the elapsed time between the time rainfall begins and the time water begins to pond on the soil surface. A South African study by Blight *et al.,* (2001) measured steady state infiltration rates varying from 0.28 mm/hour to 27.3 mm/hour through a double ring and single ring infiltrometer which are not different from the present study. Abu-Hamdah *et al*., (2006) clarified that the significantly different infiltrations observed between different soils suggested that texture impacts hydrological differences between soil types. These differences determine to a large extent, whether a soil is prone to runoff and erosion as infiltration plays a vital role in the infiltration process.

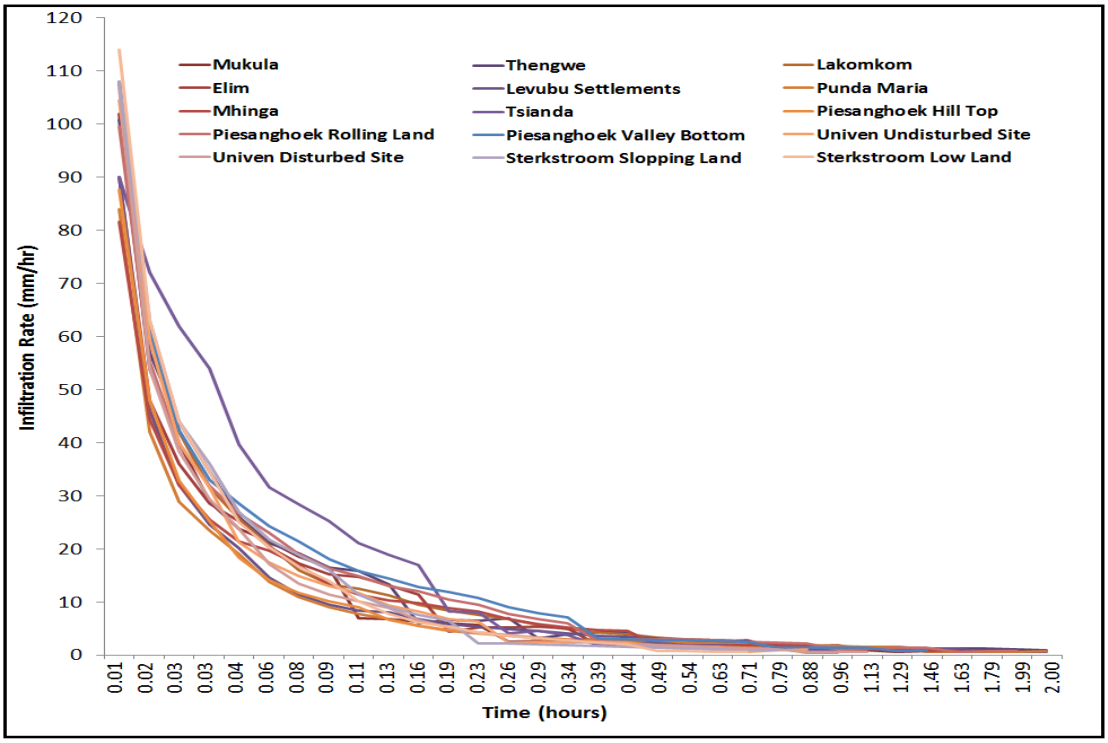

Figure 4.83: Infiltration rates at selected sampling sites

The high infiltration rates obtained in this study showed that there was high potential for groundwater recharge and reduced runoff in the study area. Some areas in the catchment were characterised by steep slopes which ease and improve runoff to be settled in lower gentle slopes giving more time for water to infiltrate into the ground. The water tends to infiltrate less and flow quickly down to rivers as overland flow. Other areas were characterised by flat slopes, where slow runoff enhances infiltration. Such areas were mostly characterised by sparsely vegetation which decreases runoff and soil erosion. This is due to the fact that vegetation acts as a shock absorber and traps the velocity of rain drops. In flat areas, infiltration of water is favoured due to high porosity under vegetation. Some areas were of sloppy terrain which increases runoff and soil erosion and reduces water infiltration. Other areas had gentle undulating relief which consist of rolling and slopping lands and hills, which impede infiltration and enhance runoff generation. The characteristics of the surface topography of each sampling site were highlighted in the methodology of this study. This shows that the relief of the land together with spatial variability

can have an impact on soil water infiltration. It can be assumed that the soil stores infiltrated water to become soil moisture, and then it recharges to groundwater level if the soil is saturated.

4.7 Impact of Land Cover Change on Hydrology and Water Resources in LRC

The impact of land cover change was determined from the overall effects as they affected peak runoff and the stream flow in the catchment. These were exposed during the analysis of hydrometeorological data as well in comparison with the state of the land cover during the study period. The detection and analysis of land cover and land use change showed that the conversion of land cover from forest to agriculture and grassland disrupted the hydrological cycle of the drainage basin, increasing evaporation and consequently, the runoff response of the area. It was observed that subsistence agriculture had extended to the steeper slopes and in the riparian areas of the catchment. The practice of continuous cultivation was impoverishing the soils as little or no land was left to fallow even as it lost fertility. The SWAT model observed sheet and rill erosion in Tshakuma and Tsianda areas in the Levubu valley and gullies were beginning to develop along foot paths. Direct expansion method showed that the higher surface albedo, the lower surface aerodynamic roughness, the lower leaf area and the shallower rooting depth of pasture reduced evapotranspiration as compared to forests which increase discharge in the long-term. In addition, low-productivity grasses like natural grassland pasture had lower leaf area and produced less litter than the original vegetation. With a lower leaf area, the pasture did not intercept as much rainfall as the forest did, making a higher fraction to reach the ground. With less litter, the capacity of surface detention was decreased, and a greater proportion of the rainfall run-off as overland flow. If surface runoff increases substantially and infiltration is critically reduced, soil moisture may also decrease, contributing to a further reduction in the ET_o. In addition, the shift from sub-surface flow to overland storm flows that often accompanies deforestation followed by adverse land use may produce dramatic changes in the catchment peak flows as well. Furthermore, if the change in infiltration associated with the land use change overrides the effect of reduced evaporation, then a shift in the river's flow regime may be expected with increased peaks during the rainy season and lowered flows during the dry season**.**

Urbanisation was associated with a proliferation of impervious surfaces such as paved roads, parking lots, and rooftops and created an environment whose impervious surfaces exceeded 80

percent of land cover in townships. The effect of such surfaces was two fold; first, it increased the velocity of runoff, with rain water being channeled to streams much more rapidly than under conditions of natural vegetation cover, secondly, infiltration was reduced, which reduced the groundwater levels and therefore the base flow of streams, such that the steady state stream flows that would be fed by groundwater between precipitation events were disturbed. Under such conditions, streams were stripped of their natural character, and flood runoff peaked dramatically after rainfall events.

The complex interactions between land use and stream flows were not fully established by the end of the research. Part of the difficulty was isolating the effects of local and regional land cover from other factors, such as atmospheric circulations that led to the El Nino rains. A strategy of preserving natural forests and investing in sustainable agriculture, especially in uplands, could significantly reduce potential losses caused by the effects of degradation.

4.8 The Contribution of the Study to the Economy

4.8.1 Contribution to knowledge

One of the major contributions of this study is the new shapefile map of Luvuvhu River catchment. It is different from the older map which showed the catchment to have a sharp and hook-like outline near the mouth. Furthermore, the catchment can now be availed on digital platforms as a virtual catchment. This presents the opportunity for hydrologists and other stake holders to perform multifaceted scenario analysis for optimal utilization of the land and water resources.

The relative sensitivity analysis identified the parameters that influenced the predicted discharge, sediment loading and nutrient content of surface and ground water. The results can be used by farmers and stakeholders to mitigate against the negative effects of agricultural activities during the rainy season in the months of October to April. Application of manure from livestock production and direct runoff can lead to acidification of soils due to the volatilization of ammonia which may increase the solubility of metals in the soil.

4.8.2 Contribution to Planning and Policy

The basic cause of problems in water catchments is pressure of population on land. The rapid growth of population increases dependence on subsistence agriculture and livestock keeping by methods that are not viable.

In order to plan and properly manage development in the catchment, the outcomes of this study could be used to inform policy on land use and development of new human settlements in the catchment. Water resources planning should involve setting modalities for a systematic and sustainable development of land and water resources with a view to averting their depletion and degradation.

The predicted volumes and peak runoff rates should be used as a function of the probability that the design storm will be exceeded during the life of structures in the catchment. It is important to relate the probability of a given sized event occurring in any year to the exceedance interval or return period. Water resources should be managed and used efficiently and effectively so as to promote its conservation and future availability in sufficient quantity and quality.

All programmes related to water use should be implemented in a manner that mitigates environmental degradation. The allocation of water should be designed in a manner that recognizes the resource not only as a human right but also an economic good, to achieve maximum benefit to the whole country. The government shall facilitate the participation of stakeholders, both in the public and private sectors to ensure that the needs of their relevant interests are taken into account.

Long-term management policies should address floods and droughts which are intrinsic features of climatic variability and climate change. Both can be alleviated by good land use planning which will control the movement of sediment and debris, thus protecting investments in reservoirs including Albasini and Nandoni. Improvements in land and water resources management can reduce poverty and destruction of resource and help the local and national governments achieve economic growth in LRC.

CHAPTER 5
CONCLUSION AND RECOMMENDATIONS

5.1 Conclusion

The study mainly aimed at evaluating the impact of land cover changes on the hydrology and water resources of LRC using GIS, remotely sensed imagery and ancillary data, mainly DEM derived data. The objectives of the study were informed by the need to detect and quantify land cover and land use changes and examine their impact on the hydrology and water resources in the catchment; extract and analyse morphologic and hydrologic properties and evaluate their effects on the hydrologic processes; analyse hydrometeorological trends for a period of 50 years and evaluate the annual flood frequency; gain a better understanding of the hydrologic phenomena operating in a catchment and of how changes in the catchment may affect those phenomena; and generate synthetic sequence of hydrological data for facility design or for use in forecasting. The objectives of this study were met and specific results and conclusions are presented in the subsequent paragraphs.

The use of multi-temporal remotely sensed data showed that the LRC had undergone significant changes in land cover over decades. The satellite time series analysis of 1980's, 1990's and 2000's showed the pre-change and post-change cover types. The predominant land cover classes selected for the study included agriculture, natural forest, bare ground, shrub and grasslands, plantation, and water bodies. At the level of individual classes, the best results were obtained for bananas with a coefficient of variation of 10.22% and a regression coefficient of 5.07%. The eucalyptus plantations had the lowest reliability with a coefficient of variation of 70.65. Throughout the 2000's, land use change revealed a decrease in natural forest from 29.34% to 20.67% and giving rise to agriculture which rose to 38.57% in 2010. Reduction of forest cover and rapid increase in human settlements had impacted negatively on the hydrology and water resources in the catchment; resulting in reduced baseflow, increased surface runoff and an increase in evaporation rates.

The Natural Resource Conservation-Curve Number (NRCS-CN) related the detected land cover changes to runoff using the physically derivable curve number parameter. Results indicated that

land cover changes affected the hydrological response of the basin leading to increased peak discharges and runoff volumes. The increase was more in the upstream sub-catchments where deforestation was rampant and led to dwindling soil moisture retention capabilities and rates of infiltration. The deforestation in this area was related to indigenous population growth, with increased demands for fuelwood and timber for house construction; tree cutting for cooking, clear-cutting for agriculture, ranching and development, and degradation due to climate change. Given the rapid land use changes in the catchment, a significant rise in water levels would lead to an increase in potential flood damages, particularly for flood events of lower to medium extremity, reducing flood security for existing protection facilities.

The flood peak discharges in the whole basin was noted to have increased by at least 17% over the period of 1980 -2009. In some cases, changes in the peak discharges in the sub-catchments were also noted to decrease with increase in the rainfall amounts indicating the possibility that the land cover changes may not have a very strong influence during large storm events. The flood volumes were also noted to have increased by at least 11% over the same period of time. The flood time to peak indicated a decreasing trend, in the range of 0.5 to 1 hour within the years. When severe floods occur, people who live close to rivers are at the risk of losing their lives; while their houses and farms may be destroyed. The variation of suspended sediment load was significantly affected by the human activities and the rainfall and runoff in the catchment. The SWAT model was applied to the Tsakhuma-Levubu sub-catchment in the Upper LRC for the purpose of simulating the rainfall-runoff process in the sub-basin. The model was found to be suitable for predicting the location of runoff-generating areas in the sub-catchment.

The analysis of flood frequency showed increasing discharges at higher probabilities of exceedance for all return periods. The results showed that an increase in the peak discharges was to be expected, especially for small and middle floods. However, a distribution with the best goodness of fit could be used as a powerful tool for estimating and calculating the return period for the floods anywhere along rivers in the catchment. The EVI and LP3 models predicted the highest discharges which could be taken as the estimated limiting values for design purposes, especially for the 100 and 200 year return periods.

Results show that the proposed conceptual framework is a useful tool to support land planning and forest management, adapting the provision of hydrological services to the regional biophysical and social conditions. The information on land cover change and associated hydrological impacts were addressed. The overall results showed that the changes in land cover influenced the hydrologic processes in the LRC. The main cause of land cover change in the catchment was rapid population growth in which rapid land use, mainly deforestation and agricultural practices were prominent. The general trends derived showed that conversion from forest to agricultural fields was dominant. Understanding how the changes in land use and cover influence hydrology and water resources can enhance the ability of planners, practitioners, researchers and farmers to formulate and implement sound policies to minimize undesirable future impacts and devise management alternatives. The information obtained in this study should therefore be used as a baseline study for future studies in the catchment or elsewhere.

5.2 Recommendations

1. There should be further research employing remotely sensed data of higher spatial and temporal resolution from different sensors to detect and quantify land cover changes. The spectral signatures generated from such studies should be applied in monitoring environmental processes with the aim of understanding the interactions between hydrological regimes and the physiographic characteristics of the catchment. Advanced techniques utilising the science of hyperspectroscopy should be used in soil moisture studies and suspended sediment monitoring.

2. Higher resolution Digital Elevation Models should be generated by using a combination of different interpolation techniques to enable advanced analysis of hot-spot areas. The hilly terrain in the catchment should be modeled using a higher density of spot heights whereas plains and rolling land could be modeled by sparse spot heights. This would improve the sensitivity of the models which would then make the analysis of the soil-landscape relationships more accurate. Terrain attributes derived from land elements could then be used as indicator variables for risk and pollution arising from developments.

3. The collection of hydrometeorological data should be intensified by using automatic field measuring equipment as much as possible. The spatial distribution of weather stations should cover the different micro-climatic zones of the catchment in order to provide representative data. More research should be carried out to determine whether the increase in flood frequency and magnitude may also be related to climate change. There should be more inter-agency collaboration in the area of data gathering and analysis in order to access and utilize the best resources in the country.

4. There should be close monitoring and sustained enforcement of the rural land use regulations to prevent the conversion of land to urban land use. A participatory approach involving all stakeholders should be employed to promote sustainable developments in the catchment. Uncontrolled developments disrupt the hydrological cycle and impact on the catchment response. The higher surface albedo which results from paving and land clearing; lower leaf area and shallower rooting depth of pasture and grasses lead to reduced evapotranspiration. The low-productivity open lands that replace cleared grounds produce less litter. With less litter, the capacity of surface detention decreases, and a greater proportion of the rainfall goes as overland flow.

REFERENCES

Abdullahi, A.S., Ahmad, D., Amin, M.S.M. and Aimrun, W. (2013) Spatial and Temporal Aspects of Evapotranspiration in Tanjung Karang Paddy Field, Peninsular Malaysia. *International Journal of Science, Engineering and Technology Research* 2(2): 473-479, ISSN 2278-7798.

Abu-Hamdah, N., Abo-Qudais, A. and Othman, A.M. (2006) Effect of soil aggregate size on infiltration and erosion characteristics. *European Journal of Soil Sciences*, 57: 609-616.

Ackermann, E.R. (2011) Sequential land cover classification. Published Msc thesis, University of Pretoria, 129p.

AgriInfo, (2011) Methods of Soil Moisture Estimation Laboratory & Field Methods. Available at *http://www.agriinfo.in/default.aspx/*, 25 January 2011

Ahmed, A.A. and Fawzi, A. (2011) Meandering and bank erosion of the River Nile and its environmental impact on the area between Sohag and El-Minia, Egypt. *Arabian Journal of Geosciences*, 4(1): 1-11.

Ahrens, C.D., Jackson, P.L., Jackson, C.E.J. and Jackson, C.E.O. (2012) Meteorology Today: An Introduction to Weather, Climate and the Environment, Cengage Learning, Boston, 640p.

Akbarimehr, M. and Naghdi, R. (2012) Assessing the relationship of slope and runoff volume on skid trails (Case study: Nav 3 district). *Journal of Forest Science*, 58(8): 357–362

Akrasi, S.A. (2011) Sediment Discharges from Ghanaian Rivers into the Sea. *West African Journal of Applies Ecology*, volume 18: 1-13, ISSN: 0855-4307.

Albhaisi, M., Brendonck, L. and Batelaan, O. (2013) Predicted impacts of land use change on groundwater recharge of the upper Berg catchment, South Africa. *Water SA*, vol.39, no.2, Pretoria, ISSN 1816-7950.

Alemaw, B.F. and Chaoka, T.R. (2006) The 1950–1998 warm ENSO events and regional implication to river flow variability in southern Africa. *Water SA*, 32:459–463.

Alexander, W.J.R. (1990) Flood Hydrology for Southern Africa. SANCOLD, Pretoria, RSA.

Alexander, W.J.R. (2001) Flood Risk Reduction Measures. University of Pretoria, Pretoria, RSA.

Alhassoun, R.A. (2009) Studies on factors affecting the infiltration capacity of agricultural soils. Published PhD Thesis, Carol Wilhelmina Technical University, Braunschweig, Germany. 173p.

Allen, J.D. and Hanuschak, G.A. (1988) The Remote Sensing Applications Program of the National Agricultural Statistics Service 1980-1987. *National Agricultural Statistics Service staff report no. SRB-88-08*, United States Department of Agriculture, National Agricultural Statistics Service.

Allen, R.G., Pereira, L.S., Raes, D. and Smith, M. (1998) Crop evapotranspiration: guidelines for computing crop water requirement. *FAO Irrigation and Drainage Paper* No. 56, Rome, Italy.

Allred, K.O. (2001) Multi-objective spatial decision support for protection of streams in urbanizing watersheds. Published MSc Thesis, Southern Illinois University, Carbondale, USA, 69p.

Alonso, F.G., Soria, S.L. and Gozalo, J.C. (1991) Comparing two methodologies for crop area estimation in Spain using Landsat TM images and ground-gathered data. *Remote Sensing of Environment*, 35(1) :29-35. DOI: 10.1016/0034-4257(91)90063.

Andersen, F.H. (2008) Hydrological modeling in semi-arid area using remote sensing data. Published PhD Thesis, University of Copenhagen, Denmark.

Anderson, J. R. (1977) Land use and land cover changes: A framework for monitoring. *Journal of Research by the Geological Survey*, 5: 143-153.

Angino, E.E. and O'Brien, W.J. (1968) Effects of suspended material on water quality, *in* Proceedings of Symposium on Geochemistry, Precipitation, Evaporation, Soil Moisture, Hydrometry, General Assembly of Bern, September–October 1967: *International Association of Science Hydrology*, no. 78: 120–128.

Angliss, M., Ashton, P., Cook, C., Deacon, A., Foord, S., Fouche, P., Henning, D., Kleynhans, N., Rodgers, S., Roux, D., Strydom, W., Vink, D., Van Der Waal, B., Van Wyk, E. and Vlok, W. (2001) State of rivers report (2001). Letaba and Luvuvhu Systems. WRC report no: TT 165/01, Water Research Commission, Pretoria.

Angstrom, A. (1924) "Solar terrestrial radiation," Quarterly Journal of the Royal Meteorological Society, 50: 121–126.

Anornu, G.K., Kabo-bah, A. and Kortatsi, B.K. (2012) Comparability Studies of High and Low Resolution Digital Elevation Models for Watershed Delineation in the Tropics: Case of Densu River Basin of Ghana *International Journal of Cooperative Studies*, 1(1): 9-14.

Arnold, G.J., Srinivasan, R., Muttiah, R.S. and. Williams, J.R (1998) Large area hydrologic modelling and assessment Part I: Model development. *J. Am. Water Resour. Assoc.* 34(1): 73–89.

ASCE, (1996) *Hydrology Handbook*. 2nd Edition, ASCE Manuals and Report on Engineering Practice, No 28. Task Committee on Hydrology Handbook, American Society of Civil Engineers, USA.

ASTM, (2007) D4410, in terminology for fluvial sediment, annual book of standards, water and environmental technology: West Conshohocken, Pennsylvania, ASTM International, 7p.

Badhwar, G.D., Chhikara, R.S. and Pitts, D.E. (1986) Field size distribution for selected agricultural crops in the United States and Canada. *Remote Sensing of Environment,* 19: 25-45.

Bagnold, R.A. (1966) An approach to the sediment transport problem from general physics. Online USGS professional paper 422-1, U.S. Govt.Print.Off, 37p.

Baldyga, T.J., Miller, S.N., Shivoga, W. and Maina-Gichaba, C. (2004) assessing the impact of land cover change in Kenya using remote sensing and hydrologic modeling. ASPRS Annual Conference Proceedings May 2004, Denver, Colorado, *ASPRS.*

Bansode, S. and Patil, K. (2016) Water balance assessment using Q-SWAT. *International Journal of Engineering Research*, 5(6): 515-518.

Bayliss, A.C. and Reed, D.W. (2001) The use of historical data in flood frequency estimation. A report to the Ministry of Agriculture, Fisheries and Food (MAFF), Centre of Ecology and Hydrology, Oxfordshire, UK.

Beckedahl, H.R., Bowyer-Bower, T.A.S., Dardis, G.F. and Hanvey, P.M. (1988) Geomorphic effects of soil erosion. In: Moon, B.P. and Dardis, G.F. (Eds), The Geomorphology of Southern Africa, Southern Book Co. Johannesburg, p249-277.

Benson, M.A. (1960) Characteristics of frequency curves based on a theoretical 1,000-year record, in Dalrymple, Tate, Flood frequency analyses: U.S. Geol. Survey Water-Supply Paper 1543-A, 80p.

Berry, B. J.L. and Baker, A.M. (1968) *Geographic sampling, Spatial Analysis: A Reader in Statistical Geography*. (B.J.L. Berry and D.F. Marble, Eds.), Prentice Hall, Englewood Cliffs, N.J., p91-100.

Beven, K.J. (2012) Rainfall-runoff modeling: The primer. 2nd Edition, Willey and Sons, New York, New York, 479p.

Beven, K.J. (2004) Robert E. Horton's perceptual model of infiltration processes. *Hydrological Processes*, 18: 3447–3460.

Bisri, M., Othman, F. and Sholichin, M. (2008) Determination of runoff value using Kineros Model: Case study in Sumpil Catchment, Indonesia, *ICCBT 2008 - D - (15)* - p157-168.

Blight, G.E., Fourie, A.B. and James, C.S. (2001) *Measurements of infiltration and evaporation characteristics of soils in the Nylsvlei Flood-Plain*, 4th Environmental Management, Technology and Development Conference.

Bolch, T., Kamp, U. and Olsenholler, J. (2005) Using ASTER and SRTM DEMs for studying geomorphology and glaciation in high mountain areas. New strategies for European Remote Sensing. M. Oluic (Ed.) Millpress, Rotterdam, p119-127.

Bosch, J.M. and Hewlett, J.D. (1982) A review of catchment experiments to determine the effect of vegetation changes on water yield and evapotranspiration. *Journal of Hydrology*, 55: 3-23.

Brady, N.C. and Weil, R.R. (2002) Elements of the nature and properties of soils. 2nd Edition, Prentice Hall, New Jersey.

Brandl, G. (1999) A The Soutpansberg Group Catalogue of South African Lithostratigraphic Units, South African Committee for Stratigraphy, Council for Geoscience, p639-641.

Brandl, G. (Ed.) (2000) Alldays 1:250 000 Geological Map. Council for Geoscience, Pretoria, South Africa.

Brandl, G. (2002) The geology of the Alldays area. Explanation Sheet Geological Survey 2228, South Africa, 71p.

Briassoulis, H. (2000) Analysis of land use change: Theoretical and modeling approaches. In S. Loveridge (Ed.), The web book of regional sciences, Regional Research Institute, West Virginia University, Morgantown, West Virginia, USA.

Bruijnzeel, L.A. (1990) Hydrology of Moist Forests and the Effects of Conversion: A State of Knowledge Review, Free University, Amsterdam, p224.

Bumby, A.J. (2000) The geology of the Blouberg formation: Waterberg and Soutpansberg groups in the area of Blouberg mountain, Northern Province, South Africa. Published PhD Thesis, University of Pretoria, South Africa, 323p.

Bunce, R.G.H., Barr, C.J. and Fuller, R.M. (1992) Integration of methods for detecting land use change, with special reference to Countryside Survey 1990. In Whitby M C (Ed.) *Land use change: the causes and consequences*. London, Her Majesty's Stationery Office: p69–78.

Burges, S.J. Wigmosta, M.S. and Meena, J.M. (1998) Hydrologic effects of land-use change in a zero-order catchment. *Journal of Hydrologic Engineering*, 3: 86-97.

Burgy, R. H. and Luthin, J. N. (1957) Discussion of "A Test of the single- and double-ring types of infiltrometers". *Transactions, American Geophysical Union*, 38(2): 260-261.

Burrough, P.A. and McDonneL, R.A. (1998) *Principles of Geographical Information System*. Oxford University Press, New York, 332p.

Burrough, O.A. (1986) Principles of geographic information systems for Land Resource Assessment. *Monographs on soil and resources survey*, no 12, Oxford Science Publications, New York.

Butt, A., Shabbir, R., Ahmad, S.S. and Aziz, N. (2015) Land use change mapping and analysis using Remote Sensing and GIS: A case study of Simly watershed, Islamabad, Pakistan. *The Egyptian Journal of Remote Sensing and Space Sciences*, 18(2): 251–259.

Calder, I.R. (1992) Hydrological effects of land use change: In Handbook of Hydrology. D.R Maidment (Ed.), McGraw Hill, New York, p13.11-13.15.

Calder, I.R. (2005) Blue Revolution II: Land use and integrated water resources management, Earthscan, London, 327p.

Campos, J.N.B. (2010) Modeling the Yield–Evaporation–Spill in the Reservoir Storage Process: The Regulation Triangle Diagram. *Water Resources Manage*ment, 24: 3487–3511.

Carpenter, L.G. (1999) The loss of water from reservoirs by seepage and evaporation. *Agricultural Experiment Station Bulletin*, No. 45, 32p.

Central Statistical Agency of Ethiopia, (2008) *Training course on Land Cover Mapping in Support of Area Frame Statistical Analysis.* Case study of West Showa (Ethiopia). Addis Ababa.

Central Statistical Agency of Ethiopia, (2010) Combining enumeration area maps and satellite images (land cover) for the development of area frame (multiple frames) in an African country: preliminary lessons from the experience of Ethiopia. A. Tariku Abaye (Ed.), Addis Ababa.

Central Statistical Agency of Ethiopia, (2011) Comparative Study Between Area Frame and List Frame for Agricultural Survey. *Twenty-Second Session of African Commission on Agricultural Statistics*, Addis Ababa.

Central Statistical Agency of Ethiopia, (2012) Development of Master Sampling Frames for agricultural and rural statistics. The experience of Ethiopia. *Global strategy to improve agricultural and rural statistics. High Level Stakeholders Meeting on the Global Strategy - From Plan to Action. Master Sampling Frames (MSF) for Agricultural and Rural Statistics*, FAO, Rome.

CEP, 2011: Runoff Coefficient factsheet: *The Clean Water Team Guidance Compendium for Watershed Monitoring and Assessment State Water Resources Control Board 5.1.3 FS-(RC). http://www.waterboards.ca.gov/water_issues/programs/swamp/docs/cwt/guidance/513.pdf.*

Chapman, D.C. and Lake, D.W, Jr. (2003) Computing Runoff. Section 4. New York Standards and Specifications for Erosion and Sediment Control. Available at *http://www.cdrpc.org/NET/WQ/ErosANDsed/4comp_runoff_17_38.pdf*.

Chen, L., Shao, Y. and Ren, Z. (1994) Climate change in China during the past 70 years and its relation to the monsoon variations. In Zepp, R. G. (Ed.), *Climate Biosphere Interaction: Biogenic Emission and Environmental Effects of Climate Change*, John Wiley and Sons, New York, p31–49.

Chiew, F.H.S. and McMahon, T.A. (1995) Trends and changes in historical annual stream flow volumes and peak discharges of rivers in the world. Proc. Int. Congress on Modeling and Simulation, November 1995, Newcastle, Australia (in press).

Chiew, F.H. and McMahon, T.A. (2002) Modeling the impacts of climate change on Australian stream flow. *Hydrological Processes*, 16: 1235–1245.

Cho, J., Barone, V.A. and Mostaghimi, S. (2009) Simulation of land use impacts on groundwater levels and streamflow in a Virginia watershed. *Agricultural Water Management* 9 6: 1-11.

Chow, V.T. Maidment, D. R. and Mays. L. W. (1988) *Applied Hydrology*. McGraw-Hill, Inc., 572p.

Chunzhen, L. (2009) Research advances in impacts of natural climate variability and anthropogenic climate change on streamflow. *Advance in Climate Change Research,* 5 (Suppl.), 47J53.

Clarke, K.C. (1988) Scale-Based Simulation of Topographic Relief. *American Cartographer,* 15(2): 173–181.

Cochran, W.G. (1977) *Sampling Techniques*, 3rd Ed., John Wiley and Sons, Inc., New York.

Cohen, I. (1960) A coefficient agreement of nominal scales. *Educational and Psychological Measurement*, 20: 37–46.

Conaghan, K. (2010) Assessing the Hydrologic Implications of Land Use Change for the Upper Neuse River Basin. MSc Thesis, Duke University, 57p.

Coppin, P., Jonckheere, I., Nackaerts, K. and Muys, B. (2004) Digital change detection methods in ecosystem monitoring: a review. *International Journal of Remote Sensing*, 25: 1565-1596.

Costa, M. and Foley, J. (1997) Water balance of the Amazon Basin: dependence on vegetation cover and canopy conductance. *Journal of Geophysical Research*, 102 (D20), 17p.

Coutu, G.W. and Vega, C. (2007) Impacts of land use changes on runoff generation in the east branch of the Brandywine Creek watershed using a GIS-based hydrologic model. *Middle States Geographer*, 40:142-149.

Cunge, J.A. (1969) On the Subject of a Flood Propagation Computation Method (Muskingum Method). *Journal of Hydraulic Research*, 7(2): 205-230.

Cunnane, C. (1989) Statistical Distributions for Flood Frequency Analysis. *Operational Hydrology Report* no. 33, World Meteorological Organization.

Dadhwal, V.K., Aggarwal, S.P. and Misra, N. (2010) Hydrological Simulation of Mahanadi River Basin and Impact of Landuse/Landcover Change on Surface Runoff Using A Macro Scale Hydrological Model. In W. Wagner and B. Szekely, (Eds). *Proceedings of ISPRS TC VII Symposium - 100 years ISPRS,* Vienna, Austria, July 5 - 7, ISPRS, XXXVIII (7B), p165 - 170.

Dagada, K., 2012. Long-term and seasonal changes in evaporation and links to climate change and land use in Luvuvhu River Catchment. Unpublished BSc Hons dissertation in Hydrology, University of Venda, 76p.

Dance, K.W. and Hynes, H.R.N. 1980. Some effects of agricultural land use on stream insect communities. *Environmental Pollution*, 22(Series A): 14-28.

Das, G. (2002) *Hydrology and Soil conservation Engineering*. Prentice Hall of India, New Delhi, 481p.

Das, M.M. and Saikia, M.D. (2012) *Watershed Management*. PHI Learning Pvt. Ltd., 30 Oct 2012 - *Technology & Engineering*, p10.

Das, S., Maitra, A. and Shukla, A.K. (2010) Rain attenuation modeling in the 100 GHz frequency using drop size distributions for different climatic zones in tropical India. *Progress in Electromagnetics Research B*, 25: 211-224.

Daubin, K.W. and Beach, D.W. (1981) Crop monitoring using Landsat. *Proceedings of the 2nd Australasian Landsat Conference*, September 1981, Canberra, Australia.

Davies, B. and Day, J. (1998) *Vanishing Waters*. University of Cape Town Press, South Africa.

Delidjakova, K. Bello, R. and McMillan, G. (2014) Measurements of evapotranspiration across different land cover types in the Greater Toronto area. Sustainable Technologies Evaluation Program, Toronto and Region Conservation Authority, Toronto, Ontario, 49p.

Deng X, Zhao C, Yan H (2013) Systematic modelling of impacts of land use and land cover changes on regional climate: a review. *Advances in Meteorology*, Volume 2013, Article ID 317678, 11p.

Deodhar, M.J. (2009) *Elementary Engineering Hydrology*. Dorling Kindersley Pvt. Ltd, New Delhi, India, 397p.

DeVantier, B., Feldman, A. and Ca, H.E.C.D. (1993) Review of GIS applications in hydrologic modeling. *Journal of Water Resources Planning and Management*, 119: 246-261.

Diamond, J. (2003) Infiltration rate assessment of some major soils. *Irish Geography*, 36(1): 32-46.

Di Gregorio, A. and Jansen, L.J.M. (Eds). (2000) Land Cover Classification System (LCCS): Classification Concepts and User Manual. Environment and Natural Resources Service, GCP/RAF/287/ITA Africover - East Africa Project and Soil Resources, Management and Conservation Service, FAO, 179p.

Di Gregorio, A. and Jansen, L.J.M. (2005) *Land Cover Classification System* (LCCS): *Classification concepts and user manual Software version 2*. Rome: FAO, ISBN 92-5-105327-8.

Dilley, M., Chen, R.S., Deichmann, U., Lerner-Lam, A.L., Arnold, M., Agwe, J., Buys, P., Kjekstad, O., Lyon, B. and Yetman, G. (2005) *Natural Disaster Hotspots: A Global Risk Analysis*. World Bank, Washington, DC.

Dinçergök, T. (2007) The role of dam safety in dam-break induced flood management, *International Congress on River Basin Management*, Antalya, Turkey, 23-25 May 2007, p682-697.

Duaibe, K. (2009) Human activities and flood hazards and risks in the south west Pacific: a case study of the Navua catchment area, Fiji Islands. Published MSc thesis, University of Wellington, New Zealand.

Dube, L.T. (2002) Structure and precursors of the 1992/93 drought in KwaZulu-Natal, South Africa from NCEP reanalysis data. *Water SA*, 29(2): 201-207.

Dunn, S.M. and Mackay, R. (1995) Spatial variation in evapotranspiration and influence of land use on catchment hydrology. *Journal of Hydrology*, 171: 49-73.

DWA (1999) Resource directed measures for protection of water resources, Volume 1, Integration Manual Version 1.0, Department of Water Affairs and Forestry, Pretoria. p78-100.

DWA (2001) State of Rivers Report: South African River Health Programme: Letaba and Luvuvhu River Systems. DWAF, Resource Quality Services. *A report to the Water Research Commission*, WRC Report no 165/01.

DWA (2002) A proposed National Water Resources Strategy for South Africa. Proposed First Edition, Department of Water Affairs and Forestry, Pretoria, South Africa.

DWA (2003) Luvuvhu and Letaba Water Management Area. Overview of water resources availability and utilization. Department of Water Affairs and Forestry, Pretoria, South Africa.

DWA (2004) Directorate: National Water Resource Planning. Internal strategic perspective Luvuvhu/Letaba Water Management Areas. Department of Water Affairs, Pretoria, Report No. PWMA 01/000/00/0304.

DWA (2013) Development of a reconciliation strategy for the Luvuvhu and Letaba water supply system: Demographic and Economic Development Potential. DWA Report Number PWMA 02/B810/00/1412/17. Department of Water Affairs, Directorate: National Water Resource Planning, Republic of South Africa.

Dyson, L.L. (2000) A dynamical forecasting perspective on synoptic weather systems over southern Africa. Published MSc Thesis in Meteorology, University of Pretoria, South Africa.

Dyson, L.L. and Van Heerden, J. (2001) The heavy rainfall and floods over the north-eastern interior of South Africa during February 2000. *South African Journal of Science*, 97: 80-86.

Dyson, L.L. and van Heerden, J. (2002) A model for the identification of tropical weather systems. *Water SA*, 28(3): 249-258.

Dyson, L.L., van Heerden, J. and Marx, H.G. (2002) Short term weather forecasting techniques for heavy rainfall. *A Report to the Water Research Commission by Department of Geography, Geoinformatics and Meteorology*, University of Pretoria. WRC Report NO 1011/1/02.

Earle, A. Goldin, J. and Phemo, K. (2005) Domestic water provision in the democratic South Africa- Changes and challenges , AWRU, GPS, University of Pretoria, South Africa.

Ellis, E. (2013) *Land-use and land-cover change*: In: Encyclopedia of Earth. Eds. Cutler J. Cleveland. First published in the Encyclopedia of Earth April 18, 2010; Last revised Date May 7, 2012; Available at *http://www.eoearth.org/article/Land-use_and_land-cover_change*, February 22, 2013

EPA (2012) Watershed Modeling Approach Recommendation: Lake Champlain Phosphorus TMDL. Prepared for: U.S. EPA Region 1 – New England by Tetra Tech, Inc. February 7, 2012, 16p.

ESRI (2011a) Hydrologic analysis sample applications. Available at *http://help.arcgis.com/en/arcgisdesktop/10.0/help/index.html#//009z0000005z000000.htm*.

ESRI (2011b) ArcGIS desktop: Release 10. Environmental Systems Research Institute, Redlands, CA.

ESRI (2011c) Arc Hydro Tools Overview. Environmental Systems Research Institute, Redlands, CA.

FAO (1992) CROPWAT: A computer program for irrigation planning and management. Smith M. (Ed.), *Irrigation and Drainage Paper 46*, Rome, Italy.

FAO (2002a) Deficit Irrigation Practices. Food and Agriculture Organization of the United Nations, Rome, ISBN 92-5-104768-5.

FAO, (2002b) Land use impacts on water resources: a literature review. Benjamin Kiersch (Ed.), In: *Land-water linkages in rural watersheds*. Land and Water Development Division, Food and Agriculture Organization, Rome, Italy.

FAO (2003) Water Resources, Development and Management Service. CLIMWAT: A climatic database for CROPWAT. FAO Land and Water Development Division.

FAO (2004) Drought-resistant soils: Optimization of soil moisture for sustainable plant production. FAO Land and Water Development Division, Rome.

FAO, (2012) The ETo Calculator: Evapotranspiration from a reference surface. Reference Manual Version 3.2, Edited by Dirk Raes, Food and Agriculture Organization of the United Nations Land and Water Division, Via delle Terme di Caracalla, 00153 Rome, Italy.

FAO (2014) Compendium on methods and tools to evaluate impacts of, and vulnerability and adaptation to, climate change. UN framework Conventuin on climate change, FAO, Rome.

FAO-ISSS-ISRIC (1998) World reference base for soil resources. World Soil Resources Report No. 84. Rome.

Fischer, C., Roscher, C., Jensen, B., Eisenhauer, N., Baade, J., Attinger, S., Scheu, S., Weisser., W.W., Schumacher, J. and Hildebrandt, A. (2014) How Do Earthworms, Soil Texture and Plant Composition Affect Infiltration along an Experimental Plant Diversity Gradient in Grassland? Andrew Hector (Ed), *PLoS One*, 9(6): e98987.

Forsyth, T. (2005) Land Use Impacts On Water Resources – Science, Social and Political Factors. M. Anderson (Ed), *Encyclopedia of Hydrological Sciences*, John Wiley & Sons, Ltd., p1-14.

Frederiksen, P. (1981) Terrain analysis and accuracy prediction by means of the Fourier transformation. *Photogrammerrica*, *36,* Boulder, Co, p145-157.

Gallego, F.J. (1995) *Sampling frames of squaresegments.* Report EUR 16317, office of publications of the E.C. Luxembourg, 68p. ISBN92-827-5106-6.

Gallego, F.J. (1999) Crop area estimation in the MARS project. Agriculture and Regional Information Systems, Space Application Institute, JRC, TP. 262/21020, Ispara, Italy.

Garbrecht, J. and Martz, L.W. (1999a) Digital Elevation Model Issues In Water Resources Modeling. In: Proceedings from invited water resources sessions, ESRI International User Conference, p1-7.

Garbrecht, J. and Martz, L.W. (1999b) An automated digital landscape analysis tool for topographic evaluation, drainage identification, watershed segmentation, and subcatchment parameterization. Grazinglands Research Laboratory, USDA, Agricultural Research Service, El Reno, Oklahoma.

Garen, D. and Moore, D.S. (2005) Curve number hydrology in water quality modeling: use, abuses and future directions. *Journal of American Water Resource Association*, 41(2): 377–388.

Gary, G.L. (1973) Hydrology Manual. National Weather Service, California. Available at *www.sbcounty.gov/dpw/floodcontrol/pdf/HydrologyManual.pdf*.

Gee, G.W, and Bauder, J.W. (1986) Particle-size analysis. p. 383-411. In A Klute (Ed.) Methods of Soil Analysis, Part 1. Physical and Mineralogical Methods. *Agronomy Monograph* No. 9 (2nd Ed.), *American Society of Agronomy/Soil Science Society of America*, Madison, WI.

Gerber, R., Smit, N.J., van Vuren, Johan H.J., Nakayama, S.M.M.,Yohannes, Y.B., Ikenaka, Y., Ishizuka, M. and Wepener, V. (2015) Application of a Sediment Quality Index for the assessment and monitoring of metals and organochlorines in a premier conservation area. *Environmental Science and Pollution Research*, 22(24): 19971–19989.

Giertz, S. and Diekkruger, B. (2003) Analysis of hydrological processes in a small headwater catchment in Benin, West Africa. *Physics and Chemistry of the Earth*, 28(33-36), 1333-1341.

Githui, F., Mutua, F. and Bauwens, W. (2009) Estimating the impacts of land cover changes on runoff using the soil water and assessment tool (SWAT): case study of Nzoia catchment, Kenya. Hydrological Sciences Journal, 54(5): 899-908.

Gomez, B., Mertes, L.A., K., Phillpe, J.D., Magilligan, F.J. and James. L.A. (1995) Sediment characteristics of an extreme flood: 1993 upper Mississippi River valley. *Geology*, 23(11): 963 – 966.

Gondwe, M.P. and Jury, M.R. (1997) Sensitivity of vegetation (NDVI) to climate over Southern Africa: Relationships with summer rainfall and OLR, *South African Geographical Journal*, 79: 52-60.

Gordon, N.D., McMahon, T.A. and Finlayson, B.L. (2004) *Stream Hydrology: An Introduction for Ecologists*. 2nd Ed, John Wiley and Sons, England.

Gray, J.R. and Simões, F.J.M. (2008) Estimating Sediment Discharge: Appendix D. Available at *http://doc-oc-as-docsviewer.googleusercontent.com/viewer/securedown/*, 22 January 2011.

Green, W.H. and Ampt, G. (1911) Studies of Soil Physics: Part 1- The flow of air and water through soils. *Journal of Agricultural Science*, 4: 1-24.

Griscom, H.P., Ashton, P.M.S. and Berlyn, G.P. (2004) Seedling survival and growth of native tree species in pastures: Implications for dry tropical forest rehabilitation in central Panama. *Forest Ecology and Management*, 218: 306–318.

Griscom, H.R., Gyedu-Ababio, T. and Miller, S.N. (2009) Revealing the Impacts of Dams and Land Cover Change on Luvuvhu River Baseflows. Published oral presentation at the 5th Annual Kruger Network Meeting 2007.

Griscom, H.R., Miller, S.N., Gyedu-Ababio, T. and Sivanpillai, R. (2010) Mapping land cover change of the Luvuvhu catchment, South Africa for environmental modeling. *GeoJournal* 75:163–173.

Gumbel, E.J. (1941) The return period of flood flows. *Ann. Math. Statist*, 12(2): 163-190.

Güntner, A. and Bronstert, A. (2004) Representation of landscape variability and lateral redistribution processes for large-scale hydrological modeling in semi-arid areas, *Journal of Hydrology*, 297: 136-161.

Gupta, S.C., Kessler, A. C., Brown, M.K. and Zvomuya, F. (2015) Climate and agricultural land use change impacts on streamflow in the upper midwestern United States. *Water Resources Research*, 51(7): 5301–5317.

Gupta, S.K. (2011) *Modern Hydrology and Sustainable Water Development*. John Wiley & Sons, 464p.

Gush, M., Scott, D., Jewitt, G., Schulze, R., Lumsden, T., Hallowes, L. and GÖrgens, A. (2002) Estimation of stream flow reductions resulting from commercial afforestation in South Africa. Water Research Commission Report TT 173/02, Pretoria, South Africa.

Guswa, A.J, Celia, M.A and Rodriguez-Iturbe, I. (2002) Models of soil dynamics in ecohydrology: A comparative study. *Water Resources Research*, 38(9): 1166-1181.

Gutu, S.Z. (2009) Experience of Ethiopia in Implementing an Integrated Survey Program and Advanced Technology, in *21st Session of the African Commission on Agricultural Statistics*, Accra, Ghana.

Haan, C.T. (1977) Statistical methods in Hydrology, Iowa State University Press, Ames, Iowa, USA.

Haarhoff, J. and Cassa, A.M. (2009). *Introduction to flood hydrology*. Juta and Co, Ltd, Cape Town, South Africa, p165.

Hall, D.O., Scurlock, J.M.O., Bolhär-Nordenkampf, H.R., Leegood, R.C. and Long, S.P. (Eds) (2013) Photosynthesis and Production in a Changing Environment: A field and laboratory manual. A Reprint: Springer-Science and Business Media, B.V., Hong Kong, p58.

Harding, S.T. (1962) Evaporation from Pyramid and Winnemucca Lakes. Journal of Irrigation and Drainage Division, ASCE.

Harris, R.R. (1985) Relationships between fluvial geomorphology and vegetation on Cottonwood Creek, Tehama and Shasta Counties, California. Published Ph.D. Dissertation, Department of Forestry, University of California, Berkeley, 329p.

Harris, R.R. (1987) Occurrence of vegetation on geomorphic surfaces in the active floodplain of a California alluvial stream. *American Midland Naturalist*, 118: 393-405.

Harrison, M.S.J, (1984) A generalized classification of South African summer rain-bearing synoptic systems. *International Journal of Climatology*, 4: 547-560.

Harrower, M.J. (2010) Geographic Information Systems (GIS) hydrological modeling in archaeology: an example from the origins of irrigation in Southwest Arabia (Yemen). *Journal of Archaeological Science*, 37: 1447–1452.

HEC, 2000, Hydrologic Modeling System-HEC-HMS: Technical Reference Manual. US Army corps of Engineers Hydrologic Engineering Center, Davis, California, USA.

Hejduk, A. and Banasik, K. (2010) Suspended sediment concentration and yield in snowmelt flood events in a small lowland river. *Land Reclamation*, 42(1): 61–68.

Helsel, D.R. and Hirsch, R.M. (2010) Statistical Methods in Water Resources. U.S. Geological Survey, Investigations Book 4, Chapter A3. U.S. Geological Survey.

Hernandez, M., Miller, S.N., Goodrich, D.C., Goff, B.F., Kepner, W.G., Edmonds, C.M. and Jones, K.B. (2000) Modeling runoff response to land cover and rainfall spatial variability in semi-arid watersheds. *Environmental Monitoring and Assessment*, 64: 285-298.

Herold, M. Goldstein, N. C. and Clarke, K. C. (2003) The spatiotemporal form of urban growth: measurement, analysis and modeling. *Remote Sensing of Environment*, 86: 286-302.

Hillel, D. (1980) *Fundamentals of Soil Physics*. Academic Press, New York, 413p.

Holland, T. (2012) USDA-NASS Sampling Frames for Agriculture: List, Area and Multiple Frames. *Global strategy to improve agricultural and rural statistics. High Level*

Stakeholders Meeting on the Global Strategy - From Plan to Action. Master Sampling Frames (MSF) for Agricultural and Rural Statistics, FAO, Rome.

Holtan, H.N. (1961) *A concept for infiltration estimates in watershed engineering.* USDA Agricultural Research Service, ARS 41-51.

Hong, S.H., Mladenoff, D.J., Radeloff, V.C. and Crow, T.R. (1998) Integration of GIS data and classified satellite imagery for regional forest assessment. *Ecological Applications,* 8(4): 1072–1083.

Hope, R.A. Jewitt, G.P.W. and Gowing, J.W. (2004) Linking the hydrological cycle and rural livelihoods: A case study in the Luvuvhu catchment, South Africa. *Physics and chemistry of the Earth*, 29: 1209–1217.

Hossain, F., Degu, A.M., Yigzaw, W., Burian, S., Niyogi, D., Shepherd, J.M. and Pielke, R. (2012) Climate feedback-based provisions for dam design, operations and water management in the 21st century. *Journal of Hydrologic Engineering*, 17(8): 837-850.

Hubbard, V.C., Jordan, D. and Stecker, J.A. (1999) Earthworm response to rotation and tillage in Missouri claypan soil. *Biol Fertil Soils*, 29: 343-7.

Hutchinson, M.F. (1989) A new procedure for gridding elevation and stream line data with automatic removal of spurious pits. *Journal of Hydrology*, 106: 211-232.

Hutchinson, M.F. (1996) A locally adaptive approach to the interpolation of Digital Elevation Models. *Proceedings of the 3rd International Conference on Intergrating GIS and Environmental Modelling*. National Centre for Geographic Information and Analysis, Santa Fe, NM. January 21-26, 1996.

Illgner, P. (2004) Environmental Impact Assessment for the proposed Matimba-Witkop No.2 400KV Transmission Line, Limpopo Province. Rhodes University document, South Africa.

IPCC, (2001) Climate Change 2001: Working Group II: Impacts, Adaptation and Vulnerability: Contribution of Working Group II to the Third Assessment Report of the Intergovernmental Panel on Climate Change. McCarthy, J.J, (Ed.) Cambridge University Press, UNEP, WMO, 271p.

Ippoliti, E., Clementini, E. and Natali, S. (2012) Automatic generation of land use maps from land cover maps. Proceedings of the AGILE'2012 International Conference on Geographic Information Science, Avignon, April, 24-27, 2012, ISBN: 978-90-816960-0-5.

ISRIC, (2016) Land Degradation Assessment in Drylands: GEF-UNEP-FAO program Land Degradation in Drylands, the Global Assessment of Land Degradation and Improvement (GLADA). ISRIC - World Soil Information, http://www.isric.org/projects/land-degradation-assessment-drylands-glada.

IUSS, (2006) World Reference base for soil resources. 2nd Ed, World Soil Resources Report No 103, FAO, Rome.

ITT Visual Information Solutions, (2008) "ENVI user's guide", Version 4.5, 2008.

Jain, S.K., Agarwal, P.K. and Singh, V.P. (2008) Hydrology and water resources in India. Springer publisher, India, 1258p.

Jäntschi, L. and Bolboacă, S.D. (2009) Distribution Fitting 2. Pearson-Fisher, Kolmogorov-Smirnov, Anderson-Darling, Wilks-Shapiro, Cramer-von-Misses and Jarque-Bera statistics. *Bulletin of University of Agricultural Sciences and Veterinary Medicine Cluj-Napoca Horticulture*, 66(2): 691-697.

Jovanovic, N., Mu, Q., Bugan, R.D.H. and Zhao, M. (2015) Dynamics of MODIS evapotranspiration in South Africa. *Water SA*, 41(1): 79-90. ISSN 1816-7950.

Jensen, J.R. (2005) Digital image processing, 3rd Ed. Upper Saddle River, NJ: Prentice Hall, 526p.

Jewitt, G.P.W. and Garratt, J.A. (2004) Hydrological modeling in the Luvuvhu catchment. CAMP Technical Report 2. BEEH, RSA, CLUWRR, RSA, Pietermaritzburg, RSA, Newcastle, UK. 27 pp. Available at *www.cluwrr.ncl.ac.uk*.

Jewitt, G.P.W., Garratt, J.A., Calder, I.R. and Fuller, L. (2004) Water resources planning and modeling tools for the assessment of land use change in the Luvuvhu Catchment, South Africa. *Physics and Chemistry of the Earth*, 29: 1233–1241.

Jewitt, G.P.W., Lorentz, S.A., Gush, M.B., Thornton-Dibb, S., Kongo, V., Wiles, L., Blight, J., Stuart-Hill, S.I., Versfeld, D. and Tomlinson, K. (2009) Methods and Guidelines for the Licensing of SFRAs with Particular Reference to Low Flows. Water Research Commission Report No. 1428/1/09. Pretoria, South Africa.

Jianfeng, X. and Kenneth, G. (2008) Effect of Rainfall Intensity on Infiltration into Partly Saturated Slopes. *Geotechnical and Geological Engineering*, 26(2): 199-209.

Jinguji, I. (2012) How to Develop Master Sampling Frames using Dot Sampling Method and Google Earth. *Global strategy to improve agricultural and rural statistics - High Level Stakeholders Meeting on the Global Strategy - From Plan to Action, Master Sampling Frames (MSF) for Agricultural and Rural Statistics*, FAO, Rome.

Johnston, K., Ver Hoef, J., Krivoruchko, K. and Lucas, N. (2001) Using Geostatistical Analyst. ESRI, 300p.

Junk, W.J., An, S., Finlayson, C.M., Gopal, B., Květ, J., Mitchell, S.A., Mitsch, W.J. and Robarts, R.D. (2013) Current state of knowledge regarding the world's wetlands and their future under global climate change: a synthesis. *Aquatic Sciences*, 75: 151–167.

Jury, M.R. (1997) Inter-annual climate modes over southern Africa from satellite cloud OLR 1975-1994. *Theoretical Applied Climatology*, 57: 155-163.

Jury, M.R., Weeks, S. and Gondwe, M.P. (1997) Satellite-observed vegetation as an indicator of climate variability over southern Africa. *South African Journal of Science*, 93: 34–38.

Kabanda, T.A. (2004) Climatology of long term Drought in the Northern Region of the Limpopo Province of South Africa. Doctoral thesis in Climatology, University of Venda, South Africa.

Kamtukule, S.L. (2008) Investigating impacts of sedimentation on water availability in small dams: Case study of Chamakala II Small Earth dam, Malawi. Published MSc Thesis in Integrated Water Resources Management, University of Zimbabwe, 71p.

Kanyanga, J.K. (2008) El Niño Southern Oscillation (ENSO) and atmospheric circulation over southern Africa. Published PhD Thesis, University of Johannesburg, South Africa, 153p.

Karamouz, M. Nazif, S. and Falahi, M. (2012) *Hydrology and Hydroclimatology: Principles and Applications*. 1st Ed, CRC Press, 740p, ISBN: 1466512199.

Kelbe, B.E. (1984) Cumulus cloud characteristics of the eastern Transvaal Lowveld. *Water SA*, 10: 81-90.

Kepner, W.G., Bassett, S.D., Mouat, D.A. and Goodrich, D.C. (2004) Scenario analysis for the San Pedro River: analyzing hydrological consequences of a future environment. *Environmental Monitoring Assessment*, 94: 115-127.

Keskin, M.E. Terzi, Ö. and Küçüksille, E.U. (2009) Data mining process for integrated evaporation model. *Journal of Irrigation and Drainage Engineering*, 135(1): 39-43.

Kiersch, B. (2000) Land use impacts on water resources: a literature review. FAO workshop on Land-Water Linkages in Rural Watersheds. Available at *http://www.fao.org/ag/agl/watershed/watershed/en/mainen/index.stm*.

Kleynhans, C.J. (1996). A qualitative procedure for the assessment of the habitat integrity status of the Luvuvhu River (Limpopo system, South Africa). *Journal of Aquatic Ecosystem Health* 5: 41-54.

Knighton, D. (1998) *Fluvial Forms and Processes: A New Perspective*. Arnold, London, 383p.

Köhl, M., Magnussen, S.S. and Marchetti, M. (2006) *Sampling methods, remote sensing and GIS multiresiurce forest inventory*. Springer-Verlag, Berlin, Heidelberg, 373p.

Kohler, M.A., Nordenson, T.J. and Fox, W.E. (1955) Evaporation from pans and lakes. U.S. Weather Bureau Research Paper, 38, Washington DC.

Kuells, C., Leibundgut, C.H., Schwarz, U. and Schick, A. P. (1995) Channel infiltration study using dye tracers. *Application of Tracers in Arid Zone Hydrology: Proceedings of the Vienna Symposium*, August 1994. IAHS Publ. no. 232: 429-436.

Lee, C. (2005) Application of Rainfall Frequency Analysis on Studying Rainfall Distribution Characteristics of Chia-Nan Plain Area in Southern Taiwan. *Crop, Environment & Bioinformatics*, 2: 31-38.

Lee, J., B. R. Lintner, C. K. Boyce, and P. J. Lawrence, 2011: Land use change exacerbates tropical South American drought by sea surface temperature variability. *Geophysics Research Letter*, 38, L19706, doi:10.1029/2011GL049066.

Le Maitre, D., Van Wilgen, B.W., Chapman, R.A. and McKelly, D.H. (1996) Invasive plants in the Western Cape, South Africa: Modelling the consequences of a lack of management. *Journal of Applied Ecology*, 33: 161-172.

Le Maitre, D.C., Van Wilgen, B.W., Gelderblom, C.M., Bailey, C., Chapman, R.A. and Nel, J.A. (2000) Invasive alien trees and water resources in South Africa: case studies of the costs and benefits of management, *Forest Ecology And Management*, 160: 143–159.

Le Maitre, D. and Görgens, A. (2001) Potential impacts of invasive alien plants on reservoir yields in South Africa. *Proc. 10th S. Afr. National. Hydrology. Symposium*, September 2001, Pietermaritzburg, South Africa.

Lewis, M. J., Singer, M. J. and Tate, K. W. (2000) Applicability of SCS curve number methods for a California oak woodlands watershed. *Journal of Soil and Water Conservation*, 20: 226–230.

Li, J., Li, G., Zhou, S. and Chen, F. (2014) Quantifying the Effects of Land Surface Change on Annual Runoff Considering Precipitation Variability by SWAT. *Water Resources Management*, 30: 1071-1084.

Li, P., Li, Z. and Lu, K. (2004) Effect of vegetation cover types on soil infiltration under simulating rainfall. ISCO 2004 - 13th International Soil Conservation Organisation Conference, Brisbane, July 2004.

Linsley, R.K, Kohler, M.A. and Paulhus, J. L. H. (1958) *Hydrology for engineers*. McGraw-Hill, Inc., 689p.

Liu, X. and Li, J. (2008) Applications of SCS model in estimation of runoff from small watershed in Loess Plateau of China. *Chinese geographic science*, 18(3): 235-241.

Lull, H.W. and Reinhart K.G. (1955) Soil moisture measurement U.S. Forest Serv. Southern For. Exp. Sta. Occas. Paper 140, 56p.

Macdonald, D., Gomez-Perez, I., Franzese, J., Spalleti, L., Lawver, L., Gahagan, L., Dalziel, I., Thomas, C., Trewin, N., Hole, M. and Paton, D. (2003) Mesozoic break-up of SW Gondwana: Implications for regional hydrocarbon potential of the southern South Atlantic. *Marine and Petroleum Geology*, 20: 287-301.

Maidment, D.R. (1992) GIS and hydrological modeling. *Proceeding of the first International Symposium/workshop on GIS and Environmental Modelling*, September 1991, Boulder, Colorado.

Maidment, D.R. (1996) GIS and Hydrologic Modeling - an Assessment of Progress. *Proceedings of the Third International Conference on GIS and Environmental Modeling*, January 22-26, 1996, Santa Fe, New Mexico.

Maidment, D.R. (Ed). (2002) *Arc Hydro: GIS for Water Resources*. ESRI Press, Redlands, New York, 208p.

Maktav, D. and Erbek, F.S. (2005) Analysis of urban growth using multi-temporal satellite data in İstanbul, Turkey. *International Journal of Remote Sensing*, 26: 797–810.

Mallory, S.J.L., Versfeld, D. and Nditwani T. (2011) Estimating stream-flow reduction due to invasive alien plants: Are we getting it right? Department of Water Affairs, South Africa.

Malunjkar, V.S., Shinde, M.G., Ghotekar, S. S. Atre A. A. (2015) Estimation of Surface Runoff using SWAT Model. *International Journal of Inventive Engineering and Sciences* 3 Issue-4, ISSN: 2319–9598, March 2015

Mangangka, I.R. (2008) The Decline of Soil Infiltration Capacity Due To High Elevation Groundwater. *Civil Engineering Dimension*, Vol. 10, No. 1, p35-39, ISSN 1410-9530.

Maramba, T.R. (2011) An investigation of the influence of temperature on rainfall variability in the Luvuvhu River Catchment. Unpublished BSc Hon dissertation in Hydrology, University of Venda, 52p.

Maragatham, R.S. (2012) Trend analysis of rainfall data -a comparative study of existing methods. *International Journal of Physics and Mathematical Sciences,* Vol. 2 (1) January-March, pp.13-1, ISSN: 2277-2111 (Online).

Marek, M.A. (2011) Hydraulic Design Manual Manual Notice: 2011-1.Texas Department of Transportation (TxDOT). Design Division (DES) Publisher. Available at *http://onlinemanuals.txdot.gov/txdotmanuals/hyd/manual_notice.htm*.

Martyn, D. (1992) *Climates of the world*: Developments in atmospheric science. Elsevier, New York, New York, USA.

Martz, L.W. and Garbrecht, J. (1992) Numerical Definition of Drainage Network and Subcatchment Areas from Digital Elevation Models. Computers and Geosciences, 18(6): 747-761.

Mason, S.J. (1996) Rainfall trends over the Lowveld of South Africa. *Climatic Change*, 32: 35–54.

Mason, S.J., Joubert, A.M., Cosijn, C. and Crimp, S.J. (1996) Review of seasonal forecasting techniques and their applicability in Southern Africa. *Water South Africa*, 22: 203–209.

Mason, S.J. and Joubert, A.M. (1997).Simulated changes in extreme rainfall over southern Africa. *International Journal of Climatology*, 17(3): 291–301.

Matano, A., Gelder, F.B., Dida, G.O., Kanangire, C.K., Anyona, D.N., Abuom, P.O., Owuor, P.O. and Ofulla, A.V.O. (2015) Effects of Land Use Change on Land Degradation Reflected by Soil Properties along Mara River, Kenya and Tanzania. *Open Journal of Soil Science*, 5: 20-38

MathWave Technologies (2011) *EasyFit Software Version 5.5*, USA.

Mavima, G.A., Sopora, G., Makurira, H. and Dzvario, W. (2011) Sedimentation impacts on reservoir as a result of land use on a selected catchment in Zimbabwe. *International Journal of Engineering Science and Technology*, Vol. 3, No. 8, ISSN: 0975-5462.

Mays, L.W. (2001) *Water Resources Engineering*. 1st Ed, John Wiley and Sons, Inc, India, 890p.

McColl, C. and Aggett, G. (2007) Land use forecasting and hydrologic model integration for improved land-use decision support. *Journal of Environmental Management*, 84(4): 494-512.

McGee, T.J. (1991) *Water supply and sewerage*. 6th Ed. McGraw-Hill International Editions, Singapore, 602p.

McGlinchey, M.G. and Inman-Bamber, N.G. (2002) Robust estimates of evapotranspiration for sugarcane. *Proceedings of the Annual Congress - South African Sugar Technologists' Association*, p245-249.

McKenzie, N., Coughlan, K. and Cresswell, H. (2002) Soil properties measurement and interpretation for Land Evaluations. CSIRO Publishing, Melbourne. http;//www.usyd.edu/agric/.

McKenzie, N., Jacquier, D., Isbell, R. and Brown, K. (2004) Australian Soils and Landscapes: An lllustrated Compendium. CSIRO Publishing.

McMahon, T.A. and Adeloye, A.J., (2005) *Water Resources Yield*, Highlands Ranch, CO: Water Resources Publications, 234p.

Meijerink, A.M.J., de Brouwer, H.A.M., Mannaerts, C.M. and Valuenzela, C.R. (1994) Introduction to the use of Geographic Information Systems for practical hydrology, *ITC Publication* No. 23, Enschede, 243p.

Merwade, V. (2006) Frequency Analysis Reading: Applied Hydrology Chapter 12 - PPT Presentation. Retrieved: *www.powershow.com/.../Frequency_Analysis_Reading_Applied_Hy.*

Merz, R. and Blöschl, G. (2009) A regional analysis of event runoff coefficients with respect to climate and catchment characteristics in Austria. *Water Resources Research*, 45(1), DOI: 10.1029/2008WR007163.

Meyer, C., Rooseboom, A., Retief, M.J. and Cloete, G.C. (2000) Discharge measurement in terms of pressure differences at bridge piers. A Report to the Water Research Commission. WRC Report No 980/3/00.

Meyer-Roux, J. (1992). The development of the agriculture project of the EEC, Proceedings of the Conference on the Application of Remote Sensing to Agricultural Statistics (F. Toselli and J. Meyer-Row, editors), Institute for Remote Sensing Applications, Joint Research Centre, Ispra. Villa Carlotta, Belgirate, Lake Maggiore, Italy, 26-27 November 1991, p31-39.

Middleton, B.J. and Bailey, A.K. (2008) Water resources of South Africa, 2005 study (WR2005). Water Research Commission report no. TT381/08. Pretoria, South Africa.

Miline, A.K. (1998) Change direction analysis using Landsat Imagery: a review of methodologies. In: Proceedings of the IGARSS'88 Symposium in Edinburgh, Scotland, ESA SP-284, Noordwijk, Netherlands: ESA, p541-544.

Miller, S.N., Semmens, D.J., Goodrich, D. C., Hernandez, M.R. Miller, C. Kepner, W.G. and Guertin, D.P. (2007) The automated geospatial watershed assessment tool. *Environmental Modelling and Software*, 22(3): 365-377.

Miller, S.N., Semmens, D.J., Miller, R.C., Hernandez, M., Goodrich, D.C., Miller, W.P., Kepner, W.G. and Ebert, D. (2002) GIS-based Hydrologic Modeling: The Automated Geospatial Watershed Assessment Tool. Proceedings of the 2nd Federal Interagency Hydrologic Modeling Conference, Las Vegas, NV, USA, p12.

Moghaddamnia, A., Ghafari, M., Piri, J. and Han, D. (2008) Evaporation Estimation Using Support Vector Machines Technique. *World Academy of Science, Engineering and Technology*, 43: 14-22.

Mölders, N. (2011) Land-Use and Land-Cover Changes: Impact on Climate and Air Quality. Springer, 210p.

Moolchan, E. (2010) The impact of the 2007 Hurricane season operations for Trinidad and Tobago. Trinidad and Tobago Meteorological services, Piarco, Trinidad.

Moore, I.D., Grayson, R.B. and Ladson, A.R. (1991) Digital Terrain Modelling: A Review of Hydrological, Geomorphological and Biological Applications. *Hydrological Processes*, 5(1): 3-30.

Moreira, M.A., Chen, S.C. and Batista, G.T. (1986) Wheat area estimation using digital LANDSAT MSS data and aerial photograph, *Int. Journal of Remote Sensing*, 7(9): 1109-1120.

Mostert, T.H.C., Bredenkamp, G.J., Klopper, H.L., Verwey, C., Mostert, R.E. and Hahn, N. (2008) Major vegetation types of the Soutpansberg conservancy and the Blouberg Nature Reserve, South Africa. Koedoe vol. 50, Pretoria, ISSN 0075-6458.

Mueller, E.N., Francke, T., Batalla, R.J. and Bronstert, A. (2009) Modelling the effects of landuse change on runoff and sediment yield for a meso-scale catchment in the Southern Pyrenees. *Catena*, 79: 288-296.

Mukheibir, P. (2005) Local Water Resource Management Strategies for Adaptation to Climate Induced Impacts in South Africa. Energy Research Centre, University of Cape Town, South Africa.

Mukheibir, P. and Sparks, D. (2003) Water resource management and climate change in South Africa: visions, driving factors and sustainable development indicators; report for Phase I of the Sustainable Development and Climate Change Project. University of Cape Town, Rondebosch, South Africa.

Murty, V.N.S. (2009) Geotechnical Engineering: Principles and Practices of soil mechanics and Foundation Engineering. A Reprint by CRC Press, Marcel Decker Inc, New York, 1029p.

Mwangi, H.M., Julich, S., Patil, S.D., McDonald, M.A. and Feger, K. (2016) Relative contribution of land use change and climate variability on discharge of upper Mara River, Kenya. *Journal of Hydrology: Regional Studies*, 5(1): 244-260.

Nassor, A. and Jury, M.R. (1998) Intra-Seasonal Climate Variability of Madagascar. Part 1: Mean Summer Conditions. *Meteorology and Atmospheric Physics*, 65: 31-41.

Ncube, M. and Taigbenu, A.E. (2008). Application of the SWAT model to assess the impact of land cover and land use on the hydrologic response in the Olifants Catchment. Proceedings of the 2007 Waternet/WARFSA Symposium, Lusaka, Zambia, 31 Oct-2 Nov 2007.

Ndlovu, H., Ndambuki, J.M. and Kibiiy, J. (2012) Modelling the effects of land-use changes on existing stormwater infrastructure. Published online, available at *www.ewisa.co.za/literature/files/ID23%20Paper15%20Ndlovu%20H.pdf*.

Ndiritu, J., Odiyo, J. O., Makungo, R., Ntuli C. and Mwaka B. (2011) Yield–reliability analysis for rural domestic water supply from combined rainwater harvesting and run-of-river abstraction. *Hydrological Sciences Journal*, 56(2): 238-248.

Neitsch, S.L., Arnold, J.G., Kiniry, J.R., Williams, J.R. and King, K.W. (2002) *Soil and Water Assessment Tool Theoretical documentation*: Version 2000. TWRI Report TR-191, Texas Water Resources Institute, USA.

Neitsch, S.L., Arnols, J.G., Kiniry, J.R. and Williams, J.R. (2011) *Soil and Water Assessment Tool Theoretical Documentation*: version 2009. Texas A&M University: College Station, TX, USA.

Nieuwolt, S. (1997) *Tropical Climatology: An Introduction to the Climates of Low Latitudes*. John Wiley, New York, p85-88.

NOAA, (2011) Flood Frequency Estimates for New England River Restoration Projects: Considering Climate Change in Project Design. US.DOC/NOAA fisheries services, USA.

Nordin, C.F. Jnr. (1985) The sediment loads of rivers. In Rodda, J.C. (Ed.) Facets of Hydrology, vol II, Chapter 7, John Wiley, Chichester.

NRCS, (1999) Runoff Curve Number – Module 204. Engineering Hydrology Training Series, Natural Resources Conservation Service – United States Department of Agriculture, National Employee Development Centre, Published July 1999.

NRCS, (2007) *Stream Hydrology*. Part 654 Stream Restoration Design National Engineering Handbook, Natural Resources Conservation Service - United States Department of Agriculture, 210–VI–NEH.

O'Callaghan, J.F. and Mark, D.M. (1984) The extraction of drainage networks from digital elevation data. *Computer Graphics and Image Processing,* 28: 323–344.

O'Keeffe, J., Uys, M. and Bruton, M.N. (1992) *Freshwater Systems*, in Fuggle, R.F. and Rabie, M.A. (Eds.) 1992. *Environmental Management in South Africa*. Johannesburg: Juta & Co.

Obiero, J.P.O., Hassan, M.A. and Gumbe, L.O.M. (2011) Modelling of Streamflow of a Catchment in Kenya. *Journal of Water Resource and Protection*, 3: 667-677.

Odongo, V.O. (2014) Quantifying the effect of land use/cover change on its water quantity and quality in Lake Naivasha Basin. Published PhD thesis, International Institute for Geo-Information Science and Earth Observation, Enschede, the Netherlands.

Olaleye, J. B., Abiodun, O. E. and Asonibare, R. O. (2012) Land-use and land-cover analysis of Ilorin Emirate between 1986 and 2006 using Landsat imageries. *African Journal of Environmental Science and Technology*, 6(4): 189-198.

Olofintoye, O.O., Sule, B.F. and Salami, A.W. (2009) Best–fit Probability distribution model for peak daily rainfall of selected Cities in Nigeria**.** *New York Science Journal*, 2(3): 1-12.

Oosterbaan, R.J. (1994) Frequency and regression analysis of hydrologic data. in: H.P. Ritzema (Ed.), *Drainage Principles and Applications*, Publication 16, 2nd revised edition, International Institute for Land Reclamation and Improvement (ILRI), Wageningen, The Netherlands. ISBN 90 70754 3 39.

Palamuleni, L.G., Ndomba, P.M. and Annegarn, H. J. (2011) Evaluating land cover change and its impact on hydrological regime in Upper Shire River Catchment, Malawi. Reg Environ Change 11:845- 855, DOI 10.1007/s10113-011-0220-2.

Pao-Shan Y., Yu-Chi, W. and Chun-Chao, K. (2003) Effects of land-use change on runoff response in the ungauged Ta-Chou basin, Taiwan. Available at *http://itia.ntua.gr/hsj/redbooks/279/iahs_279_0117.pdf*.

Parissopoulos, G.A. and Wheater, H.S. (1991) Effects of Wadi flood hydrograph characteristics on infiltration. *Hydrology Journal*, 126(3-4): 247-263.

Pathak, P. (1991) Runoff sampler for small agricultural watersheds. *Agricultural Water Managemen*t, 19: 105-115.

Pavelsky, T.M. and Smith, L.C. (2009) Remote sensing of suspended sediment concentration, flow velocity, and lake recharge in the Peace-Athabasca Delta, Canada. *Water Resources Research*, 45(11), DOI: 10.1029/2008WR007424.

Pegram, G. and Parak, M. (2004) A review of the regional maximum flood and rational formula using geomorphological information and observed floods. *Water SA*, 30(3): 377-384.

Peng G., Pasternack, G.B., Bali, K.M. and Wallender, W.W. (2006) Suspended-sediment transport in an intensively cultivated watershed in southeastern California. *Catena*, 69: 239–252.

Pfannkuch, H.O. and Paulson, R. (2005) *Grain size distribution and hydraulic properties,* Available at *http://www.cs.pdx.edu/~ian/geology2.5.html*.

Philip, J.R. (1957) Theory of infiltration: 4. *Soil Science*, 84: 257-264.

Pilon, P.J. (2004) Guidelines for reducing flood losses. United Nations Inter-Agency Secretariat of the International Strategy for Disaster Reduction (UNISDR), Geneva, CH.

Pitman, W V (1973): A mathematical model for generating monthly river flows from meteorological data in South Africa. Hydrological Research Unit, Univ. of the Witwatersrand, Report No. 2/73.

Podobnikar, T. (2010) Geomorphic Analysis of the low quality digital elevation Model. Proceedings of the13th AGILE International Conference on Geographic Information Science 2010, Guimarães, Portugal.

Poff, N.L. and Hart, D.D. (2002) How Dams Vary and Why It Matters for the Emerging Science of Dam Removal. *BioScience*, 52(8): 659-738.

Ponce, V.M. (1989) Flood of the binational cottonwood creek- Arroyo Almar, California and Baja California, Web version 1.05 [050509], *http://ponce.tv/alamar/alamarenglish.html*.

Prachansri, S. (2007) Analysis of soil and land cover parameters for flood hazard assessment. Published Msc Thesis, International Institute for Geo-Information Sciences and Earth Observation, The Netherlands, 92p.

Prenzel, B. (2004) Remote sensing-based quantification of land-cover and land-use change for planning. *Progress in Planning*, 61: 281–299.

Price, K., Jackson, C.R. and Parker A.J. (2010) Variation of surficial soil hydraulic properties cross land uses in the southern Blue Ridge Mountains, NC, USA, *Journal of Hydrology*, 383: 265-268.

Putuhena, W.M. and Cordery, I. (2000) Some hydrological effects of changing forest cover from eucalypts to Pinus radiata. *Agricultural and Forest Meteorology*, 100: 59-72.

Rahman, A., Haddad, K., Ishak, E., Weinmann, E. and Kuczera G. (2010) Regional Flood Estimation in Australia: An Overview of the Study in Relation to the Upgrade of Australian Rainfall and Runoff, Flood Management Authorities (FMA), Gosford, NSW.

Rango, A. (1994) Application of remote sensing methods to hydrology and water resources. *Hydrological Sciences Journal*, 39(4): 309-320.

Reason, C.J.C., Allan, R.J., Lindesay, J.A. and Ansell T.J. (2000) ENSO and climatic signals across the Indian Ocean Basin in the global context: Part I, Interannual Composite Patterns. *International Journal of Climatology*, 20: 1285–1327.

Reason, C.J.C., Hachigonta, S. and Phaladi, R.F. (2005) Interannual variability in rainy season characteristics over the Limpopo region of South Africa. *International Journal of Climatology*, 25: 1835-1853.

Reddy, P.J.R. (2011) *A textbook of Hydrology*. University Science Press: Laxmi Publications Pvt. Ltd, New Delhi, India, 509p.

Reshma, T., Kumar, P.S., Babu, M.J. R. and Kumar, K.S. (2010) Simulation of runoff in watersheds using SCS-CN and Muskingum-Cunge methods using remote sensing Geographical Information Systems. *International Journal of Advanced Science and Technology*, 25: 31-42.

Reuter, H.I., Nelson, A. and Jarvis, A. (2007) An evaluation of void filling interpolation methods for SRTM data. *International Journal of Geographic Information Science*, 21(9): 983-1008.

Reynolds, S.G. (1970a) The gravimetric method of soil moisture determination part I: a study of equipment, and methodological problems. *Journal of Hydrology*, 11: 258-273.

Reynolds, S.G. (1970b) The gravimetric method of soil moisture determination part II: typical required sample sizes and methods of reducing variability. *Journal of Hydrology*, 11: 274-287.

Reynolds, S.G. (1970c) The gravimetric method of soil moisture determination part III: an examination of factors influencing soil moisture variability. *Journal of Hydrology*, 11: 288-300.

Rietkerk, M., Ketner, P., Burger, J., Hooren, B. and Olff, H. (2000) Multiscale soil and vegetation patchiness along a gradient of herbivore impact in a semi-arid grazing system in West Africa. *Plant Ecology*, 148: 207–224.

Rippl, W. (1883) *The capacity of storage reservoirs for water supply*. Proc. Inst. Civil Engineers, London, 71: 270-278.

Robock, A., Vinnikov, K.Y., Srinivasan, G., Entin, J. K., Hollinger, S. E., Speranskaya, N. A., Liu, S. and Namkhai, A. (2000) The global soil moisture data bank, *Bulletin of the American Meteorological Society*, 81: 1281–1299.

Rooseboom, A. and Annandale, G. W. (1981) Techniques applied in determining sediment loads in South African rivers. In *Erosion and Sediment Transport Measurement. Proc. Florence Symp*, June 1981. IAHS Publ. No. 133: 219–224.

Rogasik, J., Panten, K., Schnug, E. and Rogasik, H. (2004) Infiltration Management Factors. *Encyclopedia of Soil Science*, DOI: 10.1081 /E-ESS-120019048.

Ryerson, R.A., Dobbins, R.N. and Thibault, C. (1985) Timely crop area estimates from Landsat. *Photogrammetric Engineering and Remote Sensing*, 51: 1735-1743.

Saghafian, B., Farazjoo, H., Bozorgy, B., and Yazdandoost, F. (2007) Flood Intensification due to changes in land use. *Water Resources Management* 22: 1051–1067.

Samad, M.H., Chauhdry, M., Ashraf, M., Saleem, Q., Hamid, U., Babar, H., Tariq, H. and Farid, M.S. (2016) Sediment yield assessment and identification of check dam sites for Rawal Dam Catchment. *Arabian Journal of Geosciences*, 9(6): 1-14.

SANRAL (2006) *Drainage Manual*. 5th Ed. South African National Road Agency Limited, Pretoria, South Africa.

Santillan, J.R., Makinano, M.M. and Paringit, E.C. (2010) Intergration of GIS, remote sensing and hydrologic models for predicting land cover change impacts on surface runoff and sediment yield in a critical watershed in Mindanao, Philippines. *International Archives of the Photogrammetry, Remote Sensing and Spatial Information Sciences*, volume XXX VIII, Part 8, Kyoto, Japan.

SAWS (2001) Current Weather Conditions for Thohoyandou. South African Weather Services ©2001, Pretoria.

Saxton, K.E., Rawls, W.L., Rosenberger, J.S. and Papendick, R.I. (1986) Estimating generalized soil water characteristics from texture. *Soil Science Society of American Journal*, 50: 1031-1036.

Schaffer, C.H. (2005) Investigating the Importance of Land Cover on Evapotranspiration. Published Msc Thesis in Geogaphy, Northern Illinois University, 85p.

Schiariti, P. (2010) Basic Hydrology: Curve Numbers. Mercer County Soil Conservation District. Available at *njscdea.ncdea.org/CurveNumbers.pdf*.

Schindl, G., Studnicka, M., Eckelhart, A. and Summer, W. (2005) Hydrological and Instrumentation aspects of monitoring and analyzing suspended sediment transport crossing international borders. *International Association of Hydrological Science*. IAHAS Publication 291, ISBN 1-901502-87-2, the Netherlands.

Schmidt, O., Clements, R.O. and Donaldson, G. (2003) Why do cereal-legume intercrops support large earthworm populations? *Soil ecology*, 22(2): 181-190.

Schulze, R.E. (1965) General survey: Climate of South Africa. Weather Bureau Department of Environmental Affairs, Pretoria.

Schulze R.E. (1995) Hydrology and Agrohydrology: A Text to Accompany the ACRU 3.00 Agrohydrological Modelling System. WRC Report No. TT 69/95, Water Research Commission, Pretoria. 552p.

Schulze, R.E. (2008) South African Atlas of Climatology and Agrohydrology, WRC Report, South Africa, Rep No. 1489/1/08.

Schulze, R.E., Lorentz, S., Kienzle, S.W. and Perks, L. (2004) Modelling the impacts of land-use and climate change on hydrological responses in the mixed underdeveloped / developed

Mgeni catchment, South Africa. BAHC-IGBP Publication, Springer, Research Commission, South Africa, Rep. 1155/1/04, 37–50, 2004, 17p.

Schumm, S.A. (1977) *The fluvial System*. New York, John Wiley & Sons, 338p.

Scipal, K., Scheffler, C. and Wagner, W. (2005) Soil Moisture Runoff Relation at the catchment scale as observed with Coarse Revolution Microwave Remote Sensing. *Hydrology and Earth System Sciences*, *Discussion*, 2: 417-448.

SCS (1986) U.S. Soil Conservation Service. Technical Release 55: Urban Hydrology for Small Watersheds. USDA (U.S. Department of Agriculture). June 1986. Available at *http://www.info.usda.gov/CED/ftp/CED/tr55.pdf*.

Senseman, G.M., Bagley, C. F. and Tweddale, S.A. (1995) Accuracy Assessment of the Discrete Classification of Remotely-Sensed Digital Data for Landcover Mapping. US Army Corps of Engineers, USACERL Technical Report EN-95/04.

Shadeed, S. and Almasri, M. (2010) Application of GIS-based SCS-CN method in West Bank catchments. *Palestine Water Science and Engineering*, 3(1): 1-13.

Sharma, R.K. and Sharma, T.K. (2002) *Irrigation engineering*. 1st Ed. Chad & Co. Ltd, New Dehli, India. 768p.

Sheldrick, B. H. and Wang, C. (1993) Particle-size Distribution. In: Carter, M. R. (Ed.), *Soil Sampling and Methods of Analysis*, Canadian Society of Soil Science, Lewis Publishers, Ann Arbor, MI. p499-511.

Sheng, T.C., Barrett, R.E. and Mitchell, T.R. (1997) Using Geographic Information Systems for watershed classification and rating in developing countries. *Journal of Soil and Water Conservation*, 55(2): 84-89.

Shi, P., Yuan, Y. and Chen, J. (2001) The effect of land use on runoff in Shenzhen City of China. *Acta Ecologica Sinica*, 21(7): 1041–1049.

Shit, P.K., Bhunia, G.S. and Maiti, R. (2014) Vegetation Influence on Runoff and Sediment Yield in the Lateritic Region: An Experimental Study. *J. Geogr Nat Disast* 4: 116. doi:10.4172/2167-0587.1000116.

Shivhare, V., Goel, M.K, Singh, C.K. (2014) Simulation of surface runoff for upper Tapi subcatchment area (Burhanpur watershed) using SWAT. *The International Archives of the Photogrammetry, Remote Sensing and Spatial Information Sciences*, Volume XL-8, 2014 ISPRS Technical Commission VIII Symposium, 09-12 December 2014, Hyderabad, India.

Shongwe, M.E. (2007) Performance of recalibration systems of GCM forecasts over southern Africa. Published MSc Dissertation, University of Pretoria, 85p.

Singh, V.P. (Ed.) (1995) *Computer Models of Watershed Hydrology*. Water Resources Publications, Highland Ranch, Colorado.

Singh, V.P. and Xu, Y.J. (2006) Coastal Hydrology and Processes: Proceedings of the AIH 25th Anniversary Meeting & International Conference, "*Challenges in Coastal Hydrology and and Water Quality*", International Conference "Challenges in Coastal Hydrology and Water Quality" (2006: Baton Rouge, La.), Highland Ranch, Colo., Water Resources Publications, p163.

Singo, L.R. (2008) Temporal characteristics of rainfall and their influence on river discharge: the case of Luvuvhu River Catchment in Limpopo Province of South Africa. Published MSc Hydrology Thesis, University of Venda, 107p.

Singo L.R., Kundu, P.M., Odiyo, J.O., Mathivha, F.I. and Nkuna, T.R. (2012) Flood Frequency Analysis of Annual Maximum Stream flows for Luvuvhu River Catchment, Limpopo

Province, South Africa. *Proceedings of the 16th SANCIAHS National Hydrology Symposium*, Pretoria, South Africa, 1-3 October 2012.

Singo, T.E. (2010) Effects of land use and soil types on infiltration rate and implication on groundwater yield in Khalavha Village, Limpopo Province. Unpublished Bsc Hons Hydrology dissertation, University of Venda, 59p.

Siriwardena, L., Finlayson, B.L. and McMahon, T.A. (2006) The impact of land use change on catchment hydrology in large catchments: The Comet River, Central Queensland, Australia. *Journal of Hydrology*, 326(1-4): 199-214.

Sivakami, C., Meenakshi, S. M. and Sundram, A. (2010) Application of RS and GIS for land use/land cover mapping and change detection in Madurai District, TN. Indian Geotechnical Conference, December 16–18, 2010, IGS Mumbai Chapter & IIT Bombay.

Slabbert, N. (2007) The potential impact of an inter-basin water transfer on the Modder and Caledon River systems. Published PhD Thesis, University of Free State.

Slatyer, R.O. (1967) Plant-Water Relationships. London, New York, 366p.

Sloan, P.G. and Moore, I.D. (1984) Modeling subsurface stormflow on steeply sloping forested watersheds. *Water Resources Research*, 20(12): 1815-1822.

Smithers, J.C. and Schulze, R.E. (1995) ACRU Hydrological Modelling System: User manual Version 3.00. *A Report to the Water Research Commission*, Pretoria, Report No TT70/95.

Smithers, J.C. and Schulze, R.E. (2002) Design rainfall and flood estimation in South Africa. School of Bioresources Engineering and Environmental Hydrology- *Report to the Water Research Commission*, WRC Project No: K5/1060, University of Kwazulu-Natal, South Africa.

Smithers J.C., Chetty, K.T., Frezghi, M.S., Knoesen, D.M. and Tewolde, M.H. (2006) Development and Assessment of a Continuous Simulation Modelling System for Design Flood Estimation. *A Report to the Water Research Commission*, Pretoria, WRC Report No. 1318/1/07.

Snyder, R.L. (2001) Converting solar radiation to hours of bright sunshine. Reagents of the University of Carlifornia, USA, 1 November 2001.

Sodov, K., Nyamtseren, M.; Nasanbat, E. and Doljin, D. (2015) Land cover change during last decade in Mongolia. 3rd UNCCD Scientific conference, 9-12 March 2015, Cancún, Mexico.

Soliman, M.M. (2010) Engineering Hydrology of Arid and Semi-Arid Regions. 1st Edition, CRC Press, Taylor and Francis Group, New York, 411p.

Solín, L., Feranec, J. and Nováček, J. (2011) Land cover changes in small catchments in Slovakia during 1990–2006 and their effects on frequency of flood events. *Natural Hazards*, 56: 195-214.

Sørensen, H.R., Klucovska, J., Topolska, J., Clausen, T. and Refsgaard, J.C. (1996) An Engineering Case Study – Modeling the Influences of the Gabcikovo Hydropower Plant on the Hydrology and Ecology in the Slovakian Part of the River Branch System of Zitny Ostrov. In: *Distributed Hydrological Modeling*, Abbott, M.B. and Refsgaard, J.C. (Eds.), Kluwer Academic Publishers, p233-254.

Stisen, S., Jensen, K.H., Sandholt I. and Grimes, D. (2008) A remote sensing driven distributed hydrological model of the Senegal River basin. *Journal of Hydrology*, *354*(1-4): 131-148.

Strahler, A. and Strahler, A. (2006). *Introducing Physical Geography*. 3rd Edition, Wiley & Sons, Boston, 368p.

Strom, S., Nathan K. and Woland, J. (2013) Site Engineering for Landscape Architects. 6th Edition, Hoboken, N.J (Ed.), John Wiley & Sons, Inc., 368p.

Subramanya, K., 2013. *Engineering Hydrology*. 3rd Ed, Tata McGraw Hill, New Delhi, India, 242p.

Sumi, T., Morita, S., Ochi, T. and Komiya, H. (2002. Development of the Suspended-Sediment Concentration Measuring System with Differential Pressure Transmitter in Rivers and Reservoirs. Hydraulic Measurements and Experimental Methods: p1-10. doi: 10.1061/40655(2002)32.

Suprit, K., Shankar, D., Venugopal, V. and Bhatkar, N.V. (2012) Simulating the daily discharge of the Mandovi River, west coast of India. *Hydrological Science Journal*, 57(4): 686-704.

Sylla, L., Xiong, D., Zhang, H.Y. and Bangoura, S.T. (2012) A GIS technology and method to assess environmental problems from land use/cover changes: Conakry, Coyah and Dubreka region case Study. *The Egyptian Journal of Remote Sensing and Space Sceinces*, 15: 31-38.

Syvitski, J.P.M., Reidy, C.A. and Wilkinson, B.H. (2005) Impact of humans on the flux of terrestrial sediment to the global coastal ocean. *Science*, 308: 376-380.

Takara, K. (2009) Frequency analysis of hydrological extreme events and how to consider climate change. Disaster Prevention Research Institute, Kyoto University, Japan.

Taljaard, J.J. (1994) Atmospheric circulation systems, synoptic climatology and weather phenomena of South Africa. South African Weather Bureau Technical Paper, No. 27, 45p.

Tanaka, S. and Takara, K. (2002) A study on threshold selection in POT analysis of extreme floods: The Extremes of the Extremes: Extraordinary Floods. *Proceedings of International symposium on Extreme Floods*, Reykjavik, Iceland. July 2000. IAHS Publ. no. 271. 2002.

Taylor J.C. and Eva, H.D. (1992) Regional Inventories on Beds, Cambs and Northants (UK), *1992-final report to CEC-JRC*, Silsoe College ISBN 1 871564522, 70p.

Taylor, C.M., Lambin, E.F., Stephenne, N., Harding, R.J. and Essery R.L.H. (2002) The Influence of Land Use Change on Climate in the Sahel. *Journal of Climate*, 15: 3615–3629.

Thomas, D.S.G. and Goudie, A.S. (Eds.) (2000) *The Dictionary of Physical Geography* [*Paperback*]. John Wiley & Sons, 624p.

Thorvat, A.R. and Mujumdar, M.M. (2010) Regional Flood Frequency Analysis of Upper Krishna Basin. India 2010 Conference at a Glance, 5-7 January 2010, Indian Institute of Technology, Madras, Chennai, India.

Trinh, D.H. and Chui, T.F.M. (2013) Assessing the hydrologic restoration of an urbanized area via an integrated distributed hydrological model. *Hydrology and Earth System Science*, 17: 4789-4801.

Tsheko, R. (2006) Comparison between the United States Soil Conservation Service (SCS) and the two models commonly used for estimating rainfall-runoff in south-eastern Botswana. *Water SA* vol. 32 No. 1, ISSN 0378-4738.

Tshehla, C.E. (2009) Climatology of air mass transport to Cape Point. Published Master of Science thesis in the School of Environmental Sciences, University of KwaZulu-Natal, Durban, p17.

Tshikolomo, K.A., Walker, S. and Nesamvuni, A.E. (2013) Prospect for Developing Water Storage through Analysis of Runoff and Storage Capacity of Limpopo and Luvuvhu-Letaba Water Management Areas of South Africa. *International Journal of Applied Science and Technology*, 3(3): 70-79.

Turner, B.L. and Meyer, B.L. (Eds) (1994) "Global Land Use and Land Cover Change: An Overview." In *Changes in Land Use and Land Cover: A Global Perspective*, 3-10. Cambridge: Cambridge University Press.

Tyson, P.D. (1984) The Atmospheric Modulation of Extended Wet and Dry Spells over Southern Africa, 1958-1978. *Journal of Climatology*, 4: 621-635.

Tyson, P.D. (1986) *Climate change and variability in Southern Africa*. Oxford University Press, Cape Town, 220p.

Tyson, P.D. and Preston-Whyte, R.A. (2000) *The Weather and Climate of Southern Africa*, 2nd Ed, Oxford University Press, Cape Town, South Africa, p233-236.

United Nations Development Programme (UNDP), (2004) "*A global report: Reducing disaster risk- A challenge for development*", John S. Swift Co. USA. ISBN 92-1-126160-0.

USACE (1981) "*The new HEC-1 flood hydrograph package*", U.S Army Corps of Engineers, Hydrological Engineering Centre, Technical Paper Report No TP-82, Davies, CA.

USEPA (2001) *BASINS Version 3.0*: The Better Assessment Science Integrating Point and Nonpoint Sources. U.S. Environmental Protection Agency, EPA 82/ 8/01 001.

USEPA (2007) Fundamentals of urban runoff management: Technical and institutional issues. 2nd Edition, Shaver, E., R. Horner, J. Skupien, C. May, and G. Ridley (Eds)., U.S. Environmental Protection Agency, CA.

USGS (2003) "*Peak flow frequency estimates for US geological stream flow gauging stations in Connecticut*", Ahearn E.A (Ed.), USGS Federal Center, Denver, USA.

USGS (2010) "*100-Year Flood–It's All About Chance*", Robert R. Holmes, Jr. and Karen Dinicola (Eds.), General Information Product 106, U.S. Geological Survey, Virginia.

USGS, (2012) *Global data explorer*. Retrieved April 12, 2012 from *http://gdex.cr.usgs.gov/*.

USWRC (1981) *Floodplain Management Handbook.* Prepared by Flood Loss Reduction Associates. Washington, D.C: US Government Printing Office. United States Water Resources Council, 69 p.

Valimba, P. (2004) Rainfall variability in southern Africa, its influences on stream flow variations and its relationships with climatic variations. Published PhD thesis, Rhodes University, South Africa.

VanShaar, J.R., Haddeland, I. and Lettenmaier, D.P. (2002) Effects of land-cover changes on the hydrological response of interior Columbia River basin forested catchments. *Hydrological Processes*, 16: 2499-2520, DOI: 10.1002/hyp.1017.

Van Zyl, J.L. (Ed.) (1988) Response of grapevine roots to soil water regimes and irrigation systems. In: The Grapevine Root and Its Environment. *Tech. Comm.* 215. Department of Agricultural Development, Pretoria, SA, p30-43.

Van Zyl, K. (2006) A study on a Disaster Risk Management plan for the South Africa. Agricultural Sector. AGRI SA, NAFU SA, TAU SA, Pretoria.

Vesilind, P.A., Morgan, S.M. and Heine, L.G. (2009) *Introduction to Environmental Engineering*, Cengage Learning Publisher, USA, 606p.

Vieux, B.E. (2004) *Distributed Hydrologic Modeling Using GIS*. Kluwer Academic Publishers, Dordrecht, The Netherlands, 289pp.

Von Hagen, C.R. (2001). Use of an Area Sampling Frame to identify the spatial distribution of livestock in the Gauteng province. Msc Dissertation, Rand Afrikaans University, South Africa, 109p.

von Hagen, C.R., van der Meigden, J. and van der Zel, G. (2002) Using an Area Sampling Frame to calculate livestock statistics in the Gauteng Province, South Africa, within a GIS. ARC-ISCW, Pretoria, South Africa.

Walling, D.E. (1977a) Assessing the accuracy of suspended sediment rating curves for a small basin. *Water Resource Research*, 13: 531-538.

Walling, D.E. (1977b) Limitations of the rating curve technique for estimating suspended sediment loads, with particular reference to British rivers. In: *Erosion & Solid Matter Transport in Inland Waters* (Proc. Paris Symp., July 1977), IAHS Publ. 122: 34-48.

Walling, D.E. and Webb, B.W. (1981) The reliability of suspended sediment load data. In: *Erosion and Sediment Transport Measurements* (Proc. Florence Symp., June 1981), IAHS Publ. 133: 177-194.

Walmsley, R.D. and Bruwer, C.A. (1980) Water transparency characteristics of South African impoundments. *Journal of Limnological Society of South Africa*, 6(2): 69-76.

Wagner, W., Lemoine, G. and Rot, H. (1999) A Method for Estimating Soil Moisture from ERS Scatterometer and Soil Data. *Journal of Remote Sensing and Environment*, 70: 191–207.

Ward, R.C. and Robinson, M. (1990) *Principles of Hydrology*. McGraw-Hill, London, 365pp.

Ware, R. and Lad, F. (2003) Flood Frequency Analysis of the Waimakariri River. Available online at *http://www.math.canterbury.ac.nz/research/ucdms2003n17.pdf*.

Waring, R.H. and Running, S.W. (1998) *Forest Ecosystems: Concepts and Management*, 2nd Ed. Academic Press, London.

Watson, B.M., Ghafouri, M. and Selvalingam, S. (2003) Application of SWAT to model the water balance of the Woady Yaloak River catchment, Australia. *2nd International SWAT conference*, Bari Italy. TWRI Tech. Report 266: 94-110.

Weiner, C. (2006) Limiting factors for the short-term recruitment of savanna trees at woodland islands in the Western Soutpansberg, South Africa. Published Msc Thesis, University of Bremen, München, GRIN Verlag GmbH, 74p.

Western, A.W., Rodger, B., Grayson, R.B. and Blöschl, G. (2002) Scaling of Soil Moisture: A Hydrologic Perspective. *Annual Review of Earth Planet Sciences*, 30: 149-180.

Wetzel, R.G. and Likens, G.E. (2009) *Limnological Analyses*. 5th Edition. Springer-Verlag New York Inc. 429 pp.

White, E.D., Easton, Z.M., Fuka, D.R., Collick, A.S., McCartney, M., Awulachew, S.B. and Steenhuis, T.S. (2009) A Water Balance-Based Soil and Water Assessment Tool (SWAT) for Improved Performance in the Ethiopian Highlands. In: S.B. Awulachew, et al. (Ed.):

Improved water and land management in the Ethiopian highlands: Its impact on downstream stakeholders dependent on the Blue Nile. 2009 *IWMI Workshop*, Addis Ababa, Ethiopia.

White, M.D. and Greer, K.A. (2006) The effects of watershed urbanization on the stream hydrology and riparian vegetation of Los Penasquitos, Creek, California. *Landscape and Urban Planning*, 74(2): 125-138.

Wilkinson, B.H. (2004) Humans as geologic agents: A deep-time perspective. *Geological Society of America meeting*. Nov. 7-10. Denver.

Wilson, E.M. (1990) *Engineering Hydrology*. 4th Edition, Palgrave Macmillan Publisher, New York, 347pp.

WMO, (1994) *Guide to hydrological practices*. Data acquisition and processing, analysis, forecasting and other applications, WMO-No. 168, World Meteorological Organization, Geneva.

Wolock, D.M. and Price, C.V. (1994) Effects of digital elevation model map scale and data resolution on a topography-based watershed model. *Water Resources Research* 30(11): 3041-3052.

Xiaohong, R. and jiying, Q. (2004) Analysis of impact of large dams on river ecosystem, New Developments in Dam Engineering, Taylor and Francis group, London, p757.

Yang, J. and Wang, Y. (2011) Estimating evapotranspiration fraction by modeling two-dimensional space of NDVI/albedo and day–night land surface temperature difference: A comparative study. *Advances in Water Resources*, doi:10.1016/j.advwatres.2011.01.006.

Yuan, F., Sawaya, K.E., Loeffelholz, B.C. and Bauer, M.E. (2005) Land cover classification and changes analysis of the twin cities (Minnesota) Metropolitan Area by

multitemporal Landsat remote sensing. *Journal of Remote Sensing and Environment*, 98: 317-328.

Yeh, A. (1999) Urban planning and GIS. In: Geographical Information Systems—Management Issues and Applications. Longley, P., Goodchild, M., Maguire, D. and Rhind, D. (Eds.), John Wiley & Sons, New York, p877–888.

Zacharias, I., Dimitriou, E. and Koussouris, T.H. (2003) Estimating land cover changes and associated environmental impacts on wetlands by coupling remote sensing and hydrological modeling. *Water Resources Systems—Water Availability and Global Change* (Proceedings of symposium HS02a held during IUGG2003 al Sapporo, July 2003). IAHS Publ. no. 280: 247-254.

Zevenbergen, L.W. and Thorne, C.R. (1987) Quantitative analysis of land surface topography. *Earth Surface Processes and Landforms*, 12: 47–56.

Zeng, N., Needlin, J.D., Lau, K.M. and Tucker, C.J. (1999) Enhancement of climate variability in the Sahel by vegetation interaction. *Science,* 286: 1537-1540.

Zhang, T., Zhang, X., Xia, D. and Liu, Y. (2014) An Analysis of Land Use Change Dynamics and Its Impacts on Hydrological Processes in the Jialing River Basin. *Water*, 6: 3758-3782, doi: 10.3390/w6123758.

Zieglar, A.D. (2004) Hydrological consequences of landscape fragmentation in mountainous northern Vietnam: Evidence of accelerated overland flow generation. *Journal of Hydrology*, 287: 124-146.

Zilassi, P., Jordan, G., Kovacs, Fe., van Rompaey, A. and Van Dessel, W. (2010) Investigating the link between soil quality and agricultural land use change. A case study in the Lake Balaton Catchment, Hungary. Carpathian Journal of Earth and Environmental Sciences, 5(2): 61-70.

Zimmermann, B., Elsenber, H. and De Moraes, J.M. (2000) The influence of land use change on soil hydraulic properties: Implication for runoff generation. *Forest Ecology and Management*, 222(1-3): 29-38.

APPENDICES

APPENDIX 1: CLIMATE/ETO DATA

Climate/ETO data for Levubu

CropWat 4 Windows Ver 4.3 Climate and ETo (grass) Data

Country : South Africa Station : Levubu
Altitude: 610 meter(s) above M.S.L.
Latitude: -23.08 Deg. (South) Longitude: 30.28 Deg. (East)

Month	MaxTemp (deg.C)	MiniTemp (deg.C)	Humidity (%)	Wind Spd. (Km/d)	SunShine (Hours)	Solar Rad. (MJ/m2/d)	ETo (mm/d)
January	28.4	18.6	65.6	88.8	5.4	19.2	4.25
February	27.4	18.4	64.2	79.8	5.0	17.9	3.88
March	26.7	17.4	63.9	73.2	5.1	16.5	3.45
April	25.6	15.2	62.4	71.6	5.5	14.8	2.88
May	24.2	12.4	57.8	81.1	6.1	13.2	2.45
June	21.9	9.8	53.8	95.6	5.9	11.8	2.22
July	22.1	9.6	53.6	100.0	6.1	12.5	2.37
August	23.6	11.2	52.4	105.0	6.0	14.4	2.94
September	26.0	13.7	53.0	115.0	5.8	16.5	3.70
October	26.3	15.4	58.3	118.5	5.2	17.5	3.99
November	27.0	16.7	61.6	103.4	5.2	18.6	4.15
December	27.8	18.0	63.3	96.3	5.1	18.8	4.23
Average	25.6	14.7	59.2	94.0	5.5	16.0	3.38

Pen-Mon equation was used in ETo calculations with the following values for Angstrom's Coefficients:
a = 0.25 b = 0.5

Climate/ETO data for Lwamondo

CropWat 4 Windows Ver 4.3 Climate and ETo (grass) Data

Country : South Africa Station : Lwamondo
Altitude: 648 meter(s) above M.S.L.
Latitude: -23.04 Deg. (South) Longitude: 30.37 Deg. (East)

Month	MaxTemp (deg.C)	MiniTemp (deg.C)	Humidity (%)	Wind Spd. (Km/d)	SunShine (Hours)	Solar Rad. (MJ/m2/d)	ETo (mm/d)
January	29.5	19.9	65.6	85.1	6.6	21.1	4.62
February	27.7	19.1	59.8	73.3	6.1	19.6	4.16
March	28.3	18.7	67.8	71.0	6.4	18.5	3.78
April	26.8	16.1	65.3	69.0	6.8	16.5	3.11
May	24.1	12.2	58.8	74.1	7.3	14.6	2.47
June	22.2	10.2	56.3	77.6	6.7	12.7	2.10
July	23.0	10.1	58.1	84.3	7.4	13.9	2.33
August	25.0	11.8	55.9	98.9	7.7	16.5	3.11
September	25.9	13.4	52.7	103.9	7.1	18.3	3.78
October	28.0	16.3	58.8	110.7	6.7	19.8	4.37
November	28.4	17.9	61.5	96.5	6.0	19.9	4.41
December	29.4	19.3	63.6	88.7	6.2	20.6	4.58
Average	26.5	15.4	60.4	86.1	6.8	17.7	3.57

Pen-Mon equation was used in ETo calculations with the following values for Angstrom's Coefficients:
a = 0.25 b = 0.5

Climate/ETO data for Madzivhandila

CropWat 4 Windows Ver 4.3 Climate and ETo (grass) Data

Country : South Africa Station : Madzivhandila
Altitude: 517 meter(s) above M.S.L.
Latitude: -22.98 Deg. (South) Longitude: 30.55 Deg. (East)

Month	MaxTemp (deg.C)	MiniTemp (deg.C)	Humidity (%)	Wind Spd. (Km/d)	SunShine (Hours)	Solar Rad. (MJ/m2/d)	ETo (mm/d)
January	30.6	19.1	45.7	6.0	6.5	21.0	3.90
February	28.5	19.4	64.1	7.0	3.7	15.8	3.13
March	29.0	18.7	47.1	5.5	6.1	18.0	3.14
April	27.5	15.0	45.6	0.0	5.6	14.9	2.22
May	26.3	10.0	57.2	0.0	6.6	13.8	1.71
June	24.9	8.4	58.4	2.9	6.0	12.0	1.38
July	24.0	7.5	57.0	5.8	5.6	12.0	1.45
August	26.2	9.5	57.2	6.8	6.8	15.4	2.12
September	28.5	13.4	38.2	7.9	4.4	14.6	2.42
October	29.0	15.2	51.5	20.4	4.6	16.6	3.18
November	28.9	18.2	56.6	0.0	4.3	17.2	3.25
December	30.9	18.9	56.7	0.0	4.2	17.4	3.40
Average	27.9	14.4	52.9	5.2	5.4	15.7	2.61

Pen-Mon equation was used in ETo calculations with the following values for Angstrom's Coefficients:
a = 0.25 b = 0.5

Climate/ETO data for Thohoyandou

CropWat 4 Windows Ver 4.3 Climate and ETo (grass) Data

Country : South Africa Station : Thohoyandou
Altitude: 730 meter(s) above M.S.L.
Latitude: -22.94 Deg. (South) Longitude: 30.49 Deg. (East)

Month	MaxTemp (deg.C)	MiniTemp (deg.C)	Humidity (%)	Wind Spd. (Km/d)	SunShine (Hours)	Solar Rad. (MJ/m2/d)	ETo (mm/d)
January	28.8	20.3	69.7	77.8	8.6	24.3	5.00
February	29.9	20.3	65.1	88.1	7.0	21.0	4.60
March	28.4	19.1	66.4	69.6	8.1	21.0	4.15
April	26.3	17.1	65.2	65.7	2.2	10.4	2.40
May	25.5	15.4	56.5	61.6	4.6	11.5	2.26
June	23.6	13.5	53.9	69.6	3.1	8.9	1.94
July	22.2	12.5	54.6	69.3	2.6	8.7	1.90
August	25.2	13.9	50.8	79.9	1.8	9.2	2.42
September	28.2	16.3	51.3	100.7	3.0	12.6	3.36
October	28.5	17.6	59.0	108.4	3.6	15.1	3.80
November	28.9	18.6	64.4	94.6	4.2	17.0	4.01
December	28.7	19.9	69.2	84.8	1.0	12.3	5.31
Average	27.0	17.0	60.5	80.8	4.2	14.3	3.43

Pen-Mon equation was used in ETo calculations with the following values for Angstrom's Coefficients:
a = 0.25 b = 0.5

Climate/ETO data for Univen

CropWat 4 Windows Ver 4.3 Climate and ETo (grass) Data

Country : South Africa Station : University of Venda (Univen)
Altitude: 712 meter(s) above M.S.L.
Latitude: -22.97 Deg. (South) Longitude: 30.44 Deg. (East)

Month	MaxTemp (deg.C)	MiniTemp (deg.C)	Humidity (%)	Wind Spd. (Km/d)	SunShine (Hours)	Solar Rad. (MJ/m2/d)	ETo (mm/d)
January	29.6	19.8	66.9	92.6	2.6	14.7	3.69
February	30.6	20.0	66.6	106.6	3.4	15.4	3.91
March	28.7	18.1	69.1	87.3	9.0	22.3	4.41
April	27.0	15.4	67.8	74.1	2.6	11.0	2.52
May	26.1	11.9	62.5	75.7	5.3	12.3	2.40
June	24.1	9.9	60.3	85.0	9.8	16.0	2.41
July	23.5	9.2	58.8	83.5	7.6	14.2	2.36
August	25.9	10.7	53.9	109.9	0.1	7.1	2.56
September	26.0	16.0	50.3	129.1	3.2	12.9	3.52
October	25.9	19.4	57.4	132.7	3.9	15.6	3.90
November	29.3	18.0	64.3	109.2	3.9	16.6	4.06
December	29.8	19.5	64.4	104.0	4.8	18.3	4.38
Average	27.2	15.7	61.9	99.1	4.7	14.7	3.34

Pen-Mon equation was used in ETo calculations with the following values for Angstrom's Coefficients:
a = 0.25 b = 0.5

Climate/ETO data for Mhinga

CropWat 4 Windows Ver 4.3 Climate and ETo (grass) Data

Country : South Africa Station : Mhinga
Altitude: 460 meter(s) above M.S.L.
Latitude: -22.79 Deg. (South) Longitude: 30.84 Deg. (East)

Month	MaxTemp (deg.C)	MiniTemp (deg.C)	Humidity (%)	Wind Spd. (Km/d)	SunShine (Hours)	Solar Rad. (MJ/m2/d)	ETo (mm/d)
January	31.1	20.5	70.0	32.8	1.7	13.3	3.09
February	32.6	19.8	64.5	35.6	2.5	14.0	3.25
March	32.2	18.5	63.8	33.5	1.6	11.4	2.69
April	29.0	15.8	65.0	30.8	0.4	8.1	1.93
May	28.2	12.0	61.9	32.7	1.5	8.0	1.74
June	26.5	8.9	59.2	36.6	3.0	8.8	1.66
July	25.0	8.4	59.9	40.4	3.4	9.6	1.74
August	27.6	9.6	55.9	46.7	0.0	7.0	1.94
September	31.1	14.0	51.9	58.8	1.0	9.8	2.73
October	31.9	17.8	56.2	58.8	1.4	11.7	3.12
November	31.5	19.0	62.8	49.4	1.2	12.3	3.10
December	31.3	20.2	67.1	38.4	1.2	12.6	3.05
Average	29.8	15.4	61.5	41.2	1.6	10.5	2.50

Pen-Mon equation was used in ETo calculations with the following values for Angstrom's Coefficients:
a = 0.25 b = 0.5

APPENDIX 2: TOTAL AND EFFECTIVE RAINFALL AND EVAPORATION DATA

Total and Effective Rainfall and Evaporation data for Levubu

CropWat 4 Windows Ver 4.3 Total & Effective Rainfall and Evaporation Data for Levubu

Month	Total Rainfall (mm/month)	Effective Rain (mm/month)	A-Pan Evaporation (mm/month)
January	172.4	124.8	151.6
February	206.7	138.3	130.6
March	122.1	98.2	130.8
April	44.9	41.7	106.8
May	26.1	25.0	104.4
June	14.2	13.9	93.3
July	11.0	10.8	98.3
August	15.9	15.5	115.7
September	36.4	34.3	142.9
October	76.5	67.1	156.8
November	125.6	100.4	152.5
December	135.2	106.0	149.1
Total (mm/Year)	987.0	776.0	1532.95

N.B. To convert to mm/day data was divided by the number of days in each month

Effective rainfall calculated using the USSCS formulas:

Effective R. = (125 - 0.2 * Total R.)* Total R. / 125 ... (Total R. < 250 mm/month),
Effective R. = 0.1 * Total R. - 125 ... (Total R. > 250 mm/month).

Total and Effective Rainfall and Evaporation data for Lwamondo

CropWat 4 Windows Ver 4.3 Total & Effective Rainfall and Evaporation Data for Lwamondo

MMonth	Total Rainfall (mm/month)	Effective Rain (mm/month)	A-Pan Evaporation (mm/month)
January	109.4	90.3	127.3
February	153.8	116.0	115.2
March	72.4	64.0	126.8
April	33.3	31.5	122.0
May	9.2	9.1	98.0
June	11.5	11.3	81.5
July	7.7	7.6	92.6
August	5.7	5.6	121.7
September	11.2	11.0	135.4
October	48.1	44.4	157.0
November	81.1	70.6	139.3
December	102.2	85.5	119.8
Total (mm/Year)	645.6	546.9	1436.83

N.B. To convert to mm/day data was divided by the number of days in each month

Effective rainfall calculated using the USSCS formulas:

Effective R. = (125 - 0.2 * Total R.)* Total R. / 125 ... (Total R. < 250 mm/month),
Effective R. = 0.1 * Total R. - 125 ... (Total R. > 250 mm/month).

Total and Effective Rainfall and Evaporation data for Madzivhandila

CropWat 4 Windows Ver 4.3 Total & Effective Rainfall and Evaporation Data for Madzivhandila

Month	Total Rainfall (mm/month)	Effective Rain (mm/month)	A-Pan Evaporation (mm/month)
January	22.1	21.3	157.2
February	31.5	29.9	166.6
March	45.9	42.5	144.1
April	7.8	7.7	130.6
May	0.4	0.4	117.4
June	1.9	1.9	97.6
July	0.9	0.9	103.2
August	0.7	0.7	94.8
September	3.3	3.3	127.8
October	7.0	6.9	141.7
November	29.2	27.8	144.3
December	12.9	12.6	164.2
Total (mm/Year)	163.6	155.9	1589.56

N.B. To convert to mm/day data was divided by the number of days in each month

Effective rainfall calculated using the USSCS formulas:

Effective R. = (125 - 0.2 * Total R.)* Total R. / 125 ... (Total R. < 250 mm/month),

Effective R. = 0.1 * Total R. - 125 ... (Total R. > 250 mm/month).

Total and Effective Rainfall data for Thohoyandou

CropWat 4 Windows Ver 4.3 Total & Effective Rainfall Data for Thohoyandou

Month	Total Rainfall (mm/month)	Effective Rain (mm/month)
January	25.3	24.3
February	9.7	9.5
March	13.5	13.2
April	7.4	7.3
May	1.2	1.2
June	1.6	1.6
July	3.5	3.5
August	1.1	1.1
September	3.1	3.1
October	5.3	5.3
November	25.4	24.4
December	31.6	30.0
Total (mm/Year)	128.7	124.5

N.B. To convert to mm/day data was divided by the number of days in each month

Effective rainfall calculated using the USSCS formulas:

Effective R. = (125 - 0.2 * Total R.)* Total R. / 125 ... (Total R. < 250 mm/month),

Effective R. = 0.1 * Total R. - 125 ... (Total R. > 250 mm/month).

Where,

Month 1= January	Month 5= May	Month 9= September
Month 2= February	Month 6=June	Month 10= October
Month 3= March	Month 7= July	Month 11= November
Month 4= April	Month 8= August	Month 12= December

Total and Effective Rainfall data for Univen

CropWat 4 Windows Ver 4.3 Total & Effective Rainfall Data for Univen

Month	Total Rainfall (mm/month)	Effective Rain (mm/month)
January	32.7	31.0
February	23.3	22.4
March	16.8	16.3
April	8.0	7.9
May	1.4	1.4
June	2.0	2.0
July	2.7	2.7
August	1.6	1.6
September	3.2	3.2
October	5.0	5.0
November	29.1	27.7
December	39.4	36.9
Total (mm/Year)	165.2	158.1

N.B. To convert to mm/day data was divided by the number of days in each month

Effective rainfall calculated using the USSCS formulas:

Effective R. = (125 - 0.2 * Total R.)* Total R. / 125 ... (Total R. < 250 mm/month),
Effective R. = 0.1 * Total R. - 125 ... (Total R. > 250 mm/month).

Total and Effective Rainfall data for Mhinga

CropWat 4 Windows Ver 4.3 Total & Effective Rainfall Data for Mhinga

Month	Total Rainfall (mm/month)	Effective Rain (mm/month)
January	22.0	21.2
February	9.2	9.1
March	6.4	6.3
April	8.9	8.8
May	4.2	4.2
June	0.7	0.7
July	2.0	2.0
August	0.6	0.6
September	2.3	2.3
October	1.8	1.8
November	16.8	16.3
December	27.8	26.6
Total (mm/Year)	102.7	99.9

N.B. To convert to mm/day data was divided by the number of days in each month

Effective rainfall calculated using the USSCS formulas:

Effective R. = (125 - 0.2 * Total R.)* Total R. / 125 ... (Total R. < 250 mm/month),
Effective R. = 0.1 * Total R. - 125 ... (Total R. > 250 mm/month).

APPENDIX 3: TOTAL AND EFFECTIVE RAINFALL DISTRIBUTION

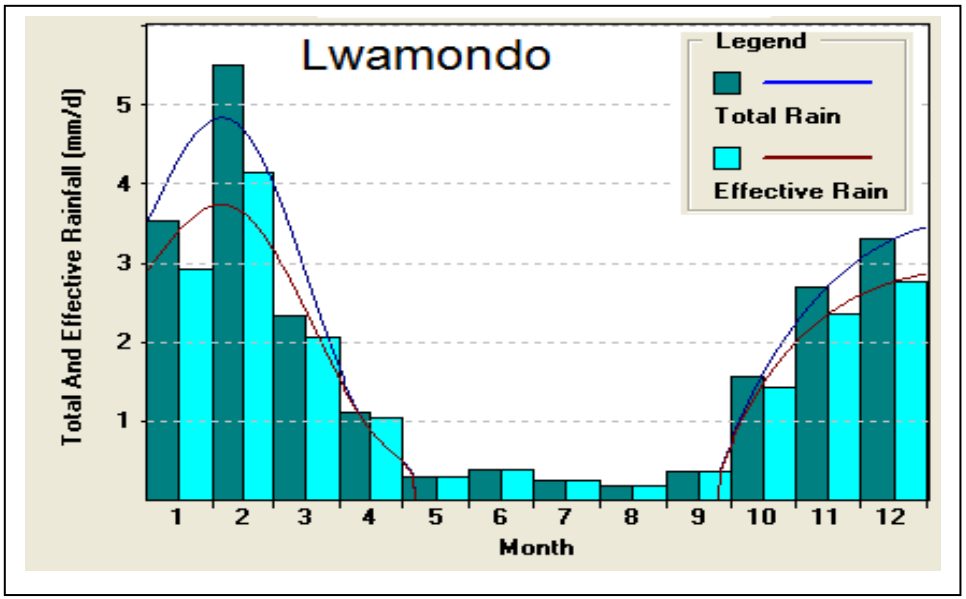

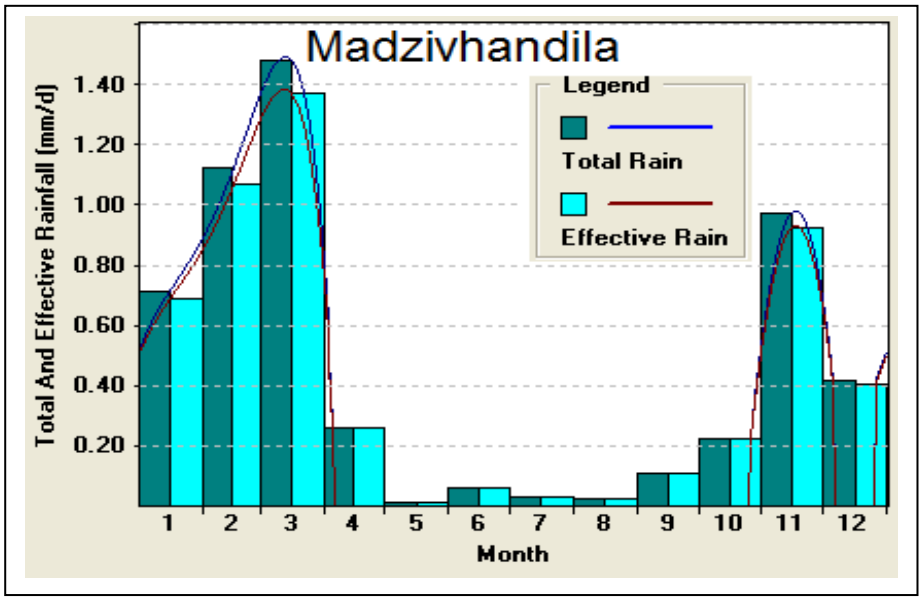

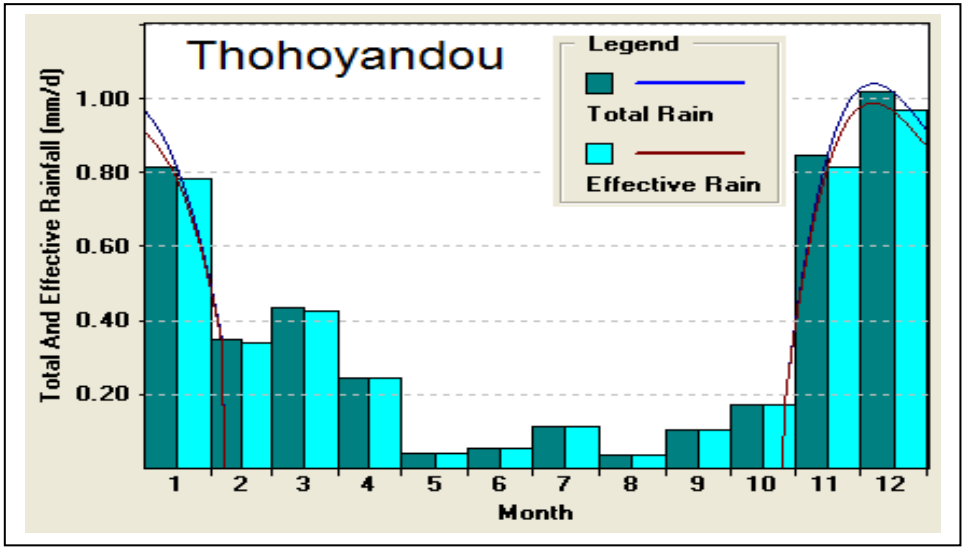

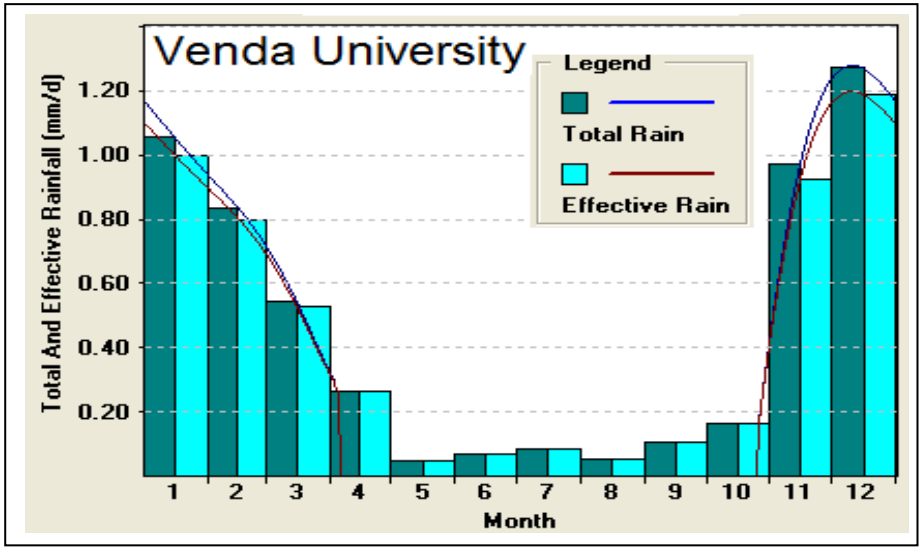

APPENDIX 4: AVERAGE MONTHLY MINIMUM AND MAXIMUM TEMPERATURES

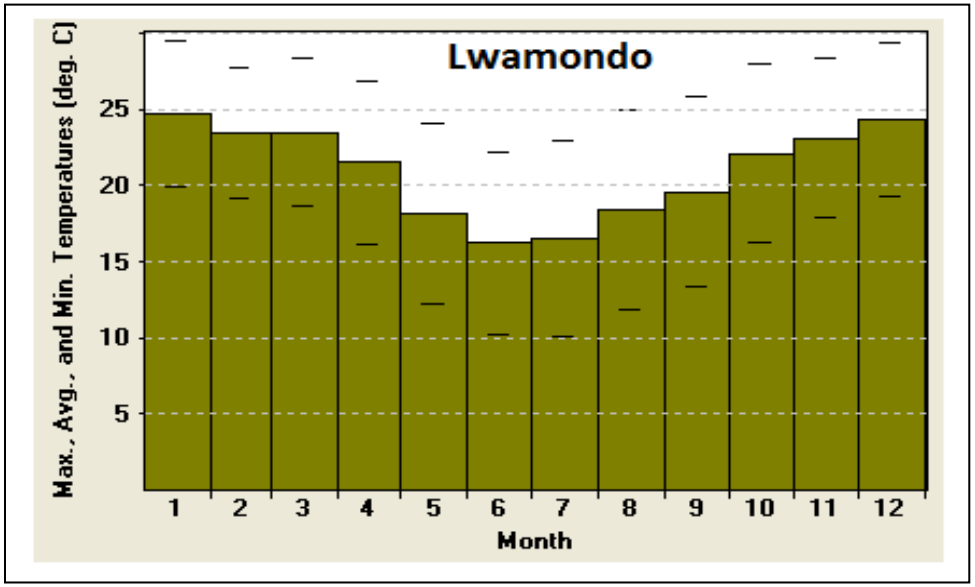

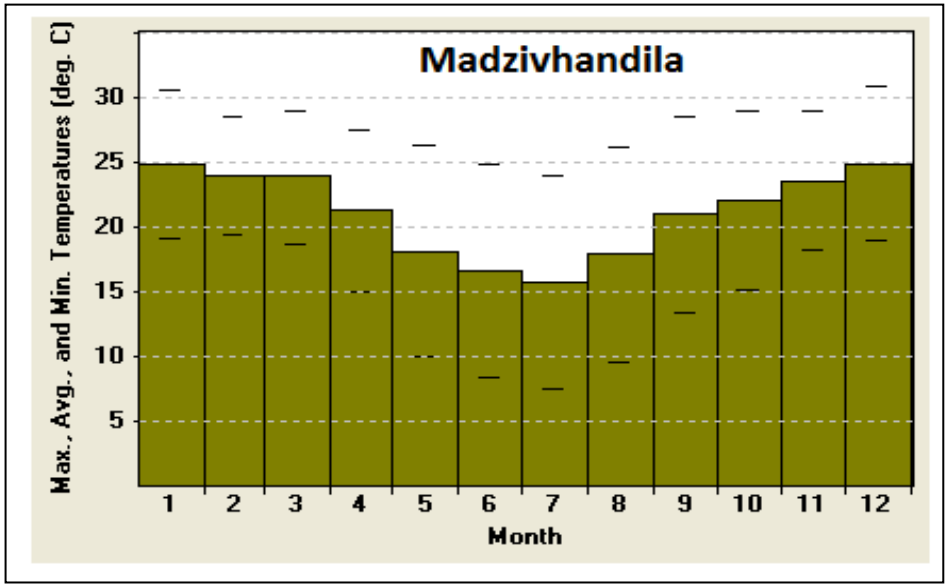

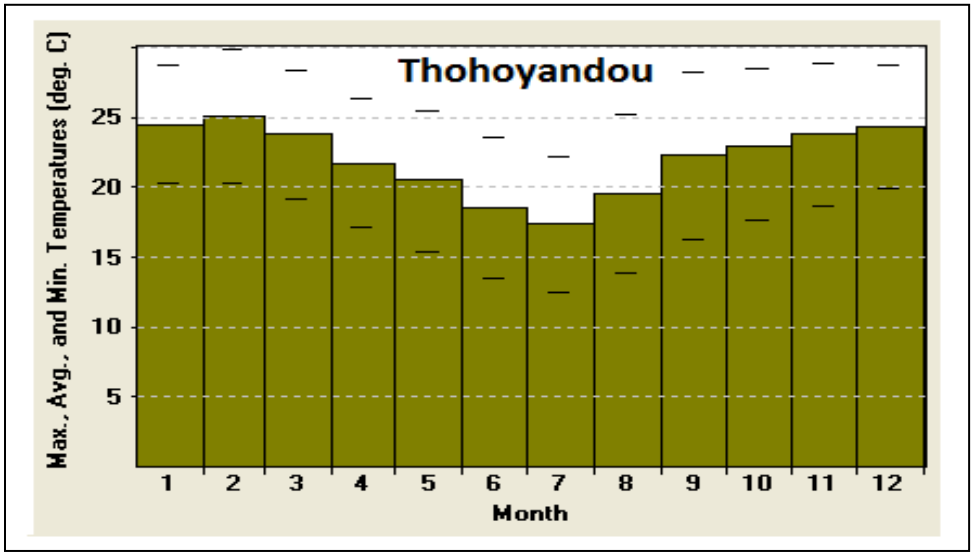

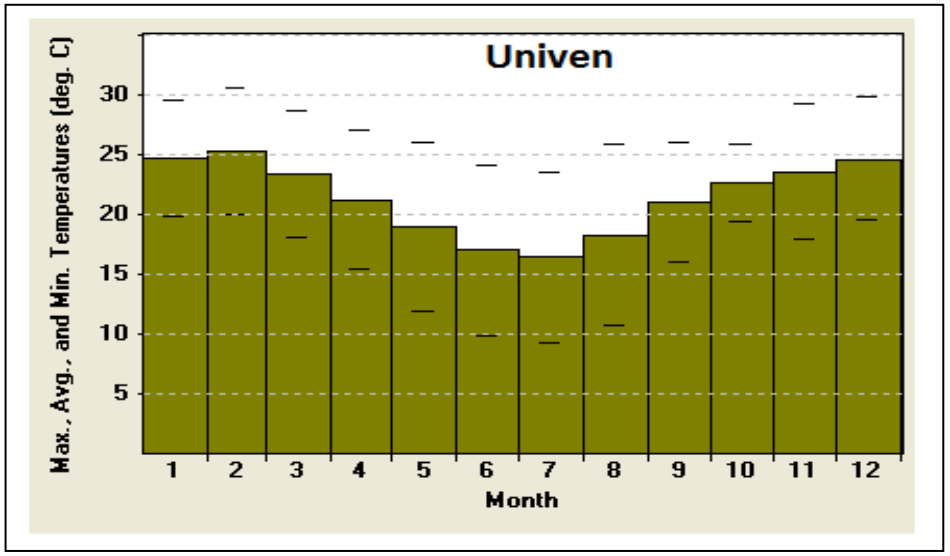

APPENDIX 5: AVERAGE MONTHLY WIND SPEED

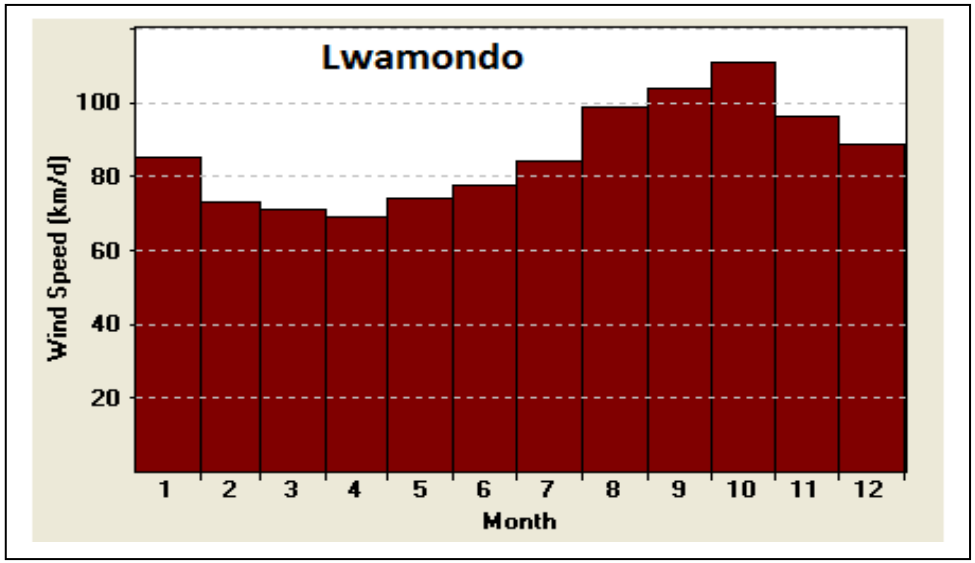

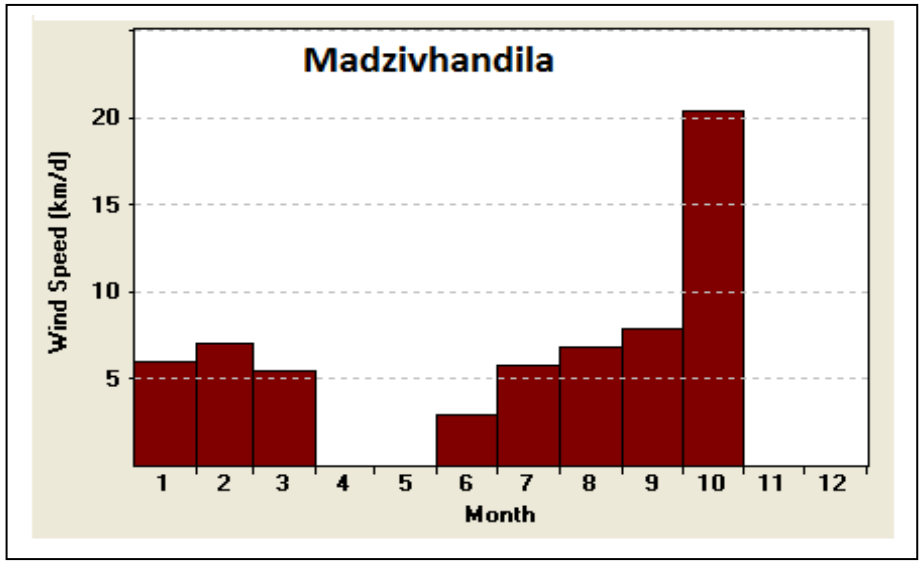

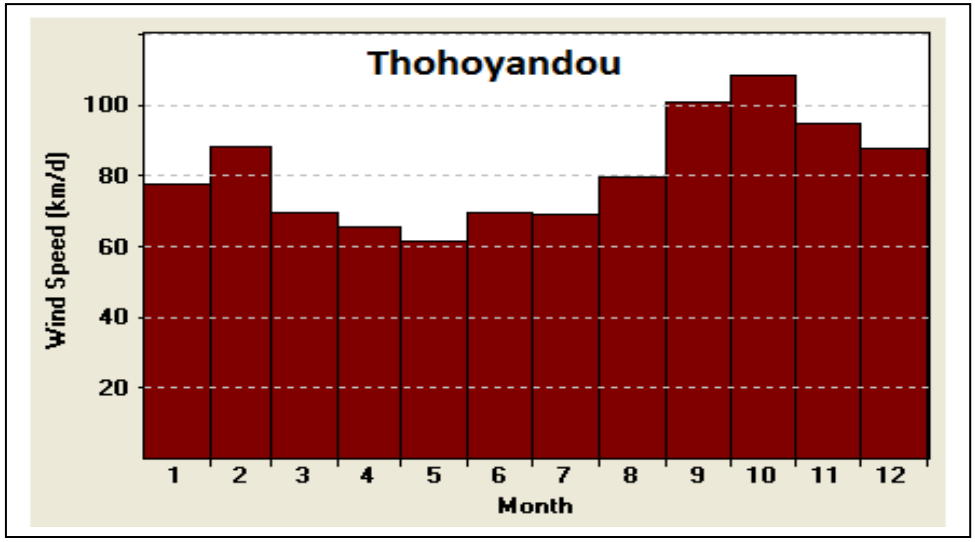

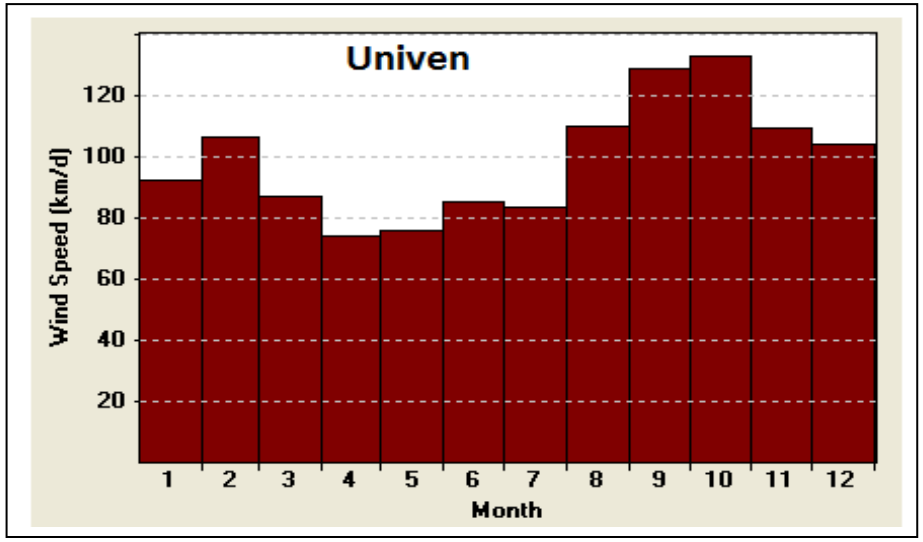

APPENDIX 6: AVERAGE MONTHLY HUMIDITY

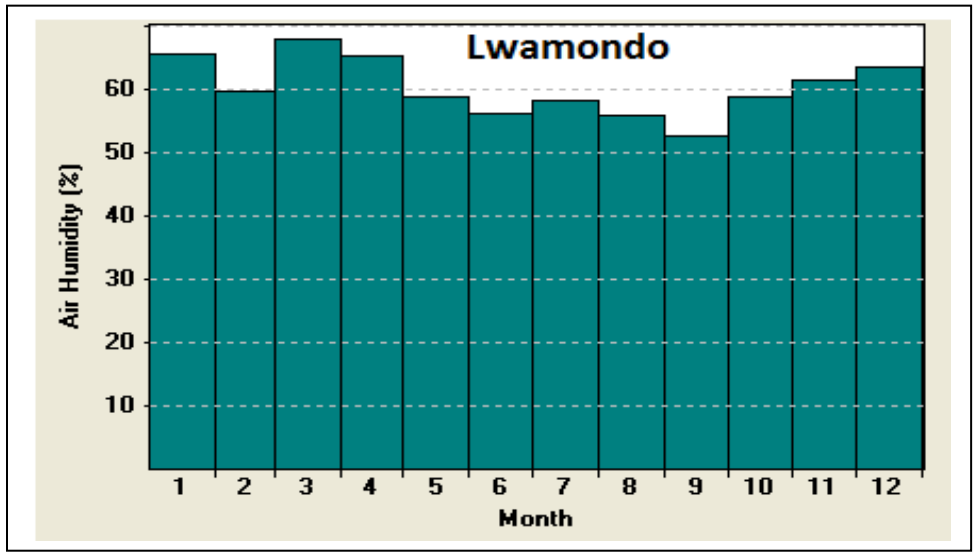

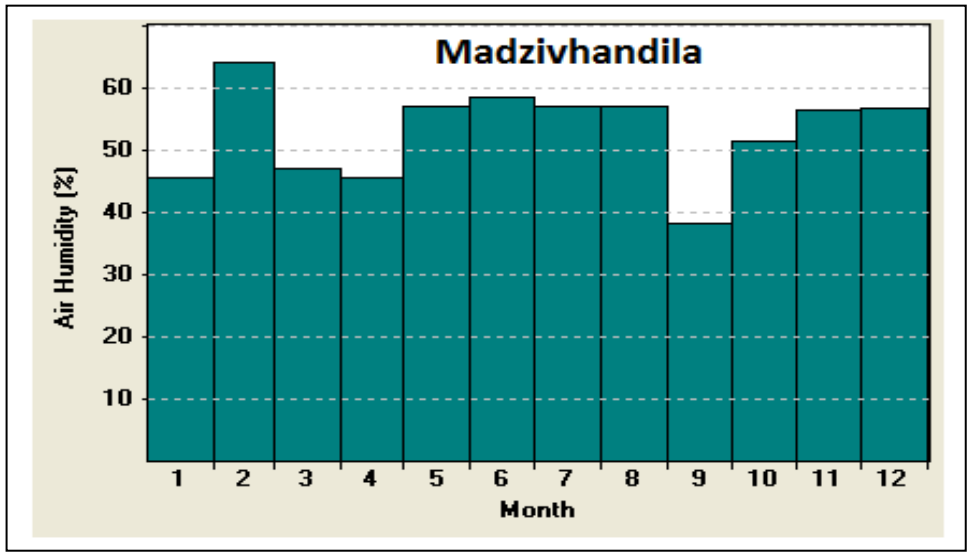

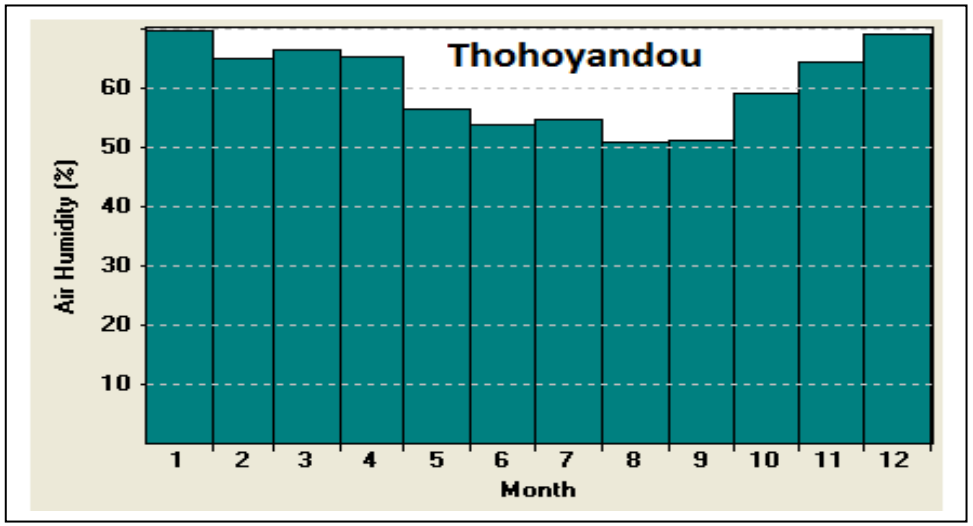

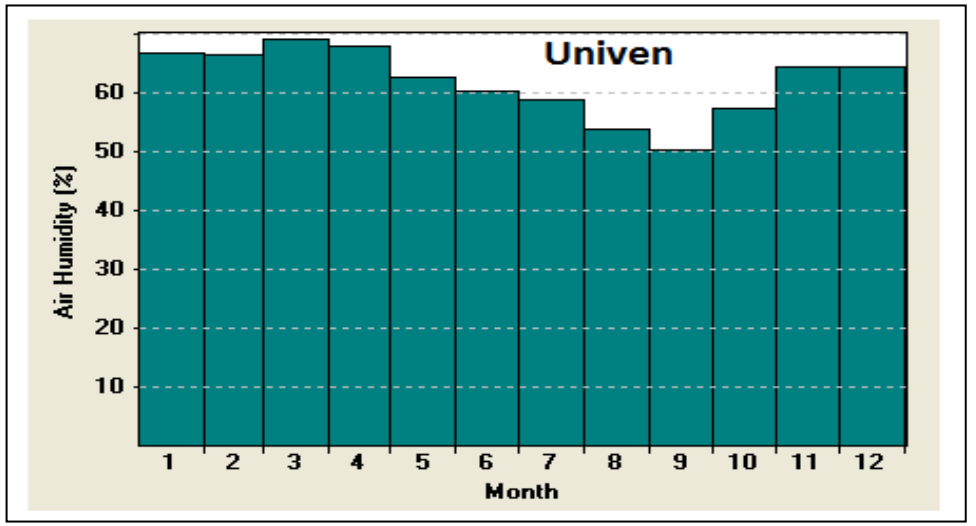

APPENDIX 7: AVERAGE MONTHLY SOLAR RADIATION

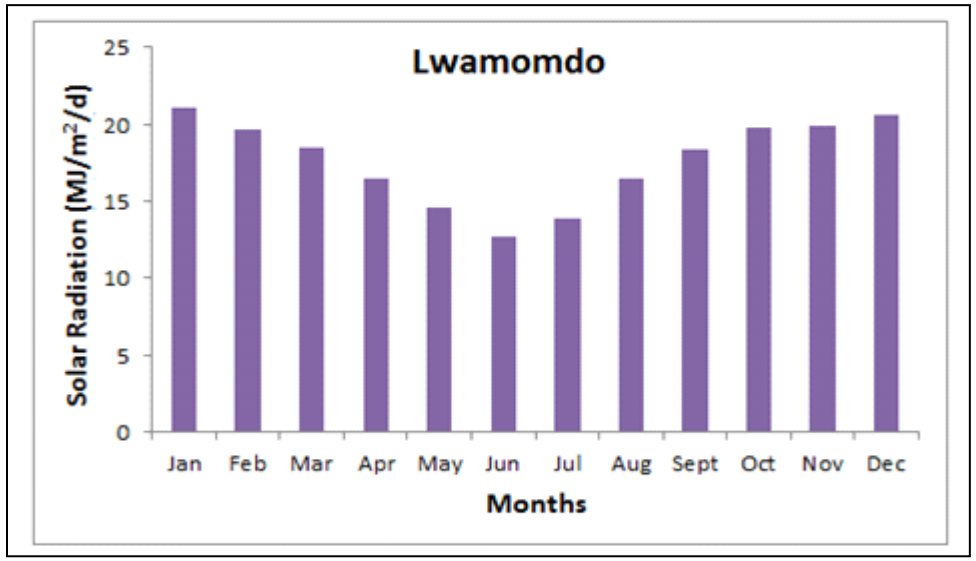

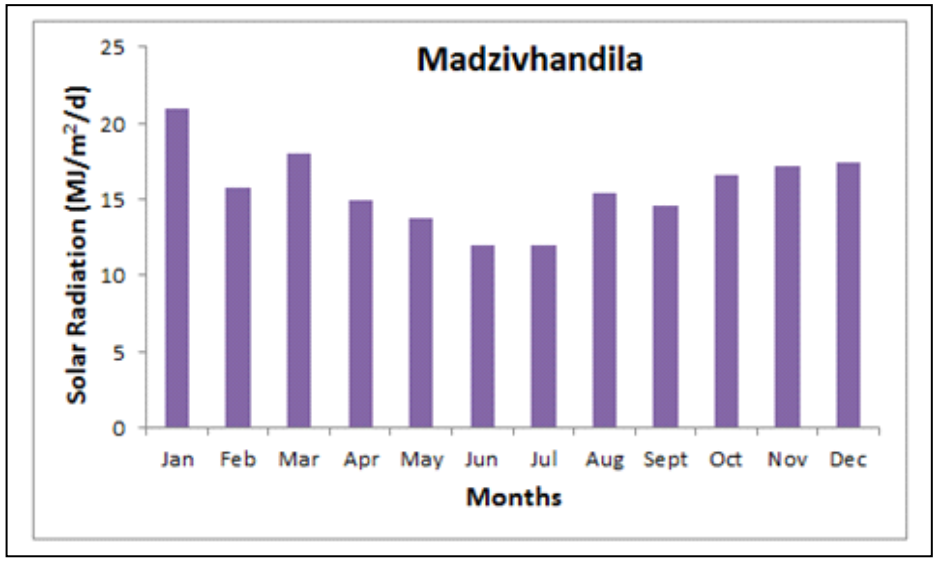

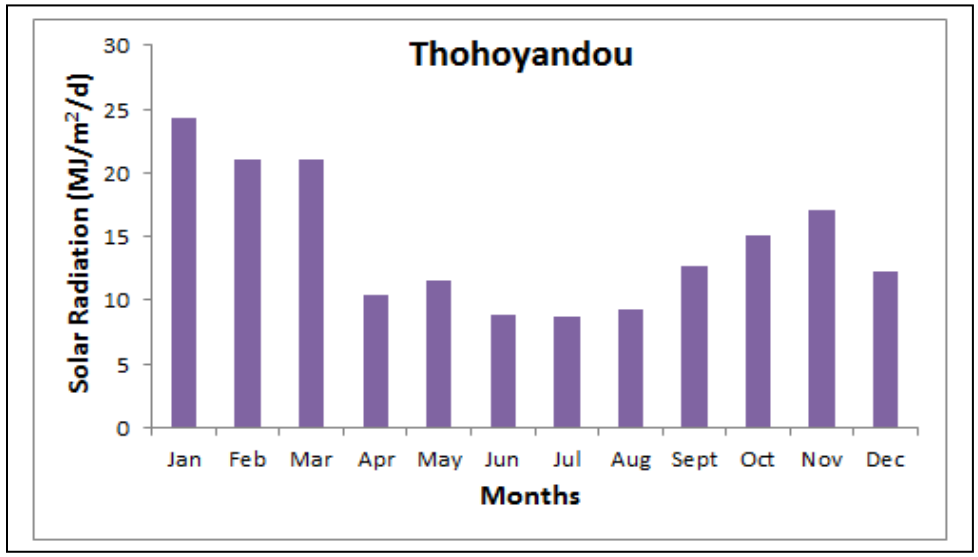

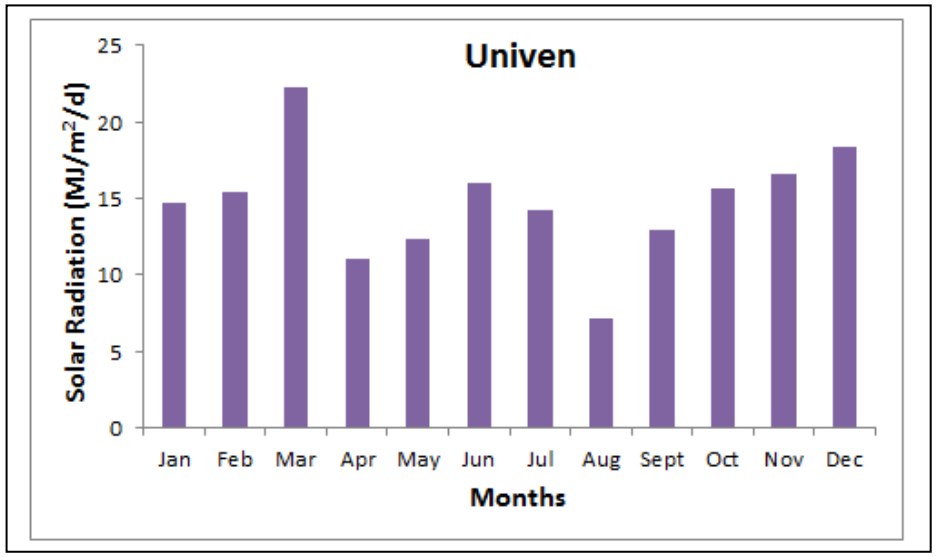

APPENDIX 8: AVERAGE MONTHLY SUNSHINE HOURS

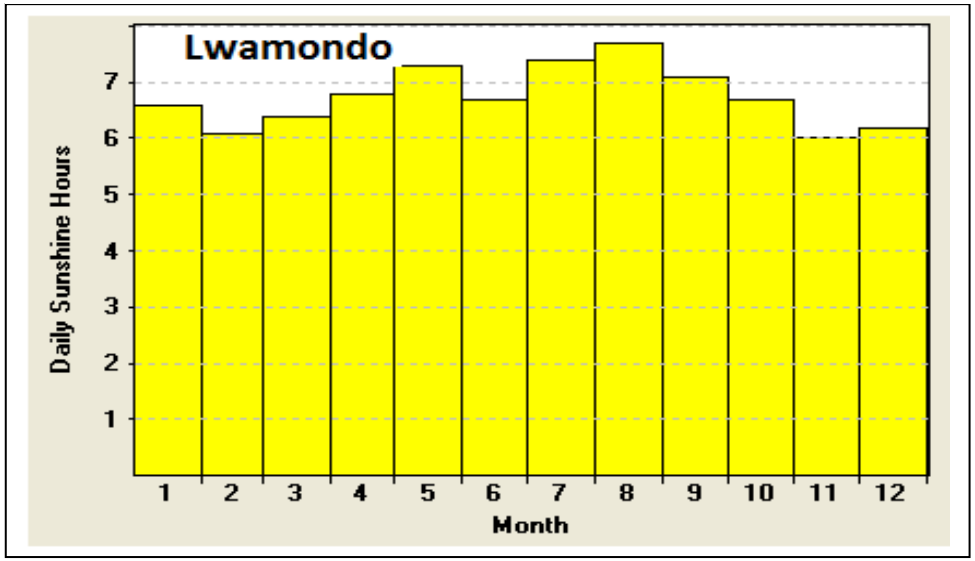

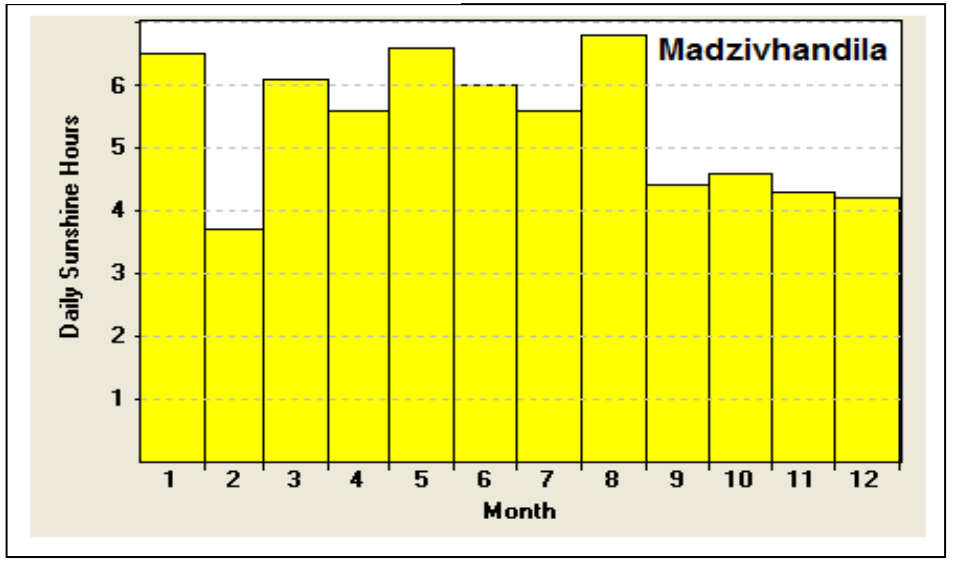

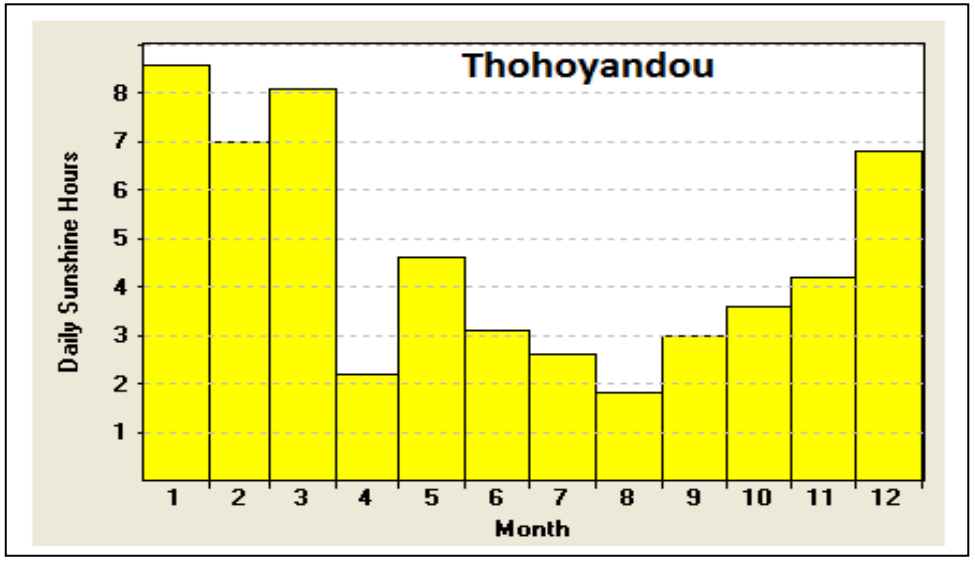

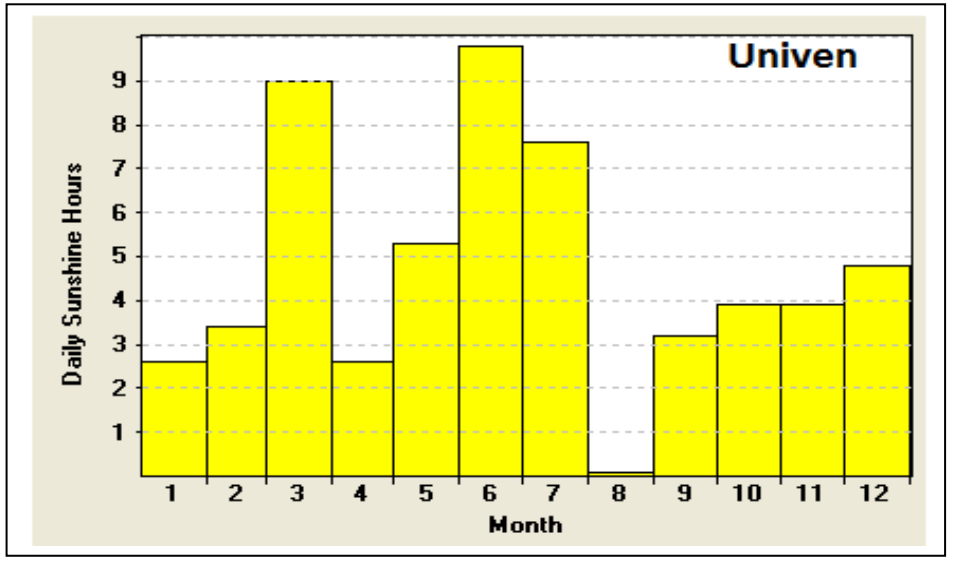

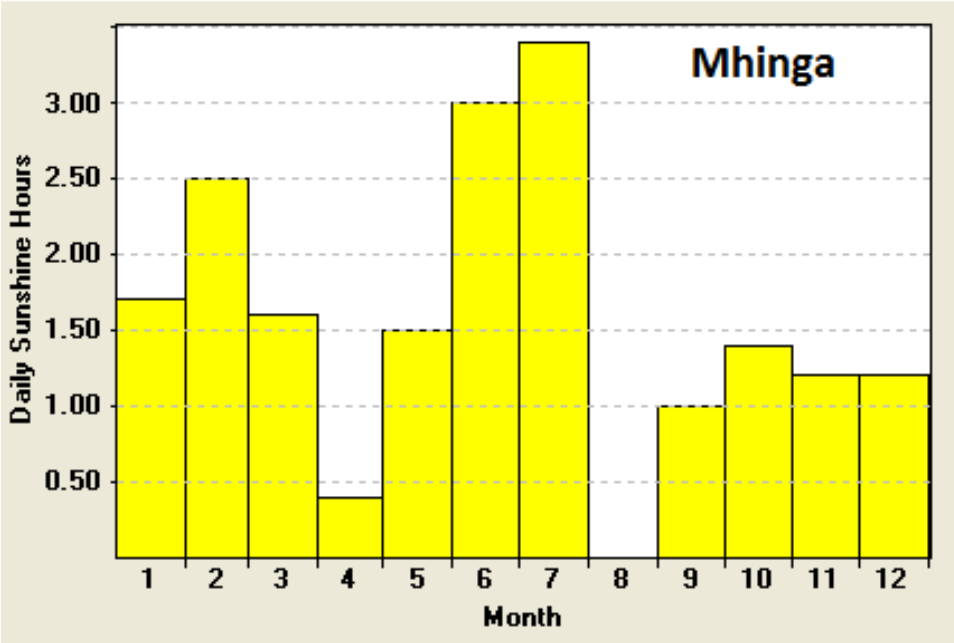

Where,

Month 1= January	Month 7= July
Month 2= February	Month 8= August
Month 3= March	Month 9= September
Month 4= April	Month 10= October
Month 5= May	Month 11= November
Month 6=June	Month 12= December

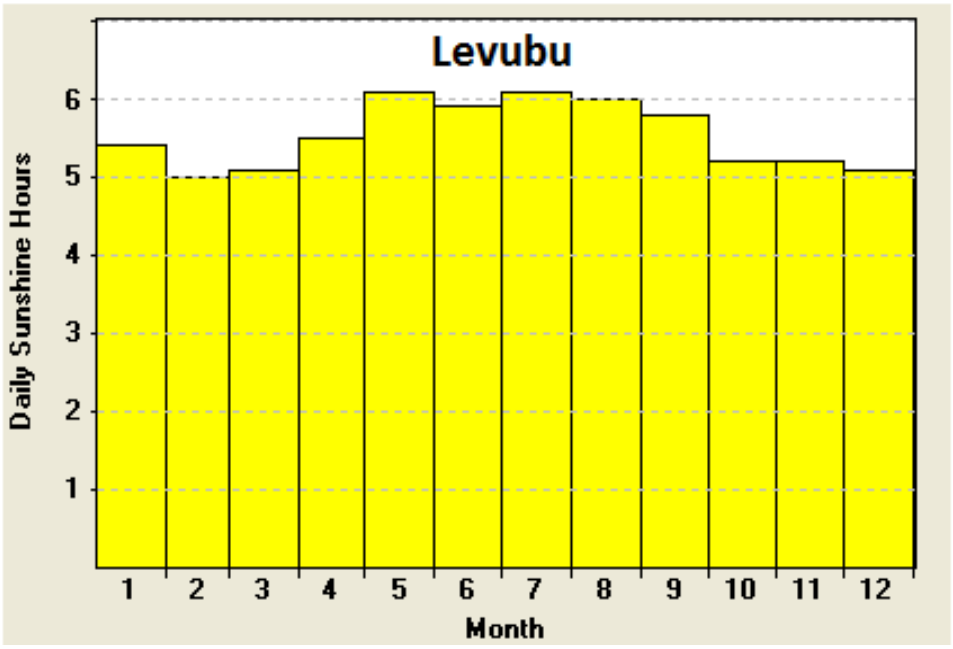

APPENDIX 9: AVERAGE MONTHLY ET_O

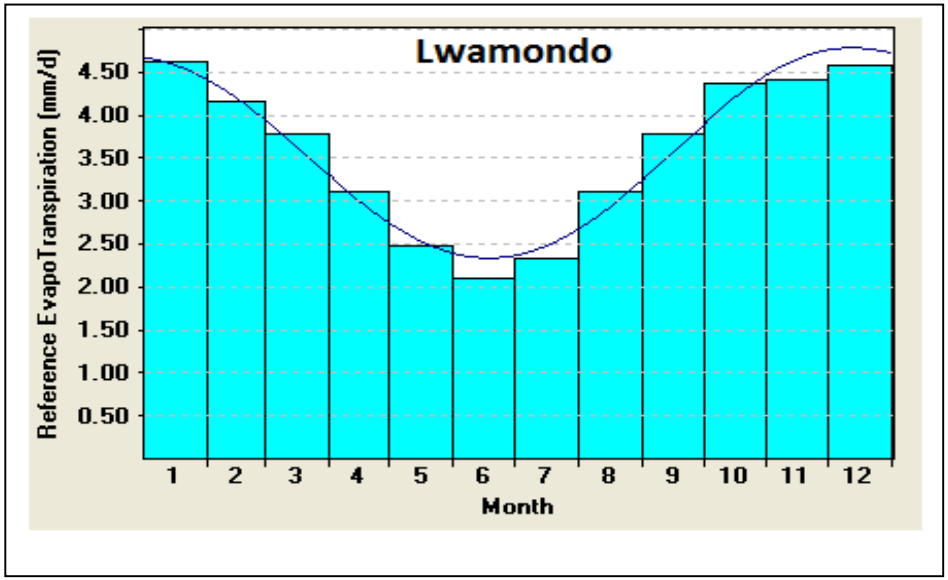

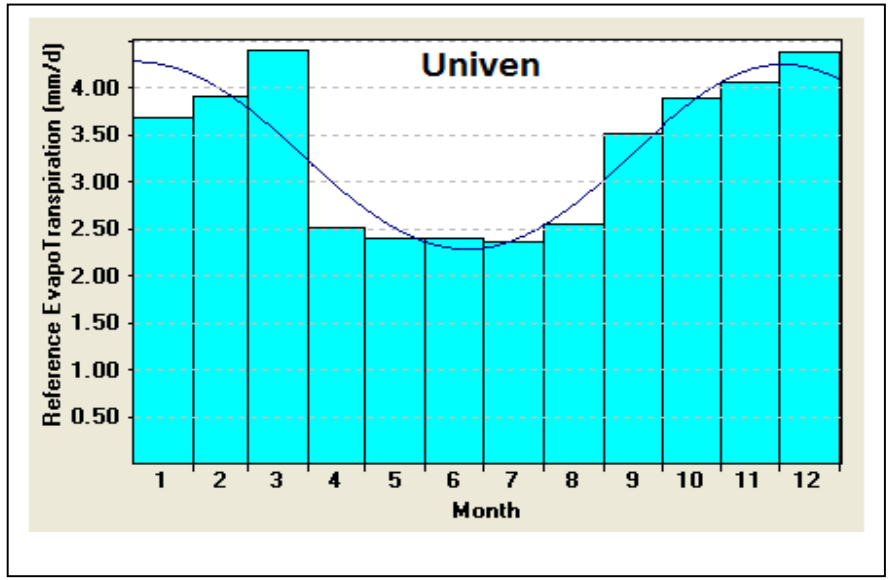

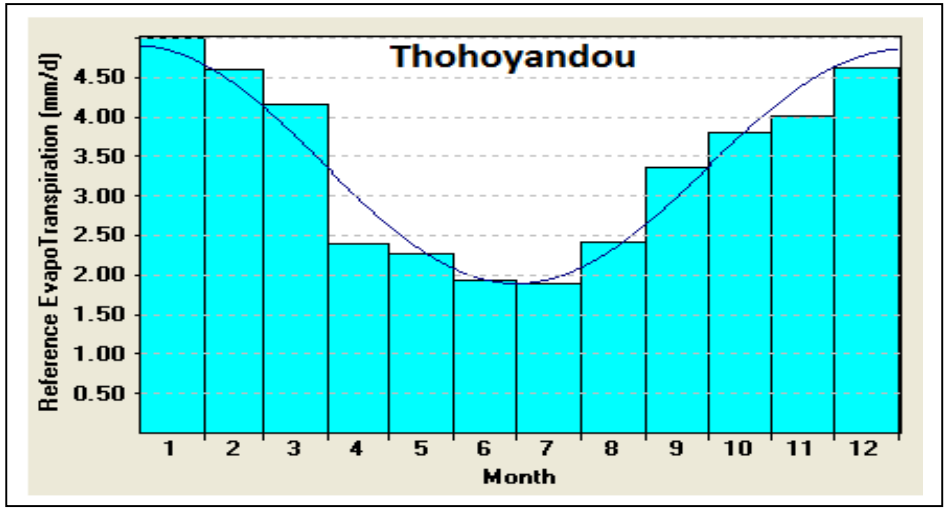

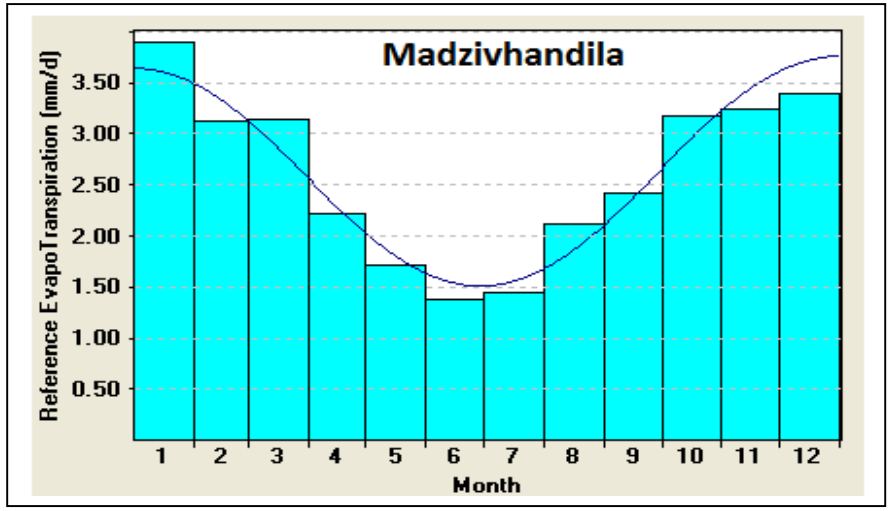

APPENDIX 10: AVERAGE ANNUAL RUNOFF TRENDS DURING THE 1960-1985 PHASE

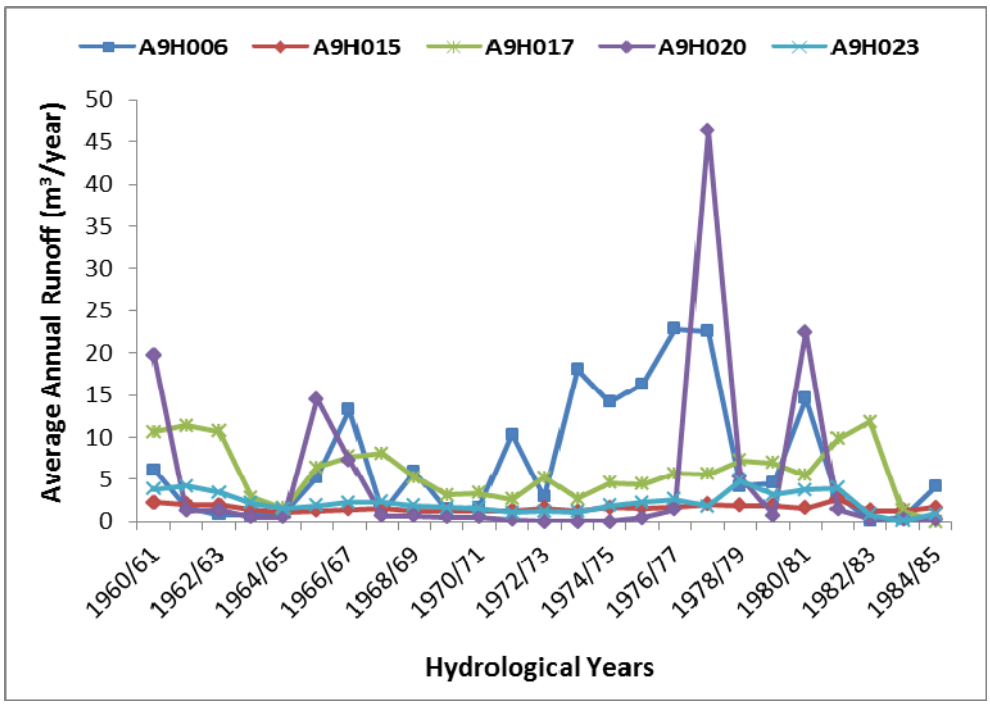

APPENDIX 11: AVERAGE ANNUAL RUNOFF TRENDS DURING THE 1985-2010 PHASE

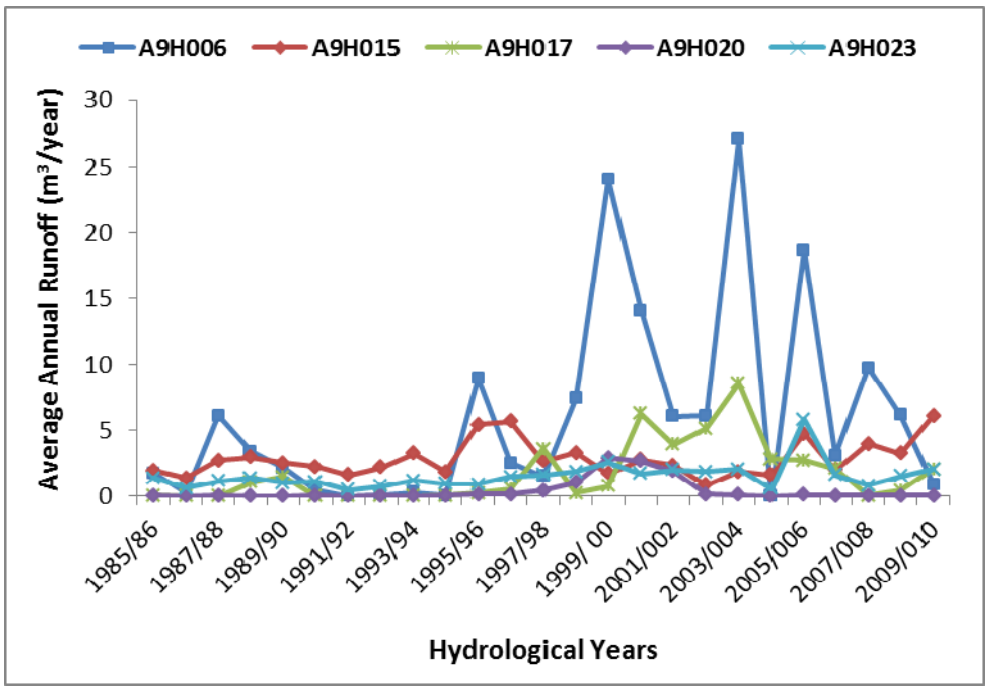

APPENDIX 12: OBSERVED AND SIMULATED RUNOFF VOLUMES AT DIFFERENT SUB-CATCHMENTS

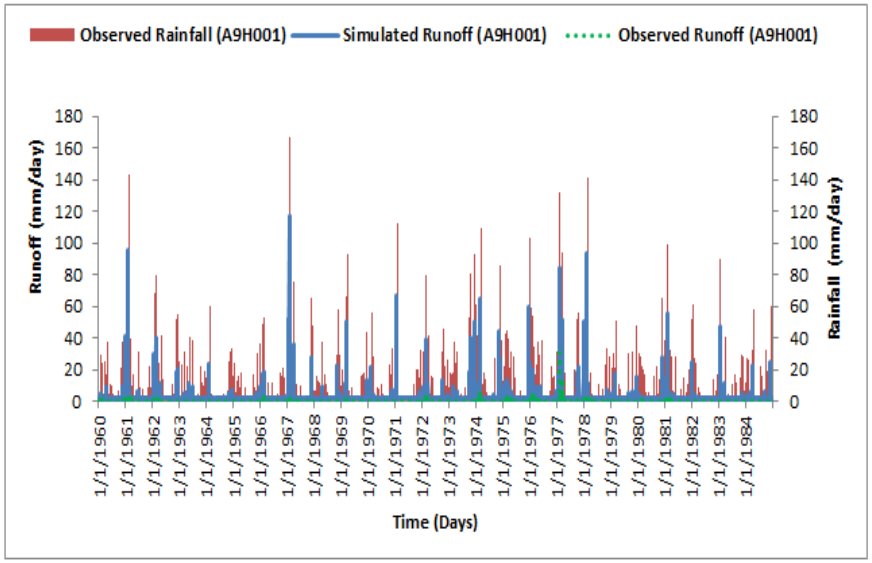

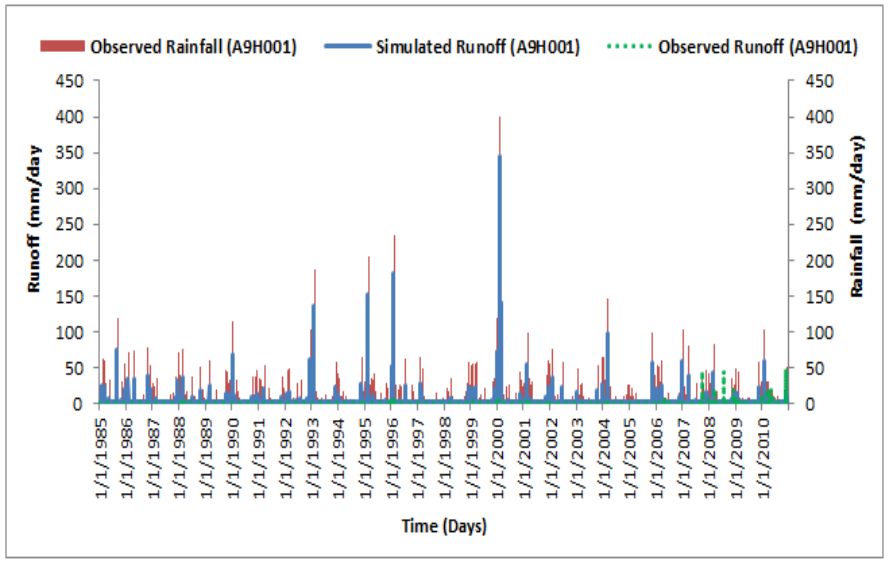

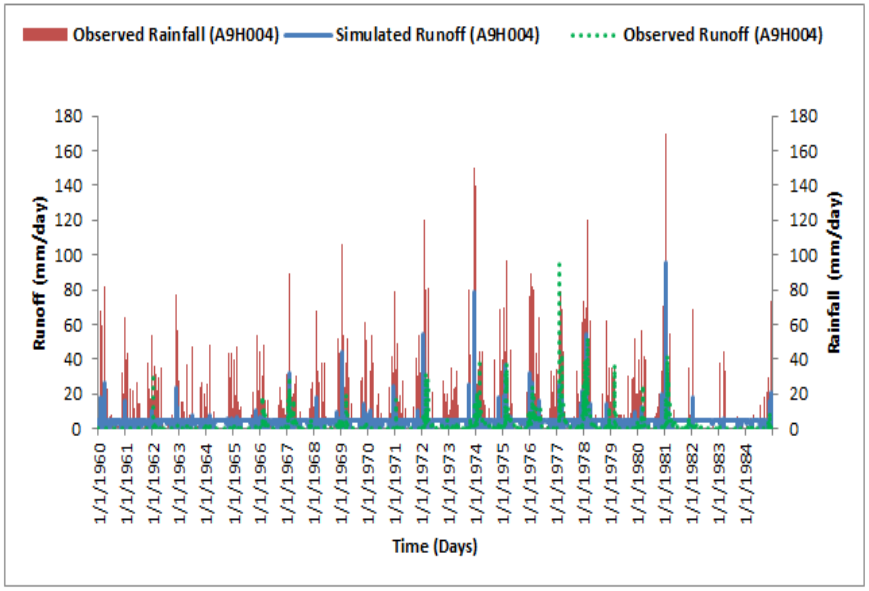

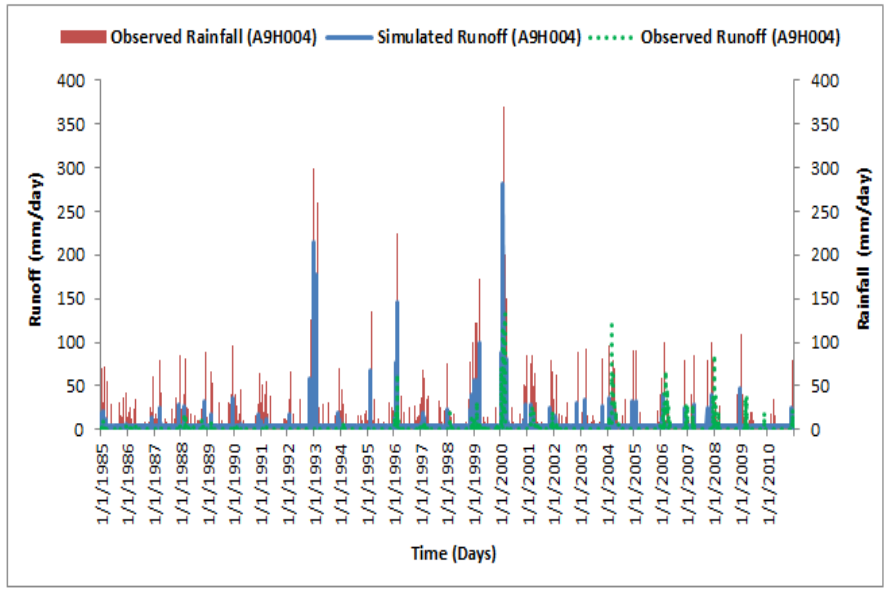

APPENDIX 13: RELATIONSHIP BETWEEN OBSERVED AND SIMULATED RUNOFF VOLUMES AT DIFFERENT SUB-CATCHMENTS

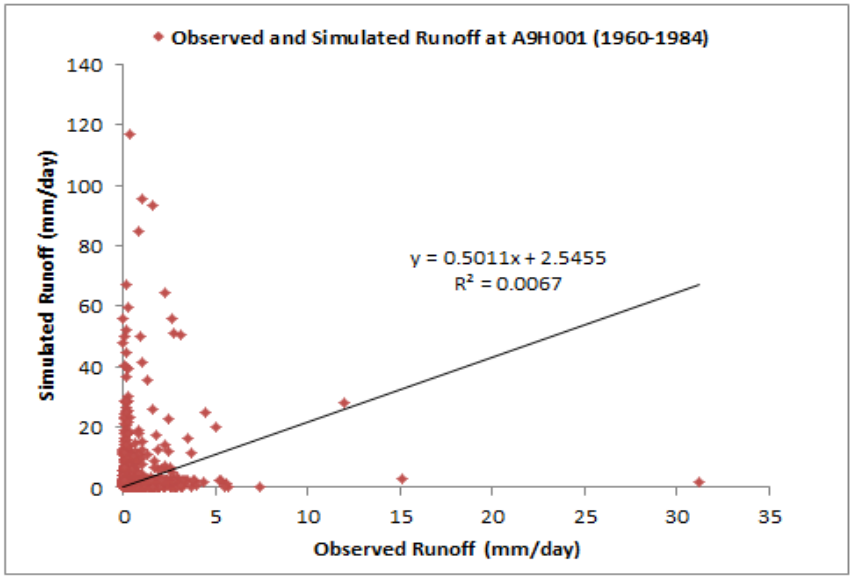

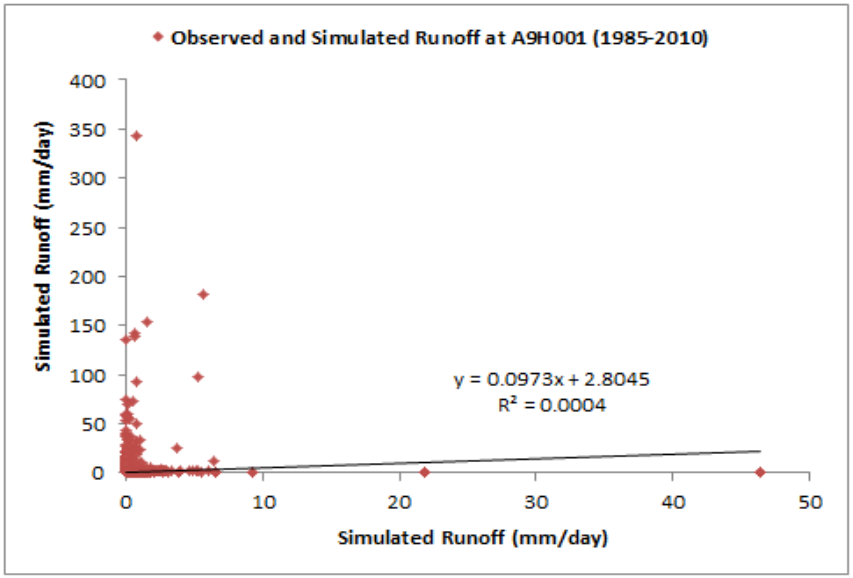

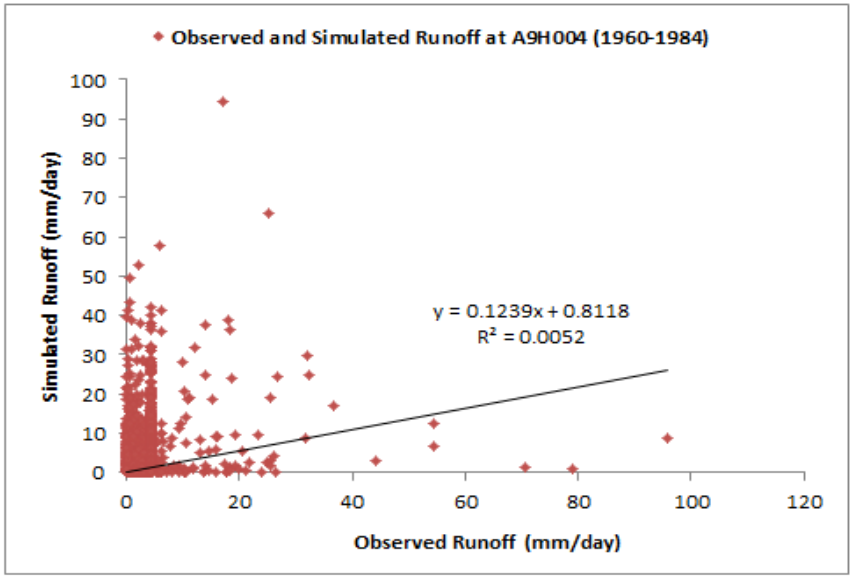

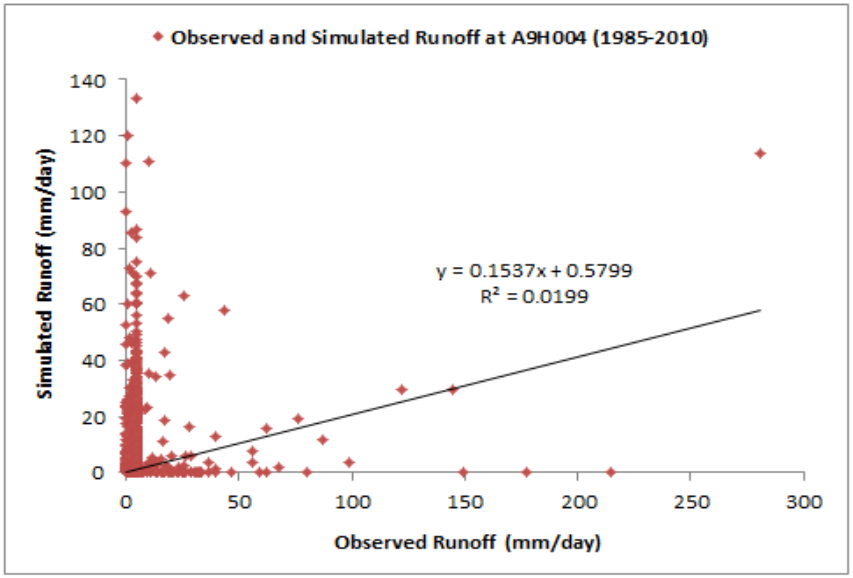

APPENDIX 14: STREAM FLOW TRENDS DURING THE 1960-1985 PHASE

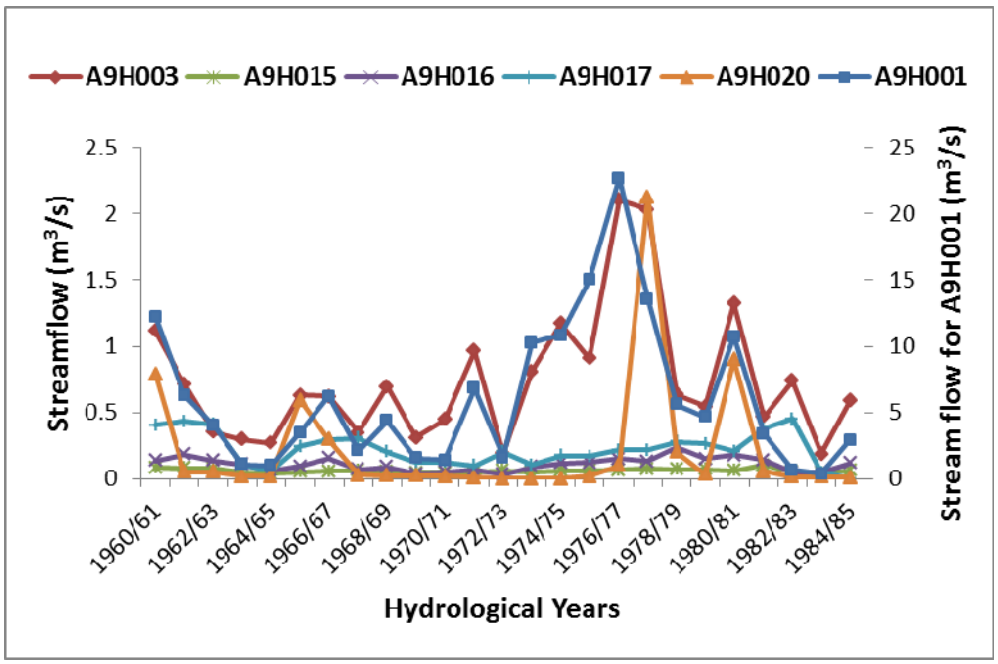

APPENDIX 15: STREAM FLOW TRENDS DURING THE 1985-2010 PHASE

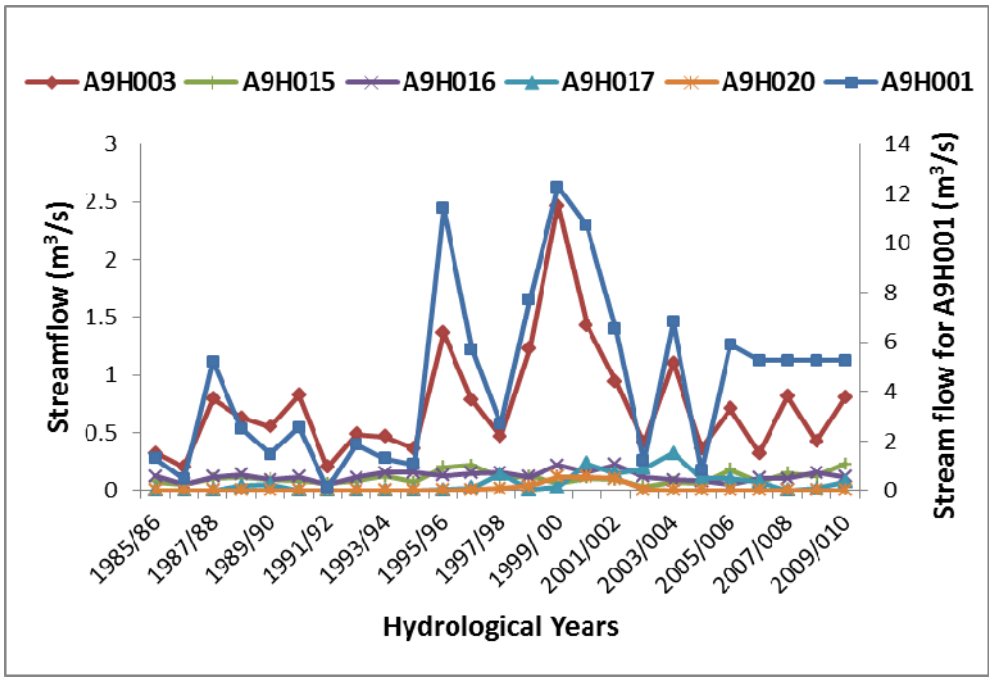

APPENDIX 16: ANNUAL MAXIMUM RAINFALL SERIES

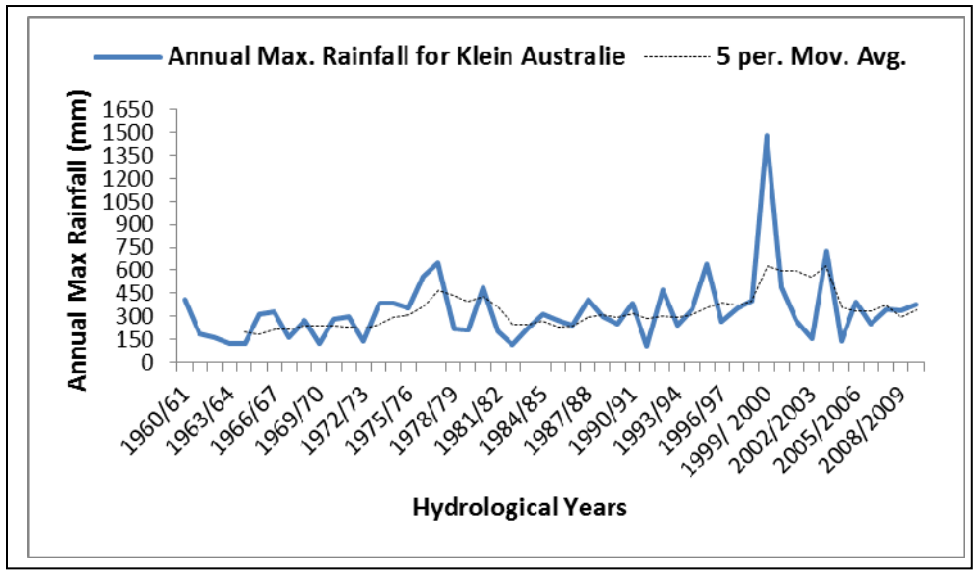

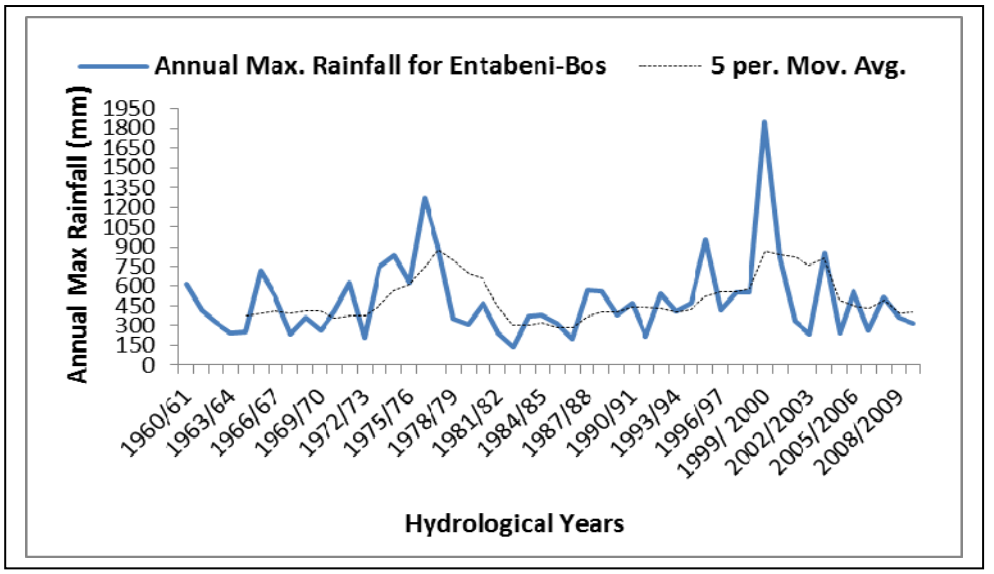

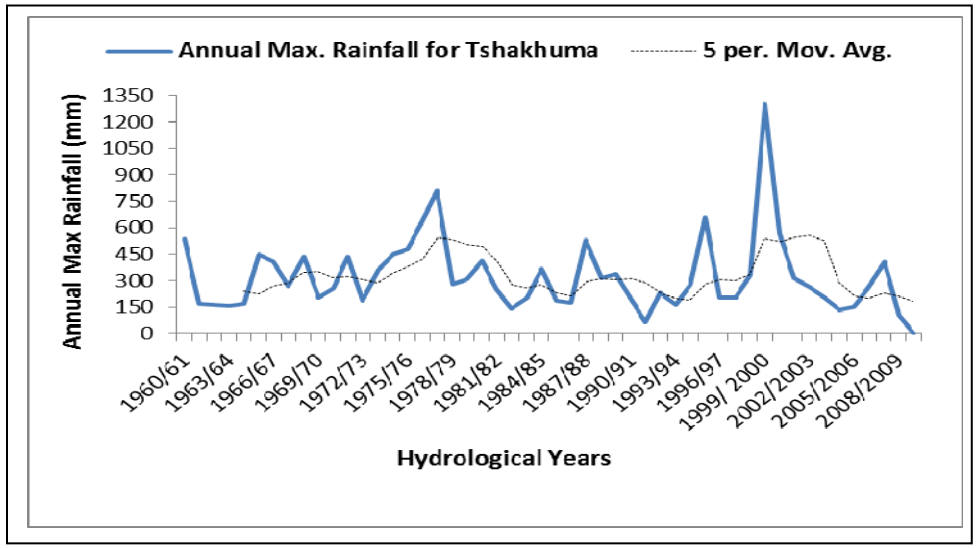

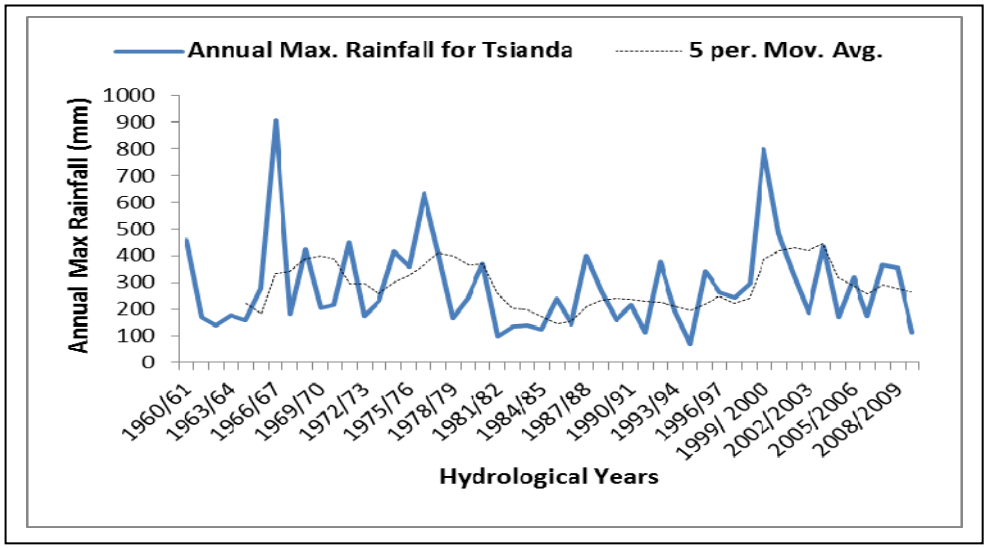

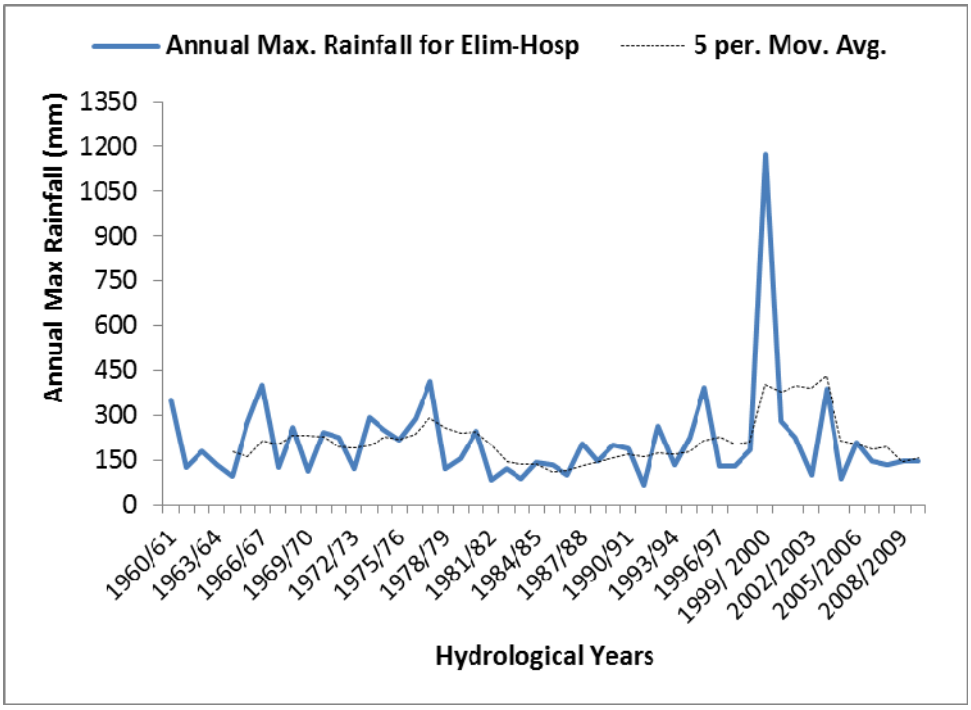

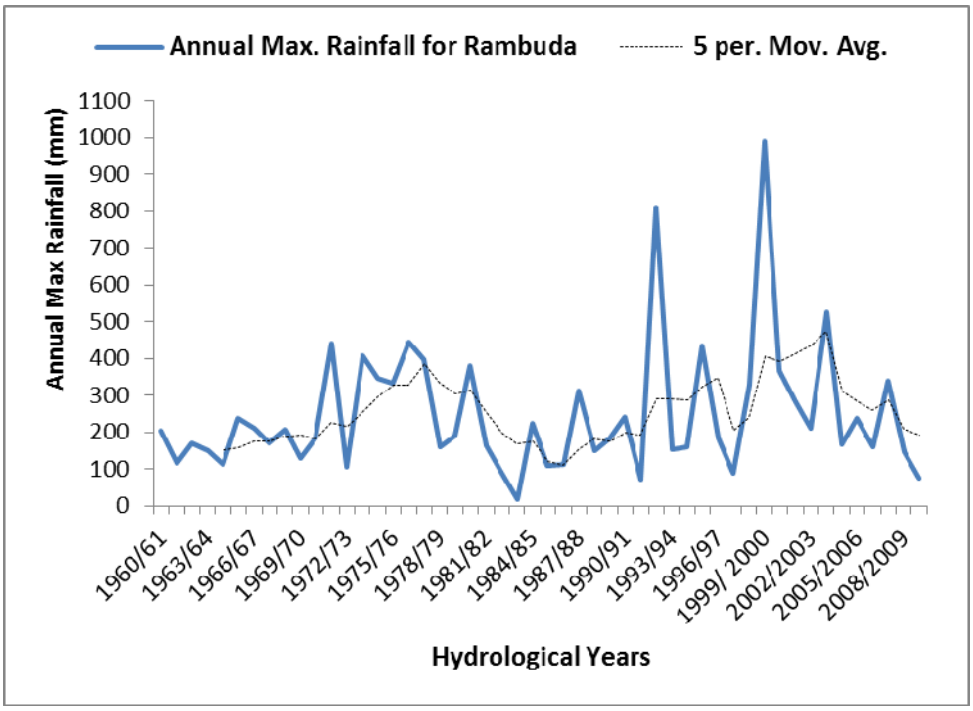

APPENDIX 17: ANNUAL MAXIMUM STREAM FLOW SERIES

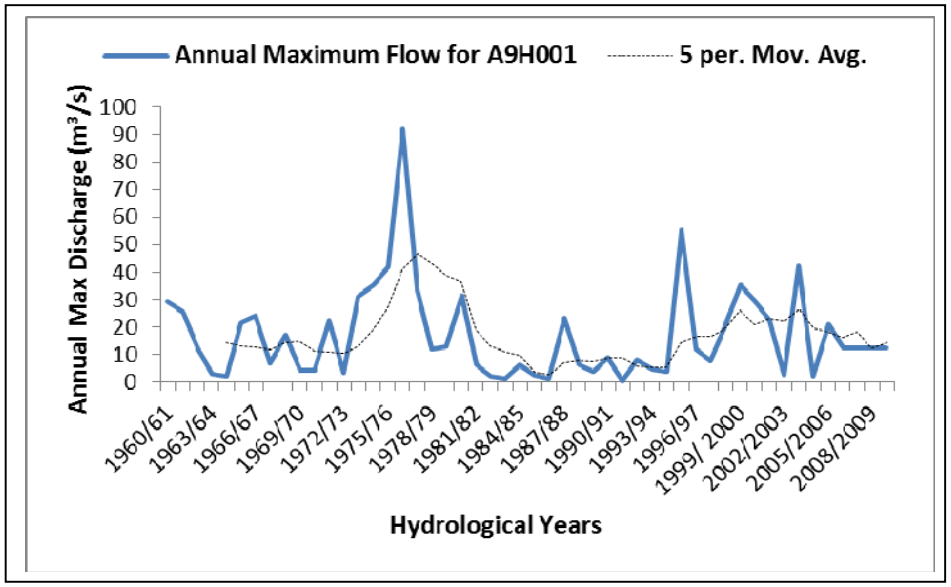

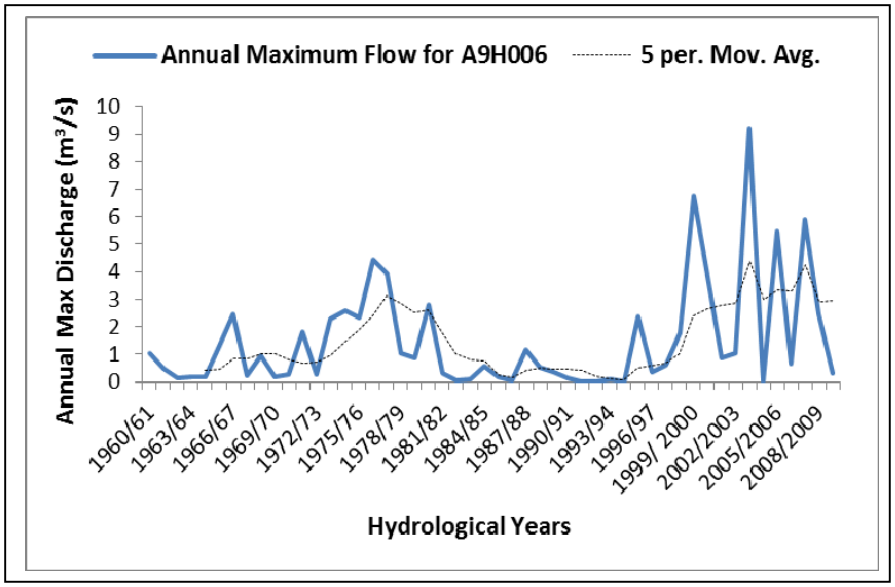

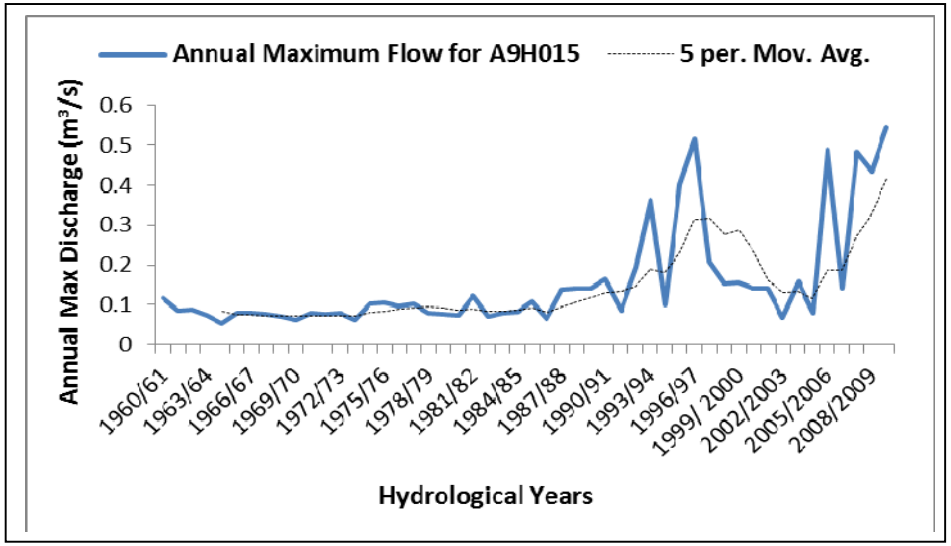

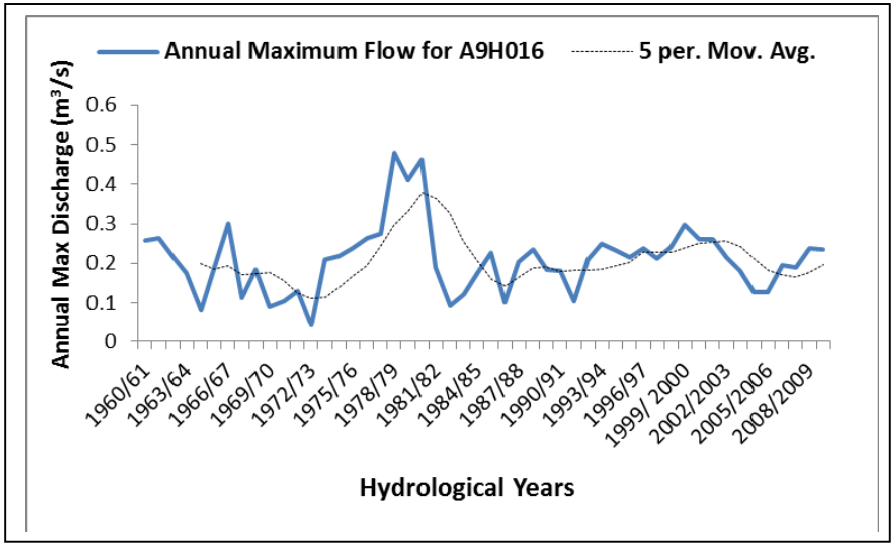

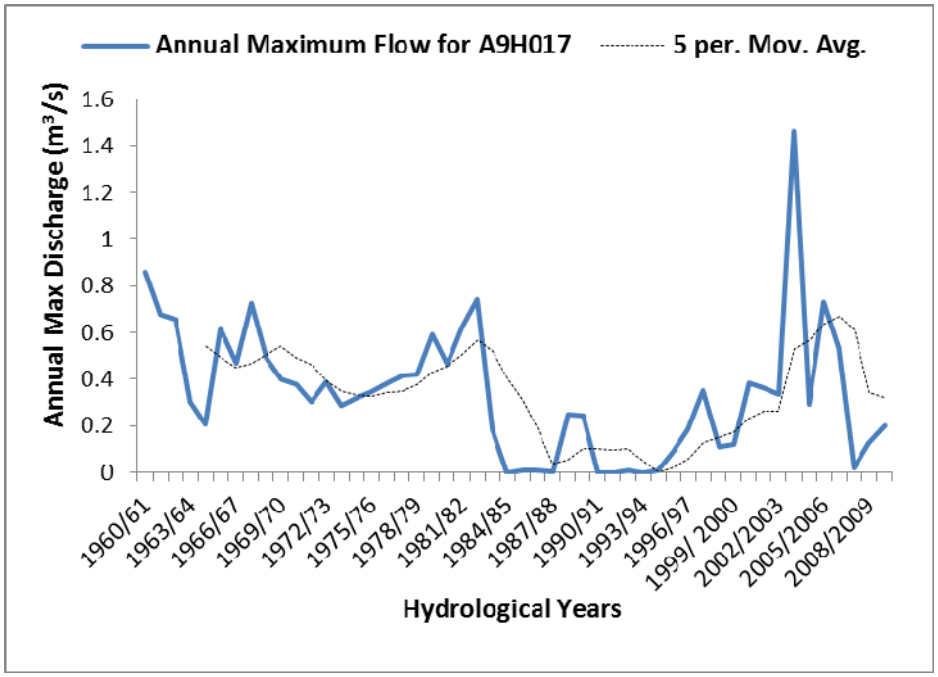

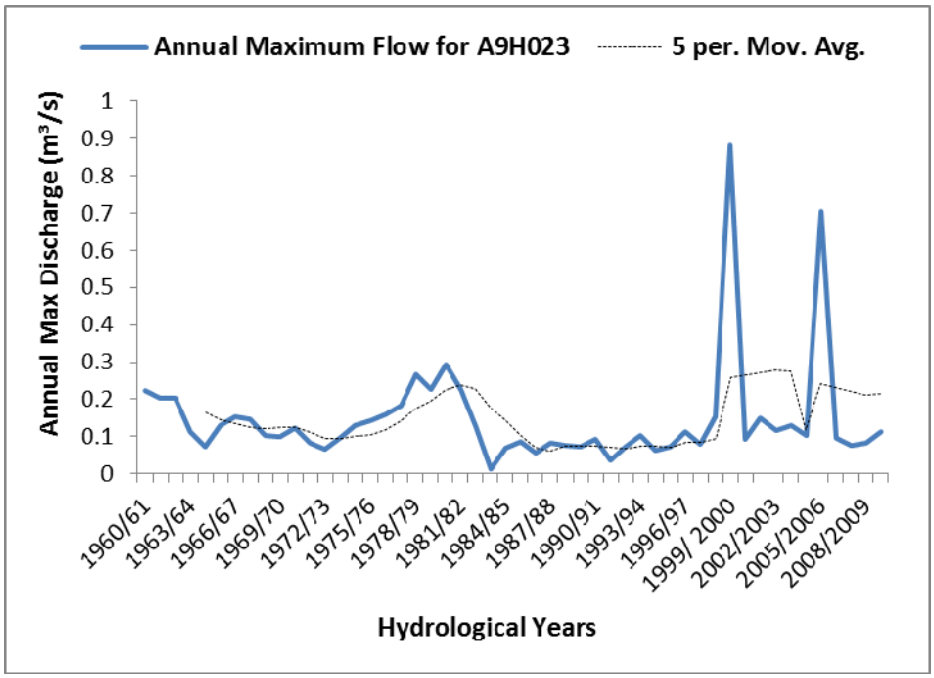

APPENDIX 18: RETURN PERIODS FOR ANNUAL MAXIMUM RAINFALL

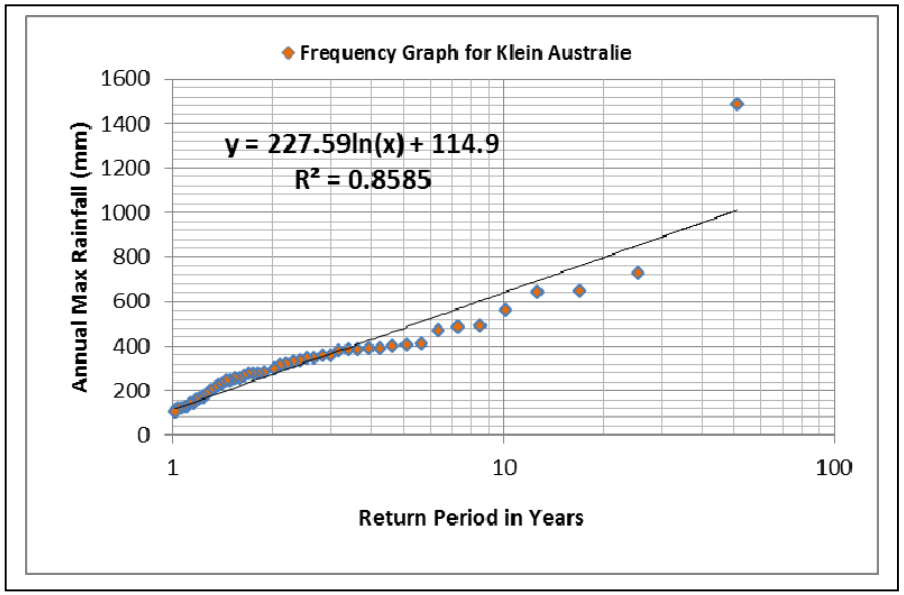

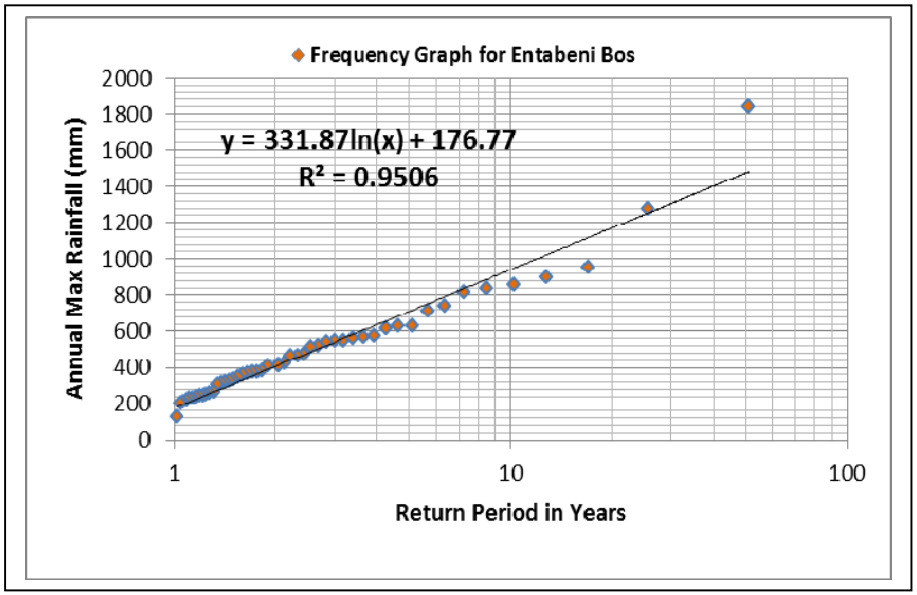

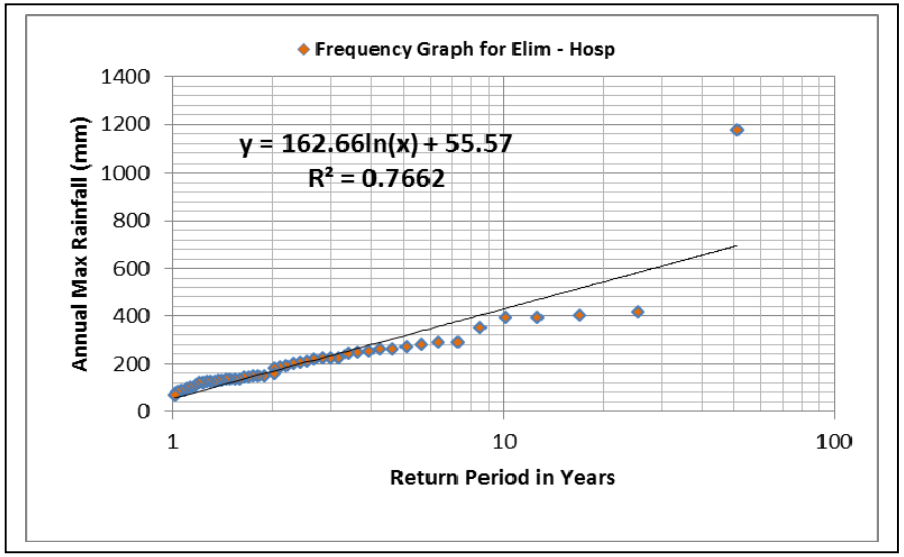

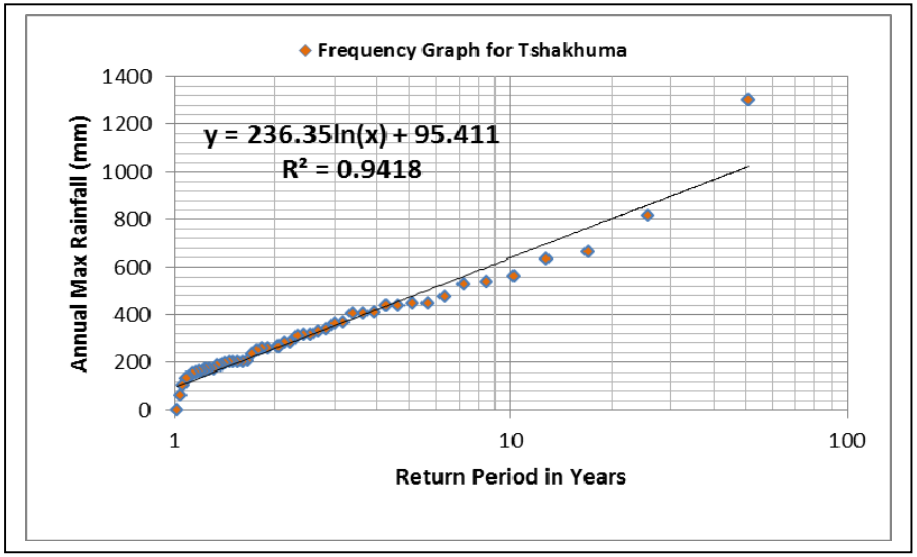

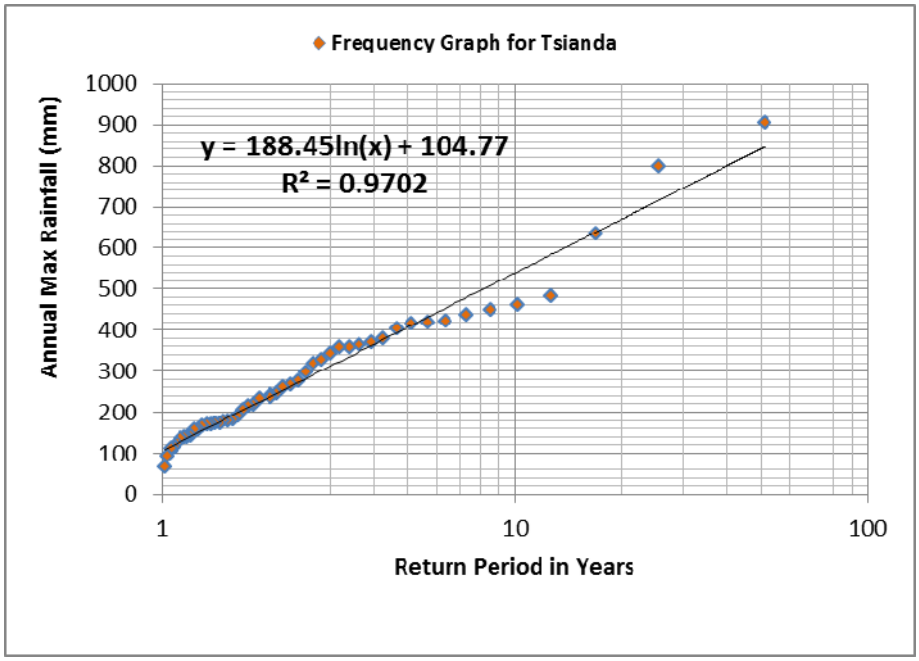

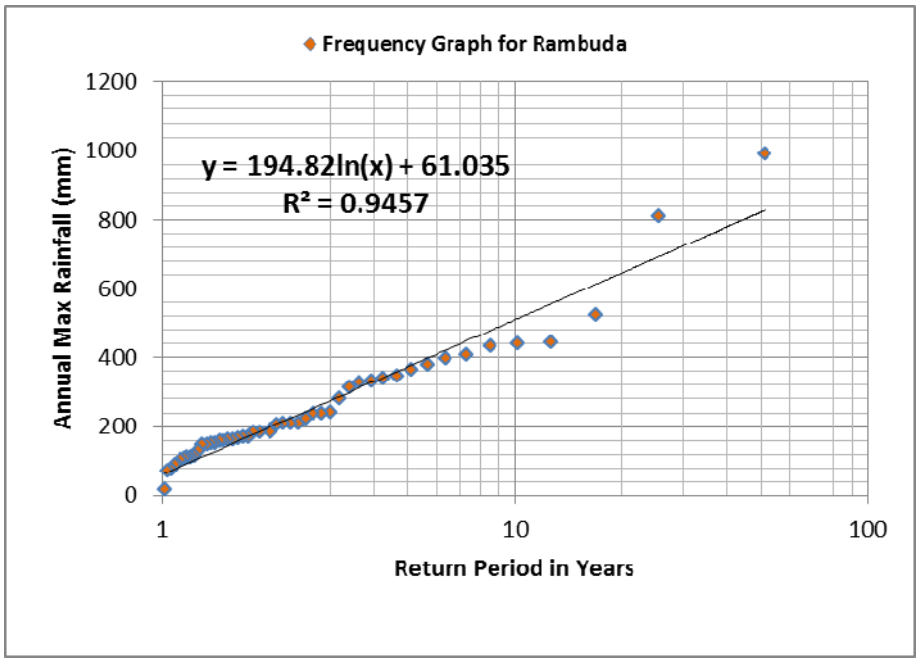

APPENDIX 19: RETURN PERIODS FOR ANNUAL MAXIMUM STREAM FLOW

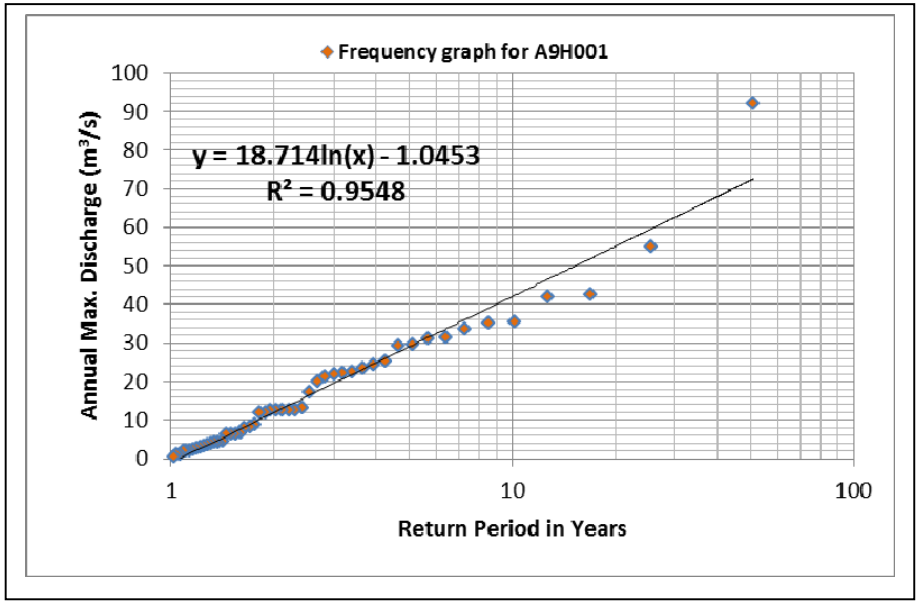

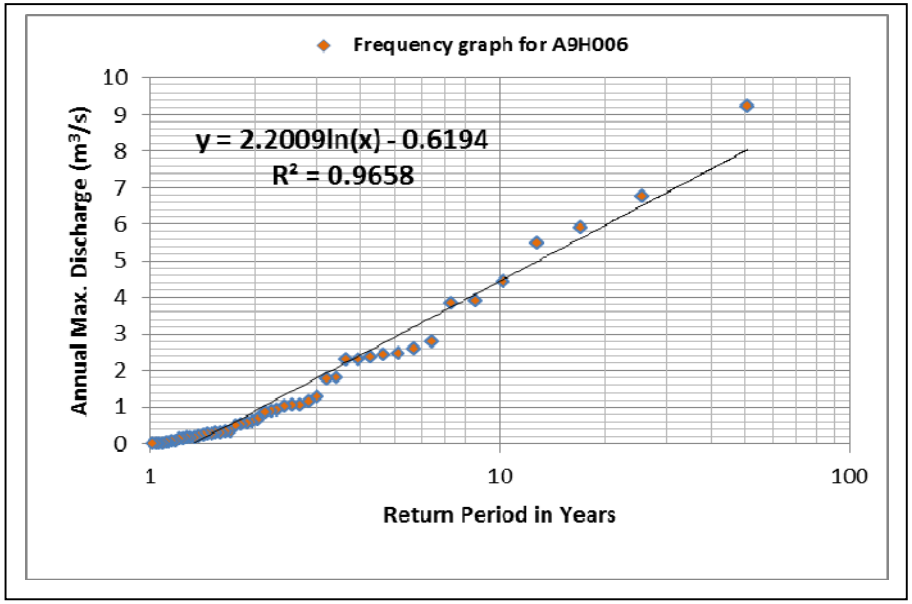

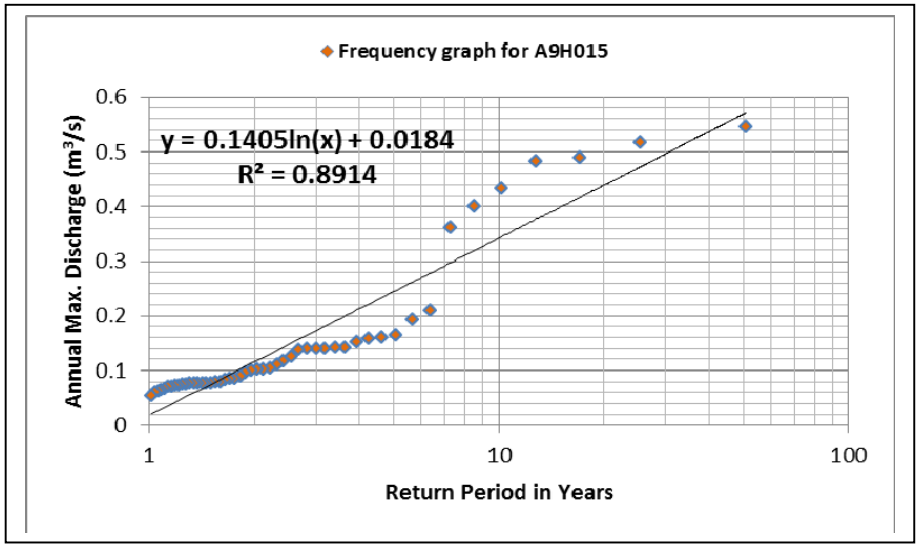

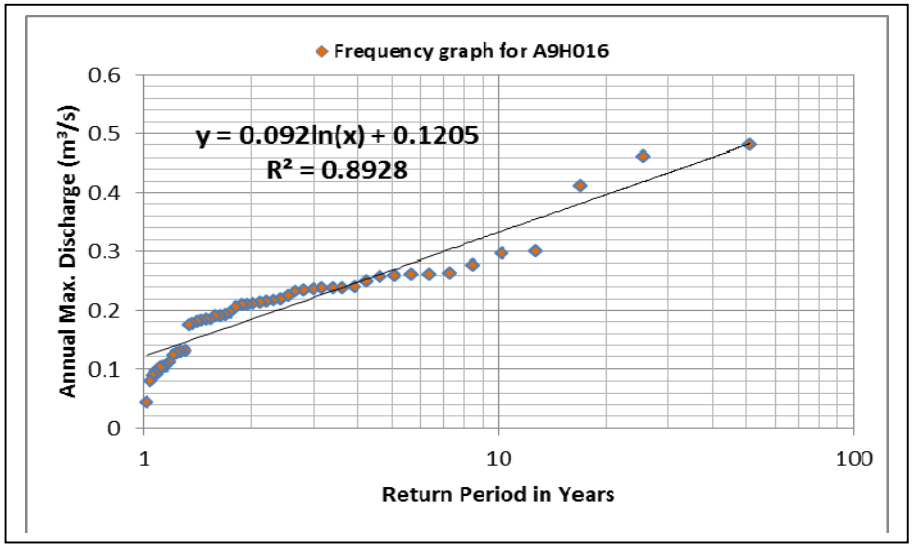

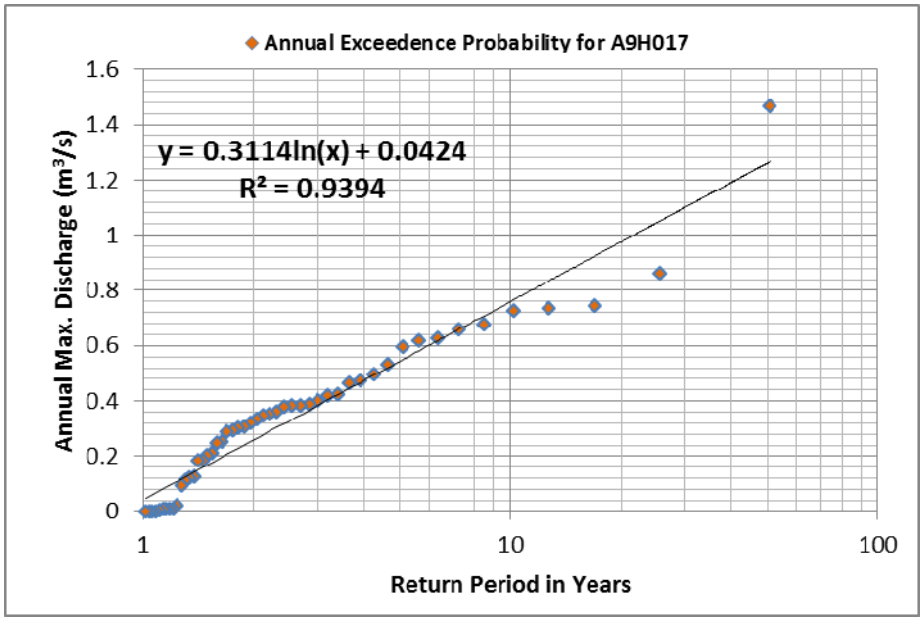

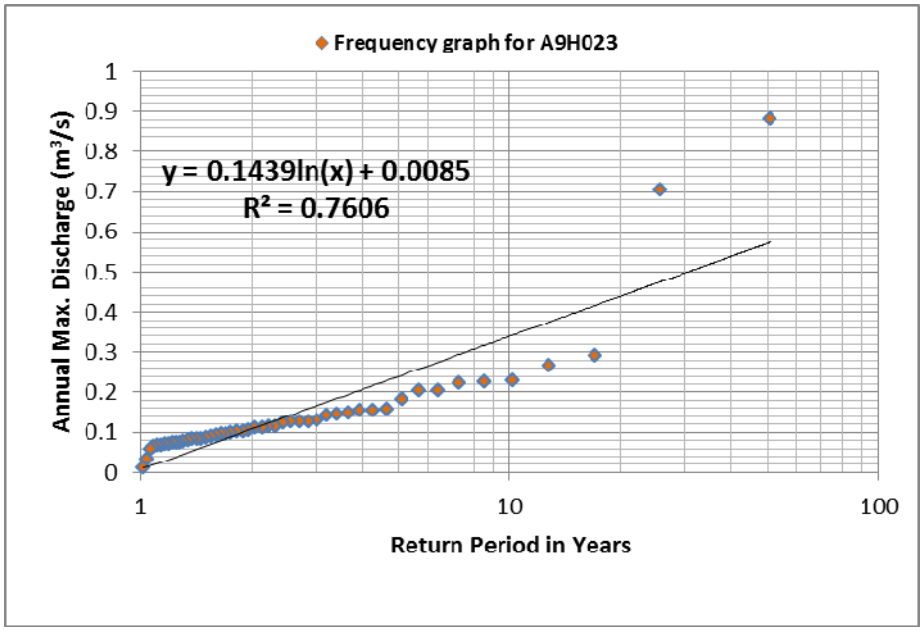

APPENDIX 20: COMPUTED PEAK FLOOD FOR THE 2-, 5-, 10-, 25-, 50-, 100- AND 200- YEAR RETURN PERIODS USING LP3 DISTRIBUTION

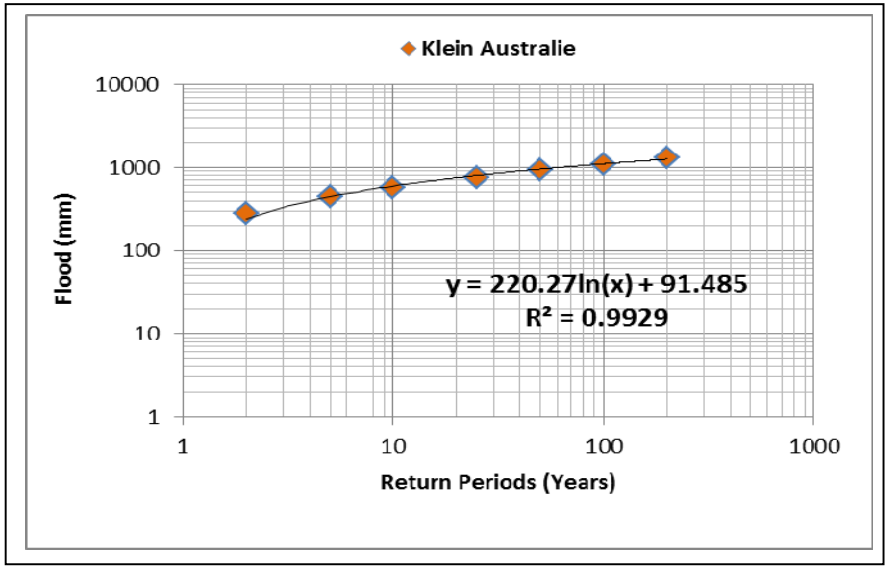

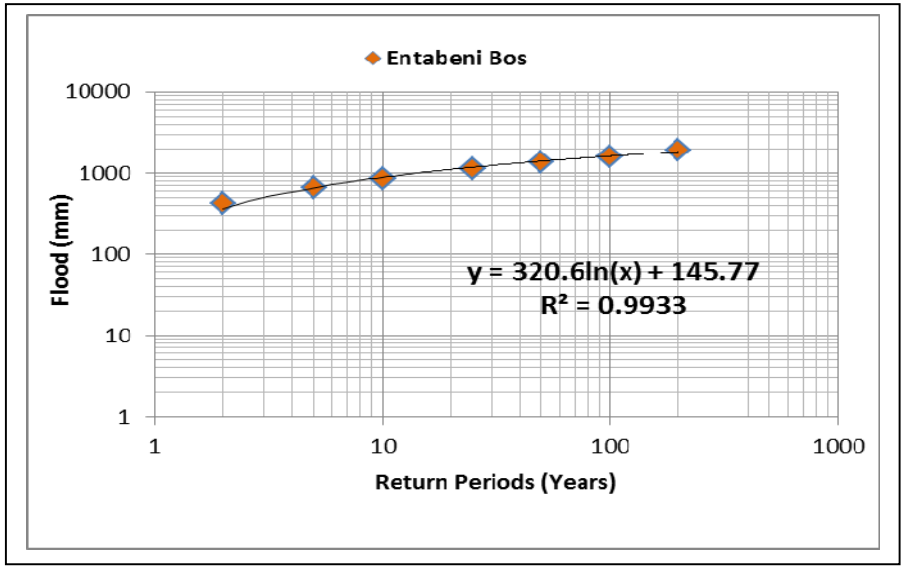

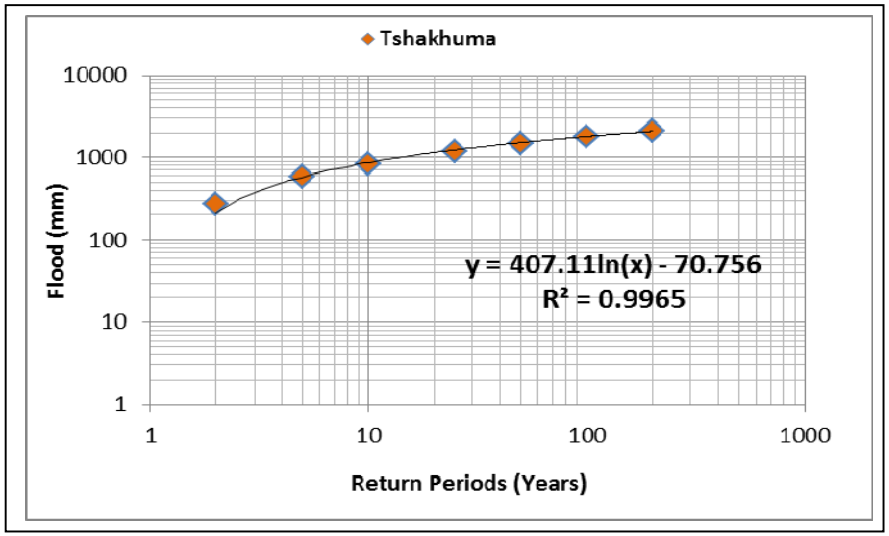

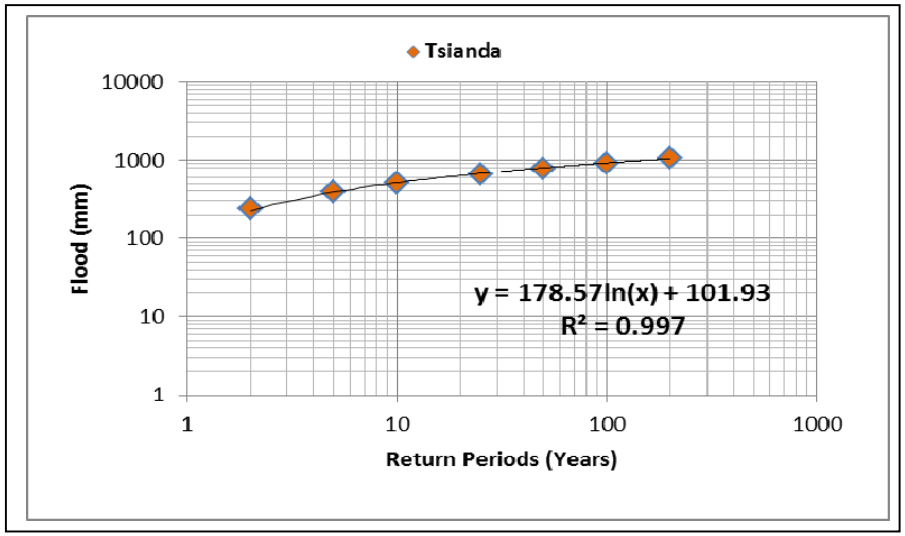

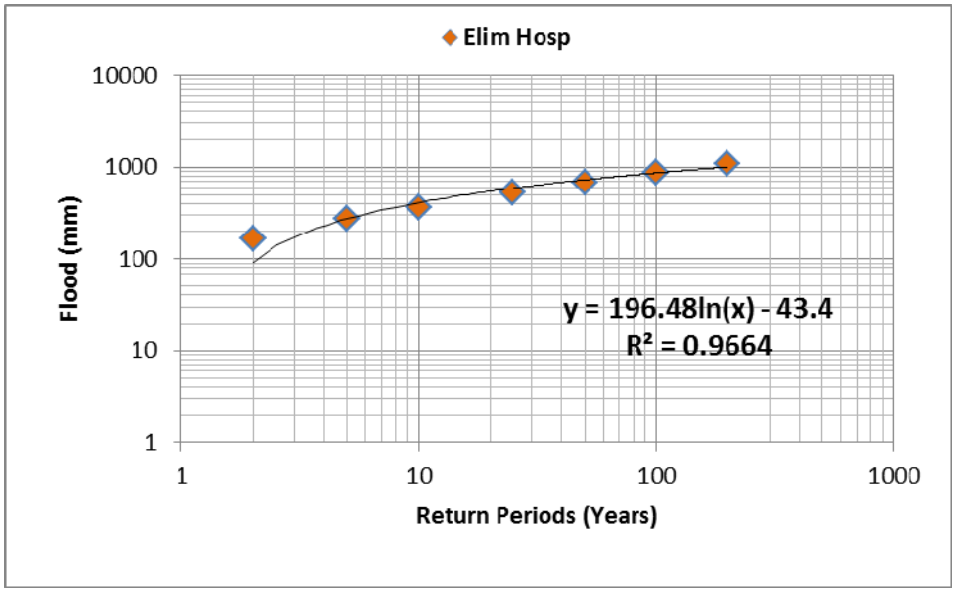

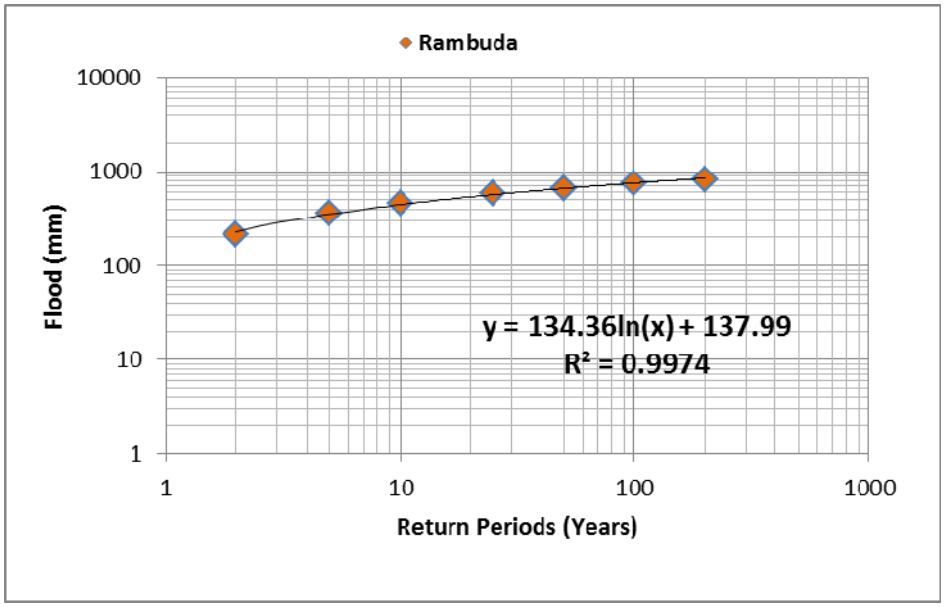

APPENDIX 21: COMPUTED PEAK FLOWS FOR THE 2-, 5-, 10-, 25-, 50-, 100- AND 200- YEAR RETURN PERIODS USING LP3 DISTRIBUTION

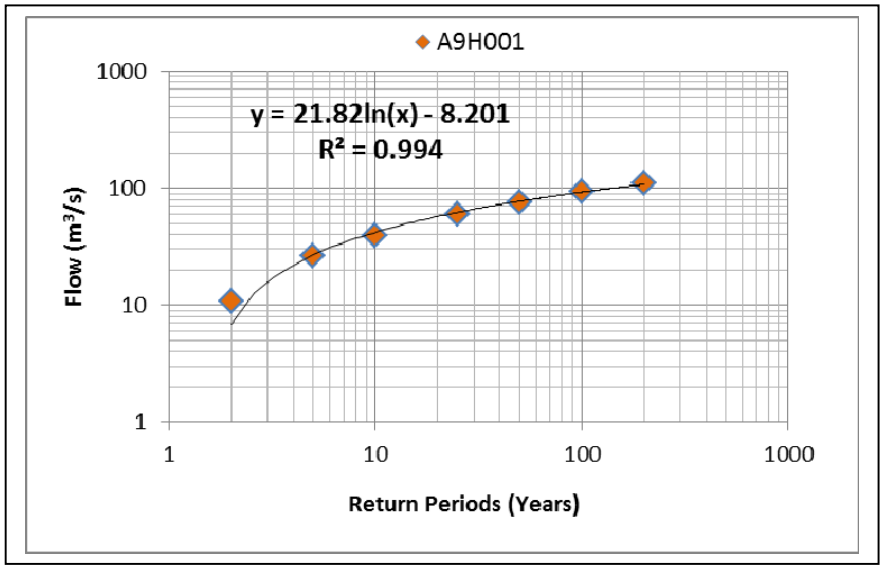

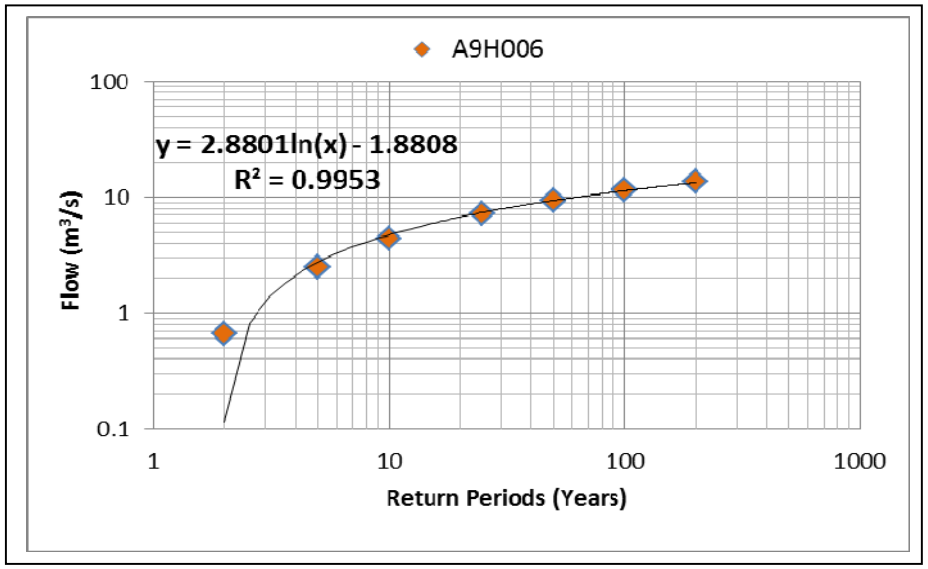

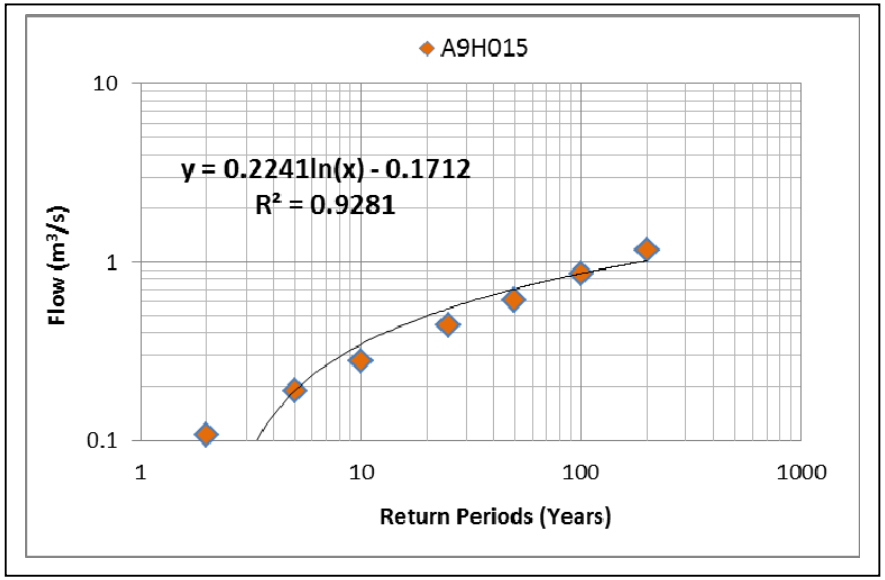

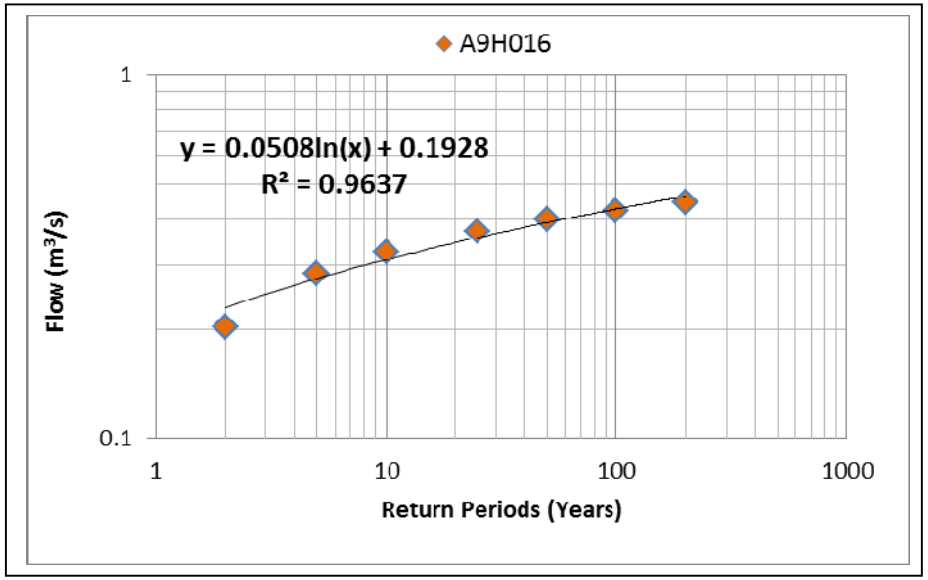

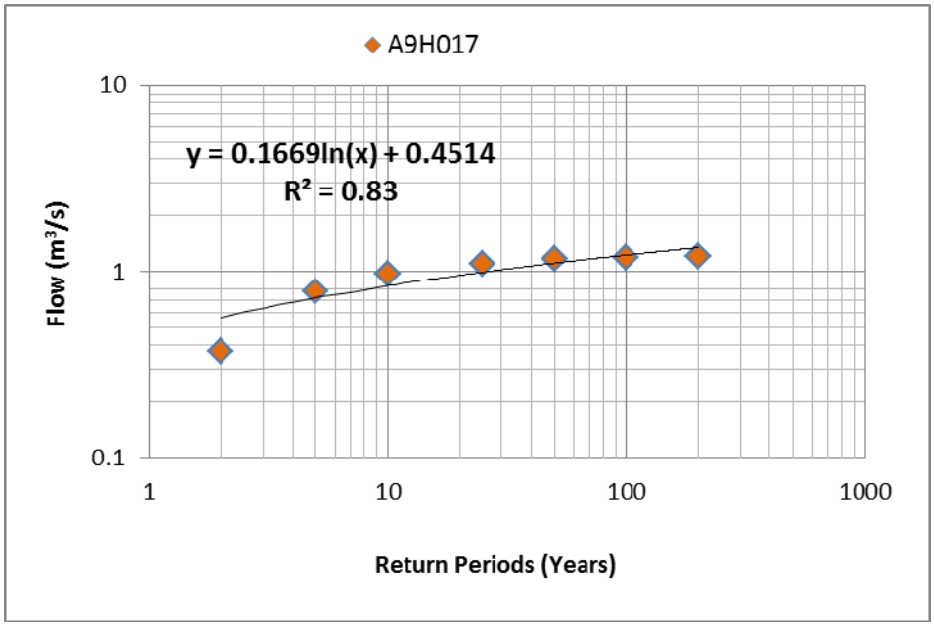

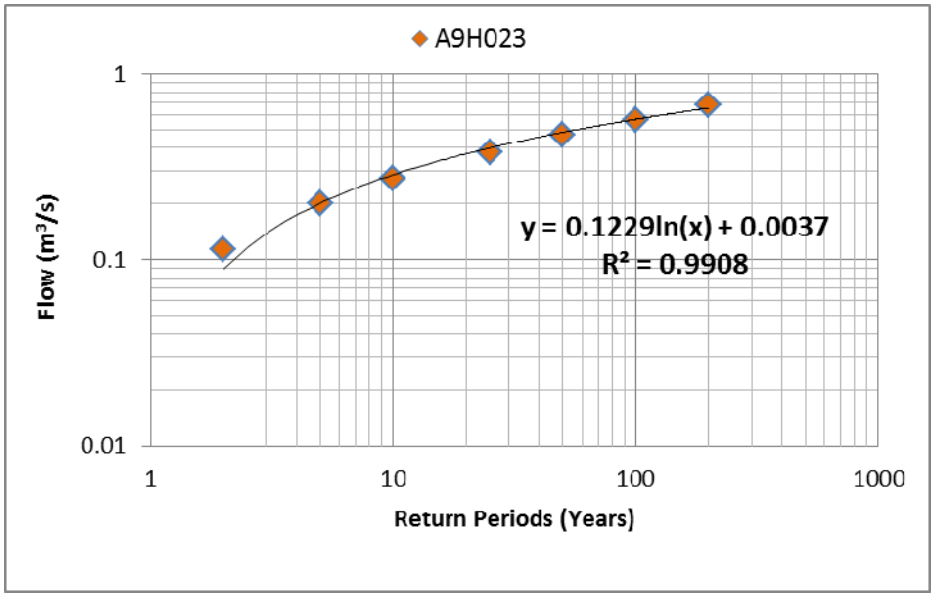

APPENDIX 22: COMPUTED PEAK FLOOD FOR THE 2-, 5-, 10-, 25-, 50-, 100- AND 200- YEAR RETURN PERIODS USING GUMBEL'S DISTRIBUTION

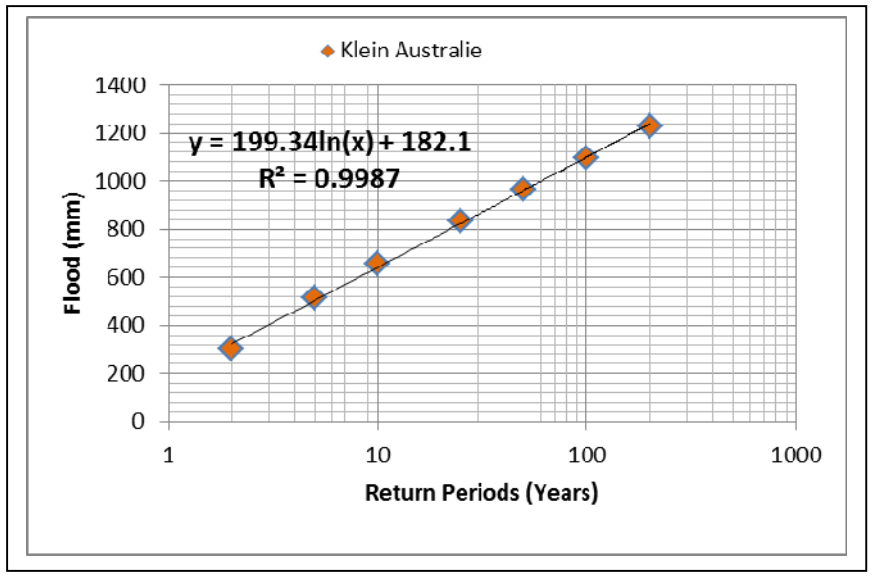

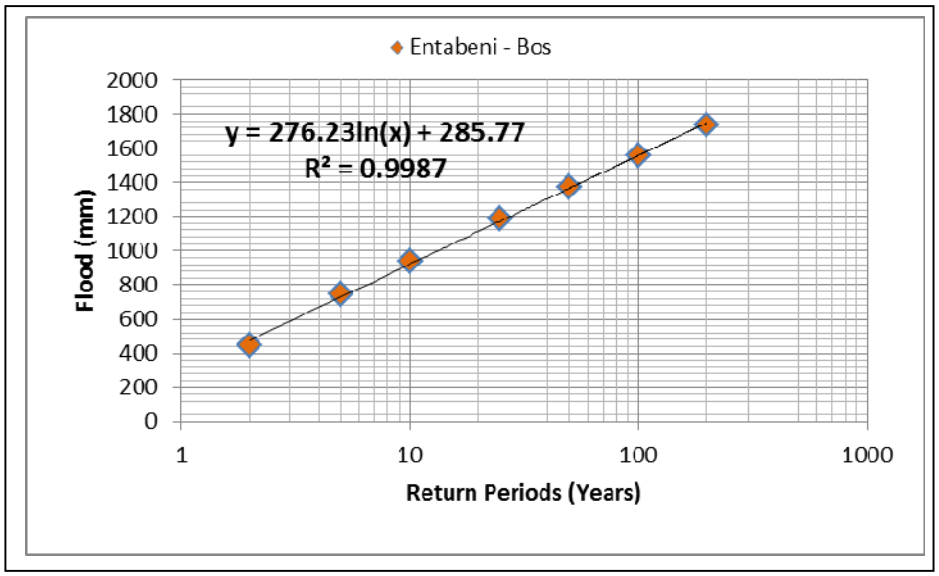

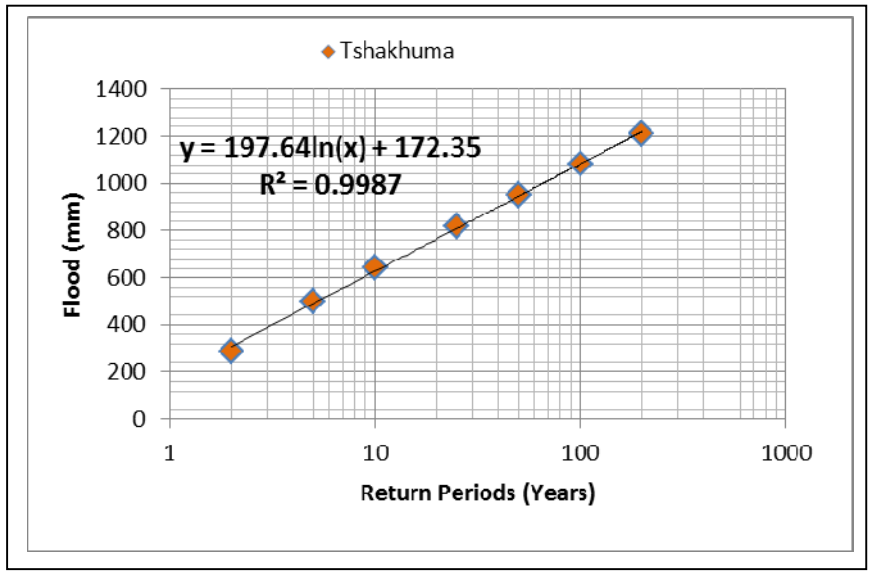

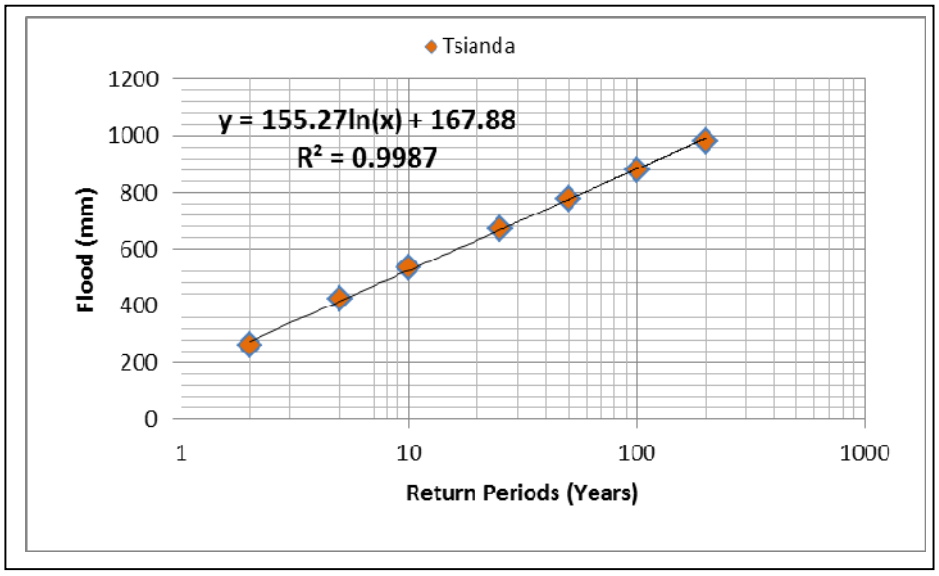

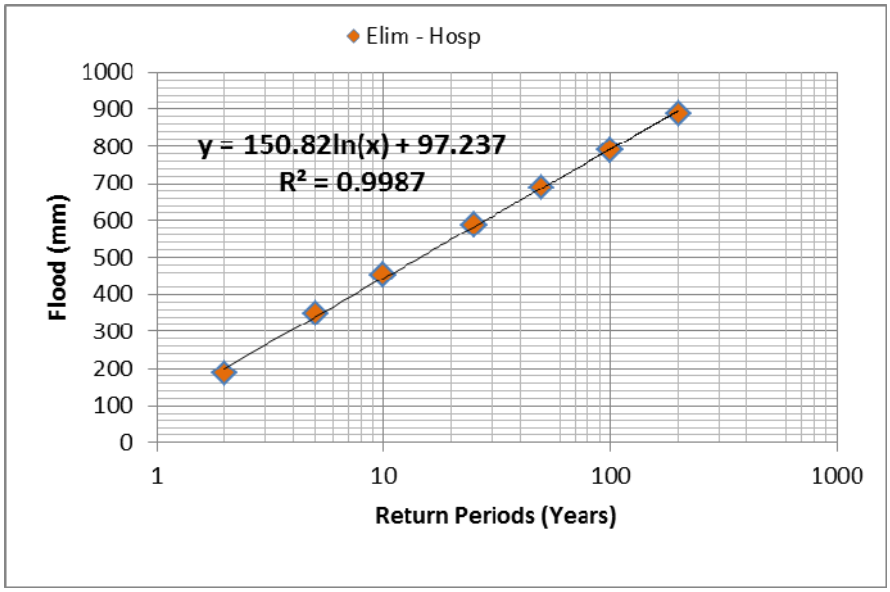

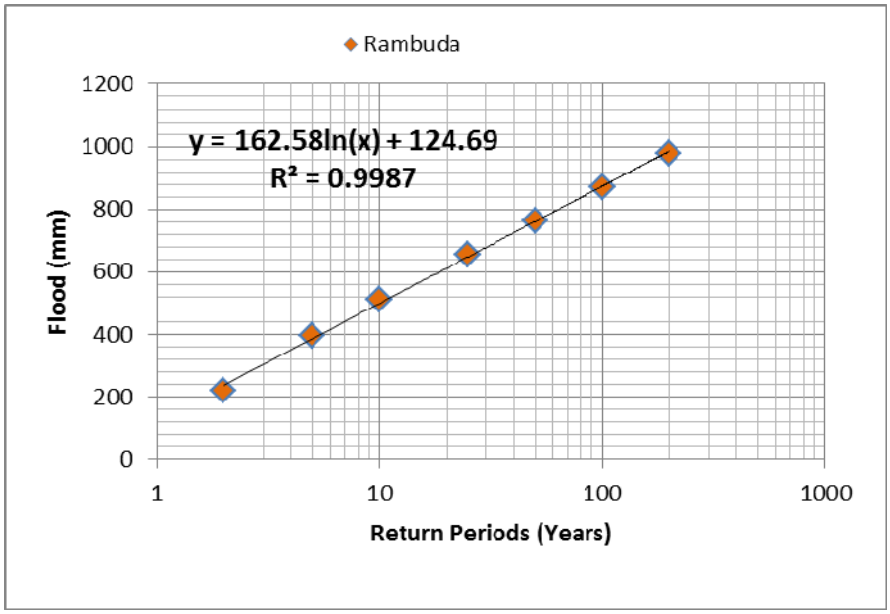

APPENDIX 23: COMPUTED PEAK FLOWS FOR THE 2-, 5-, 10-, 25-, 50-, 100- AND 200- YEAR RETURN PERIODS USING GUMBEL'S DISTRIBUTION

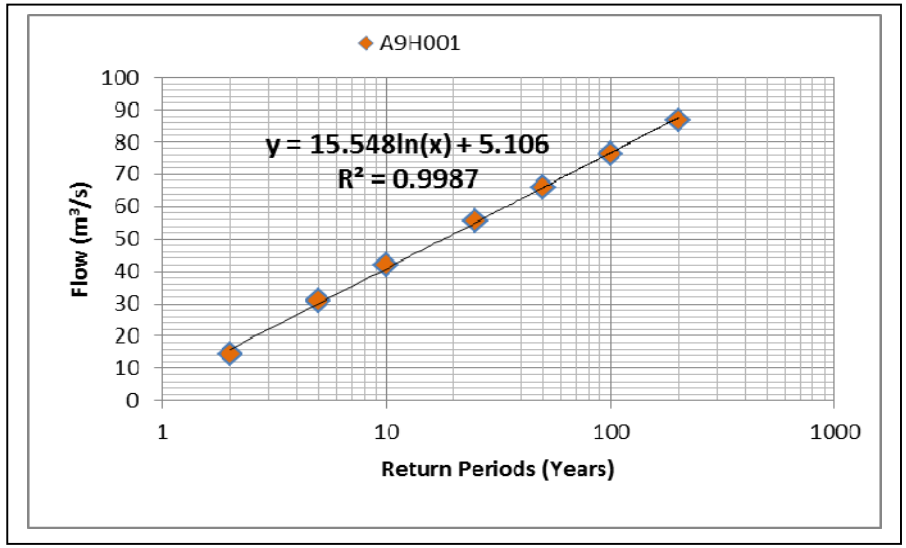

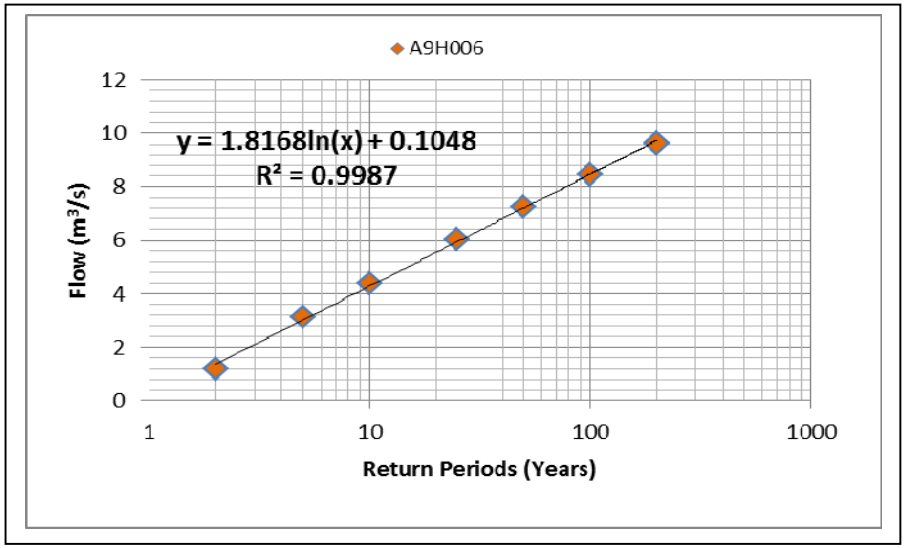

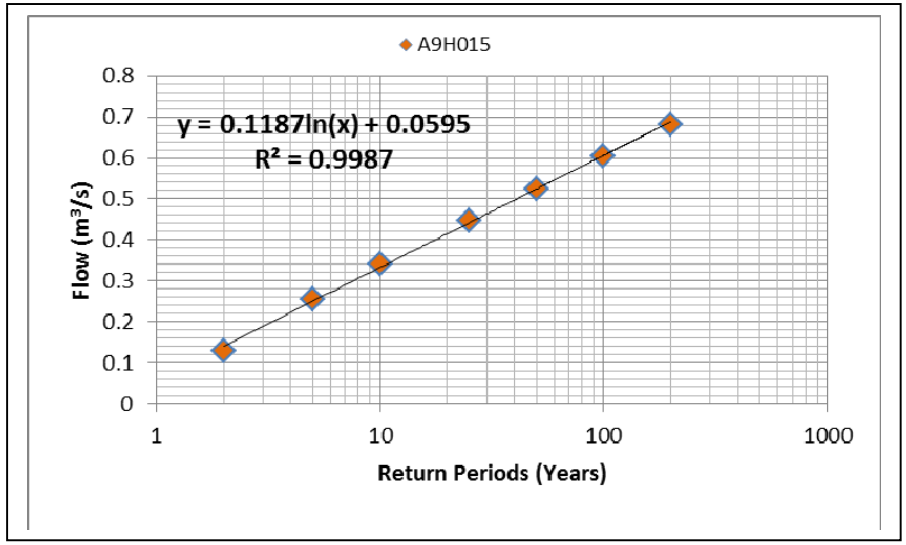

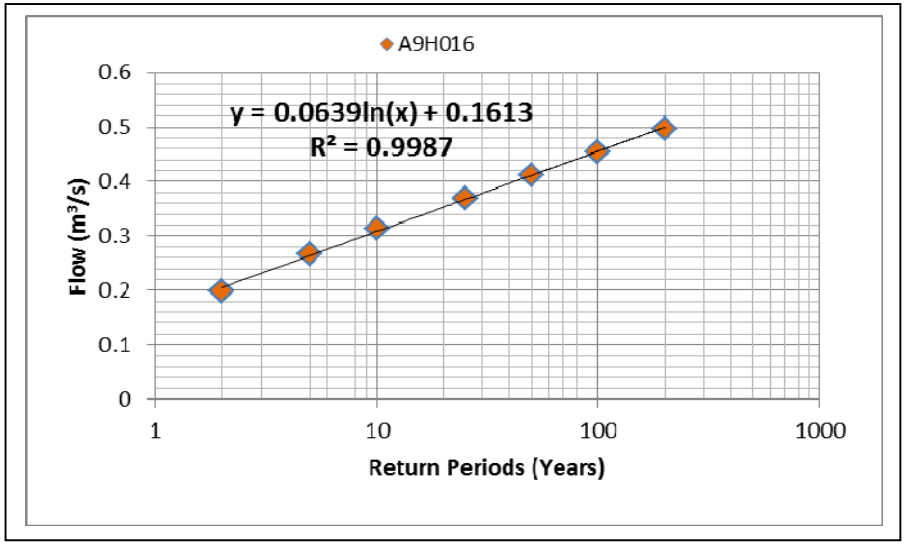

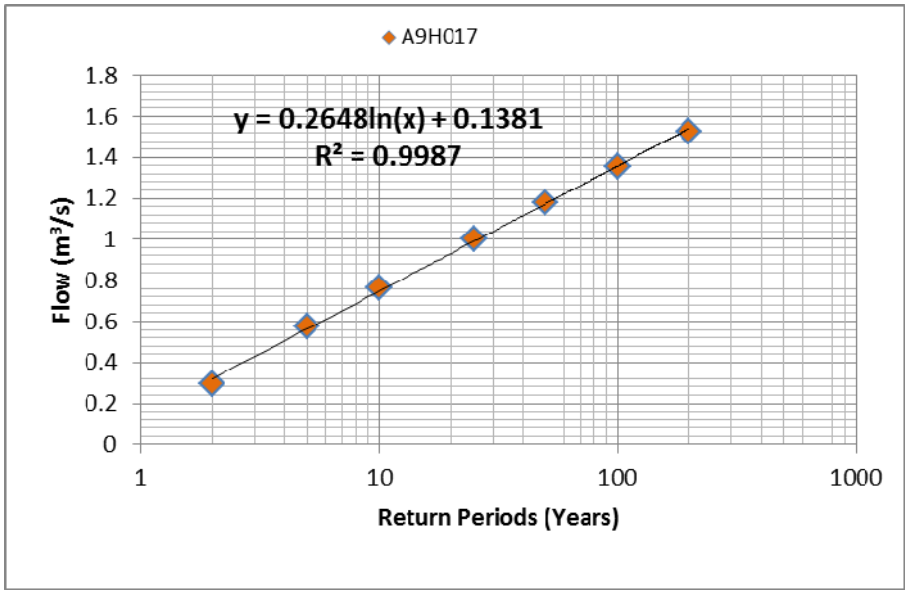

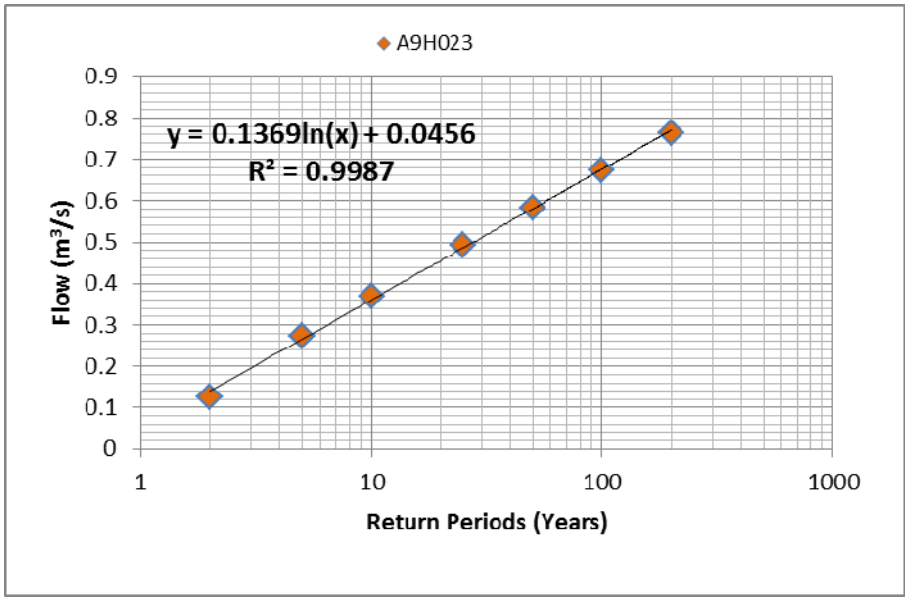

APPENDIX 24: GRAIN SIZE DISTRIBUTION CURVES

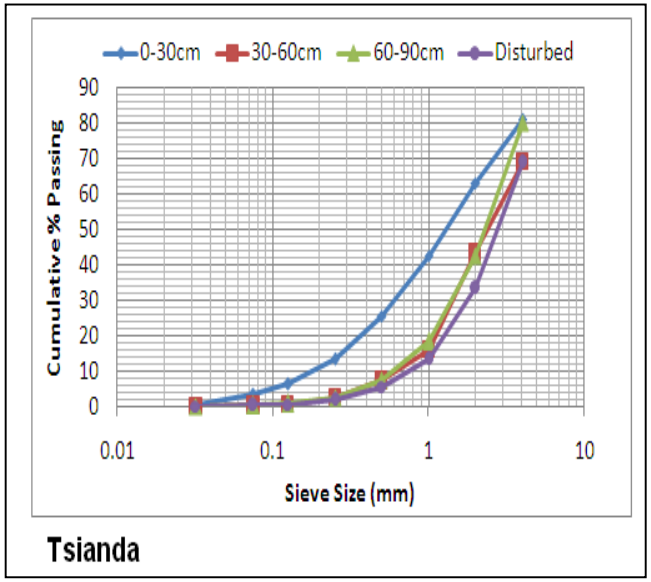

Tsianda

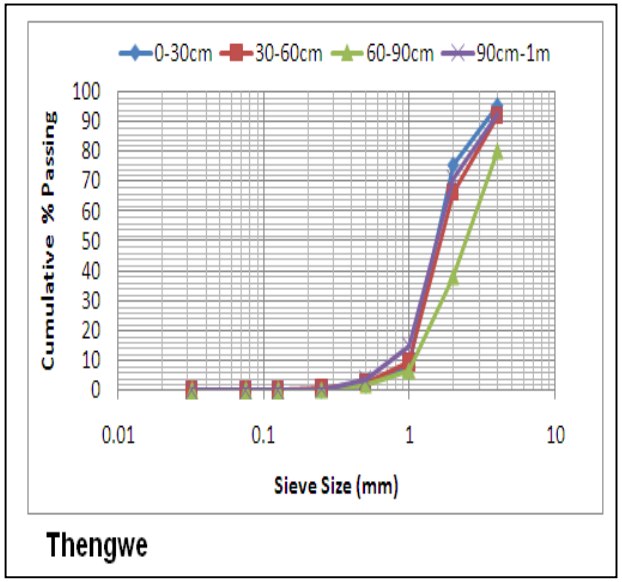

Thengwe

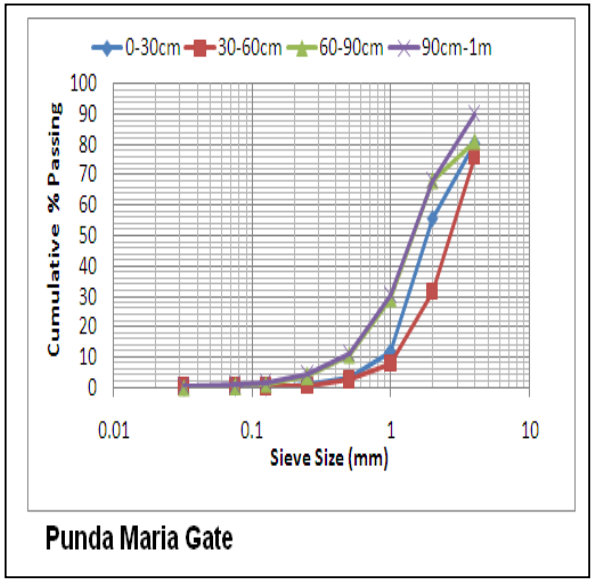

Punda Maria Gate

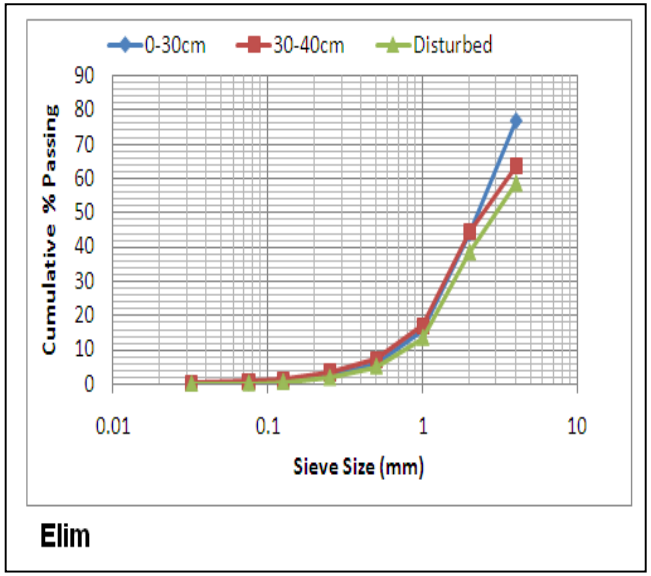

Elim

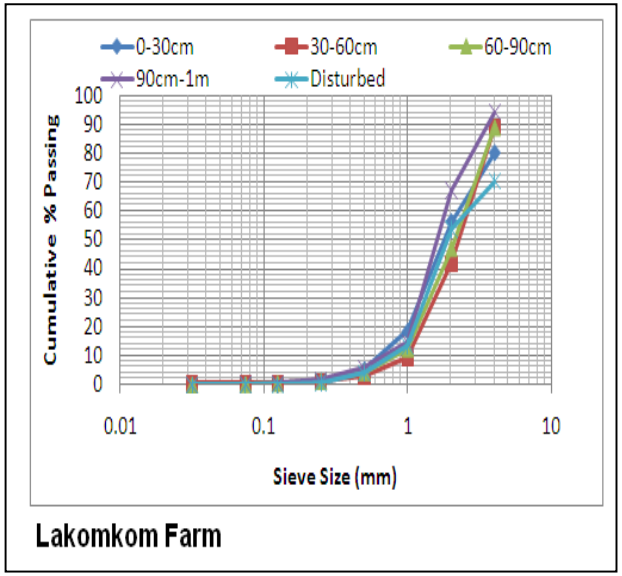

Lakomkom Farm

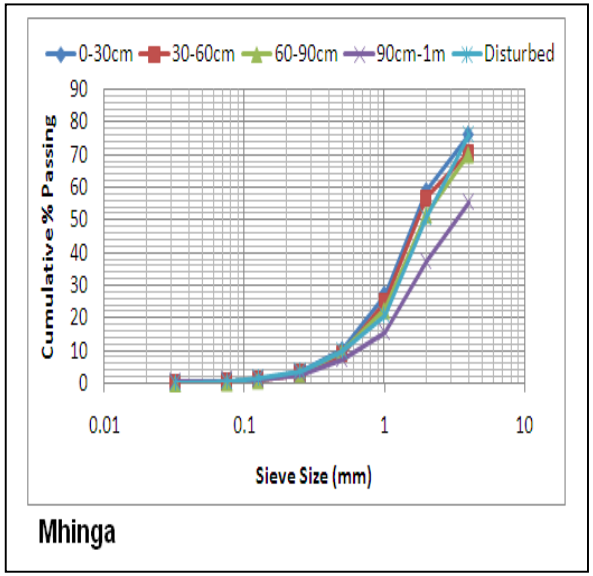

Mhinga

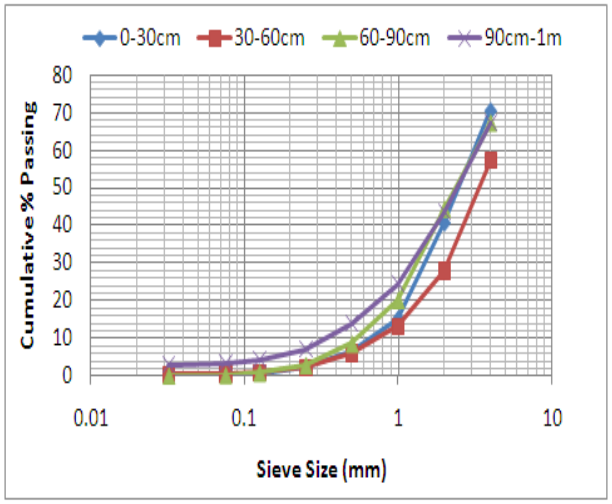

Univen Undisturbed Site

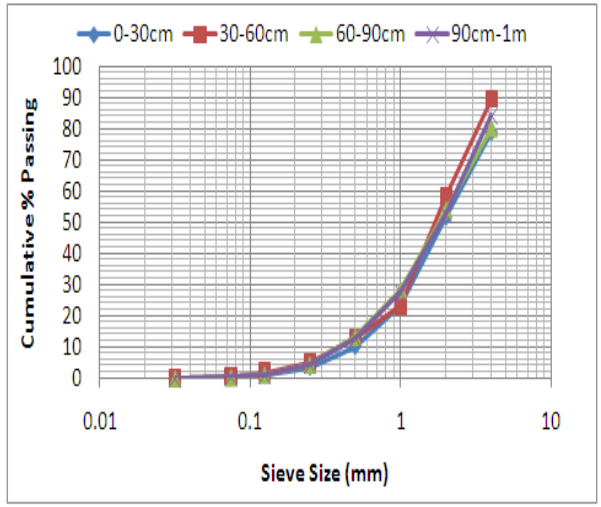

Univen Disturbed Site

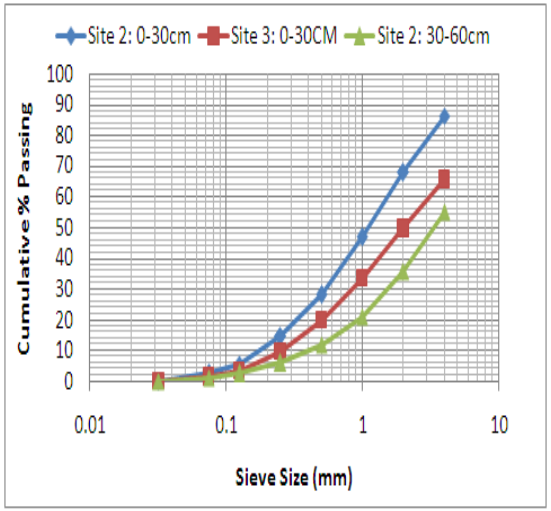

Piesanghoek Hill Top

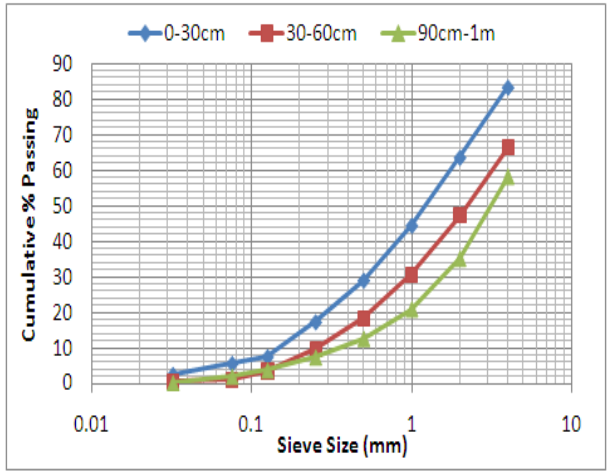

Piesanghoek Valley Bottom

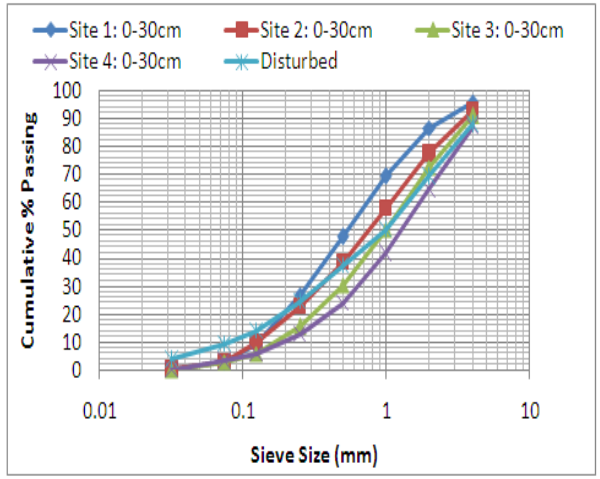

Piesanghoek Slopping Land

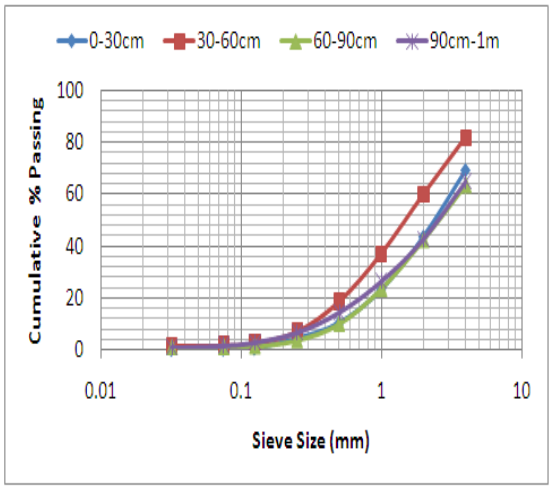

Sterkstroom Low Land